1-1-2014

Part I: Nitroalkane Transformations: Synthesis of Vicinal Diamines and Arylnitromethanes Part II: Quantification of Electrophile Lumo-Lowering via Colorimetric Probes

Ryan R. Walvoord
University of Pennsylvania, rrwalvoord@gmail.com

Part I: Nitroalkane Transformations: Synthesis of Vicinal Diamines and Arylnitromethanes Part II: Quantification of Electrophile Lumo-Lowering via Colorimetric Probes

Abstract

Part I of this dissertation focuses on the synthetic chemistry of arylnitromethanes as both products and reactants. Use of these compounds as key building blocks in the synthesis of vicinal diamines was explored via a catalytic aza-Henry strategy. These studies resulted in the identification of simple cinchonidinium acetate as an effective catalyst for the asymmetric synthesis of syn-1,2-diarylethylenediamines with excellent diastereocontrol. Difficulties in synthesizing arylnitromethanes from existing techniques provided impetus for the development of an improved method of greater generality. Ultimately, successful conditions were identified for the palladium-catalyzed cross coupling of nitromethane with readily available aryl halide partners, providing facile access to an array of functionalized arylnitromethanes. A tandem reductive Nef process was incorporated to provide a one-pot transformation directly to aryl aldehyde or oxime, thereby exploiting the use of nitromethane as a formylation equivalent. Application of the nitromethylation conditions to vinyl halides resulted in the discovery of a unique tandem cross-coupling/π-allylation nitroethylation reaction.

Part II of this dissertation focuses on the use of colorimetric sensors for the quantitative measurement of catalyst strength via LUMO-lowering of electrophiles. Despite rampant growth in catalyst synthesis and application, understanding of controlling factors of catalyst activity, particularly for those functioning through hydrogen-bonding, remains limited. A simple pyrazinone chromophore was found to exhibit hypsochromic shifts upon binding to an array of known hydrogen-bond catalysts. These wavelength shifts showed high correlation to relative rate enhancement of the catalysts in Diels Alder and Friedel Crafts reactions. Acidity values, often used to estimate hydrogen-bond strength, were illustrated to be poor indicators of catalytic activity, in contrast to that of the wavelength shifts. The results establish the catalyst-sensor wavelength is a useful tool with which to gauge catalyst strength and also reveal catalyst structure-activity relationships. Current efforts for measuring stronger BrÃ¸nsted and Lewis Acid catalysts with an alternate colorimetric sensor are also described.

Degree Type
Dissertation

Degree Name
Doctor of Philosophy (PhD)

Graduate Group
Chemistry

First Advisor
Marisa C. Kozlowski

Keywords
Hydrogen Bonding, Organocatalysis, Palladium Catalysis

Subject Categories
Organic Chemistry

PART I: NITROALKANE TRANSFORMATIONS: SYNTHESIS OF VICINAL

DIAMINES AND ARYLNITROMETHANES

PART II: QUANTIFICATION OF ELECTROPHILE LUMO-LOWERING VIA

COLORIMETRIC PROBES

Ryan Richard Walvoord

A DISSERTATION

in

Chemistry

Presented to the Faculties of the University of Pennsylvania

in

Partial Fulfillment of the Requirements for the

Degree of Doctor of Philosophy

2014

Supervisor of Dissertation

_____

Marisa C. Kozlowski, Professor of Chemistry

Graduate Group Chairperson

_____

Gary A. Molander
Hirschmann-Makineni Professor of Chemistry

Dissertation Committee:

Patrick J. Walsh, Professor of Chemistry
Amos B. Smith III, Rhodes-Thompson Professor of Chemistry
Gary A. Molander, Hirschmann-Makineni Professor of Chemistry

ACKNOWLEDGEMENT

The following dissertation is the culmination of nearly six years of work, and there are numerous people to whom I owe sincere thanks. First, to my research advisor, Professor Marisa Kozlowski, for taking a bit of a chance on a then long-haired, barely 21-year old who had asked if there was extra time in grad school to also study German language. Her willingness to allow me to pursue multiple interesting projects, often simultaneously, has been critical for helping me learn to be an independent scientist. I also want to thank her for her continued patience and help, particularly with my transition into physical organic chemistry, in which I had previously had very little training or experience.

The projects described in this thesis, particularly in Chapters 2 and 3, received important contributions from other researchers who are gratefully thanked. Dr. Simon Berritt performed and assisted with many high-throughput experimentation screens and conducted several key early experiments for the nitromethylation chemistry. Dr. Rosaura Padilla and Sergei Tcyrulnikov optimized and explored the nitroethylation reaction. Coworker Phuong Huynh spent a large amount of time investigating optimal conditions for kinetic analysis of the Diels Alder reaction and established much of the early rate studies with hydrogen-bonding catalysts. I also want to acknowledge the aid of Dr. Patrick Carroll for solving X-ray crystal structures, as well as Drs. George Furst and Jun Gu for NMR assistance and company while collecting data points.

I am thankful to my labmates in the Kozlowski group with whom I have worked over these years for being great scientists and excellent persons. The approachability and cooperation of the group, combined with the distinct lack of drama has made research

both more productive and enjoyable. A special thanks is appropriate for Dr. Barbara Jane Morgan for having a very tough-love, hands-on approach to my initial training. Thank you to Alison and Kelsey for talking chemistry (and fun/space facts) over lunch. I also need to thank John for being a fantastic labmate and friend for the past five years, and I have greatly benefitted from his ability to identify critical questions across many areas of research.

Finally, I want to thank my friends and family, especially Jason Melvin, my brother, my parents, and of course Anna, for continued support and love through the stresses of graduate school.

ABSTRACT

PART I: NITROALKANE TRANSFORMATIONS: SYNTHESIS OF VICINAL

DIAMINES AND ARYLNITROMETHANES

PART II: QUANTIFICATION OF ELECTROPHILE LUMO-LOWERING VIA

COLORIMETRIC PROBES

Ryan Richard Walvoord

Professor Marisa C. Kozlowski

Part I of this dissertation focuses on the synthetic chemistry of arylnitromethanes as both products and reactants. Use of these compounds as key building blocks in the synthesis of vicinal diamines was explored via a catalytic *aza*-Henry strategy. These studies resulted in the identification of simple cinchonidinium acetate as an effective catalyst for the asymmetric synthesis of *syn*-1,2-diarylethylenediamines with excellent diastereocontrol. Difficulties in synthesizing arylnitromethanes from existing techniques provided impetus for the development of an improved method of greater generality. Ultimately, successful conditions were identified for the palladium-catalyzed cross coupling of nitromethane with readily available aryl halide partners, providing facile access to an array of functionalized arylnitromethanes. A tandem reductive Nef process was incorporated to provide a one-pot transformation directly to aryl aldehyde or oxime, thereby exploiting the use of nitromethane as a formylation equivalent. Application of the nitromethylation conditions to vinyl halides resulted in the discovery of a unique tandem cross-coupling/π-allylation nitroethylation reaction.

Part II of this dissertation focuses on the use of colorimetric sensors for the quantitative measurement of catalyst strength via LUMO-lowering of electrophiles.

Despite rampant growth in catalyst synthesis and application, understanding of controlling factors of catalyst activity, particularly for those functioning through hydrogen-bonding, remains limited. A simple pyrazinone chromophore was found to exhibit hypsochromic shifts upon binding to an array of known hydrogen-bond catalysts. These wavelength shifts showed high correlation to relative rate enhancement of the catalysts in Diels Alder and Friedel Crafts reactions. Acidity values, often used to estimate hydrogen-bond strength, were illustrated to be poor indicators of catalytic activity, in contrast to that of the wavelength shifts. The results establish the catalyst-sensor wavelength is a useful tool with which to gauge catalyst strength and also reveal catalyst structure-activity relationships. Current efforts for measuring stronger Brønsted and Lewis Acid catalysts with an alternate colorimetric sensor are also described.

TABLE OF CONTENTS

Part I. NITROALKANE TRANSFORMATIONS: SYNTHESIS OF VICINAL DIAMINES AND ARYLNITROMETHANES

1. STEREOSELECTIVE SYNTHESIS OF 1,2-DIARYLETHYLENEDIAMINES VIA ASYMMETRIC *AZA*-HENRY REACTION

1.1. Background

1.1.1. Significance of 1,2-Diamines

Molecules containing contiguous nitrogen-bearing carbon atoms are pervasive in multiple areas of chemistry.[1] This vicinal, or 1,2-diamine moiety is a central structural feature of many biologically relevant molecules (Figure 1.1), including the essential cofactor biotin (vitamin H). The motif has found great utility in areas of medicinal chemistry ranging from molecular imaging tools to pharmaceuticals possessing anticancer, antidepressant, antipsychotic, and other properties.[2] A tangible example includes the plati n series of anticancer agents[3], wherein several successful analogs, such as oxaliplatin, have replaced the two monodentate ammine ligands from the parent cisplatin with a bidentate 1,2-diamine ligand.[4] The potent p53-MDM2 inhibitor Nutlin-3 also features a chiral 1,2-diamine unit in its central imidazole core.[5]

1) Lucet, D.; Le Gall, T.; Mioskowski, C. "The Chemistry of Vicinal Diamines" *Angew. Chem. Int. Ed.* **1998**, *37*, 2580-2627.
2) Michalson, E. T.; Szmuszkovicz, J. "Medicinal agents incorporating the 1,2-diamine functionality" *Prog. Drug. Res.* **1989**, *33*, 135-149.
3) (a) Wang, D.; Lipard, S. J. "Cellular Processing of Platinum Anticancer Drugs" *Nat. Rev. Drug Discovery* **2005**, *4*, 307-320. (b) Jamieson, E. R.; Lippard, S. J. "Structure, Recognition, and Processing of Cisplatin–DNA Adducts" *Chem. Rev.* **1999**, *99*, 2467-2498.
4) (a) Raymond, E.; Chaney, S. G.; Taamma, A.; Cvitkovic, E. "Oxaliplatin: A review of preclinical and clinical studies" *Ann. Oncol.* **1998**, *9*, 1053-1071. (b) Wheate, N. J.; Walker, S.; Craig, G. E.; Oun, R. "The status of platinum anticancer drugs in the clinic and in clinical trials" *Dalton Trans.* **2010**, *39*, 8113-8127.
5) (a) Lowe, S. W.; Cepero, E.; Evan, G. "Intrinsic tumour suppression" *Nature* **2004**, *432*, 307-315. (b) Fischer, P. M.; Lane, D. P. "Small-molecule inhibitors of the p53 suppressor HDM2: have protein-protein interactions come of age as drug targets?" *Trends Pharmacol. Sci.* **2004**, *25*, 343-346.
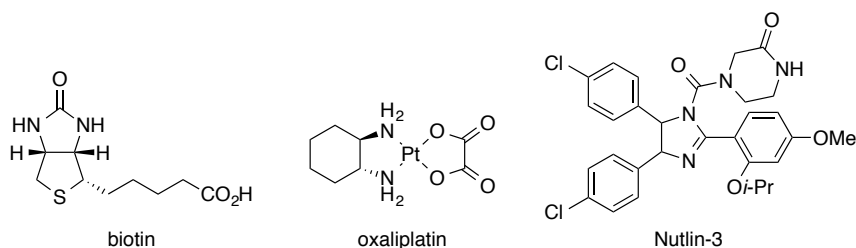
Figure 1.1 Examples of 1,2-diamines in biologically active molecules.

Perhaps most notable is the use of chiral, nonracemic 1,2-diamines as the critical stereocontrol element in myriad catalytic, asymmetric transformations (Figure 1.2). The motif may be incorporated in the ligand of a metal catalyst, as evidenced by the privileged Schiff base or salen structures, in which the diamine is condensed with aryl aldehydes and subsequently coordinated with a variety of metals. These catalysts have proven effective for a large breadth of reaction motifs, and continue to be widely investigated and employed.[6] Alternatively, 1,2-diamines have been incorporated into numerous organocatalyst structures, with the amine groups functioning as basic sites and/or hydrogen bond donors. Takemoto's thiourea-based catalyst, capable of asymmetric Michael addition of malonates into nitroolefins,[7] distinctly illustrates this strategy.
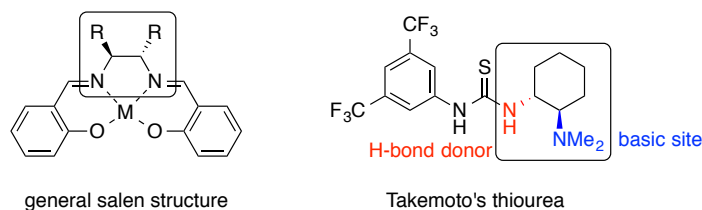
Figure 1.2 Examples of 1,2-diamines in chiral catalyst structures.

6) Gupta, K. C.; Sutar, A. K. "Catalytic activities of Schiff base transition metal complexes" *Coord. Chem. Rev.* **2008**, *252*, 1420-1450.
7) Okino, T.; Hoashi, Y.; Takemoto, Y. "Enantiosleletive Michael Reaction of Malonates to Nitroolefins Catalyzed by Bifunctional Organocatalysts" *J. Am. Chem. Soc.* **2003**, *125*, 12672-12673.

Previous work in the Kozlowski group has detailed the design, synthesis, and utility of a doubly cationic bisamidinium catalyst **1.01**, which displays rate enhancement of nearly two orders of magnitude for the Claisen rearrangement of simple monodentate allyl vinyl ether **1.02** (Scheme 1.1).[8] Initial studies employing the chiral bisamidinium **1.04** afforded the anticipated ketone **1.03** in low enantiomeric excess, demonstrating that enantiocontrol can be effected with this type of catalyst scaffold (Scheme 1.2).[9]

Scheme 1.1 Bisamidinium-catalyzed Claisen rearrangement.
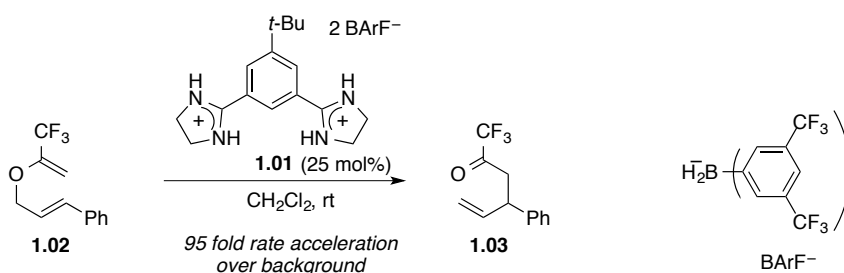
Scheme 1.2 Preliminary asymmetric rearrangement using a chiral bisamidinium.
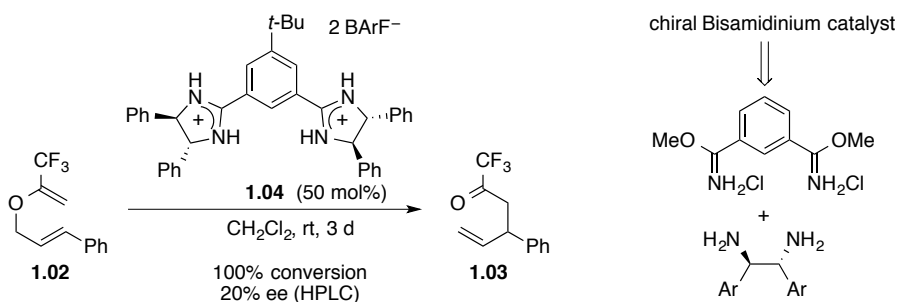
Electronic and steric tuning of the catalyst structure would be accomplished via selection of the 1,2-diarylethylenediamine incorporated. Unfortunately, these efforts were severely hindered by the general inaccessibility of this class of molecules. Specifically, the few variations of the parent compound commercially available are prohibitively expensive, and, as will be discussed in greater detail in the subsequent

---

8) Annamalai, V. R.; Linton, E. C.; Kozlowski, M. C. "Design of a Bisamidinium Claisen Rearrangement Catalyst for Monodentate Substrates" *Org. Lett.* **2009**, *11*, 621-624.

9) Annamalai, V. R.; Linton, E. C.; Walvoord, R. R.; Kozlowski, M. C. *unpublished results*.

section, current methods for their synthesis remain impractical. As a consequence to these limitations, exploration of catalyst activity *via* systematic changes to the critical diamine moiety continues to be largely unfeasible. Development of a direct, robust method for the synthesis of both symmetrical and unsymmetrical 1,2-diarylethylenediamines represents a challenging and worthwhile goal.

1.1.2. Previous Synthetic Access to 1,2-Diarylethylenediamines

Due to the considerable interest in exploring diamine modulation, several methods have been developed for the synthesis of chiral, nonracemic 1,2-diarylethylenediamines. Stereoselective reductive dimerization or reduction of bis-imines are the most studied reaction profiles (Scheme 1.3). Corey and coworkers described the reduction of benzil-derived bis-imines under Birch conditions to afford the racemic diamines.[10] This method affords the products in good yield and selectivity, but is limited by the availability of benzil precursors. The reductive dimerization of *N*-TMS imines with niobium(IV) to provide the *anti*-diamine products in highly selectivity was reported by Pedersen and coworkers.[11] Although this process requires two equivalents of Nb for each product generated, a diverse array of starting imines are readily available via aryl aldehydes. The above examples can provide racemic products in good efficiency but require a subsequent resolution to afford enantiopure diamines. Such resolutions have

10) (a) Corey, E. J.; Lee, D.-H.; Sarshar, S. "Convenient Routes to Symmetrical Benzils and Chiral 1,2-Diaryl-1,2-diaminoethanes, Useful Controllers and Probes for Enantioselective Synthesis" *Tetrahedron: Asymmetry* **1995**, *6*, 3-6. (b) Pikul, S.; Corey, E. J. "(1R,2R)-(+)- and (1S,2S)-(−)-1,2-diphenyl-1,2-ethylenediamine" *Org. Synth.* **1998**, *71*, 22-26.
11) Roskamp, E. J.; Pedersen, S. F. "Convenient Routes to Vicinal Diamines. Coupling of Nitriles or *N*-(Trimethylsilyl)imines Promoted by NbCl4(THF)2" *J. Am. Chem. Soc.* **1987**, *109*, 3152-3154.

been demonstrated to be substrate-dependent and often low-yielding,[12] rendering these processes unsuitable for rapidly generating nonracemic diamine libraries. A resolution can be avoided if a chiral, enantioenriched imine is employed. Specifically, *N*-sulfinyl imines can be coupled using SmI$_2$ with HMPA, revealing the enantiopure, *anti*-diamine products after acid removal of the sulfinyl group.[13] The method affords the products in very good stereoselectivity but variable yields, and requires two equivalents of the costly *tert*-butylsulfinamide chiral building block (1 g ~ $70).

Scheme 1.3 Imine reduction routes for chiral diamines.
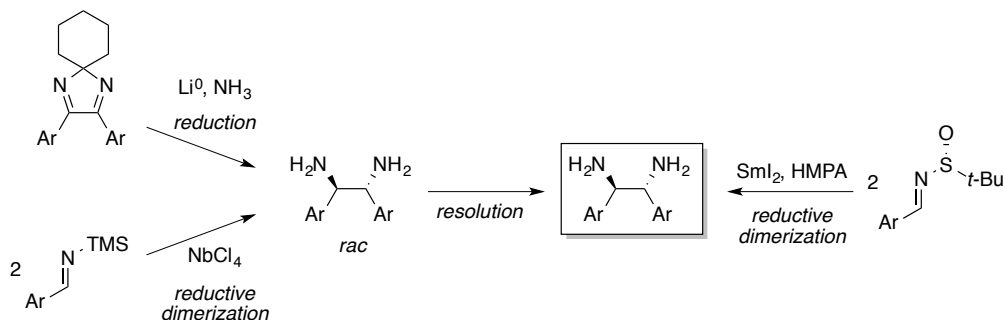
An alternative approach, as illustrated in Scheme 1.4, utilizes the power of the Sharpless asymmetric dihydroxylation[14] of stilbenes, followed by nitrogen substitution using azide chemistry. This process has been used only sparingly,[15] likely due to

12) Denmark, S. E.; Su, X.; Nishigaichi, Y.; Coe, D. M.; Wong, K.-T.; Winter, S. B. D.; Choi, J. Y. "Synthesis of Phosphoramides for the Lewis Base-Catalyzed Allylation and Aldol Addition Reactions" *J. Org. Chem.* **1999**, *64*, 1958-1967.

13) Zhong, Y.-W.; Izumi, K.; Xu, M.-H.; Lin, G.-Q. "Highly Diastereoselective and Enantioselective Synthesis of Enantiopure C$_2$-Symmetrical Vicinal Diamines by Reductive Homocoupling of Chiral *N*-*tert*-Butansulfinyl Imines" *Org. Lett.* **2004**, *6*, 4747-4750.

14) Kolb, H. C.; VanNieuwenhze, M. S.; Sharpless, K. B. "Catalytic Asymmetric Dihydroxylation" *Chem. Rev.* **1994**, *94*, 2483-2547.

15) (a) Sasaki, H.; Irie, R.; Hamada, T.; Suzuki, K.; Katsuki, T. "Rational Design of Mn-Salen Catalyst (2): Highly Enantioselective Epoxidation of Conjugated *cis*-Olefins" *Tetrahedron* **1994**, *50*, 11827-11838. (b) Hilgraf, R.; Pfaltz, A. "Chiral Bis(*N*-sulfonylamino)phosphine- and TADDOL-Phosphite-Oxazoline Ligands: Synthesis and Application in Asymmetric Catalysis" *Adv. Synth. Catal.* **2005**, *347*, 61-77.

unavailability of geometrically pure stilbene substrates and limited functional group tolerance in the substitution chemistry.

Scheme 1.4 Chiral diamine synthesis *via* asymmetric dihydroxylation/substitution.
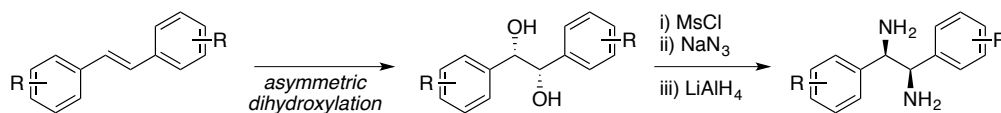
Chin and coworkers have more recently developed an elegant method for the stereospecific synthesis of enantiopure 1,2-diarylethylenediames through a diaza-Cope rearrangement (Scheme 1.5).[16] The enantiopure "mother" diamine **1.05** is condensed with the desired aldehyde to form initial bis-imine **1.06a** and subsequently rearranged via a process termed a resonance-assisted hydrogen-bond directed diaza-Cope.

Scheme 1.5 Chin's diaza-Cope method for chiral diamine synthesis.
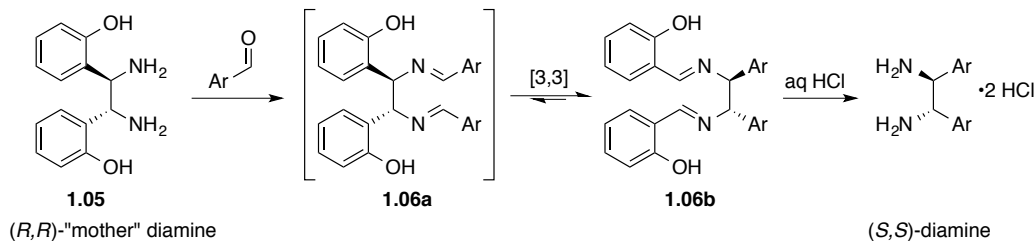
The rearrangement proceeds under mild conditions and with excellent stereocontrol, affording (*S,S*)-diamine products after hydrolysis in >99% *ee* when starting with >99% ee (*R,R*)-**1.05**. Overall, a broad array of enantiopure diamines can be accessed in high yields (70-90%) without the need of a chiral resolution. Although the

---

16) (a) Chin, J.; Mancin, F.; Thavarajah, N.; Lee, D.; Lough, A.; Chung, D. S. "Controlling Diaza-Cope Rearrangement Reactions with Resonance-Assisted Hydrogen Bonds" *J. Am. Chem. Soc.* **2003**, *125*, 15276-15277. (b) Kim, H.-J.; Kim, H.; Alhakimi, G.; Jeong, E. J.; Thavarajah, N.; Studnicki, L.; Koprianiuk, A.; Lough, A. J.; Suh, J.; Chin, J. "Preorganization in Highly Enantioselective Diaza-Cope Rearrangement Reaction" *J. Am. Chem. Soc.* **2005**, *127*, 16370-16371. (c) Kim, H.; Nguyen, Y.; Yen, C. P.-H.; Chagal, L.; Lough, A. J.; Kim, B. M.; Chin, J. "Stereospecific Synthesis of *C₂* Symmetric Diamines from the Mother Diamine by Resonance-Assisted Hydrogen-Bond Directed Diaza-Cope Rearrangment" *J. Am. Chem. Soc.* **2008**, *130*, 12184-12191.

mother diamine is now commercially available, it remains costly[17], and its synthesis (through Corey's reductive method described previously) requires several steps including a chiral resolution.

1.1.3. Asymmetric, Catalytic aza-Henry Reactions

An appealing approach for a concise synthesis of 1,2-diamines focuses on the stereoselective carbon-carbon bond formation between two smaller nitrogen-containing subunits. The nucleophilic addition of nitroalkanes and imines, known as the *aza*-Henry (or nitro-Mannich) reaction, is a powerful method for the direct formation of β-nitroamines, which may be readily reduced and deprotected to reveal the 1,2-diamine moiety. Consequently, our initial efforts centered on the development of a stereoselective *aza*-Henry reaction of arylnitromethanes with aryl imines to afford the *anti*-nitroamine products (Figure 1.3). A notable advantage of this approach is the ability to prepare diamines with unsymmetric aryl substitution, as opposed to oxidative or reductive dimerization sequences.
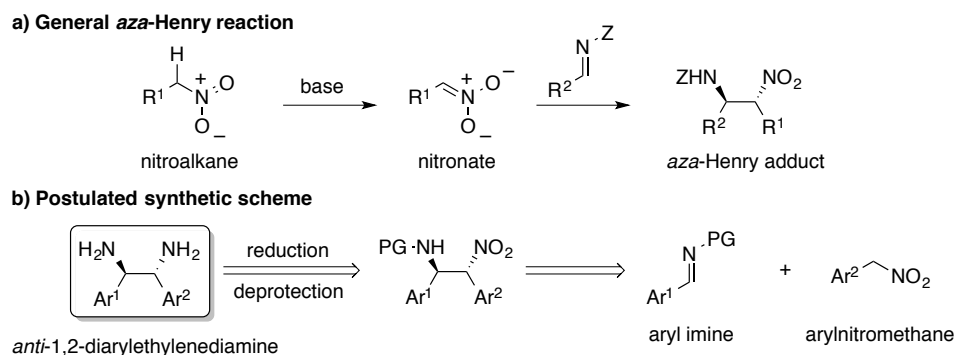
Figure 1.3 *Aza*-Henry strategy for 1,2-*anti*-diarylethylenediamines.

---

17) From Sigma-Aldrich: 1 g of (1R,2R)-1,2-bis(2-hydroxyphenyl)ethylenediamine = $130.50 (1/24/14).

The *aza*-Henry reaction provides versatile *β*-nitroamine adducts that may be further transformed into diamines, *α*-amino acid derivatives, and other useful building blocks. Consequently, the reaction has received considerable investigation, particularly in asymmetric variants over the past 15 years.[18] The first such example was reported by Shibasaki and coworkers in 1999, in which a Yb-K heterobimetallic 2,2-binaphthol (BINOL) complex catalyzed the addition of nitromethane into *N*-phosphinoyl aryl imines.[19] Since then, successful asymmetric methods have been developed employing a variety of metal-based systems.[20] Beginning with Takemoto's use of a bifunctional thiourea catalyst[21], significant effort has also focused on asymmetric organocatalyzed methods. In addition to thioureas[22], amidinium[23], ammonium betaine[24], chiral Brønsted

18) (a) Marques-Lopez, E.; Merino, P.; Tejero, T.; Herrera, R. P. "Catalytic Enantioselective Aza-Henry Reactions" *Eur. J. Org. Chem.* **2009**, 2401-2420. (b) Westermann, B. "Asymmetric Catalytic Aza-Henry Reactions Leading to 1,2-Diamines and 1,2-Diaminocarboxylic Acids" *Angew. Chem. Int. Ed.* **2003**, *42*, 151-153.

19) Yamada, K.; Harwood, S. J.; Gröger, H.; Shibasaki, M. "The First Catalytic Asymmetric Nitro-Mannich-Type Reaction Promoted by a New Heterobimetallic Complex" *Angew. Chem. Int. Ed.* **1999**, *38*, 3504-3506.

20) Select examples of metal catalyzed *syn*-selective methods: (a) Knudsen, K. R.; Risgaard, T.; Nishiwaki, N.; Gothelf, K. F.; Jørgensen, K. A. "The First Catalytic Asymmetric Aza-Henry Reaction of Nitronates with Imines: A Novel Approach to Optically Active *β*-Nitro-*α*-Amino Acid- and *α*,*β*-Diamino Acid Derivatives" *J. Am. Chem. Soc.* **2001**, *123*, 5843-5844. (b) Anderson, J. C.; Howell, G. P.; Lawrence, R. M.; Wilson, C. S. "An Asymmetric Nitro-Mannich Reaction Applicable to Alkyl, Aryl, and Heterocyclic Imines" *J. Org. Chem.* **2005**, *70*, 5665-5670. (c) Trost, B. M; Lupton, D. W. "Dinuclear Zinc-Catalyzed Enantioselective Aza-Henry Reaction" *Org. Lett.* **2007**, *9*, 2023-2026.

21) Okino, T.; Nakamura, S.; Furukawa, T.; Takemoto, Y. "Enantioselective Aza-Henry Reaction Catalyzed by a Bifunctional Organocatalyst" *Org. Lett.* **2004**, *6*, 625-627.

22) Select examples of thiorea catalyzed *syn*-selective methods see: (a) Yoon, T. P.; Jacobsen, E. N. "Highly Enantioselective Thiourea-Catalyzed Nitro-Mannich Reactions" *Angew. Chem. Int. Ed.* **2005**, *44*, 466-468. (b) Robak, M.; Trincado, M.; Ellman, J. A. "Enantioselective Aza-Henry Reactions with an *N*-Sulfinyl Urea Organocatalyst" *J. Am. Chem. Soc.* **2007**, *129*, 15110-15111. (c) Rampalakos, C.; Wulff, W. D. "A Novel Bis-Thiourea Organocatalyst for the Asymmetric Aza-Henry Reaction" *Adv. Synth. Catal.* **2008**, *350*, 1785-1790.

23) Nugent, B. M.; Yoder, R. A.; Johnston, J. N. "Chiral Proton Catalysis: A Catalytic Enantioselective Direct Aza-Henry Reaction" *J. Am. Chem. Soc.* **2004**, *126*, 3418-3419.

24) Uraguchi, D.; Koshimoto, K.; Ooi, T. "Chiral Ammonium Betaines: A Bifunctional Organic Base Catalyst for Asymmetric Mannich-Type Reaction of *α*-Nitrocarboxylates" *J. Am. Chem. Soc.* **2008**, *130*, 10878-10879.

acid[25], and *cinchona* alkaloid-based catalysts[26] have been reported. Many of these investigations have focused on asymmetric addition of nitromethane as the nucleophile. Secondary nitroalkanes, which form an additional stereocenter, have been studied to a lesser extent, leading to several doubly stereoselective methods for the preparation of the *syn*[27] adducts in high enantiopurity.

Despite these considerable advances, notable challenges remain, particularly with regard to synthesis of *anti*-1,2-diarylethylenediamine precursors. Specifically, in contrast to *syn*-selective processes, only two asymmetric methods have been reported for the *anti* diastereomer. Shibasaki and coworkers elegantly detailed the design of a Cu-Sm heterobimetallic Schiff base catalyst[28] for the *anti*-selective addition of nitroethane and nitropropane into *N*-Boc benzaldimines.[29]

25) Reuping, M.; Antonchick. A. P. "Brønsted-Acid-Catalyzed Activation of Nitroalkanes: A Direct Enantioselective Aza-Henry Reaction" *Org. Lett.* **2008**, *10*, 1731-1734.
26) Cinchonidinium-catalyzed reactions of amidosulfones: (a) Fini, F.; Sgarzani, V.; Pettersen, D.; Herrera, R. P.; Bernardi, L.; Ricci, A. "Phase-Transfer-Catalyzed Asymmetric Aza-Henry Reaction Using *N*-Carbamoyl Imines Generated In Situ from α-Amido Sulfones" *Angew. Chem. Int. Ed.* **2005**, *44*, 7975-7978. (b) Palomo, C.; Oiarbide, M.; Laso, A.; Lopez, R. "Catalytic Enantioselective Aza-Henry Reaction with Broad Substrate Scope" *J. Am. Chem. Soc.* **2005**, *127*, 17622-17623. (c) Gomez-Bengoa, E.; Linden, A.; Lopez, R.; Mugica-Mendiola, I.; Oiarbide, M.; Palomo, C. "Asymmetric Aza-Henry Reaction Under Phase Transfer Catalysis: An Experimental and Theoretical Study" *J. Am. Chem. Soc.* **2008**, *130*, 7955-7966. (d) Wei, Y.; He, W.; Liu, Y.; Liu, P.; Zhang, S. "Highly Enantioselective Nitro-Mannich Reaction Catalyzed by *Cinchona* Alkaloids and *N*-Benzotriazole Derived Ammonium Salts" *Org. Lett.* **2012**, *14*, 704-707.
27) The *anti* configuration is defined as shown in Figure 1.3. Opposite nomenclature is used in other references, notably the Shibasaki publications.
28) In a somewhat ironic testament to their importance in asymmetric catalysis, a chiral 1,2-diamine is used here as the stereocontrol element in a method developed for generating chiral 1,2-diamine precursors.
29) Handa, S.; Gnanadesikan, V.; Masunaga, S.; Shibasaki, M. "*syn*-Selective Catalytic Asymmetric Nitro-Mannich Reactions Using a Heterobimetallic Cu–Sm–Schiff Base Complex" *J. Am. Chem. Soc.* **2007**, *129*, 4900-4901.

Table 1.1 Shibasaki's *anti*-selective heterobimetallic *aza*-Henry method.

R	yield (%)	dr (*anti*:syn)	% ee
Me	98	>95:5	93
Et	83	>95:5	99
n-Pr	**trace**	-	-
PhCH$_2$	80	>95:5	**11**

A subsequent report[30] described an improved procedure for catalyst generation, which broadened the scope to include sterically hindered and aliphatic imines. However, a large excess of nucleophile partner was necessary, and, more importantly, the scope remained severely limited (Table 1.1). For example, employing nitrobutane or 2-nitropropane yielded only trace product and 1-nitro-2-phenylethane afforded low (11% ee) enantioselectivity. Following Shibasaki's report, Wang and coworkers described a rosin-derived thiourea catalyst effective for the asymmetric aza-Henry reaction with nitromethane.[31] Limited experiments employing nitroethane provide moderate selectivity for the *anti* diastereomer. The other primary challenge lay in developing a method capable of tolerating the bulkier and weakly nucleophilic arylnitromethane group. Previous utilization of arylnitromethanes in *aza*-Henry reactions is limited to two examples with α-iminoesters, with both providing much lower selectivity (particularly diastereoselectivity) compared with smaller nitroalkanes.[20a,25] As seen in Shibasaki's system previously described, bulkier nitroalkanes have widely demonstrated poor

30) Handa, S.; Gnanadesikan, V.; Matsunaga, S.; Shibasaki, M. "Heterobimetallic Transition Metal/Rare Earth Metal Bifunctional Catalysis: A Cu/Sm/Schiff Base Complex for *Syn*-Selective Catalytic Asymmetric Nitro-Mannich Reaction" *J. Am. Chem. Soc.* **2010**, *132*, 4925-4934.

31) Jiang, X.; Zhang, Y.; Wu, L.; Zhang, G.; Liu, X.; Zhang, H.; Fu, D.; Wang, R. "Doubly Stereocontrolled Asymmetric Aza-Henry Reaction with *in situ* Generation of *N*-Boc-Imines Catalyzed by Novel Rosin-Derived Amine Thiourea Catalysts" *Adv. Synth. Catal.* **2009**, *351*, 2096-2100.
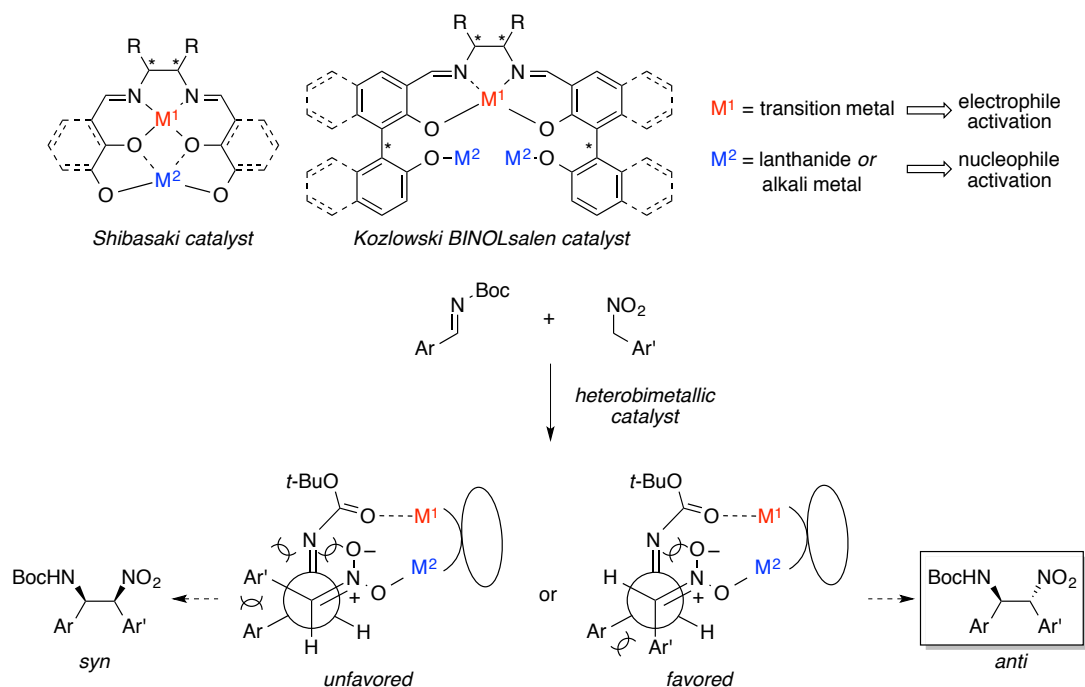
enantioselectivity, diastereoselectivity, and efficiency compared to smaller nitroalkanes in otherwise highly selective processes. It is pertinent to note that attempts in our lab to employ Shibasaki's Cu-Sm bimetallic system with phenylnitromethane were met with little success, resulting in low *anti* selectivity (2.5:1) and racemic products.

Previous efforts in the Kozlowski group had investigated the synthesis, structure, and catalytic capabilities of BINOL-derived salen complexes – a novel bifunctional catalyst motif.[32] A variety of transition metals can be stably inserted into the N_2O_2 binding pocket, and the remaining phenols can be deprotonated *in* situ with alkali metals. Consequently, the BINOLsalen scaffold provides a highly tunable platform for heterobimetallic catalysis, featuring well-defined sites for electrophile and nucleophile activation. Based on the similar design of Shibasaki's heterobimetallic system, we postulated that our BINOLsalen catalysts might possess the correct dual-binding array for preferential formation of the desired *anti* adducts. Specifically, Lewis acid activation of the Boc carbonyl with the inner metal and concomitant deprotonative activation of the nitroalkane with the outer metal-phenoxide should favor the chelation-controlled model in Figure 1.4.

---

32) (a) DiMauro, E. F.; Kozlowski, M. C. "BINOL-Salen Metal Catalysts Incorporating a Bifunctional Design" *Org. Lett.* **2001**, *3*, 1641-1644. (b) DiMauro, E. F.; Kozlowski, M. C. "Late-Transition-Metal Complexes of BINOL-Derived Salens: Synthesis, Structure, and Reactivity" *Organometallics* **2002**, *21*, 1454-1461. (c) Annamalai, V.; DiMauro, E. F.; Carroll, P. J.; Kozlowski, M. C. "Catalysis of the Michael Addition Reaction by Late Transition Metal Complexes of BINOL-Derived Salens" *J. Org. Chem.* **2003**, *68*, 1973-1981.

Figure 1.4 Postulated transition state models with heterobimetallic catalysts.

This transition state model was similarly used to rationalize the stereoselectivity observed by Shibasaki. The BINOLsalen catalysts possess additional chiral centers (BINOL and diamine backbone), allowing further variation in stereocontrol elements for developing a highly enantiospecific addition of the nitronate nucleophile. Whereas Shibasaki's catalyst was incompatible with larger nitroalkanes, we envisioned the putatively larger nucleophile binding pocket of the BINOLsalen catalysts would allow for incorporation of the bulkier arylnitromethanes.

1.2. Results

Initial investigation of the desired *aza*-Henry transformation focused on the addition of phenylnitromethane **1.08a** with the *N*-Boc-protected benzaldimines. This particular group was selected due to its proposed binding mode with the inner metal of

12

the BINOLsalen catalyst, high reactivity with weaker nucleophiles, and ease of removal for diamine formation. The two reaction components can be accessed with relative synthetic ease. In particular, aryl imines are readily obtained from condensation of the desired aldehyde with *tert*-butyl carbamate and sodium benzenesulfinate. The resulting bench-stable adducts are converted to the corresponding imines with mild base. Thorough investigation of reported methods revealed Kornblum's nitrite displacement of benzyl bromides using $AgNO_2$ as the most effective process for the synthesis of arylnitromethanes[33], although generation of electron-rich or sterically hindered substrates (*ortho*-substitution) could not be accessed (see section 2.1.2. for further discussion of arylnitromethane synthesis).

Relative stereochemistry was assigned following Scheme 1.6. Treatment of **1.08a** and benzaldehyde-derived imine **1.07a** with triethylamine smoothly afforded nitrocarbamate adduct **1.09aa** in good yield as a 7:1 mixture of racemic diastereomers. Careful consideration of the nitro reduction was necessary to avoid competitive hydrogenolysis of the relatively weak benzyl–benzyl C–C bond or $C–NO_2$ bond.[34] Successful formation of the amine was afforded by employing $NiCl_2$ with $NaBH_4$ at low temperatures. Subsequent acidic removal of the Boc group revealed the 1,2-diamine moiety. Switching the order of these transformations was unsuccessful. Acidic removal of the Boc group triggered a retro-Henry process, releasing **1.08a** and hydrolyzed benzaldehyde. ^{1}H NMR comparison with commercially-obtained *syn*(meso) and *anti-*

33) Kornblum, N.; Taub, B.; Ungnade, H. E. "The Reaction of Silver Nitrite with Primary Alkyl Halides" *J. Am. Chem. Soc.* **1954**, *76*, 3209-3211.
34) Fessard, T. C.; Motoyoshi, H.; Carreira, E. M. "Pd-catalyzed cleavage of benzylic nitro bonds: New opportunities for asymmetric synthesis" *Angew Chem. Int. Ed.* **2007**, *46*, 2078-2081.

1,2-diphenylethylenediamine established the major product **1.10aa** as the *syn* diastereomer.

Scheme 1.6 Assignment of relative stereochemistry.
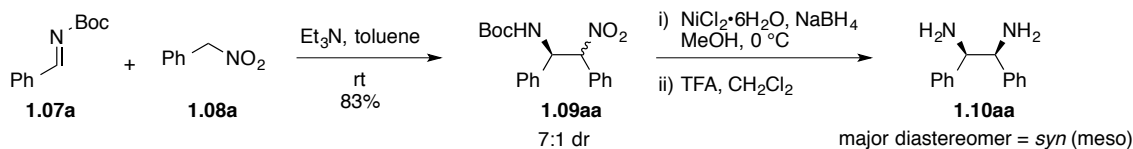
Investigation of the proposed catalyst system on the *aza*-Henry reaction commenced using a series of BINOLsalen structures, as prepared according to the general synthetic route in Scheme 1.7.

Scheme 1.7 Synthesis of BINOLsalen catalysts.
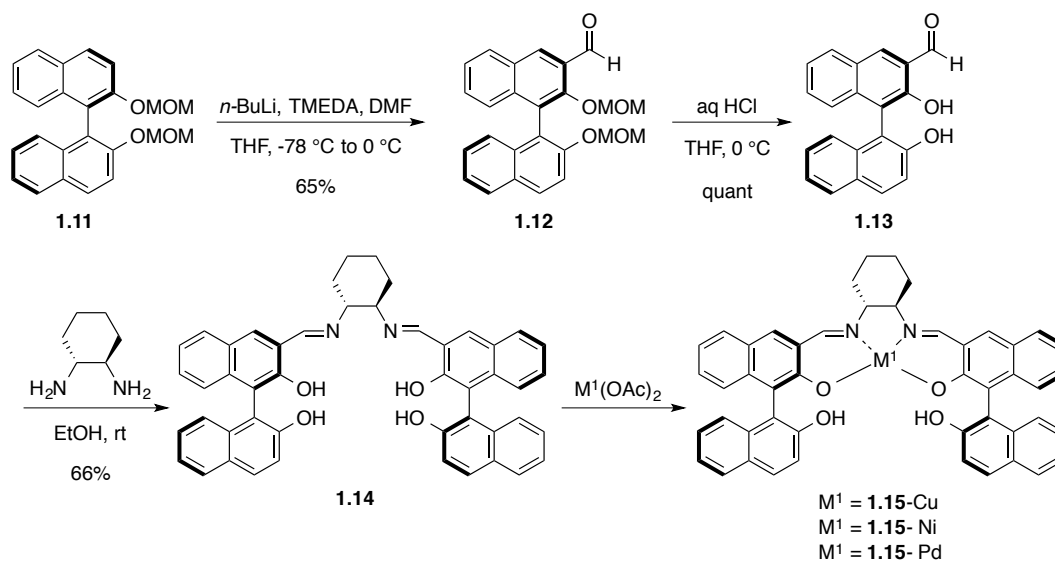
Lithiation of MOM-protected BINOL **1.11** and quenching with DMF afforded monoformylated product **1.12**, which was subsequently deprotected under acidic conditions. Condensation of the resultant aldehyde with 1,2-cyclohexanediamine produced the BINOLsalen scaffold **1.14**. Various metals can be inserted into the N_2O_2 binding pocket using the desired metal acetates. For all reactions employing these

14

catalysts, the outer metal phenoxide was preformed *in situ* by reacting the catalyst with the desired alkali metal base for 2 h prior to substrate addition.

Table 1.2 Effects of BINOLsalen inner and outer metal.

catalyst[a]	M[1]	base	dr (*anti*:syn)[b]	% ee (*anti*)[c]
(*R,R,R,R*)-**1.15**	Cu	Li_2CO_3	6:94	ND
(*R,R,R,R*)-**1.15**	Cu	$BaCO_3$	5:95	ND
(*R,R,R,R*)-**1.15**	Cu	K_2CO_3	50:50	26
(*R,R,R,R*)-**1.15**	Cu	CsOH	50:50	20
(*R,R,R,R*)-**1.15**	Cu	Cs_2CO_3	50:50	28
(*R,R,R,R*)-**1.15**	Pd	Cs_2CO_3	48:52	18
(*S,S,S,S*)-**1.15**	Ni	Cs_2CO_3	58:42	-6
(*S,S,S,S*)-**1.15**	Ni	Na_2CO_3	6:94	ND

[a]Catalyst,base, and THF were stirred under Ar at rt for 2 h before substrate addition. [b]Determined by ^{1}H NMR. [c]Determined by HPLC after reduction.

Initial investigations varied inner and outer metals (Table 1.2). For the latter, smaller alkali metals, as well as barium, provided poor conversions and were mostly selective for the *syn* isomer, while cesium and potassium afforded higher conversion and near equal ratios of diastereomers. Catalysts with copper, palladium, or nickel as the inner metal demonstrated similar levels of diastereoselectivity, with copper providing the highest level of enantioinduction. In general, the results suggest the outer metal is largely responsible for diastereoselectivity, while inner metal plays a key role in enantioinduction. Although unsatisfactory selectivities were observed with all of the catalysts, these experiments demonstrated that the BINOLsalen catalysts were capable of enantiodiscrimination using arylnitromethane coupling partners.

Table 1.3 Solvent effects using BINOLsalen catalysts.

solvent[a]	yield (%)	dr (anti:syn)[b]	% ee (anti)[c]
THF	47	44:56	14
CH$_2$Cl$_2$	46	50:50	37
toluene	52	40:60	31
PhCF$_3$	62	11:89	ND
MeCN	83	62:38	0
Et$_2$O	92	20:80	ND
2-Me-THF	80	42:58	27

[a]Catalyst,base, and solvent were stirred under Ar at rt for 2 h before substrate addition. [a]Determined by ^{1}H NMR. [b]Determined by HPLC after reduction.

A solvent screen using the copper/cesium BINOLsalen system failed to significantly improve product selectivity to the *anti* diastereomer, although dichloromethane provided improved enantioselectivity (Table 1.3). Interestingly, acetonitrile afforded high reaction efficiency and greater *anti* selectivity (62:38), yet provided racemic product.

Table 1.4 Structural variation of BINOLsalen catalysts.

catalyst[a]	dr (anti:syn)[b]	% ee (anti)
(R,S,S,R)-**1.15**-Cu	1.3:1	6
(R,S,S,R)-**1.15**-Ni	1.3:1	11
(S,S)-**1.16**-Pd	1:1.1	-17
R-BINOL	1.3:1	46

[a]Catalyst,base, and THF were stirred under Ar at rt for 2 h before substrate addition. [b]Determined by ^{1}H NMR. [c]Determined by HPLC after reduction.

Variation of the diamine backbone in the BINOLsalen structures allowed analysis of the stereodefining elements (Table 1.4). Specifically, diastereomeric *R,S,S,R*-**1.15** catalysts were synthesized as described in Scheme 1.7 using 1,2-*S,S*-cyclohexanediamine. These catalysts proved to be the mismatch, providing similar *anti* selectivity but lower levels of enantioselectivity with Cu as the inner metal. Notably, the *R,S,S,R*-Ni catalyst provided the *anti* product with opposite absolute stereochemistry compared to the *S,S,S,S*-Ni catalyst, implicating the BINOL backbone as the key stereodefining element. This hypothesis was confirmed through ethylenediamine-derived catalyst *S,S*-**1.16**, which provided the *anti* product in similar magnitude but opposite absolute enantioinduction in comparison to the *R,R,R,R*-**1.15** analogue. Surprisingly, simple use of BINOL with cesium carbonate provided the *aza*-Henry adduct in similar dr and significantly improved ee compared to the more complex BINOLsalen catalysts. Performing the reaction in dichloromethane with a 2:1 BINOL:cesium carbonate ratio afforded the *anti* product in promising 60% ee, albeit with only a slight preference toward the *anti* isomer.

A series of modified BINOL structures were tested as catalysts for the desired transformation, resulting in generally similar levels of diastereoselectivity (~1:1), but large variations in asymmetric induction (Table 1.5).

Table 1.5 Modified BINOL and BINOL analogues as catalysts.

catalyst[a]	base	dr (anti:syn)[b]	% ee (anti)[c]
R-BINOL	Cs_2CO_3	57:43	60
1.17	Cs_2CO_3	60:40	40
1.18	Cs_2CO_3[d]	60:40	-16
1.19	Cs_2CO_3	50:50	4
1.20	Cs_2CO_3	49:51	4
1.21	Cs_2CO_3	29:71	-4
1.22	Cs_2CO_3[e]	55:45	-4
1.23	Cs_2CO_3	51:49	0
1.24	$CsOH \cdot H_2O$	37:63	-20
1.25	$CsOH \cdot H_2O$	37:63	0
1.26	$CsOH \cdot H_2O$	49:51	0

[a]Catalyst, base, and solvent were stirred under Ar at rt for 2 h before substrate addition. [b]Determined by ^{1}H NMR. [c]Determined by HPLC after reduction. [d]25 mol% Cs_2CO_3 used. [e]100 mol% Cs_2CO_3 used.

Modification of the dihedral biaryl bond using H_8-BINOL **1.17** afforded the *anti* product in slightly lower ee, whereas the monomethylated **1.18** provided only minor enantioinduction, indicating the importance of the dual phenoxide motif. Similarly, substitution at the 3,3'-positions proved deleterious, providing racemic product. Triflate and acetate-modified BINAM structures **1.21** and **1.22** also afforded racemic product despite having similar or more acidic protons with respect to the phenols of BINOL. Other chiral, nonracemic compounds possessing dihydroxy [35] or dicarboxylate functionality were tested as catalysts, with only the protected tartrate derivative **1.24** imparting any enantiodiscrimination.

---

35) The stronger $CsOH \cdot H_2O$ base was employed to form the putative deprotonated metal-alkoxy catalyst.

Table 1.6 Base variation with BINOL as catalyst.

base[a]	mol %	dr (*anti*:syn)[b]	% ee (*anti*)[c]
Li[d]	50	20:80	0
Et$_3$N	50	57:43	0
KO*t*-Bu	50	55:45	60
K$_2$CO$_3$	50	9:91	ND
Ag$_2$CO$_3$	50	-[e]	-
Rb$_2$CO$_3$	50	55:45	60
Cs$_2$CO$_3$	25	60:40	54
Cs$_2$CO$_3$	50	57:43	60
Cs$_2$CO$_3$	100	55:45	68[f]
Cs$_2$CO$_3$	250	43:57	63

[a]Catalyst, base, and solvent were stirred under Ar at rt for 2 h before substrate addition. [b]Determined by ^{1}H NMR. [c]Determined by HPLC after reduction. [d]Preformed S-Li$_2$BINOLate used. [e]No product formation detected. [f]-71 % ee was obtained when S-BINOL used.

Examination of the base additive (Table 1.6) revealed the larger cesium and rubidium carbonates to be optimal, with potassium *tert*-butoxide also providing similar results. Use of the organic base triethylamine resulted in racemic product, as did use of a preformed dilithium BINOLate salt.[36] Greater success resulted from varying the base to BINOL ratio, with a 4:1 yielding the highest enantioselection. This result is surprising considering that an apparent excess of inorganic base would be expected to facilitate nonselective background reaction. Limited solubility of cesium carbonate in

---

36) Jerome Robinson (Schelter/Walsh Groups) is thanked for providing (*S*)-Li$_2$BINOLate.

dichloromethane, or formation of a BINOLate complex of greater than 2:1 base:BINOL stoichiometry[37] may account for this observation.

Table 1.7 Effects of 6,6'-BINOL substitution and base variation.

catalyst[a]	base	dr (*anti*:syn)[b]	% ee (*anti*)[c]	% ee (*syn*)[c]
BINOL	Cs_2CO_3	45:55	67	57
1.27	Cs_2CO_3	45:55	68	61
1.28	Cs_2CO_3	43:57	53	47
BINOL	Li_2CO_3	-[d]	-	-
BINOL	Na_2CO_3	-[d]	-	-
BINOL	KOH	30:70	65	56
BINOL	Mg(*n*-Bu)$_2$	-[d]	-	-

[a]Catalyst, base, and solvent were stirred under Ar at rt for 2 h before substrate addition. [b]Determined by ^{1}H NMR. [c]Determined by HPLC. [d]Only trace product was formed.

Additional structural and base exploration was undertaken on the more soluble *tert*-butyl adduct **1.09ab**, which could be analyzed via chiral HPLC directly, without nitro group reduction (Table 1.7). Importantly, both sets of diastereomers were resolved, revealing formation of the *syn* product in slightly lower ee compared to the *anti* isomer. Bromine substitution at the 6,6' positions of BINOL gave slightly improved results, whereas phenyl substitution significantly decreased enantioselectivity. In all cases, diastereoselectivity was not affected. As in previous systems, smaller alkali metals gave very only trace amounts of product, including formation of the putative magnesium-BINOLate with di-*n*-butyl magnesium. Potassium hydroxide yielded nearly identical

---

37) Preliminary mass spectrometry experiments were unsuccessful in identifying the stoichiometry of the active catalyst.

enantioselectivity but increased *syn* selectivity compared to cesium carbonate. Further

examination of temperature, concentration, and water content failed to provide improved

results.

Table 1.8 Solvent effect on the optimized Cs-BINOL catalyst.

solvent[a]	dr (*anti*:syn)[b]	% ee (*anti*)[c]	% ee (*syn*)[c]
CH$_2$Cl$_2$	45:55	67	57
toluene	43:57	75	36
chlorobenzene	33:67	72	42
p-xylene	67:33	33	48
1,2-dichloroethane	42:58	60	52

[a]Catalyst, base, and solvent were stirred under Ar at rt for 2 h before
substrate addition. [b]Determined by ^{1}H NMR. [c]Determined by HPLC.

Performing the optimized coupling in different solvents provided varied results

(Table 1.8). Interestingly, *p*-xylene provided the highest *anti* selectivity (2:1) but with

significantly decreased enantioselectivity. Conversely, both toluene and chlorobenzene

yielded increased *anti* ee, but were more selective towards the *syn* diastereomer (3:1 and

2:1 *syn*, respectively). Diastereoselectivity and enantioselectivity for the *anti* product

decreased using 1,2-dichloroethane.

Table 1.9 Scope of the Cs-BINOL catalyst.

|	**1.09aa**	**1.09ab** (t-Bu)	**1.09ac** (CF$_3$)	**1.29**	**1.30**
dr (anti:syn)[a]	55:45	45:55	42:58	25:75[b]	55:45
ee (anti)[c]	68	67	70	0	11
ee (syn)[c]	ND	57	63	0	28

[a]Determined by ^{1}H NMR. [b]Relative stereochemistry not assigned. [c]Determined by HPLC.

Substitution of the nitroalkane yielded similar dr (~1:1) and enantioselectivity (~70% *anti*, ~60% *syn*) for the phenyl, 4-*t*-butylphenyl, and 4-trifluoromethylphenyl adducts **1.09aa**, **1.09ab**, and **1.09ac**, respectively (Table 1.9). Slightly higher levels of enantioinduction were observed for both diastereomers of the more electron-withdrawing arylnitromethane. Substitution of the Boc imine protecting group with *N*-tosyl resulted in a 3:1 mixture of racemic diastereomers. Interestingly, nitroethane displayed adequate reactivity but provided much poorer enantioselectivity. Preliminarily, the pK_a of the nitroalkyl nucleophile appears to play a critical role in the asymmetric induction afforded by the BINOLate catalyst, with more acidic arylnitromethanes (pK_a ~8) displaying superior results compared to aliphatic nitroalkanes (pK_a ~10). Although further experiments are necessary to validate this observation, these results mirror previous reports of arylnitromethanes possessing unique reactivity in comparison to the linear, aliphatic nitroalkanes commonly studied in *aza*-Henry reaction methodology.

Asymmetric coupling of amidosulfones with nitromethane can be accomplished directly *via in situ* formation of the imine with strong base, as first reported by both

Herrara[26a] and Palomo[26b,c] using a phase transfer catalyst. Along with the operational

ease of using bench-stable solid amidosulfones, this process has the advantage of

tolerating enolizable aliphatic imine precursors (Scheme 1.8). By changing the base

additive to the stronger potassium hydroxide, the optimized BINOLate system smoothly

afforded the anticipated adduct **1.09ab** when employing an amidosulfone precursor.

Comparable levels of enantioinduction were observed for both diastereomers in

comparison to the preformed imine substrates, and diastereoselectivity remained poor.

Scheme 1.8 BINOLate catalyzed *aza*-Henry reaction using an amidosulfone.

Scheme 1.8 BINOLate catalyzed *aza*-Henry reaction using an amidosulfone.
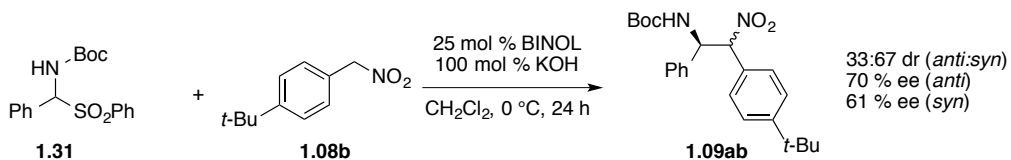
Synthetically useful levels of enantioselectivity for the *aza*-Henry reaction with

arylnitromethane nucleophiles had been realized using BINOLate catalysts. However,

systematic variation of reaction conditions failed to improve the diastereoselectivity

much beyond a 1:1 ratio. The proposed dual-binding model for the BINOLsalen catalysts

proved nonviable, with observed diastereoselectivity largely independendent of catalyst

structure. Indeed, performing the coupling with cesium carbonate alone provided the

adduct in nearly identical stereoselectivity as with either BINOLsalen or BINOLate

catalyst (Scheme 1.9).

**Scheme 1.9** Nonselective aza-Henry coupling with cesium carbonate.
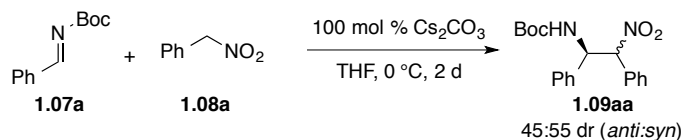
Monitoring the reaction by ^{1}H NMR critically revealed that the product dr was significantly changing over the course of the reaction (Scheme 1.10). When conducted with 50 mol % cesium carbonate in CDCl$_3$, a large excess of the *syn* product was initially formed, later reaching an apparent 62:38 *anti:syn* equilibrium by 18 h.

**Scheme 1.10** Change in diastereomeric ratio with time for the *aza*-Henry coupling.

t (h)	dr (*anti:syn*)^a
0.5	17:83
2	30:70
18	62:38
48	62:38

^{a}Determined by ^{1}H NMR.
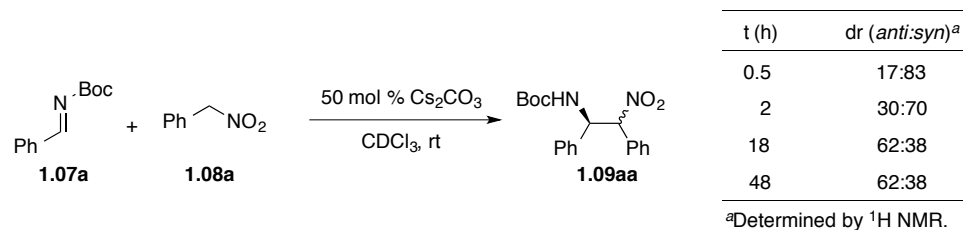
The observed change in diastereoselectivity can be hypothesized to occur *via* two distinct mechanisms, both ostensibly occurring through product deprotonation events (Figure 1.5). In one pathway (path a), deprotonation of the carbamate N–H proton can release both imine and nitronate precursors in a retro-*aza*-Henry process. If the *syn* adduct is kinetically favored, but *anti* is thermodynamically similar, a retro-recombination process can occur to provide the observed change in selectivity over time. Alternatively, deprotonation of the α-nitro proton is also possible (path b), resulting in epimerization of the center to the observed equilibratium ratio. A critical difference in these pathways is that stereoretention at the β-nitro carbon is only expected for path b.
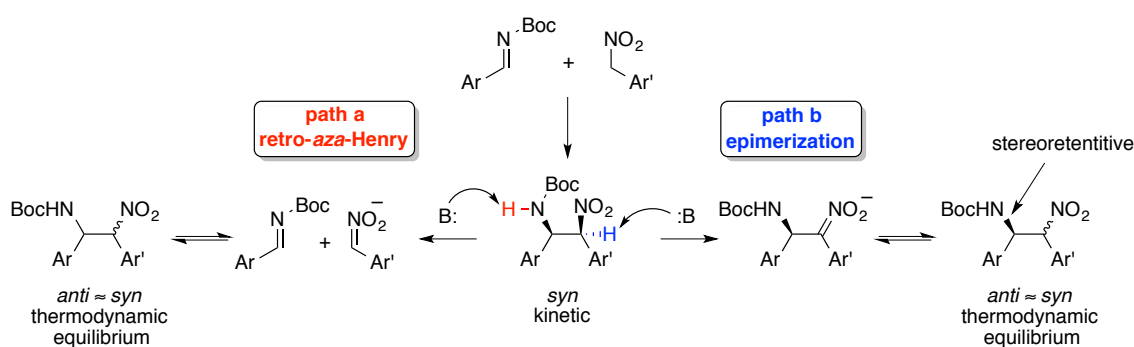
Figure 1.5 Possible mechanisms for the change in diastereomeric ratio with time.

To probe the mechanism, a 7:1 racemic mixture of *syn*:*anti* **1.09aa** was subjected to the optimal asymmetric BINOLate conditions (Scheme 1.11). After 24 h, the dr had changed, as expected, to a slight favoring of the *anti* isomer. More significantly, no asymmetric induction was observed for the formed *anti* diastereomer, lending support for the epimerization pathway.

Scheme 1.11 Treatment of racemic **1.09aa** to asymmetric coupling conditions.
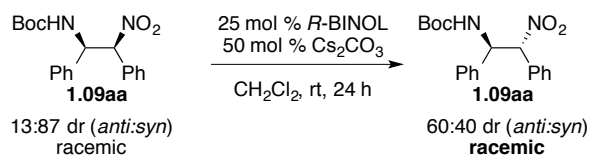
Substantiating evidence for epimerization was found when highly enantioenriched (92 % ee) *syn*-**1.09ab**[38] was subjected to cesium carbonate for 4 h (Scheme 1.12). A 4:1 mixture of *syn*:*anti* resulted, with stereoretention of the remaining *syn* isomer, along with an equivalent level of ee for the newly formed *anti* isomer. Favorable deprotonation of

---

38) This material was obtained through *cinchona* alkaloid catalysis and recrystallization (see Section 1.2.2.).

the α-nitroalkyl proton vs N–H carbamate proton is also rationalized on the basis of pK_a, despite the kinetic barrier associated with nitronate formation.[39]

Scheme 1.12 Stereoretentive epimerization of *syn*-**1.09ab**.
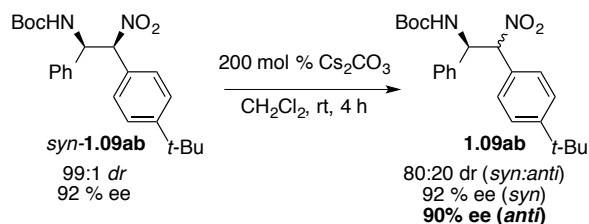
Given the continued difficulty in accessing the *anti* products, these mechanistic results hint at the potential utility of a stereoretentive epimerization strategy, in which the absolute configuration of the β-nitro center is first established through a *syn*-selective asymmetric *aza*-Henry addition. Efficient epimerization could then afford the enantioenriched *anti* isomer, providing ready access to all four possible stereoisomers through catalyst configuration and/or epimerization. Further epimerization studies are discussed in Section 1.2.3.

1.2.2. Use of Cinchona Alkaloids as Catalysts
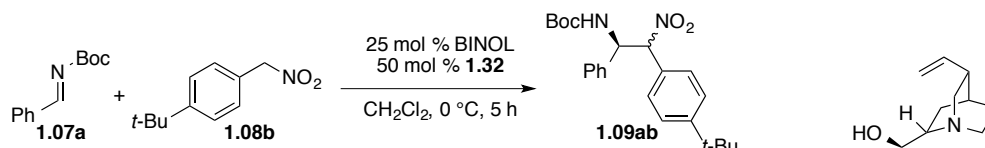
During the course of studying the BINOL-catalyzed *aza*-Henry reaction, cinchonidine (**1.32**) was added as a chiral organic base additive, with the goal of forming a more enantiodiscriminating BINOLate system (Table 1.10). Performing the reaction with either enantiomer of BINOL in combination with cinchonidine favored the *syn*

---

39) Nitroalkanes deprotonate slower than expected based on acidity. See Ando, K.; Shimazu, Y.; Seki, N.; Yamataka, H. "Kinetic Study of Proton-Transfer Reactions of Phenylnitromethanes. Implication for the Origin of Nitroalkane Anomaly" *J. Org. Chem.* **2011**, *76*, 3937-3945 and references therein.
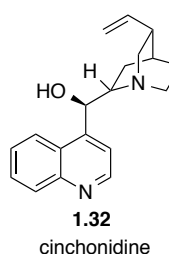
product with the same (−)-absolute stereochemistry independent of BINOL enantiomer.

Indeed, cinchonidine alone provided higher levels of enantioinduction and *syn* selectivity.

**Table 1.10** Cinchonidine-controlled *aza*-Henry reaction.

catalyst system	dr (*syn:anti*)[a]	ee % (*syn*)[b]	ee % (*anti*)[b]
R-BINOL + cinchonidine	72:28	-34	10
S-BINOL + cinchonidine	75:25	-33	16
cinchonidine	78:22	-45	-11

[a]Determined by ^{1}H NMR. [b]Determined by HPLC.
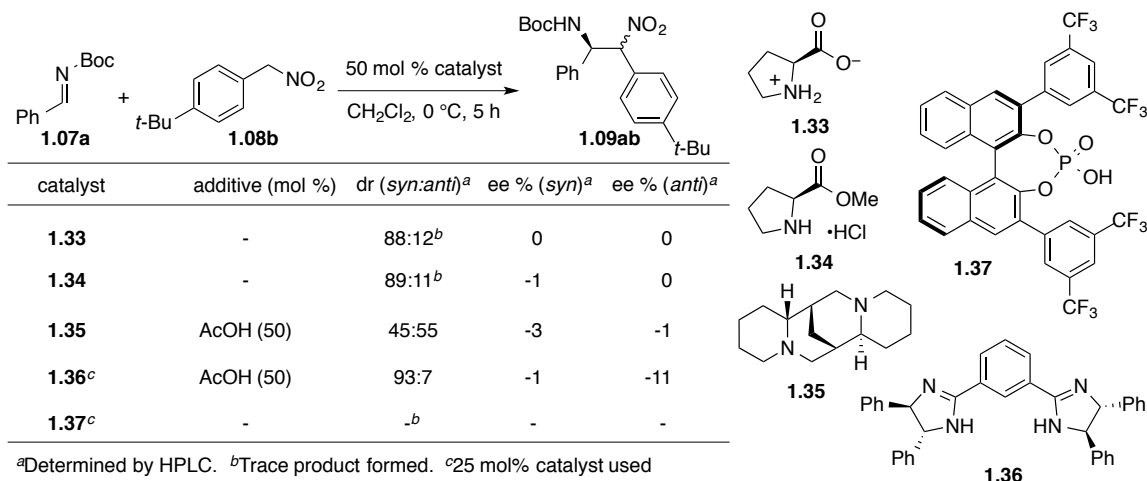
Further investigation was undertaken with the goal of identifying a complimentary *syn*-selective asymmetric *aza*-Henry reaction for the synthesis of *syn*-1,2-diarylethylenediamines. Development of a selective epimerization process, as previously discussed, would render the method viable for accessing either diastereomer in high optical purity. A key discovery was serendipitously found when performing the cinchonidine-catalyzed coupling in the presence of equimolar amounts of acetic acid (Scheme 1.13). This simple catalyst system, putatively *in situ* formation of cinchonidinium acetate *via* protonation of the quinuclidine nitrogen, smoothly provided the *syn* adduct in high selectivity and promising levels of enantioinduction (61% ee).

Scheme 1.13 Increased selectivity of cinchonidine with an acid additive.
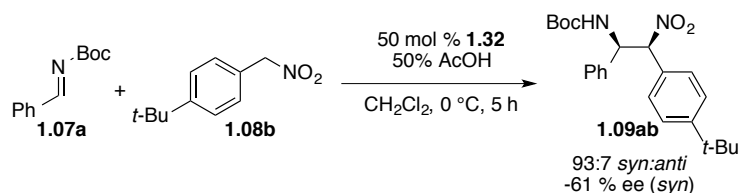
Testing various chiral amine/ammonium compounds proved cinchonidine to be uniquely selective for the desired transformation (Table 1.11). Although amino ester **1.34** and chiral bisamidine **1.36** displayed high diastereoselectivity, all catalysts tested provided essentially racemic product. 3,3'-Substituted BINOLphosphate **1.37**, an effective asymmetric catalyst for several Brønsted acid-catalyzed transformations,[40] provided only trace amounts of product.

Table 1.11 Chiral amines/ammoniums/Brønsted acids as alternative catalysts.

catalyst	additive (mol %)	dr (*syn:anti*)[a]	ee % (*syn*)[a]	ee % (*anti*)[a]
1.33	-	88:12[b]	0	0
1.34	-	89:11[b]	-1	0
1.35	AcOH (50)	45:55	-3	-1
1.36[c]	AcOH (50)	93:7	-1	-11
1.37[c]	-	-[b]	-	-

[a]Determined by HPLC. [b]Trace product formed. [c]25 mol% catalyst used

Substitution of acetic acid with other organic acids of similar or greater strength resulted in similar diastereoselectivity, but lower levels of enantioselectivity (Table 1.12). For example, addition of chiral phosphate **1.38** did not provide a matched system of higher selectivity. Notably, the strongest acids tested, *p*-toluenesulfonic acid and triflic
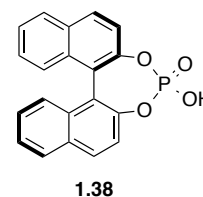
40) Select examples: (a) Akiyama, T.; Morita, H.; Itoh, J.; Fuchibe, K. "Chiral Brønstend Acid Catalyzed Enantioselective Hydrophosphonylation of Imines: Asymmetric Synthesis of α-Amino Phosphonates" *Org. Lett.* **2005**, *7*, 2583-2585. (b) Henseler, A.; Kato, M.; Mori, K.; Akiyama, T. "Chiral Phosphoric Acid Catalyzed Transfer Hydrogenation: Facile Synthetic Access to Highly Optically Active Trifluoromethylated Amines" *Angew. Chem. Int. Ed.* **2011**, *50*, 8180-8183. (c) Jiang, J.; Xu, H.-D.; Xi, J.-B.; Ren, B.-Y.; Lv, F.-P.; Guo, X.; Jiang, L.-Q.; Zhang, Z.-Y.; Hu, W.-H. "Diastereoselectively Switchable Enantioselective Trapping of Carbamate Ammonium Ylides with Imines" *J. Am. Chem. Soc.* **2011**, *133*, 8428-8431. (d) Cai, Q.; Liu, C.; Liang, X.-W.; You, S.-L. "Enantioselective Construction of Pyrroloindolines via Chiral Phosphoric Acid Catalyzed Cascade Michael Addition–Cyclization of Tryptamines" *Org. Lett.* **2012**, *14*, 4588-4590.

acid, exhibited significant product inhibition. Greater success resulted from lowering the reaction temperature, which elevated both diastereo- and enantioselectivity for the *syn* product. Reaction at −30 °C yielded near perfect diastereocontrol. Increased ee was observed at even lower temperature, but conversion became problematic, with no product forming at −78 °C after several days. Increasing acetic acid:catalyst stoichiometry to 3:1 inhibited reactivity, while a 1:3 ratio resulted in slightly poorer product dr and ee. A brief solvent survey revealed 1,2-dichlorethane to be comparable with dichloromethane, but diastereocontrol was limited due to its higher melting point.   Both toluene and benzotrifluoride provided good *syn*-selectivity, but poorer enantioselectivity.

Table 1.12 Acid and temperature effects with the cinchonidine catalyst.

additive	solvent	temperature (°C)	dr (*syn:anti*)[a]	ee % (*syn*)[a]	ee % (*anti*)[a]
BzOH	CH_2Cl_2	0	93:7	-31	-1
(*R*)-**1.38**	CH_2Cl_2	0	88:12	-21	-44
(*S*)-**1.38**	CH_2Cl_2	0	88:12	-37	-45
TFA	CH_2Cl_2	0	86:14	-33	-25
p-TsOH	CH_2Cl_2	0	-[b]	-	-
4-aminobenzoic acid	CH_2Cl_2	-45	96:4	-31	-
TfOH	CH_2Cl_2	-45	-[b]	-	-
AcOH	CH_2Cl_2	0	93:7	-61	-
AcOH	CH_2Cl_2	-15	95:5	-68	-
AcOH	CH_2Cl_2	-30	97:3	-71	-
AcOH	CH_2Cl_2	-45	99:1	-74	-
AcOH	CH_2Cl_2	-78	-[b]	-	-
AcOH (150 mol %)	CH_2Cl_2	-45	-[b]	-	-
AcOH (17 mol %)	CH_2Cl_2	-45	98:2	-70	-
AcOH	$PhCF_3$	0	92:8	-48	-50
AcOH	toluene	-45	99:1	-41	-
AcOH	DCE	-20	97:3	-73	-

[a]Determined by HPLC. [b]Trace product formed.

Effects of catalyst structure were explored using the other *cinchona* alkaloids (Table 1.13). All unmodified *cinchona* compounds exhibited near perfect *syn* diastereoselectivity. As anticipated, the pseudoenantiomer of cinchonidine, cinchonine, afforded the product with similar levels of enantioselectivity but for the opposite absolute configuration. Quinine and quinidine are isostructural to cinchonine and cinchonidine, respectively, except for methoxy substitution at the 7 position of the quinoline ring. However, these catalysts provided noticeably lower enantioselection compared to their unsubstituted analogues, along with an unanticipated change in product absolute configuration. This effect was further probed via synthetic manipulation of quinidine to afford **1.42** and **1.43**, which contain phenol and methanesulfonyl substitution, respectively. Interestingly, the relatively deactivated sulfonate **1.43** did not translate into enhanced selectivity, instead negating enantioinduction altogether. Phenol-substituted **1.42** gave only trace product and also led to an inversion in absolute stereochemistry of the product. Trimethylsilyl protected cinchonidine **1.44** afforded excellent diastereocontrol but minimal enantioinduction. Catalysts **1.45** and **1.45**, dihydroquinine- and dihydroquinidine-derived dimers, respectively, yielded poor results.

Table 1.13 Structural variation effects with cinchona alkaloids catalysts.

catalyst	dr (*syn:anti*)[a]	ee % (*syn*)[a]
1.32 (cinchonidine)	99:1	-74
1.39 (cinchonine)	99:1	+71
1.40 (quinine)	98:2	+44
1.41 (quinidine)	98:2	-37
1.42	95:5[b]	+12
1.43[c]	96:4	-1
1.44	99:1	-15
1.45[d]	91:9	+4
1.46[d]	76:24	-13

R^1 = H   R^2 = H   **1.32** (cinchonidine)
R^1 = OMe R^2 = H   **1.40** (quinine)
R^1 = OH   R^2 = H   **1.42**
R^1 = OMs R^2 = H   **1.43**
R^1 = H   R^2 = TMS **1.44**

R = H   **1.39** (cinchonine)
R = OMe **1.41** (quinidine)

[a]Determined by HPLC. [b]Trace product formed. [c]Run with 25 mol% catalyst and AcOH. [d]Run at 0 °C with 100 mol % AcOH.

1.45 ((DHQ)$_2$PYR)

1.46 ((DHQD)$_2$AQN)
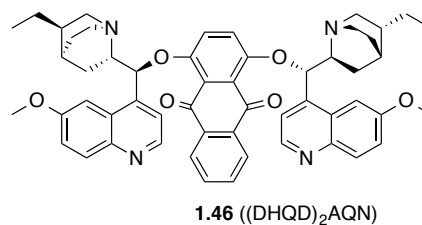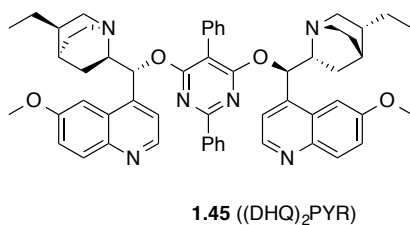
The pseudo-meta position of the 7-substituent affects the basicity of the quinoline nitrogen only slightly (quinolinium pKa of cinchonidinium = 4.17, quinidinium = 4.32). Consequently, steric influence of the substituent may play a significant role in the enantiodetermining step of the mechanism, rather than strictly modulating nitrogen quinoline basicity. Other binding modes, particularly for catalyst **1.42** may also occur. An alternate activation mechanism involving hydrogen bonding of the phenol to imine substrate may predominate with this structure. Based on the results from the dimeric catalysts and particularly **1.44**, the free secondary hydroxyl group is also critical for high levels of enantioselection. Notably, employing *N*-benzylated catalyst **1.47** led to reaction

inhibition and poor selectivities,[41] confirming the importance of the free quinuclidine moiety (Scheme 1.14). Using pK_a values, formation of a protonated quinuclidinium species appears critical for higher enantioinduction (pK_a acetic acid = 4.76, pK_a cinchonidinium–H$^+$ = 8.40).[42]

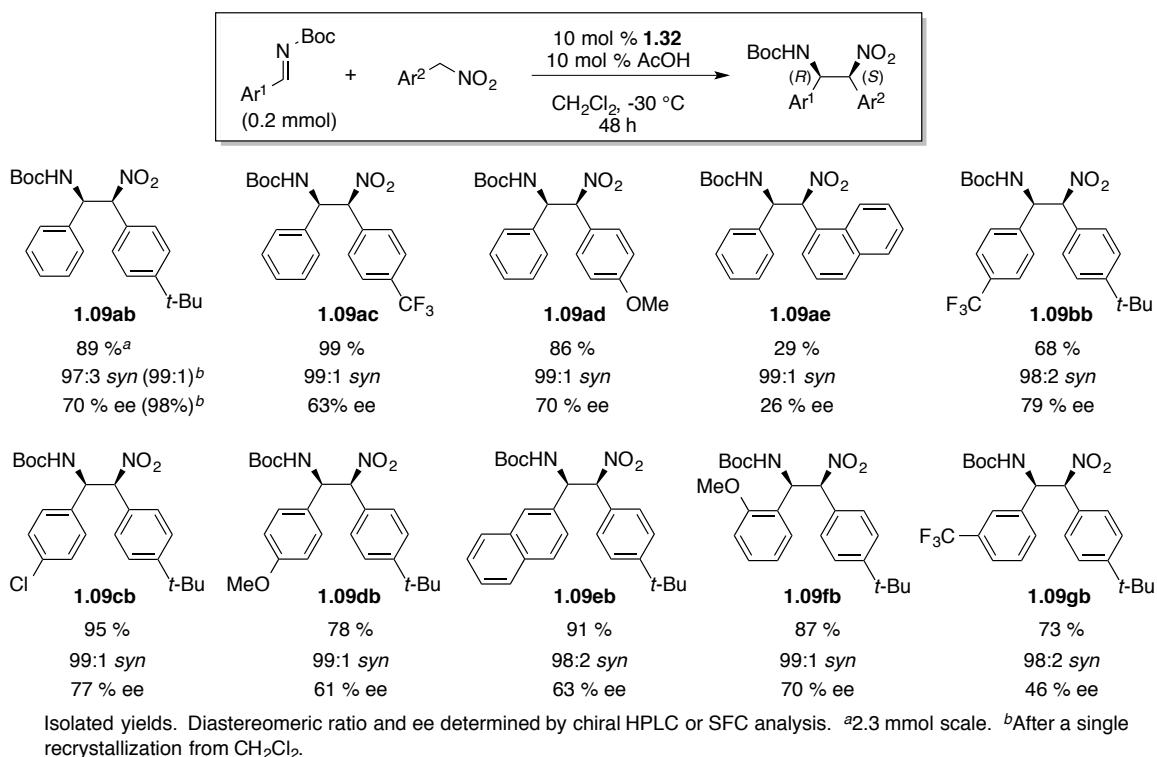**Scheme 1.14** Reaction inhibition using *N*-benzylated cinchonidine.

1.09ab
trace product
88:12 dr (*syn*)
-13 % ee (*syn*)

1.47
N-benzylcinchonidinium chloride
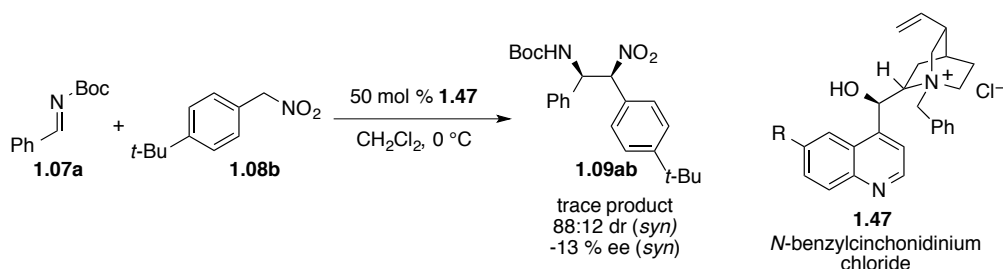
Performing the reaction at −30 °C with lowered catalyst and acetic acid loadings (10 mol %) provided reasonable rates and a minimal decrease in selectivity. The generality of the method was explored under these optimized conditions as illustrated in Table 1.14. Both electron-withdrawing and electron-donating substitution of the arylnitromethane moiety was tolerated, providing adducts **1.09ac** and **1.09ad** in excellent diastereoselectivity and moderate enantioselectivity. Steric hindrance on the nucleophile was deleterious, with 1-nitromethylnaphthalene providing product **1.09ae** in low conversion and poor selectivity. The method proved general for a variety of imines, providing good results for electron rich, electron poor, and naphthyl-based substrates, as well as those possessing *ortho*-substitution. In contrast, *meta*-trifluoromethyl product **1.09gb** was obtained in poorer enantioselectivity, but with good diastereoselectivity and

---

41) *N*-alkylated *cinchona* alkaloids have been successful catalysts in asymmetric *aza*-Henry reactions using nitromethane and nitroethane with amidosulfones (see references 26b-d). Thorough experimentation to employ them with arylnitromethanes were unsuccessful, yielding poor dr and ee.

42) Jencks, W. P.; Regenstein, J. "Ionization Constants of Acids and Bases" In *Handbook of Biochemistry and Molecular Biology*, 3rd ed.; Fassman, G. D., Ed.; CRC Press: Ohio, 1975; Vol. 1, pp 305-351.

efficiency. Based on the higher levels of enantioinduction for **1.09bb** and **1.09cb** (79 %

and 77%, respectively), best results are obtained with electron poor imines. Accordingly,

p-methoxy adduct **1.09db** was obtained in decreased ee (61%). In general, the method

affords excellent yields of the *syn* diastereomer in synthetically useful enantiomeric

excess.

Table 1.14 Substrate scope for the cinchonidinium acetate catalyzed *aza*-Henry reaction.

1.09ab	**1.09ac**	**1.09ad**	**1.09ae**	**1.09bb**
89 %[a]	99 %	86 %	29 %	68 %
97:3 *syn* (99:1)[b]	99:1 *syn*	99:1 *syn*	99:1 *syn*	98:2 *syn*
70 % ee (98%)[b]	63% ee	70 % ee	26 % ee	79 % ee
1.09cb	**1.09db**	**1.09eb**	**1.09fb**	**1.09gb**
95 %	78 %	91 %	87 %	73 %
99:1 *syn*	99:1 *syn*	98:2 *syn*	99:1 *syn*	98:2 *syn*
77 % ee	61 % ee	63 % ee	70 % ee	46 % ee

Isolated yields. Diastereomeric ratio and ee determined by chiral HPLC or SFC analysis. [a]2.3 mmol scale. [b]After a single recrystallization from CH_2Cl_2.

It is critical to note that the product ee can be easily enhanced via recrystallization

of the solid products. For example, the model reaction was performed on a 2.3 mmol

scale, affording **1.09ab** in 70% ee. Single recrystallization from dichloromethane

provided nearly enantiopure product (98% ee), and no *anti* isomer was detected by

HPLC. Crystallization *via* slow evaporation also provided samples of **1.09ab** suitable for

X-ray crystallographic analysis (Figure 1.6), confirming relative and absolute

configuration.[43]   The exceptional diastereocontrol displayed by the acetic acid-cinchonidine catalyst system is remarkable, considering the highly acidic α-nitro proton of the products. This system is ostensibly selective for deprotonation of the nitroalkane substrate while avoiding epimerization of the product to the thermodynamic mixture found under the BINOLate-derived catalysts. The perfect diastereocontrol of highly acidic product **1.09ac** is of particular note.
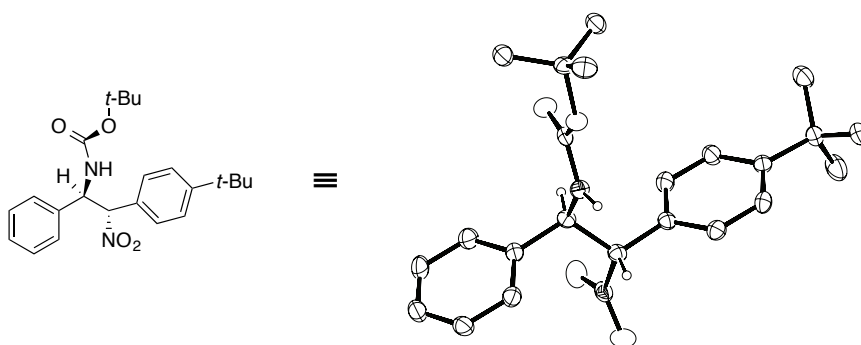
Figure 1.6 X-ray crystal structure of *aza*-Henry adduct **1.09ab**.

Overall, a simple method for the generation of *syn*-1,2-diarylethylenediamine precursors in synthetically useful enantiomeric excess was developed. An array of imine and arylnitromethane substrates is tolerated, including highly acidic nitroalkanes, and enantiopure material can be obtained via simple recrystallization of the products. During the course of our investigations, Johnston and coworkers reported the first asymmetric *aza*-Henry reaction of arylnitromethanes, in which a complex pyrrolidine-bisamidine catalyst afforded the *syn* products in high yield and ee.[44] This methodology was

43) Crystals analyzed by X-ray crystallography were 99:1 *syn:anti*, 98% ee.
44) Davis, T. A.; Johnston, J. N. "Catalytic, enantioselective synthesis of silbene *cis*-diamines: A concise preparation of (–)-Nutlin 3, a potent p53/MDM2 inhibitor" *Chem. Sci.* **2011**, *2*, 1076-1079.

employed in an elegant and concise synthesis of p53-MDM2 inhibitor (−)-Nutlin-3.[45] The described cinchonidine-based system herein provides a complimentary method to that reported by Johnston that does not require a complex catalyst synthesis. Higher diastereoselectivity is also observed with this system, particularly for highly acidic nitroalkanes, which display poor selectivity with the pyrrolidine-bisamidine catalyst.

1.2.3. Epimerization of Products to Afford the Anti Stereoisomer

Despite the discovery of a highly *syn*-selective *cinchona*-catalyzed asymmetric *aza*-Henry method, the original goal for an efficient synthesis of the *anti* isomer remained unrealized. Development of suitable epimerization conditions from *syn* to *anti* provides an alternative strategy as opposed to catalyst-controlled diastereoselectivity, which had thus far proven unsuccessful. Such a process became particularly enticing in light of the *syn*-selective process described above, since ready access to all four possible stereoisomers would be possible via catalyst configuration and/or epimerization. Initial experimentation confirmed an epimerization process, as opposed to a retro-Henry sequence, when subjecting *syn* adducts to mild inorganic bases (see end of Section 1.2.1). Promising results were obtained using cesium carbonate, which isomerized *syn* adduct **1.09ab** to a 60:40 *anti*:*syn* ratio (see Scheme 1.11). Subsequent efforts focused on further favoring the *anti* adduct.

---

45) Davis, T. A.; Vilgelm, A. E.; Richmond, A.; Johnston, J. N. "Preparation of (−)-Nutlin-3 Using Enantioselective Organocatalysis at Decagram Scale" *J. Org. Chem.* **2013**, *78*, 10605-10616.

Table 1.15 Epimerization with amine bases of varying strength.

base	pK_a[a]	dr (*syn:anti*)[b]	% ee *syn* (*anti*)[b]
pyridine	5.4	98:2	97
DMAP	9.9	44:56	97 (97)
DBU	11.6	62:38	97 (97)

[a]Refers to dissociation constants of the protonated amine in H_2O. [b]Determined byHPLC.

Amine bases were surveyed with a range of pK_a values[46] for the isomerization of pure *syn* product of high enantiopurity (Table 1.15). No epimerization was observed after treatment with pyridine, likely due to its weak basicity. However, pK_a is not the sole determining factor, as DMAP provided better results and favored the *anti* diastereomer, as compared to the stronger DBU. No erosion of enantioselectivity was detected; the epimerized product was formed with equal levels of enantioselectivity. This observation proved consistent in all epimerization experiments.

Table 1.16 Epimerization using triethylamine or Hünig's base.

base	time (h)	solvent	dr (*syn:anti*)[a]
(*i*-Pr)$_2$NEt	3	CH_2Cl_2	89:11
(*i*-Pr)$_2$NEt	24	CH_2Cl_2	89:11
Et$_3$N	24	CH_2Cl_2	44:56
Et$_3$N	3	toluene	96:4
Et$_3$N	3	DMAc	89:11

[a]Determined by HPLC.

Other amine bases possessing similar pK_a to DMAP afforded disparate results (Table 1.16). The bulkier Hünig's base yielded only minor epimerization, even after 24 h, while triethylamine gave similar results to DMAP. Performing the reaction in nonpolar or polar aprotic solvents inhibited epimerization.

---

46) Cecchi, L.; De Sarlo, F.; Machetti, F. "1,4-Diazabicyclo[2.2.2]octane (DABCO) as an Efficient Reagent for the Synthesis of Isoxazole Derivatives from Primary Nitro Compounds and Dipolarophiles: The Role of the Base" *Eur. J. Org. Chem.* **2006**, 4852-4860.

Scheme 1.15 HTE screen for epimerization with inorganic base.
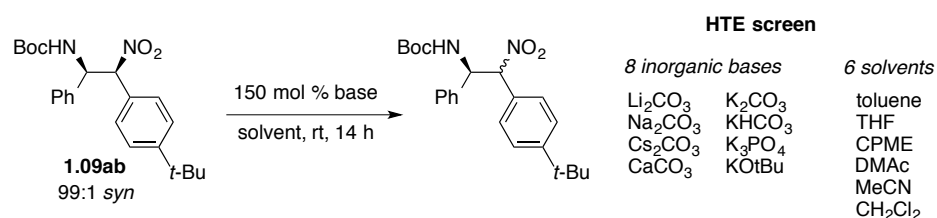
A large screen of inorganic bases, including a series of metal carbonates, and potassium bases of varying strengths was examined in tandem with six different solvents (Scheme 1.15). Although accurate analysis for all trials was complicated by decomposition products, general conclusions were obtained. Lithium, sodium, and calcium carbonates yielded minimal (sodium) or no change to the starting material, whereas significant byproducts or decomposition was observed for potassium *t*-butoxide and carbonate. The best results were obtained with potassium bicarbonate, potassium phosphate, or cesium carbonate, although none of the experiments indicated epimerization greater than a 1:1 *syn*:*anti* ratio. In general, solvents provided similar results according to base, except for *N,N*-dimethylacetamide, which produced minor epimerization with the otherwise inactive lithium and sodium carbonates. With other bases, this solvent exacerbated decomposition pathways.

The studies simply employing organic or inorganic bases for epimerization of the *syn* diastereomer confirmed that the two product diastereomers were thermodynamically similar in energy, leading to ~1:1 ratios under the best conditions. A different approach, focused on metal chelation-controlled epimerization, was postulated to shift this equilibrium in favor of the *anti* diastereomer (Figure 1.7).
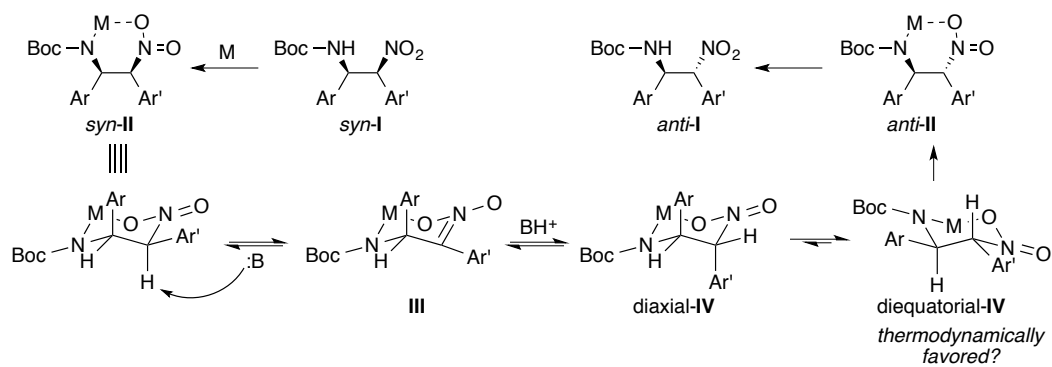
Figure 1.7 Postulated mechanism for chelation-controlled epimerization.

Specifically, a 6-membered metal-chelate **II** may form *via* coordination of the metal to the nitro and amine groups. Subsequent base-mediated epimerization forms the diequatorial aryl-aryl conformer **IV**, which should be lower in energy and thermodynamically favored. Decomplexation then affords the desired isomerized product. Initial experiments focused on *in situ* complexation with various oxophilic or azaphilic acids followed by triethylamine addition (Table 1.17). In all cases, the metal additive provided lower epimerization levels that triethylamine alone, and magnesium perchlorate and scandium triflate completely inhibited the process. In combination with titanium(IV) isopropoxide, increasing the amount of triethylamine or employing inorganic base (potassium phosphate) led to poorer results.

Table 1.17 Attempted chelation-controlled epimerization with Lewis acids.

metal	dr (*syn:anti*)[a]
Mg(ClO$_4$)$_2$	97:3[b]
Sc(OTf)$_3$	97:3[b]
Ni(acac)$_2$	85:15
Cu(acac)$_2$	72:27
Ti(O*i*-Pr)$_4$	78:22[b]
Ti(O*i*-Pr)$_4$[c]	82:18
Ti(O*i*-Pr)$_4$[d]	91:9

[a]Determined by HPLC. [b]Analysis at 24 h yielded no change in dr. [c]Added 5 equiv Et$_3$N. [d]50 mol % K$_3$PO$_4$ used instead of Et$_3$N.

A microscale high-throughput experimentation (HTE) screen was performed to further explore the chelation-controlled epimerization (Table 1.18). The effect of 12 different Lewis acids was examined with either triethylamine or DMAP in THF or dichloromethane (48 unique conditions).

Table 1.18 HTE screen of chelation-controlled epimerization.

conditions:

A - Et$_3$N + THF
B - DMAP + THF
C - Et$_3$N + CH$_2$Cl$_2$
D - DMAP + CH$_2$Cl$_2$

conditions	Ti(O*i*-Pr)$_4$	Eu(OTf)$_3$	Al(O*i*-Pr)$_3$	Bi(OTf)$_3$	Fe(acac)$_3$	Zn(OTf)$_2$
A	5:1	NR	4:1	N/A	5:1	NR
B	6:1	NR	2:1	N/A	1:1	NR
C	5:1	NR	2:1	N/A	1:1	NR
D	6:1	NR	2:1	N/A	1:1	NR

conditions	CrCl$_2$	In(OTf)$_3$	Sn(OTf)$_2$	Co(acac)$_2$	Yb(OTf)$_3$	VO(acac)$_2$
A	NR	N/A	N/A	N/A	NR	6:1
B	NR	N/A	N/A	8:1	NR	6:1
C	NR	N/A	N/A	N/A	NR	1:1
D	5:1	N/A	N/A	6:1	NR	1:1

Ratios refer to syn:anti ratio as determined by SFC analysis. NR indicates no measurable change in dr. N/A indicates significant decomposition or byproduct formation with only trace SM detected.

The resulting diastereomeric ratios were highly dependent on Lewis acid employed. For several additives, neither product isomer was detected after the reaction,

indicating large amounts of byproduct formation and/or decomposition.[47] Surprisingly, europium, ytterbium, and zinc triflates provided no change in selectivity, despite being very strong Lewis acids. In contrast to metal additive, base and solvent variation minimally affected epimerization levels. In general, dichloromethane provided slightly improved results. The highest levels of isomerization were observed using iron(III) acetylacetonate or oxovanadium(V) acetylacetonate in dichloromethane. Unfortunately, these conditions again afforded the product in a ~1:1 ratio, indicating that the metal may simply not be participating in the reaction. None of the Lewis acids improved selectivity compared to base alone. The inhibiting effect of several additives may be explained via coordination of the amine bases to the metals, rather than coordination of the substrate. Further experimentation, including use of noncoordinating inorganic bases in combination with Lewis acids is relevant.

1.3. Conclusions

Significant research has been undertaken for the synthesis of 1,2-diarylethylenediamines using an *aza*-Henry reaction approach. Exploration of BINOLsalen and BINOLate catalysts demonstrated that these catalysts can provide moderate levels of enantioselectivity, although diastereoselection was poor, affording thermodynamic mixtures (~1:1) of *syn* and *anti* products *via* base-catalyzed epimerization. In contrast, employing the cheap and readily available *cinchona* alkaloid cinchonidine with AcOH allows facile synthesis of the *syn* diastereomer with exceptional

---

47) The possibility that substrates remained chelated with these additives and therefore not analyzed cannot be disregarded.

diastereocontrol and moderate to good enantioselectivity for a range of substrates. In tandem with subsequent recrystallization, this method provides an attractive route toward optically pure products.

Attempts to access the *anti* products via epimerization, with or without an added Lewis acid for chelation, have thus far proven ineffective. This approach remains attractive for accessing all diamine stereoisomers, and other epimerization strategies are worthwhile, including altering the chelation model by varying imine protecting group, and screening for solubility differences in the product diastereomers. Computational analysis of energy differences between free and/or chelated diastereomers may provide additional guidance.

1.4. Experimental Section

General Considerations

All reactions were carried out under an atmosphere of dry argon unless otherwise noted. When necessary, solvents were distilled prior to use. Dichloromethane, acetonitrile, and triethylamine were distilled from CaH_2, THF and diethyl ether were distilled from sodium/benzophenone ketyl, toluene was distilled from metallic sodium, and Hünig's base was distilled from KOH. Reactions were monitored by thin layer chromatography (TLC) using Silicycle glass-backed TLC plates with 250 μm silica and F254 indicator. Visualization was accomplished with UV light, ninhydrin stain, or *p*-anisaldehyde stain. Flash column chromatography was performed using Silicycle Silaflash P60 silica gel (40-63 μm particle size).

NMR spectra were recorded on Brüker AM-500, Brüker DRX-500, Brüker DMX-360, and Brüker DMX-300 Fourier transform NMR spectrometers. Chemical shifts are reported relative to the solvent resonance peak δ 7.27 (CDCl$_3$) for ^{1}H and δ 77.23 (CDCl$_3$) for ^{13}C. Data are reported as follows: chemical shift, multiplicity (s = singlet, d = doublet, t = triplet, q = quartet, bs = broad singlet, m = multiplet), coupling constants, and number of protons. High resolution mass spectra were obtained using a Waters LC-TOF LCT-XE Premier model mass spectrometer with an ionization mode of either ESI or CI. Infrared spectra were recorded using a Perkin-Elmer 1600 series or JASCO FT/IR-480 spectrometer. Melting points were obtained on a Thomas Scientific Unimelt apparatus and are uncorrected. Enantiomeric excesses were determined using CSP-HPLC on an Agilent 1100 Series HPLC, or using CSP-SFC on a JASCO SF-2000 SFC. Optical rotations were measured on a JASCO polarimeter with a sodium lamp.

Amidosulfones and imines,[22c,48] BINOLsalen catalysts **1.15**,[32] modified BINOL catalysts **1.21**,[49] **1.27**,[50] **1.28**,[51] bisamidine **1.36**,[8] and cinchona catalysts **1.42**,[52] **1.44**[53] were prepared as previously described.

48) Wenzel, A. G.; Jacobsen, E. N. "Asymmetric Catalytic Mannich Reactions Catalyzed by Urea Derivatives: Enantioselective Synthesis of β-Aryl-β-Amino Acids" *J. Am. Chem. Soc.* **2002**, *124*, 12964-12965.

49) Mikami, K.; Kakuno, H.; Aikawa, K. "Enantiodiscrimination and Enantiocontrol of Neutral and Cationic Pt^{II} Complexes Bearing the *Tropos* Biphep Ligand: Application to Asymmetric Lewis Acid Catalysis" *Angew. Chem. Int. Ed.* **2005**, *44*, 7257-7260.

50) Cui, Y.; Evans, O. R.; Ngo, H. L.; White, P. S.; Lin, W. "Rational Design of Homochiral Solids Based on Two-Dimensional Metal Carboxylates" *Angew. Chem. Int. Ed.* **2002**, *41*, 1159-1162.

51) Kumaraswamy, G.; Sastry, M. N. V.; Jena, N.; Kumar, K. R.; Vairamani, M. "Enantioenriched (*S*)-6,6'-diphenylBinol-Ca: a novel and efficient chirally modified metal complex for asymmetric epoxidation of α,β-unsaturated enones" *Tetrahedron: Asymmetry* **2003**, *14*, 3797-3803.

52) Hallet, A. J.; Kwant, G. J.; de Vries, J. G. "Continuous Separation of Racemic 3,5-Dinitrobenzoyl-Amino Acids in a Centrifugal Contact Separator with the Aid of Cinchona-Based Chiral Host Compounds" *Chem. Eur. J.* **2009**, *15*, 2111-2120.

53) Lindholm, A.; Maki-Arvela, P.; Toukonitty, E.; Pakkanen, T. A.; Hirvi, J. T.; Salmi, T.; Murzin, D. Y.; Sjöholm, R.; Leino, R. "Hydrosilylation of cinchonidine and 9-*O*-TMS-cinchonidine with triethoxysilane: application of 11-(triethoxysilyl)-10-11-dihydrocinchonidine as a chiral modifier in the
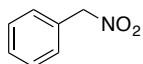
Phenylnitromethane (1.08a)

Benzyl bromide (0.50 mL, 4.18 mmol) was added slowly to a slurry of silver nitrite (2.50 g, 16.7 mmol) and deionized water (8 mL), and the resulting mixture was stirred at rt in the dark. After 4 h, the mixture was passed through Celite and extracted with EtOAc (3 x 20 mL). The combined organics were washed with brine, dried over Na_2SO_4, filtered, and concentrated. Purification by chromatography (4% EtOAc/Hexanes) afforded the title compound as a colorless oil (187 mg, 33%): ^{1}H NMR (500 MHz, CDCl$_3$) δ 7.45-7.48 (m, 5H), 5.46 (s, 2H). Spectroscopic data match those reported in the literature.[54]

General Procedure A - Synthesis of Arylnitroalkanes:

Silver nitrite (1.0 g, 6.5 mmol) was added to a flame-dried flask in the dark and placed under argon. The vessel was covered with aluminium foil, then charged with Et$_2$O (7 mL) and appropriate benzyl bromide (5.42 mmol) and stirred vigorously at rt. After 14 h, the mixture was filtered through Celite, rinsed with EtOAc, and concentrated. Purification by chromatography afforded the desired arylnitromethane.
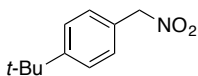
1-(*tert*-Butyl)-4-(nitromethyl)benzene (1.08b)

enantioselective hydrogenation of 1-phenylpropane-1,2-dione" *J. Chem. Soc., Perkin Trans. 1* **2002**, 2605-2612.

54) Greger, J. G.; Yoon-Miller, S. J. P.; Bechtold, N. R.; Flewelling, S. A.; MacDonald, J. P.; Downey, C. R.; Cohen, E. A.; Pelkey, E. T. "Synthesis of Unsymmetrical 3,4-Diaryl-3-pyrrolin-2-ones Utilizing Pyrrole Weinreb Amides" *J. Org. Chem.* **2011**, *76*, 8203-8214.

General Procedure A was performed on 4-(*tert*-butyl)benzyl bromide (10.9 mmol scale) for 14 h. Purification by chromatography (3% to 6% EtOAc/Hexanes) afforded the titled compound as a colorless oil (979 mg, 46%): ^{1}H NMR (300 MHz, CDCl$_3$) δ 7.47 (d, J = 8.4 Hz, 2H), 7.40 (d, J = 8.4 Hz, 2H), 5.43 (s, 2H), 1.34 (9H). Spectroscopic data match those reported in the literature.[55]
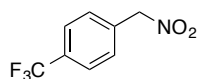
1-(Nitromethyl)-4-(trifluoromethyl)benzene (1.08c)

General Procedure A was performed on 4-(trifluoromethyl)benzyl bromide for 14 h. Purification by chromatography (3% to 6% EtOAc/Hexanes) afforded the titled compound as a white solid (746 mg, 67%): ^{1}H NMR (300 MHz, CDCl$_3$) δ 7.72 (d, J = 8.4 Hz, 2H), 7.61 (d, J = 8.1 Hz, 2H), 5.52 (s, 2H). Spectroscopic data match those reported in the literature.[56]
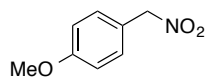
1-Methoxy-4-(nitromethyl)benzene (1.08d)

55) Barr, L.; Easton, C. J.; Lee, K.; Lincoln, S. F. "Aminocyclodextrins to facilitate the deprotonation of 4-*tert*-butyl-α-nitrotoluene" *Org. Biomol. Chem.* **2005**, *3*, 2990-2993.
56) Walvoord, R. R.; Berritt, S.; Kozlowski, M. C. "Palladium-Catalyzed Nitromethylation of Aryl Halides: An Orthogonal Formylation Equivalent" *Org. Lett.* **2012**, *14*, 4086-4089.

Synthesized from 4-methoxybenzaldehyde oxime using a reported procedure[57] in 13% yield: ^{1}H NMR (500 MHz, CDCl$_3$) δ 7.39 (d, J = 8.7 Hz, 2H), 6.95 (d, J = 8.7 Hz, 2H), 5.38 (s, 2H), 3.83 (s, 3H). Spectroscopic data match those reported in the literature.[58]
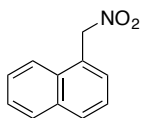
1-(Nitromethyl)naphthalene (1.08e)

General Procedure A was performed on 1-(bromomethyl)naphthalene for 5 d. Purification by chromatography (2% to 5% EtOAc/Hexanes) afforded the titled compound as a yellow solid (104 mg, 10%): mp 64-66 °C; ^{1}H NMR (500 MHz, CDCl$_3$) δ 8.04 (d, J = 8.3 Hz, 1H), 7.97 (d, J = 8.2 Hz, 1H), 7.94 (d, J = 8.2 Hz, 1H), 7.63 (td, J = 7.6, 1.3 Hz, 1H), 7.56-7.62 (m, 2H), 7.52 (td, J = 7.7, 1.0 Hz, 1H), 5.91 (s, 2H); ^{13}C NMR (125 MHz, CDCl3) δ 133.9, 131.8, 131.2, 130.7, 129.1, 127.7, 126.6, 125.9, 125.4, 122.9, 77.8; IR (film) 3059, 2912, 1552, 1367, 780 cm^{-1}; HRMS (CI) calcd for C$_{11}$H$_9$ [M-(NO$_2$)]$^+$ m/z = 141.0704, found 141.0701.
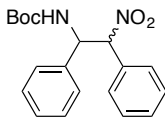
tert-Butyl (2-nitro-1,2-diphenylethyl)carbamate (1.09aa)

A flame-dried Schlenk tube was charged with **1.07a** (80 mg, 0.39 mmol), Et$_3$N (27 μL, 0.20 mmol), and toluene (2.0 mL). To the resulting solution, **1.08a** (80 mg, 0.59 mmol)

57) Base, S.; Vanajatha, G. "A Versatile Method for the Conversion of Oximes to Nitroalkanes" *Synth. Commun.* **1998**, *28*, 4531-4535.

58) Hauser, F. M.; Baghdanov, V. M. "A Convenient Preparation of Ring-Methoxylated Phenylnitromethanes" *J. Org. Chem.* **1998**, *53*, 2872-2873.

was added, and the reaction stirred under argon for 20 h at rt, whereupon the reaction was quenched with 1 M HCl (5 mL) and extracted with EtOAc (3 x 10 mL). The combined organics were dried over Na_2SO_4, filtered, and concentrated, and the resulting solid was triturated with Hexanes to afford the title compound as white solid as a 7:1 *syn*:anti mixture of diastereomers (92 mg, 69%): ^{1}H NMR (300 MHz, $CDCl_3$) major isomer: δ 7.56-7.61 (m, 2H), 7.40-7.44 (m, 3H), 7.32-7.40 (m, 5H), 5.79 (d, J = 10.1 Hz, 1H), 5.69 (dd, J = 9.7, 9.7 Hz, 1H), 4.80 (d, J = 9.1 Hz, 1H), 1.26 (s, 9H).
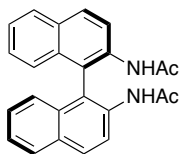
(*R*)-2,2'-bis(acetamido)-1,1'-binaphthyl (1.22)

To a solution of (*R*)-BINAM (50 mg, 0.176 mmol) in CH_2Cl_2 (2.0 mL) was added acetic anhydride (40 μL, 0.42 mmol) and the mixture was stirred at rt for 16 h. The reaction was then quenched with sat aq $NaHCO_3$ (20 mL) and extracted with CH_2Cl_2 (3 x 20 mL). The combined organics were washed with brine, dried over Na_2SO_4, filtered, and concentrated. Trituration with Hexanes afforded the title compound as a white solid in quantitative yield: ^{1}H NMR (300 MHz, $CDCl_3$) δ 8.37 (d, J = 9.0 Hz, 2H), 8.06 (d, J = 9.0 Hz, 2H), 7.95 (d, J = 8.1 Hz, 2H), 7.47 (ddd, J = 7.4, 6.9, 1.2 Hz, 2H), 7.29 (ddd, J = 7.5, 6.9, 1.2 Hz, 2H), 7.04 (d, J = 8.4 Hz, 2H), 6.91 (bs, 2H), 1.85 (s, 6H). Spectroscopic data match those reported in the literature.[59]

59) Miyano, S.; Nawa, M.; Mori, A.; Hashimoto, H. "Axially Dissymmetric Bis(aminophosphine)s Derived from 2,2'-Diamino-1,1'-binaphthyl. Synthesis and Application to Rhodium(I)-Catalyzed Asymmetric Hydrogenations" *Bull. Chem. Soc. Jpn.* **1984**, *57*, 2171-2176.

General Procedure B - *aza*-Henry reaction with BINOLsalen catalysts:

Catalyst (24 μmol) and base (49 μmol) were added to a dry microwave vial, placed under argon, and THF (0.7 mL) was added. After stirring for 2 h, the mixture was cooled to 0 °C, and imine (49 μmol in 0.2 mL THF) was added followed by nitroalkane (73 μmol in 0.2 mL THF). The mixture was stirred at 0 °C for 2 d, then concentrated *in vacuo*, and passed through a silica plug, eluting with 30% EtOAc/Hexanes to remove the catalyst. Analysis by ^{1}H NMR afforded the diastereomeric ratio based on integrations of the *tert*-butyl (Boc) groups.

The *aza*-Henry adduct was dissolved in MeOH (1 mL) and cooled to 0 °C under argon. NiCl$_2$•6H$_2$O (12 mg, 50 μmol) was added, followed by NaBH$_4$ (18 mg, 480 μmol) producing a black mixture and observable hydrogen evolution. After stirring 30 min at 0 °C, the mixture was quenched with sat aq NH$_4$Cl (10 mL), extracted with CH$_2$Cl$_2$ (3 x 10 mL). The combined organics were dried over Na$_2$SO$_4$, filtered and concentrated. Preparatory thin layer chromatography (10% MeOH/CH$_2$Cl$_2$) afforded the diastereomeric products as a colorless oil. Enantiomeric excess for the *anti* diastereomer was determined by HLPC: Chiralpak IA column (5% *i*-PrOH/Hexanes, 1.0 mL/min, λ = 220 nm) t$_R$(*anti*, major) = 27.8 min, t$_R$(*anti*, minor) = 30.6 min, t$_R$(*syn*, unseparated) = 19.9 min.

General Procedure C - Cs-BINOLate catalyzed *aza*-Henry reaction (Table 1.9**):**

An oven-dried microwave vial was charged with (*R*)-BINOL (3.5 mg, 12.2 μmol) and Cs$_2$CO$_3$ (40 mg, 122 μmol), placed under argon, and CH$_2$Cl$_2$ (0.7 mL) was added. After stirring at rt for 2 h, the reaction was cooled to 0 °C and the imine (49 μmol in 0.2 mL

CH$_2$Cl$_2$) and nitroalkane (73 µmol in 0.2 mL CH$_2$Cl$_2$) were added. The mixture was stirred for 20 h at 0 °C, after which it was passed through a silica plug, eluting with 30% EtOAc/Hexanes to remove the catalyst. Analysis by ^{1}H NMR afforded the diastereomeric ratio based on integration of the *tert*-butyl (Boc) groups.
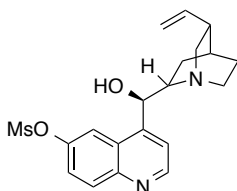
4-((*R*)-hydroxy((1*S*,2*R*,4*S*,5*R*)-5-vinylquinuclidin-2-yl)methyl)quinolin-6-yl methanesulfonate (1.43)

To a solution of **1.42** (75 mg, 0.242 mmol) in CH$_2$Cl$_2$ (1.6 mL) was added Et$_3$N (34 µL, 0.242 mmol). After cooling the resulting solution to 0 °C, methansulfonyl chloride (19 µL, 0.242 mmol) was added dropwise, and the mixture was stirred for 20 min at 0 °C. The mixture was quenched with sat aq NaHCO$_3$ (10 mL) and extracted with CH$_2$Cl$_2$ (3 x 20 mL). The combined organics were dried over Na$_2$SO, filtered, and concentrated *in vacuo*. Purification via chromatography (95:5:1 CH$_2$Cl$_2$:MeOH:Et$_3$N) and trituration with Hexanes afforded the title compound as a white solid (54 mg, 57%): mp 81-84 °C; ^{1}H NMR (360 MHz, CDCl$_3$) δ 8.79 (d, J = 4.5 Hz, 1H), 8.07 (d, J = 9.3 Hz, 1H), 8.02 (d, J = 2.6 Hz, 1H), 7.60 (d, J = 4.4 Hz, 1H), 7.53 (dd, J = 9.2, 2.5 Hz, 1H), 5.71 (ddd, J = 17.5, 10.6, 7.5 Hz, 1H), 5.57 (d, J = 4.5 Hz, 1H), 5.51 (bs, 1H), 4.99-4.89 (m, 2H), 3.51, 3.40 (m, 1H), 3.18 (s, 3H), 3.16-3.08 (m, 1H), 2.98 (dd, J = 13.9, 10.2 Hz, 1H), 2.70-2.63 (m, 1H), 2.62-2.51 (m, 1H), 2.31-2.22 (m, 1H), 1.86-1.79 (m, 3H), 1.61-1.53 (m, 1H); ^{13}C NMR (90 MHz, CDCl$_3$) δ 150.9, 149.8, 146.8, 146.8, 141.4, 132.5, 126.2, 124.2, 119.7,

116.3, 114.9, 71.5, 60.7, 56.5, 43.1, 39.7, 37.8, 27.9, 22.2; IR (film) 3076, 2931, 2868, 1510, 1367, 1186, 1149, 930, 818 cm^{-1}; HRMS (ESI) calcd for $C_{20}H_{25}N_2O_4S$ [M+H]$^+$ m/z = 389.1535, found 389.1546; $[\alpha]_D^{24}$ = –63.0 (c 0.40, CH_2Cl_2).

General Procedure D - cinchonidine-AcOH catalyzed *aza*-Henry reaction (Table 1.14**):**

An oven-dried microwave vial was charged with cinchonidine (5.9 mg, 0.020 mmol) and placed under argon. CH_2Cl_2 (3 mL) and glacial AcOH (0.020 mmol, 0.2 M in CH_2Cl_2) were added, and the solution was cooled to –30 °C. Imine (0.24 mmol, 0.6 M in CH_2Cl_2) was added, followed by dropwise addition of arylnitromethane (0.20 mmol, 0.5 M in CH_2Cl_2). The mixture was stirred for 48 h at –30 °C, whereupon it was passed through a silica plug with CH_2Cl_2 and concentrated. Trituration with Hexanes then removed unreacted arylnitromethane and afforded the pure title compound. The diastereomeric ratio and optical purity were determined by chiral HPLC or SFC analysis.
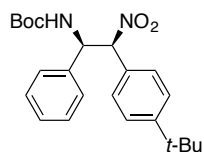
***tert*-Butyl ((1*R*,2*S*)-2-(4-(*tert*-butyl)phenyl)-2-nitro-1-phenylethyl)carbamate (1.09ab)**

General Procedure D was performed on a 2.28 mmol scale and afforded the title compound as a white solid (806 mg, 89%, 97:3 *syn*:*anti*, 70% ee): mp 194-195 °C (dec.); ^{1}H NMR (500 MHz, CDCl$_3$) δ 7.52 (d, J = 8.2 Hz, 2H), 7.44 (d, J = 8.3 Hz, 2H), 7.31-7.41 (m, 5H), 5.70 (m, 2H), 4.70 (bs, J = 8.9 Hz, 1H), 1.32 (s, 9H), 1.24 (s, 9H); ^{13}C

NMR (125 MHz, CDCl$_3$) δ 154.4, 153.7, 137.9, 129.2, 128.9, 128.7, 128.7, 127.4, 126.0, 94.4, 80.5, 56.8, 35.0, 31.4, 28.3; IR (film) 3429, 2974, 1699, 1552, 1514, 1367, 1159 cm^{-1}; HRMS (ESI) calcd for C$_{23}$H$_{30}$N$_2$O$_4$Na [M+Na]$^+$ m/z = 421.2103, found 421.2104; $[\alpha]_D^{24}$ = –26.6 (c 0.50, 98% ee, CH$_2$Cl$_2$); HPLC Chiralpak IA (10% i-PrOH/Hexanes, 1.0 mL/min, λ = 220 nm): t$_R$($anti$, major) = 9.8 min, t$_R$(syn, major) = 11.9 min, t$_R$(syn, minor) = 25.1 min, t$_R$($anti$, minor) = 28.8 min. Recrystallization from CH$_2$Cl$_2$ afforded 329 mg of product (99:1 syn:$anti$, 98% ee); concentrating the mother liquor afforded 404 mg of product (96:4 syn:$anti$, 51% ee).
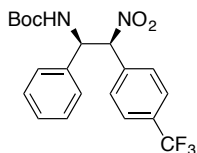
tert-**butyl   ((1R,2S)-2-nitro-1-phenyl-2-(4-(trifluoromethyl)phenyl)ethyl)carbamate (1.09ac)**

General Procedure D afforded the title compound as a white solid (87.0 mg, 99%, 99:1 syn:$anti$, 63% ee): mp 181.5-184 °C (dec.); ^{1}H NMR (500 MHz, CDCl$_3$) δ 7.74 (d, J = 8.2 Hz, 2H), 7.69 (d, J = 8.3 Hz, 2H), 7.34-7.42 (m, 5H), 5.87 (bd, J = 8.5 Hz, 1H), 5.70 (bs, 1H), 4.84 (bs, 1H), 1.24 (s, 9H); ^{13}C NMR (125 MHz, CDCl$_3$) δ 154.3, 136.9, 135.4, 132.4 (q, J = 32.7 Hz), 129.5, 129.4, 129.2, 127.3, 125.8 (q, J = 3.6 Hz), 123.8 (q, J = 273.1 Hz), 93.7, 80.8, 57.0, 28.1; IR (film) 3398, 2989, 1684, 1552, 1522, 1336, 1166 cm^{-1}; HRMS (ESI) calcd for C$_{20}$H$_{20}$F$_3$N$_2$O$_4$ [M-H]$^-$ m/z = 409.1375, found 409.1370; $[\alpha]_D^{24}$ = –32.2 (c 0.51, 63% ee, CH$_2$Cl$_2$); HPLC Chiralpak IA (10% i-PrOH/Hexanes, 1.0

mL/min, λ = 220 nm): $t_R(anti1)$ = 10.7 min, $t_R(syn$, minor) = 12.0 min, $t_R(syn$, major) = 15.3 min, $t_R(anti2)$ = 52.5 min.
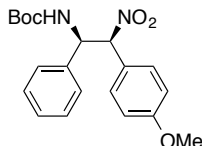
tert-butyl ((1_R_,2_S_)-2-(4-methoxyphenyl)-2-nitro-1-phenylethyl)carbamate (1.09ad)

General Procedure D afforded the title compound as a white solid (64.0 mg, 86%, 99:1 _syn:anti_, 70% ee): mp 183-185 °C (dec.); ^{1}H NMR (500 MHz, CDCl$_3$) δ 7.51 (d, J = 8.7 Hz, 2H), 7.31-7.38 (m, 5H), 6.93 (d, J = 8.7 Hz, 2H), 5.72 (bs, 1H), 5.66 (bs, 1H), 4.90 (bs, 1H), 3.82 (s, 3H), 1.28 (s, 9H); ^{13}C NMR (125 MHz, CDCl$_3$) δ 161.1, 154.5, 137.9, 130.4, 129.1, 128.8, 127.3, 123.7, 114.3, 94.1, 80.5, 56.7, 55.5, 28.2; IR (film) 3406, 2981, 2935, 1692, 1552, 1522, 1174 cm^{-1}; HRMS (ESI) calcd for C$_{20}$H$_{24}$N$_2$O$_5$Na [M+Na]$^+$ _m/z_ = 395.1583 , found 395.1601; $[\alpha]_D^{24}$ = –3.4 (_c_ 0.50, 70% ee, CH$_2$Cl$_2$); HPLC Chiralpak IA (10% _i_-PrOH/Hexanes, 1.0 mL/min, λ = 220 nm): $t_R(anti1)$ = 15.7 min, $t_R(syn$, major) = 17.7 min, $t_R(syn$, minor) = 22.4 min, $t_R(anti2)$ = 39.0 min.
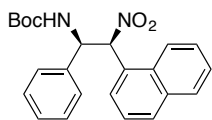
tert-butyl ((1_R_,2_S_)-2-(naphthalen-1-yl)-2-nitro-1-phenylethyl)carbamate (1.09ae)

General Procedure D afforded the title compound as a white solid (24.0 mg, 29%, 99:1 _syn:anti_, 26% ee): mp 151-155 °C (dec.); ^{1}H NMR (500 MHz, CDCl$_3$) δ 8.23 (d, J = 8.5 Hz, 1H), 8.00 (d, J = 7.5 Hz, 1H), 7.95 (d, J = 8.4 Hz, 1H), 7.93 (d, J = 8.4 Hz, 1H), 7.63

(t, J = 7.6 Hz, 1H), 7.57 (d, J = 7.7 Hz, 1H), 7.55 (d, J = 7.8 Hz, 1H), 7.34-7.46 (m, 5H),

6.78 (bd, J = 8.0 Hz, 1H), 5.93 (bs, 1H), 4.93 (bd, J = 8.0 Hz, 1H), 1.21 (s, 9H); ^{13}C

NMR (125 MHz, CDCl$_3$) δ 154.5, 137.8, 134.0, 131.9, 130.9, 129.4, 129.1, 128.9, 127.6,

127.5, 127.3, 126.7, 126.3, 125.5, 122.2, 89.0, 80.5, 56.6, 28.1; IR (film) 3375, 3059,

2981, 1676, 1552, 1522, 1359, 1166 cm^{-1}; HRMS (ESI) calcd for C$_{23}$H$_{24}$N$_2$O$_4$Na

[M+Na]$^+$ m/z = 415.1634, found 415.1651; [α]$_D^{24}$ = −3.0 (c 0.23, 26% ee, CH$_2$Cl$_2$);

HPLC Chiralpak IA (10% i-PrOH/Hexanes, 1.0 mL/min, λ = 220 nm): t$_R$(syn, major) =

12.8 min, t$_R$(syn, minor) = 15.5 min, t$_R$($anti$1) = 17.3 min, t$_R$($anti$2) = 19.9 min.
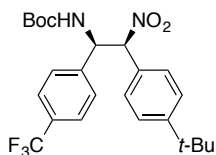
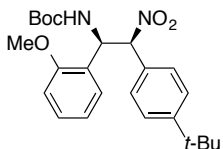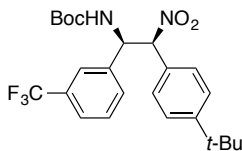**_tert_-butyl ((1_R_,2_S_)-2-(4-(_tert_-butyl)phenyl)-2-nitro-1-(4-(trifluoromethyl)phenyl)ethyl)carbamate (1.09bb)**

General Procedure D afforded the title compound as a white solid (63 mg, 68%, 98:2

syn:$anti$, 79% ee): mp 195-197 °C; ^{1}H NMR (500 MHz, CDCl$_3$) δ 7.63 (d, J = 8.3 Hz,

2H), 7.51 (d, J = 8.5 Hz, 2H), 7.50 (d, J = 8.6 Hz, 2H), 7.45 (d, J = 8.6 Hz, 2H), 5.76 (m,

2H), 4.92 (bs, 1H), 1.33 (m, 9H), 1.26 (s, 9H); ^{13}C NMR (125 MHz, CDCl$_3$) δ 154.4,

154.0, 141.9, 131.0 (q, J = 32.7 Hz), 128.5, 128.2, 127.9, 126.1, 126.1 (q, J = 3.6 Hz),

123.9 (q, J = 271.9 Hz), 93.8, 80.8, 56.5, 34.9, 31.3, 28.2; ^{19}F (282 MHz, CDCl$_3$) δ -

62.75; IR (film) 3422, 2974, 1692, 1552, 1514, 1328, 1166, 1128 cm^{-1}; HRMS (ESI)

calcd for C$_{24}$H$_{29}$F$_3$N$_2$O$_4$Na [M+Na]$^+$ m/z = 489.1977, found 489.1989; [α]$_D^{24}$ = −16.1 (c

0.50, 79% ee, CH$_2$Cl$_2$); HPLC Chiralpak IA (10% *i*-PrOH/Hexanes, 1.0 mL/min, λ = 220

nm): t$_R$(*syn*, major) = 11.8 min, t$_R$(*anti*1+2) = 12.9 min, t$_R$(*syn*, minor) = 17.1 min.
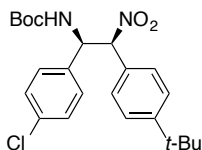
***tert*-butyl**   **((1*R*,2*S*)-2-(4-(*tert*-butyl)phenyl)-1-(4-chlorophenyl)-2-**

nitroethyl)carbamate (1.09cb)

General Procedure D afforded the title compound as a white solid (82.0 mg, 95%, 99:1

syn:*anti*, 77% ee): mp 185-188 °C (dec.); ^{1}H NMR (500 MHz, CDCl$_3$) δ 7.49 (d, *J* = 8.7

Hz, 2H), 7.44 (d, *J* = 8.5 Hz, 2H), 7.33 (d, *J* = 8.7 Hz, 2H), 7.30 (d, *J* = 8.7 Hz, 2H), 5.71

(bs, 1H), 4.88 (bs, 1H), 1.33 (s, 9H), 1.25 (s, 9H); ^{13}C NMR (125 MHz, CDCl$_3$) δ 154.4,

153.8, 136.4, 134.7, 129.3, 128.8, 128.5, 128.3, 126.0, 94.1, 80.6, 56.2, 34.9, 31.3, 28.2;

IR (film) 3414, 2974, 1692, 1552, 1514, 1159 cm^{-1}; HRMS (ESI) calcd for

C$_{23}$H$_{29}$ClN$_2$O$_4$Na [M+Na]$^+$ *m/z* = 455.1714, found 455.1700; [α]$_D^{24}$ = –24.0 (*c* 0.51, 77%

ee, CH$_2$Cl$_2$); SFC Chiralcel OJ-H (10% MeOH/CO$_2$, 2.0 mL/min, 40 °C, λ = 220 nm):

t$_R$(*anti*1) = 5.0 min, t$_R$(*anti*2) = 6.5 min, t$_R$(*syn*, major) = 7.7 min, t$_R$(*syn*, minor) = 10.9

min.
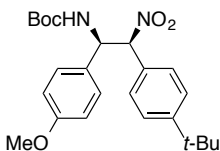
***tert*-butyl**   **((1*R*,2*S*)-2-(4-(*tert*-butyl)phenyl)-1-(4-methoxyphenyl)-2-**

nitroethyl)carbamate (1.09db)

General Procedure D afforded the title compound as a white solid (67.0 mg, 78%, 99:1

syn:*anti*, 61% ee): mp 194-196 °C; ^{1}H NMR (500 MHz, CDCl$_3$) δ 7.52 (d, J = 8.4 Hz,

2H), 7.43 (d, J = 8.5 Hz, 2H), 7.29 (d, J = 8.7 Hz, 2H), 6.89 (d, J = 8.7 Hz, 2H), 5.71 (d,

J = 10.0 Hz, 1H), 5.63 (bs, 1H), 4.79 (d, J = 9.3 Hz, 1H), 3.80 (s, 3H), 1.32 (s, 9H), 1.24

(s, 9H); ^{13}C NMR (125 MHz, CDCl$_3$) δ 159.8, 154.4, 153.4, 129.9, 128.8, 128.7, 128.5,

125.8, 114.5, 94.5, 80.3, 56.4, 55.4, 34.5, 31.3, 28.2; IR (film) 3422, 2966, 1692, 1552,

1514, 1251, 1166 cm^{-1}; HRMS (ESI) calcd for C$_{24}$H$_{32}$N$_2$O$_5$Na [M+Na]$^+$ m/z = 451.2209,

found 451.2209; $[\alpha]_D^{24}$ = −18.0 (*c* 0.51, 61% ee, CH$_2$Cl$_2$); HPLC Chiralpak IA (10% *i*-

PrOH/Hexanes, 1.0 mL/min, λ = 220 nm): t_R(*anti*1) = 13.3 min, t_R(*syn*, major) = 14.6

min, t_R(*syn*, minor) = 28.0 min, t_R(*anti*2) = 36.3 min.
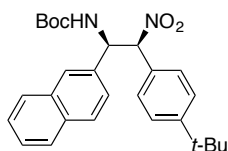
tert*-butyl **((1*R*,2*S*)-2-(4-(*tert*-butyl)phenyl)-1-(naphthalen-2-yl)-2-
nitroethyl)carbamate (1.09eb)**

General Procedure D afforded the title compound as a white solid (81.7 mg, 91% yield,

98:2 *syn*:*anti*, 63% ee): mp 199-201 °C; ^{1}H NMR (500 MHz, CDCl$_3$) δ 7.87 (d, J = 8.5

Hz, 1H), 7.81-7.85 (m, 3H), 7.56 (d, J = 8.2 Hz, 2H), 7.49-7.53 (m, 2H), 7.43-7.48 (m,

3H), 5.87 (bs, 2H), 4.86 (bs, 1H), 1.34 (s, 9H), 1.25 (s, 9H); ^{13}C NMR (125 MHz, CDCl$_3$)

δ 154.5, 153.7, 135.2, 133.5, 133.4, 129.3, 128.8, 128.7, 128.5, 128.4, 127.9, 126.9,

126.8, 126.0, 124.6, 94.3, 80.5, 57.0, 35.0, 31.4, 28.4; IR (film) 3419, 2966, 2925, 1693,

1547, 1510, 1365, 1165 cm^{-1}; HRMS (ESI) calcd for C$_{23}$H$_{25}$N$_2$O$_4$ [M-*t*Bu]$^+$ m/z =

393.1814, found 393.1814; $[\alpha]_D^{24} = -24.7$ (*c* 0.50, 63% ee, CH$_2$Cl$_2$); HPLC Chiralpak IA

(10% *i*-PrOH/Hexanes, 1.0 mL/min, $\lambda = 220$ nm): $t_R(anti1) = 11.6$ min, $t_R(syn,$ major) =

13.7 min, $t_R(anti2) = 30.5$ min, $t_R(syn,$ minor) = 34.5 min.

tert-butyl **((1R,2S)-2-(4-(tert-butyl)phenyl)-1-(2-methoxyphenyl)-2-nitroethyl)carbamate (1.09fb)**

General Procedure D afforded the title compound as a white solid (74.2 mg, 87%, 99:1

syn:anti, and 70% ee): mp 186-188 °C; ^{1}H NMR (500 MHz, CDCl$_3$) δ 7.59 (d, *J* = 8.0

Hz, 2H), 7.43 (d, *J* = 8.2 Hz, 2H), 7.29-7.35 (m, 2H), 6.92-6.97 (m, 2H), 5.98 (d, *J* = 10.6

Hz, 1H), 5.82 (t, *J* = 10.6 Hz, 1H), 5.53 (d, *J* = 10.3 Hz, 1H), 3.97 (s, 3H), 1.32 (s, 9H),

1.20 (s, 9H); ^{13}C NMR (125 MHz, CDCl$_3$) δ 157.3, 154.5, 153.1, 131.6, 130.2, 129.2,

128.8, 125.5, 124.6, 121.4, 111.3, 93.1, 79.7, 56.1, 55.7, 34.8, 31.3, 28.2; IR (film) 3445,

2966, 1715, 1552, 1498, 1367, 1244, 1166, 1020 cm^{-1}; HRMS (ESI) calcd for

C$_{24}$H$_{32}$N$_2$O$_5$Na *m/z* = 451.2209, found 451.2226; $[\alpha]_D^{24} = -26.4$ (*c* 0.49, 70% ee,

CH$_2$Cl$_2$); HPLC Chiralpak IA (10% *i*-PrOH/Hexanes, 1.0 mL/min, $\lambda = 220$ nm): $t_R(anti1)$

= 7.4 min, $t_R(syn,$ minor) = 9.8 min, $t_R(anti2) = 15.8$ min, $t_R(syn,$ major) = 23.1 min.

tert-butyl ((1*R*,2*S*)-2-(4-(*tert*-butyl)phenyl)-2-nitro-1-(3-(trifluoromethyl)phenyl)ethyl)carbamate (1.09gb)

General Procedure D afforded the title compound as a white solid (68.3 mg, 73%, 98:2 *syn:anti*, 46% ee): mp 155-156 °C; ^{1}H NMR (500 MHz, CDCl$_3$) δ 7.60 (d, J = 7.9 Hz, 1H), 7.58 (d, J = 7.9 Hz, 1H), 7.57 (s, 1H), 7.42-7.51 (m, 5H), 5.75 (bs, 2H), 4.99 (bs, 1H), 1.33 (m, 9H), 1.27 (s, 9H); ^{13}C NMR (125 MHz, CDCl$_3$) δ 154.4, 153.9, 138.9, 131.7 (q, J = 32.7 Hz), 131.0, 129.6, 128.5, 128.1, 126.1, 125.6 (q, J = 3.6 Hz), 124.2 (q, J = 3.4 Hz), 123.9 (q, J = 273.0), 93.8, 80.9, 56.7, 34.9, 31.3, 28.1; ^{19}F NMR (282 MHz, CDCl$_3$) δ -62.67; IR (film) 3368, 2974, 1699, 1552, 1367, 1328, 1166, 1128 cm^{-1}; HRMS (ESI) calcd for C$_{24}$H$_{29}$F$_3$N$_2$O$_4$Na [M+Na]$^{+}$ m/z = 489.1977, found 489.1966; $[\alpha]_D^{24}$ = –4.7 (*c* 0.50, 46% ee, CH$_2$Cl$_2$); HPLC Chiralpak IA (5% *i*-PrOH/Hexanes, 1.0 mL/min, λ = 220 nm): t$_R$(*anti*1) = 10.6 min, t$_R$(*syn*, major) = 11.7 min, t$_R$(*syn*, minor) = 19.5 min, t$_R$(*anti*2) = 20.7 min.

General Base-Mediated Epimerization of _aza_-Henry Adducts:

An oven-dried 1 d vial was charged with or **1.09ab** and CH$_2$Cl$_2$. The desired base was added as a solution in CH$_2$Cl$_2$ (0.5 equiv), and the vials were sealed and stirred at rt for the indicated time, whereupon the mixture was passed directly through a short pad of silica gel, eluting with excess CH$_2$Cl$_2$. After concentrating, the resulting residues were analyzed by HPLC.

HTE Screen for Epimerization with Inorganic Base (Scheme 1.15**):**

Suspensions of all bases in THF were prepared (~25 mg/ mL) and dosed as slurries to the appropriate vials in a 96 well plate (15 μmol base). After removing the solvent under vacuum, **1.09ab** was added as a 0.1 M solution in the desired solvent to the appropriate vial (10 μmol substrate, 100 μL reaction volume). The plate was sealed and stirred at rt for 14 h, after which each vial was quenched with AcOH (500 μL, 0.04 M in MeCN) and stirred for an additional hour at rt. After allowing the solids to settle, each mixture was directly analyzed by SFC: Chiralcel OJ-H (7.5% $MeOH/CO_2$ 0-7 min, ramp to 10% $MeOH/CO_2$ 7-12 min, 2.0 mL/min, 40 °C, λ = 220 nm): $t_R(anti1)$ = 5 min, $t_R(anti2)$ = 6.5 min, $t_R(syn1)$ = 7.5 min, $t_R(syn2)$ = 10 min.

Epimerization of *aza*-Henry Adducts with Lewis Acid Chelation (Table 1.17**):**

An oven-dried vial was charged with **1.09ab** (5.0 mg, 17 μmol), Lewis acid (34 μmol), placed under argon, and CH_2Cl_2 (250 μL) was added. After stirring for 15 min at rt, Et_3N (100 μL, 0.084 M in CH_2Cl_2) was added, and the reaction stirred under argon at rt for 3 h, after which the reaction was quenched with AcOH (10 μL) and passed through small pad of silica gel, eluting with excess CH_2Cl_2. After concentrating, the resulting residues were analyzed by HPLC.

HTE Screen for Chelation-Controlled Epimerization (Table 1.18**):**

Lewis acids were plated out as solutions in THF [Eu(OTf)$_3$, Al(OiPr)$_3$], toluene (CrCl$_2$), or MeCN [Bi(OTf)$_3$, Fe(acac)$_3$, Zn(OTf)$_2$, In(OTf)$_3$, Sn(OTf)$_2$, Co(acac)$_2$, Yb(OTf)$_3$, VO(acac)$_2$] to the appropriate vials in a 96 well plate (20 μmol Lewis acid). After removing solvent under vacuum, **1.09ab** (10 μmol) was added as a solution in appropriate solvent, followed by base (5 μmol) as a solution in the same solvent (100 μL reaction volume). The plate was sealed and stirred at rt for 22 h, after which each vial was quenched with AcOH (500 μL, 0.04 M in MeCN) and stirred for an additional hour at rt. After allowing solids to settle, each mixture was directly analyzed by SFC.

2. NITROMETHANE AS A COUPLING PARTNER IN NOVEL PALLADIUM-CATALYZED REACTIONS

2.1. Background

2.1.1. Synthetic Utility of Nitroalkanes

Aliphatic nitro groups, i.e. nitroalkanes, play a unique and versatile role in organic synthesis.[60] Owing to the strong electron-withdrawing properties of the nitro group (σ_{para} = 0.78)[61] α-deprotonation of nitroalkanes readily occurs with relatively mild bases (pK_a nitromethane = 10.2).[42] The resulting nitronate anion can be utilized in a variety of powerful carbon–carbon bond forming processes, reacting with various electrophiles such as aldehydes (Henry reaction), imines (*aza*-Henry reaction), or enones (conjugate addition reaction), as illustrated in Scheme 2.1. As these processes largely occur with formation of at least one chiral center, significant research has resulted in stereoselective and/or asymmetric variants of these transformations.[18a,62]

60) (a) Ono, N. *The Nitro Group in Organic Synthesis*; Wiley-VCH: New York, 2001. (b) Feuer, H., Nielsen, A. T., Eds. In *Nitro Compounds: Recent Advances in Synthesis and Chemistry*; VCH Publishers: New York, 1990; Chapters 1-2. (c) Rosini, G.; Ballini, R. "Functionalized Nitroalkanes as Useful Reagents for Alkyl Anion Synthons" *Synthesis* **1988**, 833-847.

61) McDaniel, D. H.; Brown, H. C. "An Extended Table of Hammett Substituent Constants Based on the Ionization of Substituted Benzoic Acids" *J. Org. Chem.* **1958**, *23*, 420-427.

62) (a) Ballini, R.; Bosica, G.; Fiorini, D.; Palmieri, A.; Petrini, M. "Conjugate Additions of Nitroalkanes to Electron-Poor Alkenes: Recent Results" *Chem. Rev.* **2005**, *105*, 933-971. (b) Luzzio, F. A. "The Henry reaction: recent examples" *Tetrahedron* **2001**, *57*, 915-945.

Scheme 2.1 Utility of nitroalkanes in C–C bond formation.
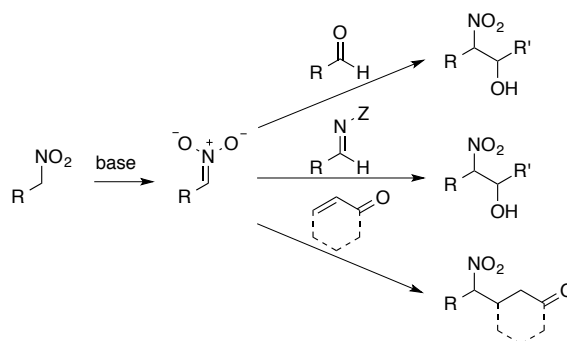
Further utility of these compounds is engendered by the extensive functional group modification available to the nitroalkyl moiety (Scheme 2.2). Specifically, the nitro group may be directly converted to carbonyl, amine, nitrile, nitrile oxide, and other functionality,[63] or reacted intermolecularly through dipolar additions to form isoxazole or furoxan heterocycles.[64]

Scheme 2.2 Potential nitro group transformations.
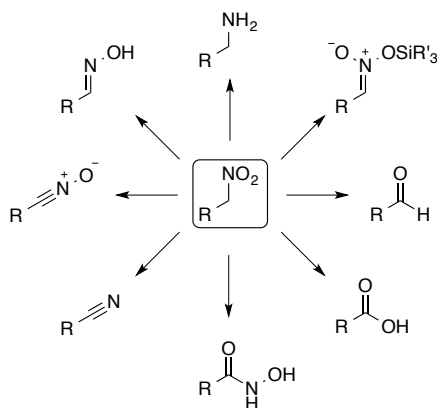
63) (a) Seebach, D.; Colvin, E. W.; Lehr, F.; Weller, T. "Nitroaliphatic Compounds – Ideal Intermediates in Organic Synthesis" *Chimia* **1979**, *33*, 1–18. (b) Ballini, R.; Palmieri, A.; Righi, P. "Highly efficient one- or two-step sequences for the synthesis of fine chemicals from versatile nitroalkanes" *Tetrahedron* **2007**, *63*, 12099–12121.

64) (a) Padwa, A. In *1,3-Dipolar Cycloaddition Chemistry*; Taylor, E. C., Weissberger, A., Eds.; Wiley & Sons: New York, 1984; Chapter 10. (b) Cecchi, L.; De Sarlo, F.; Machetti, F. "1,4-Diazabicyclo[2.2.2]octane (DABCO) as an Efficient Reagent for the Synthesis of Isoxazole Derivatives from Primary Nitro Compounds and Dipolarophiles: The Role of the Base" *Eur. J. Org. Chem.* **2006**, 4852-4860.

The ability of the nitroalkyl unit to stereoselectively form C–C bonds and subsequently transform into various other functional handles has secured the motif as a potent tool in organic synthesis. This importance has been demonstrated in the use of advanced nitroalkanes as key intermediates in the synthesis of biologically significant small molecules. Recent examples include the asymmetric synthesis of nutlin-3 by Johnston and coworkers[45] and manzamine A by the Dixon laboratory.[65] The latter synthesis particularly highlights the utility of the nitroalkyl moiety, as illustrated in Scheme 2.3.

Scheme 2.3 Use of nitroalkanes as key intermediate in Dixon's manzamine A synthesis.
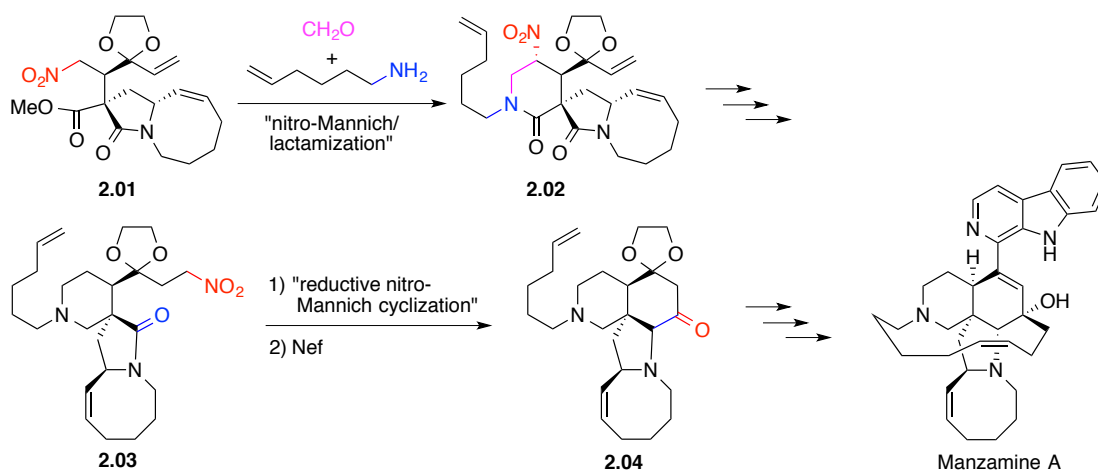
The first key step involves an addition of a nitronate anion into an *in situ* formed imine (nitro-Mannich/*aza*-Henry) with concomitant lactamization of the nearby ester, constructing the piperidine ring and necessary alkenyl unit in **2.02** for future cross metathesis. Later in the synthesis, nitroalkane **2.03** undergoes a reductive nitro-Mannich to form the fused tetracyclic core, and the nitro group is transformed into ketone **2.04** *via*

65) Jakubec, P.; Hawkins, A.; Felzmann, W.; Dixon, D. J. "Total Synthesis of Manzamine A and Related Alkaloids" *J. Am. Chem. Soc.* **2012**, *134*, 17482-17485.

Nef reaction. Subsequently Grignard addition and alkene metathesis establishes the final ring system of the manzamine framework.

2.1.2. Previous Synthetic Access to Arylnitromethanes

Our interest in nitroalkanes, and arylnitromethanes specifically, stemmed from the exploration of asymmetric diamine synthesis using these compounds as a key building block (see Chapter 1). While simple members of the family, such as the parent phenylnitromethane could be prepared in a straightforward manner in modest yield, attempts to access compounds possessing even subtle structural variation proved surprisingly difficult utilizing known synthetic methods. Indeed, despite their considerable synthetic utility, nitroalkane syntheses are largely limited to the classical Meyer reaction,[66] the displacement of halides with metal nitrites. Studies by Kornblum and coworkers in the 1950's further examined conditions for halide displacement with either silver or sodium nitrite, and established much of the current understanding and protocols for the reaction.[67] Notably, reaction of primary bromides and iodides affords useful yields of the nitroalkane products, but steric hindrance deleteriously impacts secondary, tertiary, and benzylic substrates. The ambient nature of the nitrite nucleophile is of critical importance, which consequently provides nitroalkyl or nitrite ester products by *N*- or *O*-alkylation, respectively. Kornblum's studies methodically described the increased preference of nitrite ester formation with increasing electron

66) Meyer, V.; Stüber, O. "Vorläufige Mittheilung" *Chem. Ber.* **1872**, *5*, 203-205.

67) (a) Kornblum, N.; Taub, B.; Ungnade, H. E. "The Reaction of Silver Nitrite with Primary Alkyl Halides" *J. Am. Chem. Soc.* **1954**, *76*, 3209-3211. (b) Kornblum, N.; Larson, H. O.; Blackwood, R. K.; Mooberry, D. D.; Oliveto, E. P.; Graham, G. E. "A new Method for the Synthesis of Aliphatic Nitro Compounds" *J. Am. Chem. Soc.* **1956**, *78*, 1497-1501. (c) Kornblum, N.; Powers, J. W. "Synthesis of Aliphatic Nitro Compounds" *J. Org. Chem.* **1957**, *22*, 455-456

density of the parent benzyl bromide substrate (cf. 16% for *p*-nitrobenzyl bromide vs 61% for *p*-methoxybenzyl bromide). [68] Combined, these steric and electronic considerations largely limit efficient formation of arylnitromethanes using metal nitrites to unhindered, electron-deficient substrates. Facile formation of undesired byproducts, including benzyl alcohol and aldehyde (via hydrolysis and/or Nef processes) further complicate this approach. Results for representative substrates using the Meyer/Kornblum reaction are shown in Scheme 2.4.

Scheme 2.4 Meyer/Kornblum synthesis of select benzyl bromide substrates.
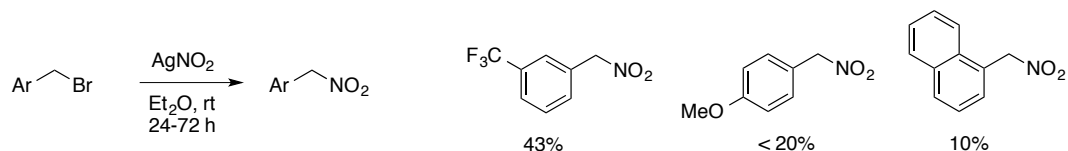
Limited examples of benzylic amine[69] or oxime[70] oxidation to provide the nitro products have been reported, but employ harsh conditions or oxidants, such as HOF•MeCN or peroxytrifluoroacetic acid, which do not tolerate many functional groups. Alternatively, synthesis of arylnitromethanes from benzyl cyanides occurs in reasonable yields via treatment of the deprotonated substrate with methyl nitrate and subsequent hydrolysis and decarboxylation. [71] However, this method suffers from the obvious

68) Kornblum, N.; Smiley, R. A.; Blackwood, R. K.; Iffland, D. C. "The Mechanism of the Reaction of Silver Nitrite with Alkyl Halides. The Contrasting Reactions of Silver and Alkali Metal Salts with Alkyl Halides. The Alkylation of Ambident Anions" *J. Am. Chem. Soc.* **1955**, *77*, 6269-6280.

69) Rozen, S.; Kol, M. "Oxidation of Aliphatic Amines by HOF•CH₃CN Complex Made Directly from F₂ and Water" *J. Org. Chem.* **1992**, *57*, 7342-7344.

70) (a) Emmons, W. D.; Pagano, A. S. "Peroxytrifluoroacetic Acid. VI. The Oxidation of Oximes to Nitroparaffins" *J. Am. Chem. Soc.* **1955**, *77*, 4557-4559. (b) Bose, D. S.; Vanajatha, G. "A Versatile Method for the Conversion of Oximes to Nitroalkanes" *Synth. Commun.* **1998**, *28*, 4531-4535.

71) (a) Black, A. P.; Babers, F. H. "Phenylnitromethane" *Org. Synth.* **1939**, *19*, 73-76. (b) Ando, K.; Shimazu, Y.; Seki, N.; Yamataka, H. "Kinetic Study of Proton-Transfer Reactions of Phenylnitromethanes. Implication for the Nitroalkane Anomaly" *J. Org. Chem.* **2011**, *76*, 3937-3945.

limitation in substrate availability and a multistep sequence. Perhaps of greater concern is the use of methyl nitrate, which is a volatile, highly explosive compound.[72]

Scheme 2.5 Synthesis of arylnitromethanes via nitration of benzyl cyanides.
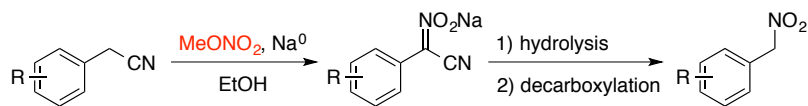
In agreement with the above summary and our own findings, a survey of recent reports utilizing arylnitromethanes provides numerous examples[44,54] highlighting the surprising difficulty for the preparation of what appear to be rather simple molecules. Accordingly, development of an efficient, robust method for synthesizing these compounds from inexpensive and available precursors would comprise a worthwhile contribution to the community.

2.2. 1st Generation Coupling in Neat Nitromethane[56]

2.2.1. Nitroalkyl Coupling Approach and Relevant Precedent

Prior synthetic strategies have focused on utilizing benzylic substrates and adding the nitro functionality to arrive at the desired compounds. An alternative approach, shown in Scheme 2.3, retrosynthetically disconnects the nitromethyl unit from the arene to yield a functionalized aryl unit and a nitromethyl fragment. As demonstrated in receiving the Nobel Prize in Chemistry in 2010, palladium-catalyzed cross-coupling has

---

72) Ray, J. D.; Ogg, Jr., R. A. "The Heat of Formation of Methyl Nitrate" *J. Phys. Chem.* **1959**, *63*, 1522-1523.

become extraordinarily powerful in the arena of C–C bond construction.[73] We hypothesized that a synthesis of arylnitromethanes may be viable by exploiting this reaction modality on an aryl and nitromethyl fragment. Considering the high availability and low cost of aryl halides and nitromethane (a common organic solvent), the union of these substrates would present an attractive and general method to prepare these compounds.

Scheme 2.6 Retrosynthetic analysis and potential coupling strategy of arylnitromethanes.
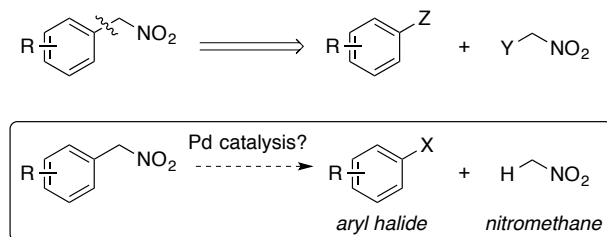
Precedent for the coupling of aryl halides with acidic carbons possessing electron-withdrawing α-substituents,[74] such as 1,3-dicarbonyl compounds of similar acidity to nitromethane, supported the potential of the proposed transformation. The most analogous example was reported by Buchwald and coworkers, in which nitroalkanes were successfully coupled with aryl bromides and chlorides in good yields using a di-*tert*-butylbiphenyl phosphine ligand with a palladium catalyst (Scheme 2.7).[75]

---

73) Select reviews: (a) Nicolaou, K. C.; Bulger, P. G.; Sarlah, D. "Palladium-Catalyzed Cross-Coupling Reactions in Total Synthesis" *Angew. Chem. Int. Ed.* **2005**, *44*, 4442-4489. (b) Miyaura, N.; Suzuki, A. "Palladium-Catalyzed Cross-Coupling Reactions of Organoboron Compounds" *Chem. Rev.* **1995**, *95*, 2457-2483. (c) Beletskaya, I. P.; Cheprakov, A. V. "The Heck Reaction as a Sharpening Stone of Palladium Catalysis" *Chem. Rev.* **2000**, *100*, 3009-3066.

74) Prim, D.; Campagne, J.-M.; Joseph, D.; Andrioletti, B. "Palladium-catalysed reactions of aryl halides with soft, non-organometallic nucleophiles" *Tetrahedron* **2002**, *58*, 2041-2075.

75) (a) Vogl, E. M.; Buchwald, S. L. "Palladium-Catalyzed Monoarylation of Nitroalkanes" *J. Org. Chem.* **2002**, *67*, 106-111. (b) Fox, J. M.; Huang, X.; Chieffi, A.; Buchwald, S. L. "Highly Active and Selective Catalysts for the Formation of α-Aryl Ketones" *J. Am. Chem. Soc.* **2000**, *122*, 1360-1370.

Interestingly, the coupling partner in these reports was limited to secondary, unhindered nitroalkanes, and attempts to couple nitromethane proved unsuccessful in their studies.

Scheme 2.7 Cross-coupling of secondary nitroalkanes with aryl halides.
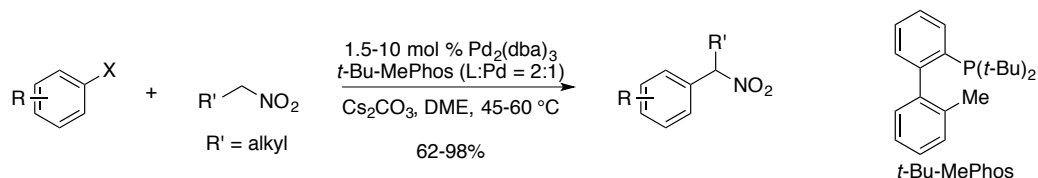
Recently, coworker Alison Metz of the Kozlowski group demonstrated that highly acidic (pK$_a$ <6) nitroacetates can be coupled with aryl bromides under palladium-catalysis (Scheme 2.8).[76] Notably, reaction conditions previously successful for malonates and nitroalkanes proved completely ineffective for this system. Investigation revealed that the highly bulky *tert*-butyl XPhos ligand is required for the transformation, putatively favoring the *C*-bound nitronate intermediate for subsequent reductive elimination.

Scheme 2.8 Cross-coupling of nitroacetates with aryl bromides.
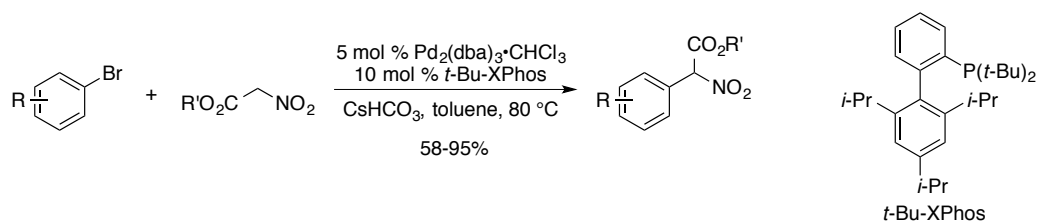
Due to the variety of functional handles for further manipulation, the resulting arylnitroacetates constitute a useful group of synthetic intermediates.[77] Of particular relevance here, arylnitromethanes may be accessed from these products via saponification of the ester and subsequent acid-catalyzed decarboxylation (Scheme 2.9).

76) Metz, A. E.; Berritt, S.; Dreher, S. D.; Kozlowski, M. C. "Efficient Palladium-Catalyzed Cross-Coupling of Highly Acidic Substrates, Nitroacetates" *Org. Lett.* **2012**, *14*, 760-763.
77) Metz, A. E.; Kozlowski, M. C. "2-Aryl-2-nitroacetates as Central Precursors to Aryl Nitromethanes, α-Ketoesters, and α-Amino Acids" *J. Org. Chem.* **2013**, *78*, 717-722 .

This route, however, requires three steps from the aryl halide and employs the more expensive nitroacetate coupling partner. The discovery of a direct coupling with nitromethane represents a more ideal preparation for the desired arylnitromethanes.

Scheme 2.9 Conversion of arylnitroacetates to arylnitromethanes.
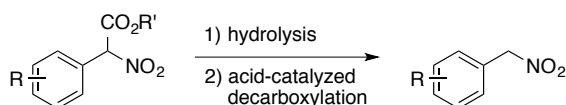
When the optimized conditions for the coupling of arylnitroacetates was applied to nitromethane and 1-bromonaphthalene as a test reaction, Alison Metz discovered that the desired nitromethylated product was formed in 10% conversion, importantly demonstrating that the overall strategy was indeed viable.

2.2.2. High-Throughput Experimentation and Reaction Optimization

Combined with the ineffectiveness of catalysts and conditions for ostensibly related transformations, the large number of reaction variables for the proposed coupling highlighted the utility of High-Throughput Experimentation (HTE).[78] Initial efforts, performed in collaboration with Dr. Simon Berritt, explored the coupling of *p*-bromoanisole (**2.05a**) as a model substrate. Utilizing the technology of the UPenn-Merck High Throughput Experimentation Laboratory, a screen of 19 different phosphine ligands, 4 bases of varying strength, and 4 solvents was performed, in total allowing examination of 304 individual reaction conditions on a 10 μmol scale. Product to internal

78) Dreher, S. D.; Dormer, P. G.; Sandrock, D. L.; Molander, G. A. "Efficient Cross-Coupling of Secondary Alkyltrifluoroborates with Aryl Chlorides–Reaction Discovery Using Parallel Microscale Experimentation" *J. Am. Chem. Soc.* **2008**, *130*, 9257-9259.

standard ratios are presented in Figure 2.1 as a bubble chart, with larger circles corresponding to larger conversions.
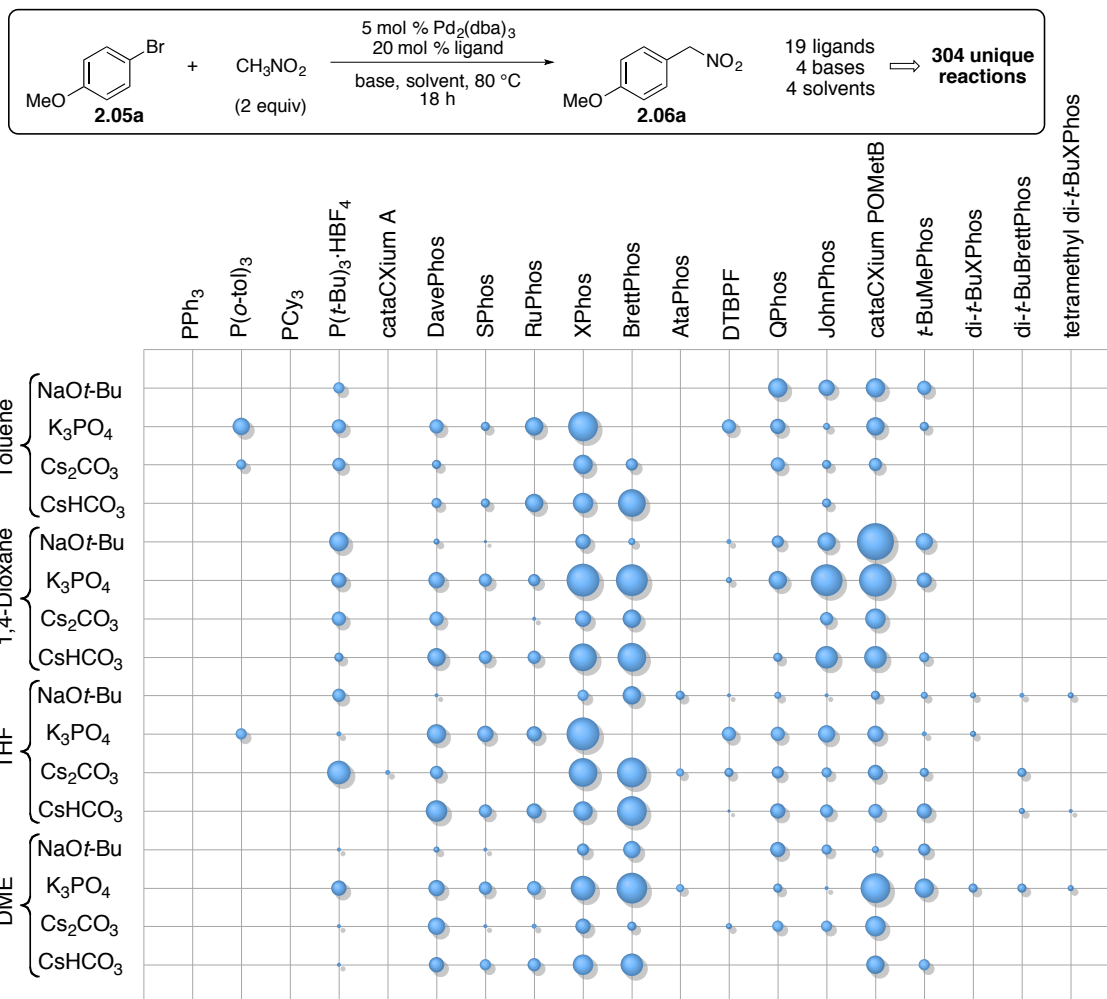
Figure 2.1 High Throughput Experimentation for the coupling **2.05a** with nitromethane.

The graphical representation of conversion in Figure 2.1 reveals several trends. Along with cataCXium POMetB, the bis-cyclohexylbiphenyl ligands XPhos and BrettPhos showed the highest reactivity through a variety of conditions. These results are surprising, considering that the bulkier *tert*-butyl variants were necessary in the aforementioned couplings of nitroalkanes[75] and nitroacetates.[76] Since nitromethane is an even smaller coupling partner, a bulky ligand around the palladium center would have

been predicted to favor the *C*-bound over *O*-bound form of the nitronate to palladium prior to reductive elimination. Polar, ethereal solvents, THF and 1,4-dioxane in particular, proved more effective than toluene. The optimal window for base strength appeared to be pK_{HA} ~9-13 based on the results of cesium carbonate and potassium phosphate. Bicarbonate and *tert*-butoxide provided poor conversion or high levels of decomposition, respectively. Analysis of the HPLC chromatograms revealed significant byproduct formation, including des-bromo and aldehyde compounds (via Nef reaction of the product), as well as decomposition. Table 2.1 illustrates the disparity of product versus impurity formation for the lead hits as determined by HPLC.

Table 2.1 Product and impurity formation for lead hits in the **Figure 2.1** HTE screen.

ligand	solvent	base	Prod/IS	Impurities/IS
cataXCium POMetB	1,4-Dioxane	NaO*t*-Bu	2.40	2.96
XPhos	THF	K_3PO_4	1.96	2.48
XPhos	1,4-Dioxane	K_3PO_4	1.93	2.86
cataXCium POMetB	1,4-Dioxane	K_3PO_4	1.93	3.21
JohnPhos	1,4-Dioxane	K_3PO_4	1.87	4.22
BrettPhos	1,4-Dioxane	K_3PO_4	1.82	3.33
BrettPhos	DME	K_3PO_4	1.75	2.30
BrettPhos	THF	Cs_2CHO_3	1.66	3.08
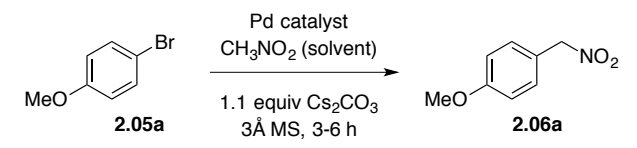
Increasing the concentration of nucleophile (nitromethane) in the reaction was postulated to improve the rate of product formation and minimize competitive decomposition pathways. A screen conducted by Dr. Simon Berritt analyzed the effect of nitromethane concentration on the reaction using the XPhos ligand and THF as the cosolvent. Indeed, as displayed in Figure 2.2, employing ≥25 equiv nitromethane

provided dramatic increases in product formation for bromobenzene, and reactivity with

chlorobenzene was even observed at 50 °C.
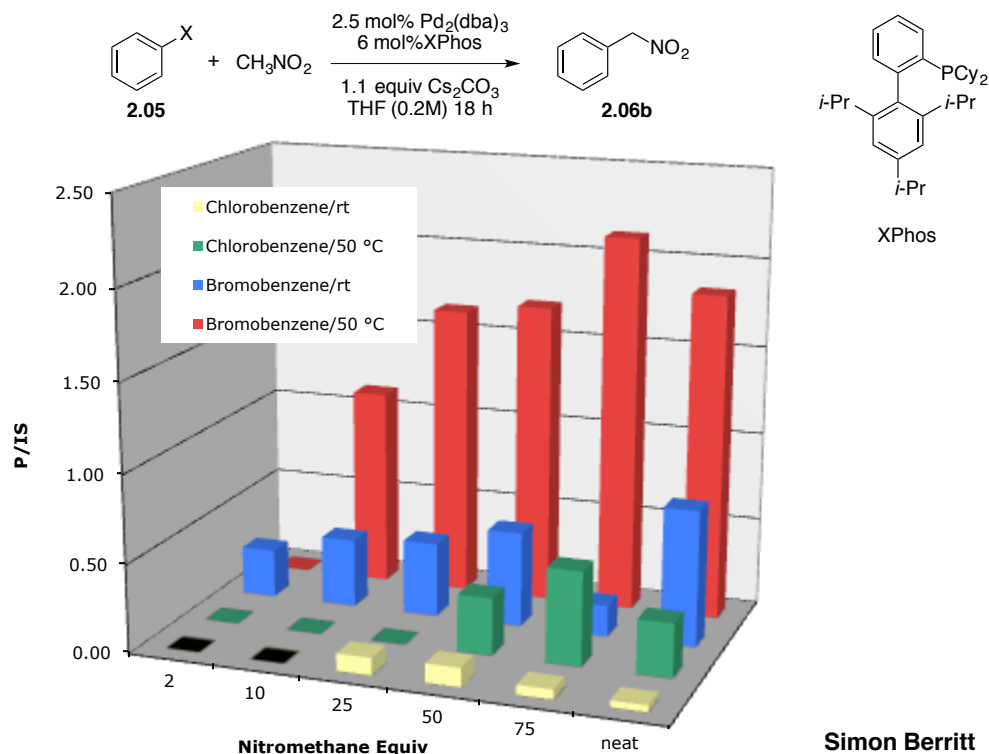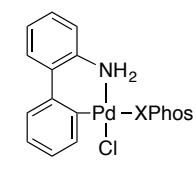
Figure 2.2 Effects of nitromethane concentration on coupling conversion.

Performing the coupling reactions with nitromethane as solvent provided greatly

enhanced reactivity, providing excellent conversions in short reaction times (<6 h) and

mild temperatures (50 °C). Aldehyde byproducts, which require water, were suppressed

via addition of 3Å molecular sieves. Scale-up experiments (Table 2.2) employing a

preformed palladium-XPhos catalyst exhibited no improvements in reaction performance,

and the carbazole byproduct complicated product isolation. A critical improvement was

discovered when the reaction was performed at lower concentrations of aryl halide.

Lower concentrations provided a cleaner reaction profile, and increased the yield

dramatically (57% at 0.2 M vs. 93% at 0.1 M).

Table 2.2 Bench-scale coupling optimization using nitromethane as solvent.

Pd catalyst	concentration (M)	yield (%)[a]
5 mol% **2.07**	0.2	59
5 mol% **2.07**	0.1	89
5 mol% Pd$_2$dba$_3$ + 12 mol% XPhos	0.2	57
2.5 mol% Pd$_2$dba$_3$ + 6 mol% XPhos	**0.1**	**93**

[a]Isolated yield after column chromatography.

2.2.3. Substrate Scope and Limitations

With optimized conditions in hand, the scope of the method was explored with a variety of aryl halides (Table 2.3). Electron rich and electron poor substrates performed well, as seen with similar efficiencies using trifluoromethyl or methoxy substrates **2.05d** or **2.05a**. An array of functionality was tolerated by the method, including ester, ketone, and nitro substitution. Notably, the desired transformation occurs in the presence of ketones bearing α-protons, which are known to couple under similar conditions.[79] Nitrogen-containing heterocycles, including pyridine **2.05k**, indole **2.05l**, and pyrazole **2.05m**, also performed well. *ortho*-Substitution did not hinder reactivity, as best demonstrated by the high reactivity and efficiency of 2-bromomesitylene (**2.05j**) when subjected to the standard reaction conditions. Aryl triflates, iodides, and chlorides can also be employed, although the latter require more forcing conditions. The disparity in reactivity between bromide and chloride is such that selective reactivity can be achieved, as observed for substrate **2.05o**. A larger scale reaction (5 mmol) performed on substrate

---

79) (a) Culkin, D. A.; Hartwig, J. F. "Palladium-catalyzed alpha-arylation of carbonyl compounds and nitriles." *Acc. Chem. Res.* **2003**, *36*, 234-245. (b) Biscoe, M. R.; Buchwald, S. L. "The Selective Monoarylation of Acetate Esters and Aryl Methyl Ketones Using Aryl Chlorides." *Org. Lett.* **2009**, *11*, 1773-1775.

71

2.05a afforded the anticipated product in 74% yield. Slight differences in the heating (oil bath instead of IKA plate) may have contributed to the observed erosion in yield via decomposition.

Table 2.3 Substrate scope for the nitromethylation of aryl halides.

2.05a	**2.05b**	**2.05c**	**2.05d**	**2.05e**	**2.05f**
93%	77%	93%	87%	77%	61%
2.05g	**2.05h**	**2.05i**	**2.05j**	**2.05k**	**2.05l**	**2.05m**
91%	89%	93%	97%	83%	76%[a]	77%[b]
2.05n	**2.05a-OTf**	**2.05k-Cl**	**2.05o**	**2.05p**	**2.05q**
70%	78%	44%[b]	69%	58%[c]	48%
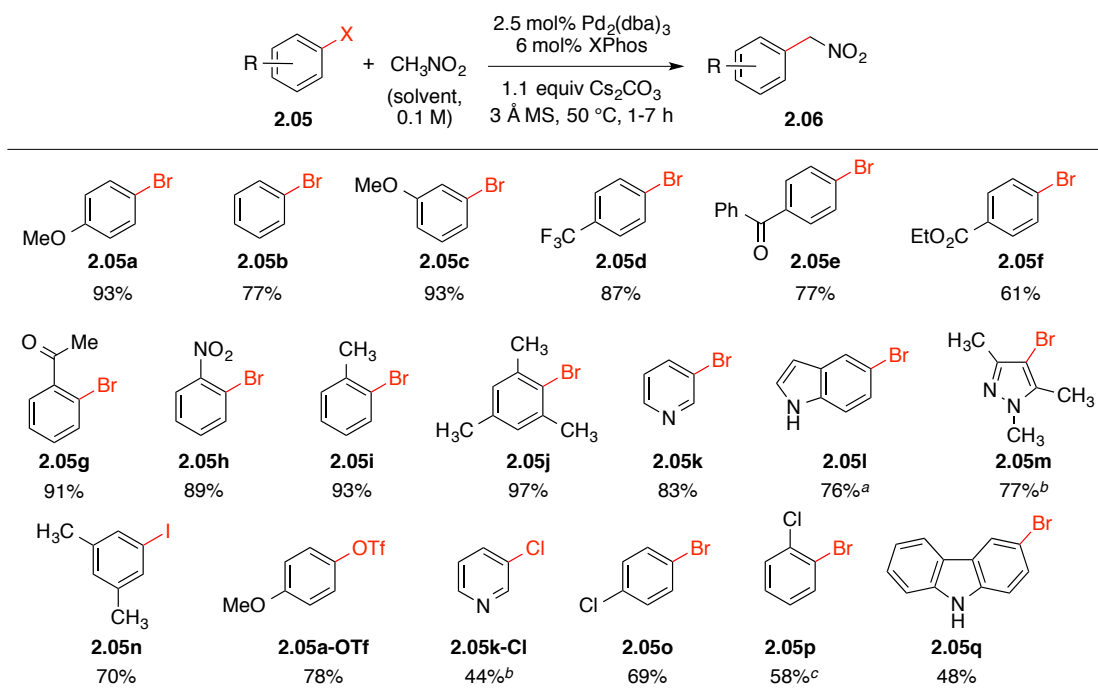
[a]At 70 °C. [b]At 80 °C using 5 mol% Pd$_2$(dba)$_3$ and 12 mol% XPhos. [c]At 50 °C using 5 mol% Pd$_2$(dba)$_3$ and 12 mol% XPhos.

In summary, a robust and direct method was developed that allows facile access to an array of arylnitromethanes, a class of compounds for which a general preparation was previously absent in the community.[80] The process employs relatively low amounts of an inexpensive, common ligand and palladium source, particularly in comparison to the more costly stoichiometric silver nitrite. As demonstrated in Chapter 1, the products

---

80) After completion of this work, we discovered a single related reaction in the Supporting Information of: Burkhard, J. A.; Tchitchanov, B. H.; Carreira, E. M. "Cascade Formation of Isoxazoles: Facile Base-Mediated Rearrangement of Substituted Oxetanes" *Angew. Chem. Int. Ed.* **2011**, *50*, 5379–5382. The conditions described therein (10 equiv of MeNO2, 1.5 mol % Pd$_2$dba$_3$, 6 mol % *t*-Bu-MePhos, 1.1 equiv of Cs$_2$CO$_3$, DME, 50 °C, 16.5 h) provided lower yields over longer reaction times (16.5 vs 5 h) with *p*-bromoanisole (74% vs 93%) and much lower yields with 2-bromomesitylene (<17% vs 97%).

are useful building blocks for an array of synthetic applications, owing to their unique reactivity and potential functional group manipulations.

2.3. Tandem Formylation via Nef Reaction of Arylnitromethanes

2.3.1. Current Formylation Methods

Aldehydes are among the most useful functional groups due to their high reactivity with a range of nucleophiles. Alternate reactivity profiles, including cycloadditions and umpolung chemistry, further the utility of aldehydes. Due to their inherent reactivity, aldehydes are often installed at specific points in a synthetic scheme rather than carried through several consecutive steps. As noted in Section 2.1.1, the nitromethylene unit is capable of several transformations to other useful functionality. The Nef reactions, first discovered in 1894,[81] is a general reaction for the conversion of a nitro group to the corresponding carbonyl. Having discovered an efficient means to synthesize an array of arylnitromethanes, it was envisioned that identification of suitable Nef conditions for these products would extend the utility of this method to access aryl aldehydes (Scheme 2.10).

Scheme 2.10 Nitromethylation-Nef stategy for arene formylation.

---
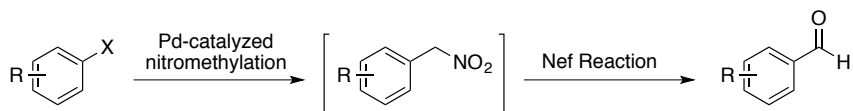
81) Nef, J. U. "Ueber die Constitution der Salze der Nitroparaffine" *Liebigs Ann. Chem.* **1894**, *280*, 263-291.

Standard methods for introducing a formyl group onto an arene can be broadly categorized into two types of reactions, as outlined in Figure 2.3. The first class effectively consists of electrophilic aromatic substitution reactions with various latent formylating agents. Commonly used examples include the Vilsmeier-Haack, Duff, Gattermann, and Reimer-Tiemann reactions and the Fries rearrangement.[82] Although these methods are useful in many synthetic schemes, their application is restricted to π-basic substrates void of acid-labile functionality (except the Reimer-Tiemann, which proceeds via a dichlorocarbene intermediate). Control of regioselectivity can also be problematic. The second class of reaction treats an aryl halide with an alkyl lithium reagent and traps the intermediate aryl lithium with dimethylformamide. The aldehyde moiety is then revealed upon hydrolysis.[83] This process controls regioselectivity, but due to the harsh lithiation conditions, certain functional groups are not tolerated.
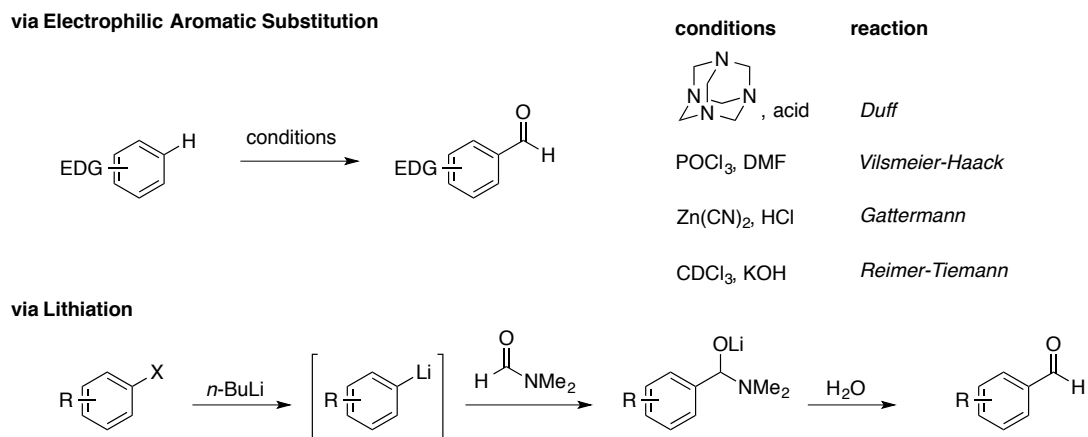
Figure 2.3 Common methods for arene formylation.

82) For a general review of formylation methods, see: (a) Olah, G. A.; Ohannesian, L.; Arvanaghi, M. "Formylating Agents" *Chem. Rev.* **1987**, *87*, 671-686. (b) Kantlehner, W. "New Methods for the Preparation of Aromatic Aldehydes" *Eur. J. Org. Chem.* **2003**, 2530-2546.
83) (a) Wakefield, B. J. *Organolithium Methods*; Academic Press: San Diego, CA, 1988. (b) Sice, J. "Preparation and Reactions of 2-Methoxythiophene" *J. Am. Chem. Soc.* **1953**, *75*, 3697-3700.

More recent efforts have focused on the formylation of aryl halides via palladium-catalysis with carbon monoxide as the formylating agent.[84] While these investigations have resulted in several promising methods,[85] this approach is inherently limited due to the use of carbon monoxide, which is toxic and often operationally challenging, and, more importantly, the use of stoichiometric amounts of reducing reagent. In light of the various constraints for current formylating methods, developing a process for the synthesis of aryl aldehydes from aryl halides via the arylnitromethane would constitute a useful alternative approach.

2.3.2. Hydrolytic and Oxidative Nef Reactions

The classical mechanism for the Nef reaction proceeding via hydrolysis is presented in Scheme 2.11.[86] Deprotonation of the acidic α-carbon yields the nitronate, which upon subsequent treatment with acid, undergoes double protonation to form the nitronic acid. This species is then susceptible to hydrolysis, expelling hyponitrous acid, water, and the corresponding carbonyl compound.

84) (a) Shoenberg, A.; Heck, R. F. "Palladium-Catalyzed Formylation of Aryl, Heterocyclic, and Vinylic Halides" *J. Am. Chem. Soc.* **1974**, *96*, 7761-7764. (b) Baillargeon, V. P.; Stille, J. K. "Palladium-Catalyzed Formylation of Organic Halides with Carbon Monoxide and Tin Hydride" *J. Am. Chem. Soc.* **1986**, *108*, 452-461.

85) (a) Skoda-Foeldes, R.; Kollar, L. "Synthetic Applications of Palladium Catalysed Carbonylation of Organic Halides" *Curr. Org. Chem.* **2002**, *6*, 1097-1119. (b) Klaus, S.; Neumann, H.; Zapf, A.; Strübing, D.; Hübner, S.; Almena, J.; Riermeier, T.; Gross, P.; Sarich, M.; Krahnert, W.-R.; Rossen, K.; Beller, M. "A General and Efficient Method for the Formylation of Aryl and Heteroaryl Bromides" *Ang. Chem. Int. Ed.* **2006**, *45*, 154-158.

86) Ballini, R.; Petrini, M. "Recent synthetic developments in the nitro to carbonyl conversion (Nef reaction)" *Tetrahedron* **2004**, *60*, 1017-1047.

Scheme 2.11 Mechanism of the hydrolytic Nef reaction.
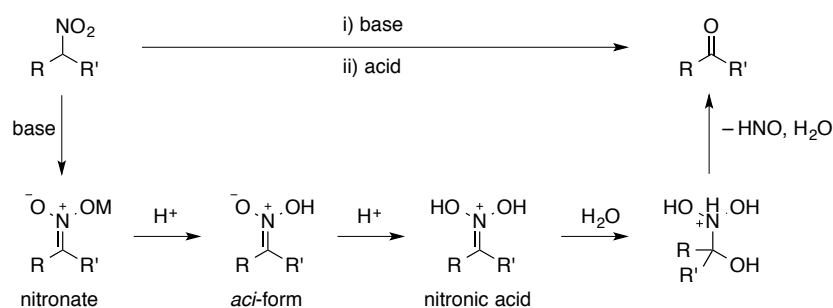
Initial efforts attempting to employ standard base and acid mediated Nef transformations on the product arylnitromethanes are summarized in Scheme 2.12. Even when employing the strongest conditions, only trace amounts of the desired aldehyde were observed. Starting material was recovered with varying amounts of decomposition. These observations are in accord with a smaller, related study conducted by Kornblum with benzylic nitro compounds.[87] Indeed, Nef reactions are more commonly performed on secondary substrates (resulting in ketones), in part due to the comparative instability of aldehyde products under the strong acid/base conditions.[86]

Scheme 2.12 Attempts at a hydrolytic Nef reaction of arylnitromethanes.
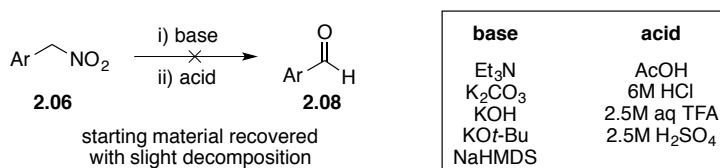
Deuterium studies were undertaken to determine whether initial deprotonation was occurring. Indeed, treating the substrate with potassium *tert*-butoxide and quenching with aqueous deuterium chloride resulted in recovery of substrate with α-deuterium

---

87) (a) Kornblum, N.; Graham, G. E. "The Regeneration of Nitroparaffins from Their Salts" *J. Am. Chem. Soc.* **1951**, *73*, 4041-443. (b) Kornblum, N.; Brown, R. A. "The Action of Acids on Nitronic Esters and Nitroparaffin Salts. Concerning the Mechanisms of the Nef and the Hydroxamic Acid Forming Reactions of Nitroparaffins" *J. Am. Chem. Soc.* **1965**, *87*, 1742-1747.

incorporation, indicating successful formation of the nitronate intermediate (Scheme 2.13). However, combining these deprotonation conditions with even concentrated sulfuric acid failed to yield product, indicating that for these substrates, either protonation to form the nitronic acid or the subsequent hydrolysis are unfavorable.

Scheme 2.13 Formation and unreactivity of the arylnitromethane nitronate to hydrolysis.
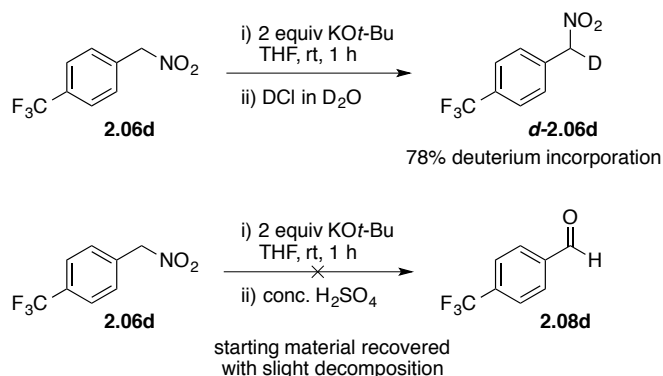
Postulating that the requisite nitronic acid species was not forming under the reaction conditions, the test substrate was exposed to *O*-alkylating conditions to afford the related nitronic ester, which hydrolyze more readily.[87b] After formation, the nitronic ester **2.09** was directly subjected to typical hydrolysis conditions (Scheme 2.14). Although conversion to aldehyde occurred, the major product observed was overoxidized ester **2.10**.

Scheme 2.14 Nitronic ester formation and attempted hydrolysis.
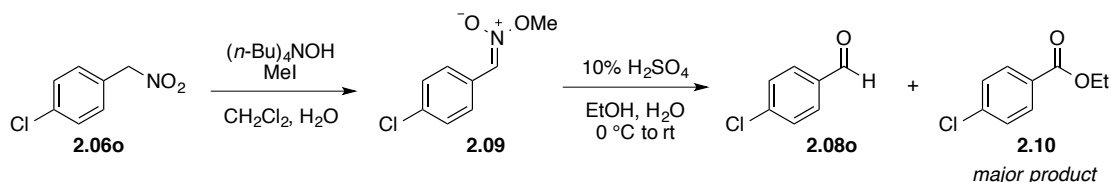
Numerous conditions exist for effecting the Nef reaction that focus on oxidative or reductive pathways.[86,88] Of these, peroxy and permanganate reagents are most commonly encountered for oxidative methods. Attempts employing buffered hydrogen peroxide or sodium percarbonate on the arylnitromethanes resulted in either minimal conversion, or overoxidation of the desired aldehyde to the corresponding acid. The sensitivity of the intermediate aldehyde further highlights the difficulty in identifying effective conditions for the desired Nef reaction on the arylnitromethane substrates. Greater success was encountered employing buffered potassium permanganate under basic conditions. Treating *p*-chloro substrate **2.06o** to these conditions at low concentrations afforded the desired aldehyde in good yields, although reproducibility proved somewhat problematic (Scheme 2.15). Despite these encouraging results, performing the reaction at higher concentrations revealed competitive formation of compound **2.11** via 2-electron oxidative dimerization of the starting nitroalkane.[89] Analysis of these conditions on a variety of substrates revealed increased levels of dimerization with electron neutral or electron rich arylnitromethanes (Table 2.4). Attempts to minimize this pathway via dilution proved unsuccessful, with significant formation of the oxidative dimer (~40% conversion) even at 0.01 M concentrations.

88) Select examples: (a) Olah, G. A.; Arvanaghi, M.; Vankar, Y. D.; Prakash, G. K. S. "Synthetic Methods and Reactions; 89. Improved Transformation of Nitro Compounds into Carbonyl Compounds by Hydrogen Peroxide/Potassium Carbonate" *Synthesis* **1980**, 662-663. (b) Kornblum, N.; Erickson, A. S.; Kelly, W. J.; Henggeler, B. "Conversion of Nitro Paraffins into Aldehydes and Ketones" *J. Org. Chem.* **1982**, *47*, 4534-4538. (c) Zhang, Z.; Yu, A.; Zhou, W. "Synthesis and structure-activity relationship of 7-(substituted)-aminomethyl-4-quinolone-3-carboxylic acid derivatives" *Bioorg. Med. Chem.* **2007**, *15*, 7274-7280.
89) (a) Do, H.-Q.; Tran-Vu, H.; Daugulis, O. "Copper-Catalyzed Homodimerization of Nitronates and Enolates under an Oxygen Atmosphere" *Organometallics* **2012**, *31*, 7816. (b) Asaro, M. F.; Nakayama, I.; Wilson, Jr., R. B. "Formation of Sterically Hindered Primary Vicinal Diamines from Vicinal and Geminal Dinitro Compounds" *J. Org. Chem.* **1992**, *57*, 778-782. (c) Pagano, A. H.; Shechter, H. "Oxidation of Nitronates with Persulfate and with Silver Ions" *J. Org. Chem.* **1970**, *35*, 295-303.

Scheme 2.15 KMnO$_4$-mediated oxidative Nef reaction of **2.06o**.

i) KOH, MeOH, 0 °C

ii) KMnO$_4$, MgSO$_4$
H$_2$O (0.02M)

68-82%

2.06o → **2.08o**
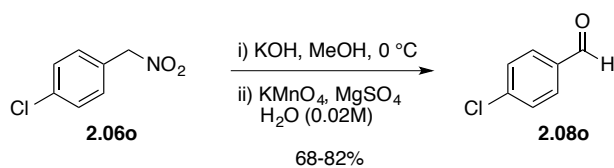
Table 2.4 Competitive oxidative dimerization of arylnitromethanes with KMnO$_4$.

i) KOH, MeOH, 0 °C

ii) KMnO$_4$, MgSO$_4$
H$_2$O

2.06 → **2.08** + **2.11**
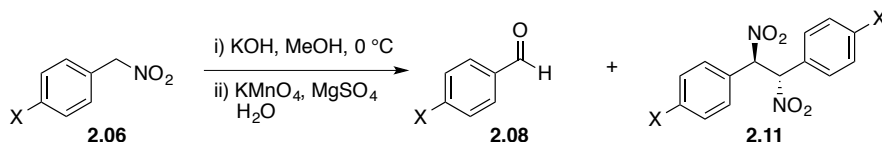
X	concentration	2.08 : 2.11[a]
CF$_3$	0.02 M	1:0
Cl	0.02 M	1:0
Cl	0.20 M	1.8:1
t-Bu	0.01 M	3:1
OMe	0.01 M	3:1

[a]Determined by ^{1}H NMR.

2.3.1. Development of a Sn(II)-Mediated, One-Pot Formylation/Oximation Method

Having exhausted more conventional methods for nitro to carbonyl conversion, reductive procedures were investigated. An effective approach for the reduction of nitro groups to oximes by a Sn(II) complex had been reported by Urpi and Vilarassa.[90] This method was extended to further reduce the oxime to the aldehyde, although only for a small number of unfunctionalized substrates.[91] Gratifyingly, an adapted procedure proved effective on an array of arylnitromethanes, providing moderate to good yields for both electron rich and poor substrates (Table 2.5). The method notably tolerates ketone

90) Bartra, M.; Romea, P.; Urpi, F.; Vilarrasa, J. "A Fast Procedure for the Reduction of Azides and Nitro Compounds Based on the Reducing Ability of Sn(SR)$_3^-$ Species" *Tetrahedron* **1990**, *46*, 587-594.
91) Urpi, F.; Vilarrasa, J. "New Synthetic 'Tricks'. A Novel One-Pot Procedure for the Conversion of Primary Nitro Groups into Aldehydes" *Tetrahedron Lett.* **1990**, *31*, 7499-7500.

and ester functionalities, which typically are not compatible with electrophilic aromatic substitution or lithiation-formylation chemistry. Poorer conversion of the oxime intermediate to aldehyde was observed for the indole substrate.

Table 2.5 Sn(II)-Mediated Nef reaction of arylnitromethanes.
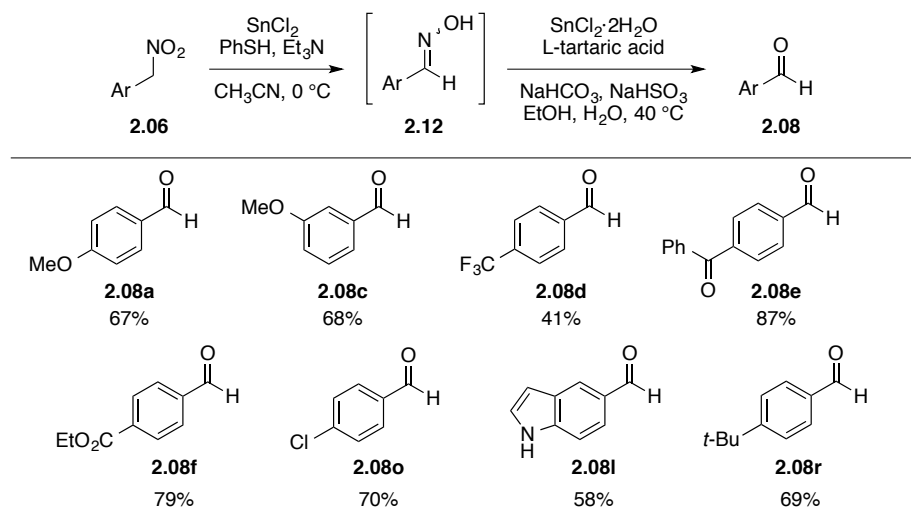
Envisioning the potential utility of a tandem nitromethylation/Nef process, **2.05a** was reacted under the standard nitromethylation conditions. Upon full conversion to the arylnitromethane, the solvent was removed, and the Sn(II) reducing Nef conditions were applied. The corresponding aldehyde was produced in 71% yield, representing a one-pot formylation of aryl halides under mild conditions (Scheme 2.16). Notably, the reduction of the arylnitromethane can be halted at the oxime intermediate, as demonstrated in the direct oximation of **2.05i** in 74% yield. To the best of our knowledge, this represents the first one-pot formation of oximes from aryl halides.

Scheme 2.16 One-pot formylation or oximation of aryl halides.
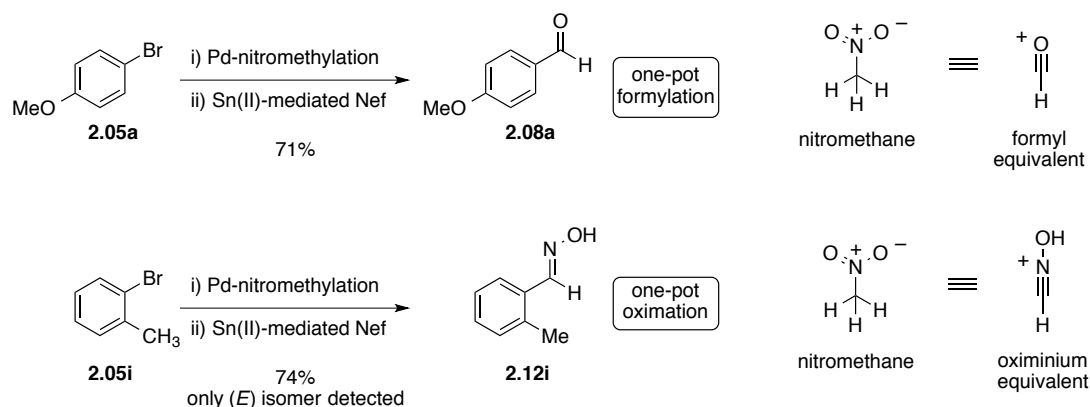
In summary, suitable conditions were identified for the Nef reaction of arylnitromethanes to provide the aryl aldehyde products in good yield across a range of substrates. This process could be incorporated into a one-pot tandem nitromethylation/Nef method, in which nitromethane is used as a masked carbonyl equivalent. The resulting formylation/oximation processes constitute effective approaches complimentary to conventional methods.

2.4 2nd Generation Coupling Using 2 or 10 Equivalents of Nitromethane[92]

2.4.1. Safety Concerns of Nitromethane and Reinvestigation of the Original Coupling

Section 2.2 describes the development of the palladium-catalyzed nitromethylation of aryl halides. Due to its relatively poor nucleophilicity, nitromethane is used as solvent (0.1 M, ~185 equiv) to improve reactivity and yield in this first generation procedure. Nitromethane is stable at ambient temperature and pressures and is routinely employed as a polar organic solvent in small-scale synthesis. However, under

---

92) Walvoord, R. R.; Kozlowksi, M. C. "Minimizing the Amount of Nitromethane in Palladium-Catalyzed Cross-Coupling with Aryl Halides" *J. Org. Chem.* **2013**, *78*, 8859-8864.

elevated temperature and/or very high pressures, nitromethane can be explosive.[93] Furthermore, particular caution must be exercised when performing reactions with nitromethane under basic conditions to avoid isolation of dry nitronate salts, as these compounds are shock and heat sensitive (Figure 2.4). [94] Methazonic acid (nitroacetaldehyde oxime) or fulminates may also be formed under basic conditions, and these compounds are known to detonate with heat, shock, or friction.[95] These potential safety concerns provided sufficient impetus for a reinvestigation of the nitromethylation of aryl halides, with the goal of minimizing nitromethane loading while retaining high reaction efficiency.
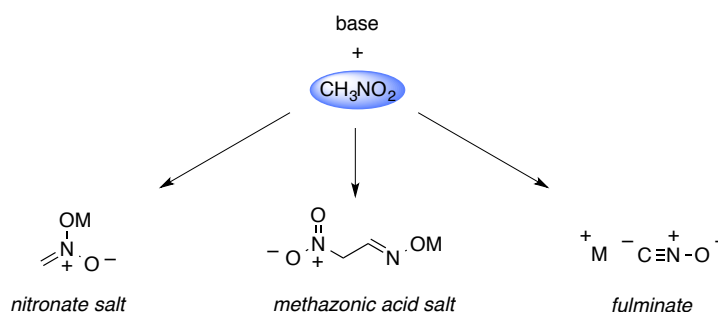
Figure 2.4 Hazardous byproducts potentially formed with nitromethane and base.

In order to identify conditions engendering adequate reactivity to minimize decomposition pathways, a focused HTE screen was designed using lead hits from the previous investigation. Specifically, a limited number of ligands were analyzed while varying ethereal solvents and bases (Figure 2.5, Table 2.6). JohnPhos provided

93) (a) McKittrick, D. S.; Irvine, R. J.; Bergsteinsson, I. "Nitromethane – Potential Hazards in Use" *Ind. Eng. Chem., Anal. Ed.* **1938**, *10*, 630-631. (b) Piermarini, G. J.; Block, S.; Miller, P. J. "Effects of pressure on the thermal decomposition kinetics and chemical reactivity of nitromethane" *J. Phys. Chem.* **1989**, *93*, 457-462.
94) Markofsky, S. B. "Nitro Compounds, Aliphatic", Ullmann's Encyclopedia of Industrial Chemistry, Electronic Release, Wiley-VCH, Weinheim October 2011.
95) Bretherick, L. *Bretherick's Handbook of Reactive Chemical Hazards*, 4th ed.; Butterworths: Boston, 1990.

inferior conversions compared to the other ligands, while XPhos again offered the cleanest reaction profile as determined by HPLC. Poor conversions were observed with the weaker bicarbonate and sodium carbonate bases. Potassium phosphate appeared optimal based on conversion and HPLC trace. Both THF and 1,4-dioxane provided superior rates and reaction purity in comparison to CPME.
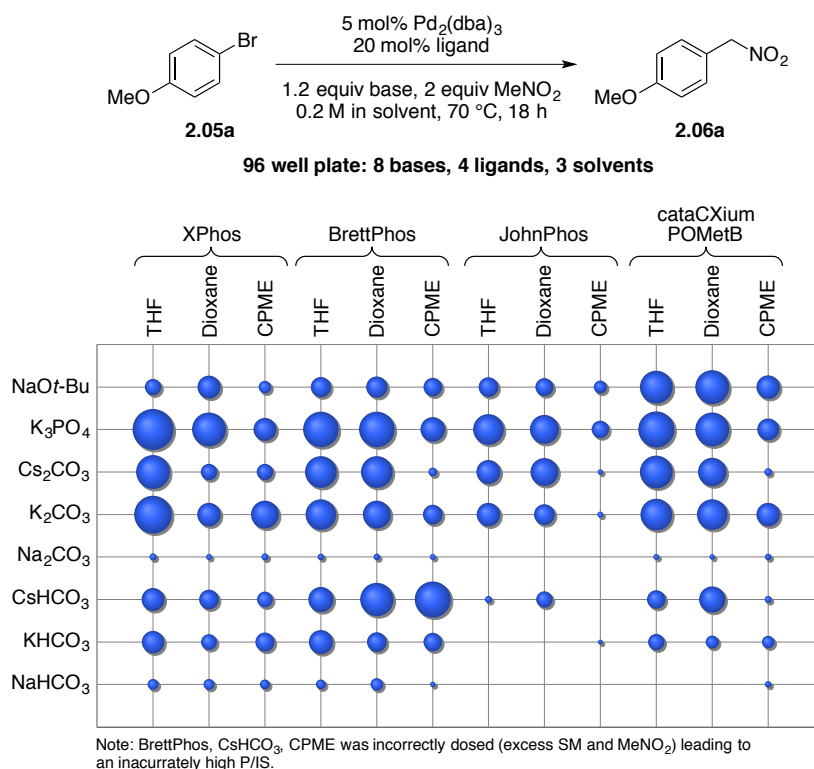
Figure 2.5 Focused HTE screen for minimizing nitromethane concentration.

Table 2.6 Lead hits from the HTE screen (**Figure 2.5**).

Ligand	Base	Solvent	P/IS
XPhos	K_3PO_4	THF	5.854
XPhos	K_2CO_3	THF	4.998
cataCXiumPOMetB	K_3PO_4	THF	4.567
BrettPhos	$CsHCO_3$	CPME	4.560
BrettPhos	K_3PO_4	THF	4.519
BrettPhos	K_3PO_4	1,4-Dioxane	4.412
XPhos	Cs_2CO_3	THF	4.062
cataCXiumPOMetB	K_3PO_4	1,4-Dioxane	4.050
XPhos	K_3PO_4	1,4-Dioxane	4.047
cataCXiumPOMetB	NaOtBu	1,4-Dioxane	4.015

Final optimization was performed via bench-scale reactions of the lead hits (Table 2.7). Surprisingly, reaction rate did not correspond well to product yield, particularly in cases employing THF or the CataCXium POMetB ligand. These conditions gave faster consumption of starting material, but led to increased amounts of decomposition by ^{1}H NMR spectroscopy. The combination of the XPhos ligand in 1,4-dioxane and potassium phosphate provided optimal yield while minimizing decomposition, affording the product in 81% yield with just 2 equivalents of nitromethane with reasonable reaction time (18 h). As anticipated, increasing nitromethane to 5 or 10 equivalents proved beneficial to both reaction rate and yield. Finally, the ligand to palladium ratio could be lowered to 1.2:1 with only minimal decrease in yield.

Table 2.7 Bench-scale results of lead HTE conditions.
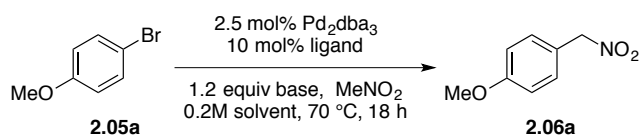
ligand	solvent	base	equiv MeNO$_2$	P:SM at 5 h[a]	% yield[b]
cataCXium POMetB	THF	K$_3$PO$_4$	2	93:7	66[c]
cataCXium POMetB	1,4-dioxane	K$_3$PO$_4$	2	89:11	67[c]
XPhos	THF	K$_3$PO$_4$	2	67:33	42
XPhos	THF	Cs$_2$CO$_3$	2	83:17	62
XPhos	THF	K$_2$CO$_3$	2	64:36	69
XPhos	1,4-dioxane	K$_3$PO$_4$	2	59:41	81
XPhos	1,4-dioxane	K$_3$PO$_4$	5	90:10	85
XPhos	1,4-dioxane	K$_3$PO$_4$	10	90:10	92
XPhos	1,4-dioxane	K$_3$PO$_4$	2	62:38	79[d]

[a]Determined by GC. [b]Isolated yield after column chromatography. [c]9 h reaction time. [d]Performed with 6 mol% ligand.

2.4.2. Substrate Scope Using 2 or 10 Equivalents of Nitromethane

Having identified suitable conditions employing significantly lower amounts of nitromethane, the substrate scope was explored. Using 10 equivalents of nitromethane, aryl bromides containing electron-donating or withdrawing groups provided high yields of the desired product (Table 2.8). Functionality including carbonyl, nitro, and indole groups was well tolerated, as well as enolizable ketones. o*rtho*-Substitution did not exhibit any deleterious effects on rate or yield of the products, as particularly demonstrated by the coupling of 2-bromomesitylene (**2.05j**). Aryl chlorides could also be employed, although more forcing conditions were generally required. The reactivity disparity between the halogen substrates is such that the bromide could be selectively coupled in the presence of a chloride, allowing for the potential of future coupling with other nucleophiles. Biphenyl triflate **2.05u** underwent smooth reaction to the desired product, representing an overall conversion of a phenol to a nitromethylene. In contrast, aryl iodides did not function well in the present transformation, a notable difference from the 1st generation protocol. These results are consistent with a mechanism in which oxidative addition is not rate-limiting. When nitroethane was employed in place of nitromethane, the coupling proceeded in excellent yield (98%), which may be partially explained by the greater stability of the secondary nitroalkyl products (Scheme 2.17). This result reveals the method is not limited to nitromethane, and can serve as a method for coupling larger nitroalkane congeners, complimentary to that reported by Buchwald.[75b]

Table 2.8 2nd Generation coupling of aryl bromides using 10 equivalents of nitromethane.

2.05a	**2.05e**	**2.05h**	**2.05j**	**2.05l**	**2.05o**
94%	82%	82%	90%	80%	86%
2.05e-Cl	**2.05s**	**2.05t**	**2.05u**	**2.05v**	
77%	77%[b]	50%[b]	86%	24%	
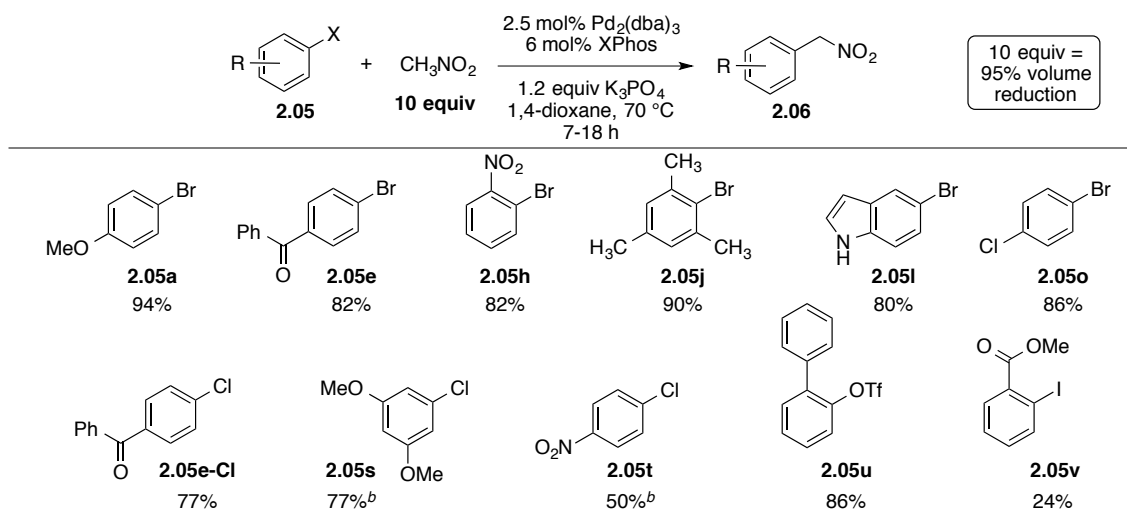
[a]Isolated yield after column chromatography. [b]At 80 °C using 5 mol% Pd₂(dba)₃ and 12 mol% XPhos.

Scheme 2.17 Cross-coupling with nitroethane.
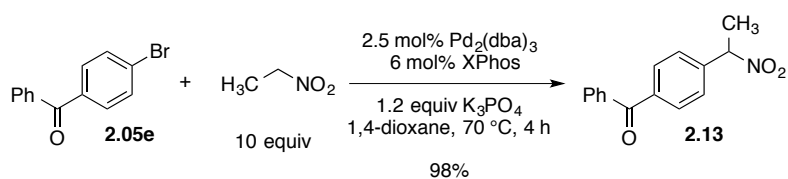
Select aryl bromides were also subjected to the optimized conditions while employing only 2 equivalents of nitromethane. The results are displayed in Table 2.9, and illustrate that the reactions produce the coupled products with similar functional group tolerance, but with more moderate yields. Longer reaction times were required under these conditions, and full conversion of starting material proved problematic for several substrates. Further extending reaction time resulted in increased product decomposition with respect to starting material conversion.

Table 2.9 2nd Generation coupling of aryl bromides using 2 equivalents of nitromethane.

2.06a	2.06e	2.06h	2.06j	2.06l	2.06o
79%	56%[b]	55%	57%[b]	65%	46%[b]
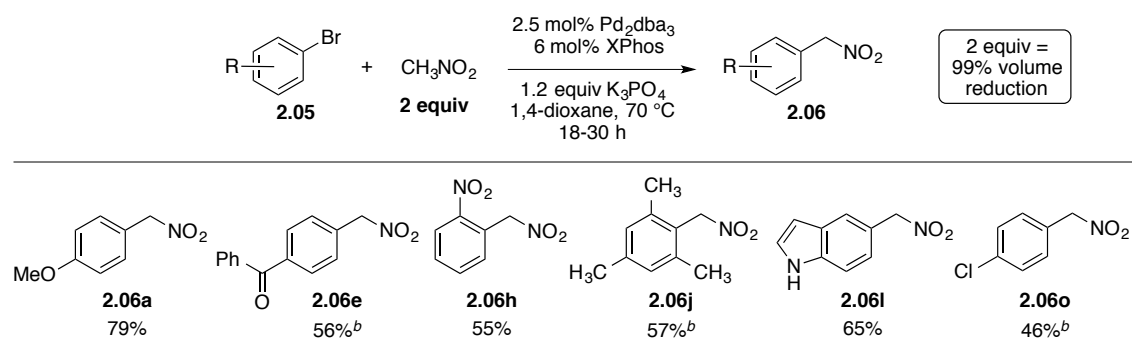
[a]Isolated yield after column chromatography. [b]Incomplete conversion.

In summary, a 2nd generation method for the coupling of aryl halides or triflates with nitromethane under palladium catalysis was developed. In this modified protocol, the amount of nitromethane has been decreased from solvent (100% v/v, 185 equiv) to 5% (10 equiv) or 1% (2 equiv) of the volume described in the original report, making this procedure considerably more attractive for large-scale processes. The method retains high functional group compatibility and tolerates significant steric encumbrance of the aryl halide or triflate, providing an array of arylnitromethane products in high yield.

2.5. Discovery of a Tandem Nitromethane Coupling/π-Allylation Reaction[96]

2.5.1. Initial Discovery and Mechanistic Investigation

During the investigation of the 1st generation coupling of nitromethane with aryl halides (Section 2.2), vinyl bromides were examined as potential substrates with which to expand the method. Specifically, these compounds were anticipated to yield allyl nitro species, a class of compounds difficult to synthesize with current methods. Upon

---

96) Padilla-Salinas, R.; Walvoord, R. R.; Tcyrulnikov, S.; Kozlowski, M. C. "Nitroethylation of Vinyl Triflates and Bromides" *Org. Lett.* **2013**, *15*, 3966-3969.

treatment of β-bromostyrene to the standard coupling conditions, however, none of the expected product was observed. Instead, nitro*ethyl*ated product **2.16** was formed in moderate yield (Scheme 2.18).

Scheme 2.18 Initial discovery of a nitroethylation reaction.
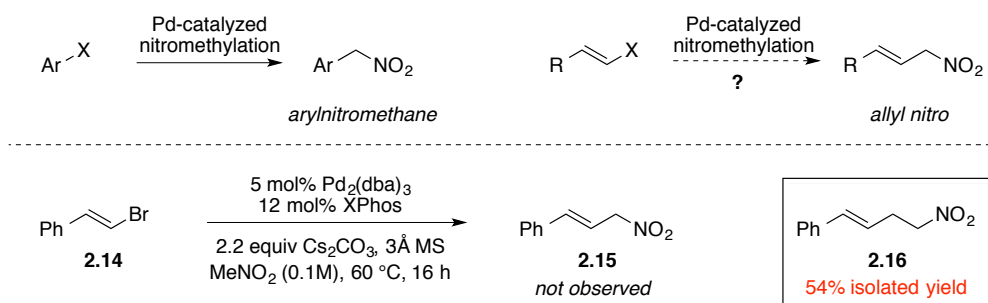
The formation of this unanticipated product indicated an alternative, double homologation pathway was possible when employing vinyl bromides. Allylic nitro species, although relatively scarce in the literature, have been reported to undergo oxidative ionization with palladium to form reactive π-allyl intermediates.[97] In addition, nitromethane, among other nitroalkanes, has been employed as a successful nucleophilic partner with π-allyls generated from allylic acetates.[98] Consequently, the formation of compound **2.16** can be postulated to arise through a unique mechanism as depicted in

97) (a) Tamura, R.; Hegedus, L. S. "Palladium(0)-catalyzed allylic alkylation and amination of allylnitroalkanes" *J. Am. Chem. Soc.* **1982**, *104*, 3727–3729. (b) Ono, N.; Hamamoto, I.; Kaji, A. "Palladium-catalysed Allylic Alkylations of Allylic Nitro-compounds" *J. Chem. Soc., Chem. Commun.* **1982**, 821–822. (c) Tamura, R.; Kamimura, A.; Ono, N. "Displacement of Aliphatic Nitro Groups by Carbon and Heteroatom Nucleophiles" *Synthesis* **1991**, 423–434.

98) (a) Wade, P. A.; Morrow, S. D.; Hardinger, S. A. "Palladium Catalysis as a Means for Promoting the Allylic C-Alkylation of Nitro Compounds" *J. Org. Chem.* **1982**, *47*, 365– 367. (b) Deardoff, D. R.; Savin, K. A.; Justman, C. J.; Karanjawala, Z. E.; Sheppeck, J. E., II; Hager, D. C.; Aydin, N. "Conversion of Allylic Alcohols into Allylic Nitromethyl Compounds via a Palladium-Catalyzed Solvolysis: An Enantioselective Synthesis of an Advanced Carbocyclic Nucleoside Precursor" *J. Org. Chem.* **1996**, *61*, 3616– 3622. (c) Rieck, H.; Helmchen, G. "Palladium Complex Catalyzed Asymmetric Allylic Substitutions with Nitromethane: Enantioselectivities Exceeding 99.9%ee*" Angew. Chem. Int. Ed.* **1996**, *34*, 2687–2689. (d) Trost, B. M.; Surivet, J. "Asymmetric Alkylation of Nitroalkanes" *Angew. Chem. Int. Ed.* **2000**, *39*, 3122–3124. (e) Uozumi, Y.; Suzuka, T. "π-Allylic C1-Substitution in Water with Nitromethane Using Amphiphilic Resin-Supported Palladium Complexes" *J. Org. Chem.* **2006**, *71*, 8644–8646

Figure 2.6. Here, nitromethane is used as a nucleophile in an initial palladium-catalyzed cross-coupling, and once again in a subsequent π-allylation sequence. Specifically, the reaction proceeds via initial oxidative addition to the vinyl halide and subsequent transmetallation with a metal nitronate to afford intermediate Pd(II) species **II**. Upon reductive elimination, the resulting allyl nitro intermediate can coordinate to Pd(0) and undergo oxidative ionization to form π-allyl intermediate **IV**. A second nitronate can act as a nucleophile on this intermediate, yielding the nitroethylated product and regenerating the active Pd(0) catalyst.
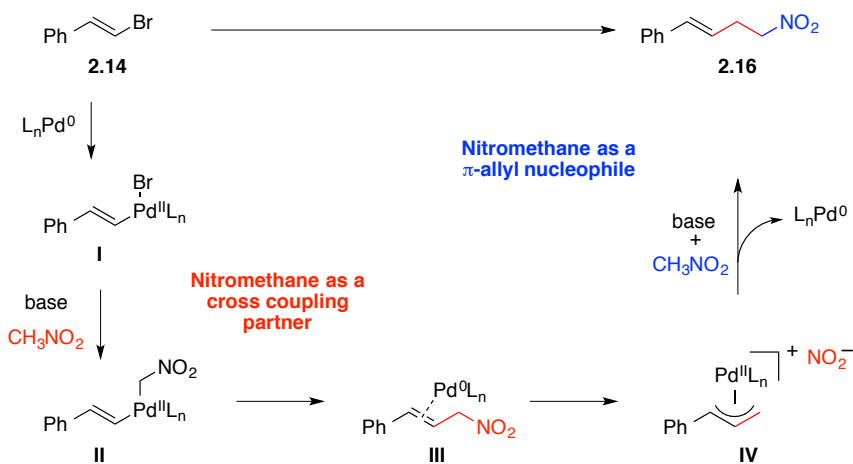
Figure 2.6 Postulated mechanism for the nitroethylation of **2.14**.

A series of experiments to further understand the nature of the transformation was undertaken. Notably, the putative allyl nitro intermediate **2.15** was never detected in the reaction, and halting the process prior to full conversion resulted only in starting material and nitroethylated product. These observations suggest that intermediate **III** rapidly undergoes ionization under the reaction conditions, and the rate-limiting step occurs in the initial cross coupling. Although allyl nitro compounds are generally difficult to synthesize, Henry condensation of β-tetralone **2.17** with nitromethane and isomerization

in the presence of ethylene diamine affords compound **2.18** in moderate yield (Scheme 2.19). [99] This particular compound provides a useful tool to test as a proposed intermediate, since the corresponding "precursor" vinyl bromide **2.21** can also be easily synthesized from tetralone **2.19**.

Scheme 2.19 Synthesis of tetralone-derived substrates.
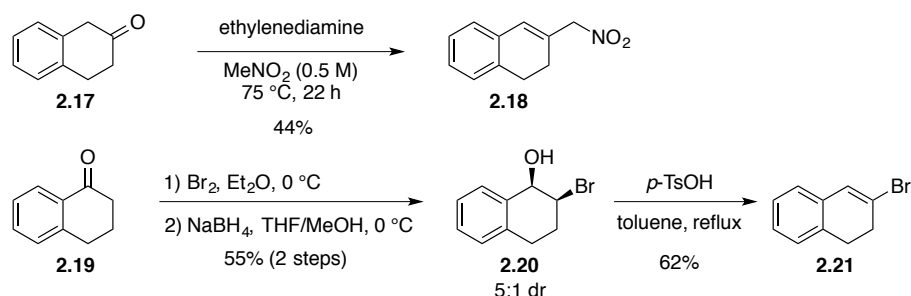
Upon treatment of vinyl bromide **2.21** to the coupling conditions, the doubly homologated product was obtained in 56% yield (Scheme 2.20). In contrast, the proposed intermediate **2.18** produced only low yield of the homoallylic product **2.22**. Significant amounts of byproducts, including dimerization were detected by LCMS.

Scheme 2.20 Coupling experiments with tetralone-derived substrates.
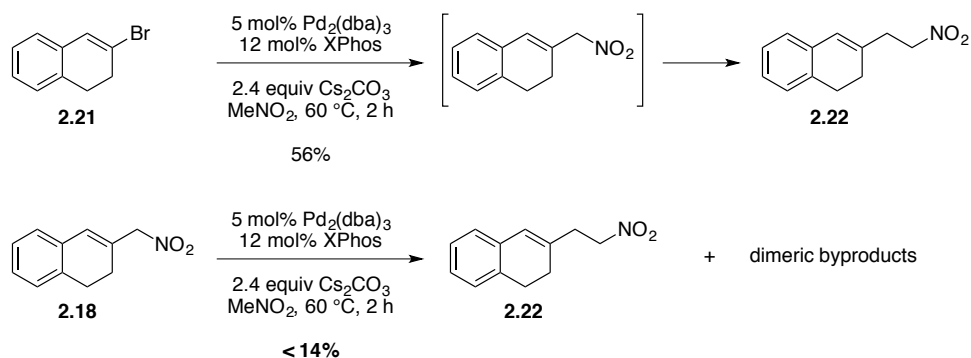
99) Barton, D. H. R.; Motherwell, W. B.; Zard, S. Z. "A simple and economic synthesis of the corticosteroid side chain from 17-oxo-steroids" *Bull. Soc. Chim. Fr.* **1983**, 61-65.

The reaction with vinyl bromide **2.21** proved sensitive to nitromethane loading. Employing 10 equivalents of nitromethane with 1,4-dioxane cosolvent, the reaction was sluggish and yielded small amounts (24%) of product along with larger amounts of decomposition and dimerized products. This result further points towards initial transmetallation of intermediate **I** with nitronate as the rate-limiting step. Morpholine and sodium *p*-toluenesulfinate, commonly employed nucleophiles in π-allylation chemistry, were used to as alternative coupling partners with **2.18** (Scheme 2.21). The formation of both of the substituted products, although in moderate yields, confirms **2.18** as capable of π-allylation chemistry. For the nitroethylation reaction, slow formation of the allyl nitro intermediate appears necessary for achieving high yields and avoiding alternate reaction pathways. In all of the aforementioned π-allyl reactions, the alternative branched regioisomeric products were not detected by ^{1}H NMR analysis.

Scheme 2.21 Allylic substitution of **2.18** with alternate nucleophiles.
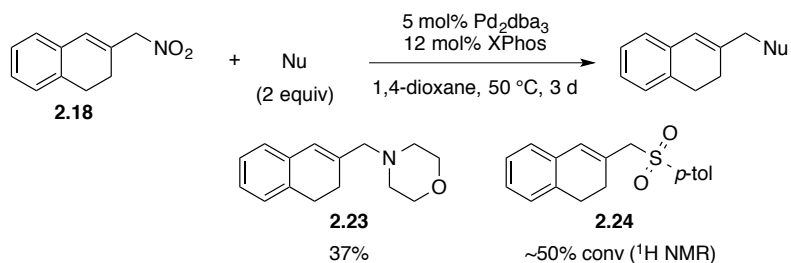
Interestingly, subjecting 2-bromonaphthalene to the reaction conditions revealed formation of the nitroethylated product **2.26** in very low yield (Scheme 2.22). This reaction ostensibly proceeds in a similar manner, here undergoing ionization to form the η^3-Pd benzyl intermediate.

Scheme 2.22 Evidence for nitroethylation of a naphthyl bromide.
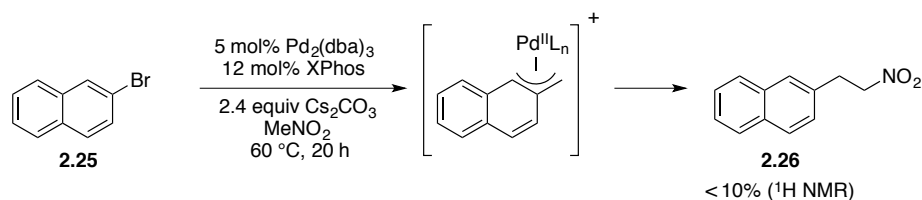
2.5.2. Development of a Nitroethylation Method for Vinyl Bromides and Triflates

After the initial experiments and mechanistic studies were conducted, coworkers Rosaura Padilla-Salinas and Sergei Tcyrulnikov moved forward with the goals of improving reaction efficiency and extending the process to a range of vinyl bromides and triflates, the latter of which are often more synthetically accessible. Challenges presented by the preliminary studies include: 1) instability of the products to sustained exposure to the reaction conditions, leading to significant decomposition, 2) ability of the allyl nitro intermediate to undergo alternative (e.g. dimerization) pathways, and 3) identification of a suitable catalyst system to perform well in both steps of the overall reaction. Specifically, the two individual coupling reactions proceed via dissimilar mechanisms, and typically utilize unrelated ligand structures. Triarylphosphines, commonly employed for π-allylation chemistry, do not facilitate the requisite initial nitromethylation,[56] while biaryl monophosphines are rarely effective in π-allyl substitution chemistry. Through rigorous exploration of potential reaction variables, aided by HTE experimentation, a general set of conditions was discovered for the efficient nitroethylation of an array of

vinyl bromides and triflates (Table 2.10).[100] As partially anticipated from the challenges above, different substrate classes performing optimally with different ligands.

Table 2.10 Substrate scope of the nitroethylation of vinyl bromides and triflates.
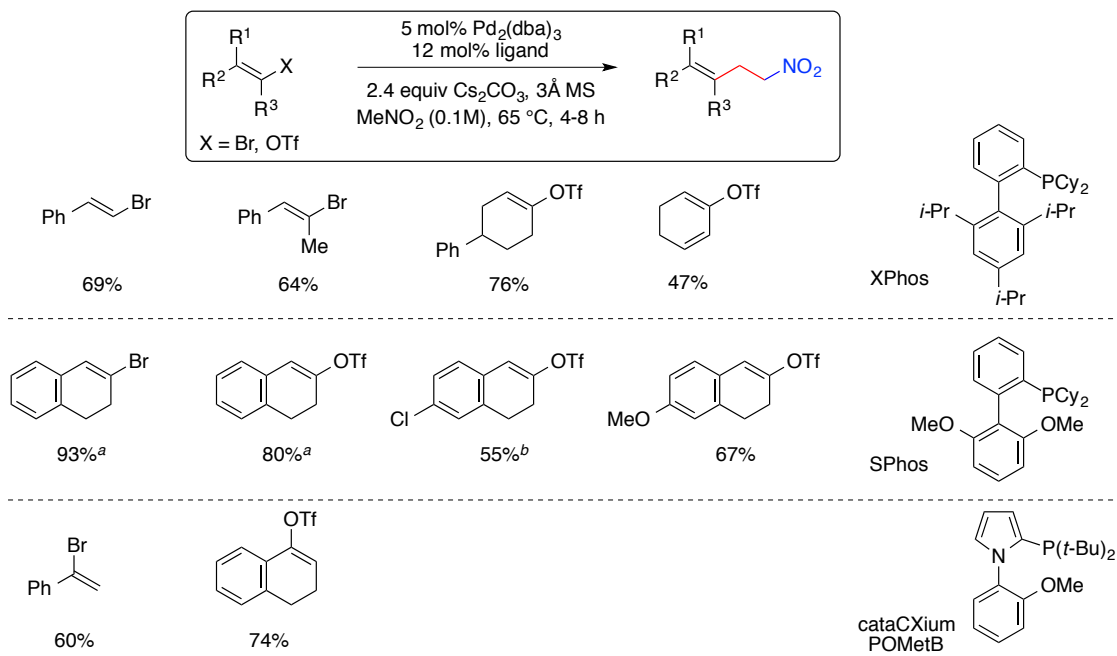
^{a}10 equiv KCl added. ^{b}Determined by ^{1}H NMR.

Rosaura Padilla & Sergei Tsyrulnikov

The resulting tandem cross-coupling/π-allylation represents an overall two-carbon homologation process for vinyl bromides and triflates. This mechanism exploits the unique nature of nitromethane as a traceless coupling partner in the first step, forming the π-allyl intermediate via nitrite displacement. This method proceeds in generally high yield under relatively mild conditions, allowing novel entry to homoallylic nitro compounds, valuable building blocks for traditional nitronate chemistry, as well as useful precursors to homoallylic amines and β,γ-unsaturated carbonyls.

100) Padilla-Salinas, R. Part II: Nitroethylation of Vinyl Triflates and Vinyl Bromides. Ph.D. Thesis, University of Pennsylvania, Philadelphia, PA, June 2014.

2.6. Conclusions
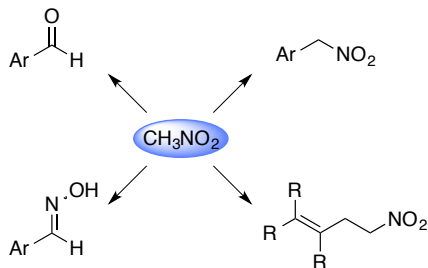
Figure 2.7 Use of nitromethane in novel coupling reactions.

In summary, a variety of novel coupling reactions employing nitromethane as the primary coupling partner with sp^2-carbons was explored (Figure 2.7). Judicious use of High-Throughput Experimentation facilitated the development of these processes, in which product formation and decomposition are often competitive. In particular, the weakly nucleophilic nature of the nitromethane anion required optimized catalyst conditions for reasonable coupling rates. These studies culminated in several useful new methods, as shown in Scheme 2.23. The palladium-catalyzed nitromethylation of aryl halides and triflates can occur under mild conditions using nitromethane as solvent (1st generation protocol) or as a reagent (2 to 10 equiv) with a cosolvent (2nd generation protocol). Nitromethane can be employed as a masked carbonyl by incorporating a reductive Nef procedure, affording aryl aldehydes or oximes in a one-pot procedure from the corresponding aryl halide. Finally, a novel tandem cross-coupling/π-allylation sequence was discovered in which nitromethane participates in both steps. The resulting method provides a convenient process for the nitroethylation of vinyl halides and triflates.

Scheme 2.23 Summary of the resulting coupling reactions of nitromethane.

1st generation Nitromethylation Protocol (Nitromethane as Solvent)

2nd generation Nitromethylation Protocol (2-10 Equiv)

1-Pot Formylation/Oximation Protocol

Nitroethylation via Tandem Cross-Coupling/π-Allylation

2.7. Experimental Section

General Considerations

All non-aqueous reactions were carried out under an atmosphere of dry argon unless otherwise noted. Commercial reagents were used as received without additional purification unless otherwise noted. Nitromethane was distilled from CaH_2 and stored at 0 °C away from light. Anhydrous 1,4-dioxane was purchased from Acros and used as received. Potassium phosphate (tribasic) was dried at 100 °C under vacuum overnight and stored in the glovebox. CH_2Cl_2 and MeCN were distilled from CaH_2, THF and Et_2O were distilled from sodium/benzophenone ketyl, Et_3N was distilled from KOH, and toluene was distilled from metallic sodium prior to use. Reactions were monitored by

thin layer chromatography (TLC) using Silicycle glass-backed TLC plates with 250 μm silica and F254 indicator. Visualization was accomplished with UV light, ceric ammonium molybdate stain, and/or 2,4-dinitrophenylhydrazine stain. Flash column chromatography was performed using Silicycle Silaflash P60 silica gel (40-63 μm particle size).

NMR spectra were recorded on Brüker AM-500, Brüker DRX-500, Brüker DMX-360, and Brüker DMX-300 Fourier transform NMR spectrometers. Chemical shifts are reported relative to the solvent resonance peak δ 7.27 (CDCl$_3$) for ^{1}H and δ 77.23 (CDCl$_3$) for ^{13}C. Data are reported as follows: chemical shift, multiplicity (s = singlet, d = doublet, t = triplet, q = quartet, bs = broad singlet, m = multiplet), coupling constants, and number of protons. High resolution mass spectra were obtained using a Waters LC-TOF LCT-XE Premier model mass spectrometer with an ionization mode of either ESI or CI. Infrared spectra were recorded using a Perkin-Elmer 1600 series or JASCO FT/IR-480 spectrometer. Melting points were obtained on a Thomas Scientific Unimelt apparatus and are uncorrected.

Aryl triflates **2.05a-OTf** and **2.05u** were prepared from the corresponding phenols using literature methods.[101] Allyl nitro **2.18**[99] and vinyl bromide **2.21**[102] were prepared as illustrated in Scheme 2.19 according to literature methods.

---

101) Kwong, F. Y.; Lai, C. W.; Chan, K. S. "Catalytic Solvent-Free Arsination: First Catalytic Application of Pd–Ar/As–Ph Exchange in the Synthesis of Functionalized Aryl Arsines" *J. Am. Chem. Soc.* **2001**, *123*, 8864-8865.
102) Voets, M.; Antes, I.; Schere, C.; Mueller-Viera, U.; Biemel, K.; Marchais-Oberwinkler, S.; Hartmann, R. W. "Synthesis and Evaluation of Heteroaryl-Substituted Dihydronaphthalenes and Indenes: Potent and Selective Inhibitors of Aldosterone Synthase (CYP11B2) for the Treatment of Congestive Heart Failure and Myocardial Fibrosis" *J. Med. Chem.* **2006**, *49*, 2222-2231.

CAUTION: While we have not experienced any problems after extensive work with nitromethane, special attention should be taken when working with nitromethane under basic conditions and heat. See references 93a and 95 for potential hazards.

General High-Throughput Experimentation Procedure: The following protocol is for the HTE experiment described in Figure 2.5 and is representative for all HTE experiments studying the nitromethylation reactions. Tabulated data for HTE screens is found in Appendix C.

Ligands (4 µmol) were dosed into the 96-well reactor equipped with 1 mL vials as solutions (50 µL, 0.08 M) in 1,2-dichloroethane. Pd_2dba_3 (1.0 µmol, 50 µL of a 0.02 M solution in benzene) was then added to the vials and the resulting solutions were evacuated to dryness on a JKem-blow-down block. Base (24 µmol, 25 mg/mL slurry in THF) was then added to the ligand/catalyst mixture, and the resulting mixture was evacuated to dryness on a JKem-blow-down block. A parylene stir-bar was added to each vial. Substrate/nitromethane/solvent solutions were prepared with 4-bromoanisole (0.2 M, 20 µmol/reaction) and nitromethane (0.4 M, 40 µmol/reaction) in the requisite solvent and then dosed in the reaction vials (100 µL reaction volume). The reactor block was sealed, removed from the glovebox and heated at 70 ºC for 18 h on an Alligator tumble stirrer (500 rpm). After cooling to ambient temperature, the reactions were quenched *via* dilution with a solution of internal standard in MeCN (2 µmol biphenyl, 0.002M, 500 µL), and the contents were stirred. Into a separate 96-well plate LC block was added 700 µL of MeCN and then 25 µL aliquots of the diluted reaction mixtures.

The 96-well plate LC block was then sealed with a polypropylene 1 mL cap mat. The reaction mixtures were analyzed using an Agilent Technologies 1200 series HPLC with a 96-well plate auto-sampler. Assay conditions: Supelco Ascentis Express C18 100 mm x 4.6 mm or ZORBAX Eclipse XDB-C8, 4.6 x 50 mm, 1.8 μm. MeCN with H_2O + 0.1 % H_3PO_4. 1.8 mL/min; 10 % in MeCN to 95 % MeCN in 6 min, hold for 2 min. Post time 2 min. Column at 40 °C; 210 nm.

Nitromethylation of Aryl Halides

General Procedure A – Cross-Coupling of Nitromethane (Nitromethane as Solvent):

In a glovebox, an oven-dried microwave vial was charged with Cs_2CO_3 (179 mg, 0.55 mmol), powdered 3 Å molecular sieves (100 mg, 200 mg/mmol), Pd_2dba_3 (11.4 mg, 0.0125 mmol), and XPhos (14.3 mg, 0.03 mmol). Nitromethane (5.0 mL) was added, followed by addition of the aryl halide (0.5 mmol). The vial was capped, removed from the glovebox, and heated to 50 °C in an IKA heating plate with vigorous stirring. Upon consumption of the aryl halide, as monitored by TLC or GC, the reaction mixture was allowed to cool to rt, diluted with CH_2Cl_2 (10 mL), and washed with saturated aq NH_4Cl (2 x 10 mL). The aqueous layer was extracted with CH_2Cl_2 (2 x 10 mL). The combined organic layers were washed with brine, dried over Na_2SO_4, filtered, and concentrated *in vacuo*. The resulting residue was purified by chromatography to afford the pure arylnitromethane.

General Procedures B and C – Cross-Coupling of Nitromethane (10 or 2 equivalents of Nitromethane):

In a glovebox, an oven-dried vial was charged with Pd_2dba_3 (11.4 mg, 0.0125 mmol), XPhos (14.3 mg, 0.030 mmol), K_3PO_4 (127 mg, 0.60 mmol), and substrate (0.50 mmol). The vial was sealed with a teflon cap, removed from the glovebox, and 1,4-dioxane (2.5 mL) was added, followed by nitromethane (270 μL, 5.0 mmol = **General Method B**, or 54 μL, 1.0 mmol = **General Method C**). The mixture was heated to 70 °C with vigorous stirring for the indicated time, then cooled to rt, diluted with CH_2Cl_2 (15 mL), and washed with 1 M aq HCl (15 mL), which was then extracted with CH_2Cl_2 (3 x 15 mL). The combined organics were dried over Na_2SO_4, filtered, and concentrated *in vacuo*. The resulting residue was purified by chromatography to afford the pure arylnitromethane.
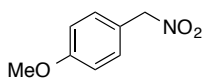
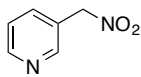**1-Methoxy-4-(nitromethyl)benzene (2.06a)**

General Procedure A was carried out on 4-bromoanisole with a reaction time of 5 h. Purification by chromatography (5% EtOAc/Hexanes) provided the title compound as a yellow oil (77.5 mg, 93%). This reaction was repeated on a 5 mmol scale following General Procedure A, heating to 50 °C for 5 h in an oil bath to afford the title compound as a yellow oil (618 mg, 74%). Slightly more decomposition was observed when heating with the oil bath vs an IKA heating plate.

General Method B was carried out on 4-bromoanisole with a reaction time of 7 h and afforded the title compound after purification as a pale yellow oil (78.4 mg, 94%): ^{1}H NMR (500 MHz, CDCl$_3$) δ 7.39 (d, *J* = 8.6 Hz, 2H), 6.95 (d, *J* = 8.7 Hz, 2H), 5.38 (s, 2H), 3.83 (s, 3H). All spectral data were in agreement with literature values.[58]

General Method C was c with a reaction time of 18 h and afforded the title compound after purification as a yellow oil (66.1 mg, 79%).
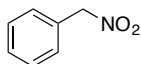
Phenylnitromethane (2.06b)

General Procedure A was carried out on bromobenzene with a reaction time of 3.5 h. Purification by chromatography (5% EtOAc/Hexanes) provided the title compound as a pale oil (53.0 mg, 77%). All spectral data were in agreement with literature values.[54]
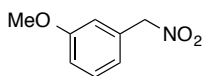
1-Methoxy-3-(nitromethyl)benzene (2.06c)

General Procedure A was carried out on 1-bromo-3-methoxybenzene with a reaction time of 5 h. Purification by chromatography (5% EtOAc/Hexanes) provided the title compound as a yellow oil (77.9 mg, 93%). All spectral data were in agreement with literature values.[58]
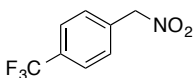
1-(Nitromethyl)-4-(trifluoromethyl)benzene (2.06d)

General Procedure A was carried out on 4-trifluoromethyl bromobenzene with a reaction time of 5 h. Purification by chromatography (5% EtOAc/Hexanes) provided the title compound as a pale yellow solid (89.5 mg, 87%): mp: 40-41 °C; ^{1}H NMR (500 MHz, CDCl$_3$) δ 7.72 (d, J = 8.2 Hz, 2H), 7.60 (d, J = 8.1 Hz, 2H), 5.52 (s, 2H); ^{13}C NMR (125

MHz, CDCl$_3$) δ 133.4, 132.4 (q, J = 32.6 Hz), 130.7, 126.3 (q, J = 3.6 Hz), 123.9 (q, J = 272.6 Hz), 79.4; IR (film) 2923, 2855, 1560, 1374, 1326, 1127, 1068 cm^{-1}; HRMS (ESI) calcd for C$_8$H$_5$NO$_2$F$_3$ [M-H]$^-$, m/z = 204.0272; found 204.0265.
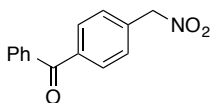
(4-(Nitromethyl)phenyl)(phenyl)methanone (2.06e)

General Procedure A was carried out on 4-bromobenzophenone with a reaction time of 6 h. Purification by chromatography (4% to 10% EtOAc/Hexanes) provided the title compound as a tan solid (93.3 mg, 77%): mp: 88-90 °C; ^{1}H NMR (500 MHz, CDCl$_3$) δ 7.87 (d, J = 8.2 Hz, 2H), 7.81 (d, J = 8.1 Hz, 2H), 7.65-7.58 (m, 3H), 7.54-7.49 (m, 2H), 5.55 (s, 2H); ^{13}C NMR (125 MHz, CDCl$_3$) δ 196.0, 139.3, 137.3, 133.5, 133.1, 130.8, 130.3, 130.1, 128.7, 79.7; IR (film) 3061, 2916, 1659, 1554, 1371, 1277 cm^{-1}; HRMS (ESI) calcd for C$_{14}$H$_{12}$NO$_3$ [M+H]$^+$, m/z = 242.0817; found 242.0820.

General Method B was carried out on 4-bromobenzophenone with a reaction time of 18 h and afforded the title compound after purification as a colorless solid (99.4 mg, 82%).

General Method B was carried out on 4-chlorobenzophenone with a reaction time of 18 h and afforded the title compound after purification as a light tan solid (93.6 mg, 77%).

General Method C was carried out on 4-bromobenzophenone with a reaction time of 30 h and afforded the title compound after purification as a tan solid (67.5 mg, 56%).
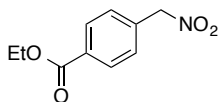
Ethyl 4-(nitromethyl)benzoate (2.06f)

General Procedure A was carried out on ethyl 4-bromobenzoate with a reaction time of 6 h. Purification by chromatography (50% to 70% EtOAc/Hexanes) provided the title compound as a white solid (63.3 mg, 61%): mp: 70-71 °C; ^{1}H NMR (500 MHz, CDCl$_3$) δ 8.11 (d, J = 8.3 Hz, 2H), 7.54 (d, J = 8.2 Hz, 2H), 5.50 (s, 2H), 4.40 (q, J = 7.1 Hz, 2H), 1.41 (t, J = 7.2 Hz, 3H); ^{13}C NMR (125 MHz, CDCl$_3$) δ 165.9, 134.1, 132.3, 130.5, 130.1, 79.7, 61.5, 14.5; IR (film) 2998, 2982, 2907, 1705, 1558, 1372, 1290, 1111 cm^{-1}; HMRS (ESI) calcd for C$_{10}$H$_{10}$NO$_4$ [M-H]$^{-}$, m/z = 208.0610; found 208.0611.

General Method B was carried out on ethyl 4-bromobenzoate with a reaction time of 18 h and afforded the title compound after purification as a colorless solid (80.7 mg, 77%).
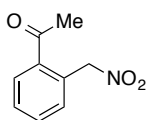
1-(2-(Nitromethyl)phenyl)ethanone (2.06g)

General Procedure A was carried out on 2'-bromoacetophenone with a reaction time of 4 h. Purification by chromatography (10% to 20% EtOAc/Hexanes) provided compound as a white solid (81.1 mg, 91%): mp: 87-89 °C; ^{1}H NMR (500 MHz, CDCl$_3$) δ 7.97-7.93 (m, 1H), 7.64-7.58 (m, 2H), 7.41-7.38 (m, 1H), 5.79 (s, 2H), 2.65 (s, 3H); ^{13}C NMR (125 MHz, CDCl$_3$) δ 200.6, 137.3, 133.5, 132.8, 130.8, 130.4, 129.3, 77.6, 28.7; IR (film) 3023, 2956, 1681, 1560, 1552, 1380, 1360, 1259 cm^{-1}; HRMS (CI) calc for C$_9$H$_{10}$NO$_3$ [M+H]$^{+}$, m/z = 180.0661; found 180.0656.

General Method B was carried out on 2'-bromoacetophenone with a reaction time of 18 h and afforded the title compound after purification as a tan solid after trituration with Hexanes (62.8 mg, 70%).
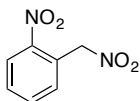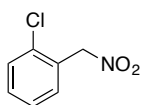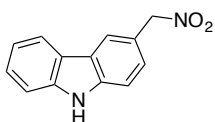

1-Nitro-2-(nitromethyl)benzene (2.06h)

General Procedure A was carried out on 1-bromo-2-nitrobenzene with a reaction time of 4 h. Purification by chromatography (10% to 25% EtOAc/Hexanes) provided the title compound as a tan solid (81.1 mg, 89%).

General Method B was carried out on 1-bromo-2-nitrobenzene with a reaction time of 18 h and afforded the title compound after purification and trituration with Hexanes as a tan solid (74.5 mg, 82%): mp: 60-63 °C; ^{1}H NMR (500 MHz, CDCl$_3$) δ 8.28 (dd, J = 8.1, 1.3 Hz, 1H), 7.77 (td, J = 7.6, 1.3 Hz, 1H), 7.71 (td, J = 8.0, 1.5 Hz, 1H), 7.52 (dd, J = 7.5, 1.3 Hz, 1H), 5.85 (s, 2H). All spectral data were in agreement with literature values.[103]

General Method C was carried out on 1-bromo-2-nitrobenzene with a reaction time of 24 h and afforded the title compound after purification as a tan solid (50.1 mg, 55%).
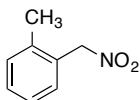
1-Methyl-2-(nitromethyl)benzene (2.06i)

103) Suzuki, H.; Murashima, T.; Kozai, I.; Mori, T. "Ozone-mediated Nitration of Alkylbenzenes and Related Compounds with Nitrogen Dioxide" *J. Chem. Soc., Perkin Trans. 1* **1993**, 1591-1597.

General Procedure A was carried out on 2-bromotoluene with a reaction time of 3.5 h. Purification by chromatography (4% EtOAc/Hexanes) provided the title compound as a yellow oil (70.2 mg, 93%): ^{1}H NMR (500 MHz, CDCl$_3$) δ 7.39-7.34 (m, 2H), 7.31-7.25 (m, 2H), 5.51 (s, 2H), 2.42 (s, 3H); ^{13}C NMR (125 MHz, CDCl$_3$) δ 138.4, 131.7, 131.1, 130.5, 128.6, 126.8, 77.9, 19.2; IR (film) 3027, 2960, 2920, 2866, 1552, 1434, 1370 cm^{-1}; HRMS (CI) calcd for C$_8$H$_9$ [M-NO$_2$]$^+$, m/z = 105.0704; found 105.0709.
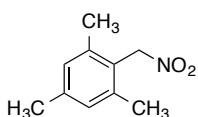
1,3,5-Trimethyl-2-(nitromethyl)benzene (2.06j)

General Procedure A was carried out on 2-bromomesitylene with a reaction time of 4.5 h. Purification by chromatography (3% EtOAc/Hexanes) provided the title compound as a colorless solid (87.0 mg, 97%): mp: 71-72 °C (lit. 70-71 °C)[5]; ^{1}H NMR (500 MHz, CDCl$_3$) δ 6.95 (s, 2H), 5.57 (s, 2H), 2.39 (s, 6H), 2.32 (s, 3H); ^{13}C NMR (125 MHz, CDCl$_3$) δ 140.2, 138.9, 129.7, 124.6, 74.0, 21.3, 19.9; IR (film) 3023, 2956, 2923, 1553, 1453, 1365 cm^{-1}; HRMS (CI) calc for C$_{10}$H$_{13}$ [M-NO$_2$]$^+$, m/z = 133.1017; found 133.1015.

General Method B was carried out on 2-bromomesitylene with a reaction time of 8 h and afforded the title compound after purification and trituration with Hexanes as pale needles (80.7 mg, 90%).

General Method C was carried out on 2-bromomesitylene with a reaction time of 24 h and afforded the title compound after purification as a colorless solid (51.3 mg, 55%).

3-(Nitromethyl)pyridine (2.06k)

General Procedure A was carried out on 3-bromopyridine on a 0.25 mmol scale (aryl halide) using 5 mol% Pd$_2$dba$_3$ and 12 mol% XPhos. The reaction was performed at 80 °C for 1.5 h. Purification by chromatography (20% to 60% EtOAc/Hexanes) provided the title compound as a pale yellow oil (28.8 mg, 83%). The above procedure was also performed on 3-chloropyridine (0.25 mmol) for 1 h to provide the title compound as a pale yellow oil (15.2 mg, 44%): ^{1}H NMR (500 MHz, CDCl$_3$) δ 8.70 (s, 2H), 7.82 (dt, $J =$ 7.9, 1.7 Hz, 1H), 7.39 (dd, $J =$ 7.8, 4.8 Hz, 1H), 5.47 (s, 2H); ^{13}C NMR (125 MHz, CDCl$_3$) δ 151.4, 151.1, 137.8, 125.8, 124.1, 77.3; IR (film) 3038, 2921, 1557, 1429, 1376 cm^{-1}; HRMS (CI) calcd for C$_6$H$_7$N$_2$O$_2$ [M+H]$^+$, $m/z =$ 139.0508; found 139.0514.
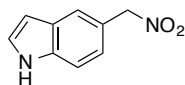
5-(Nitromethyl)-1H-indole (2.06l)

General Procedure A was carried out on 5-bromoindole with a reaction time of 2 h at 70 °C. Purification by chromatography (20% EtOAc/Hexanes) provided the title compound as a tan solid (67.2 mg, 76%): mp: 92-94 °C; ^{1}H NMR (500 MHz, CDCl$_3$) δ 8.30 (bs, 1H), 7.76 (s, 1H), 7.44 (d, $J =$ 8.4 Hz, 1H), 7.31-7.27 (m, 2H), 6.61 (m, 1H), 5.55 (s, 2H); ^{13}C NMR (125 MHz, CDCl$_3$) δ 136.6, 128.3, 125.7, 123.9, 123.3, 121.7, 111.8, 103.4, 81.1; IR (film) 3426, 2910, 1557, 1419, 1375, 1308; HRMS (CI) calcd for C$_9$H$_9$N$_2$O$_2$ [M+H]$^+$, $m/z =$ 177.0664; found 177.0659.

General Method B was carried out on 5-bromoindole with a reaction time of 7 h and afforded the title compound after purification as a tan solid (70.9 mg, 80%).

General Method C was carried out on 5-bromoindole with a reaction time of 21 h and afforded the title compound after purification as a tan solid (57.3 mg, 65%).
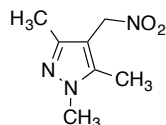
1,3,5-Trimethyl-4-(nitromethyl)-1*H*-pyrazole (2.06m)

General Procedure A was carried out on 1,3,5-trimethyl-4-(nitromethyl)-1*H*-pyrazole on a 0.25 mmol scale (aryl halide) using 5 mol% Pd$_2$dba$_3$ and 12 mol% XPhos. The reaction was performed at 80 °C for 2.5 h. Purification by chromatography (50% EtOAc/Hexanes) provided the title compound as a white solid (32.7 mg, 77%): mp: 71-72 °C; ^{1}H NMR (500 MHz, CDCl$_3$) δ 5.25 (s, 2H), 3.74 (s, 3H), 2.29 (s, 3H), 2.26 (s, 3H); ^{13}C NMR (125 MHz, CDCl$_3$) δ 147.6, 140.0, 107.0, 70.4, 36.3, 11.7, 9.9; IR (film) 2979, 2937, 1542, 1439, 1388, 1325, 1290 cm^{-1}; HRMS (ES) calcd for C$_7$H$_{12}$N$_3$O$_2$ [M+H]$^+$, *m/z* = 170.0930; found 170.0929.
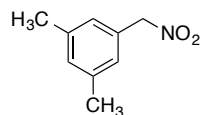
1,3-Dimethyl-5-(nitromethyl)benzene (2.06n)

General Procedure A was carried out on 1-iodo-3,5-dimethylbenzene with a reaction time of 6 h. Purification by chromatography (3% EtOAc/Hexanes) provided the title

compound as a tan solid (58.1 mg, 70%): mp: 48-50 °C; ^{1}H NMR (500 MHz, CDCl$_3$) δ 7.09 (s, 1H), 7.08 (s, 2H), 5.38 (s, 2H), 2.36 (s, 6H); ^{13}C NMR (125 MHz, CDCl$_3$) δ 139.0, 131.8, 129.8, 127.8, 80.4, 21.3; IR (film) 3018, 2921, 2852, 1555, 1374 cm^{-1}; HRMS (CI) calcd for C$_9$H$_{11}$ [M-NO$_2$]$^+$, m/z = 119.0861; found 119.0862.
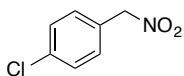
1-Chloro-4-(nitromethyl)benzene (2.06o)

General Procedure A was carried out on 1-bromo-4-chlorobenzene with a reaction time of 3 h. Purification by chromatography (4% EtOAc/Hexanes) provided the title compound as a white solid (59.1 mg, 69%): mp: 31-32 °C; ^{1}H NMR (500 MHz, CDCl$_3$) δ 7.45-7.38 (m, 4H), 5.41 (s, 2H); ^{13}C NMR (125 MHz, CDCl$_3$) δ 136.5, 131.6, 129.5, 128.2, 79.3; IR (film) 2919, 2853, 1557, 1494, 1373, 1092 cm^{-1}; HRMS (CI) calcd for C$_7$H$_6$Cl [M-NO$_2$]$^+$, m/z = 125.0158; found 125.0155.

General Method B was carried out on 1-bromo-4-chlorobenzene with a reaction time of 8 h and provided the title compound after purification as a colorless waxy material that partially melted when handling at room temperature (73.5 mg, 86%).

General Method C was carried out on 1-bromo-4-chlorobenzene with a reaction time of 30 h and afforded the title compound after purification as a colorless waxy material that partially melted when handling at room temperature (39.4 mg, 46%).

1-Chloro-2-(nitromethyl)benzene (2.06p)

General Procedure A was carried out on 2-bromo-1-chlorobenzene using 5 mol% Pd_2dba_3 and 12 mol% XPhos with a reaction time of 12 h. Purification by chromatography (4% EtOAc/Hexanes) provided the title compound as a colorless liquid (49.7 mg, 58%): ^{1}H NMR (500 MHz, $CDCl_3$) δ 7.49 (dd, $J = 8.0$, 1.2 Hz, 1H), 7.46-7.40 (m, 2H), 7.36 (ddd, $J = 7.5$, 7.5, 1.3 Hz, 1H), 5.61 (s, 2H); ^{13}C NMR (125 MHz, $CDCl_3$) δ 135.8, 132.8, 131.8, 130.2, 127.9, 127.6, 76.9; IR (film) 3065, 3020, 2918, 1557, 1372, 1059 cm^{-1}; HRMS (CI) calcd for C_7H_6Cl $[M-NO_2]^+$, $m/z = 125.0158$; found 125.0155.

3-(Nitromethyl)-9*H*-carbazole (2.06q)

General Procedure A was carried out on 3-bromocarbazole on a 0.25 mmol scale (aryl halide) with a reaction time of 2 h at 70 °C. Purification by chromatography (15% EtOAc/Hexanes) provided the title compound as a white solid (27.3 mg, 48%): mp: 145-148 °C (dec); ^{1}H NMR (500 MHz, $CDCl_3$) δ 8.19 (bs, 1H), 8.18 (s, 1H), 8.09 (d, $J = 7.8$ Hz, 1H), 7.51 (dd, $J = 8.3$, 1.7 Hz, 1H), 7.49-7.45 (m, 3H), 7.29 (m, 1H), 5.62 (s, 2H); ^{13}C NMR (125 MHz, $CDCl_3$) δ 140.3, 140.1, 127.8, 126.8, 123.9, 123.1, 122.8, 121.1, 120.7, 120.3, 111.3, 111.1, 80.9; IR (film) 3393, 1626, 1541, 1462, 1375 cm^{-1}; HRMS (ES) calcd for $C_{13}H_{10}N_2O_2Cl$ $[M+Cl]^-$, $m/z = 261.0431$; found 261.0429.
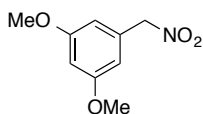
1,3-Dimethoxy-5-(nitromethyl)benzene (2.06s)

General Method B was carried out on 1-chloro-3,5-dimethoxybenzene using 5 mol% Pd$_2$dba$_3$ and 12 mol% XPhos at 80 °C with a reaction time of 5.5 h. Purification by chromatography (15% EtOAc/Hex) afforded the title compound as a tan solid (75.6 mg, 77%): mp: 56-58 °C; ^{1}H NMR (500 MHz, CDCl$_3$) δ 6.58 (d, J = 2.3 Hz, 2H), 6.52 (t, J = 2.2 Hz, 1H), 5.36 (s, 2H), 3.80 (s, 6H); ^{13}C NMR (125 MHz, CDCl$_3$) δ 161.3, 131.6, 108.0, 101.9, 80.2, 55.6; IR (film) 2916, 2848, 1597, 1551, 1456, 1430, 1372, 1206, 1153, 1066 cm^{-1}; HRMS (CI) calcd for C$_9$H$_{11}$O$_2$ [M-NO$_2$]$^+$, m/z = 151.0759; found 151.0758.
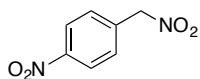
1-Nitro-4-(nitromethyl)benzene (2.06t)

General Method B was carried out on 1-chloro-4-nitrobenzene using 5 mol% Pd$_2$dba$_3$ and 12 mol% XPhos at 80 °C with a reaction time of 5 h. Purification by chromatography (12% EtOAc/Hex) afforded the title compound as a yellow solid (45.6 mg, 50%): mp: 82-86 °C (lit. 84-86 °C); ^{1}H NMR (300 MHz, CDCl$_3$) δ 8.32 (d, J = 8.7 Hz, 2H), 7.68 (d, J = 8.6 Hz, 2H), 5.57 (s, 2H). All spectral data were in agreement with literature values.[104]

---
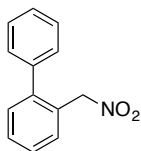
104) Bug, T.; Lemek, T.; Mayr, H. "Nucleophilicities of Nitroalkyl Anions" *J. Org. Chem.* **2004**, *69*, 7565-7576.

2-(Nitromethyl)-1,1'-biphenyl (2.06u)

General Method B was carried out on 1,1'-biphenyl-2-trifluoromethanesulfonate with a reaction time of 18 h. Purification by chromatography (3% EtOAc/Hex) afforded the title compound as a colorless oil (92.1 mg, 86%): ^{1}H NMR (300 MHz, CDCl$_3$) δ 7.36-7.56 (m, 7H), 7.28-7.34 (m, 2H), 5.42 (s, 2H); ^{13}C NMR (75 MHz, CDCl$_3$) δ 143.9, 139.8, 131.3, 130.8, 130.1, 129.2, 128.8, 128.3, 128.1, 127.5, 77.5. IR (film) 2920, 2852, 1551, 1481, 1372; HRMS (ESI) calcd for C$_{13}$H$_{11}$ [M-NO$_2$]$^+$, m/z = 167.0861; found 167.0858.
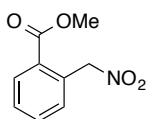
Methyl 2-(nitromethyl)benzoate (2.06v)

General Method B was carried out on methyl-2-iodobenzoate with a reaction time of 18 h. Purification by chromatography (8% EtOAc/Hexanes) afforded the title compound after trituration with Hexanes as a colorless solid (23.6 mg, 24%): mp: 66-67 °C; ^{1}H NMR (500 MHz, CDCl$_3$) δ 8.15 (dd, J = 7.7, 1.4 Hz, 1H), 7.62 (td, J = 7.5, 1.4 Hz, 1H), 7.56 (td, J = 7.6, 1.3 Hz, 1H), 7.4 (dd, J = 7.6, 1.0 Hz, 1H), 5.86 (s, 2H), 3.91 (s, 3H); ^{13}C NMR (125 MHz, CDCl$_3$) δ 166.8, 133.3, 133.2, 131.8, 130.8, 130.4, 130.2, 77.7, 52.6; IR (film) 3024, 2960, 1714, 1569, 1429, 1377, 1285, 1086 cm^{-1}; HRMS (CI) calcd for C$_9$H$_9$O$_2$ [M-NO$_2$]$^+$, m/z = 149.0602; found 149.0597.
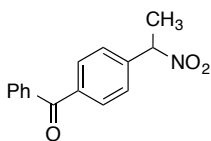
(4-(1-Nitroethyl)phenyl)(phenyl)methanone (2.13)

In a glovebox, an oven-dried vial was charged with Pd$_2$dba$_3$ (11.4 mg, 0.0125 mmol), XPhos (14.3 mg, 0.030 mmol), K$_3$PO$_4$ (127 mg, 0.60 mmol), and 4-bromobenzophenone (130.6 mg, 0.50 mmol). The vial was sealed with a teflon cap, removed from the glovebox, and 1,4-dioxane (2.5 mL) was added, followed by nitroethane (360 μL, 5.0 mmol). The mixture was heated to 70 °C with vigorous stirring for 4 h, then cooled to rt, diluted with CH$_2$Cl$_2$ (15 mL), and washed with 1 M aq HCl (15 mL), which was then extracted with CH$_2$Cl$_2$ (3 x 15 mL). The combined organics were dried over Na$_2$SO$_4$, filtered, and concentrated *in vacuo*. Purification by chromatography (10% EtOAc/Hex) afforded the title compound as a yellow oil (125.2 mg, 98%): ^{1}H NMR (500 MHz, CDCl$_3$) δ 7.84 (d, J = 8.3 Hz, 2H), 7.80 (m, 2H), 7.62 (t, J = 7.6 Hz, 1H), 7.59 (d, J = 8.4 Hz, 2H), 7.50 (t, J = 7.7 Hz, 2H), 5.71 (q, J = 7.0 Hz, 1H), 1.95 (d, J = 6.9 Hz, 3H); ^{13}C NMR (125 MHz, CDCl$_3$) δ 196.0, 139.5, 139.1, 137.3, 133.0, 130.8, 130.2, 128.6, 127.6, 85.9, 19.7; IR (film) 3058, 2927, 1654, 1546, 1446, 1276, 924 cm^{-1}; HRMS (ESI) calcd for C$_{15}$H$_{14}$O [M+H-NO$_2$]$^+$, m/z = 210.1045; found 210.1041.

Representative Procedure for the Attempted Hydrolytic Nef Reaction (Scheme 2.12):

Arylnitromethane (0.050 mmol) and base (0.10 mmol) were added to a 1-dram vial, followed by 200 μL of stock solution of solvent and mesitylene (internal standard, 0.050 mmol). The vial was capped, stirred at rt for 1.25 h, and then cooled to 0 °C. The appropriate acid (≥10 equiv) was added in one portion, and the reaction was allowed to warm to rt and stir for an addition 30 minutes, after which the vial was quenched with

500 µL EtOAc. An aliquot of the crude mixture was analyzed by GC to determine conversions.

Representative Procedure for the KMnO4 Oxidative Nef Reaction (Table 2.4**):**

A solution of arylnitromethane **2.06r** (135 mg, 0.70 mmol) in MeOH (4 mL) was cooled to 0 °C, and a solution of KOH (118 mg, 2.1 mmol) in MeOH (3 mL) was then added dropwise. After stirring the resulting mixture for 30 min at 0 °C, a solution of $KMnO_4$ (55 mg, 0.35 mmol) and $MgSO_4$ (253 mg, 2.1 mmol) in H_2O (7 mL) was added dropwise to the reaction. After 20 min, the mixture was poured into CH_2Cl_2 (20 mL) and conc aq $NaHSO_4$ (~0.2 mL) was added until the aqueous layer became colorless. The aqueous layer was extracted with CH_2Cl_2 (2 x 20 mL), and the combined organics were dried over Na_2SO_4, filtered, and concentrated. Aldehyde:oxidative dimer ratios were obtained from analysis of the crude ^{1}H NMR.

General Procedure D - Sn(II)-Mediated Nef Reaction of Arylnitromethanes:

A flame-dried 10 mL flask was charged with anhydrous $SnCl_2$ (71 mg, 0.375 mmol) and MeCN (1 mL), followed by a solution of thiophenol (115 µL, 1.12 mmol), Et_3N (174 µL, 1.25 mmol), and MeCN (0.5 mL). The resulting yellow solution was cooled to 0 °C, and the arylnitromethane (0.25 mmol) was added as a solution in MeCN (1 mL). After complete conversion to the oxime (10 min unless otherwise indicated), the solvent was removed and 95% EtOH (1 mL) was added. A slurry of $SnCl_2 \cdot 2H_2O$ (68 mg, 0.30 mmol),

L-(+)-tartaric acid (188 mg, 1.25 mmol), and $NaHCO_3$ (105 mg, 1.25 mmol) in H_2O (1 mL) was added, followed by $NaHSO_3$ (130 mg, 1.25 mmol). The resulting slurry was stirred vigorously at 40 °C for 18 h unless otherwise indicated. After cooling to rt and quenching with cold 2 N HCl (5 mL), the mixture was neutralized with saturated aq $NaHCO_3$ and extracted with CH_2Cl_2 (3 x 20 mL). The pH was raised to ~10 with 1 N NaOH, and the aqueous potion extracted with CH_2Cl_2 (20 mL). The combined organic extracts were dried over Na_2SO_4, filtered, and concentrated *in vacuo*. The resulting residue was purified by chromatography to afford the pure aldehyde. Spectroscopic data for all compounds matched literature values[105] and/or authentic samples.
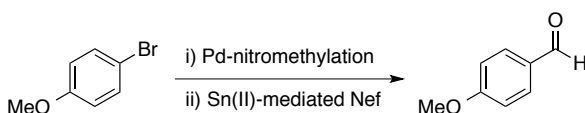
One-Pot Conversion of 2.05a to 2.08a (Scheme 2.16):

General Procedure A was followed, using 4-bromoanisole (60.2 μL, 0.5 mmoL). After 18 h at 50 °C, the reaction was cooled, and the solvent was removed. MeCN (2.5 mL) was added, and the reaction was cooled to 0 °C. A separate vial was charged with $SnCl_2$ (142 mg, 0.75 mmol), MeCN (2.5 mL), Et_3N (348 μL, 2.5 mmol), thiophenol (230 μL, 2.25 mmol). The resulting yellow slurry was cooled to 0 °C and added to the cooled crude arylnitromethane. After stirring for 1 h at 0 °C, the solvent was removed and 95% EtOH (2 mL) was added. A slurry of $SnCl_2 \cdot 2H_2O$ (136 mg, 0.60 mmol), L-(+)-tartaric acid (376 mg, 2.5 mmol), NaHCO3 (210 mg, 2.5 mmol), and H_2O (2 mL) was added to the crude oxime, followed by $NaHSO_3$ (260 mg, 2.5 mmol). The resulting slurry was

---

105) M. Pouchart, C. J. *The Alrich Library of NMR Spectra,* 2nd ed.; Aldrich Chemical Company: Milwaukee, WI, 1983; Vol. 2.

stirred vigorously at 40 °C for 17 h. After cooling to rt and quenching with cold 2 N HCl

(10 mL), the mixture was neutralized with saturated aq NaHCO$_3$ and extracted with

CH$_2$Cl$_2$ (3 x 25 mL). The pH was raised to ~10 with 1 N NaOH, and the aqueous potion

extracted with CH$_2$Cl$_2$ (25 mL). The combined organic extracts were dried over Na$_2$SO$_4$,

filtered, and concentrated *in vacuo*. The resulting residue was purified by

chromatography (5% to 10% EtOAc/Hexanes) to afford 4-anisaldehyde as a colorless

liquid (48.5 mg, 71%). All spectral data are in agreement with literature values.[105]
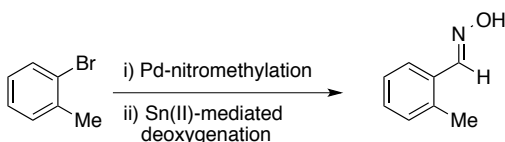
One-Pot Conversion of 2.05i to 2.012i (Scheme 2.16**):**

General Procedure A was followed, using 2-bromotoluene (60.2 μL, 0.5 mmol). After 18

h at 50 °C, the reaction was cooled, and the solvent was removed. MeCN (2.5 mL) was

added, and the reaction cooled to 0 °C. A separate vial was charged with SnCl$_2$ (142 mg,

0.75 mmol), MeCN (2.5 mL), Et$_3$N (348 μL, 2.5 mmol), thiophenol (230 μL, 2.25

mmol). The resulting yellow slurry was cooled to 0 °C and added to the cooled crude

arylnitromethane. After stirring for 30 min at 0 °C, the reaction was warmed to rt and

stirred an additional 1 h. The crude mixture was poured into saturated aq NH$_4$Cl (25

mL), and extracted with CH$_2$Cl$_2$ (3 x 25 mL). The combined organics were dried over

Na$_2$SO$_4$, filtered, and concentrated *in vacuo*. The resulting residue was purified by

chromatography (5% to 10% EtOAc/Hexanes) to afford (*E*)-2-methylbenzaldehyde

oxime as a white crystalline solid (49.7 mg, 74%): mp: 46-47 °C. All spectral data are in

agreement with literature values.[106]

Nitroethylation of Vinyl Halides
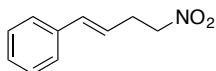
(*E*)-(4-nitrobut-1-en-1-yl)benzene (2.16)

In a glovebox, an oven-dried microwave vial was charged with Cs_2CO_3 (179 mg, 0.55

mmol), powdered 3 Å molecular sieves (50 mg), Pd_2dba_3 (11.4 mg, 0.0125 mmol), and

XPhos (14.3 mg, 0.03 mmol). Nitromethane (2.5 mL) was added, followed by addition

of β-bromostyrene (32 μL, 0.25 mmol). The vial was capped, removed from the

glovebox, and heated to 60 °C in an IKA heating plate with vigorous stirring. After 16 h,

the reaction mixture was allowed to cool to rt, diluted with CH_2Cl_2 (10 mL), and washed

with saturated aq NH_4Cl (2 x 10 mL). The aqueous layer was extracted with CH_2Cl_2 (2

x 10 mL). The combined organic layers were washed with brine, dried over Na_2SO_4,

filtered, and concentrated *in vacuo*. The resulting residue was purified by

chromatography (5% EtOAc/Hex) to afford the title compound as a colorless oil (24.1

mg, 54%): ^1H NMR (500 MHz, CDCl$_3$) δ 7.31-7.38 (m, 4H), 7.25-7.28 (m, 1H), 6.54 (d,

J = 15.8 Hz, 1H), 6.13 (dt, *J* = 15.9, 7.1 Hz, 1H), 4.51 (t, *J* = 7.0 Hz, 2H), 2.92 (ddt, *J* =

---

106) Di Nunno, L.; Vitale, P.; Scilimati, A. "Effect of the aryl group substituent in the dimerization of 3-arylisoxazoles to *syn* 2,6-diaryl-3,7-diazatricyclo[4.2.0.0^{2,5}]octan-4,8-diones induced by LDA" *Tetrahedron* **2008**, *64*, 11198-11204.

7.0, 7.0, 1.3 Hz, 2H); ^{13}C NMR (125 MHz, CDCl$_3$) δ 136.7, 134.3, 128.8, 128.0, 126.5, 123.1, 75.2, 31.0. All spectral data are in agreement with literature values.[107]
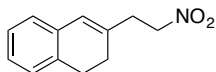
3-(2-nitroethyl)-1,2-dihydronaphthalene (2.22)

In a glovebox, an oven-dried microwave vial was charged with Cs$_2$CO$_3$ (195 mg, 0.60 mmol), Pd$_2$dba$_3$ (11.4 mg, 0.0125 mmol), and XPhos (14.3 mg, 0.03 mmol). Nitromethane (2.5 mL) was added, followed by addition of vinyl bromide **2.21** (52 mg, 0.25 mmol). The vial was capped, removed from the glovebox, and heated to 60 °C in an IKA heating plate with vigorous stirring. After 2 h, the reaction mixture was allowed to cool to rt, diluted with CH$_2$Cl$_2$ (10 mL), and washed with 1 M HCl (10 mL). The aqueous layer was extracted with CH$_2$Cl$_2$ (2 x 10 mL), and the combined organic layers were dried over Na$_2$SO$_4$, filtered, and concentrated *in vacuo*. The resulting residue was purified by chromatography (4% EtOAc/Hex) to afford the title compound as a yellow oil (28.3 mg, 56%): ^{1}H NMR (500 MHz, CDCl$_3$) δ 7.09-7.18 (m, 3H), 7.00 (m, 1H), 6.31 (s, 1H), 4.58 (t, J = 7.2 Hz, 2H), 2.92 (t, J = 7.1 Hz, 2H), 2.85 (t, J = 8.2 Hz, 2H), 2.30 (t, J = 8.2 Hz, 2H); ^{13}C NMR (125 MHz, CDCl$_3$) δ 134.9, 134.5, 133.9, 127.5, 127.3, 126.8, 126.2, 125.7, 74.1, 35.2, 28.1, 27.1; IR (film) 3016, 2925, 2830, 1550, 1376 cm^{-1}; HRMS (CI) calcd for C$_{12}$H$_{13}$NO$_2$ [M]$^+$, m/z = 203.0946; found 203.0945.

---

107) Marsh, G. P.; Parson, P. J.; McCarthy, C.; Coniquet, X. G. "An Efficient Synthesis of Nitroalkenes by Alkene Cross Metathesis: Facile Access to Small Ring Systems" *Org. Lett.* **2007**, *9*, 2613-2616.

Allyl nitro **2.18** (47 mg, 0.25 mmol) was subjected to the identical procedure using 1.2

equiv Cs_2CO_3 (98 mg, 0.30 mmol) with 2 h reaction time. Purification afforded still

impure title compound as a yellow oil (7.2 mg, <14%).
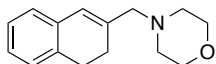
4-((3,4-dihydronaphthalen-2-yl)methyl)morpholine (2.23)

In a glovebox, an oven-dried vial was charged with Pd_2dba_3 (11.4 mg, 0.0125 mmol),

XPhos (14.3 mg, 0.030 mmol), and **2.18** (47 mg, 0.25 mmol). The vial was sealed with a

teflon cap, removed from the glovebox, and 1,4-dioxane (1.25 mL), and freshly distilled

morpholine (44 µL, 0.50 mmol) were added. The vial was then heated to 50 °C with

vigorous stirring for 3 d, then cooled to rt. The crude mixture was diluted with CH_2Cl_2

(15 mL), and washed with sat aq $NaHCO_3$ (15 mL). The aqueous later was then

extracted with CH_2Cl_2 (2 x 15 mL). The combined organics were dried over Na_2SO_4,

filtered, and concentrated *in vacuo*. The resulting residue was purified by

chromatography (10% to 40% EtOAc/Hex) to afford still impure title compound as a

yellow oil (21.0 mg, 37%): ^{1}H NMR (500 MHz, $CDCl_3$: δ 7.10-7.17 (m, 3H), 6.99-7.04

(m, 1H), 6.38 (s, 1H), 3.73 (t, J = 4.5 Hz, 4H), 3.07 (s, 2H), 2.83 (t, J = 8.1 Hz, 2H), 2.43-

2.48 (m, 4H), 2.35 (t, J = 8.2 Hz, 2H); ^{13}C NMR (125 MHz, $CDCl_3$) δ 138.2, 135.3,

134.5, 127.5, 126.9, 126.6, 126.0, 125.6, 67.3, 65.4, 54.0, 28.3, 26.1; HRMS (ESI) calcd

for $C_{15}H_{20}NO$ $[M+H]^+$, *m/z* = 230.1545; found 230.1552.

Part II. QUANTIFICATION OF ELECTROPHILE LUMO-LOWERING via COLORIMETRIC PROBES

3. QUANTIFICATION OF ELECTROPHILIC ACTIVATION BY HYDROGEN-BONDING CATALYSTS[108]

3.1. Background

3.1.1. Organocatalysis via Hydrogen-Bond Activation of Electrophiles

In 1985, pioneering efforts from Hine and coworkers described the effectiveness of 1,8-biphenylenediol **3.01** as a catalyst in the nucleophilic addition of diethylamine to phenyl glycidyl ether (Scheme 3.1).[109] The enhanced activity of **3.01** in comparison to phenol was attributed to donation of two hydrogen-bonds to the epoxide electrophile, supported by 1:1 catalyst-substrate crystallographic structures.[110] Further work by Kelly and coworkers identified modified bisphenol **3.02**, possessing acidifying and solubilizing groups, as a catalyst for the Diels Alder reaction.[111] Spurred by observations that substituted *N,N'*-diarylureas readily formed cocrystals with various Lewis bases,[112] Curran and Kuo reported in 1994 the first examples of these compounds as effective

108) (a) Huynh, P. N. H.; Walvoord, R. R.; Kozlowski, M. C. "Rapid Quantification of the Activating Effects of Hydrogen-Bonding Catalysts with a Colorimetric Sensor" *J. Am. Chem. Soc.* **2012**, *134*, 15621-15623. (b) Walvoord, R. R.; Huynh, P. N. H.; Kozlowski, M. C. *manuscript in preparation.*
109) (a) Hine, J.; Linden, S.-M.; Kanagasabapathy, V. M. "1,8-Biphenylenediol is a Double-Hydrogen-Bonding Catalyst for Reaction of an Epoxide with a Nucleophile" *J. Am. Chem. Soc.* **1985**, *107*, 1082-1083. (b) Hine, J.; Linden, S.-M.; Kanagasabapathy, V. M. "Double-Hydrogen-Bonding Catalysis of the Reaction of Phenyl Glycidyl Ether with Diethylamine by 1,8-Biphenylenediol" *J. Org. Chem.* **1985**, *50*, 5096-5097.
110) Hine, J.; Ahn, K.; Gallucci, J. C.; Linden, S.-M. "1,8-Biphenylenediol Forms Two Strong Hydrogen Bonds to the Same Oxygen Atom" *J. Am. Chem. Soc.* **1984**, *106*, 7980-7981.
111) Kelly, T. R.; Meghani, P.; Ekkundi, V. S. "Diels-Alder Reactions: Rate Acceleration Promoted by a Biphenylenediol" *Tetrahedron Lett.* **1990**, *31*, 3381-3384.
112) Etter, M. C.; Urbanczyk-Kipkowska, Z.; Zia-Ebrahimi, M.; Panunto, T. W. "Hydrogen Bond Directed Cocrystallization and Molecular Recognition Properties of Diarylureas" *J. Am. Chem. Soc.* **1990**, *112*, 8415-8426.

catalysts, including the Claisen rearrangement of simple allyl vinyl ethers.[113] These early efforts, among others, set the foundation for the application of small organic molecules containing hydrogen-bond donor arrays as catalysts.

Scheme 3.1 Early reports of hydrogen-bonding catalysis.

Hine - 1985

catalyst	k_{rel}
phenol	1
3.01	12

Kelly - 1990

mol % **3.02**	yield
0	3
40	90

Curran - 1995

k_{rel} = 5.0
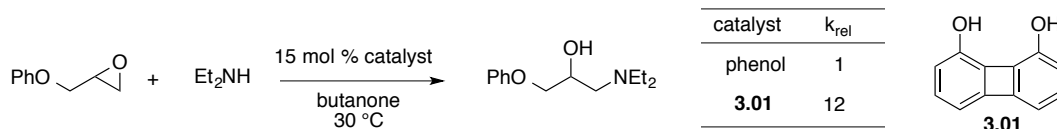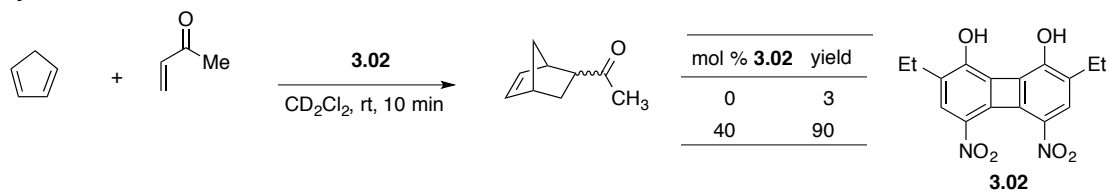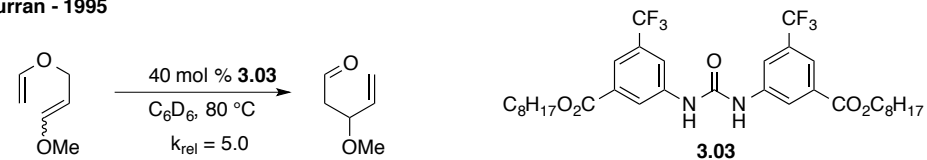
Around the turn of the century, chemists began to harness this mode of activation using chiral organocatalysts to effect asymmetric transformations. Seminal examples include the discovery of a thiourea-based catalyst for the asymmetric Strecker reaction by Jacobsen and Sigman,[114] and the use of a weakly acidic chiral diol for the asymmetric hetero-Diels Alder reaction by Rawal (Scheme 3.2).[115] Further innovation was introduced by Takemoto, who found that the introduction of a tertiary amine onto a thiourea skeleton afforded a bifunctional organocatalysts effective for the addition of

113) (a) Curran, D. P.; Kuo, L. H. "Altering the Stereochemistry of Allylation Reactions of Cyclic α-Sulfinyl Radicals with Diarylureas" *J. Org. Chem.* **1994**, *59*, 3259-3261. (b) Curran, D. P.; Kuo, L. H. "Acceleration of a Dipolar Claisen Rearrangement by Hydrogen Bonding to a Soluble Diaryl Urea" *Tetrahedron Letters* **1995**, *36*, 6647-6650.

114) Sigman, M. S.; Jacobsen, E. N. "Schiff Base Catalysts for the Asymmetric Strecker Reaction Identified and Optimized from Parallel Synthetic Libraries" *J. Am. Chem. Soc.* **1998**, *120*, 4901-4902.

115) Huang, Y.; Unni, A.K.; Thadani, A. N.; Rawal, V. H. "Single enantiomers from a chiral-alcohol catalyst" *Nature* **2003**, *424*, 146.

malonates into nitroalkenes.[7]   Since these early examples, the arena of hydrogen-bond

catalysis has seen tremendous activity over the past 15 years.[116] This intensive research

has yielded numerous catalyst structures as well as reactions for which they are effective.

Moreover, certain "privileged" catalyst motifs, including urea, thiourea, guanidine,

amidine, and squaramide-based compounds, which show more general application, have

been identified and investigated.

Scheme 3.2 Seminal examples of asymmetric hydrogen-bonding catalysis.

---
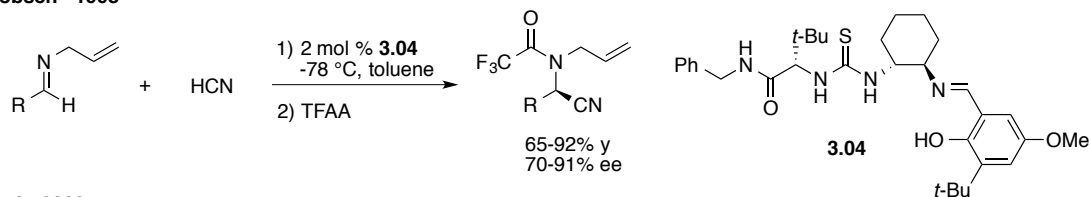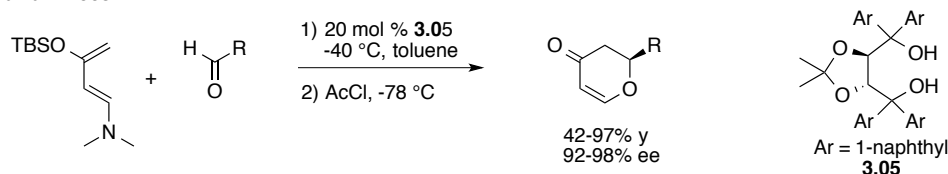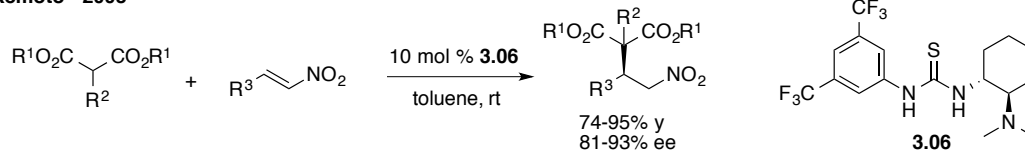
116) For select reviews, see: (a) Taylor, M. S.; Jacobsen, E. N. "Asymmetric Catalysis by Chiral Hydrogen-Bond Donors" *Angew. Chem. Int. Ed.* **2006**, *45*, 1520-1543. (b) Doyle, A. G.; Jacobsen, E. N. "Small-Molecule H-Bond Donors in Asymmetric Catalysis" *Chem. Rev.* **2007**, *107*, 5713-5743. (c) Akiyama, T. "Stronger Brønsted Acids" *Chem. Rev.* **2007**, *107*, 5744-5758. (d) Akiyama, T.; Itoh, J.; Fuchibe, K. "Recent Progress in Chiral Brønsted Acid Catalysis" *Adv. Synth. Catal.* **2006**, *348*, 999-1010. (e) Connon, S. J. "The Design of Novel, Synthetically Useful (Thio)urea-Based Organocatalysts" *Synlett* **2009**, 354-376. (f) Sohtome, Y.; Nagasawa, K. "The Design of Chiral Double Hydrogen Bonding Networks and Their Applications to Catalytic Asymmetric Carbon-Carbon and Carbon-Oxygen Bond-Forming Reactions" *Synlett* **2010**, 1-22. (g) Aleman, J.; Parra, A.; Jiang, H.; Jørgensen, K. A. "Squaramides: Bridging from Molecular Recognition to Bifunctional Organocatalysis" *Chem. Eur. J.* **2011**, *17*, 6890-6899 (h) Schenker, S.; Zamfir, A.; Freund, M.; Tsogoeva, S. B. "Developments in Chiral Binaphthyl-Derived Brønsted/Lewis Acids and Hydrogen-Bond-Donor Organocatalysis" *Eur. J. Org. Chem.* **2011**, 2209-2222. (i) Auvil, T. J.; Schafer, A. G.; Mattson, A. E. "Design Strategies for Enhanced Hydrogen-Bond Donor Catalysts" *Eur. J. Org. Chem.* **2014**, 2633-2646

In both hydrogen-bonding and more traditional, metal-based (i.e. Lewis acid) catalysis, the primary interaction responsible for rate enhancement is interaction of the catalyst with the electrophile. The resulting stabilization of the LUMO consequently lowers the activation energy of the reaction. In contrast with Lewis acids, hydrogen-bond catalysis more closely resembles Nature's use of noncovalent and electrostatic interactions to lower transition state energies, as seen in enzymes.[117] Accordingly, organocatalysis by hydrogen-bonding offers the potential for high catalyst tunability and substrate specificity. Additional advantages over Lewis acid catalysis include the lesser likelihood of signficant product inhibition and the avoidance of potentially toxic metal waste.

3.1.2. Current Approaches for Predicting Hydrogen-Bond Strengths

Metrics for gauging Lewis acid strength include the Fukuzumi parameters,[118] Irving-Williams order,[119] NMR-based measurements,[120] among others. In contrast, such predictive scales remain limited for estimation of hydrogen-bond strengths, and reports of new catalysts and reactions are fast outpacing the understanding of the specific interactions responsible for catalyst activity. The absence of comprehensive rate data for

117) Schreiner, P. R. "Metal-free organocatalysis through explicit hydrogen bonding interactions" *Chem. Soc. Rev.* **2003**, *32*, 289-296.
118) (a) Fukuzumi, S.; Ohkubo, K. "Quantitative Evaluation of Lewis Acidity of Metal Ions Derived from the *g* Values of ESR Spectra of Superoxide: Metal Ion Complexes in Relation to the Promoting Effects in Electron Transfer Reactions" *Chem. Eur. J.* **2000**, *6*, 4532-4535. (b) Fukuzumi, S.; Ohkubo, K. "Fluorescence of Maxima of 10-Methylacridone–Metal Ion Salt Complexes: A Convenient and Quantitative Measure of Lewis Acidity of Metal Ion Salts" *J. Am. Chem. Soc.* **2002**, *124*, 10270-10271.
119) (a) Irving, H.; Williams, R. J. P. "Order of Stability of Metal Complexes" *Nature*, **1948**, *162*, 746-747. (b) Irving, H.; Williams, R. J. P. "The Stability of Transition-metal Complexes" *J. Chem. Soc.* **1953**, 3192-3210.
120) (a) Deters, J. F.; McCusker, P. A.; Pilger, Jr., R. C. "A Scale of Relative Lewis Acidities from Proton Magnetic Resonance Data" *J. Am. Chem. Soc.* **1968**, *90*, 4583-4585. (b) Hilt, G.; Puenner, F.; Moebus, J.; Naseri, V.; Bohn, M. A. "A Lewis Acidity Scale in Relation to Rate Constants of Lewis Acid Catalyzed Organic Reactions" *Eur. J. Org. Chem.* **2011**, 5962-5966, and references therein.

a range of catalysts in different reactions further complicates identification of controlling factors in catalyst performance. Perhaps the most widely applied parameter for estimating hydrogen-bonding capacity is acidity. More specifically, the ΔpK_a of the donor-acceptor has been reported to provide an accurate measurement a hydrogen bond.[121] This prediction largely mirrors general acid catalysis; by the Brønsted catalysis law, the rate is directly proportional to ionization constant.[122] However, inferring catalyst strength from pK_a values ignores important secondary interactions of the catalyst to the substrate, including sterics, dual/tri-activation (multiple donor arrays), binding geometry, as well as catalyst aggregation.[8,123] Consequently, rational design of hydrogen-bond catalysts is largely reliant on systematic trial and error to achieve optimal reactivity and selectivity, despite the identification of several privileged, core structural motifs (e.g. thiourea). A recent method for asymmetric iodolactonization by Jacobsen and coworkers is shown in Scheme 3.3 and highlights the need for empirical screening.[124] In this instance, the inability to predict the superior activity of the urea vs the thiourea is striking espciall as thioureas are expected to be more reactive due to their $\sim 10^5$ *greater* acidity compared to ureas. The development of an accurate and predictive metric for gauging hydrogen-bond strengths would be a substantial contribution to the field. Such a metric

121) Gilli, P.; Pretto, L.; Bertolasi, V.; Gilli, G. "Predicting Hydrogen-Bond Strengths from Acid–Base Molecular Properties. The pK_a Slide Rule: Toward the Solution of a Long-Lasting Problem" *Acc. Chem. Res.* **2009**, *42*, 33-44.
122) Carey, F. A.; Sundberg, R. J. *Advanced Organic Chemistry*, *Part A: Structure and Mechanisms*, 5th ed.; Springer: New York, 2007; 348-354.
123) (a) Tuerkmen, Y. E.; Rawal, V. H. "Exploring the Potential of Diarylacetylenediols as Hydrogen Bonding Catalysts" *J. Org. Chem.* **2013**, *78*, 8340-8353. (b) Shokri, A.; Wang, Y.; O'Doherty, G. A.; Wang, X.-B.; Kass, S. R. "Hydrogen-Bond Networks: Strengths of Different Types of Hydrogen Bonds and An Alternative to the Low Barrier Hydrogen-Bond Proposal" *J. Am. Chem. Soc.* **2013**, *135*, 17919-17924. (c) Beletskiy, E. V.; Schmidt, J.; Wang, X.-B.; Kass, S. R. "Three Hydrogen Bond Donor Catalysts: Oxyanion Hole Mimics and Transition State Analogues" *J. Am. Chem. Soc.* **2012**, *134*, 18534-18537.
124) Veitch, G. E.; Jacobsen, E. N. "Tertiary Aminourea-Catalyzed Enantioselective Iodolactonization" *Angew. Chem. Int. Ed.* **2010**, *49*, 7332-7335.

would aid not only in catalyst design and appropriate catalyst selection for a desired transformation, but also in fundamental understanding of structure-activity relationships and mechanisms in systems with hydrogen-bonding catalysts.

Scheme 3.3 Asymmetric iodolactonization with urea versus thiourea catalysts.
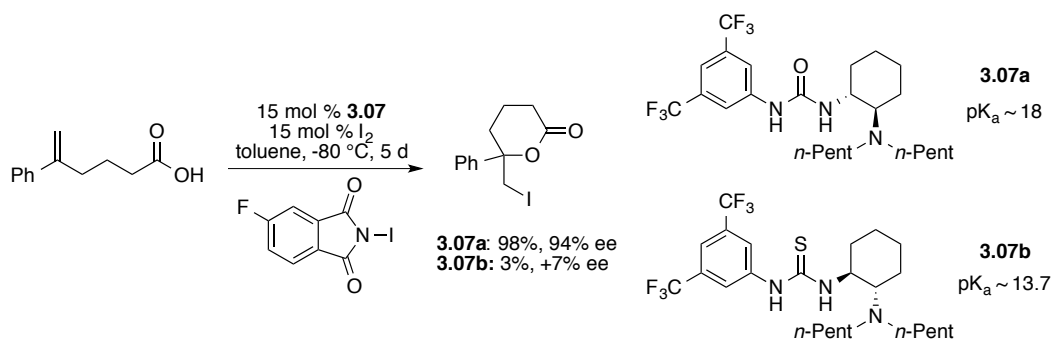
One of the main obstacles in generating such a metric is the extensive range of hydrogen bond energies (0.2 to 40 kcal/mol).[125] In particular, accurate detection of the lower register of these interactions is problematic for commonly applied spectroscopic techniques, such as NMR.[126] Indeed, initial efforts by Phuong Huynh of the Kozlowski group indicated ^{1}H NMR to be too insensitive to measure the interaction of a weak donor with an arbitrary carbonyl acceptor. At this juncture, an alternate approach was postulated, in which the sensitivity of UV-Vis spectroscopy might be employed to detect these weaker interactions. Specifically, the use of a chromophore possessing a suitable hydrogen-bonding acceptor, such as a carbonyl, was proposed to provide a measurable change in absorption spectrum upon binding with various donor molecules (Figure 3.1).

---

125) Steiner, T. "The Hydrogen Bond in the Solid State" *Angew. Chem. Int. Ed.* **2002**, *41*, 48-76.
126) For an example of detecting hydrogen bonding with a stronger thiourea catalyst, see: Lippert, K. M.; Hof, K.; Gerbit, D.; Ley, D.; Hausmann, H.; Guenther, S.; Schreiner, P. R. *Eur. J. Org. Chem.* **2012**, 5919-5927.
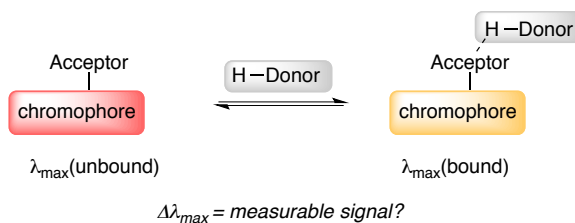
Figure 3.1 Proposed detection of hydrogen-bonding via a colorimetric sensor.

A survey of the literature for chromophores bearing a hydrogen-bond acceptor moiety revealed pyrazinone **3.08** as a potential candidate with which to test this hypothesis. This compound possesses a vinylogous amide as the acceptor with relatively minimal steric encumbrance around the carbonyl. Previous investigations led by Hirano and coworkers showed that **3.08** to exhibits solvatochromism. The particularly large changes in absorption maxima in protic versus aprotic media were encouraging for the sensitivity of the compound to hydrogen-bonding.[127] Additionally, solutions of this compound displayed significant color changes upon exposure to a limited number of Lewis Acids.[128] These prior findings pointed towards **3.08** as a potential chromophore for the UV-Vis detection of hydrogen-bonding (Scheme 3.4).

127) (a) Nakai, S.; Yasui, M.; Nakazato, M.; Iwasaki, F.; Maki, S.; Niwa, H.; Ohashi, M.; Hirano, T. "Fundamental Studies on the Structures and Spectroscopic Properties of Imidazo[1,2-*a*]pyrazin-3(7*H*)-one Derivatibes" *Bull Chem. Soc. Jpn.* **2003**, *76*, 2361-2387. (b) Takamuki, Y.; Maki, S.; Niwa, H.; Ikeda, H.; Hirano, T. "Substituent Effects on the Solvatochromism of 2-Phenylimidazopyrazinones: Effective Control of the Color Variation Range and Sensitivity toward an Indication of the Proton-donor Ability of Solvents by an Electron-withdrawing Group Substitution" *Chem. Lett.* **2004**, *33*, 1484-1485. (c) Takamuki, Y.; Maki, S.; Niwa, H.; Ikeda, H.; Hirano, T. "Substituent effects on the spectroscopic properties of solvatochromic 2-phenylimidazo[1,2-*a*]pyrazin-3(7*H*)-ones: an effective control for the colorimetric sensor properties" *Tetrahedron* **2005**, *61*, 10073-10080.

128) Sekiguchi, T.; Maki, S.; Niwa, H.; Ikeda, H.; Hirano, T. "Metal-ion complexation of imidazo[1,2-*a*]pyrazin-3(7*H*)-ones: continuous changes in absorption spectra of complexes depending on the Lewis acidity of the metal ion" *Tetrahedron Lett.* **2004**, *45*, 1065-1069.

Scheme 3.4 Proposed method for the detection of hydrogen bonding to **3.08**.

3.08
λ_{max}(unbound)

$\Delta\lambda_{max}$ observed upon binding?

3.08–HD
λ_{max}(bound)
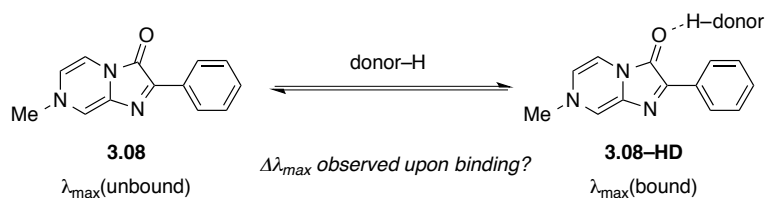
3.2. Detection of UV-Vis Perturbations via a Colorimetric Hydrogen-Bond Acceptor

Pyrazinone **3.08** was readily synthesized via condensation/cyclization of diphenylglyoxal **3.10** with pyrazine **3.09** and subsequent *N*-methylation (Scheme 3.5).[129] This route was not optimized, as only small amounts of **3.08** were needed. In the solid state, this compound exists as a bright red powder.

Scheme 3.5 Synthesis of pyrazininone chromophore **3.08**.

3.09 **3.10** 49% **3.11** 54% **3.08**

$\lambda_{max}(CH_2Cl_2) = 499$ nm
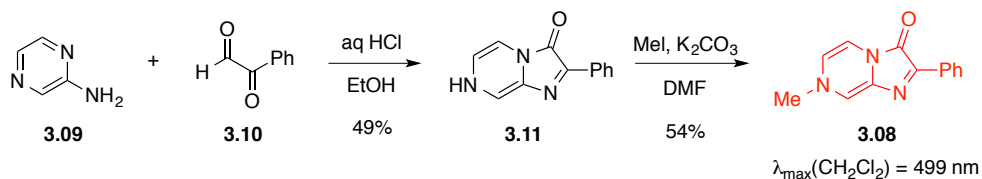
Gratifyingly, treatment of a solution of **3.08** in dichloromethane with known hydrogen-bond catalysts yielded visible color shifts of the solution (Figure 3.2), which could be monitored by UV-Vis spectroscopy. For example, incremental addition of bisamidinium **3.23** to a solution of **3.08** ([**3.08**] = 2.22 x 10^{-5} M) yielded a strong hypsochromic (blue) shift from λ_{max} = 499 nm to 465 nm upon saturation of the chromophore, as shown in Figure 3.3. This catalyst is highly active in the Claisen

129) Barlin, G. B.; Brown, D. J.; Kadunc, Z.; Petric, A.; Stanovnik, B.; Tiler, M. "Imidazo[1,2-*b*]pyridines and an Imidazo[1,2-*a*]pyrazine from Pyridazin- and Pyrazin-amines" *Aust. J. Chem.* **1983**, *36*, 1215-1220.

rearrangement, and may be presumed to be a stronger binder. Similar behavior was observed upon treatment with *N,N'*-diphenylthiourea (**3.12**), anticipated to be a relatively weak catalyst, although the color change in maximum wavelength upon catalyst saturation ($\Delta\lambda_{max}$) was significantly less (490 nm endpoint). These results validate the absorbance maximum of **3.08** as a measurable signal for the detection of hydrogen-bonding interactions.

| 3.08 | 3.08•3.12 | 3.08•3.23 |
| λ_{max} = 498.6 nm | λ_{max} = 490.0 nm | λ_{max} = 464.6 nm |
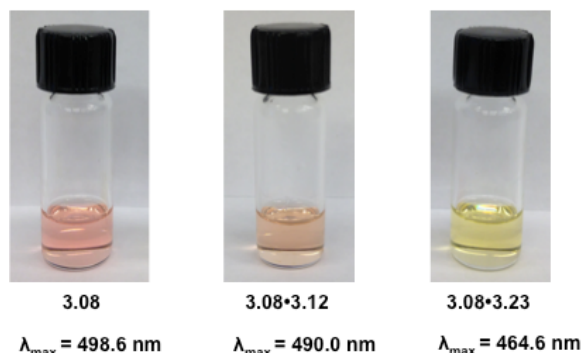
Figure 3.2 Visible color change of **3.08** upon saturation with catalysts **3.12** or **3.23**.
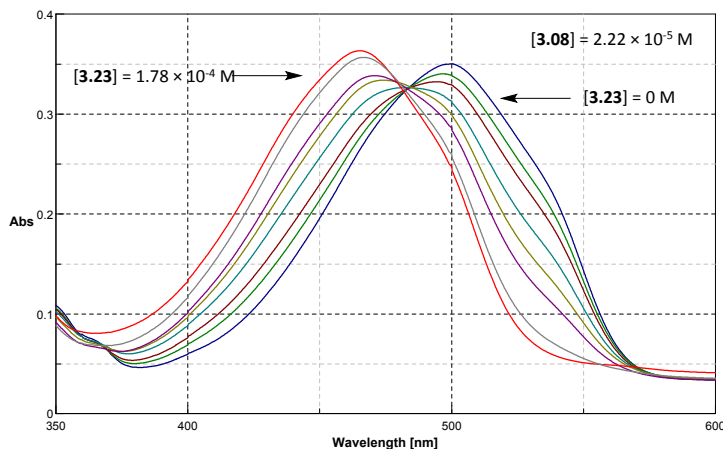
Figure 3.3 UV-titration of sensor **3.08** with increasing amounts of catalyst **3.23**.

DFT molecular orbital calculations were conducted on bound and unbound sensor **3.08** to better understand the observed change in electronic transition energy with donor

molecules.[130] The resulting HOMO-LUMO gap (lowest energy transition) energies from B3LYP/6-31(d) optimized structures are presented in Table 3.1. The calculated HOMO-LUMO gap for the free sensor closely matched the value experimentally determined for solutions in dichloromethane (cf. λ_{max} = 487 nm calculated, 499 nm experimental). More importantly, the calculations indicate that upon complexing with a hydrogen-bond donor, the energy of the HOMO-LUMO gap *increases*, thus corroborating the empirically observed hypsochromic shifts. Analysis of the magnitude of maximum wavelength shift suggests that lower λ_{max} values (i.e. larger HOMO-LUMO gap) are predicted for binders of ostensibly greater strength (e.g. phenol vs proton).

Table 3.1 Calculated HOMO–LUMO energies for bound and unbound **3.08** complexes.

binder	HOMO (eV)	LUMO (eV)	HOMO – LUMO (eV)	calculated λ_{max} (nm)
-	-4.23	-1.68	2.55	487
phenol	-5.11	-2.18	2.92	425
benzoic acid	-5.08	-2.02	3.05	407
BF_3	-5.77	-2.59	3.28	390
proton	-9.43	-6.08	3.35	370

Considering the empirical and computational results above, an energy diagram describing the interaction of pyrazinone **3.08** with hydrogen-bond donors is proposed in Figure 3.4. The lowest energy transition of the sensor may be attributed to the n to π* electronic transition, ΔE_1, and corresponds to the measured λ_{max}. Upon binding to a donor molecule, the ground state is stabilized to a greater extent compared to the excited state, i.e. $\Delta E_3 > \Delta E_2$. This resultant increase in energy ($\Delta\Delta E$) accounts for the observed hypsochromic shift of the bound sensor. For comparison, a representative energy

---

diagram for a reaction proceeding through LUMO-lowering (electrophile activation) catalysis is also presented. Here, catalyst binding activates the system through LUMO stabilization (ΔE_a), whereas the HOMO of the nucleophile, which does not bind the catalyst, is unaffected. Notably, this analysis would change if the nucleophile interacts with the hydrogen-bonding catalysts, as is the case in dual activation.[131] For the studies here, nucleophiles were selected (e.g. cyclopentadiene) that would not interact with the catalysts.

Validation of the UV-Vis sensor measurements as indicative of hydrogen-bonding capacity would occur if $\Delta E_3 - \Delta E_2$ is proportional to ΔE_a. In other words, is the change in wavelength maximum of the bound sensor•catalyst complex proportional to the rate enhancement afforded by the catalyst in hydrogen-bond mediated reactions?
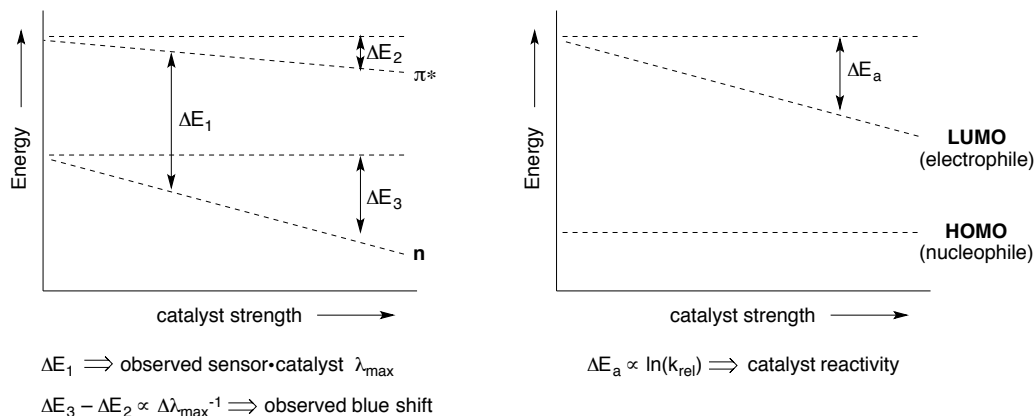
Figure 3.4 Proposed energy diagrams for catalyst interactions with sensor **3.08** and electrophiles.

131) Walsh, P. W.; Kozlowski, M. C. Fundamentals of Asymmetric Catalysis; University Science Books: Sausalito, CA, 2009.

3.3. Correlation of Sensor Wavelength Shift with Catalyst Binding and Other Physical Organic Parameters

3.3.1. Correlation of Sensor Wavelength Shift with Catalyst Binding Equilibrium

As illustrated in Figure X (UV trace of bisamidinium), addition of a hydrogen-bond donor to solution of **3.08** afforded titration-like behavior, with a continual wavelength shift until saturation of the sensor molecule with binder. The lack of two distinct peaks indicates rapid equilibrium of the bound and unbound form on the timescale of the measurement. Consequently, plots of λ_{max} versus concentration of catalyst (or catalyst equivalents) can be used to determine the binding constant (K_{eq}) of the catalyst to the sensor. A representative plot using bisamidinium catalyst **3.23** is shown in Figure 3.5.
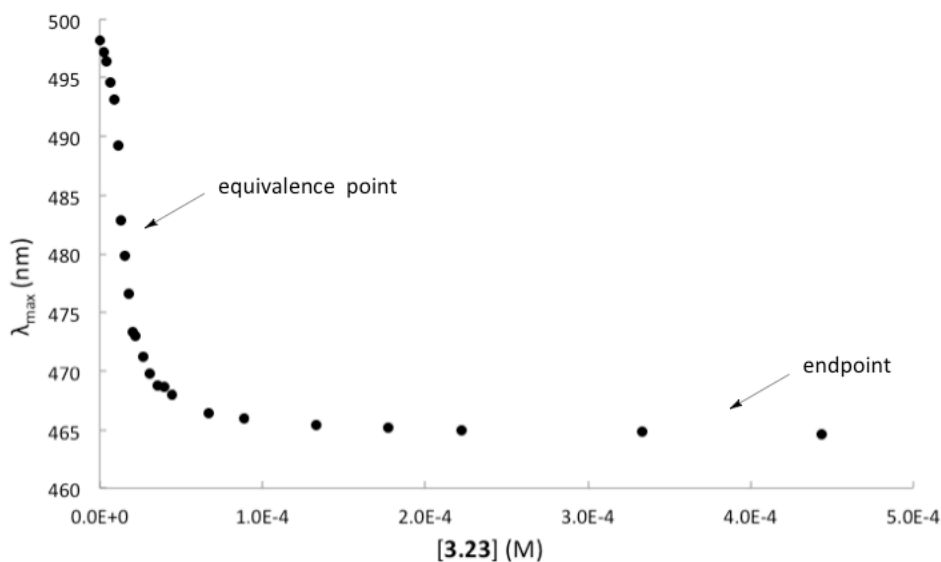
Figure 3.5 UV-titration curve of sensor **3.08** in CH_2Cl_2 with catalyst **3.23**.

The binding constant for the general equilibrium in Scheme 3.6 can be solved using the concentration of added catalyst at the equivalence point. Since, by definition,

concentrations of bound and unbound sensor are equal at the equivalence point, equation

1 simplifies to equation 2. The concentration of free catalyst, [catalyst]$_{eq}$, is equal to the

total concentration of catalyst minus the concentration bound to the sensor, which, at the

equivalence point, is half the concentration of total sensor.

Scheme 3.6 Sensor titration with a binder (catalyst).
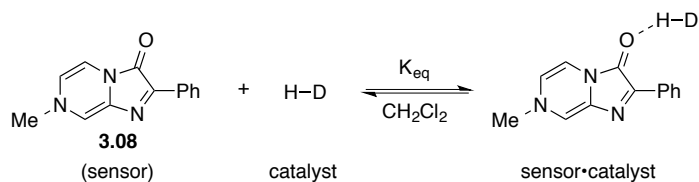
$$K_{eq} = \frac{[\text{sensor}\bullet\text{catalyst}]_{eq}}{[\text{sensor}]_{eq}\,[\text{catalyst}]_{eq}} \qquad \text{eq (1)}$$

$$K_{eq} = \frac{1}{[\text{catalyst}]_{eq}} \qquad \text{eq (2)}$$

$$[\text{catalyst}]_{eq} = [\text{catalyst}]_{total} - 0.5\,[\text{sensor}]_{total} \qquad \text{eq (3)}$$

Titrations of **3.08** in dichloromethane ([**3.08**] = 2.22 x 10^{-5} M) were conducted

using a wide array of 33 known hydrogen-bond donors, including several popular parent

scaffolds, such as thiourea, squaramide, amidinium, and silanol-based catalysts (Table

3.2). The corresponding binding constants and saturation wavelength shifts were

calculated. Notably, a broad range of blue shifts were observed for the various catalysts,

ranging from ~490 to 465 nm ($\Delta\lambda_{max}$ of 9-34 nm). In general, catalysts that produced

larger blue shifts also exhibited higher binding constants with the sensor molecule.

Indeed, good correlation was observed between the inverse $\Delta\lambda_{max}$ shift and $\ln(K_{eq})$

(Figure 3.6). It is worth nothing that this plot has values for both axes that are linearly

proportional to energy: $\Delta\lambda^{-1}$ to ΔE of sensor electronic absorption and $\ln(K_{eq})$ to ΔG of

sensor•catalyst formation. Importantly, the observed correlation reveals the sensor wavelength shift as an accurate, general indicator of binding affinity of various hydrogen-bond donors to the sensor molecule.

Table 3.2 Chart of hydrogen-bonding catalysts analyzed with sensor **3.08**. Saturated λ_{max} values (nm) are in parentheses.

3.12 (490.0) **3.13** (484.0) **3.14** (479.8) **3.15** (477.0)

3.16 (482.2) **3.17** (480.4) **3.18** (479.6) **3.19** (479.8)

3.20 (474.4) **3.21** (473.2) **3.22** (480) **3.23** (464.6)

3.24 (473.0) **3.25** (469.8) **3.26** (484.2) **3.27** (475.0) **3.28** (486.2) **3.29** (485.4) **3.30** (482.6)

Ar = 3,5-(CF$_3$)$_2$C$_6$H$_3$

3.31 (480.0) **3.32** (478.0) **3.33** (477.2) **3.34** (470.0) **3.35** (480.0)

3.36 (486.6) **3.37** (486.2) **3.38** (484.0) **3.39** (481.0)

3.40 (480.8) **3.41** (490.8) **3.42** (490.4) **3.43** (487.2) **3.44** (495.2)
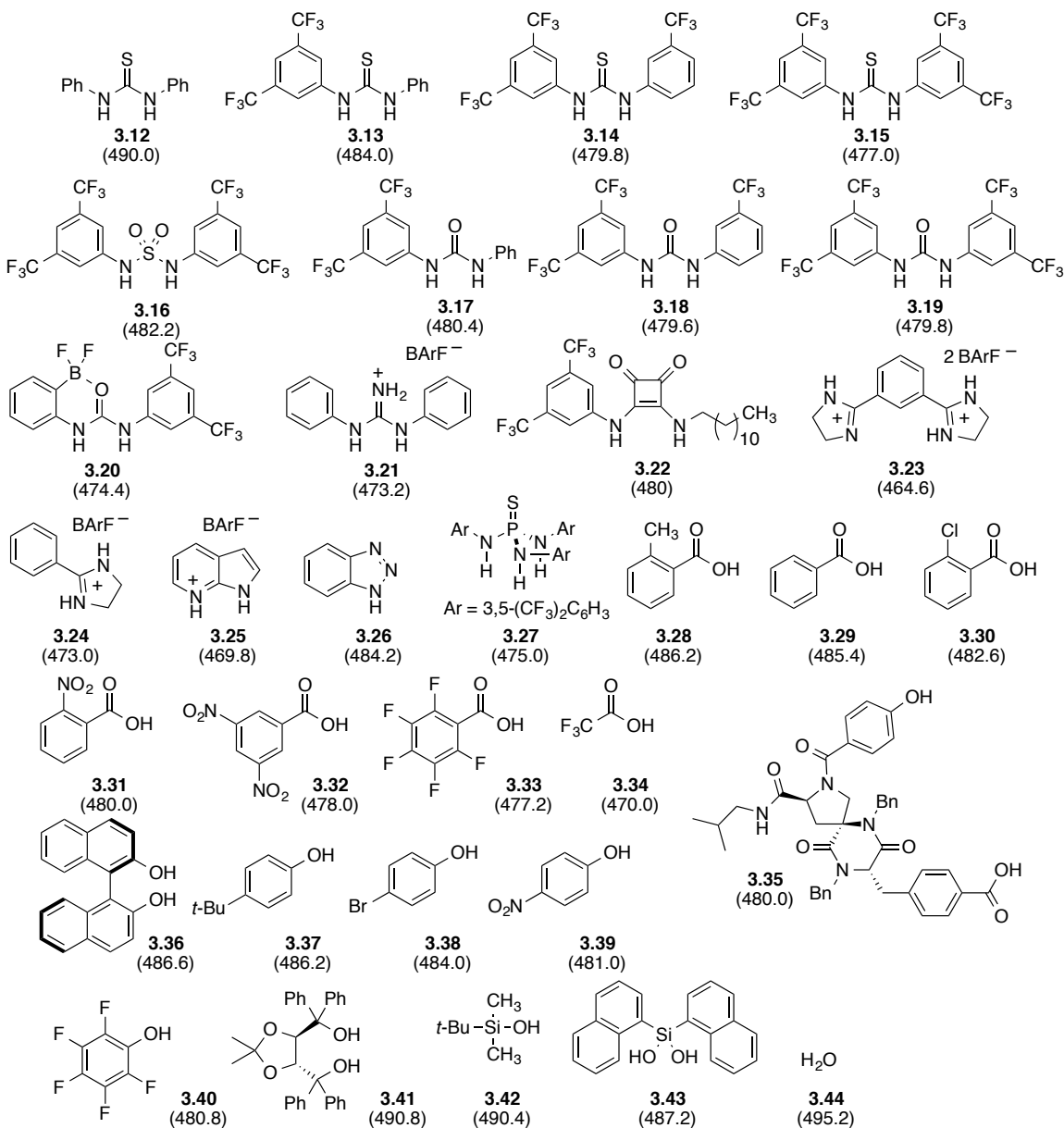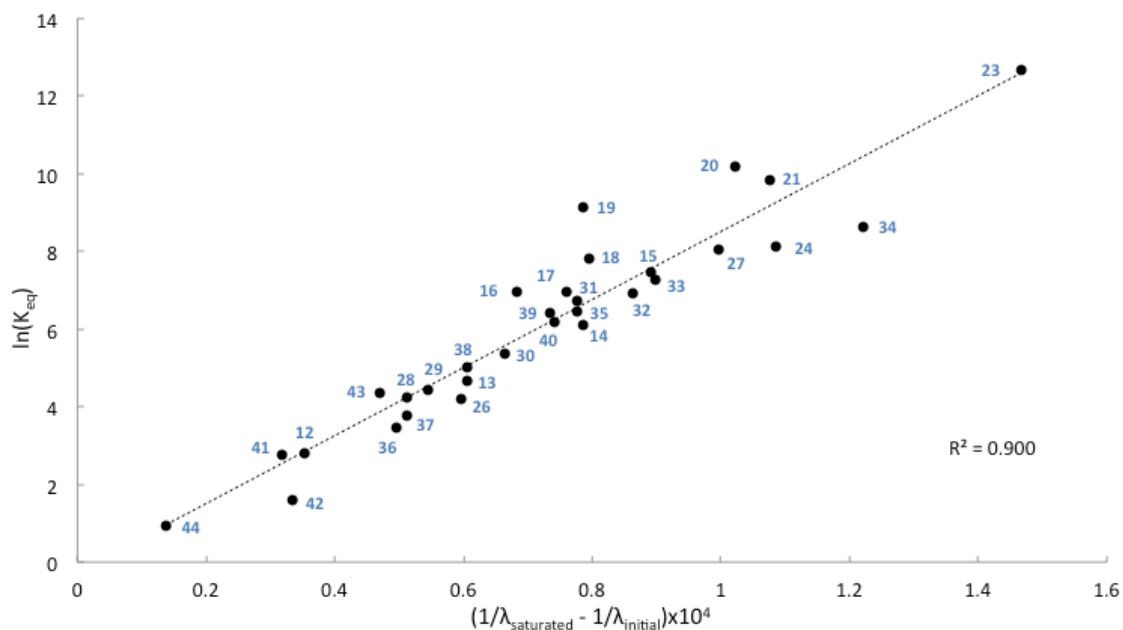
Figure 3.6 Correlation between wavelength shift and sensor•catalyst binding equilibrium constant. Catalyst chapter number prefixes have been removed for clarity (e.g. 23 refers to catalyst **3.23**).

Having verified the $\Delta\lambda_{max}$ metric as indicative of binding strength to the colorimetric sensor **3.08**, these values were assessed for the structures in Table 3.2 in the context of catalyst reactivity. Several observations are noteworthy. Despite recent studies showing good activity, silanol-based catalysts (3.42 and 3.42) exhibited very weak shifts. The increased shift of silanediol **3.43** relative to **3.42** is of note, mirroring the increased reactivity of this scaffold in comparison to related mono-silanols as reported by the Mattson[132] and Franz groups.[133] Similarly, diol-based **3.41** (TADDOL) possesses one of the smallest sensor signals. Benzoic acids and phenols spanned the intermediate range of binders, with electronic effects of aromatic substitution distinctly

132) (a) Schafer, A. G.; Wieting, J. M.; Mattson, A. E. "Silanediols: A New Class of Hydrogen Bond Donor Catalysts" *Org. Lett.* **2011**, *13*, 5228-5231. (b) Schafer, A. G.; Wieting, J. M.; Fisher, T. J.; Mattson, A. E. "Chiral Silanediols in Anion-Binding Catalysis" *Angew. Chem. Int. Ed.* **2013**, *52*, 11321-11324.
133) Tran, N. T.; Wilson, S. O.; Franz, A. K. "Cooperative Hydrogen-Bonding Effects in Silanediol Catalysis" *Org. Lett.* **2012**, *14* 186-189.

contributing to the resulting measurement. These moieties are not commonly incorporated as the critical donor component in more recent organocatalysts. However, Schafmeister and coworkers have very recently detailed the use of elegantly designed "spiroligozyme" compound **3.35** as an effective ketosteroid isomerase mimic.[134] The combination of phenolic and benzoic acid donors are carefully arranged to undergo dual-activation of a sp^3-hybridized oxygen, demonstrated by catalysis of an aromatic Claisen rearrangement. *N,N'*-Diarylureas and thioureas yielded a large range of shifts, with additional trifluoromethyl substituents correlating to greater binding. Those possessing the common 3,5-bis(trifluoromethyl) group, such as in Schreiner's catalyst **3.15**, proved among the strongest binders, reflecting the widespread incorporation of this binding structure in current organocatalysts.[135] Internally-activated BF$_2$-urea **3.20**, was the strongest binder among the (thio)ureas, which aligns very well with experimental reactivity data reported by Mattson and coworkers.[136] It is worth noting here that while the correlation of wavelength shift and binding constant was maintained for thioureas, clear deviations were observed for the weaker urea compounds **3.17-3.19**. For these cases, wavelength shift remains fairly constant, although binding constants increase as expected with greater trifluoromethyl substitution, and K$_{eq}$ may be a more accurate

134) Parker, M. F. L.; Osuna, S.; Bollot, G.; Vaddypally, S.; Zdilla, M. J.; Houk, K. N.; Schafmeister, C. E. "Acceleration of an Aromatic Claisen Rearrangement via a Designed Spiroligozyme Catalyst that Mimics the Ketosteroid Isomerase Catalytic Dyad" *J. Am. Chem. Soc.* **2014**, *136*, 3817-3827.

135) Connon, S. J. "Organocatalysis Mediated by (Thio)urea Derivatives" *Chem. Eur. J.* **2006**, *12*, 5418-5427.

136) (a) So, S. S.; Burkett, J. A.; Mattson, A. E. "Internal Lewis Acid Assisted Hydrogen Bond Donor Catalysis" *Org. Lett.* **2011**, *13*, 716-719. (b) So, S. S.; Auvil, T. J.; Garza, V. J.; Mattson, A. E. "Boronate Urea Activation of Nitrocyclopropane Carboxylates" *Org. Lett.* **2012**, *14*, 444-447. (c) Hardman, A. M.; So, S. S.; Mattson, A. E. "Urea-catalyzed Construction of Oxazinanes " *Org. Biomol. Chem.* **2013**, *11*, 5793-5797.

metric.[137] Finally, formally cationic catalysts, including amidiniums **3.23** and **3.24**, guanidinium **3.21**, and Takenaka's azaindolium catalyst **3.25**,[138] exhibited the largest wavelength shifts ($\Delta\lambda_{max}$ = 26-34 nm) and binding constants. One of the strongest binders interestingly proved to be thiophosphoramide **3.27**, which contains a pocket of three potential N–H donors. Despite apparently high binding capability, this structure has seen very limited use in the context of hydrogen-bonding catalysis,[139] ostensibly due to limited potential in asymmetric transformations.[140] Squaramide catalysts, possessing a dual N–H donor array, have found great utility as hydrogen-bond donors.[116g, 141] However, these compounds are routinely employed as heterogeneous catalysts, owing to their limited solubility in common organic solvents. Representative squaramide catalyst **3.22**, possessing the common *N*-bis(trifluoromethyl)aryl and *N'*-alkyl substitution was

---

137) Although the increased self-association of ureas compared to thioureas is well known, such a scenario would also be anticipated to affect binding constant with the sensor. Full explanation for the deviation of sensor shifts with weak ureas remains under investigation.

138) Takenaka, N.; Sarangthem, R. S.; Seerla, S. K. "2-Aminopyridinium Ions Activate Nitroalkenes through Hydrogen Bonding" *Org. Lett.* **2007**, *9*, 2819-2822.

139) (a) Rodriguez, A. A.; Yoo, H.; Ziller, J. W.; Shea, K. J. "New architectures in hydrogen bond catalysis" *Tetrahedron Lett.* **2009**, *50*, 6830-6833. (b) Borovika, A.; Tang, P.-I.; Klapman, S.; Nagorny, P. "Thiophosphoramide-Based Cooperative Catalysts for Bønsted Acid Promoted Ionic Diels–Alder Reactions" *Angew. Chem. Int. Ed.* **2013**, *52*, 13424-13428. (c) Cranwell, P.B.; Hiscock, J. R.; Haynes, C. J. E.; Light, M. E.; Wells, N. J., Gale, P. A. "Anion recognition and transport properties of sulfamide-, phosphoric triamide- and thiophosphoric triamide-based receptors" *Chem. Commun.* **2013**, *49*, 874-879.

140) The use of a chiral thiophosphorodiamide catalyst for asymmetric addition of naphthoquinonnes into nitrostyrenes has been reported: Wu, R.; Chang, X.; Lu, A.; Wang, Y.; Wu, G.; Song, H.; Zhou, Z.; Tang, C. "Chiral (thio)phosphorodiamides as excellent hydrogen bond donor catalysts in the asymmetric Michael addition of 2-hydroxy-1,4-naphthoquinone to nitroolefins" *Chem. Commun.* **2011**, *47*, 5034-5036.

141) Seminal examples: (a) Malerich, J. P.; Hagihara, K.; Rawal, V. H. "Chiral Squaramide Derivatives are Excellent Hydrogen Bond Donor Catalysts" *J. Am. Chem. Soc.* **2008**, *130*, 14416-14417. (b) Zhu, Y.; Malerich, J. P.; Rawal, V. H. "Squaramide-Catalyzed Enantioselective Michael Addition of Diphenyl Phosphite to Nitroalkenes" *Angew. Chem. Int. Ed.* **2010**, *49*, 153-156.

synthesized from dimethyl squarate and, although largely insoluble in dichloromethane, exhibited an apparent λ_{max} endpoint of ~480 nm with the sensor.[142]

The experimental ease with which the catalyst wavelength shfts are obtained greatly enhances the convenience of the method.   It is unnecessary to obtain multiple measurements for a titration curve since the endpoint wavelength shifts can be employed. Due to the weak affinity of water to the sensor ($\Delta\lambda_{max}$ ~4 nm), special precautions to exclude moisture are unnecessary. As illustrated in Scheme 3.5, colorimetric sensor **3.08** is readily prepared in two steps from commercial materials, and only microgram quantities are needed for individual titrations. Similarly, only small amounts (< 10 mg) of catalyst are necessary for sensor saturation, with exception of only the weakest of binders. These factors make the use of the sensor an attractive predictive metric with which to test new catalysts, especially compared to empirical rate measurements, which are typically more technically challenging, time-consuming, and require additional reagents.

In order to probe the binding stoichiometry of the putative catalyst•sensor adduct, the method of continuous variation (Job's method) was applied to sensor **3.08** and bisamidinium catalyst **3.23**. Such alternate binding stoichiometries were particularly in question for **3.23**, owing to its high K_{eq} and four equivalent N–H donors. The resulting Job plot is shown in Figure 3.7 and reveals a 1:1 binding stoichiometry for this system. Significantly, this result rules out alternative binding modes, including coordination of one catalyst to multiple sensor molecules.

---

142) See Experimental Section for squaramide synthesis and Appendix D for titration data. Due to the insolubility of **3.22**, an accurate binding constant value could not be determined.
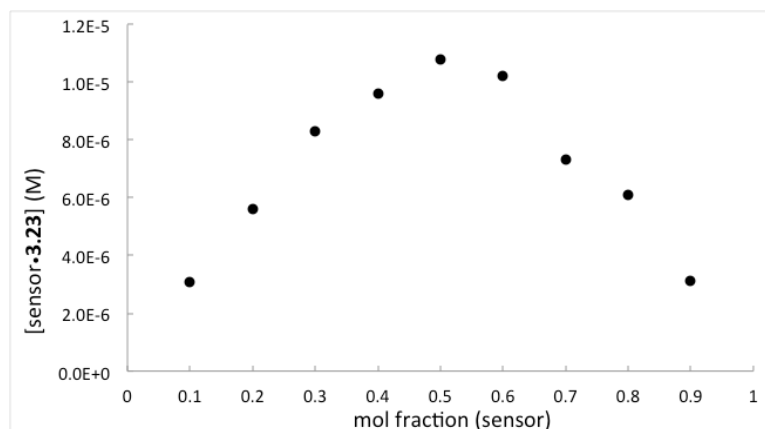
Figure 3.7 Job plot analysis of catalyst **3.23** with sensor **3.08**.

3.3.2. Analysis of Wavelength Shifts with Hammett and Acidity Parameters

The electronic modulation of arenes based on substitution has been thoroughly studied, resulting in the well-known Hammett parameters. Consequently, substituted phenols and benzoic acids offer convenient platforms to investigate the effects of electronic perturbations of the hydrogen-bond catalysts on the sensor wavelength shift. As shown in Table 3.2, a series of *para*-substituted phenols and *ortho*-substituted benzoic acids were tested with the sensor in dichloromethane. *para*-Benzoic acids were not studied due to their limited solubility. A cursory analysis of the resulting λ_{max} values clearly suggests that the sensor signal is indeed sensitive to electronic effects from aryl substituents. Moreover, a plot of the Hammett sigma constants for the arene substitutents against the inverse wavelength shift shows a quantitative correlation (Figure 3.8). To better account for *ortho*-effects, the σ_i^o parameter developed by Pytela and Liska was employed for comparison with the benzoic acid series.[143] For both sets of structures, excellent linear relationships are observed. These plots provide a convincing argument

---

143) Pytela, O.; Liska, J. "Chemometrical Analysis of Substituent Effects. V. *ortho* Effect" *Collect. Czech. Chem. Commmun.* **1994**, *59*, 2005-2021.

that the sensor absorption is particularly sensitive to the electronic nature of the binder, i.e. electronic perturbations of a catalyst structure will be accurately reflected in the λ_{max} of the sensor•catalyst complex.
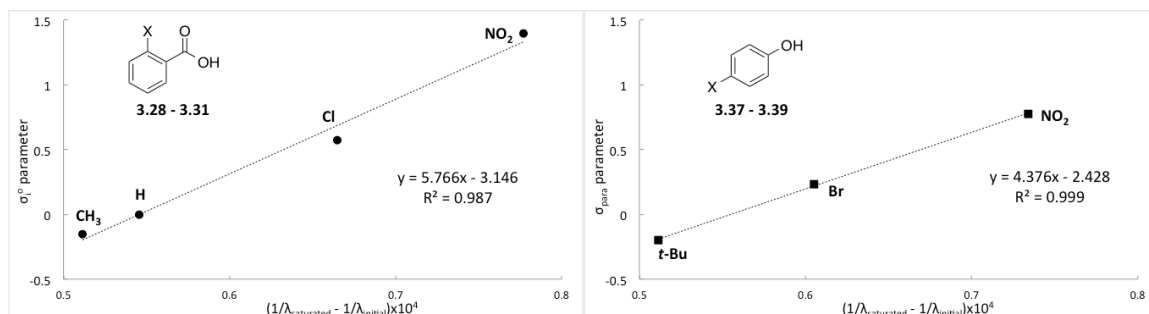
Figure 3.8 Correlation of Hammett σ parameters for *o*-benzoic acids and *p*-phenols with sensor•catalyst wavelength shifts.

An interesting corollary of this analysis is whether the sensor signal correlates with acidity values. The resulting plot comparing pK_a values with sensor wavelength shift for a series of benzoic acids, phenols, and thioureas is shown in Figure 3.9. Distinct linear correlations for acidity and wavelength shift are observed *within catalyst subtypes*, and hold for pK_a values in both water and DMSO. Interestingly, the relationships do not hold across catalysts of different parent structures, such as phenols vs benzoic acids, for example. The deviation observed for perfluorinated compound **3.40** from other phenols may be partially attributed to increased sterics around the donating O–H group. The lack of a general correlation indicates that the sensor signal is not simply a function of catalyst acidity, which has been shown to be an insufficient metric for understanding hydrogen bonding strength (see Section 3.1.2.).

137
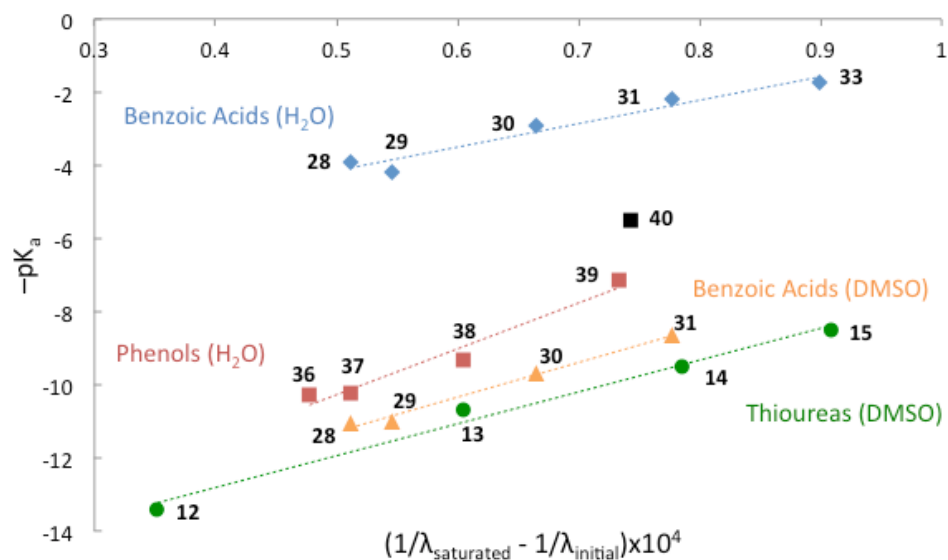
Figure 3.9 Correlation of acidity and sensor•catalyst wavelength shift within related catalyst structures. Catalyst chapter number prefixes have been removed for clarity.

The relationships discussed in this section reveal colorimetric sensor **3.08** to be a useful tool for measuring binding strength of hydrogen-bond donors, and that the observed wavelength shift is sensitive to electronic and acidity factors. However, these finding do not necessitate that the sensor is an accurate predictor for catalyst reactivity in various reactions. Specifically, alternative factors such as sterics and alternate binding geometries may predominate when the catalyst interacts with the substrate instead of the sensor.

3.4. Correlation of Sensor Wavelength Shift to Catalyzed Rate Data

3.4.1. Diels Alder

To be of general use to the community, the metric must be able to accurately predict catalyst activity. A range of reaction profiles has been identified that proceed

through electrophilic activation via hydrogen-bonding.[116] In order to best isolate reaction catalysis via hydrogen-bonding effects, an ideal reaction to study should contain only a single binding point on the electrophile. Similarly, the nucleophile should have minimal binding sites, i.e. no heteroatoms. Further desirable traits include a low background rate as well as a simple method to accurately measure the rate. The Diels Alder cycloaddition of methyl vinyl ketone (MVK) and cyclopentadiene (Cp) meets these requirements. Previous kinetic investigations of this reaction have been performed under thiourea[144] or bisphenol catalysis.[123a] Due to the structural simplicity of the reagents, catalysis occurs via hydrogen-bond donation of the catalyst to the ketone acceptor.

The hydrogen-bond catalyzed Diels Alder reaction was thus investigated under pseudo-first order conditions as illustrated in Scheme 3.7, employing catalysts varying in structure and anticipated strength. Coworker Phuong Huynh developed the reaction method and obtained the initial results. Reactions were continuously monitored by ^{1}H NMR spectroscopy by taking spectra at 5 minute intervals, and MVK concentrations were determined by comparing resonance integrations with toluene as an internal standard. All catalysts were analyzed in triplicate.

Scheme 3.7 Hydrogen-bond catalyzed Diels Alder reaction for kinetic studies.

---
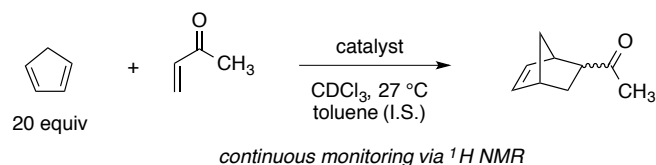
144) Wittkopp, A.; Schreiner, P. R. "Metal-Free, Noncovalent Catalysis of Diels-Alder Reactions by Neutral Hydogen Bond Donors in Organic Solvents and in Water" *Chem. Eur. J.* **2003**, *9*, 407-414.

Plotting the natural log of MVK concentration (ln[MVK]) against time provided the observed pseudo-first order rate constants k'_{obs}. The rate enhancement provided by the catalyst, normalized for catalyst loading (k_{cat}),[145] could be calculated by subtracting the background rate. Finally, the k_{rel} value provides a normalized metric for relative rate enhancement provided by the catalyst, and is a meaningful representation of catalyst strength.

$$k_{rel} = \left(\frac{k'_{obs} - k_{background}}{k_{background}} \right) N = \frac{k_{cat}}{k_{background}} \qquad \text{eq (4)}$$

Plotting the ln(k_{rel}) values against inverse wavelength shift for the tested catalysts is shown in Figure 3.10, and reveals a strong correlation. This plot again employs terms directly proportional to energy (here, the y-axis is proportional to activation energy via the Arrhenius equation). For the Diels Alder reaction, catalysts that shower greater blue shifts upon treatment with sensor **3.08** exhibit correspondingly higher reaction rates. Specifically, for the present reaction, the change in activation energy afforded by a catalyst is proportional to its change in electronic transition energy of the sensor.

145) Phuong Huynh demonstrated the Diels Alder reaction is first order in catalyst: Huynh, P. *Correlation of Reaction Rates with LUMO Lowering Ability.* M.S. Thesis, University of Pennsylvania, Philadelphia, PA, June 2012.
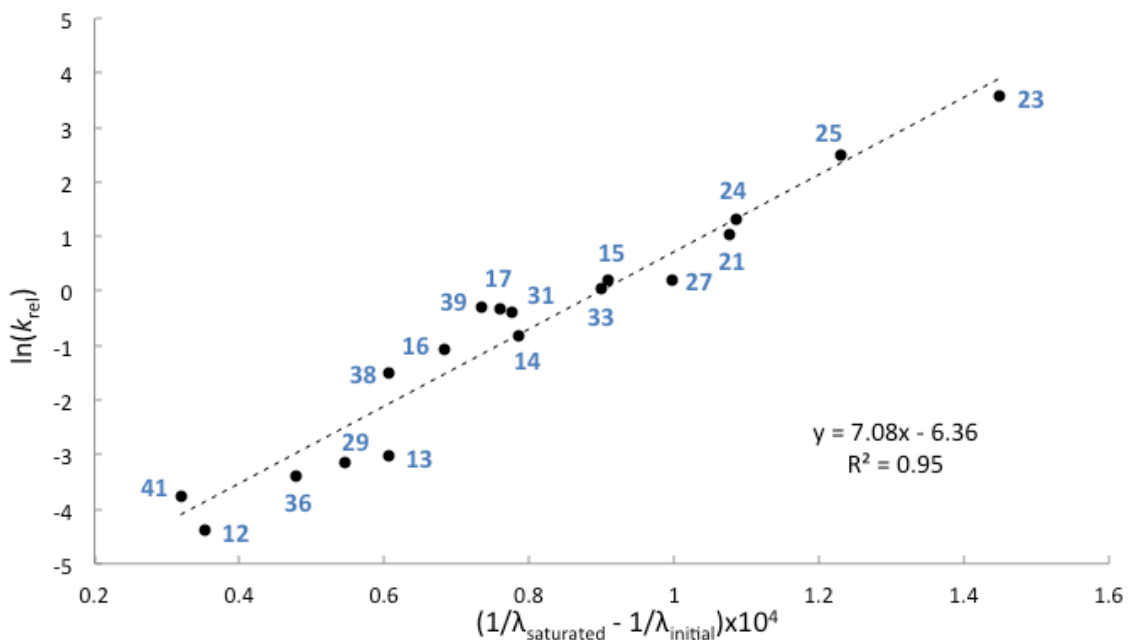
Figure 3.10 Correlation of sensor•catalyst wavelength shift and relative catalyst rate enhancement for the Diels Alder reaction shown in **Scheme 3.7**. Catalyst chapter number prefixes have been removed for clarity.

These results reveal that the sensor metric is an accurate gauge for the LUMO-lowering ability of small molecule hydrogen-bond donors in the Diels Alder reaction. The binding interactions of these catalysts with sensor closely resemble those between the catalyst and the simple carbonyl acceptor of MVK.

3.4.2. Friedel Crafts Addition with Nitroalkenes

The Friedel Crafts addition of electron-rich arenes into nitroalkenes, and β-nitrostyrenes in particular, is one of the most widely studied reactions employing hydrogen-bond catalysis and is typically used as an initial test for catalyst

activity.[123c,132a,133,136a,138,146] This reaction presents a useful platform with which to test the predictive ability of the sensor metric beyond a simple Diels Alder reaction. Notably, the carbonyl of the sensor molecule is more structurally similar to that of the ketone acceptor in MVK compared to the nitro group of a nitroalkene. Indeed, multiple reports have proposed that dual hydrogen-bond donors are capable of forming κ^2-activated intermediates. Analysis of rate data from the catalyzed Friedel Crafts addition onto nitroalkenes would address whether the carbonyl-based sensor remains valid for other acceptors (Scheme 3.8).

Scheme 3.8 Donor-acceptor binding for sensor and reaction electrophiles.

sensor carbonyl	methyl vinyl ketone	nitroalkene
$\Delta\lambda_{max}$	k_{rel} (Diels Alder)	k_{rel} (Friedel Crafts)
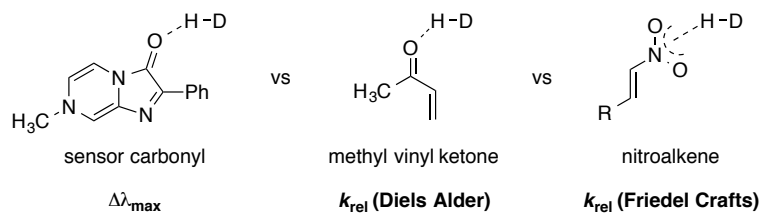
The Friedel Crafts reaction in Scheme 3.9 was elected for investigation. *N*-Methylindole (**3.45**) provides a reasonably reactive nucleophile and is not anticipated to interact with the catalysts [pK$_a$(H$_2$O) *N*-methylindolium = −1.8].[42] Similarly, substrate **3.47** should only interact via the nitro group, and is easily synthesized from Henry condensation of d_3-nitromethane with the corresponding aldehyde.

146) Fleming, E. M.; McCabe, T.; Connon, S. J. "Novel axially chiral bis-arylthiourea-based organocatalysts" *Tetrahedron Lett.* **2006**, *47*, 7037-7042.

Scheme 3.9 Hydrogen-bond catalyzed Friedel Crafts reaction for kinetic studies.
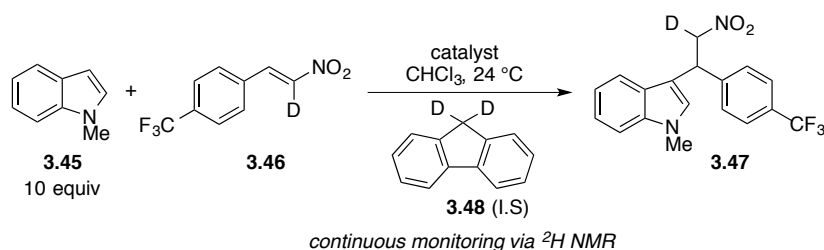
Although preliminary ^{1}H NMR studies using *proteo*-**3.46** afforded satisfactory data, the use of deuterated nitrostyrene **3.46** afforded exceptional signal isolation by ^{2}H NMR spectroscopy. Most importantly, *this method of analysis allows the investigation of any non-deuterated catalyst* without fear of catalyst signal overlapping with analyte; only starting material, internal standard (here, d_2-fluorene **3.48**), and product are observed. A representative stacked ^{2}H NMR time lapse spectrum and corresponding reaction profile using catalyst **3.23** (0.2 mol%) are shown in Figure 3.11 and Figure 3.12, respectively.
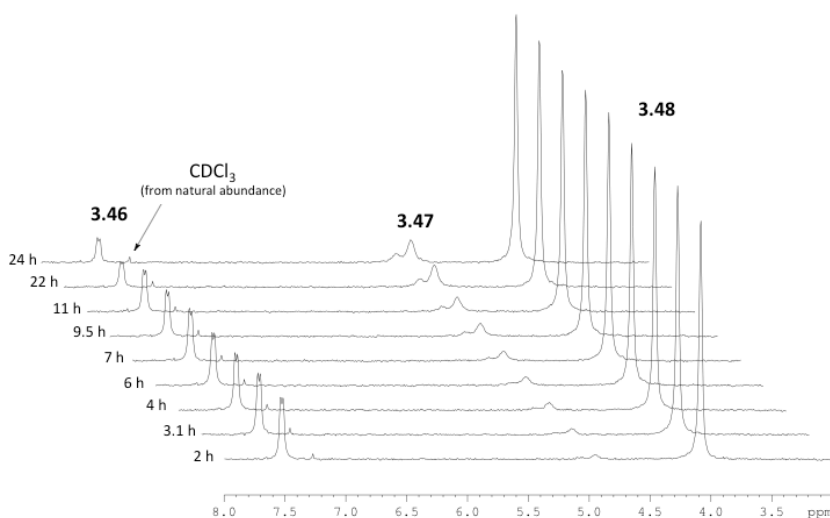
Figure 3.11 ^{2}H NMR time-lapse for the Friedel Crafts reaction catalyzed by **3.23**.

143
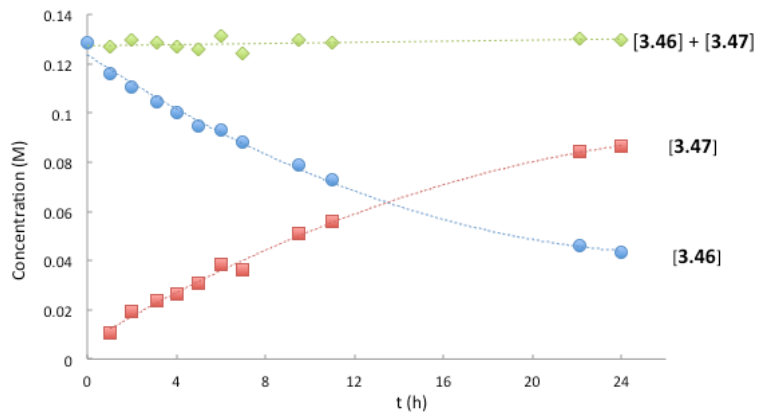
Figure 3.12 Reaction profile for the Friedel Crafts reaction catalyzed by **3.23**.

The Friedel Crafts reaction in Scheme 3.9 was thus performed under pseudo-first order conditions using an array of hydrogen-bond catalysts from Table 3.2. All catalysts were tested in duplicate, and the resulting pseudo-first order constants k'_{obs} were obtained from kinetic plots of ln[**3.46**] versus time. Separate experiments varying concentration of catalyst [**3.15**] confirmed the reaction to be first order in both catalyst and substrate. Accordingly, k_{cat} and k_{rel} values were calculated as previously described in equation 4. A plot of ln(k_{rel}) against inverse wavelength shift for catalysts in the Friedel Crafts reaction is shown in Figure 3.13.
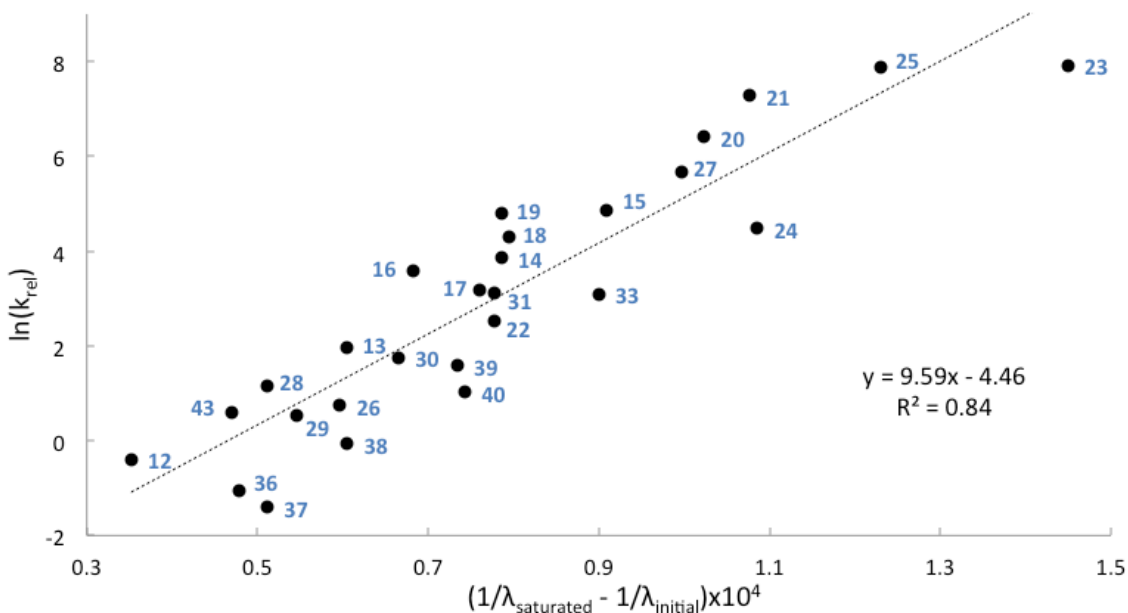
Figure 3.13 Correlation of sensor•catalyst wavelength shift and relative catalyst rate enhancement for the Friedel Crafts reaction shown in **Scheme 3.9**. Catalyst chapter number prefixes have been removed for clarity.

As observed in the Diels Alder reaction, the cationic catalysts provided the highest levels of rate enhancement, in accord with their corresponding wavelength shift with the sensor. Electron-deficient ureas and thioureas also demonstrated high reactivity. Thiophosphoramide **3.27** again proved to be among the most effective neutral catalysts. This compound, thiourea **3.15**, and sulfonamide **3.16**, and have been investigated under nearly identical reaction conditions by Shea and coworkers, and their reported k_{rel} values closely match to those found here.[139a] Interestingly, Mattson and coworkers found silanediol catalyst **3.43** to provide similar reactivity as thiourea **3.15** and urea **3.19** in the Friedel Crafts addition of indole to β-nitrostyrene.[132a] In contrast, the results here show **3.43** to be comparatively poor when using *N*-methylindole as the nucleophile. Based on these results, it may be speculated that the silanediol catalyst accelerates the reaction not

only via binding to the nitro of the electrophile, but also by interaction with the free N–H of the nucleophile.

In comparison to the Diels Alder reaction, Figure 3.13 shows a less ideal correlation between catalyst rates and sensor shifts in the Friedel Crafts reaction. A cursory analysis of these results indicates that the sensor-catalyst binding does not completely capture the different types of activation of the nitro-catalyst intermediate afforded by structurally diverse catalysts. Closer examination of the plot reveals the wavelength shift to be even more predictive of catalyst strength within catalyst groups of the same structural series (Figure 3.14). Specifically, the catalysts examined in this reaction an be placed in four general groups based on structure: benzoic acids, phenols, Y-type catalysts, and other N–H donors. The "Y-type" group consists of catalysts possessing two N–H donor groups separated by a single atom, and includes compounds such as thioureas, ureas, guanidinium **3.21**, and sulfonamide **3.16**. The other N–H donors include catalysts capable of donating only a single N–H bond (benzotriazole **3.26** or monoamidinium **3.24**) or having more than a single atom separating the donor array (as in bisamidinium **3.23** or squaramide **3.22**). Silandiol catalyst **3.43** exhibited reactivity falling in line with the benzoic acid class, potentially due to similar O–H donor geometry. Analysis of Figure 3.14 shows the inherent preference of nitroalkene towards Y-type binders. In contrast, phenols provide lower rate enhancements than other catalysts of similar strength.
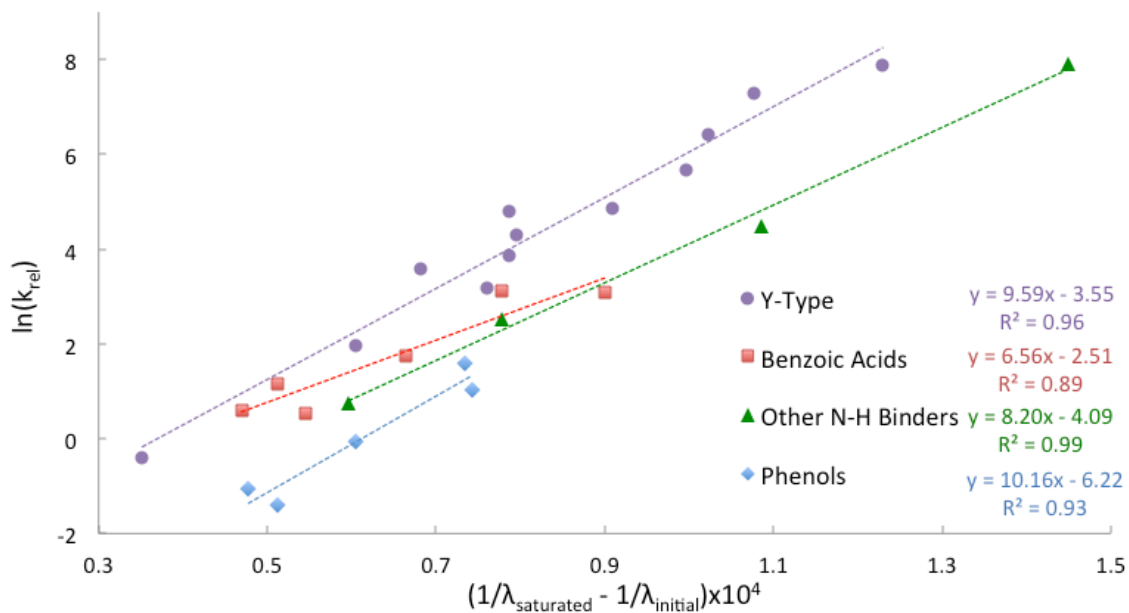
Figure 3.14 Improved correlation of sensor•catalyst wavelength shift and relative catalyst rate enhancement for the Friedel Crafts reaction based on catalyst group structure.

The experimental investigation of the hydrogen-bond catalyzed Friedel Crafts reaction indicates that interactions of the sensor carbonyl do not completely reflect those of the nitro group in the substrate. However, general trends do hold, and the wavelength shift is an accurate predictor of catalyst strength within a catalyst series. These results underline the complex nature of hydrogen-bond activation and the difficulty in making broad generalizations across different reactions. Synthesis of a colorimetric sensor containing a nitro group as the acceptor moiety is an intriguing possibility for verifying the effects of binding geometry on catalyst activity and UV shift. Such a sensor would be predicted to display λ_{max} shifts highly correlated to the Friedel Crafts rate data.

3.4.3. General Prediction of Catalyst Activity from Sensor-Catalyst Wavelength Shift

A general relationship to describe catalyst reactivity for reaction R with respect to the sensor metric ($\Delta\lambda$) is presented in equation 5. Parameter A_R represents the responsiveness of the reaction rate per unit catalyst strength, as measured by the sensor (slope). Parameter B_R represents the relative complementarity of the electrophile partner to catalyst (intercept). This equation may be further elaborated to include catalyst-group specific coefficients a_R and b_R, which may be used to account for differences in binding between the sensor and catalyst.

$$\text{Catalyst Reactivity} \propto \ln(k_{rel}) = A_R \, \Delta\lambda^{-1} + B_R \qquad \text{eq (5)}$$

$$\ln(k_{rel}) = a_R A_R \, \Delta\lambda^{-1} + b_R B_R \qquad \text{eq (6)}$$

Using the data plotted in Figure 3.10 and Figure 3.13 for the Diels Alder and Friedel Crafts reactions, parameters for both equations may be calculated (Table 3.3). All parameter values are calculated for 10 mol % catalyst (see equation 4). Comparison of the A_R parameters between the two reactions indicates that the Friedel Crafts reaction is more sensitive to catalyst strength. In other words, a particular catalyst imparts greater relative rate enhancement for this reaction as compared to the Diels Alder reaction. Since the sensor accurately models the carbonyl activation of the Diels Alder reaction (i.e. a high correlation is seen between catalyst reactivity and sensor wavelength shift), equation 5 is effective for predicting catalyzed reaction rates directly from $\Delta\lambda_{max}$ values ($a_R \approx b_R \approx$ 1). As discussed in Section *3.4.2.* the sensor-catalyst binding does not model the nitroalkene activation as accurately, and higher correlations were seen when accounting for catalyst structural series. Consequently, equations from Figure 3.14 can be used to determine a_{FC} and b_{FC} for the four catalyst subsets. The magnitudes of these coefficients

reveal effects of catalyst structure on the Friedel Crafts reaction. For example, the a_R values for Y-type and phenolic catalysts is significantly larger than those for other N–H binders and especially benzoic acids. These catalysts therefore provide comparatively greater rate enhancement as catalyst binding (as determined by the sensor-catalyst interaction) increases. The b_R coefficient here indicates inherent binding complementarity to the nitro group acceptor. Thus, Y-type binders appear to possess a better donor array for nitro group activation in comparison to either phenols or other N–H catalysts. Benzoic acids would be predicted to be active catalysts according to their b_R value, but only at the weaker binding regime, due to their relatively low sensitivity coefficient. Considering both coefficients together, Y-type catalysts are the most effective for the Friedel Crafts reaction of nitroalkenes.

Table 3.3 Equation 6 parameter values for Diels Alder and Friedel Crafts reactions.

Diels Alder		Friedel Crafts		
$A_{DA} = 7.08$ $B_{DA} = -6.36$		$A_{FC} = 9.59$ $B_{FC} = -4.46$		
		catalyst series	a_{FC}	b_{FC}
$a_{DA} \approx b_{DA} \approx 1$		Y-type	-4.23	-1.68
		benzoic acids	-5.11	-2.18
		phenols	-5.08	-2.02
		other N-H binders	-5.77	-2.59

Equation 6 provides a direct method for calculating anticipated catalyst strength for a reaction based on the sensor wavelength shift metric and accounting for catalyst structure preference. Comparison of the parameters can also reveal catalyst structure-activity relationships within a particular reaction or between separate reactions. Future investigation of additional hydrogen-bond catalyzed transformations, empirically or computationally, holds promise for expanding the quantitative predictive power of this equation across multiple catalyst structures and reactions.

3.5. Comparison of Catalyst Reactivity and Acidity

Acidity values have been a primary guiding principle in the context of hydrogen-bond catalyst design, under the presumption that a more acidic donor is capable of greater stabilization of charge buildup in the transition state. Several successful reports of optimizing catalyst activity by tuning acidity have indeed been reported, including Sigman's excellent investigation of acidity effects on both rate and enantioselectivity on a hetero-Diels Alder reaction.[147] However, even ostensibly subtle structural modulation of a catalyst can produce secondary effects that override acidity values, as illustrated in Cheng and coworkers' investigation on thiourea compounds.[148]

Considering the established utility of the sensor wavelength metric as an indicator of catalyst activity, we were interested in comparing catalyst acidity with activity. Recent efforts by Schreiner and others have determined accurate pK_a values for various common hydrogen-bond donors.[149] The large amount of rate data collected herein for the hydrogen-bond catalyzed Diels Alder and Friedel Crafts reactions offers a unique opportunity to conduct this analysis across a broad range of catalyst structures. The

147) (a) Jensen, K. H.; Sigman, M. S. "Evaluation of Catalyst Acidity and Substrate Electronic Effects in a Hydrogen Bond-Catalyzed Enantioselective Reaction" *J. Org. Chem.* **2010**, *75*, 7194-7201. (b) Jensen, K. H.; Sigman, M. S. "Systematically Probing the Effect of Catalyst Acidity in a Hydrogen-Bond-Catalyzed Enantioselective Reaction" *Angew. Chem. Int. Ed.* **2007**, *46*, 4748-4750. (c) Nickerson, D. M.; Angeles, V. V.; Auvil, T. J.; So, S. S.; Mattson, A. E. "Internal Lewis Acid Assisted Ureas: Tunable Hydrogen Bond Donor Catalysts" *Chem. Commun.* **2013**, *49*, 4289-4291.
148) Li, X.; Deng, H.; Zhang, B.; Li, J.; Zhang, L.; Luo, S.; Cheng, J.-P. "Physical Organic Study of Structure-Activity-Enantioselectivity Relationships in Asymmetric Bifunctional Thiourea Catalysis: Hints for the Design of New Organocatalysts" *Chem. Eur. J.* **2010**, *16*, 450-455.
149) (a) Jakab, G.; Tancon, C.; Zhang, Z.; Lippert, K. M.; Schreiner, P. R. "(Thio)urea Organocatalyst Equilibrium Acidities in DMSO" *Org. Lett.* **2012**, *14*, 1724-1727. (b) Ni, X.; Li, X.; Wang, Z.; Cheng, J.-P. "Squaramide Equilibrium Acidities in DMSO" *Org. Lett.* **2014**, *16*, 1786-1789.

Brønsted catalysis law (eq 7) describes the relationship of proton dissociation (K_a) and catalyst activity under general acid catalysis.

$$\log (k) = \alpha \log (K_a) + C \qquad\qquad eq\ (7)$$

Figure 3.15 and Figure 3.16 display the Brønsted catalysis equation applied to select catalyst series in the Diels Alder and Friedel Crafts reactions, respectively.
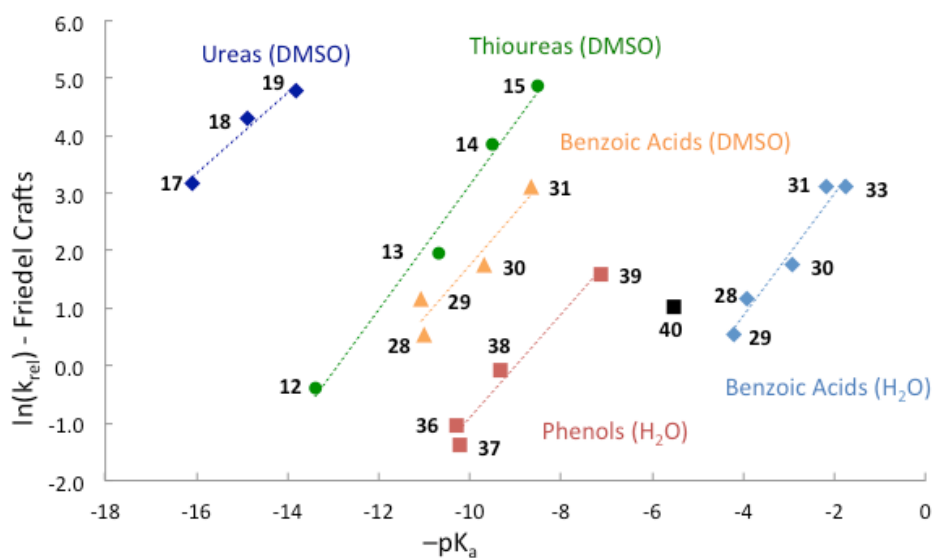
Figure 3.15 Brønsted plot for the Friedel Crafts reaction with select catalyst series. Catalyst chapter number prefixes have been removed for clarity.
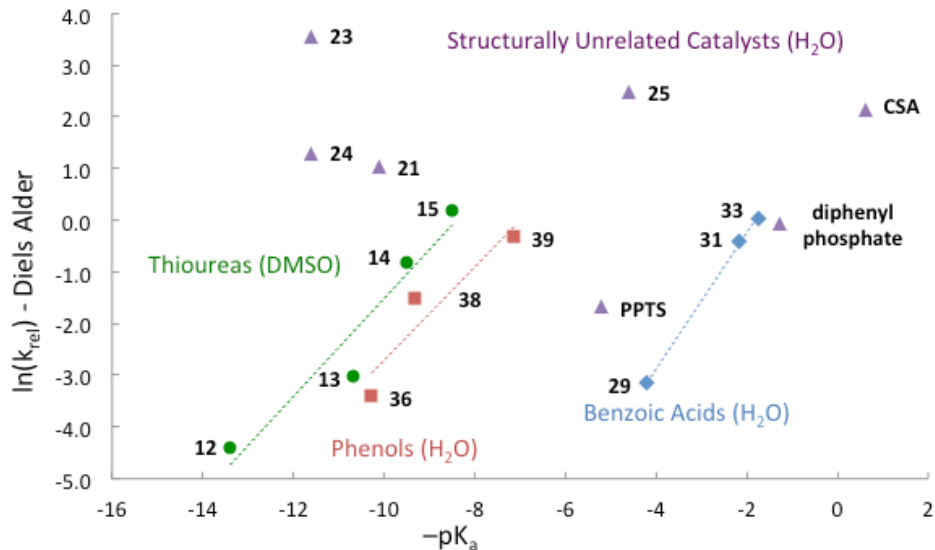
Figure 3.16 Brønsted plot for the Diels Alder reaction with select catalysts. Catalyst chapter number prefixes have been removed for clarity.

These plots establish clear linear free energy relationships (LFERs)[150] between acidity and activity *within isostructural catalyst series*. The catalysts generally show a narrow range of α values (0.39-0.47),[151] indicating a similar degree of hydrogen-bond donation in the transition state of both reactions. Deviations from this trend were found for benzoic acids in the Diels Alder ($\alpha = 0.57$) and ureas in the Friedel Crafts ($\alpha = 0.31$). These values establish that the reactions are not proceeding through formal protonation mechanisms ($\alpha = 1$). Critically, these plots highlight the inherent limitations in using pK_a values as a metric for *de novo* catalyst design. One of the clearest examples can be seen by comparing ureas and thioureas. Based solely on acidity values, thioureas would be predicted to be far more active catalysts. However, ureas proved as effective if not stronger catalysts than the corresponding thioureas (cf. **3.13**, **3.14**, **3.15** vs **3.17, 3.18,**

---

150) For a recent review on application of physical organic parameters in LFERs see: Harper, K. C.; Sigman, M. S. "Using Physical Organic Parameters to Correlate Asymmetric Catalyst Performance" *J. Org. Chem.* **2013**, *78*, 2813-2818.

151) The α values were calculated from slopes of these plots using log k_{rel} as the y-axis.

3.19). Dramatic disparities in acidity and reactivity are seen amongst the cationic catalysts, which greatly outperform far more acidic compounds. Highly reactive structurally-unrelated catalysts, including several commonly employed Brønsted acid catalysts (PPTS, diphenylphosphate, and CSA) are also included in Figure 3.16, and further highlight the inconsistency of reactivity with pK_a. Interestingly, PPTS is much less active compared to Takenaka's azaindolium catalyst **3.25**, despite very sharing similar acidities and the pyridinium N–H moiety. Dual hydrogen-bonding, available to the latter, is the most likely secondary interaction responsible for the increased reactivity. The above examples underscore the hazards of using pK_a measurements to estimate catalyst strength.

Aggregated data for all catalysts, including wavelength shift and binding constant with sensor **3.08**, k_{rel} values for both Diels Alder and Friedel Crafts, and pK_a values are presented in Table 3.4, organized by increasing sensor wavelength shift.

Table 3.4 Sensor shifts, binding constants, relative rate data, and acidity values for hydrogen-bond catalysts examined.

catalyst	λ_{max} (nm)	K_{eq} (M^{-1})	k_{rel} (Diels Alder)	k_{rel} (Friedel Crafts)	pK$_a$ (H$_2$O)	pK$_a$ (DMSO)
H$_2$O (**3.44**)	495.2	2.54	-	-	15.75	32
(*R,R*)-TADDOL (**3.41**)	490.8	1.57×10^1	0.023	-	~16	28-30
TBDMSiOH (**3.42**)	490.4	4.87	-	-	~12	-
Diphenylthiourea (**3.12**)	490.0	1.67×10^1	0.012	0.68	-	13.4
Silanediol (**3.43**)	487.2	7.88×10^1	-	1.82	11.8	-
(*R*)-BINOL (**3.36**)	487.0	3.18×10^1	0.034	0.35	10.28	17.1
4-*t*-Bu-phenol (**3.37**)	486.2	4.30×10^1	-	0.25	10.23	~18
2-Me-BzOH (**3.28**)	486.2	7.04×10^1	-	3.21	3.91	11.07
BzOH (**3.29**)	485.4	8.35×10^1	0.086	1.72	4.20	11.00
Benzotriazole (**3.26**)	484.2	6.57×10^1	-	2.12	8.38	11.9
4-Br-phenol (**3.38**)	484.0	1.50×10^2	0.224	0.93	9.34	-
(CF$_3$)$_2$-thiourea (**3.13**)	484.0	1.07×10^2	0.049	7.13	-	10.7
2-Cl-BzOH (**3.30**)	482.6	2.15×10^2	-	5.81	2.94	9.70
Sulfonamide (**3.16**)	482.2	1.04×10^3	0.337	36.4	-	<12.9
4-NO$_2$-phenol (**3.39**)	481.0	6.05×10^2	0.733	4.94	7.14	10.8
F$_5$-phenol (**3.40**)	480.8	4.92×10^2	-	2.82	5.53	-
(CF$_3$)$_2$-urea (**3.17**)	480.4	1.05×10^3	0.724	24.1	-	16.1
Squaramide (**3.22**)	~480	-	-	12.5	-	11.5-12.0
Spiroligozyme (**3.35**)	480.0	6.30×10^2	-	-	4-5	-
2-NO$_2$-BzOH (**3.31**)	480.0	8.27×10^2	0.669	22.8	2.17	8.66
(CF$_3$)$_3$-thiourea (**3.14**)	479.8	4.52×10^2	0.442	47.0	-	9.5
(CF$_3$)$_4$-urea (**3.19**)	479.8	9.38×10^3	-	120.0	-	13.8
(CF$_3$)$_3$-urea (**3.18**)	479.6	2.52×10^3	-	73.4	-	14.9
3,5-NO$_2$-BzOH (**3.32**)	478.0	1.02×10^3	-	-	-	-
F5.BzOH (**3.33**)	477.2	1.41×10^3	1.04	22.2	1.75	-
(CF$_3$)$_4$-thiourea (**3.15**)	477.0	1.77×10^3	1.22	130.6	-	8.5
Thiophosphoramide (**3.27**)	475.0	3.11×10^3	1.23	291.1	-	-
BF$_2$-urea (**3.20**)	474.4	2.65×10^4	-	603.5	-	7.5
Guanidinium (**3.21**)	473.2	1.84×10^4	2.81	1446	10.12	14
MonoAmidinium (**3.24**)	473.0	3.34×10^3	3.69	89.1	11-12	12.8-13.6
TFA (**3.34**)	470.0	5.49×10^3	-	-	0.2	-
Azaindolium (**3.25**)	469.8	-	12.2	2604	4.6	6
BisAmidinium (**3.23**)	464.6	3.22×10^5	35.1	2763	11-12	12.8-13.6
PPTS	-	-	0.190	72.7	5.2	3.4
Diphenylphosphate	-	-	0.951	26.9	1.29	-
CSA	-	-	8.53	103.3	-0.6	1.6

3.6. Conclusions

Simple pyrazinone **3.08** provides measurable wavelength shifts upon interaction with a wide variety of small molecule hydrogen bond donors. This signal, $\Delta\lambda_{max}$, was found to correlate well with binding constants of the catalysts to the sensor. Extensive kinetic analysis of Diels Alder and Friedel Crafts reactions were performed with many of these hydrogen-bonding catalysts, and the relative rate enhancements correlated well with the $\Delta\lambda_{max}$ value. These relationships establish the sensor wavelength measurements as a novel, quantitative metric with which to predict catalyst reactivity. Simply stated, hydrogen-bond donors that cause a greater blue shift when saturating sensor **3.08** are more reactive catalysts. Although relative estimates of catalyst activity may be inferred from pK_a within very closely related catalyst structures, the activity-acidity analysis provided here underlines the ineffectiveness of pK_a as a general gauge of hydrogen-bond strength. Use of the colorimetric probe as an electrophile surrogate provides a more meaningful measurement of LUMO-lowering via hydrogen-bonding.

3.7 Experimental Section

General Considerations

All non-aqueous reactions were carried out under an atmosphere of argon. All glassware was put in the oven at 85-90 °C overnight and flame-dried before use. The solvents used for the reactions and all measurements were freshly distilled prior to use: CH_2Cl_2 was distilled from CaH_2, toluene was distilled from metallic sodium, THF was

distilled from sodium/benzophenone ketyl, and $CHCl_3$ was distilled from activated powdered 4Å molecular sieves. Flash column chromatography was performed using Silicycle Silaflash P60 silica gel (40-63 μm particle size). All kinetic NMR data were recorded on a DRX-600 (600 MHz) spectrometer. Chemical shifts are reported relative to the solvent resonance peak δ 7.27 ($CDCl_3$) for ^1H NMR and δ 77.23 ($CDCl_3$) for ^{13}C. NMR spectroscopic data were reported as follows: chemical shift, multiplicity (s = singlet, d = doublet, q = quartet, b = broad, m = multiplet), coupling constants and number of protons and compared with the references. All UV spectra were obtained using a JASCO FT/IR-480 Plus from 600 nm – 350 nm. High resolution mass spectra were obtained using a Waters LC-TOF LCT-XE Premier model mass spectrometer with an ionization mode of either ESI or CI.

Synthesis of Sensor and Catalysts

Thioureas **3.13**[152] and **3.15**,[153] sulfonamide **3.16**,[139a] ureas **3.17**[149a] and **3.19**,[154] guanidinium **3.21**,[155] monoamidinium **3.24**,[8] azaindolium **3.25**,[138] and thiophosphoramide **3.27**[139a] are known compounds and were synthesized according to literature methods.

152) Li, X.; Deng, H.; Luo, S.; Cheng, J.-P. "Organocatalytic Three-Component Reactions of Pyruvate, Aldehyde, and Aniline by Hydrogen-Bonding Catalysts" *Eur. J. Org. Chem.* **2008**, 4350-4356.

153) Natarajan, A.; Guo, Y.; Arthanari, H.; Wagner, G.; Halperin, J. A.; Chorev, M. "Synthetic Studies toward Aryl-(4-aryl-4*H*-[1,2,4]triazole-3-yl)-amine from 1,3-Diarylthiourea as Urea Mimetics" *J. Org. Chem.* **2005**, *70*, 6362-6368.

154) Denoyelle, S.; Chen, T.; Chen, L.; Wang, Y.; Klosi, E.; Halperin, J. A.; Aktas, B. H.; Chorev, M. "In vitro inhibition of translation initiation by N,N'-diarylureas--potential anti-cancer agents." *Bioorg. Med. Chem. Lett.* **2012**, *22*, 402-409.

155) Uyeda, C.; Jacobsen, E. N. "Enantioselective Claisen Rearrangements with a Hydrogen-Bond Donor Catalyst" *J. Am. Chem. Soc.* **2008**, *130*, 9228-9229.
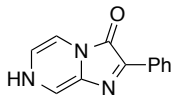
2-Phenylimidazo[1,2-a]pyrazin-3(7H)-one (3.11)

The title compound was prepared by a previously described procedure.[129] Spectral data are in good agreement with literature values. ^{1}H NMR (500 MHz, DMSO-d_6) δ 11.32 (bs, 1H), 8.47 (d, J = 7.7 Hz, 2H), 8.05 (s, 1H), 7.41-7.44 (m, 3H), 7.34 (t, J = 7.1 Hz, 1H), 6.89 (bd, J = 4.8 Hz, 1H).
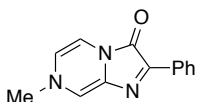
7-Methyl-2-phenylimidazo[1,2-*a*]pyrazin-3(7*H*)-one (3.08)

To a solution of **3.11** (106 mg, 0.50 mmol) in DMF (0.6 mL) were added MeI (94 μL, 1.51 mmol) and K_2CO_3 (209 mg, 1.51 mmol), and the resulting solution was stirred at room temperature for 25 min. The mixture was then diluted with CH_2Cl_2 (20 mL), washed with H_2O (2 x 10 mL), brine (1 x 10 mL), dried over Na_2SO_4, filtered, and concentrated. Purification by chromatography (4% to 10% MeOH/CH_2Cl_2) provided the title compound as a red solid (61 mg, 54%). Spectral data are in good agreement with literature values.[127a] ^{1}H NMR (500 MHz, DMSO-d_6) δ 8.46 (d, J = 7.8 Hz, 2H), 8.08 (s, 1H), 7.50 (d, J = 5.9 Hz, 1H), 7.44 (t, J = 7.7 Hz, 2H), 7.33 (td, J = 7.3, 1.2 Hz, 1H), 6.86 (dt, J = 5.8, 1.2 Hz, 1H), 3.64 (s, 3H).
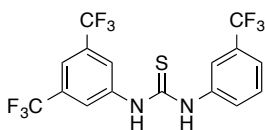
1-(3,5-bis(trifluoromethyl)phenyl)-3-(3-(trifluoromethyl)phenyl)thiourea (3.14)

To a solution of 3-(trifluoromethyl)aniline (0.175 mL, 1.4 mmol) in THF (2.0 mL) at 0 °C was added 3,5-bis(trifluoromethyl)phenyl isothiocyanate (0.270 mL, 1.4 mmol) dropwise. The solution was warmed to rt, stirred for 18 h, and concentrated in vacuo. The resulting residue was recrystallized from CH_2Cl_2/hexanes and washed with hexanes to provide the title compound as a white solid (511 mg, 86%): mp: 133-134 °C; ^{1}H NMR (500 MHz, DMSO-d_6) δ 10.45 (bs, 2H), 8.23 (s, 2H), 7.89 (s, 1H), 7.81 (s, 1H), 7.75 (d, J = 7.9 Hz, 1H), 7.60 (t, J = 7.9 Hz, 1H), 7.52 (d, J = 7.6 Hz, 1H); ^{13}C NMR (125 MHz, DMSO-d_6) δ 180.3, 141.6, 139.7, 130.1 (q, J = 32.8 Hz), 129.8, 129.3 (q, J = 31.7 Hz), 127.8, 124.0 (q, J = 273 Hz), 123.7, 123.2 (q, J = 273 Hz), 121.3 (q, J = 3.7 Hz), 120.3 (q, J = 3.7 Hz), 117.2; HRMS (ESI) calcd for $C_{16}H_8N_2F_9S$ [M-H]$^-$, m/z = 431.0264; found 431.0269.
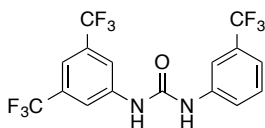
1-(3,5-bis(trifluoromethyl)phenyl)-3-(3-(trifluoromethyl)phenyl)urea (3.18)

 Synthesized using the same procedure as for **3.14**, using 3,5-bis(trifluoromethyl)phenyl isocyanate (0.242 mL, 1.4 mmol). Recrystallization from CH_2Cl_2 afforded the title compound as white solid (398 mg, 68%): mp: 166-168 °C; ^{1}H NMR (500 MHz, DMSO-d_6) δ 9.49 (bs, 1H), 9.36 (bs, 1H), 8.14 (s, 2H), 8.00 (s, 1H), 7.61-7.67 (m, 2H), 7.52 (t, J = 7.8 Hz, 1H), 7.34 (d, J = 7.5 Hz, 1H); ^{13}C NMR (125 MHz, DMSO-d_6) δ 152.5, 141.6, 140.0, 130.7 (q, J = 33.0 Hz), 129.9, 129.6 (q, J = 31.7 Hz), 124.2 (q, J = 274 Hz), 123.3

(q, J = 273 Hz) 122.5, 118.7 (q, J = 3.6 Hz), 118.3 (q, J = 3.6 Hz), 114.8 (q, J = 4.0 Hz), 114.6; HRMS (ESI) calcd for $C_{16}H_{10}N_2OF_9$ [M+H]$^+$, m/z = 417.0649; found 417.0633.
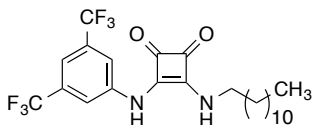
3-((3,5-bis(trifluoromethyl)phenyl)amino)-4-(dodecylamino)cyclobut-3-ene-1,2-dione (3.22)

To a solution of dodecylamine (73 mg, 0.39 mmol) in CH_2Cl_2 (3 mL) at rt was added 3-((3,5-bis(trifluoromethyl)phenyl)amino)-4-methoxycyclobut-3-ene-1,2-dione[156] (200 mg, 0.59 mmol), creating a yellow suspension. After stirring at rt for 48 h, the mixture was filtered. The resulting solid was recrystallized from MeOH and washed with cold CH_2Cl_2 to afford the title compound as a white solid (61.3 mg, 32%): mp: 188-189 °C; ^{1}H NMR (500 MHz, DMSO-d_6) δ 10.13 (bs, 1H), 8.01 (s, 2H), 7.71 (bs, 1H), 7.63 (s, 1H), 3.60 (s, 2H), 1.52-1.59 (m, 2H), 1.15-1.35 (m, 18H), 0.83 (t, J = 6.5 Hz, 3H); ^{13}C NMR (125 MHz, DMSO-d_6) δ 184.8, 180.3, 169.8, 162.2, 141.1, 131.3 (q, J = 33.0 Hz), 123.2 (q, J = 273 Hz), 117.9, 114.6, 43.8, 31.3, 30.5, 29.0, 29.0, 28.9, 28.9, 28.7, 28.5, 25.8, 22.1, 13.9; HRMS (ESI) calcd for $C_{24}H_{30}N_2O_2F_6Na$ [M+Na]$^+$, m/z = 515.2109; found 515.2100.
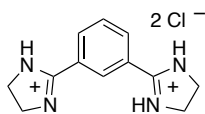
156) Konishi, H.; Lam, T. Y.; Malerich, J. P.; Rawal, V. H. "Enantioselective α-Amination of 1,3-Dicarbonyl Compounds Using Squaramide Derivatives as Hydrogen Bonding Catalysts" *Org. Lett.* **2010**, *12*, 2028-2031.

BisAmidinium Chloride (3.23-Cl)

Freshly distilled MeOH (2.0 mL) was added to a dry flask under and cooled to 0 °C. Acetyl chloride (2.0 mL) was then added dropwise, and the solution was stirred for 1 h, warmed to rt and stirred for an additional 1 h. After cooling back to 0 °C, the neutral bisamidine substrate (2-(3-(4,5-dihydro-1H-3λ^4-imidazol-2-yl)phenyl)-4,5-dihydro-1H-imidazole) (150 mg, 0.7 mmol) was added. The mixture stirred for 1 h before warming to rt and stirring for an additional 17 h. Removal of the solvent afforded the product as a light tan solid (188 mg, 94%): mp: >250 °C; ^{1}H NMR (500 MHz, DMSO-d_6) δ 11.13 (bs, 4H), 9.20 (s, 1H), 8.46 (bs, 2H), 7.92 (bs, 1H), 4.05 (bs, 8H); ^{13}C NMR (500 MHz, DMSO-d_6) δ 163.8, 133.8, 130.1, 130.0, 122.8, 44.5; IR (film) 3393, 1638, 1615, 1586, 1286 cm^{-1}.
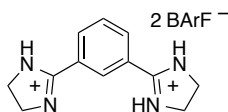
BisAmidinium BArFate (3.23)

A dry flask was charged with **3.23-Cl** (26 mg, 0.089 mmol), sodium tetrakis[3,5-bis(trifluoromethyl)phenyl]borate (150 mg, 0.169 mmol), and dry MeOH (1.5 mL). After stirring at rt for 21 h, the solvent was removed and dry CH$_2$Cl$_2$ (~2 mL) was added. The resulting mixture was passed through a plug of Celite and concentrated *in vacuo* to afford the product as a tan solid (157 mg, 96%): mp: 195-199 °C (dec); ^{1}H NMR (500 MHz, Acetone-d_6) δ 10.09 (b, 4H), 8.83 (s, 1H), 8.44 (d, J = 8.0 Hz, 2H), 8.05 (t, J = 7.9 Hz, 1H), 7.79 (s, 16H), 7.67 (s, 8H), 4.39 (s, 8H); ^{13}C NMR (125 MHz, Acetone-d_6) δ 166.6, 162.7 (q, J = 50.0 Hz), 135.6, 135.1, 132.0, 130.1 (qq, J = 31.5, 2.7 Hz), 129.7, 125.4 (q,

J = 272 Hz), 124.8, 118.5 (t, J = 3.7 Hz), 46.4; IR (film) 3460, 3237, 2998, 1357, 1279, 1124, 888 cm^{-1}.
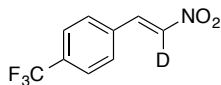
(*E*)-1-(2-Nitrovinyl-2-*d*)-4-(trifluoromethyl)benzene (3.46):

A solution of *p*-trifluoromethylbenzaldehyde (0.30 mL, 2.2 mmol) and d_3-nitromethane (0.14 mL, 2.64 mmol) in d_4-MeOD (5.0 mL) was cooled to 0 °C and a solution of NaOD in D_2O (30% wt, 0.36 mL) was added dropwise over 15 min. After stirring an additional 15 min, D_2O (1.5 mL) was added, and the reaction warmed to rt and stirred for an additional 1 h. The mixture was then cooled to 0 °C and quenched dropwise with DCl in D_2O (35% wt, 0.35 mL). The mixture was extracted with CH_2Cl_2 (3 x 15 mL), and the combined organics were dried over Na_2SO_4, filtered, and concentrated to provide the Henry adduct and a small amount of starting aldehyde as determined by ^1H NMR. The Henry adduct was dissolved in CH_2Cl_2 (11 mL), cooled to 0 °C and Et_3N (0.61 mL, 4.44 mmol) was added, followed by dropwise addition of methanesulfonyl chloride (0.34 mL, 4.44 mmol). After stirring for 15 min at 0 °C, the reaction was quenched with water (15mL) and extracted with CH_2Cl_2 (3 x 50 mL). The combined organics were dried over Na_2SO_4, filtered, and concentrated. Purification by chromatography (15% EtOAc/Hexanes) and subsequent recrystallization from CH_2Cl_2/Hexanes provided the title compound (88% deuterium incorporation as determined by ^1H NMR) as a yellow solid (286 mg, 56%): mp: 94-95 °C; ^1H NMR (500 MHz, CDCl$_3$) δ 8.02 (bs, 1H), 7.73 (d, J = 8.5 Hz, 2H), 7.68 (d, J = 8.3 Hz, 2H); ^{13}C NMR (90 MHz, CDCl$_3$) δ 139.1, 137.2, 133.9, 133.7 (q, J = 33 Hz), 129.5, 126.6 (q, J = 3.6 Hz), 123.7 (q, J = 271 Hz); IR (film)

1510, 1415, 1348, 1324, 1166, 1118, 1068 cm^{-1}; HRMS (CI) calcd for C$_9$H$_5$DF$_3$NO$_2$ [M]$^+$, m/z = 218.0413; found 218.0413.
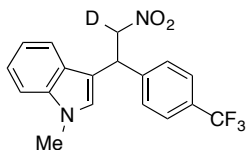
1-Methyl-3-(2-nitro-1-(4-(trifluoromethyl)phenyl)ethyl-2-*d*)-1*H*-indole (3.47):

The General Procedure for the Friedel Crafts reaction (see below) was performed on 0.10 mmol scale using 10 mol % **3.15**. After 24 h, the mixture was concentrated and purified by chromatography (10% to 15% EtOAc/Hexanes) to afford the title compound as a yellow oil (32.6 mg, 93%): ^{1}H NMR (500 MHz, CDCl$_3$) δ 7.61 (d, J = 8.0 Hz, 2H), 7.49 (d, J = 8.0 Hz, 2H), 7.44 (d, J = 7.9 Hz, 1H), 7.33 (d, J = 8.2 Hz, 1H), 7.27 (t, J = 7.6 Hz, 1H), 7.11 (t, J = 7.5 Hz, 1H), 6.88 (s, 1H), 5.24-5.29 (m, 1H), 4.93-5.11 (ABX, 1H), 3.78 (s, 3H); ^{13}C NMR (125 MHz, CDCl$_3$) δ 143.7, 137.5, 130.0 (q, J = 32 Hz), 128.4, 126.6, 126.5, 126.1 (q, J = 3.7 Hz), 124.2 (q, J = 272 Hz), 122.7, 119.9, 118.9, 112.1, 109.9, 78.9 (t, J_{C-D} = 22 Hz), 41.4, 33.1; IR (film) 3057, 2918, 1550, 1377, 1326, 1166, 1121, 1068 cm^{-1}; HRMS (ESI) calcd for C$_{18}$H$_{15}$DF$_3$N$_2$O$_2$ [M+H]$^+$; m/z = 350.1227; found 350.1223.
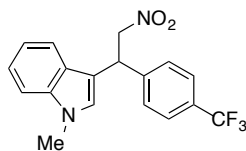
1-methyl-3-(2-nitro-1-(4-(trifluoromethyl)phenyl)ethyl)-1*H*-indole (3.47-H):

Synthesized for comparison with **3.47**. To a solution of (*E*)-1-(2-nitrovinyl)-4-(trifluoromethyl)benzene (*proteo*-**3.46**) (43.2 mg, 0.20 mmol) in DCE (0.50 mL) was added *N*-methylindole (**3.45**) (25 μL, 0.20 mmol) and benzoic acid (12.2 mg, 0.10 mmol). The mixture was sealed and heated to 50 °C for 73 h, after which the reaction was quenched with water (10 mL) and extracted with CH_2Cl_2 (3 x 10 mL). The combined organics were dried over Na_2SO_4, filtered, and concentrated. Purification of the resulting residue by chromatography (10% to 20% EtOAc/Hexanes) afforded the title compound as a yellow oil (42 mg, 60%): ^{1}H NMR (500 MHz, CDCl₃) δ 7.61 (d, *J* = 8.5 Hz, 2H), 7.49 (d, *J* = 8.0 Hz, 2H), 7.44 (d, *J* = 8.0 Hz, 1H), 7.33 (d, *J* = 8.5 Hz, 1H), 7.27 (t, *J* = 7.8 Hz, 1H), 7.12 (t, *J* = 7.5 Hz, 1H), 5.06-5.11 (ABX, 1H), 4.95-5.00 (ABX, 1H), 3.78 (s, 3H); ^{13}C NMR (125 MHz, CDCl₃) δ 143.8, 137.6, 130.1 (q, *J* = 32 Hz) 128.4, 126.6, 126.5, 126.2 (q, *J* = 3.7 Hz), 124.2 (q, *J* = 273 Hz), 122.8 , 120.0, 119.0, 112.2, 109.9, 79.3, 41.5, 33.1; IR (film) 3049, 2918, 1554, 1377, 1326, 1165, 1120, 1068 cm^{-1}; HRMS (ESI) calcd for $C_{18}H_{16}F_3N_2O_2$ [M+H]$^+$, *m/z* = 349.1164; found 349.1179.
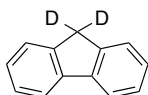
9*H*-Fluorene-9,9-*d*₂ (3.48):[157]

To a solution of fluorene (1.0 g, 6.0 mmol) in DME (9.0 mL) was added KO*t*-Bu (340 mg, 3.0 mmol), and the resulting mixture was heated to gentle reflux under argon and stirred for 14 h. The mixture was cooled to rt and poured into a mixture of water (40 mL) and glacial AcOH (2.0 mL), forming a light yellow precipitate that was filtered and

---

157) Meng, Q.; Thibblin, A. "Solvent-Promoted E2 Reaction Competing with S_N2 Reaction and Stepwise Solvolytic Elimination and Substitution Reactions" *J. Am. Chem. Soc.* **1995**, *117*, 9399-9407.

washed with water. Recrystallization from EtOH (95%) provided the title compound with 97% deuterium incorporation (d_2) as determined by ^{1}H NMR as a white solid (656 mg, 65%): mp: 114-115 °C; ^{1}H NMR (600 MHz, CDCl$_3$) δ 7.80 (d, J = 7.7 Hz, 2H), 7.56 (d, J = 7.5 Hz, 2H), 7.39 (t, J = 7.4 Hz, 2H), 7.32 (t, J = 7.5 Hz, 2H); ^{13}C NMR (150 MHz, CDCl$_3$) δ 143.4, 142.0, 127.0, 126.9, 125.3, 120.1 (d_2-benzylic carbon not observed); IR (film) 3059, 1653, 1558, 1541, 1444 cm^{-1}; HRMS (CI) calc for $C_{13}H_8D_2$ [M]$^+$; m/z = 168.0908; found 168.0905.

UV-Titration Data

General Titration Procedure

An oven-dried 10 mL volumetric flask was charged with sensor **3.08** (10.0 mg, 4.44×10^{-2} mmol) and diluted with CH$_2$Cl$_2$. A 2.22×10^{-5}M stock solution was prepared by transferring 50 µL of this initial solution to a separate 10 mL volumetric flask and diluting with CH$_2$Cl$_2$. For each UV titration experiment, 500 µL of this stock sensor solution was transferred to the UV cuvette. To a Spectrosil Quartz Starna cell 2 x 10 mm, 0.50 mL of the 2.22×10^{-5} M sensor stock solution was added and the level of the solution was marked. Aliquots of the catalyst stock solution were sequentially added and the initial 0.5 mL volume was maintained by evaporation under an argon balloon to the demarcated line. The spectrum was measured after each addition and the λ_{max} was recorded. Aliquots of the catalyst stock solution were added until the λ_{max} did not change further. The titration curves of sensor with different catalysts were made by plotting the λ_{max} vs the concentration of the catalyst after each addition.

Titration plots, raw data, and calculations of K_{eq} for all catalysts can be found in Appendix D.

Job Plot Analysis of Sensor 3.08 with catalyst 3.23

Maximum absorbance (λ_{max}) for the **3.08•3.23** complex (SC) was observed at 465 nm based on the previous titration study. Concentrations of **3.08•3.23** can be determined from measuring absorbance at 465 nm and accounting for absorbance from unbound sensor (S) using Beer's law (Abs = $b\varepsilon c$) to provide eq (8):

$$\text{Abs}_{465} = b\,\varepsilon_{465}^{SC}\,[SC] + b\,\varepsilon_{465}^{S}\,[S] \quad \text{eq (8)}$$

b = constant = 1.0 cm:

$$\text{Abs}_{465} = \varepsilon_{465}^{SC}\,[SC] + \varepsilon_{465}^{S}\,[S] \quad \text{eq (9)}$$

$$[S]_{total} = [S] + [SC]$$

$$[S] = [S]_{total} - [SC] \quad \text{eq (10)}$$

Combining eq (9) and (10):

$$\text{Abs}_{465} = \varepsilon_{465}^{SC}\,[SC] + \varepsilon_{465}^{S}\,[S]_{total} - \varepsilon_{465}^{S}\,[SC]$$

$$[SC] = \frac{\text{Abs}_{465} - \varepsilon_{465}^{S}\,[S]_{total}}{\varepsilon_{465}^{SC} - \varepsilon_{465}^{S}} \quad \text{eq (11)}$$

ε_{465}^{S} was determined from a Beer's plot of **3.08** in CH_2Cl_2:
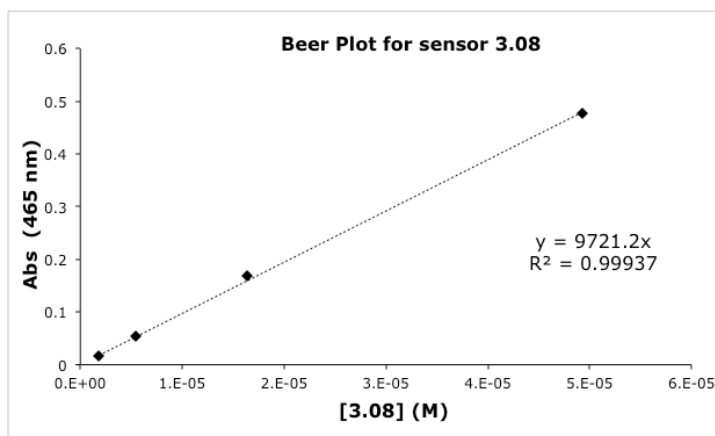
Figure 3.17. Beer Plot for **3.08** at 465 nm.

$\varepsilon_{465}{}^{S} = 9.72 \times 10^3 \ cm^{-1}M^{-1}$

$\varepsilon_{465}{}^{SC}$ was determined using absorbance measurements from the titration of **3.23** at saturation:

$Abs_{465} = 0.337$, $[SC] = 2.22 \times 10^{-5}$ M, b = 1.0 cm

$\varepsilon_{465}{}^{SC} = 1.52 \times 10^4 \ cm^{-1}M^{-1}$

Job Plot Procedure:

Catalyst **3.23** (9.7 mg) was dissolved in CH_2Cl_2 (10 mL) using a volumetric flask. 1.00 mL of this solution was diluted with CH_2Cl_2 in a separate 10 mL volumetric flask to provide the stock catalyst solution, $[\mathbf{3.23}] = 4.99 \times 10^{-5}$ M.

Sensor **3.08** (5.6 mg) was dissolved in CH_2Cl_2 (10 mL) using a volumetric flask. 200 µL of this solution was diluted with CH_2Cl_2 in a separate 10 mL volumetric flask to provide the stock catalyst solution, $[\mathbf{3.08}] = 4.97 \times 10^{-5}$ M.

Analysis was carried out as follows: To a dry cuvette, sensor solution (50 µL) was added via microsyringe, followed by catalyst solution (450 µL). The cuvette was sealed and the absorbance at 465 nm was measured. Mole fraction of sensor was varied from 0.1 to 0.9 in subsequent measurements, keeping the total volume constant at 500 µL.

Table 3.5 Data for the Job Plot analysis of **3.08** with **3.23**.

mol fraction **3.08**	Abs at 465 nm	$[3.08]_{total}$ (M)	$[3.08 \cdot 3.23]$ (M)
0.1	0.0655	5.00E-6	3.08E-6
0.2	0.1279	1.00E-5	5.60E-6
0.3	0.1913	1.50E-5	8.30E-6
0.4	0.2471	2.00E-5	9.62E-6
0.5	0.3022	2.50E-5	1.08E-5
0.6	0.3476	3.00E-5	1.02E-5
0.7	0.3803	3.50E-5	7.32E-6
0.8	0.4223	4.00E-5	6.11E-6
0.9	0.4546	4.50E-5	3.14E-6

Diels Alder Kinetic Experiments

General Procedure

MVK was dried over activated 4Å molecular sieves for 1-2 h, then over dried K_2CO_3 for at least 1 h before distilling at reduced pressure (100 torr) at 45 °C. Cp was freshly prepared from distillation of dicyclopentadiene using a Vigreaux column. Both MVK and Cp were stored at −78 °C until creating stock solutions. Toluene (internal standard) was freshly distilled from metallic sodium. $CDCl_3$ was used from a fresh bottle

and passed through plugs of dried K_2CO_3 just prior to use. All reactions were conducted in sealed NMR tubes with 0.10 M of MVK, 2.0 M (20 equiv) of Cp, 0.10 M of toluene and the indicated catalyst loading. Stock solutions of Cp (7.3 M), toluene (0.75 M), and MVK (0.75 M) with the appropriate amount of catalyst were prepared in $CDCl_3$ in flame-dried vials. Solutions were stored in a liquid N_2 bath until used. An NMR tube was charged with 350 μL $CDCl_3$, 100 μL toluene solution, and 100 μL of MVK/catalyst solution. An NMR spectrum was acquired (t = 0), after which 200 μL of Cp solution was added, the reaction was mixed, and the tube was placed in the spectrometer at 27 °C for the remainder of the experiment. After 6 min, the first spectrum was acquired, with additional spectra acquired every 5 min. Resonance integrations are as follows: δ 2.40 (s, 3H, toluene), δ 2.30 (s, 3H, MVK), 2.24 (s, 3H, exo product), 2.15 (s, 3H, endo product). Unless noted, all catalyzed reactions were performed in triplicate.

[MVK] was determined based on raw integrations of toluene and MVK and the known concentration of toluene (0.1 M):

$$\left(\frac{\text{toluene}}{\text{MVK}}\right) 0.1\text{ M} = [\text{MVK}]$$

Similarly, [P] was determined by combining raw exo and endo integrations based on toluene (0.1 M). Figure 3.18 illustrated concentration of MVK and product for one reaction.

Pseudo-first order plots were created for ln [MVK] vs t using the initial 6 data points (t = 6-31 h, see Figure 3.19 for an example). The averaged slope provided $-k'_{obs}$ for the catalyzed reaction. The k_{rel} values (Table 3.6) were determined at 0.01 M catalyst (10

mol%) and 2.0 M Cp from the pseudo-first order rate constants as described in equation

4.

Representative Data for the Diels Alder Reaction using 3.12 (20 mol%).
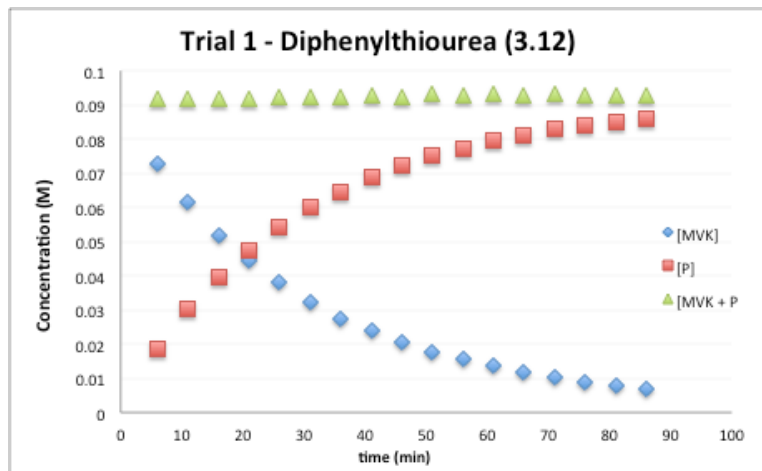
Figure 3.18 Diels Alder reaction profile using 20 mol% **3.12**.
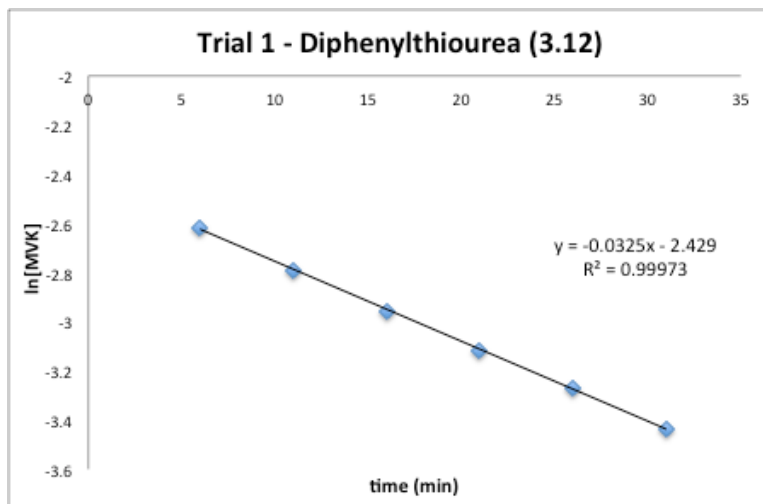
Figure 3.19 Representative first order kinetic analysis of the Diels Alder reaction.

Table 3.6 Calculation of Diels Alder k_{rel} values with error propagation for all catalysts.

catalyst	mol %	k'_{obs} (s^{-1})	k_{cat} (s^{-1})	k_{rel}	error k_{rel}	ln(k_{rel})	error ln(k_{rel})
3.12	20	3.34E-2	4.00E-4	0.012	0.0281	-4.401	2.287
3.13	10	3.42E-2	1.60E-3	0.049	0.0304	-3.014	0.620
3.14	5	3.98E-2	1.44E-2	0.442	0.0207	-0.817	0.047
3.15	5	5.24E-2	3.96E-2	1.215	0.0357	0.195	0.029
3.16	1	3.37E-2	1.10E-2	0.337	0.0136	-1.086	0.040
3.17	5	4.44E-2	2.36E-2	0.724	0.0223	-0.323	0.031
3.18	2	5.09E-2	9.15E-2	2.807	0.0556	1.032	0.020
3.19	0.25	6.12E-2	1.14E0	35.09	0.5217	3.558	0.015
3.24	5	9.27E-2	1.20E-1	3.687	0.4063	1.305	0.110
3.25	0.25	4.25E-2	3.96E-1	12.15	0.1962	2.497	0.016
3.27	2	4.06E-2	4.00E-2	1.227	0.0214	0.205	0.017
3.29	10	3.40E-2	1.40E-3	0.043	0.0336	-3.148	0.781
3.31	5	4.35E-2	2.18E-2	0.669	0.0197	-0.402	0.029
3.33	1	3.60E-2	3.40E-2	1.043	0.0559	0.042	0.054
3.36	20	3.48E-2	1.10E-3	0.034	0.0312	-3.389	0.926
3.38	20	4.72E-2	7.30E-3	0.224	0.0292	-1.496	0.130
3.39	10	5.65E-2	2.39E-2	0.733	0.0171	-0.310	0.023
3.41	20	3.41E-2	7.50E-4	0.023	0.0167	-3.772	0.726
diphenyl-phosphate	1	3.57E-2	3.10E-2	0.951	0.0390	-0.050	0.041
PPTS	5	3.57E-2	6.20E-3	0.190	0.0206	-1.660	0.108
CSA	1	6.04E-2	2.78E-1	8.528	0.1167	2.143	0.014
back-ground	-	3.26E-2	-	-	-	-	-

Friedel Crafts Kinetic Experiments

General Procedure for the Friedel Crafts Reaction

All glassware was base-washed prior to use. $CHCl_3$ was freshly distilled from 4Å molecular sieves prior to use. A stock solution (substrate solution) of nitro **3.46** (0.5 M) and internal standard **3.48** (0.5 M) in $CHCl_3$ was prepared in a flame-dried 4-dram vial. The appropriate catalyst solution (0.1 M for 10 mol% catalyst loading) in $CHCl_3$ was prepared in a separately dried vial. For each reaction, a dry NMR tube was charged with 200 µL of substrate solution, 100 µL of catalyst solution, and 325 µL CH_3Cl_3 (make-up solvent). For less soluble catalysts, more dilute catalyst solutions were used and less make-up solvent was added. For example, when 200 µL of a 0.05M catalyst solution was used, 225 µL of make-up $CHCl_3$ was added to the NMR tube. The tube was sealed with a septum and initial [**3.46**] was determined by ^2H NMR. The reaction was initiated by adding **3.45** (125 µL) and mixing the contents (total NMR tube volume = 750 µL), and the reaction tubes were stored away from light. Initial concentrations of reactants: [**3.45**] = 1.33 M, [**3.46**] = 0.133 M, [**3.48**] = 0.133 M. Reactions were analyzed at the indicated time points using ^2H NMR spectroscopy: 50 scans, d1 relaxation time = 10 s, ds = 2. Integration limits: δ 7.65-7.40 (**3.46**), 4.25-3.90 (**3.48**). All catalysts were run in duplicate from separate stock solutions.

Concentrations of starting material (**35**) were determined from the signal integrations (s) using equation 12 to account for deuteration and number of deuterons:

$$[\mathbf{X}] = \frac{s_X}{\text{\# deuterons (\% deuteration)}}$$

$$[\textbf{3.46}] = \frac{2\,[\textbf{3.48}]\,(\%d_{3.48})\,s_{3.46}}{(\%d_{3.46})\,s_{3.48}}$$

<div align="right">eq (12)</div>

Values of k_{rel} were calculated from the pseudo-first order k'_{obs} rate constants and $k_{background}$ as described for the Diels Alder reaction in equation 4 (see Figure 3.20 for a sample plot). All k_{rel} values normalized to 10 mol% catalyst (0.013 M catalyst, 0.133 M nitro substrate, 1.33 M indole substrate) are collected in Table 3.7.
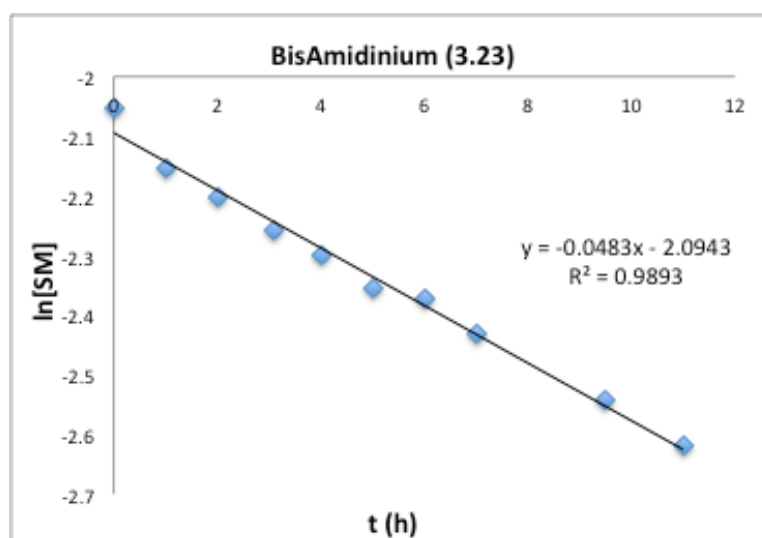
Figure 3.20 Representative first order kinetic analysis of the Friedel Crafts reaction, using 0.2 mol% **3.23** as catalyst.

Table 3.7 Calculation of Friedel Crafts k_{rel} values with error propagation for all catalysts.

catalyst	mol %	$k'_{obs}\,(s^{-1})$	k_{rel}	error k_{rel}	$\ln(k_{rel})$	error $\ln(k_{rel})$
3.12	10	1.53E-3	0.68	0.04	-0.388	0.147
3.13	10	7.41E-3	7.13	0.32	1.964	0.052
3.14	10	4.37E-2	46.95	3.58	3.849	0.078
3.15	10	1.20E-1	130.6	7.50	4.872	0.058
3.16	5	1.75E-2	36.39	0.16	3.594	0.005

3.17	5	1.19E-2	24.11	4.40	3.183	0.197
3.18	5	3.44E-2	73.39	7.37	4.296	0.103
3.19	5	5.57E-2	120.2	29.48	4.789	0.249
3.20	1	5.60E-2	603.5	129.28	6.403	0.218
3.21	0.5	6.69E-2	1446	1.53	7.277	0.001
3.22	5	6.60E-3	12.48	2.01	2.524	0.187
3.23	0.2	5.13E-2	2763	228.47	7.924	0.084
3.24	0.5	4.98E-3	89.10	10.26	4.490	0.141
3.25	0.69	1.65E-1	2604	330.77	7.865	0.128
3.26	10	2.84E-3	2.12	0.18	0.749	0.124
3.27	5	1.34E-1	291.1	36.19	5.674	0.125
3.28	10	3.84E-3	3.21	0.11	1.166	0.047
3.29	10	2.48E-3	1.72	0.13	0.544	0.123
3.30	10	6.21E-3	5.81	0.02	1.760	0.005
3.31	10	2.17E-2	22.78	2.01	3.126	0.092
3.33	10	2.12E-2	22.20	5.03	3.100	0.237
3.36	10	1.23E-3	0.35	0.03	-1.044	0.304
3.37	10	1.14E-3	0.25	0.02	-1.393	0.471
3.38	10	1.76E-3	0.93	0.02	-0.069	0.046
3.39	10	5.42E-3	4.94	0.68	1.597	0.167
3.40	10	3.48E-3	2.82	0.44	1.035	0.213
3.43	5	1.74E-3	1.82	0.62	0.600	0.718
CSA	1	1.03E-2	103.3	7.91	4.637	0.084
PPTS	1	7.54E-3	72.66	0.16	4.286	0.002
diphenyl-phosphate	5	1.32E-2	26.89	0.53	3.292	0.021
background	-	9.12E-4	-	-	-	-

4. EFFORTS TOWARD MEASURING BRØNSTED AND LEWIS ACID ACTIVATION OF ELECTROPHILES

4.1. Initial Investigations of Brønsted Acids with the Original Sensor

In Chapter 3, the utility of small pyrazinone chromophore **3.08** as a quantitative metric to measure the activating effects of hydrogen-bonding is described. A logical extension of this method is the application of the colorimetric probe to measure the strengths of Brønsted and Lewis Acid binding effects. Various techniques exist for estimating the relative strengths of these activators.[118,119,120] However, comparative strengths of hydrogen-bond donors with Lewis acids remains poorly understood beyond qualitative generalizations. Successful application of sensor **3.08** to Brønsted and Lewis Acids would result in a *unified metric* for catalysts spanning the entire range of electrophilic activation effects. Based on the general assumption that traditional Lewis and Brønsted Acids are more powerful electrophile binders, interaction of these compounds with the sensor molecule would be predicted to induce even greater hypsochromic shifts than hydrogen-bond donors (Scheme 4.1).
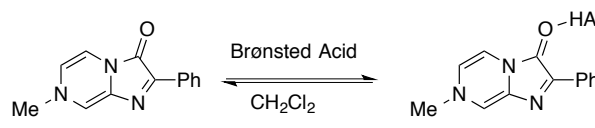
Scheme 4.1 Proposed interaction of stronger binders with sensor **3.08**.
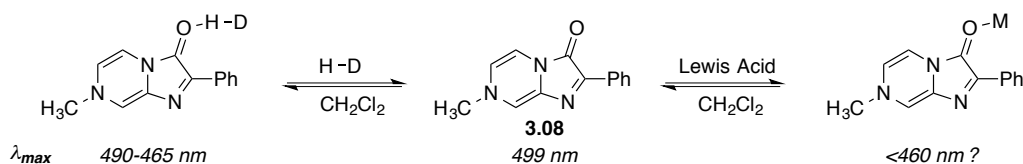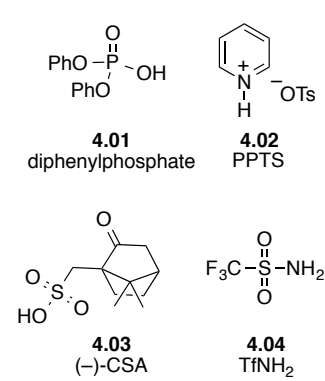
Initial studies focused on the perturbations of the UV absorption of sensor **3.08** with Brønsted acids. In contrast to the anticipated strong blue shift, incremental addition of various common acids to solutions of **3.08** in CH_2Cl_2 resulted in the appearance of a red-shifted absorption band (Table 4.1). A representative UV spectrum showing the

addition of (+)-CSA to the sensor is shown in Figure 4.1. It is worth noting that although differentiation of the magnitude of the red shift was observed, the values did not track with the relative catalyst strengths (k_{rel}) values calculated for the Diels Alder or Friedel Crafts reactions (see Section 3.4).

Table 4.1 Red shift of **3.08** upon addition of various Brønsted acids.

Brønsted Acid	saturated λ_{max} (nm)	k_{rel} (Diels Alder)	k_{rel} (Friedel Crafts)
4.01	517	0.95	27
4.02	512	0.19	73
4.03	518	8.53	103
4.04	527	-	-
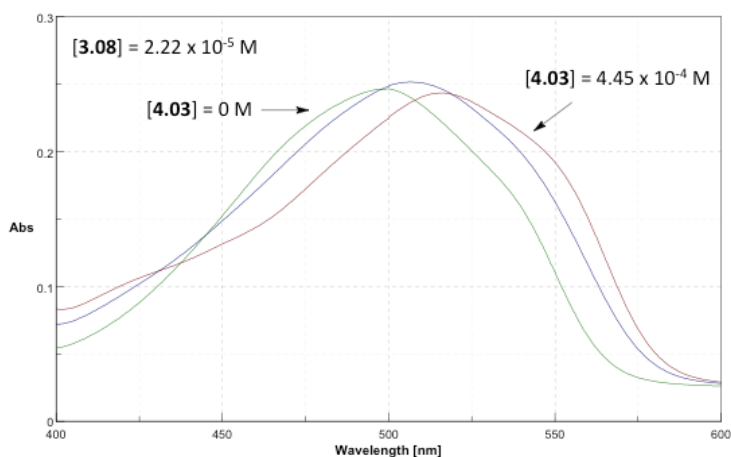
Figure 4.1 UV-titration of sensor **3.08** in CH_2Cl_2 with increasing amounts of **4.03**.

The appearance of a red shift indicates an alternate binding mode of the donor to the sensor chromophore. Since the N-7 nitrogen lone-pair is delocalized as a formally

vinylogous amide, interactions via the N-1 lone pair most likely account for the observed absorption behavior (Scheme 4.2). Further support for this interaction is provided by the hydrogen-bond found between N-1, which acts as the donor, to water in the solid state.[158]

Scheme 4.2 Proposed alternate binding interaction via N-1 of **3.08**.
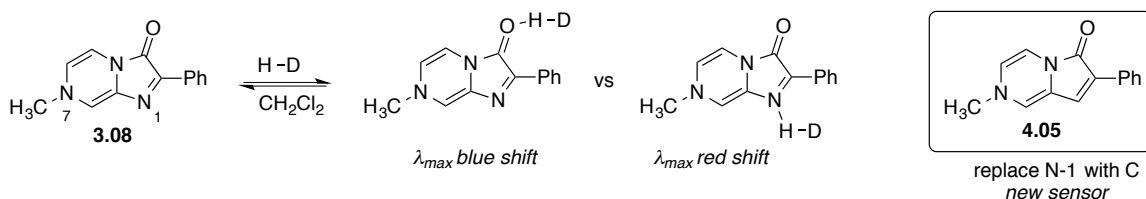
4.2. Investigation of a 2nd Generation Colorimetric Probe

4.2.1. Design and Synthesis

It was hypothesized that synthesis of compound **4.05**, which is identical in structure to **3.08** except for the replacement of the N-1 nitrogen with carbon, would obviate the competitive binding while maintaining the desired optical properties. Examples of synthetic routes to the central pyrrolo[1,2-*a*]pyrazin-6-one core proved extremely limited. However, a key report by Taylor and Cheeseman found that formation of a mixed anhydride intermediate from quinoxaline **4.06** triggered a cyclization sequence, resulting in pyrrolo[1,2-*a*]quinoxaline **4.07** (Scheme 4.3).[159] Consequently, it was envisioned that the desired compound **4.05** could be prepared via similar acetylation of an acid intermediate **4.12** and subsequent *N*-methylation (Scheme 4.4).

158) Hirano, T.; Sekiguchi, T.; Hashizume, D.; Ikeda, H.; Maki, S.; Niwa, H. "Colorimetric and fluorometric sensing of the Lewis acidity of a metal ion by metal-ion complexation of imidazo[1,2-*a*]pyrazin-3(7*H*)-ones" *Tetrahedron* **2010**, *66*, 3842-3848.
159) Taylor, E. C.; Cheeseman, G. W. H. "Synthesis and Properties of Pyrrolo(1,2-*a*)quinoxalines" *J. Am. Chem. Soc.* **1964**, *86*, 1830-1835.

Scheme 4.3 Taylor's cyclization for the synthesis of pyrrolo[1,2-*a*]quinoxaline **4.07**.
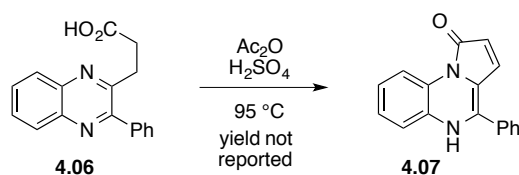
Scheme 4.4 Proposed retrosynthetic approach for pyrrolo[1,2-*a*]pyrazinone **4.05**.
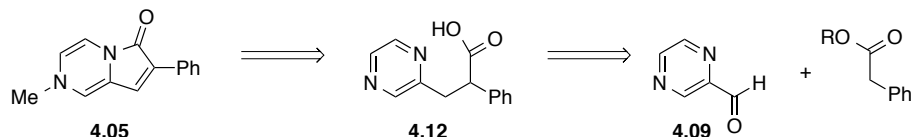
The synthesis of **4.05**, starting from commercially available pyrazinecarboxylic acid, is shown in Scheme 4.5. Fischer esterification and subsequent reduction afforded known aldehyde **4.09**, which was then treated with methyl phenylacetate in a 3-step Knoevenagel condensation sequence. Hydrogenation of alkene **4.10** and saponification afforded the key acid intermediate **4.12**. Treatment with acetic anhydride rapidly yielded a bright orange colored intermediate, proposed to be the acetylated intermediate **4.13**. Methanolysis of this intermediate provided the desired pyrrolo[1,2-*a*]pyrazinone **4.14**. Finally, *N*-methylation under typical conditions afforded desired compound **4.05** as a deep red solid possessing a single broad absorption band in CH_2Cl_2 centered at 493 nm.

Scheme 4.5 Synthesis of proposed sensor **4.05**.
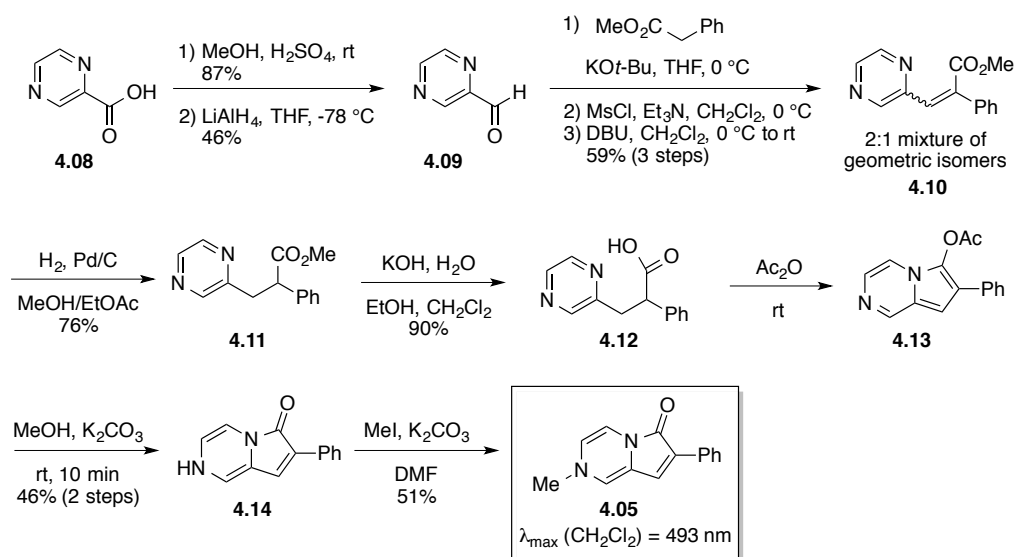
4.2.2. Solvatochromism and Initial Studies with Brønsted and Lewis Acids

Chromophore **4.05** exhibited strong solvatochromic behavior, similar to that reported for compound **3.08**. Significantly, **4.05** displayed increasing blue shifts with protic solvents. A more quantitative analysis is illustrated by comparison of the λ_{max} observed for a solvent with its Kamlet-Taft α value, an established metric for gauging the hydrogen-bond donating capability of a solvent.[160] The high correlation seen in Figure 4.2 provides evidence that compound **4.05** is sensitive to hydrogen-bond donation and affords corresponding blue shifts. Conversely, the other Taft parameters β (hydrogen-bond basicity) and π^* (polarizability) do not track well with λ_{max} (Table 4.2).

---

160) Kamlet, M. .; Abboud, J.-L. M.; Abraham, M. H.; Taft, R. W. "Linear Solvation Energy Relationship. 23. A Comprehensive Collection of the Solvatochromic Parameters, π^*, α, and β, and Some Methods for Simplifying the Generalized Solvatochromic Equation" *J. Org. Chem.* **1983**, *48*, 2877-2887.
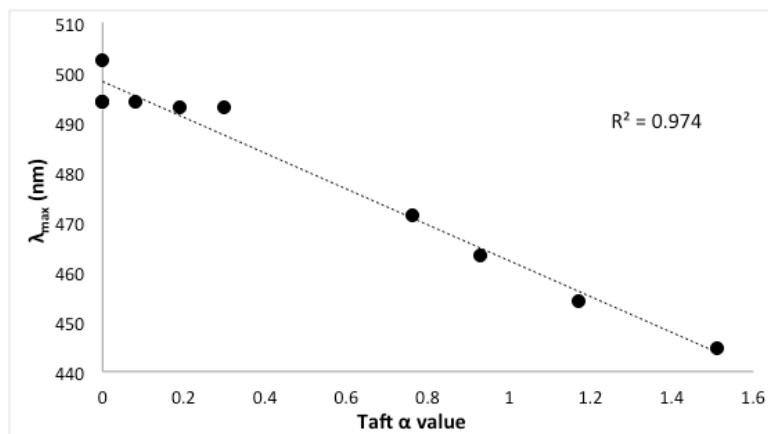
Figure 4.2 Correlation of solvatochromism and α Taft parameter for **4.05**

Table 4.2 Comparison of solvatochromism and solvent Taft parameters for **4.05**.

solvent	λ_{max} (nm)	α **(Taft)**	β (Taft)	π* (Taft)
DMSO	502.4	**0**	0.45	0.55
EtOAc	494.0	**0**	0.76	1
1,4-dioxane	494.0	**0**	0.37	0.55
acetone	494.0	**0.08**	0.48	0.71
MeCN	493.0	**0.19**	0.31	0.75
CH_2Cl_2	493.0	**0.30**	0	0.82
i-PrOH	471.2	**0.76**	0.95	0.48
MeOH	463.2	**0.93**	0.62	0.6
H_2O	454.2	**1.17**	0.18	1.09
2,2,2-trifluoroethanol	444.8	**1.51**	0	0.73

Gratifyingly, treatment of new sensor **4.05** with Brønsted acids **4.01-4.04** uniformly resulted in strong blue shifts; no red shifts were observed. Consequently, the UV absorption appears only to be perturbed via interaction with the carbonyl acceptor. With this chromophore, addition of binders gave rise to dramatic wavelength shifts of ~70 nm, along with a steady increase of a separate absorption band at 390 nm. A representative UV spectrum of **4.05** with increasing amounts of **4.03** is shown Figure 4.3.
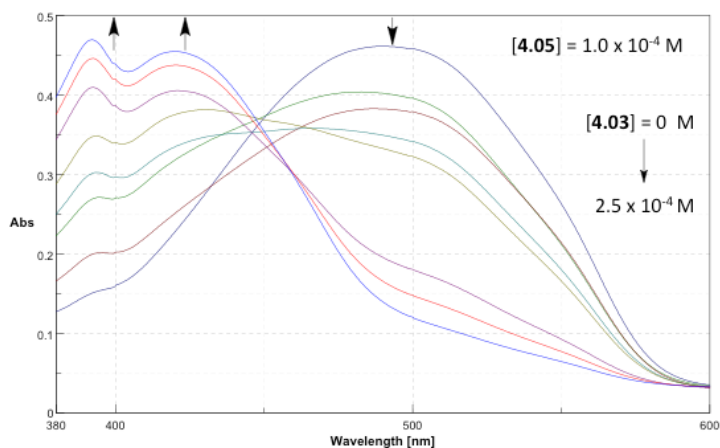
Figure 4.3 UV-titration of sensor **4.05** in CH_2Cl_2 with increasing amounts of **4.03**.

Table 4.3 Blue shifts of **4.05** upon addition of various Brønsted acids.

[4.05] = 1.0 x 10^{-4} M
λ_{max} (nm) = 493 nm

Brønsted Acid	saturated λ_{max} (nm)
4.01	424
4.02	420
4.03	420
4.04	~414

As shown in Table 4.3, the results with a limited number of Brønsted acids indicates that although the expected blue shift is indeed observed, the resulting saturated λ_{max} values span only a small range. A possible hypothesis accounting for this behavior is that these compounds are capable of full protonation of the sensor, resulting in a uniform change in the n to π* electronic transition. Again, the wavelength shifts are not predictive of catalyst activity based on the previously determined reaction rates. Preliminary studies of the new sensor with a variety of Lewis Acids, including a range of lanthanide triflate, were undertaken, using acetonitrile as the solvent to improve solubility of the metal salts. Overall, similar results were found compared to the Brønsted Acids, with appearance of broad absorption bands at λ_{max} ~ 430 or 419 along with increase in

abs at 390. Unfortunately, the relatively narrow range of wavelength endpoints currently prevents this signal from being useful for differentiation of Lewis acid strengths.

Table 4.4 Blue shifts of **4.05** upon addition of various Lewis acids.

[**4.05**] = 8.0 x 10^{-5} M
λ_{max} (nm) = 493 nm

Lews Acid	saturated λ_{max} (nm)	Lews Acid	saturated λ_{max} (nm)
Pr(OTf)$_3$	437	Dy(OTf)$_3$	434
Nd(OTf)$_3$	434	Yb(OTf)$_3$	432
Sm(OTf)$_3$	436	Sc(OTf)$_3$	418
Eu(OTf)$_3$	432	In(OTf)$_3$	~410

4.3. Conclusions and Future Efforts

Attempts to measure the activating effects of Brønsted acids with the original colorimetric sensor resulted in unanticipated red shifts due to a change in observed binding interactions. A new probe was constructed, altering the hypothesized binding acceptor site with a benign methylene unit. Although the new chromophore **4.05** exhibited a return to the originally predicted blue shifts upon treatment with either Lewis or Brønsted Acids, the magnitude of the signal could not discern between the different binders. Consequently, the wavelength shift does not appear to be a useful signal for measuring binding strengths of these catalysts. In comparison to the first sensor, **4.05** is more electron-rich due to the replacement of the N-1 nitrogen. This substitution results in a more active acceptor partner, and along with putatively stronger donors (i.e. Brønsted/Lewis Acids), may explain the observed plateauing of the new sensor signal.

Immediate efforts are focused on the measurement of binding constants of Brønsted acids with the new sensor as a comparative metric with k_{rel} values. Although similar λ_{max} endpoints are observed, the amount of catalyst needed to saturate the sensor varies, and hence the binding equilibrium may serve as a reasonable signal. Alternatively, future efforts may focus on modifications of the sensor structure to alter its binding activity while retaining its optical properties. Specifically, synthesis of an electron-deficient sensor is anticipated to provide better differentiation of the stronger activators. Thus, affecting the activity of the pseudo-amide carbonyl is critical, and modulation of this activity must be engendered without addition of other possible binding modalities. For example, an analogue with a perfluorinated aryl ring may be a worthwhile target. However, concerns regarding the aryl *ortho*-substitution, potentially rotating the aryl group out of plane or increasing steric interaction of binders, are warranted. Substitution of the N-7 group with an electron-withdrawing moiety would strongly attenuate the basicity of the carbonyl oxygen, although this presents a synthetic challenge. Ultimately, the key challenge remains to synthesize a chemical tool capable of discerning between these activators and providing a measurable signal that correlates to empirical rate enhancement. If a single compound is not identified for successfully measuring the entire spectrum of activators, two probes may be used to create a unified metric, so long as their ranges overlap.

4.4 Experimental

General Considerations

All non-aqueous reactions were carried out under an atmosphere of argon. The solvents for the reactions and all measurements were freshly distilled prior to use: CH_2Cl_2 and MeCN were distilled from CaH_2, THF was distilled from sodium/benzophenone ketyl, and Et_3N was distilled from KOH. **4.02** (acetone) and **4.03** (EtOAc) were recrystallized and dried over vacuum prior to use.   Reactions were monitored by thin layer chromatography (TLC) using Silicycle glass-backed TLC plates with 250 μm silica and F254 indicator.   Visualization was accomplished with UV light, and/or 2,4-dinitrophenylhydrazine stain.   Flash column chromatography was performed using Silicycle Silaflash P60 silica gel (40-63 μm particle size). NMR spectra were recorded on Brüker AM-500, Brüker DRX-500, Brüker DMX-360, and Brüker DMX-300 Fourier transform NMR spectrometers.   Chemical shifts are reported relative to the solvent resonance peak δ 7.27 ($CDCl_3$) for ^{1}H NMR and δ 77.23 ($CDCl_3$) for ^{13}C.   NMR spectroscopic data were reported as follows: chemical shift, multiplicity (s = singlet, d = doublet, q = quartet, b = broad, m = multiplet), coupling constants and number of protons and compared with the references. All UV spectra were obtained using a JASCO FT/IR-480 Plus from 600 nm – 350 nm.

Pyrazine-2-carbaldehyde **4.09** was synthesized from reduction of the corresponding methyl ester according to the literature.[161]
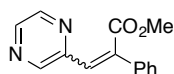
161) Ligiero, C. B. P.; Visentin, L. C.; Giacomini, R.; Filgueiras, C. A. L.; Miranda, P. C. M. L. "2,3,5,6-Tetra(pyrazin-2-yl)pyrazine: a novel bis-bidentate, bis-tridentate chelator" *Tetrahedron Lett*. **2009**, *50*, 4030-4032.

Methyl 2-phenyl-3-(pyrazin-2-yl)acrylate (4.10)

To a solution of aldehyde **4.09** (540 mg, 5.0 mmol) in THF (25 mL) at 0 °C was added methyl phenylacetate (775 μL, 5.5 mmol) followed by KO*t*-Bu (224 mg, 2.0 mmol). The reaction stirred at 0 °C for 1 h, whereupon sat aq NH_4Cl (25 mL) was added and the mixture was extracted with CH_2Cl_2 (3 x 30 mL). The combined organics were dried over Na_2SO_4, filtered, and concentrated to afford a ~5:1 mixture of alcohol diastereomers:alkene by ^{1}H NMR. The crude material was dissolved in CH_2Cl_2 (16 mL), cooled to 0 °C, and Et_3N (0.65 mL, 4.7 mmol) was added, followed by dropwise addition of methanesulfonyl chloride (0.38 mL, 4.7 mmol). After stirring for 30 min at 0 °C, the reaction was quenched with sat aq NH_4Cl (25 mL) and extracted with CH_2Cl_2 (3 x 25 mL). The combined organics were dried over Na_2SO_4, filtered, and concentrated to afford a ~5:1 mixture of mesylate diastereomers:alkene by ^{1}H NMR. The crude material was dissolved in CH_2Cl_2 (16 mL), cooled to 0 °C, and DBU (0.70 mL, 4.7 mmol) was added over 10 min. The reaction was warmed to rt and stirred for 1 h, whereupon sat aq NH_4Cl (20 ml) was added, and the mixture was extracted with CH_2Cl_2 (3 x 20 mL). The combined organics were dried over Na_2SO_4, filtered, and concentrated. Purification by chromatography (1% to 2% $MeOH/CH_2Cl_2$) afforded the title compound as a 2:1 mixture of geometric isomers by ^{1}H NMR as a white solid (711 mg, 59% over 3 steps): mp: 72-81 °C; ^{1}H NMR (500 MHz, $CDCl_3$) major isomer: δ 8.53-8.55 (m, 1H), 8.32 (d, J = 2.5 Hz, 1H), 7.98 (d, J = 1.5 Hz, 1H), 7.88 (s, 1H), 7.55-7.59 (m, 1H), 7.37-7.41 (m, 3H), 7.21-7.24 (m, 1H), 3.85 (s, 3H); ^{13}C NMR (125 MHz, $CDCl_3$) δ 169.8, 167.6, 150.6, 149.4, 146.1, 145.3, 144.5, 144.2, 143.5, 143.1, 140.4, 137.8, 137.4, 135.4, 134.7, 129.7, 129.6, 129.2, 129.1, 128.9, 126.6, 123.4, 53.0, 52.6; IR (film) 3060, 3002, 2950, 1717, 1434,

1363, 1257, 1227, 1203, 1173, 1143, 1019 cm^{-1}; HRMS (ESI) calcd for C$_{14}$H$_{13}$N$_2$O$_2$ [M+H]$^+$, *m/z* = 241.0977; found 241.0983.
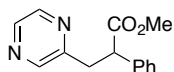
Methyl 2-phenyl-3-(pyrazin-2-yl)propanoate (4.11)

To a solution of **4.10** (121 mg, 0.50 mmol) in MeOH (3 mL) and EtOAc (3 mL) was added palladium on carbon (10 wt%, 15 mg), and the solution was sparged with hydrogen for 5 min. The reaction stirred at rt under hydrogen pressure (balloon) for 24 h, after which the mixture was filtered through Celite and concentrated. Purification by chromatography (2% MeOH/CH$_2$Cl$_2$) afforded the title compound as a white solid (92.3 mg, 76%): mp: 105-106 °C; ^{1}H NMR (500 MHz, CDCl$_3$) δ 8.44 (s, 1H), 8.32-8.35 (m, 2H), 7.19-7.29 (m, 5H), 4.23 (dd, *J* = 9.0, 6.4 Hz, 1H), 3.61 (dd, *J* = 14.7, 9.1 Hz, 1H), 3.59 (s, 3H), 3.16 (dd, *J* = 14.7, 6.4 Hz, 1H); ^{13}C NMR (125 MHz, CDCl$_3$) δ 173.6, 154.7, 145.3, 144.1, 142.6, 138.3, 129.0, 128.0, 127.7, 52.3, 50.4, 38.8; IR (film) 3029, 2950, 1727, 1428, 1228, 1167, 1018 cm^{-1}; HRMS (ESI) calcd for C$_{14}$H$_{14}$N$_2$O$_2$Na [M+Na]$^+$, *m/z* = 265.0953; found 265.0954.
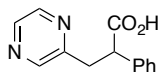
2-Phenyl-3-(pyrazin-2-yl)propanoic acid (4.12)

To a solution of **4.11** (45.6 mg, 0.188 mmol) in 95% EtOH (0.80 mL) and CH$_2$Cl$_2$ (0.20 mL) at 0 °C was added a solution of KOH (106 mg, 1.88 mmol) in water (0.80 mL). The resulting mixture was allowed to warm to rt and stirred vigorously at rt for 45 min,

whereupon it was poured into 1 M HCl (15 mL) and extracted with CH_2Cl_2 (3 x 15 mL). The combined organics were dried over Na_2SO_4, filtered, and concentrated. Purification by chromatography (2% to 4% MeOH/CH_2Cl_2) afforded the title compound as a white solid (29.3 mg, 68%): mp: 119-122 °C; ^{1}H NMR (500 MHz, CDCl$_3$) δ 11.43 (bs, 1H), 8.51 (s, 1H), 8.38 (s, 2H), 7.23-7.35 (m, 5H), 4.26 (dd, J = 8.9, 6.4 Hz, 1H), 3.64 (dd, J = 14.3, 8.9 Hz, 1H), 3.20 (dd, J = 14.6, 6.5 Hz, 1H); ^{13}C NMR (125 MHz, CDCl$_3$) δ 177.1, 155.1, 144.9, 144.3, 142.2, 138.1, 129.1, 128.1, 127.9, 50.5, 38.5; IR (film) 3030, 2928, 1718, 1406, 1232, 1174, 1132 cm^{-1}; HRMS (ESI) calcd for $C_{13}H_{13}N_2O_2$ [M+H]$^+$, m/z = 229.0977; found 229.0984.
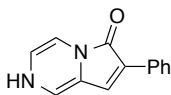
7-Phenylpyrrolo[1,2-*a*]pyrazin-6(2*H*)-one (4.14)

4.12 (90 mg, 0.39 mmol) was placed in a 20-dram vial and suspended in acetic anhydride (8.0 mL), resulting in formation of an orange precipitate within 10 min. After stirring for 1.5 h, the mixture was diluted with Et$_2$O (10 mL) and filtered, washing with Et$_2$O to afford 66 mg of crude acetylated intermediate **4.13** as tentatively assigned on the basis of ^{1}H NMR and MS data. This crude product (36 mg, 0.143 mmol) was suspended in MeOH (6 mL), and K_2CO_3 (39 mg, 0.285 mmol) was added. The resulting deep red solution stirred for 5 min, whereupon sat aq NH_4Cl (10 mL) was added, and the mixture was extracted with CH_2Cl_2 (3 x 10 mL). The combined organics were dried over Na_2SO_4, filtered, and concentrated. Purification by chromatography (8% MeOH/CH_2Cl_2) afforded the title compound as a deep red solid (24.0 mg, 53 % over 2 steps): mp: 190-

191 °C (dec.); ^{1}H NMR (500 MHz, MeOD-d_4) δ 8.03-8.06 (m, 2H), 7.55 (d, J = 9.2 Hz, 2H), 7.38 (t, J = 7.8 Hz, 2H), 7.25 (tt, J = 7.6, 1.2 Hz, 1H), 7.20 (d, J = 6.1 Hz, 1H), 6.51 (dd, J = 6.1, 1.1 Hz, 1H) N–H not observed; ^{13}C NMR (125 MHz, MeOD-d_4) δ 157.0, 135.4, 129.6, 128.4, 128.1, 127.3, 126.0, 119.4, 115.3, 114.0, 110.8; IR (film) 3198, 2924, 2853, 1619, 1551, 1507, 1175, 1119 cm^{-1}; HRMS (ESI) calcd for $C_{13}H_{11}N_2O$ [M+H]$^+$, m/z = 211.0871; found 211.0873.
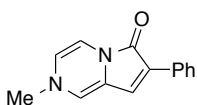
2-Methyl-7-phenylpyrrolo[1,2-a]pyrazin-6(2H)-one (4.05)

To a solution of **4.14** (17.0 mg, 0.081 mmol) in DMF (1.6 mL) was added methyl iodide (15 μL, 0.243 mmol) and K_2CO_3 (22.4 mg, 0.162 mmol). The resulting mixture stirred at rt for 15 min and an additional portion of methyl iodide (15 μL, 0.243 mmol) was added. After stirring an additional 20 min at rt, the reaction was quenched with water (15 mL) and extracted with CH_2Cl_2 (3 x 20 mL). The combined organics were washed with water (10 mL), dried over Na_2SO_4, filtered, and concentrated. Purification by chromatography (2% to 4% MeOH/CH_2Cl_2) afforded the title compound as a red solid (9.2 mg, 51%): mp: 169-170 °C (dec.); ^{1}H NMR (500 MHz, CDCl$_3$) δ 8.14 (d, J = 7.7 Hz, 2H), 7.41 (t, J = 7.7 Hz, 2H), 7.27-7.30 (m, 1H), 7.26 (s, 1H), 7.16 (d, J = 6.0 Hz, 1H), 6.74 (s, 1H), 5.87 (dd, J = 6.0, 1.1 Hz, 1H), 3.35 (s, 3H); ^{13}C NMR (125 MHz, CDCl$_3$) δ 156.8, 134.0, 128.7, 127.5, 127.0, 126.4, 125.8, 118.9, 115.8, 113.3, 110.7, 42.5; IR (film) 2924, 1671, 1594, 1484, 1420, 1135 cm^{-1}; HMRS (ESI) calcd for $C_{14}H_{13}N_2O$ [M+H]$^+$, m/z = 225.1028; found 225.1025.

UV-Titration Data

Titration of Brønsted Acids

Stock solutions of **3.08** (2.22×10^{-5} M) or **4.05** (1.0×10^{-4} M) were prepared in volumetric flasks via serial dilution in CH_2Cl_2. For each UV titration experiment, 500 µL of the stock sensor solution was transferred to a UV cuvette (Spectrosil Quartz Starna cell, 2 x 10 mm) and the level of the solution was demarcated. Aliquots of the catalyst stock solution were sequentially added and the initial volume was maintained by evaporation under an argon balloon to the demarcated line. The spectrum was measured after each addition, and the λ_{max} was recorded. Aliquots of the catalyst stock solution were added until the λ_{max} did not change further. Titration plots, and raw data for all catalysts can be found in Appendix D.

Titration of Lewis Acids

Stock solutions of Lewis Acid (5.0×10^{-2} M) were prepared by addition of the metal triflate (0.0125 mmol) and MeCN (250 µL) to a dry 1 d vial and sonicating. For $Pr(OTf)_3$, $Nd(OTf)_3$, and $Sm(OTf)_3$, slurries were formed. For each experiment, 400 µL of a stock solution of **4.04** (1.0×10^{-4} M) in MeCN was added to a UV cuvette, followed by 100 µL of the appropriate Lewis Acid stock solution. The UV absorption spectrum was measured, and the λ_{max} recorded.

APPENDIX A: Spectroscopic Data
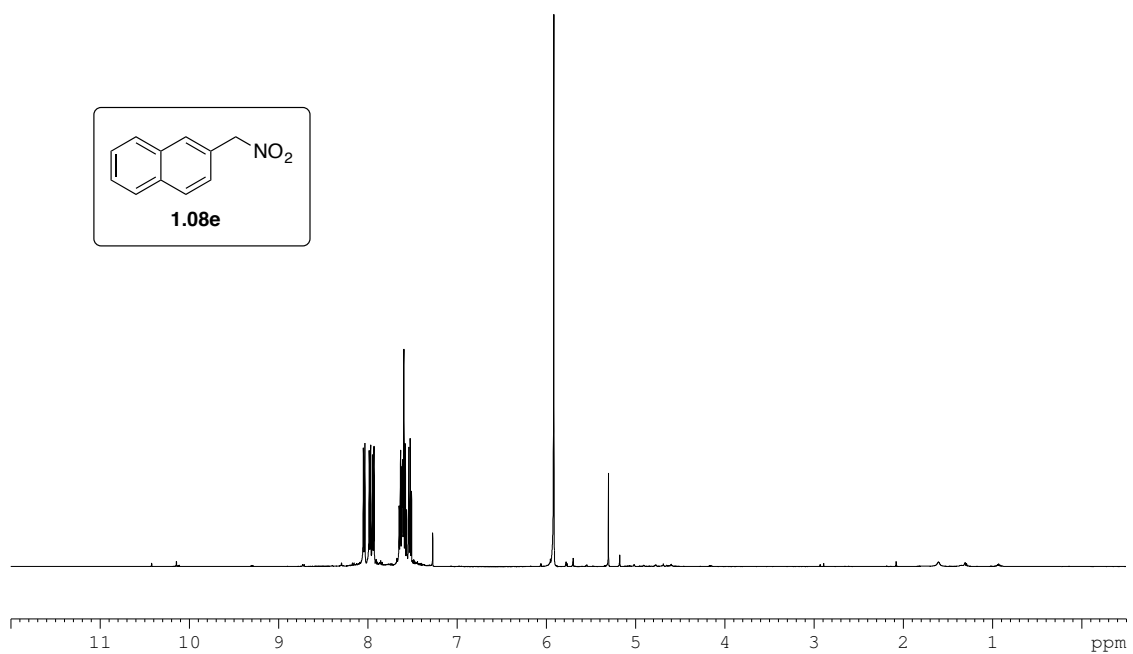
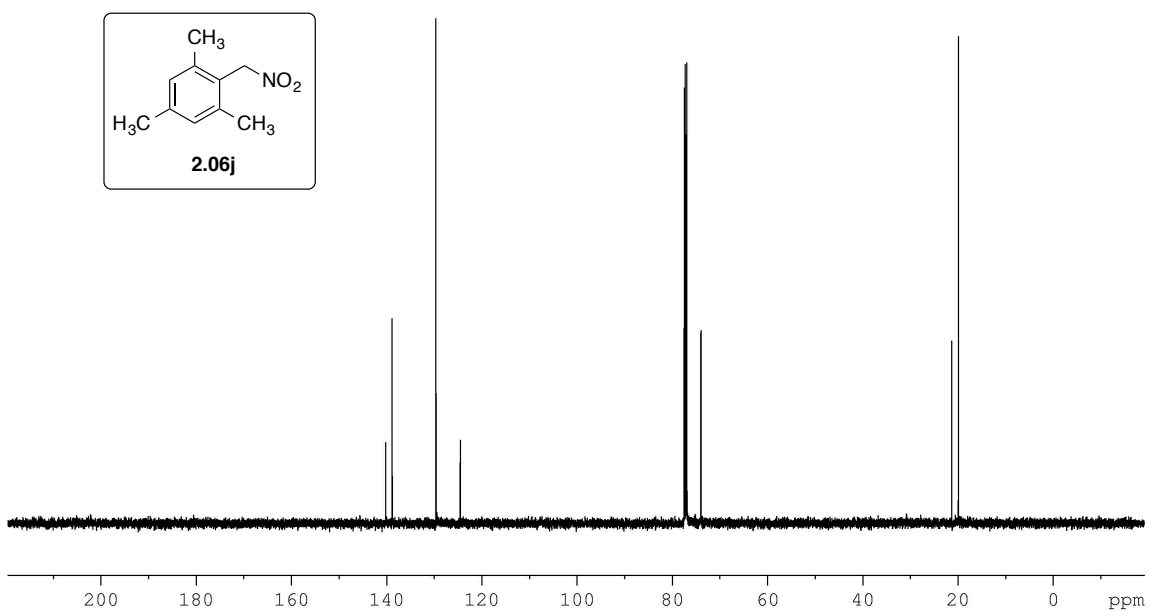**Figure A.1.08e_1** ^{1}H NMR spectrum of compound **1.08e** (500 MHz, CDCl$_3$).
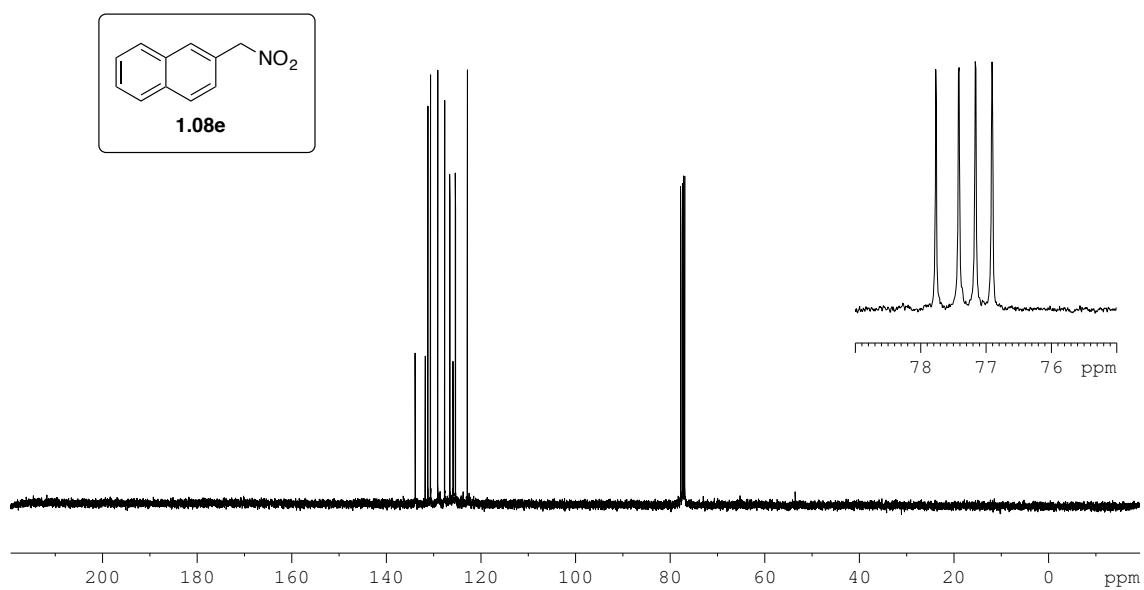
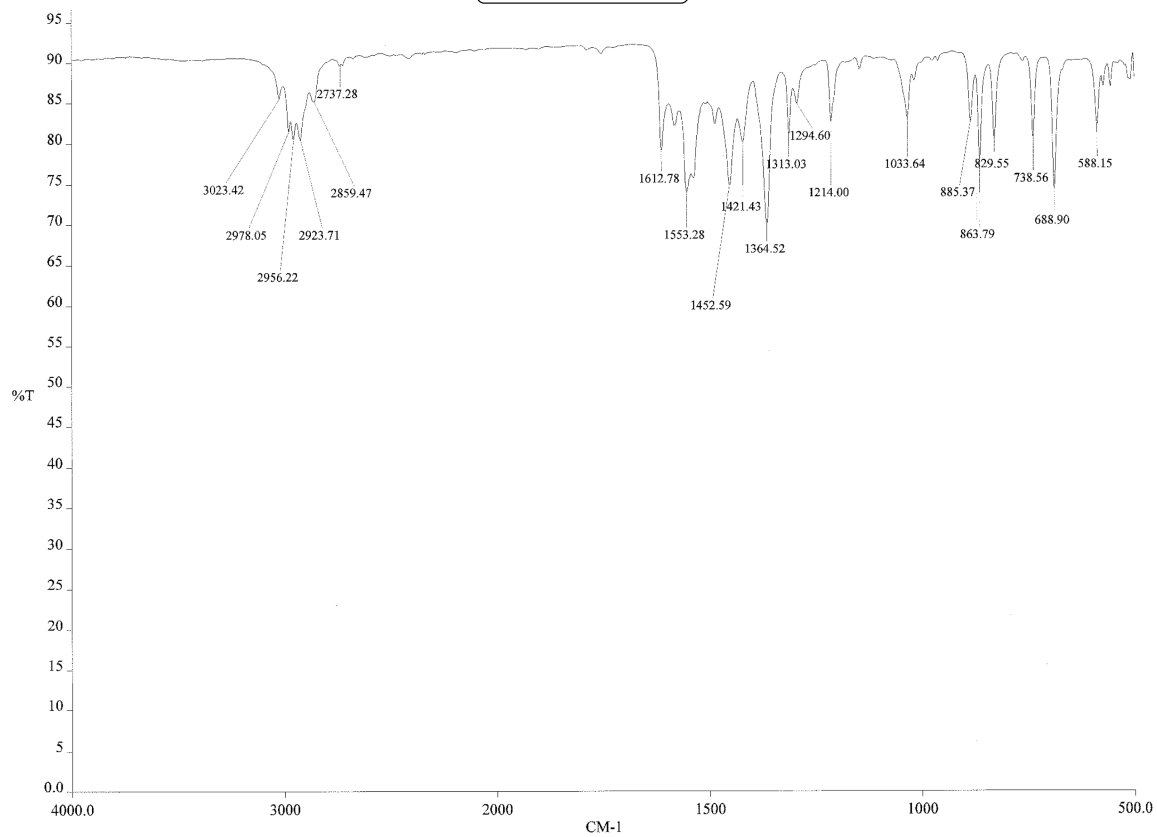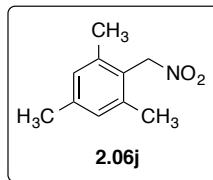**Figure A.1.08e_2** ^{13}C NMR spectrum of compound **1.08e** (125 MHz, CDCl$_3$).
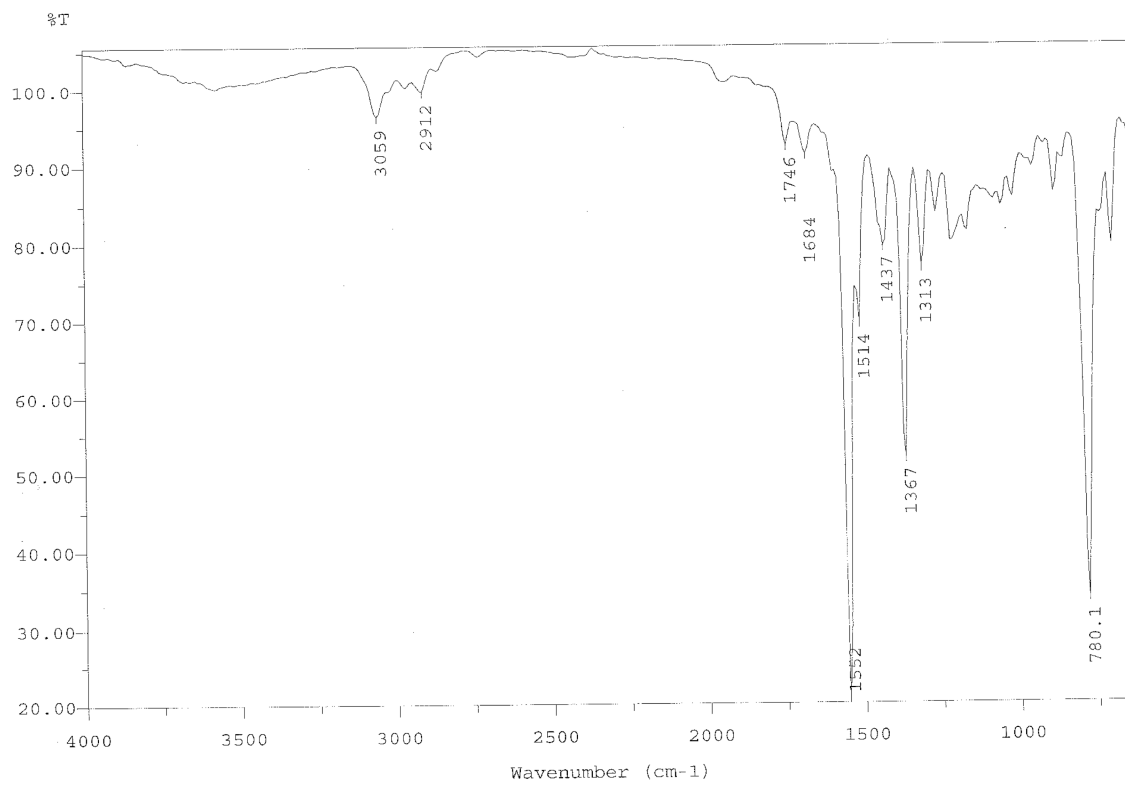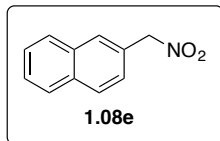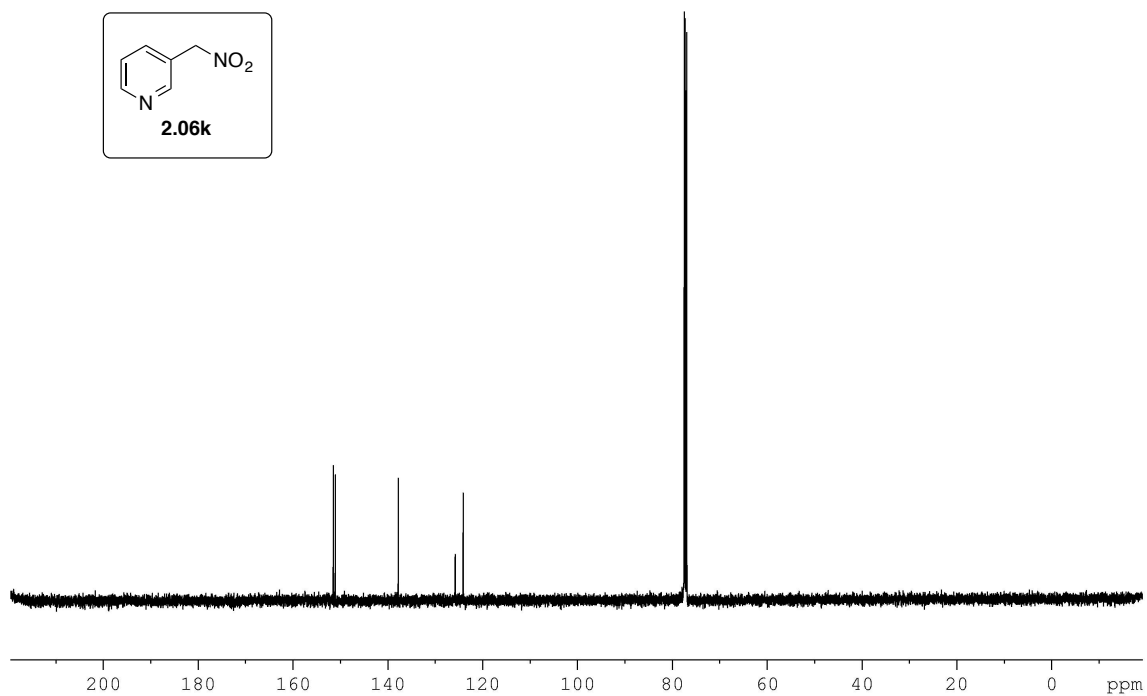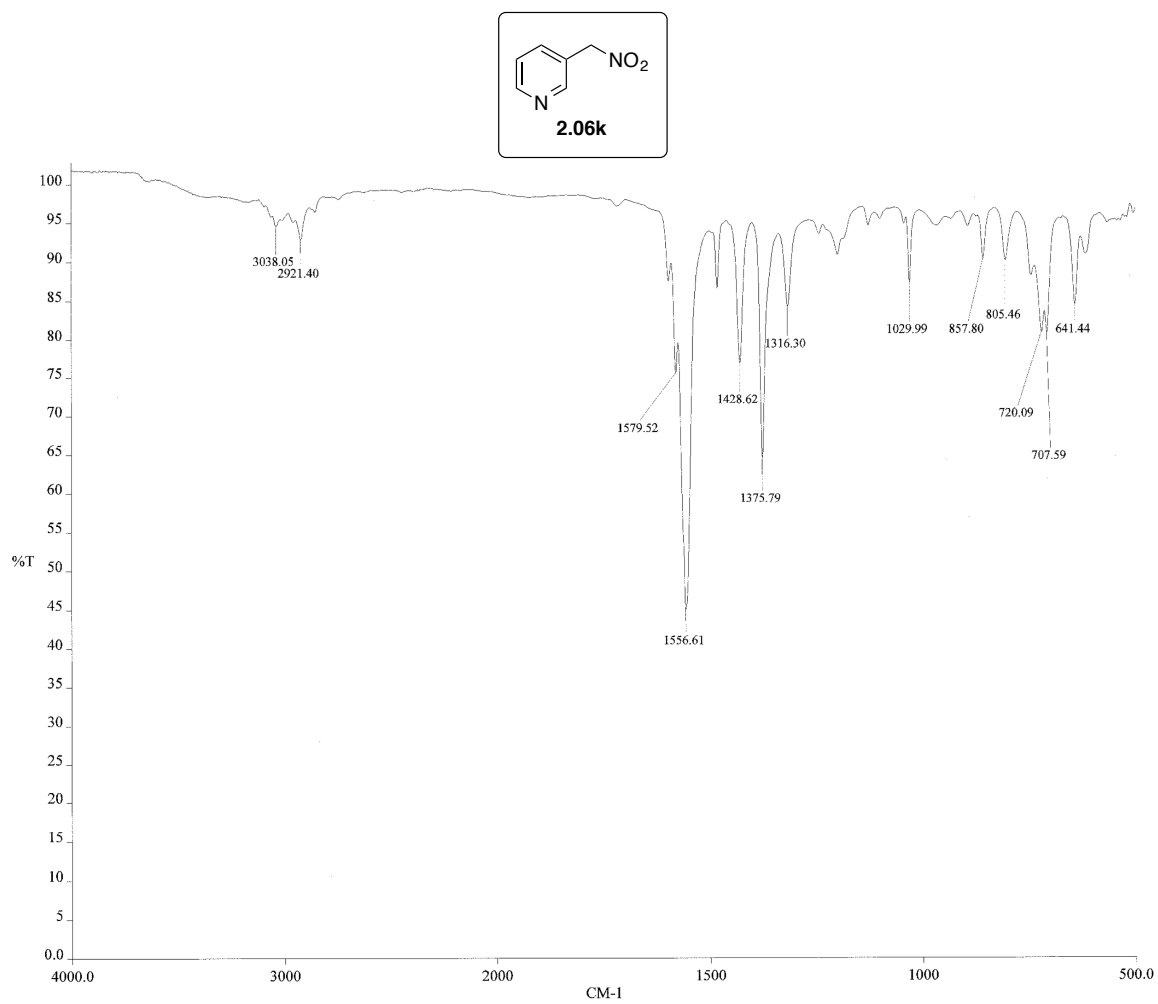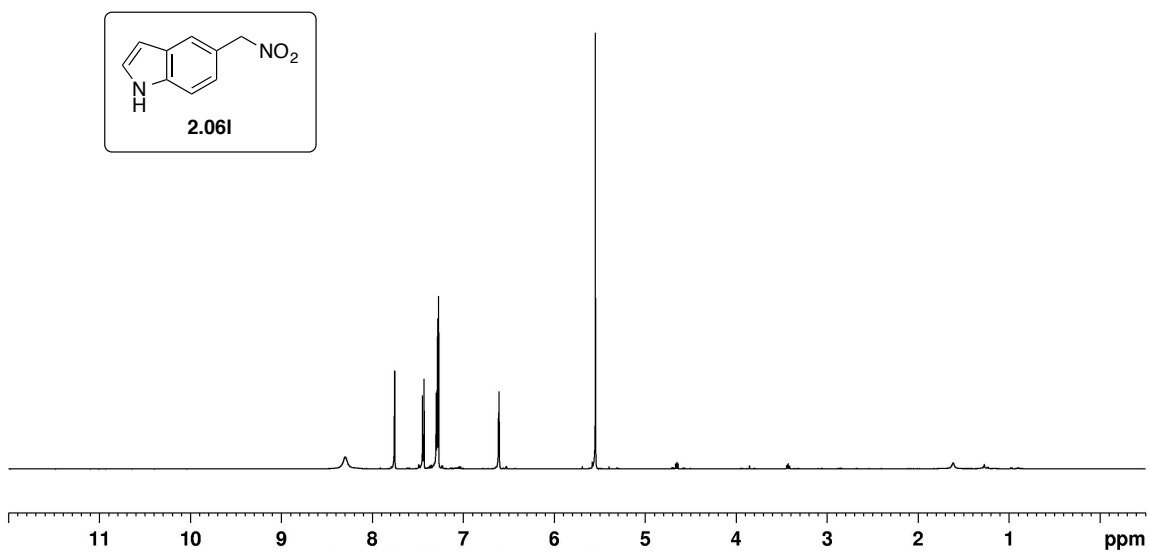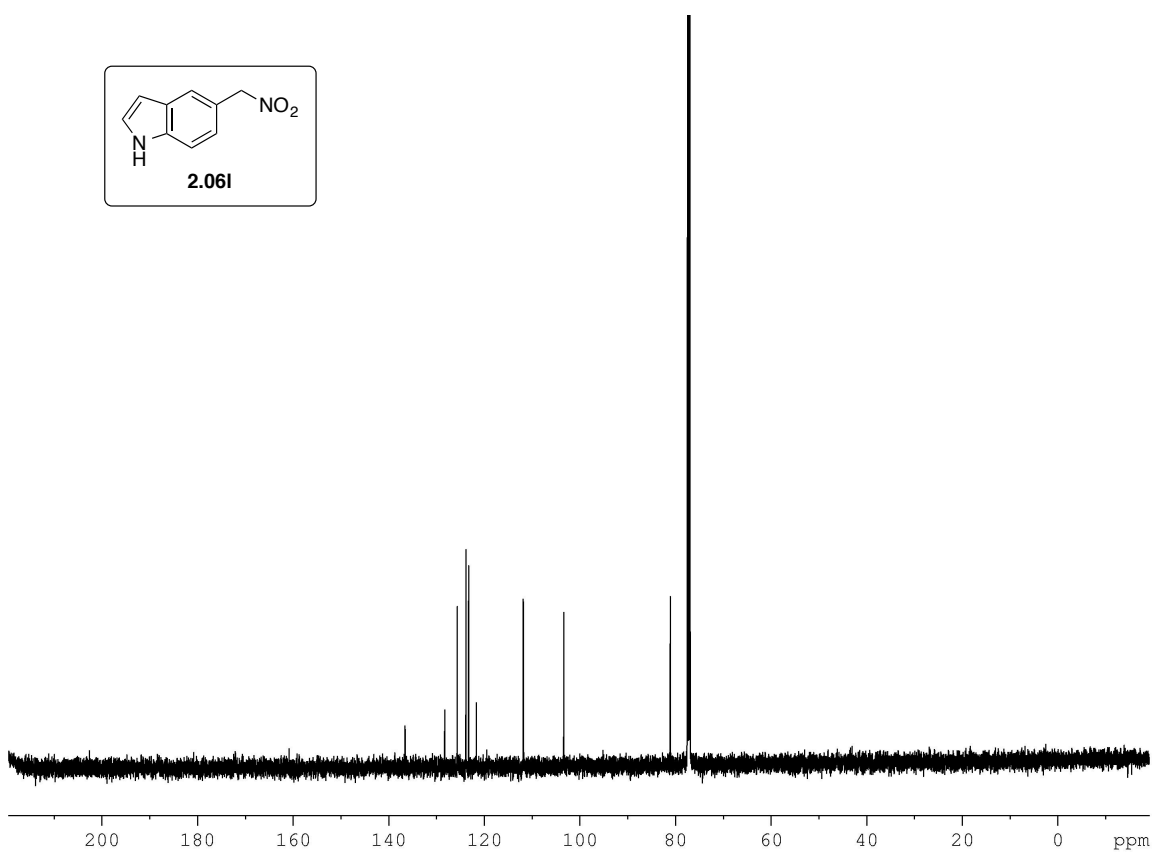
Figure A.1.08e_3 IR spectrum of compound **1.08e**.
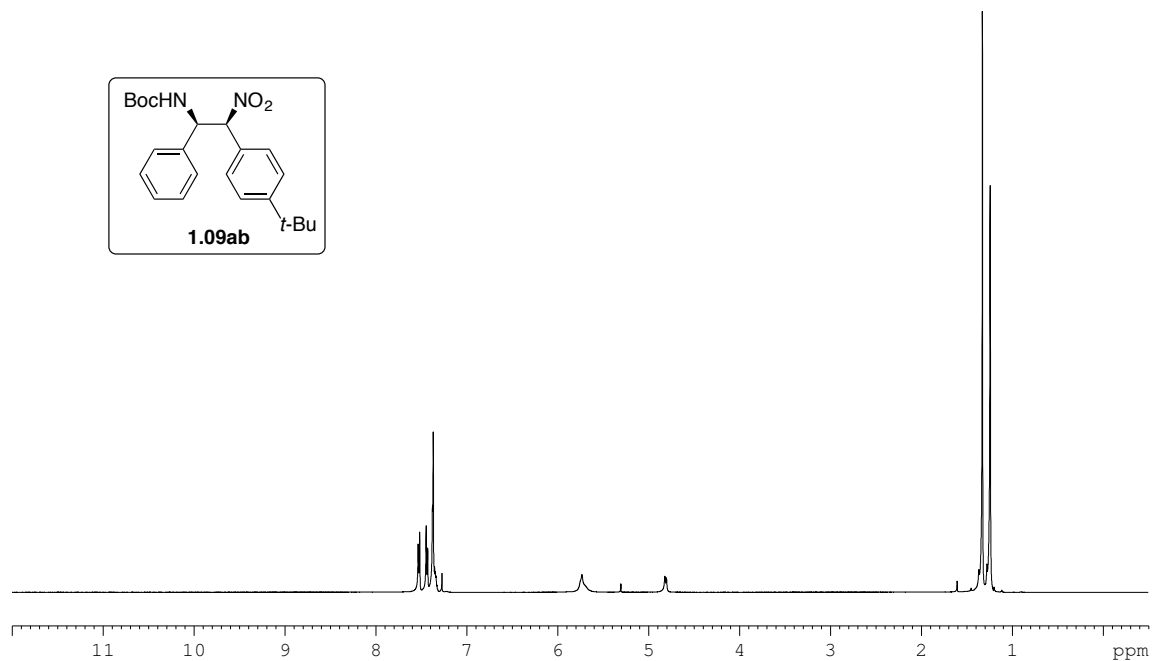
Figure A.1.09ab_1 ^{1}H NMR spectrum of compound **1.09ab** (500 MHz, CDCl$_3$).
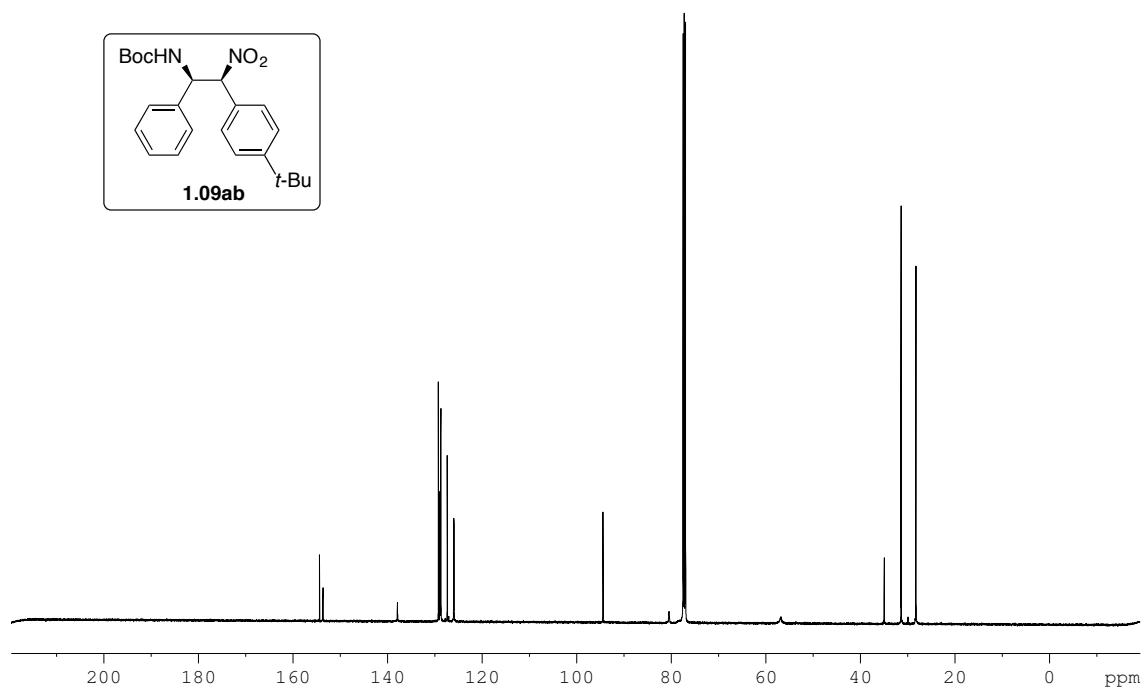
Figure A.1.09ab_2 ^{13}C NMR spectrum of compound **1.09ab** (125 MHz, CDCl$_3$).
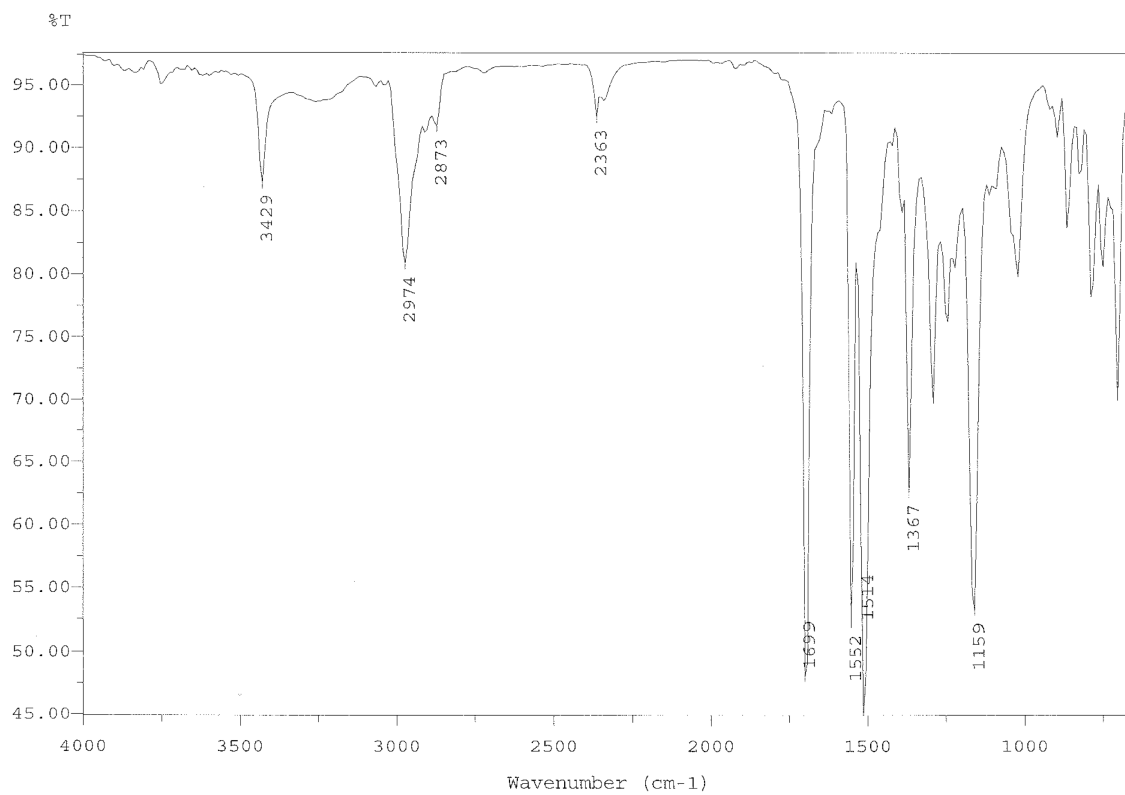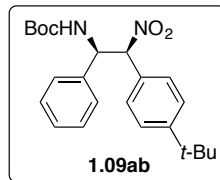
Figure A.1.09ab_3 IR spectrum of compound **1.09ab**.
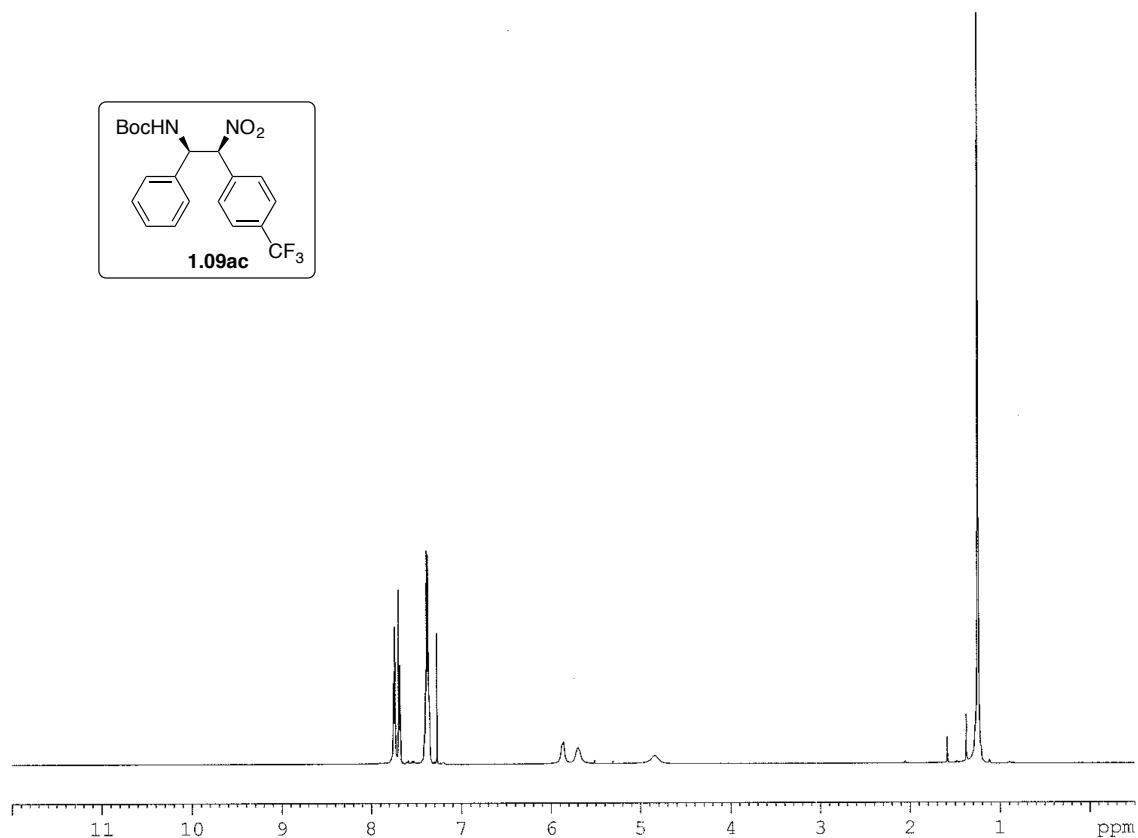
Figure A.1.09ac_1 ¹H NMR spectrum of compound **1.09ac** (500 MHz, CDCl₃).
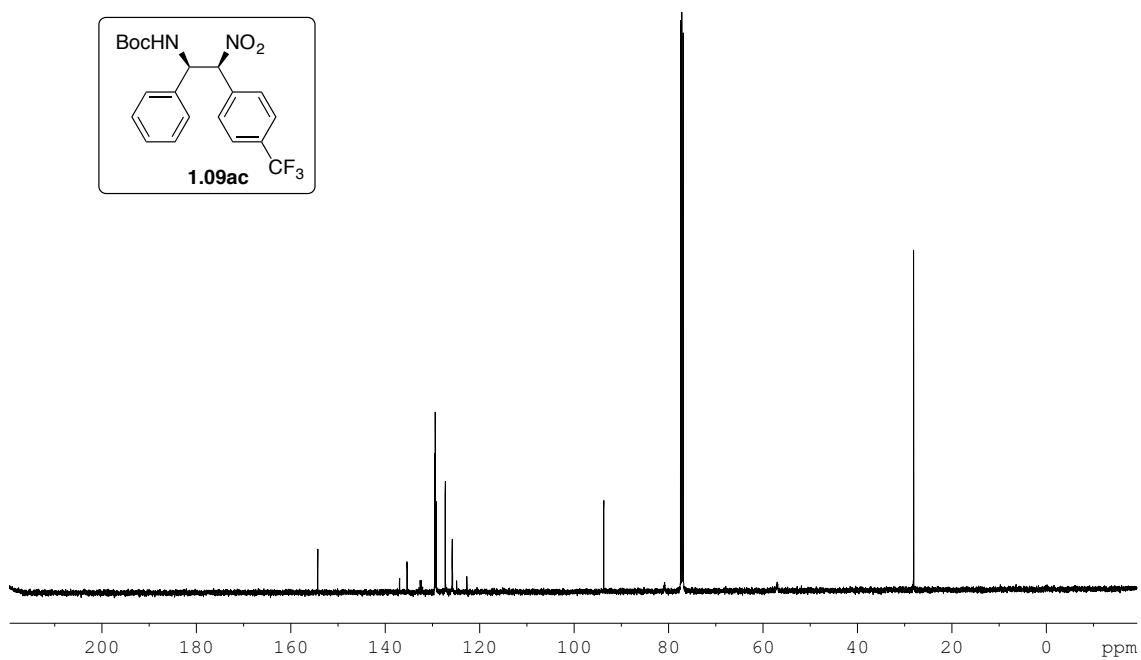
Figure A.1.09ac_2 ¹³C NMR spectrum of compound **1.09ac** (125 MHz, CDCl₃).
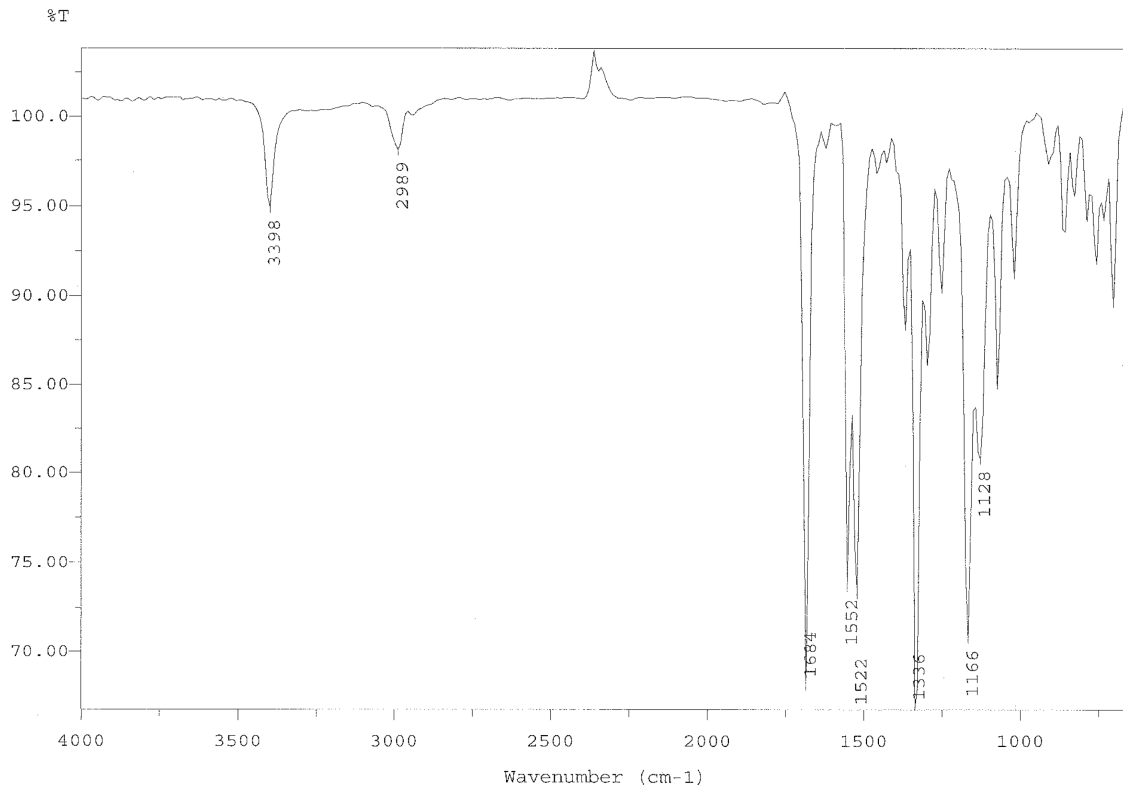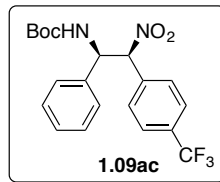
Figure A.1.09ac_3 IR spectrum of compound **1.09ac**.
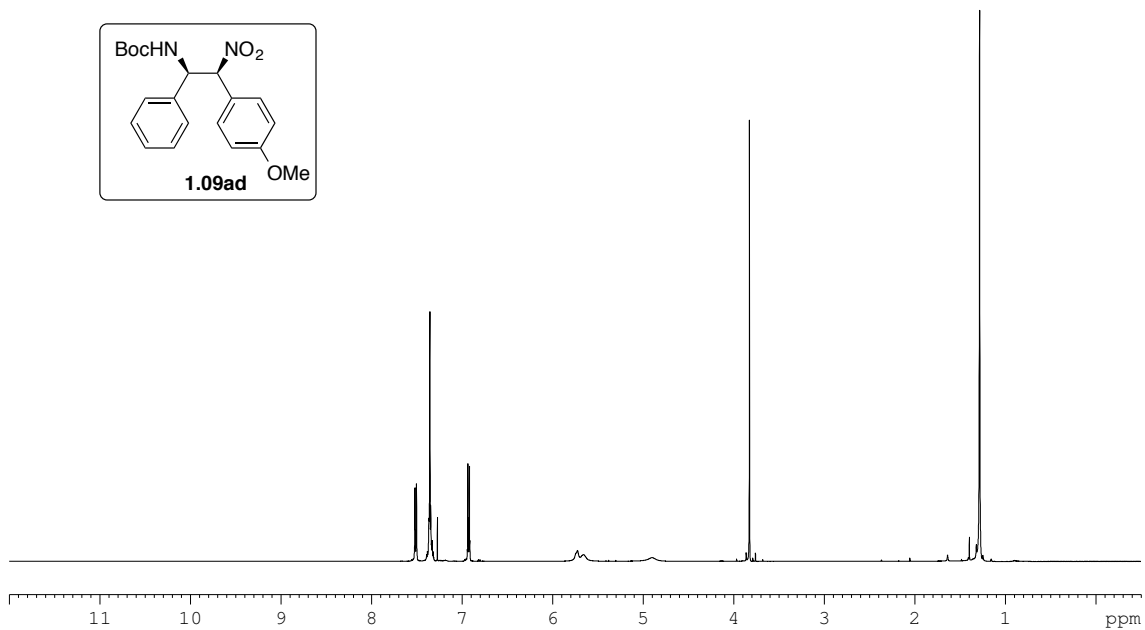
Figure A.1.09ad_1 ^{1}H NMR spectrum of compound **1.09ad** (500 MHz, CDCl$_3$).
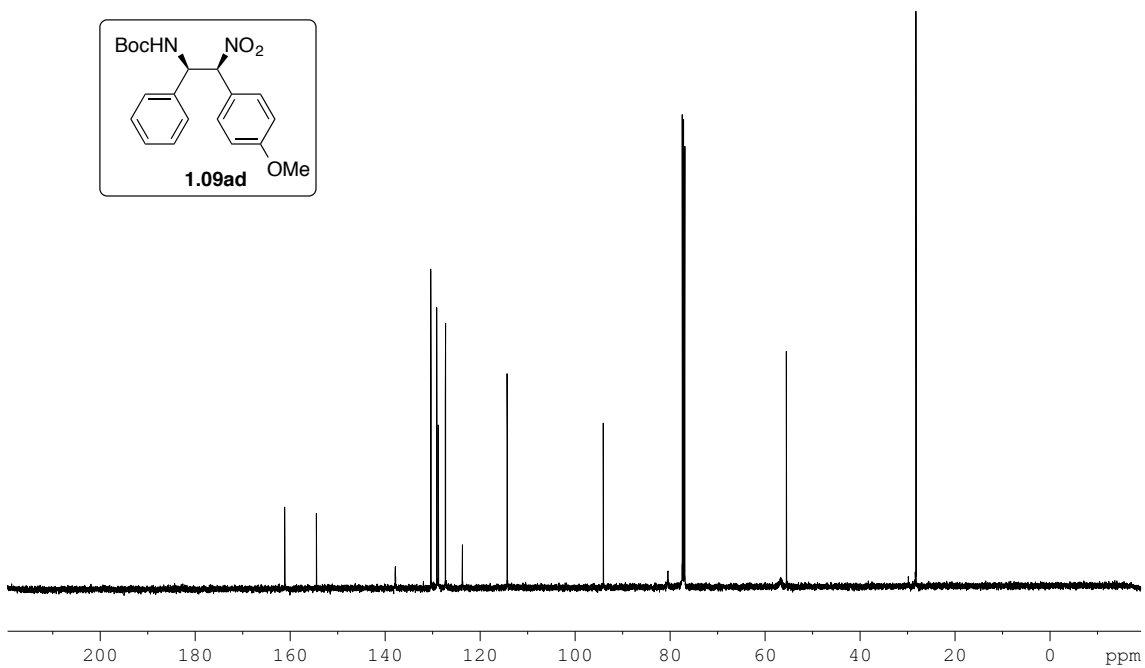
Figure A.1.09ad_2 ^{13}C NMR spectrum of compound **1.09ad** (125 MHz, CDCl$_3$).
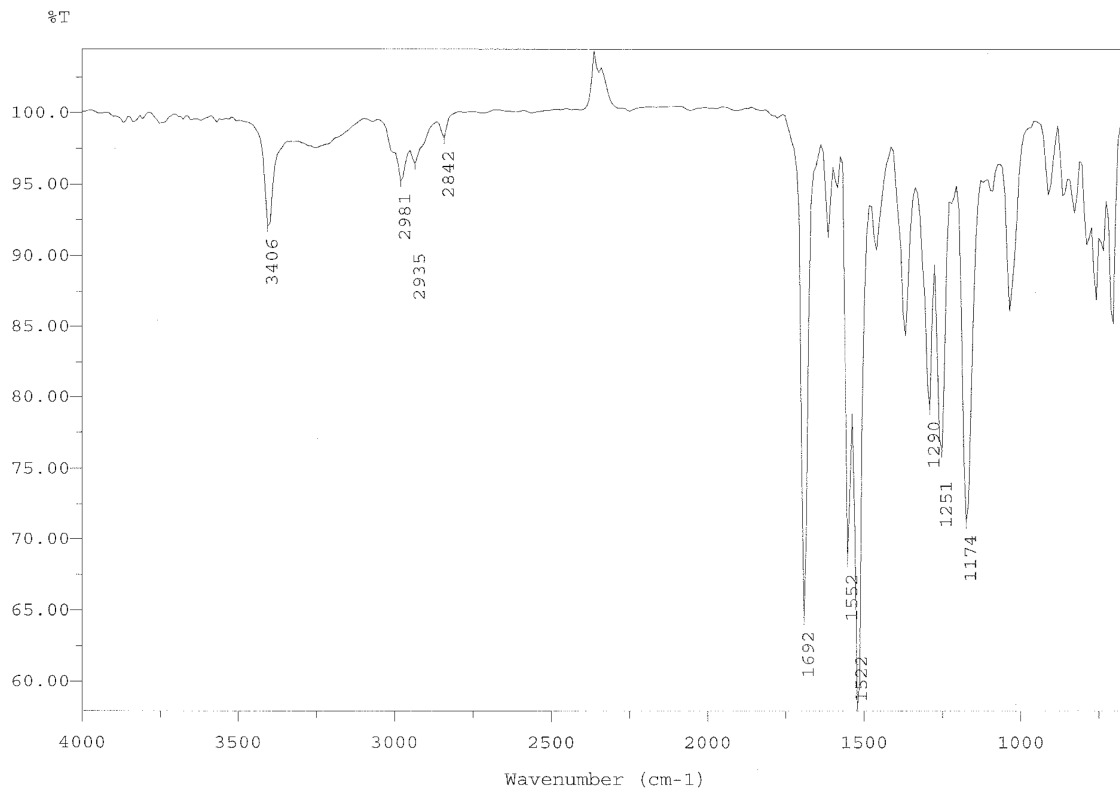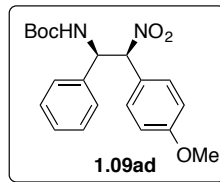
Figure A.1.09ad_3 IR spectrum of compound **1.09ad**.
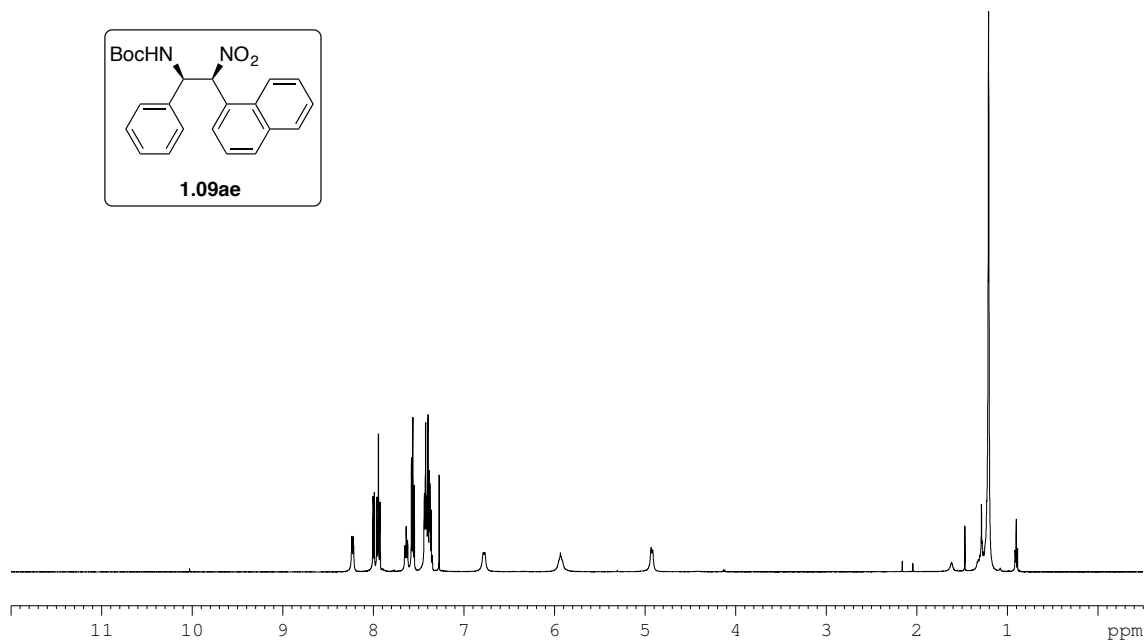
Figure A.1.09ae_1 ^{1}H NMR spectrum of compound **1.09ae** (500 MHz, CDCl$_3$).
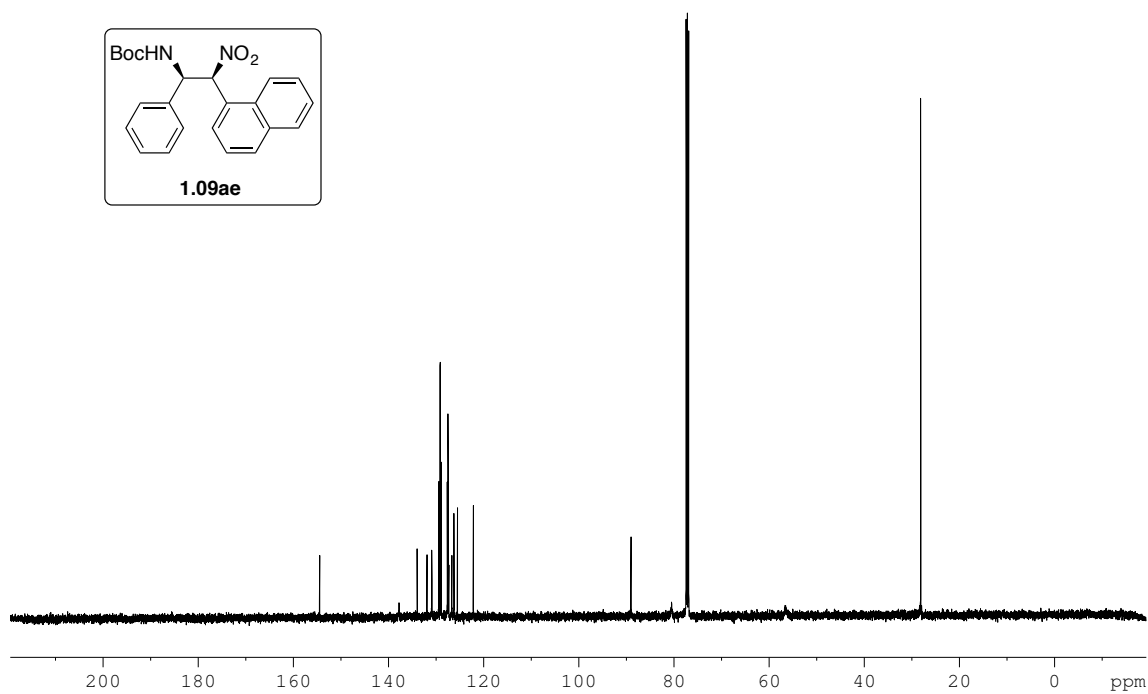
Figure A.1.09ae_2 ^{13}C NMR spectrum of compound **1.09ae** (125 MHz, CDCl$_3$).
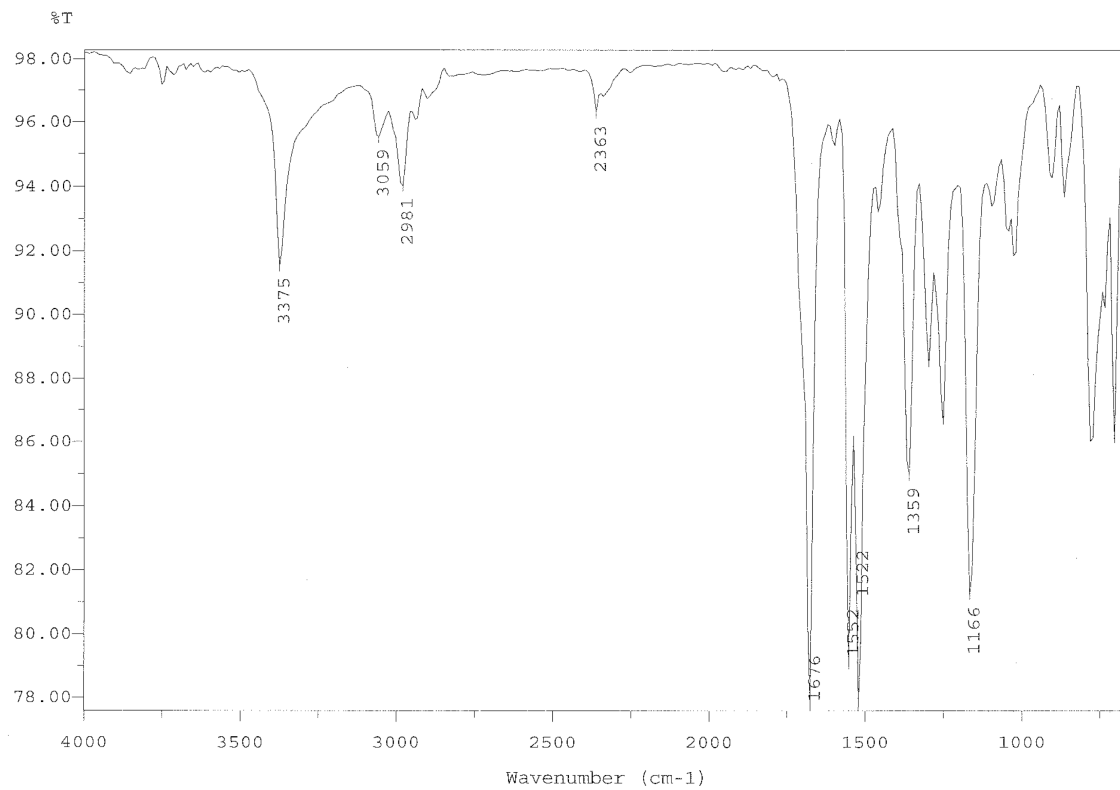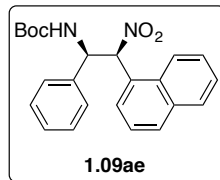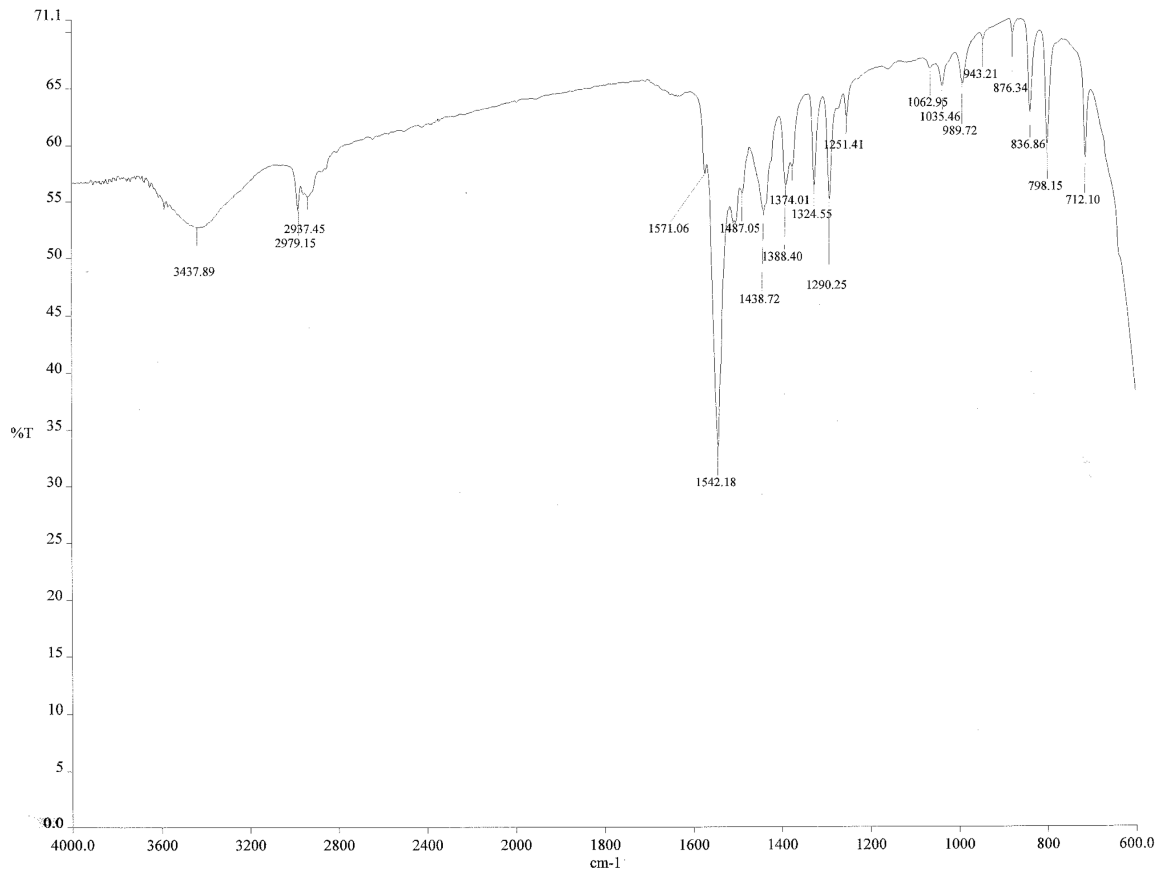
Figure A.1.09ae_3 IR spectrum of compound **1.09ae**.
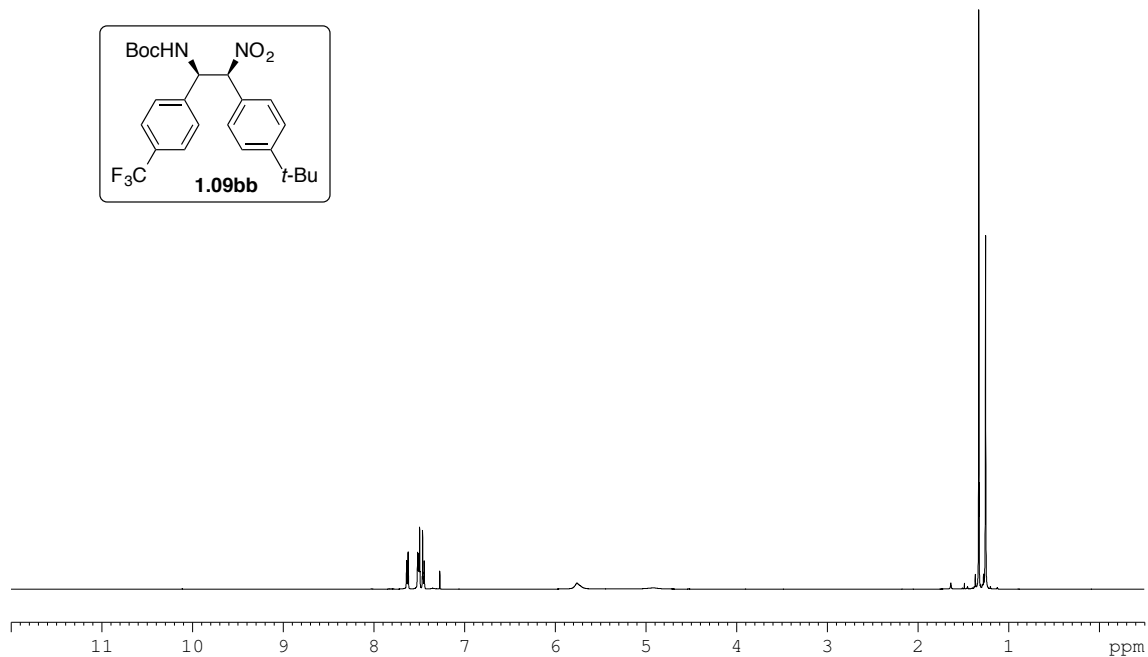
Figure A.1.09bb_1 ^{1}H NMR spectrum of compound **1.09bb** (500 MHz, CDCl$_3$).
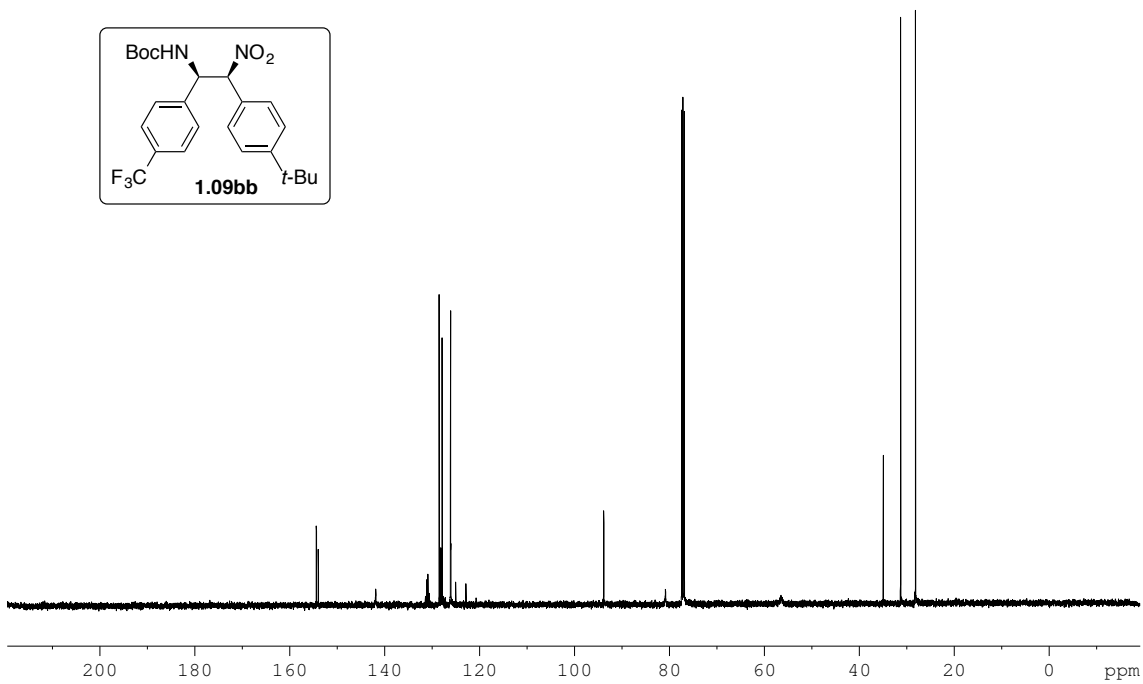
Figure A.1.09bb_2 ^{13}C NMR spectrum of compound **1.09bb** (125 MHz, CDCl$_3$).
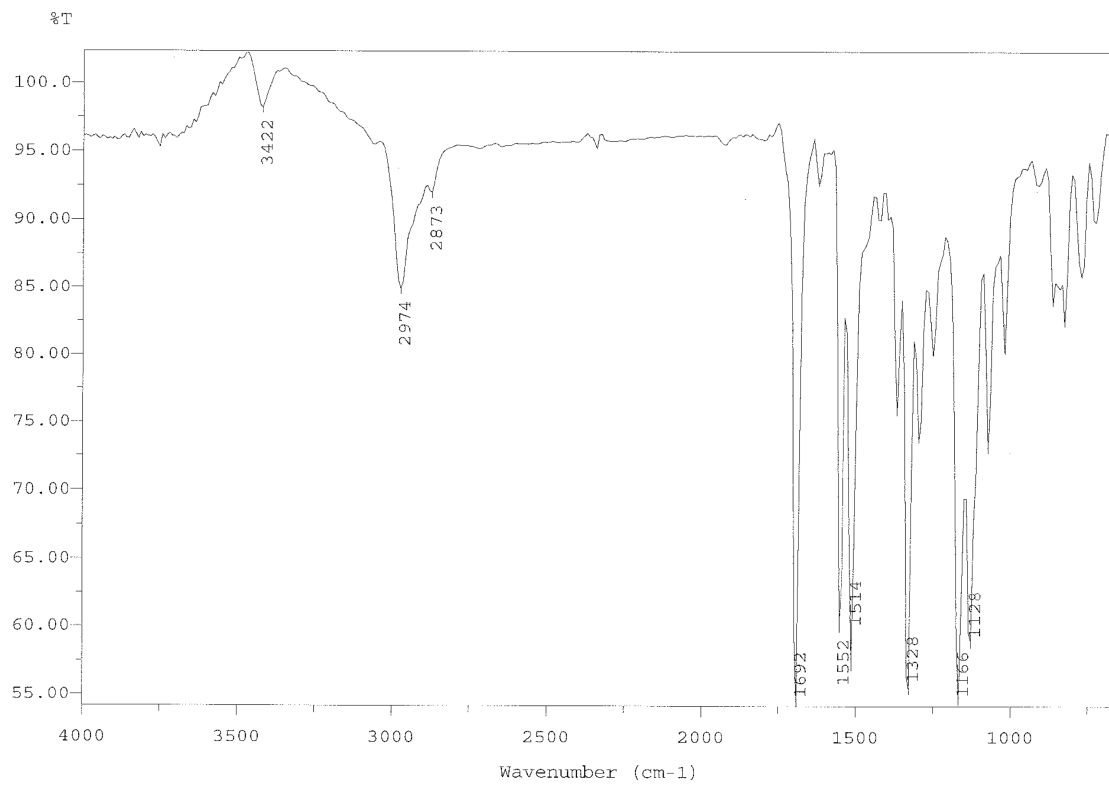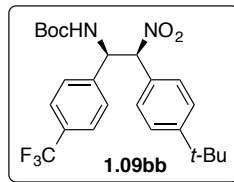
Figure A.1.09bb_3 IR spectrum of compound **1.09bb**.
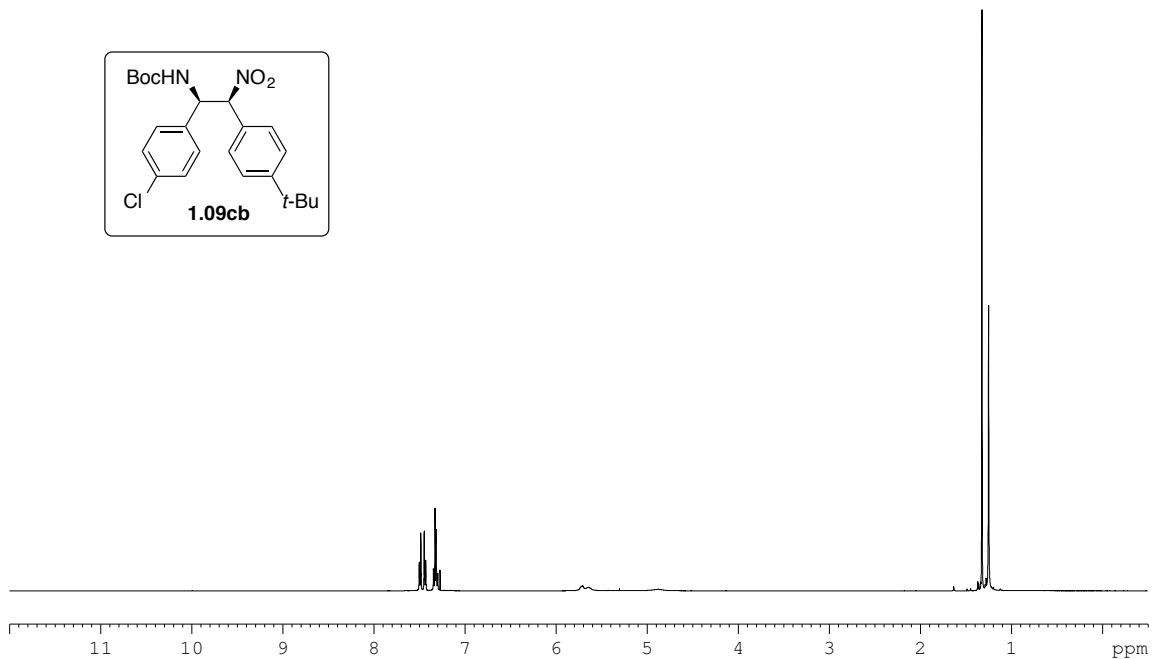
Figure A.1.09cb_1 ^{1}H NMR spectrum of compound **1.09cb** (500 MHz, CDCl$_3$).
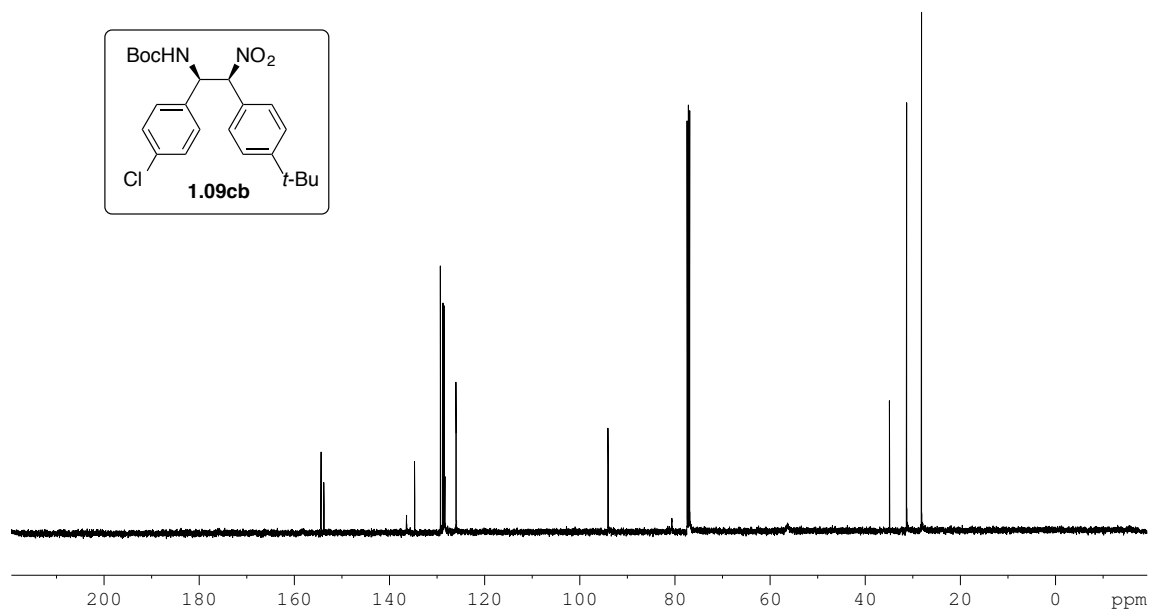
Figure A.1.09cb_2 ^{13}C NMR spectrum of compound **1.09cb** (125 MHz, CDCl$_3$).
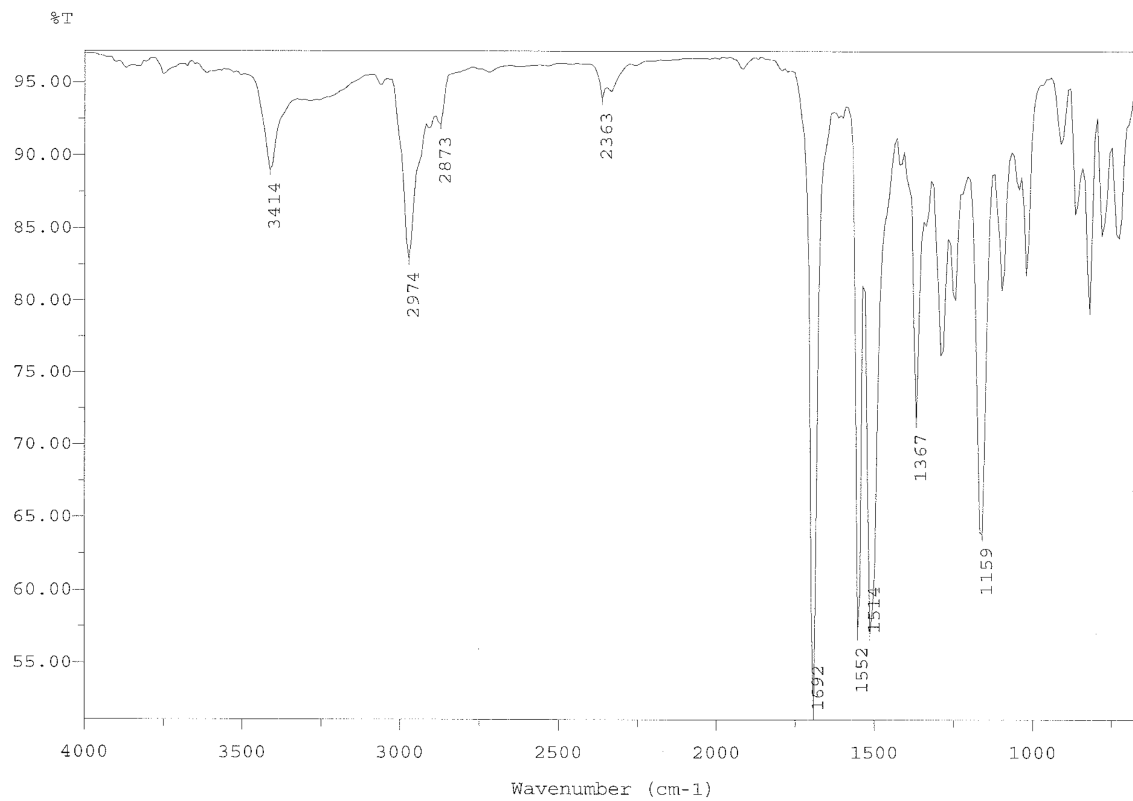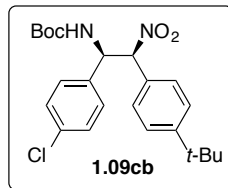
Figure A.1.09cb_3 IR spectrum of compound **1.09cb**.
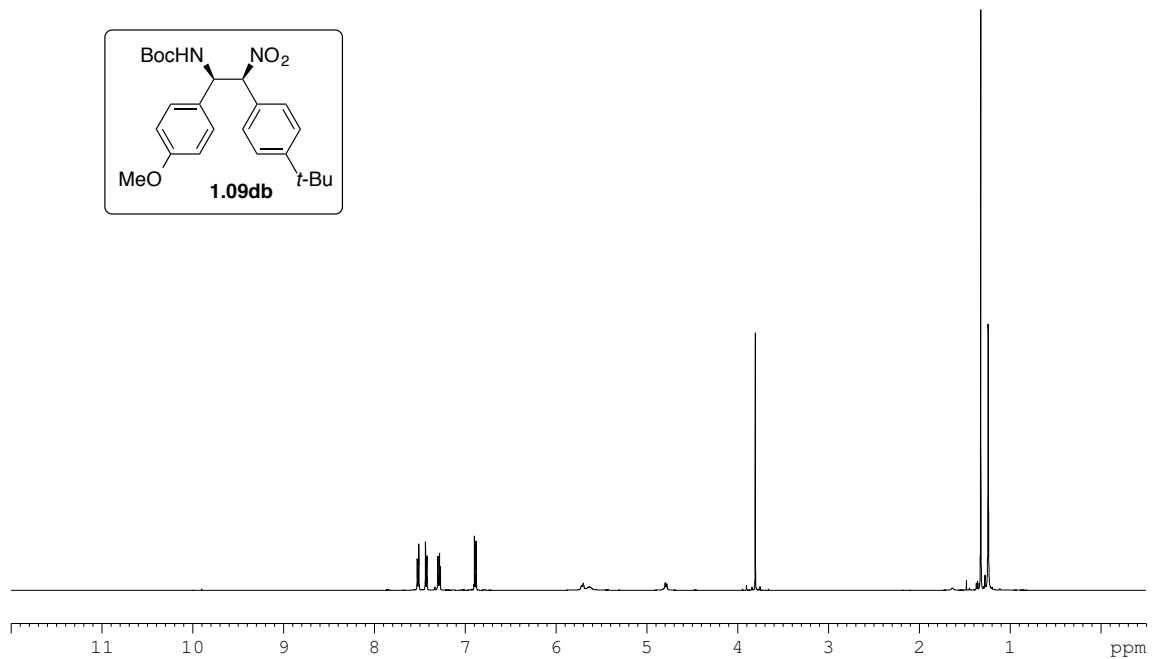
Figure A.1.09db_1 ^{1}H NMR spectrum of compound **1.09db** (500 MHz, CDCl$_3$).
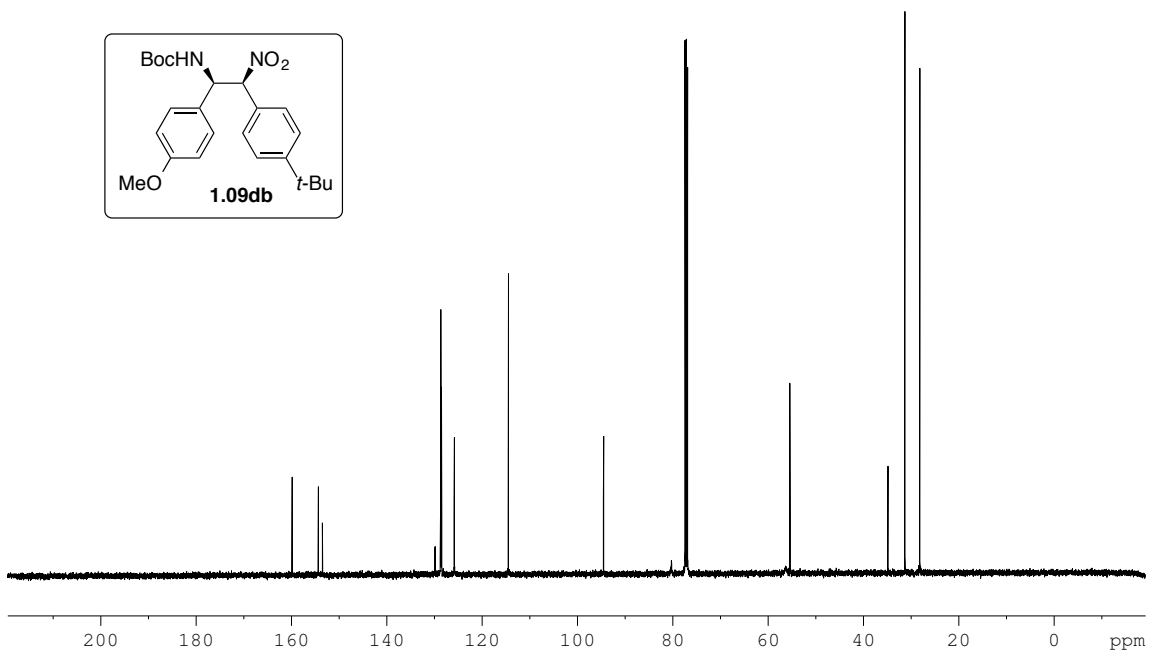
Figure A.1.09db_2 ^{13}C NMR spectrum of compound **1.09db** (125 MHz, CDCl$_3$).
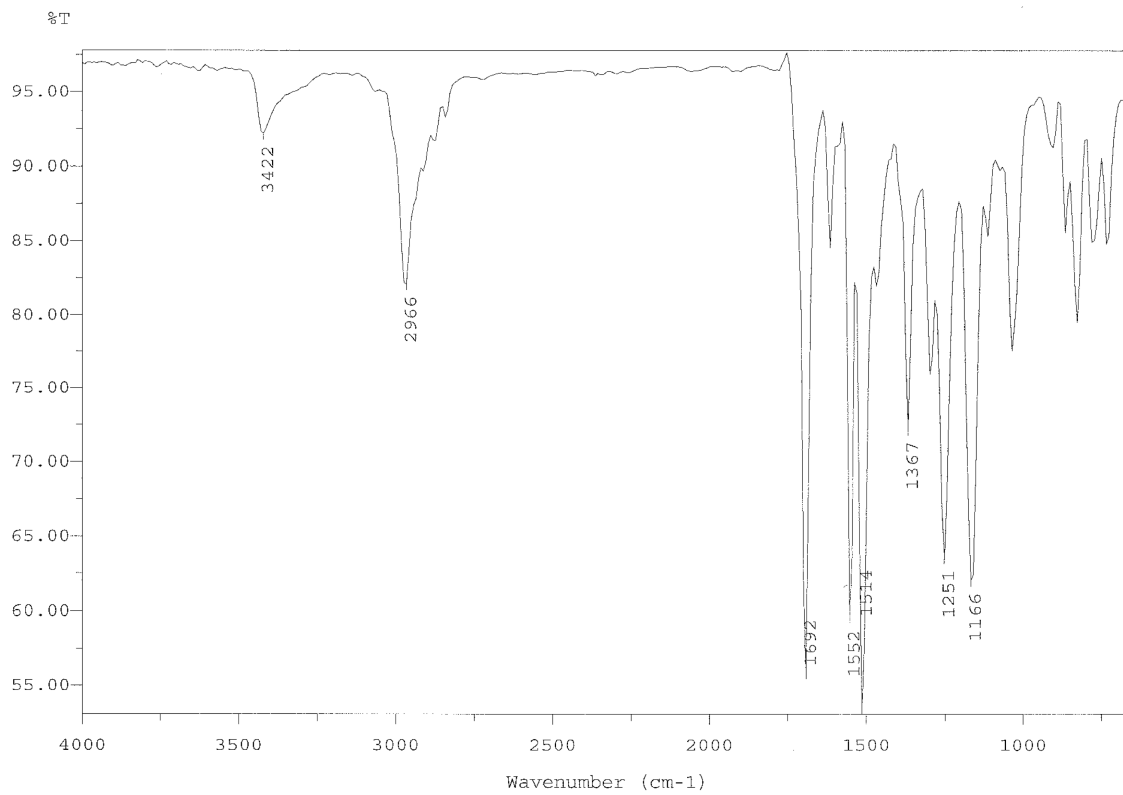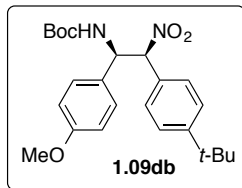
Figure A.1.09db_3 IR NMR spectrum of compound **1.09db**.
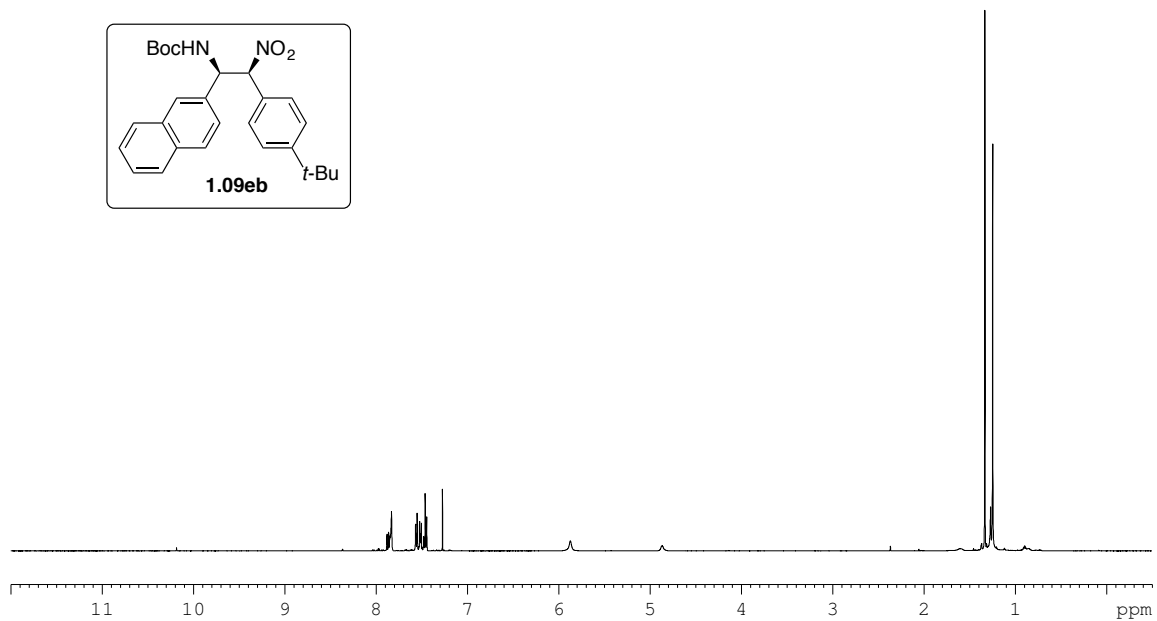
Figure A.1.09eb_1 ^{1}H NMR spectrum of compound **1.09eb** (500 MHz, CDCl$_3$).
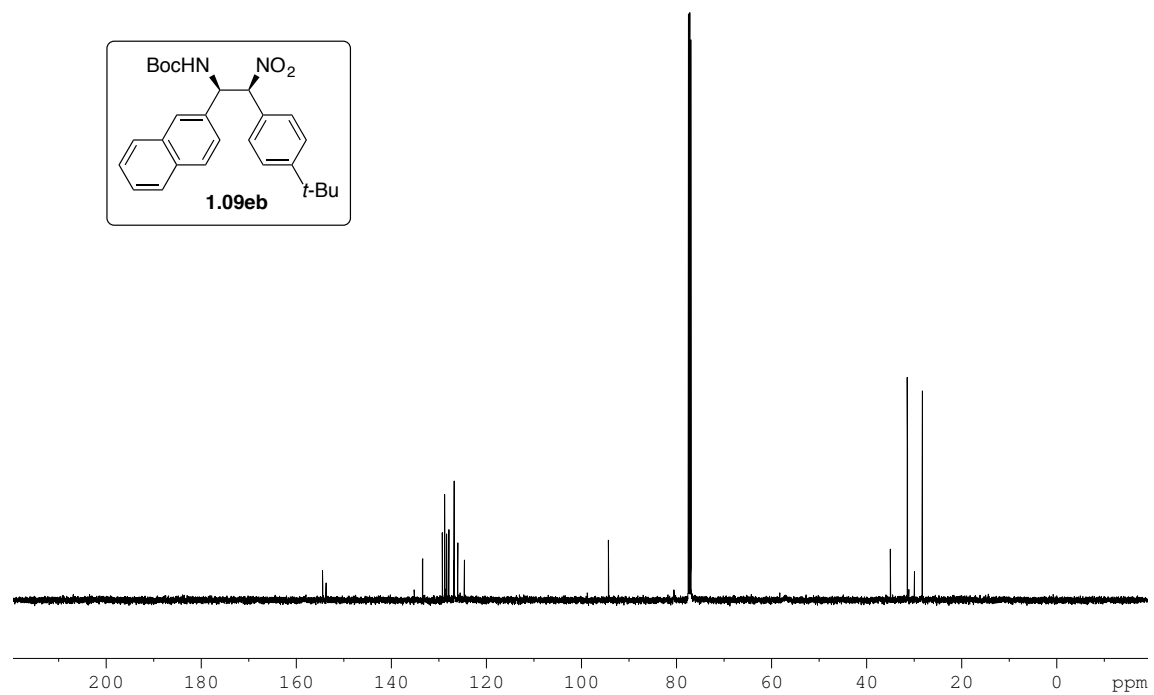
Figure A.1.09eb_2 ^{13}C NMR spectrum of compound **1.09eb** (125 MHz, CDCl$_3$).
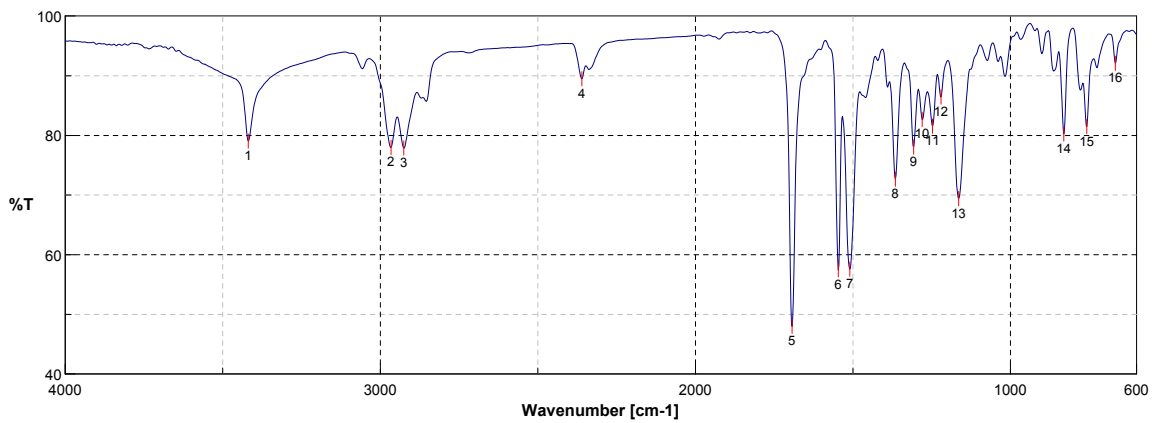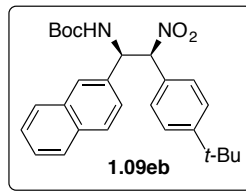
Figure A.1.09eb_3 IR spectrum of compound **1.09eb**.
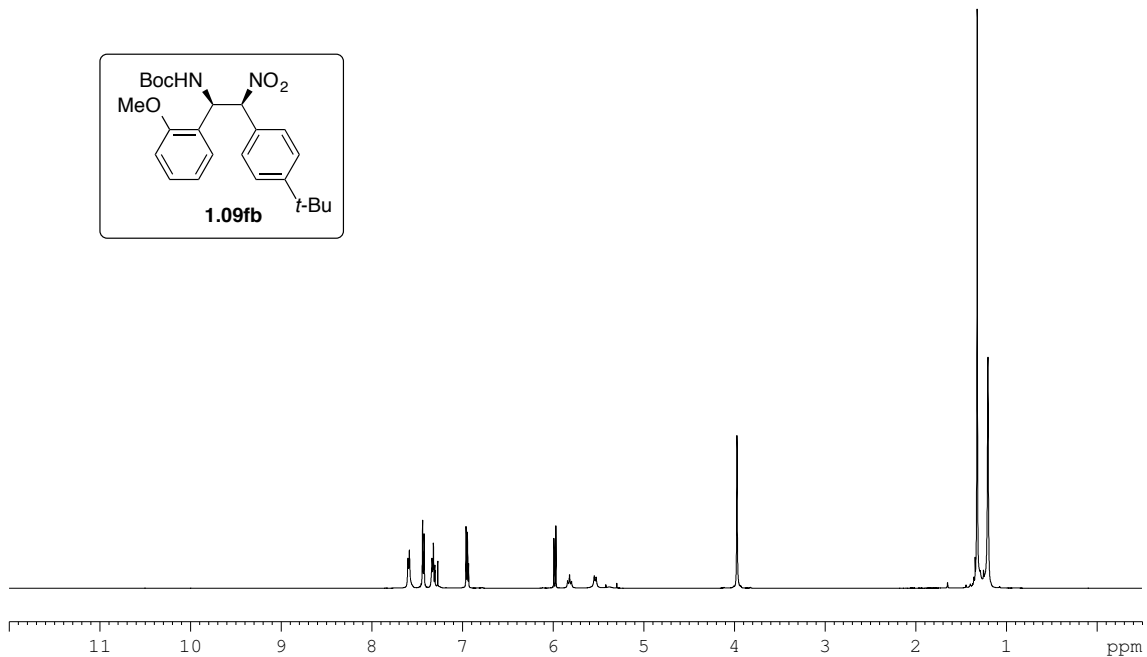
Figure A.1.09fb_1 ^{1}H NMR spectrum of compound **1.09fb** (500 MHz, CDCl$_3$).
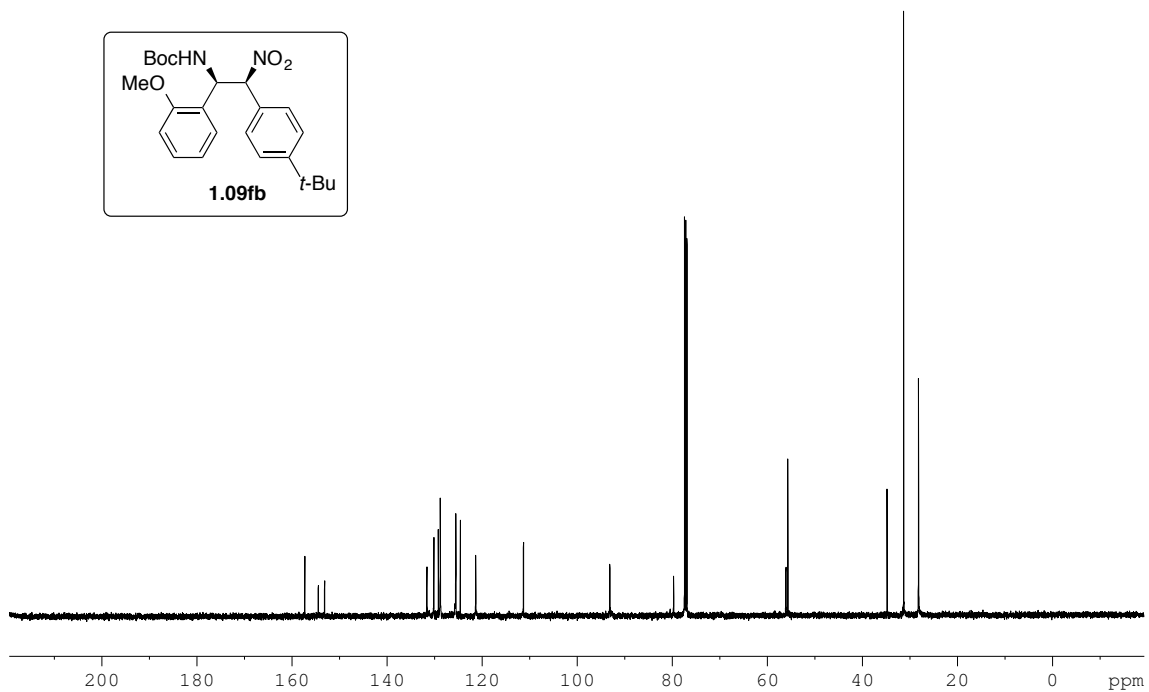
Figure A.1.09fb_2 ^{13}C NMR spectrum of compound **1.09fb** (125 MHz, CDCl$_3$).
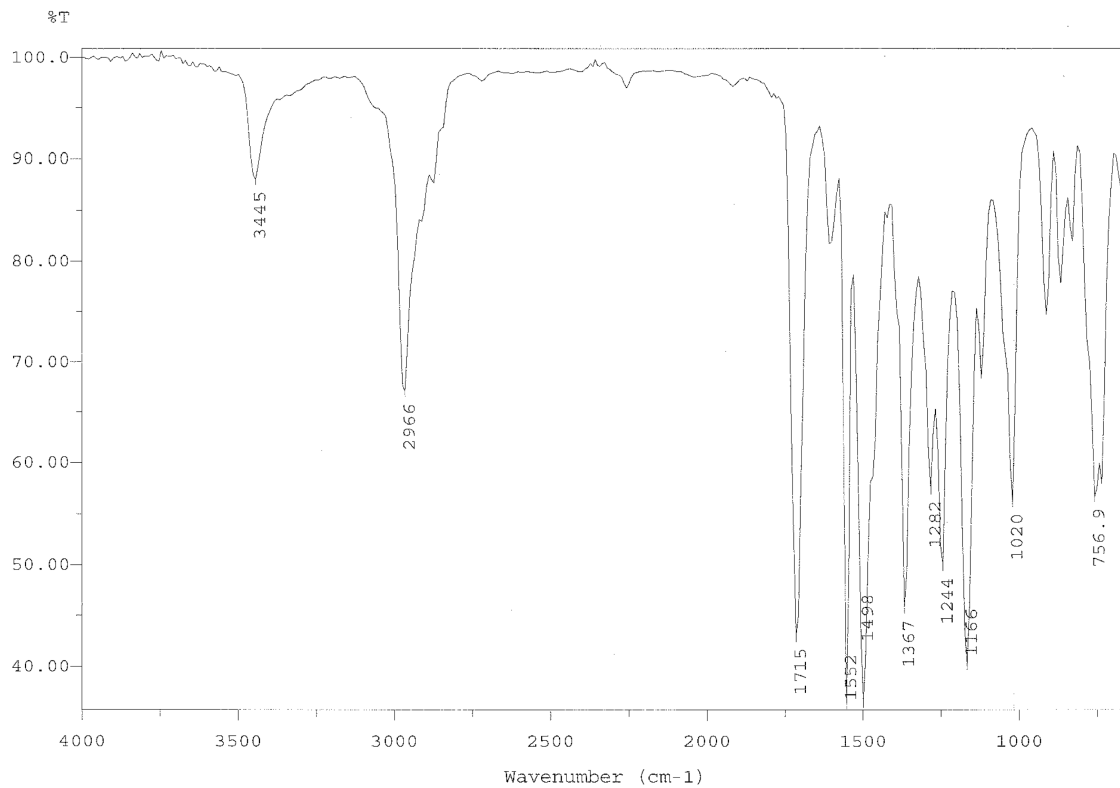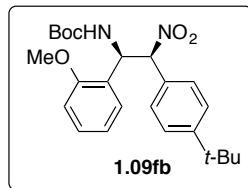
Figure A.1.09fb_3 IR spectrum of compound **1.09fb**.
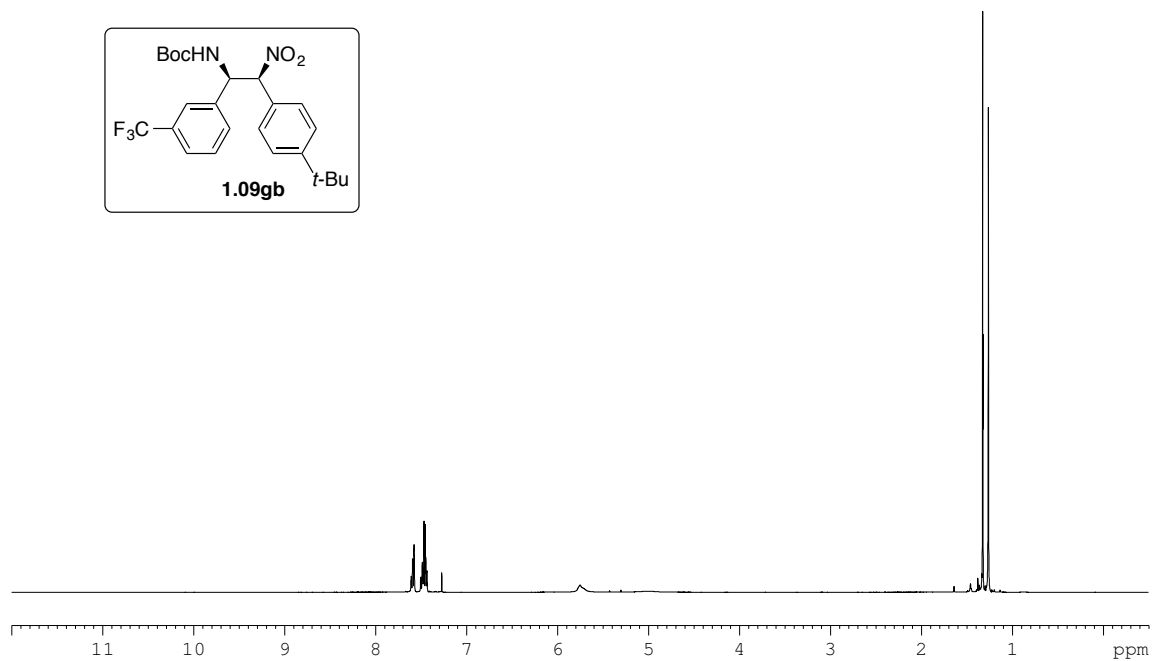
Figure A.1.09gb_1 ¹H NMR spectrum of compound **1.09gb** (500 MHz, CDCl₃).
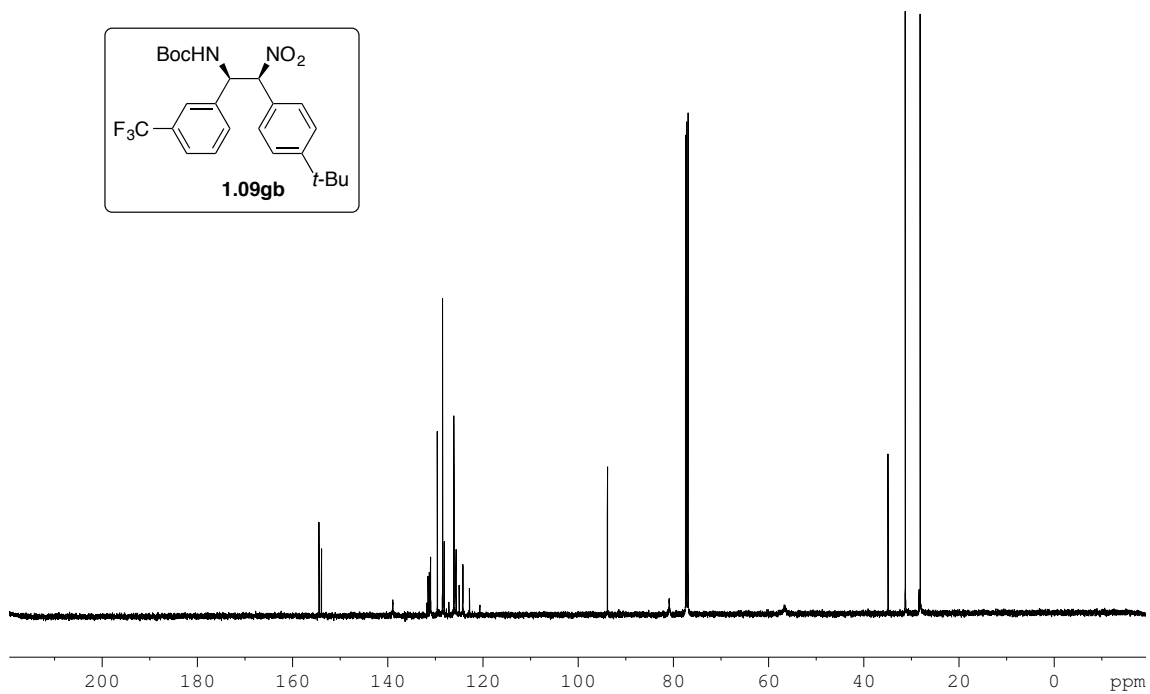
Figure A.1.09gb_2 ¹³H NMR spectrum of compound **1.09gb** (125 MHz, CDCl₃).
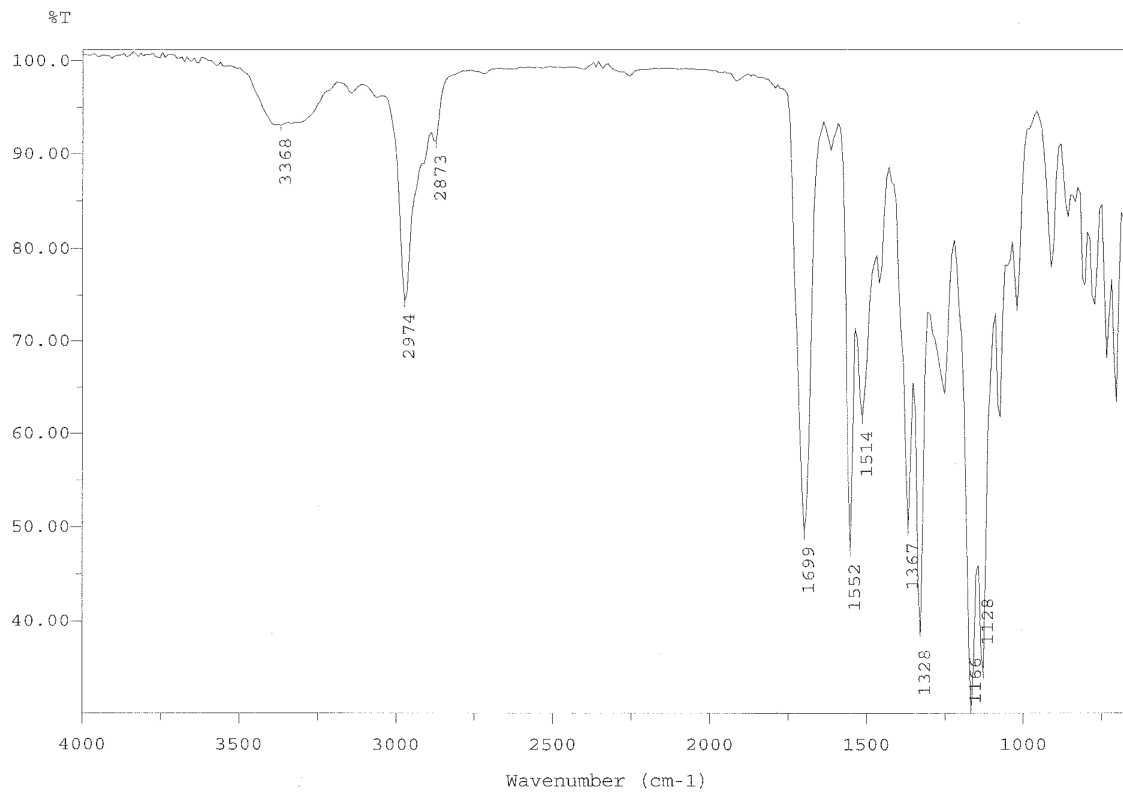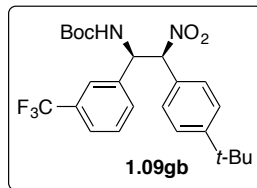
Figure A.1.09gb_3 IR spectrum of compound **1.09gb**.
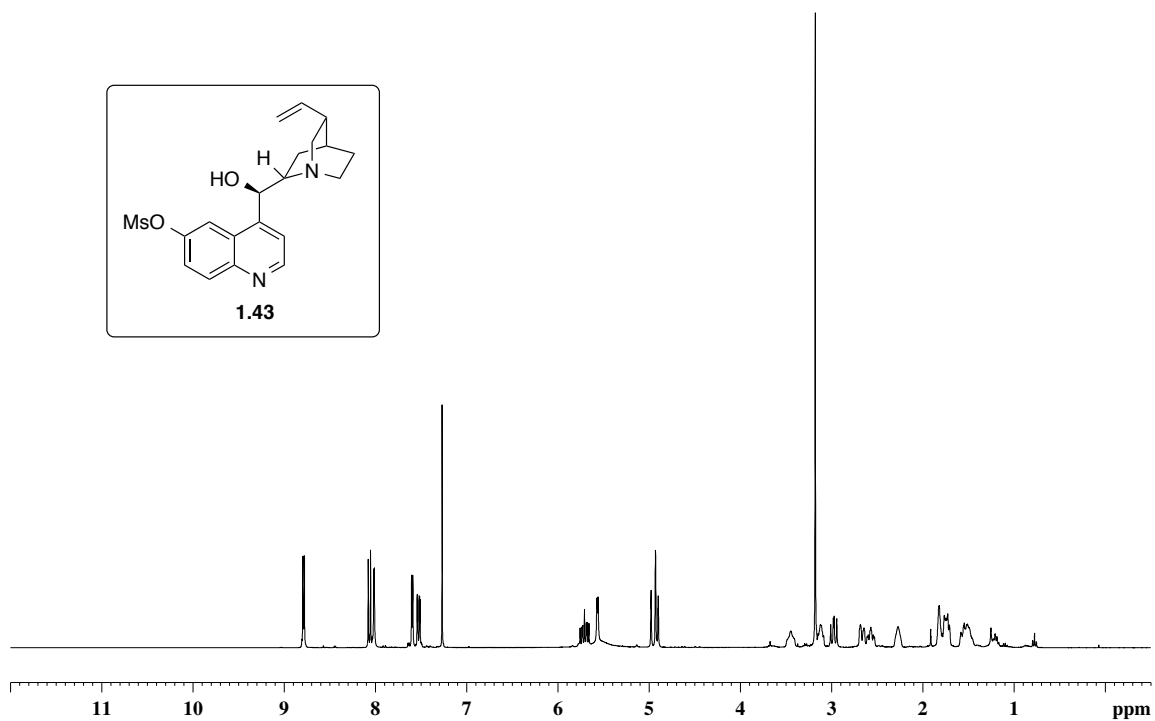
Figure A.1.43_1 ^{1}H NMR spectrum of compound **1.43** (360 MHz, CDCl$_3$).
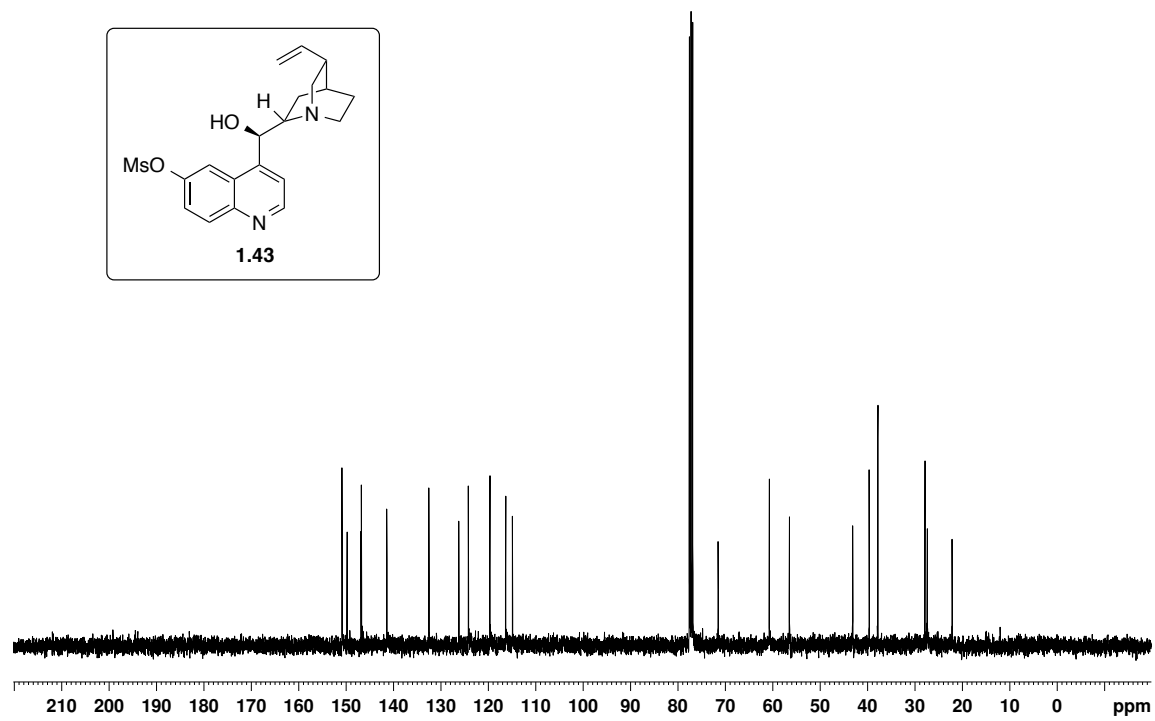
Figure A.1.43_2 ^{13}C NMR spectrum of compound **1.43** (90 MHz, CDCl$_3$).

211
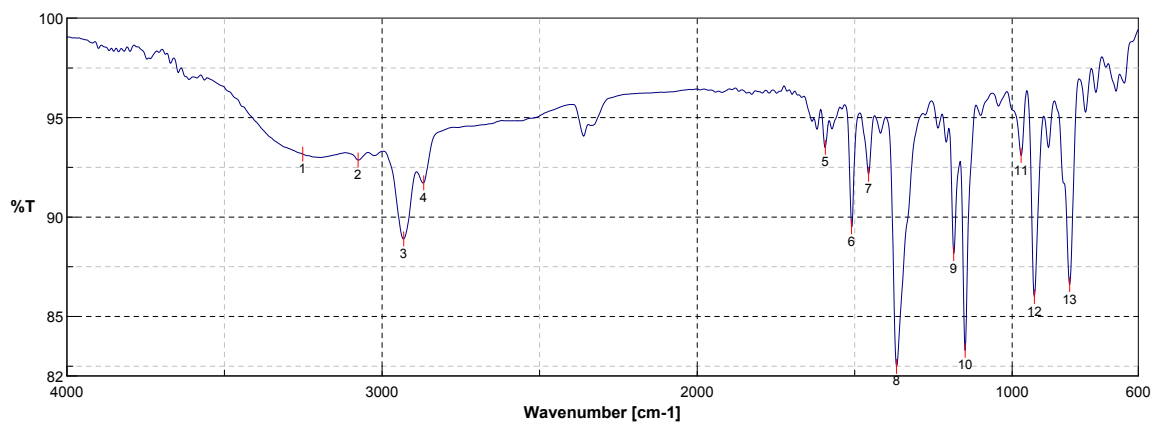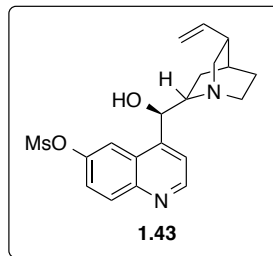
Figure A.1.43_3 IR spectrum of compound **1.43**.
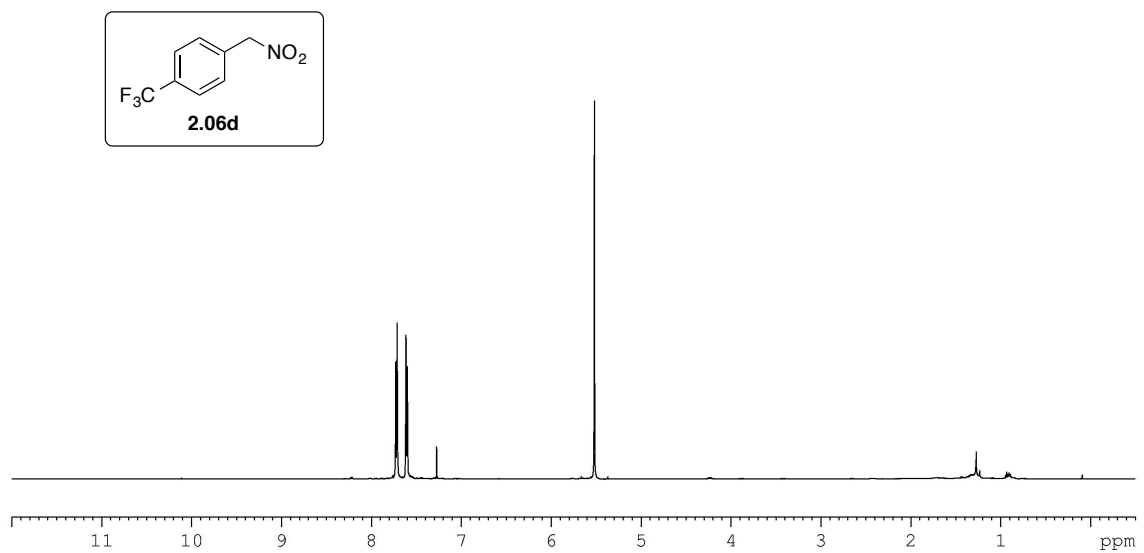
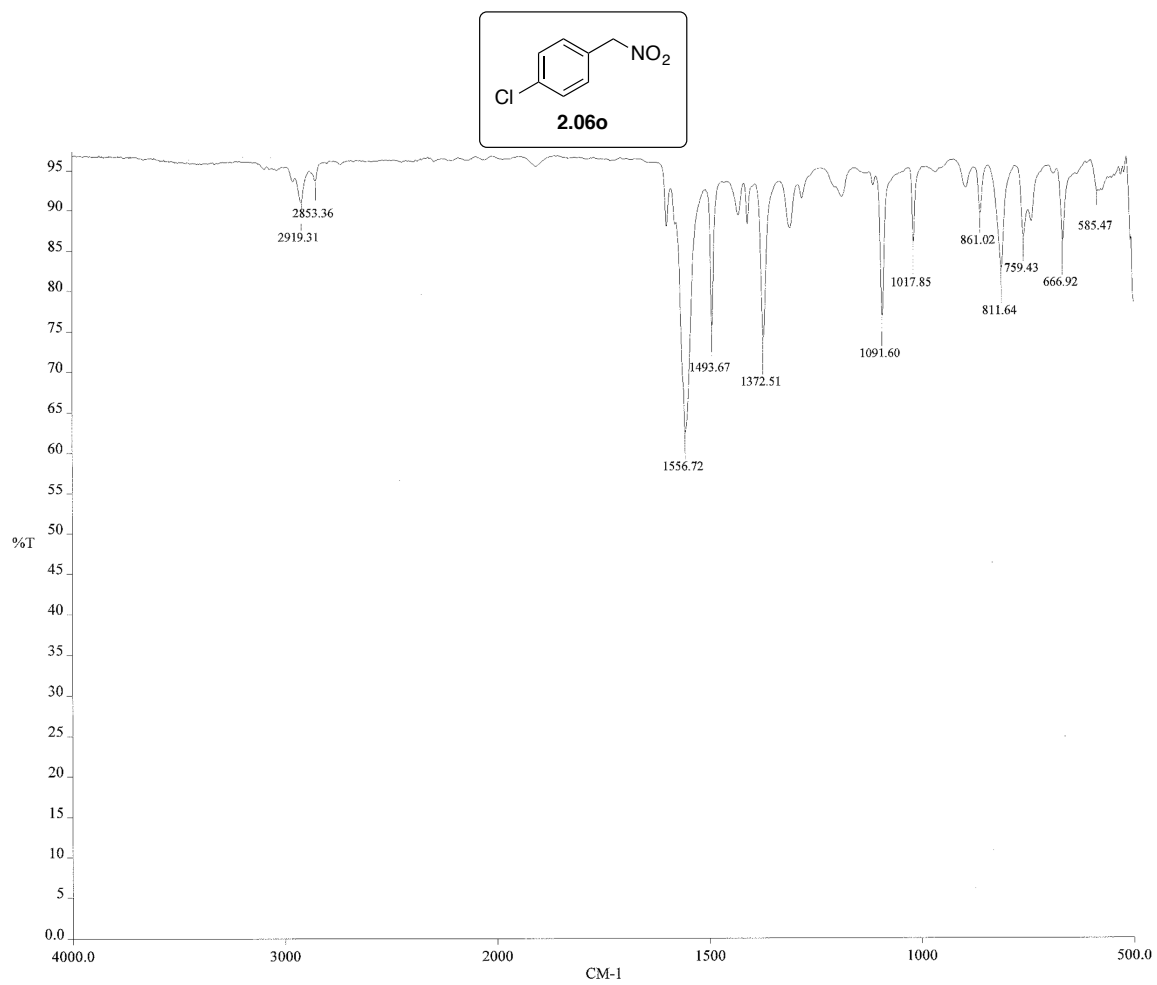**Figure A.2.06d_1** ^{1}H NMR spectrum of compound **2.06d** (500 MHz, CDCl$_3$).
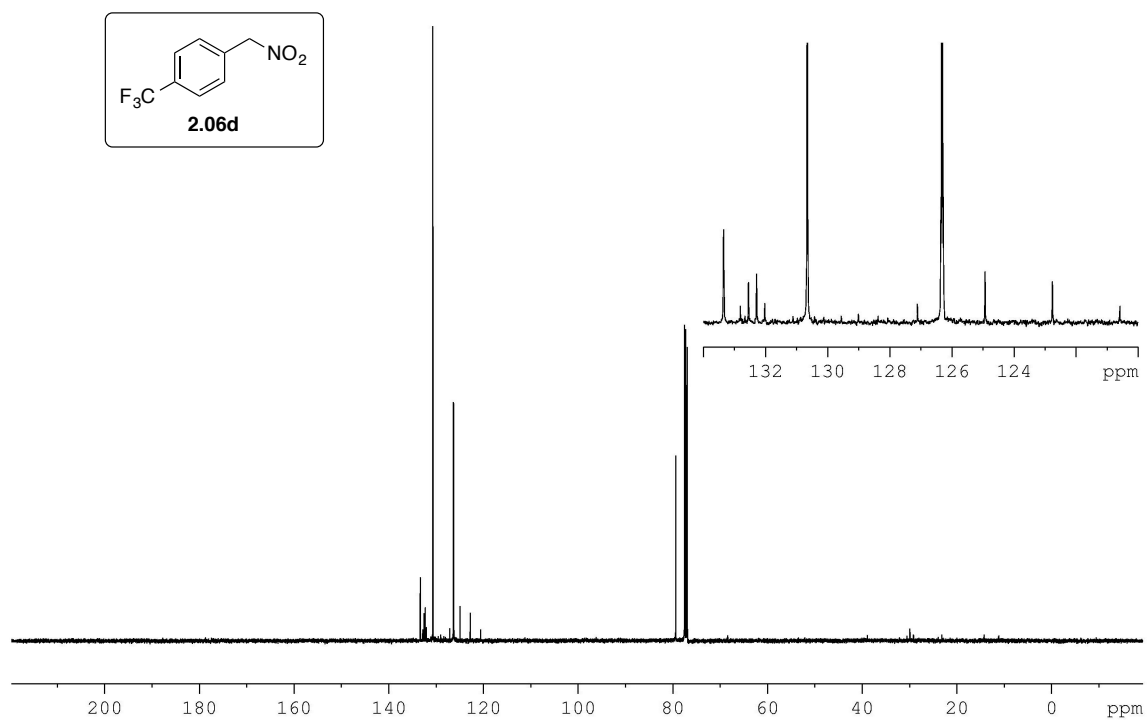
Figure A.2.06d_2 ^{13}C NMR spectrum of compound **2.06d** (125 MHz, CDCl$_3$).
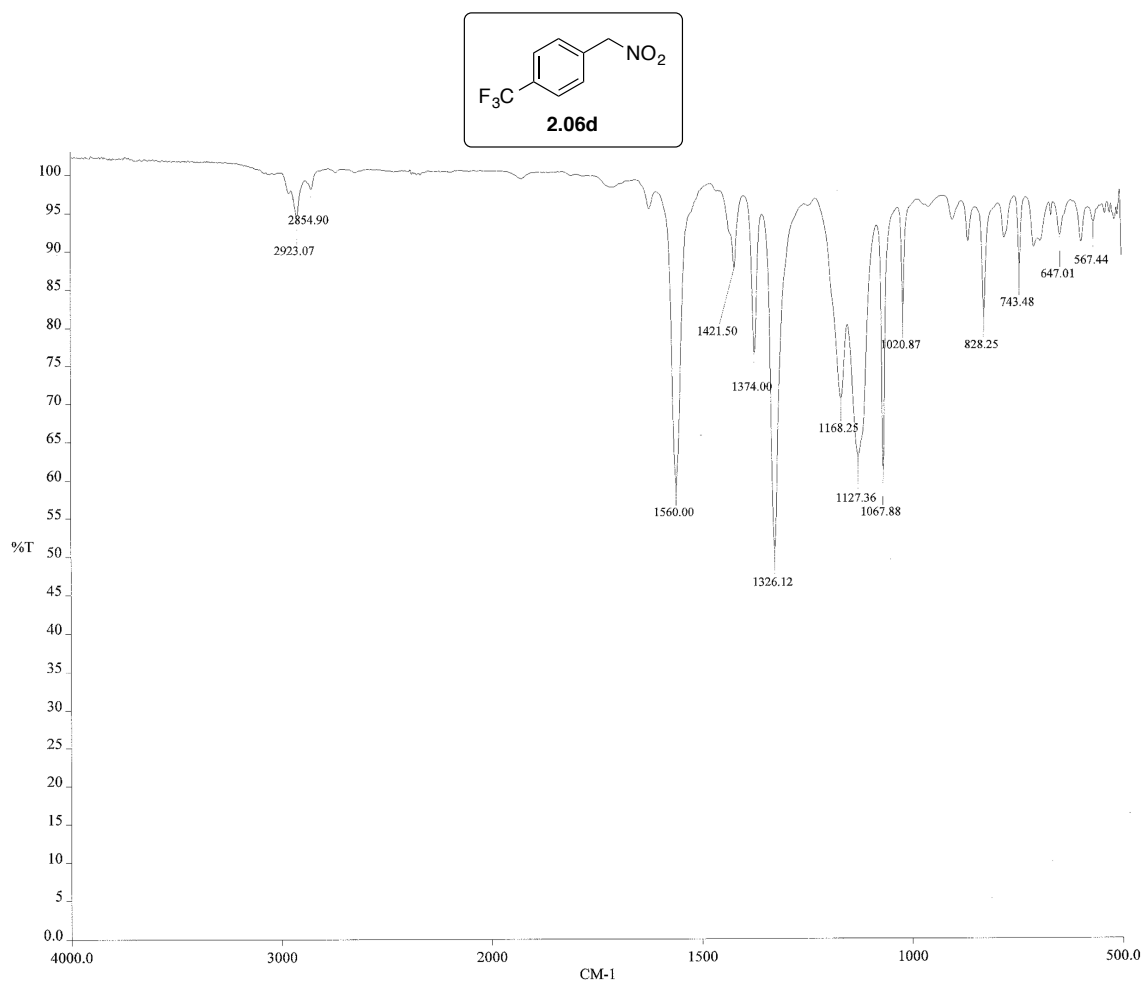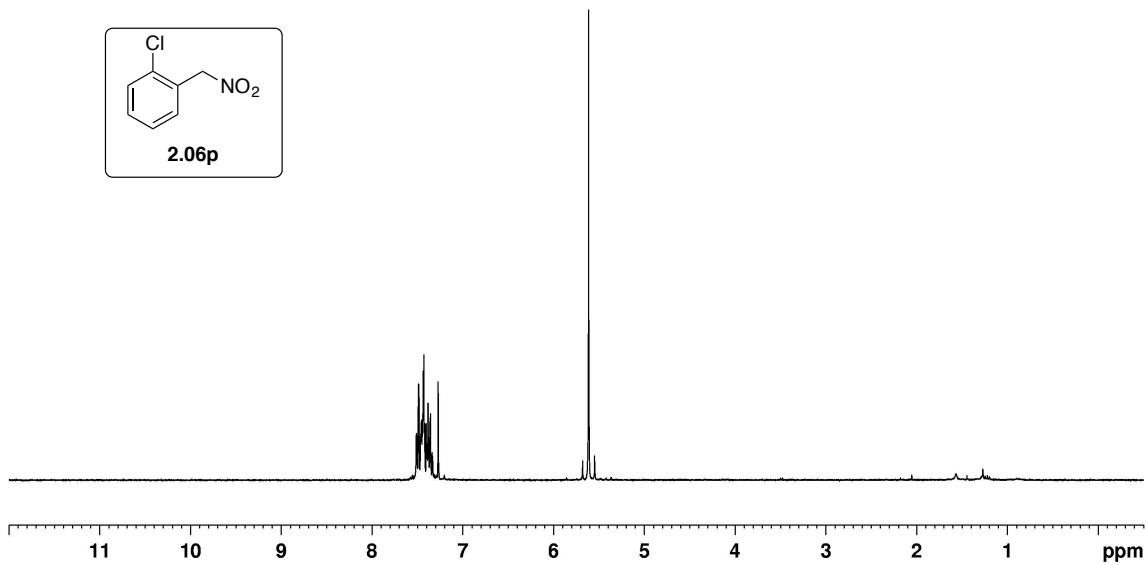
Figure A.2.06d_3 IR spectrum of compound **2.06d**.
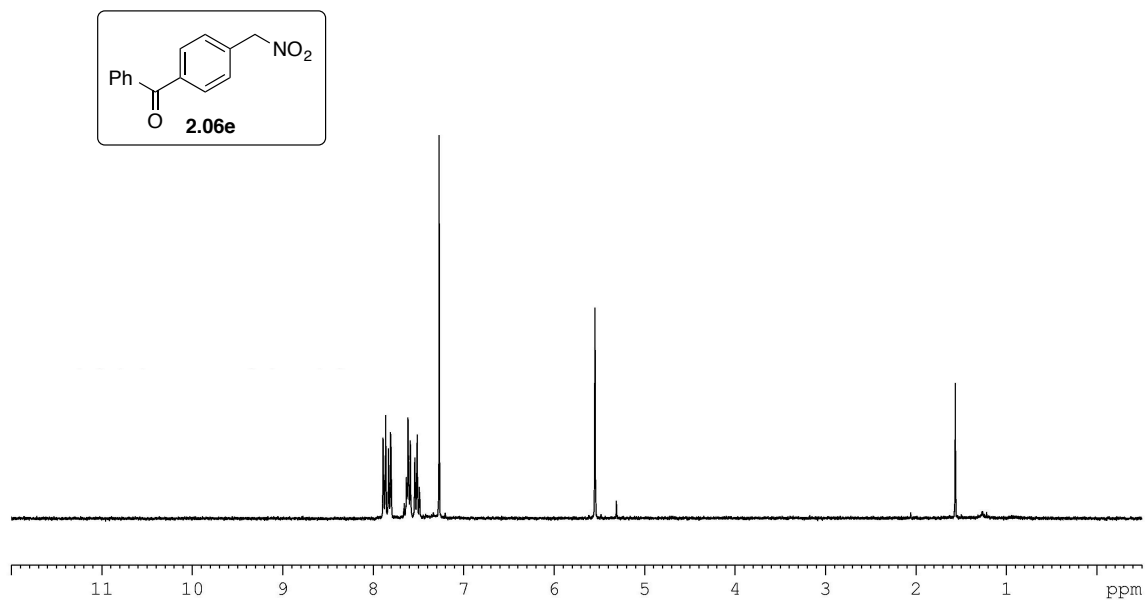
Figure A.2.06e_1 ^{1}H NMR spectrum of compound **2.06e** (500 MHz, CDCl$_3$).
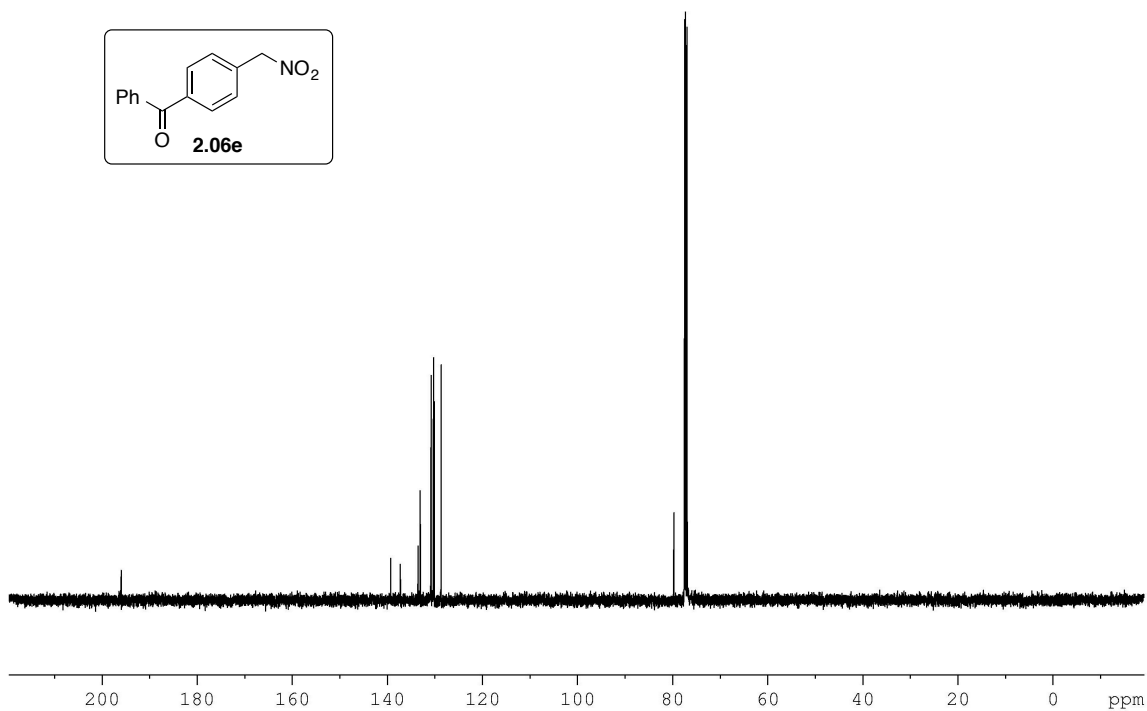
Figure A.2.06e_2 ^{13}C NMR spectrum of compound **2.06e** (125 MHz, CDCl$_3$).
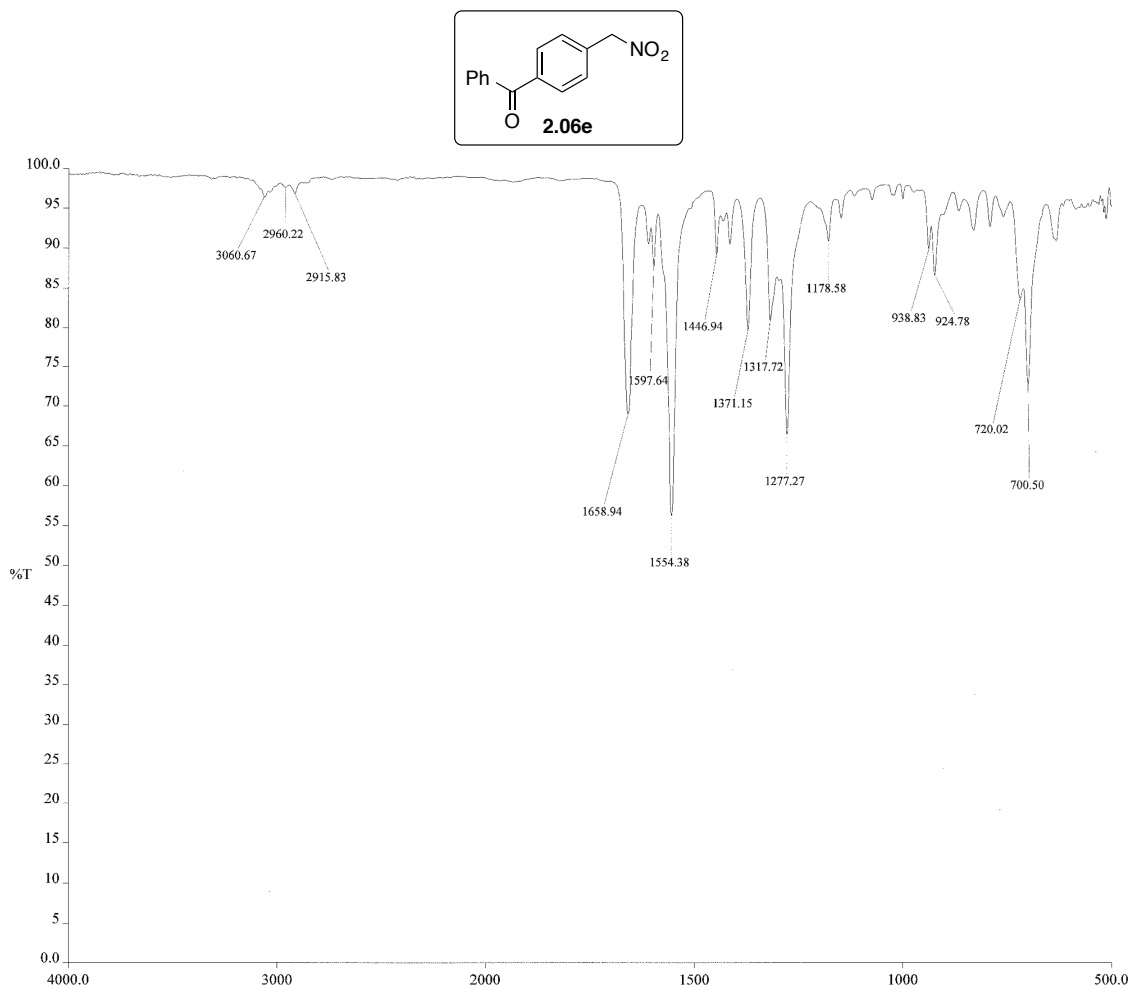
Figure A.2.06e_3 IR spectrum of compound **2.06e**.
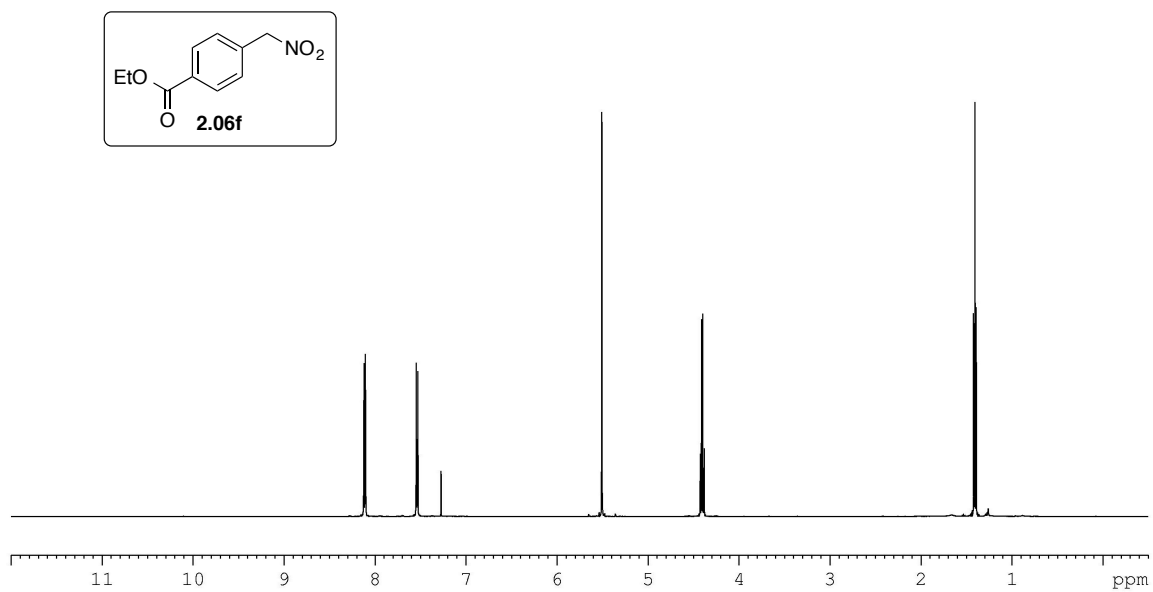
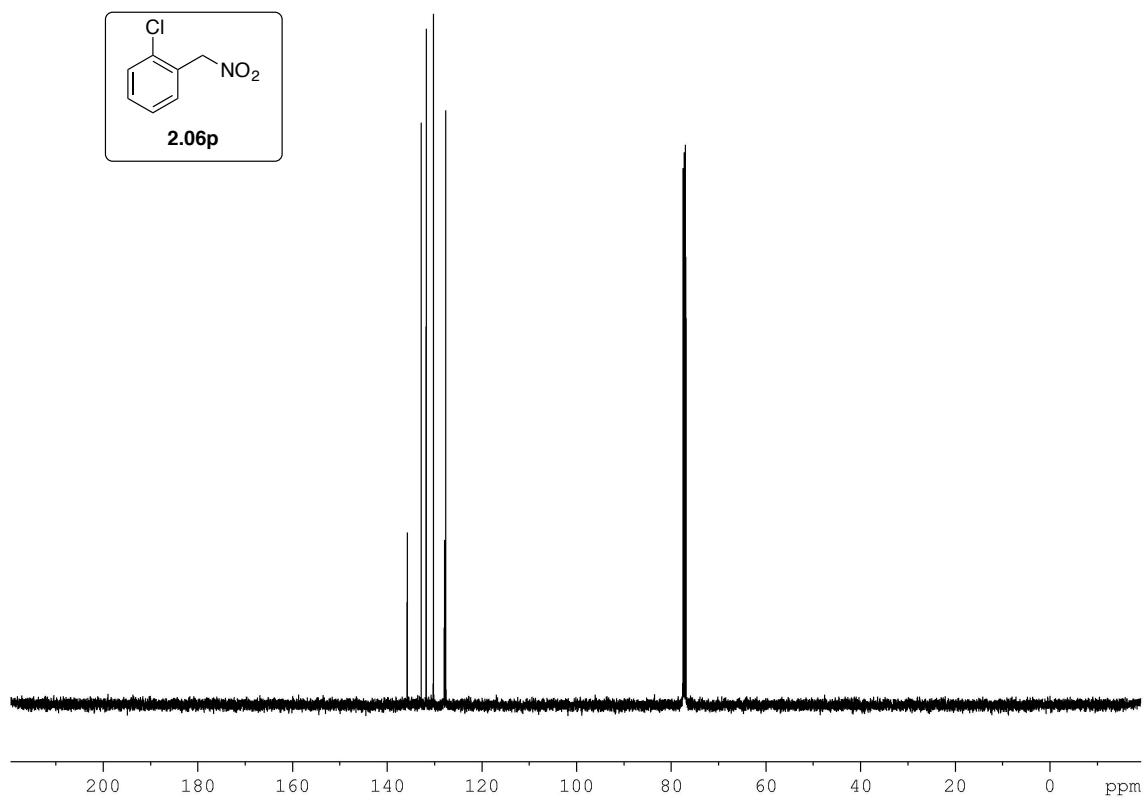**Figure A.2.06f_1** ^{1}H NMR spectrum of compound **2.06f** (500 MHz, CDCl$_3$).
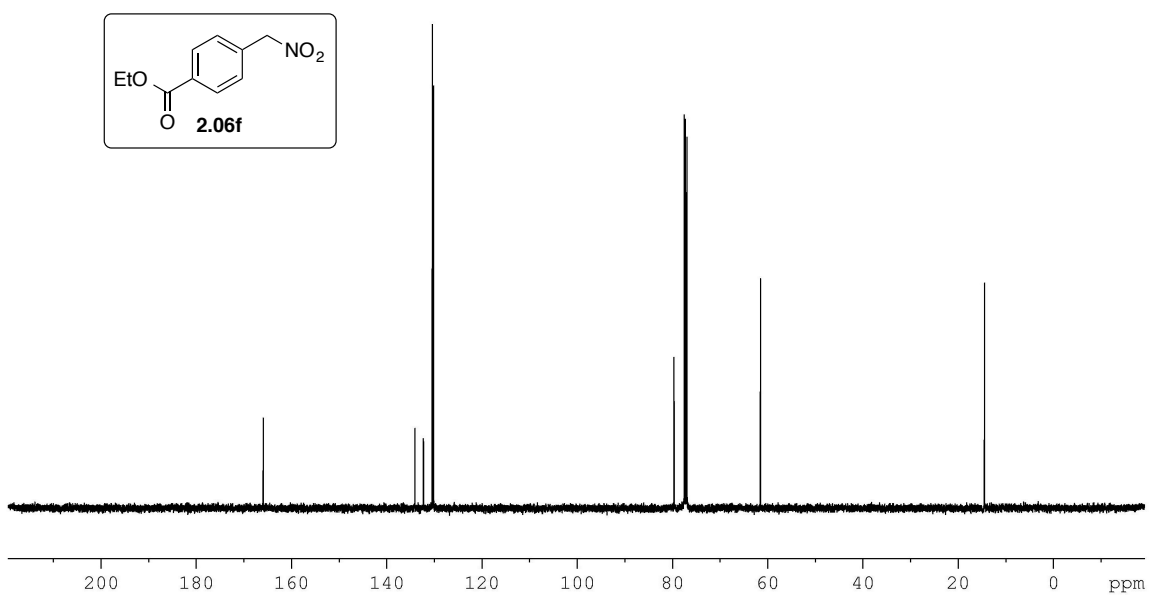
Figure A.2.06f_2 ^{13}C NMR spectrum of compound **2.06f** (125 MHz, CDCl$_3$).
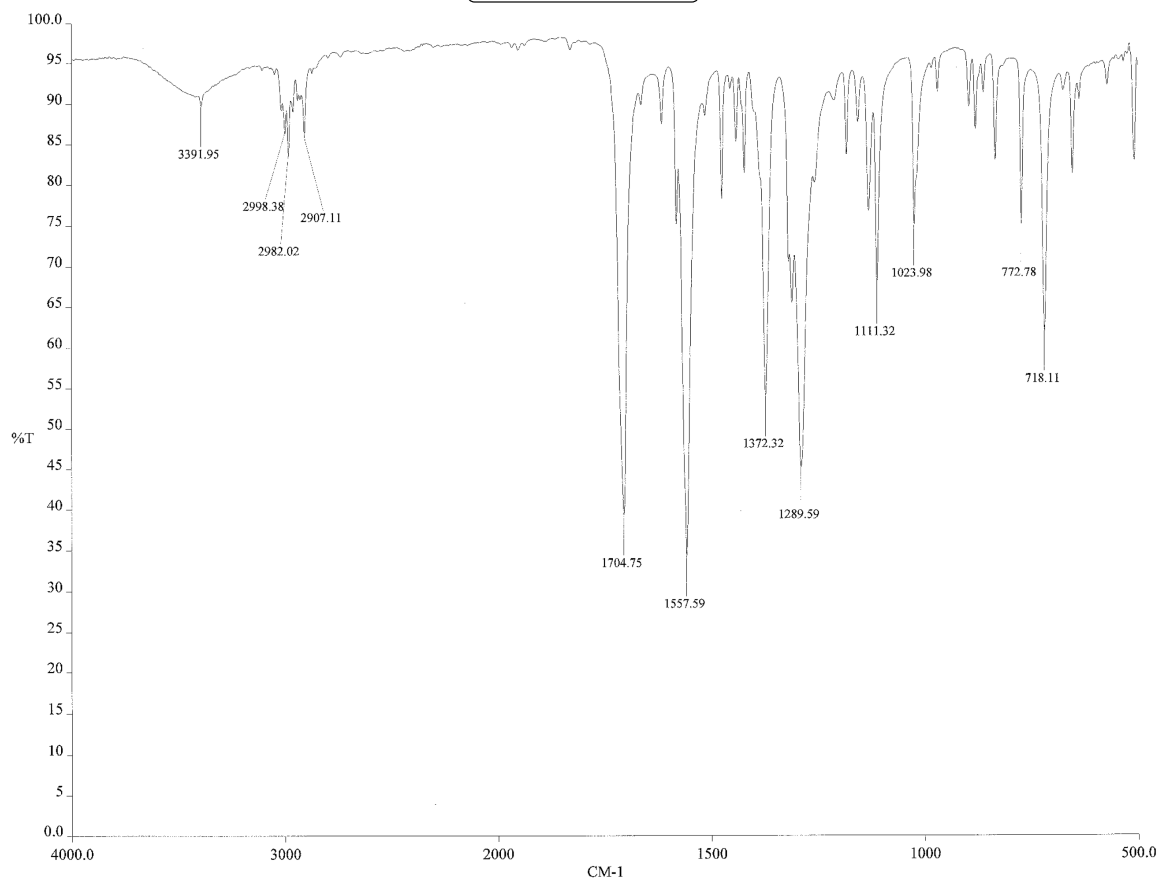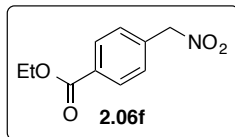
Figure A.2.06f_3 IR spectrum of compound **2.06f**.

218
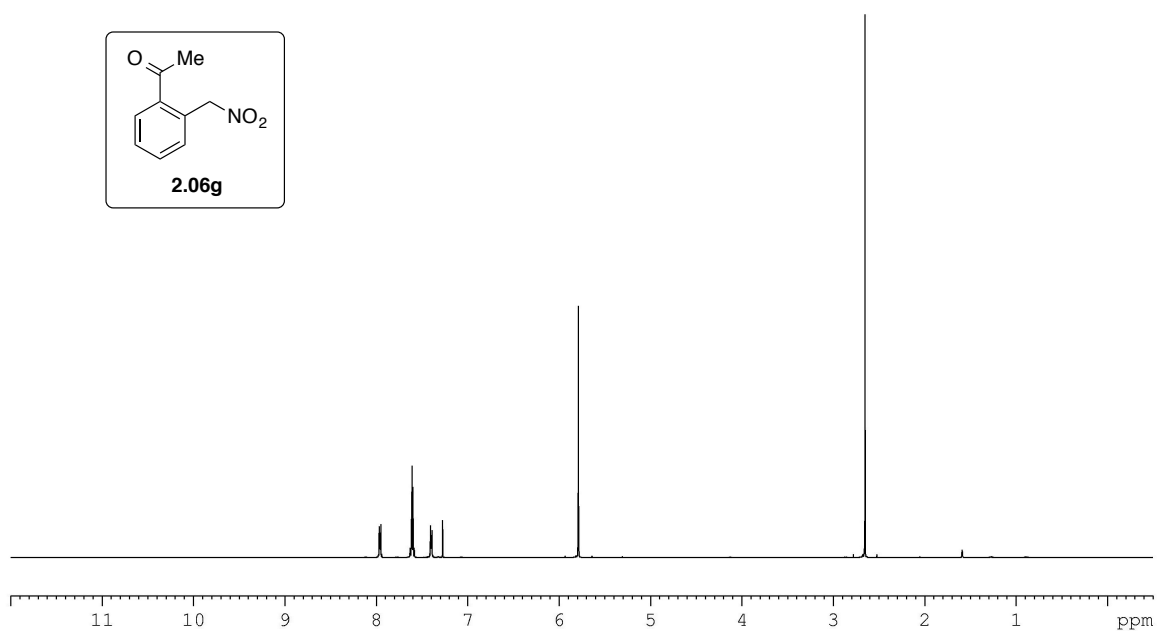
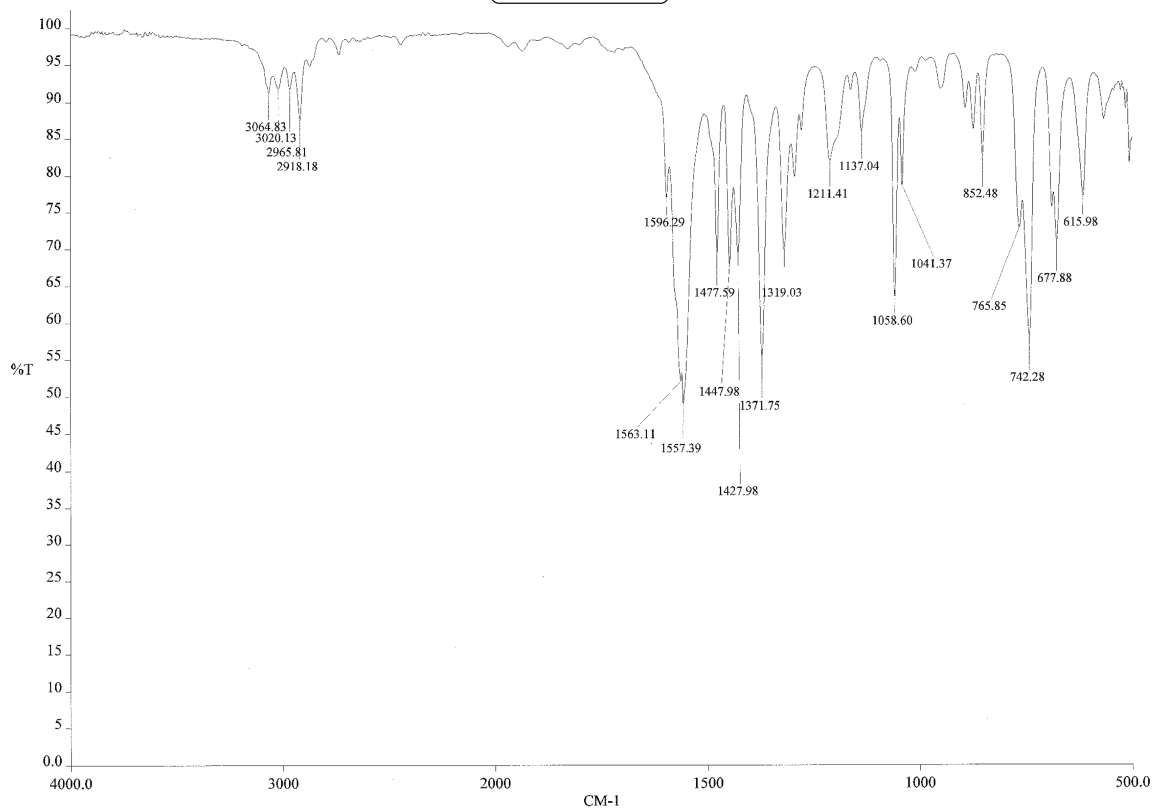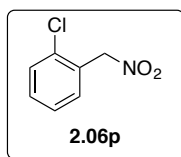**Figure A.2.06g_1** ^{1}H NMR spectrum of compound **2.06g** (500 MHz, CDCl$_3$).
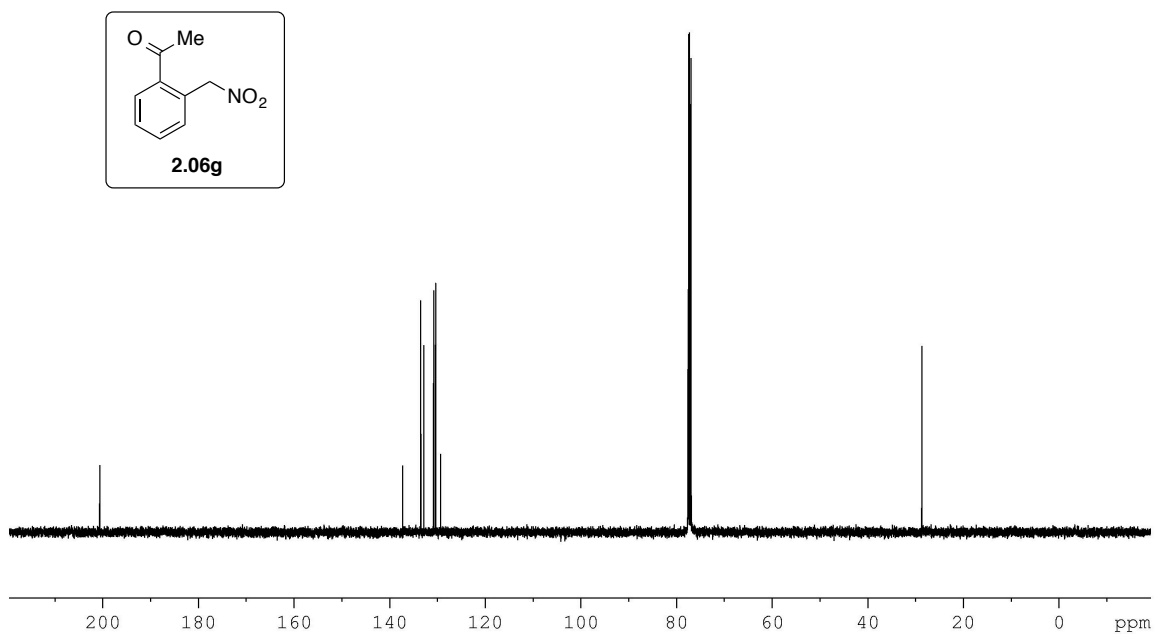
Figure A.2.06g_2 ^{13}C NMR spectrum of compound **2.06g** (125 MHz, CDCl$_3$).
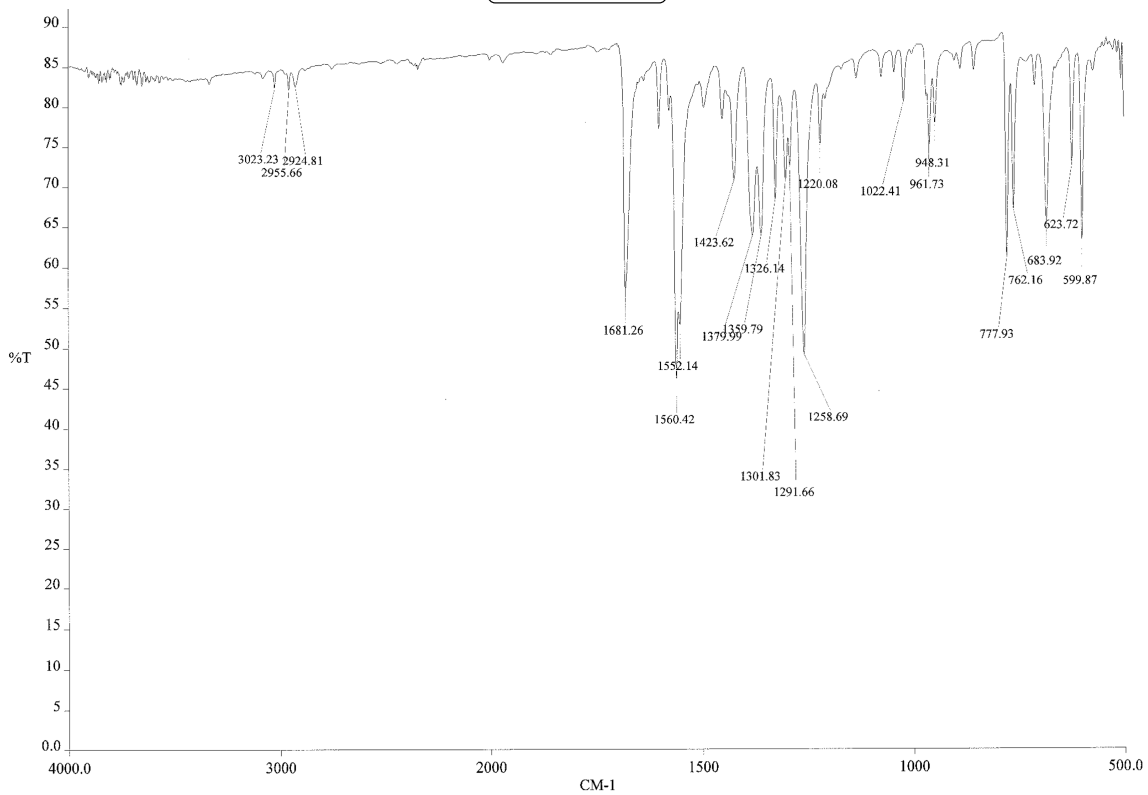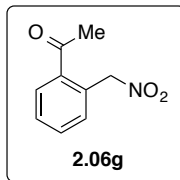
Figure A.2.06g_3 IR spectrum of compound **2.06g**.
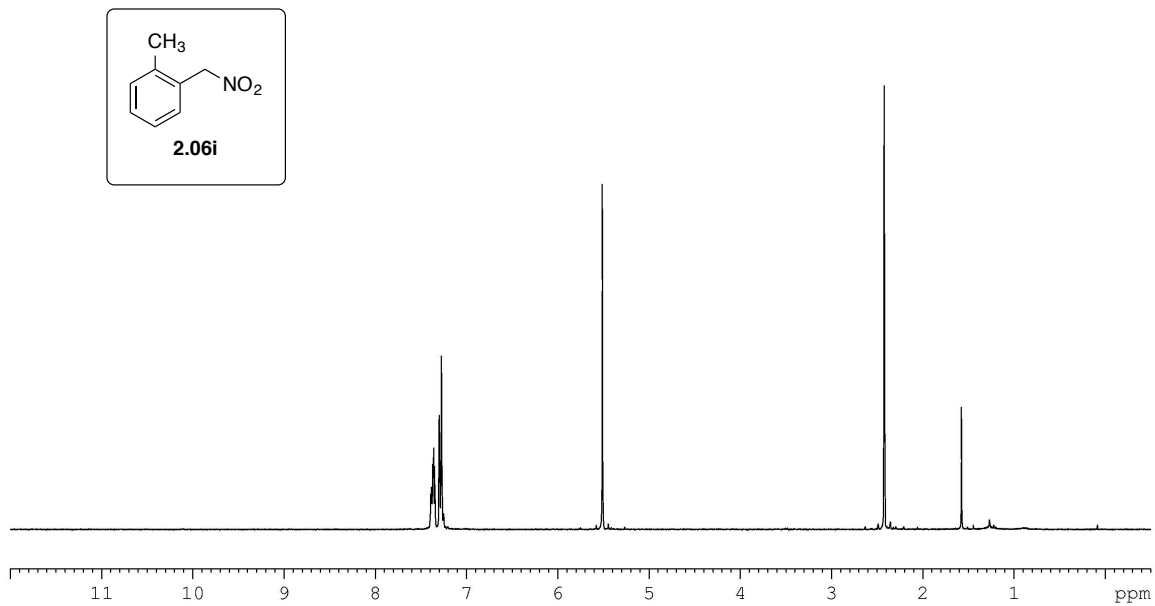
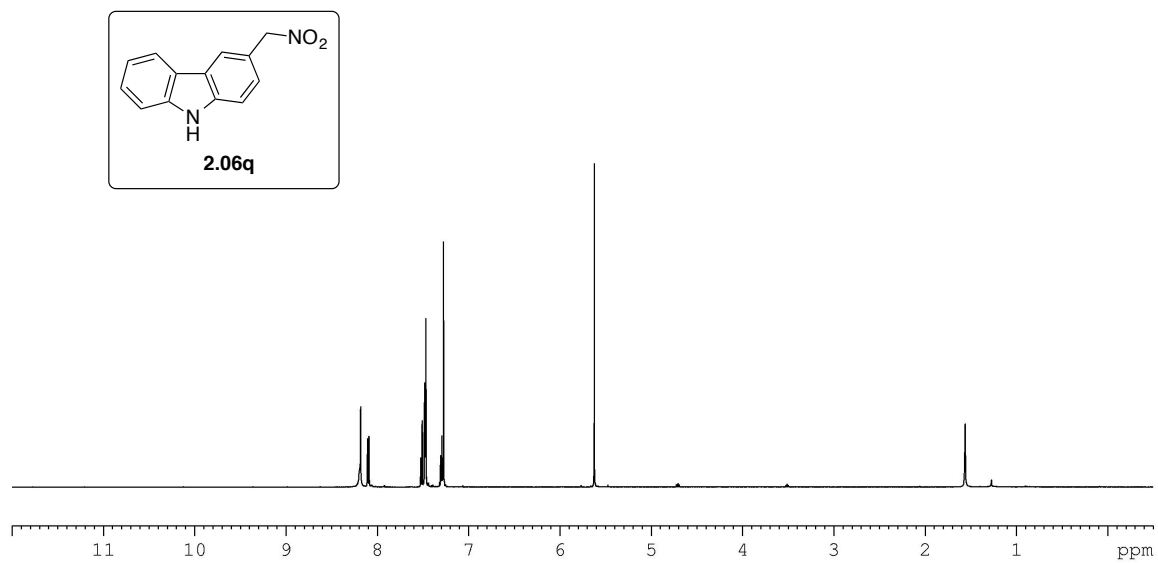**Figure A.2.06i_1** ^{1}H NMR spectrum of compound **2.06i** (500 MHz, CDCl$_3$).
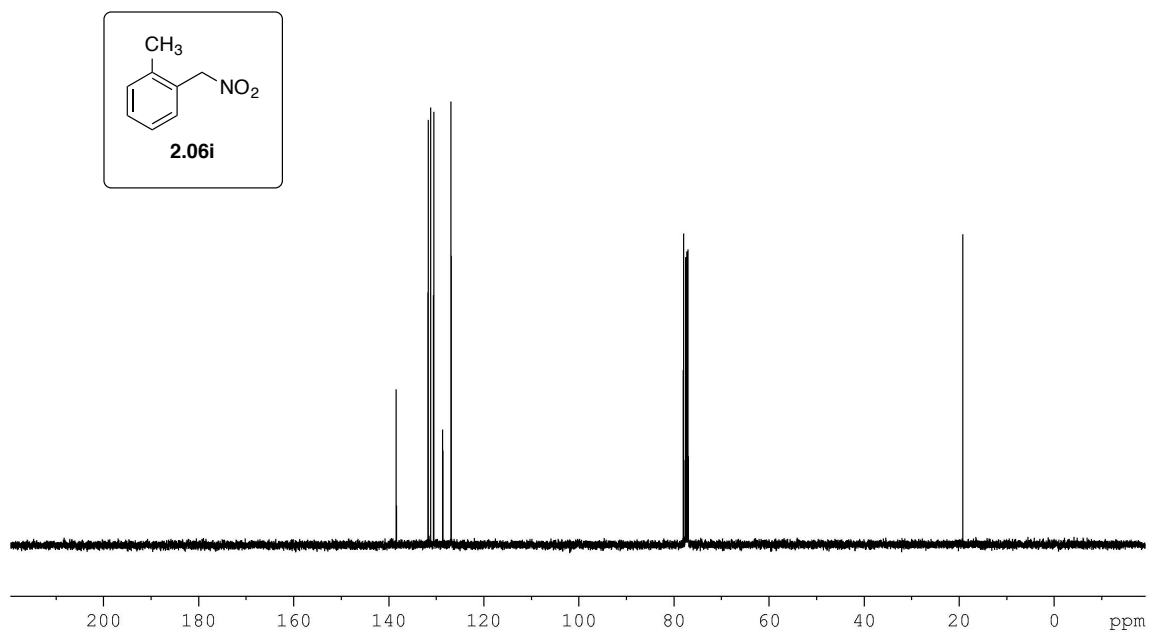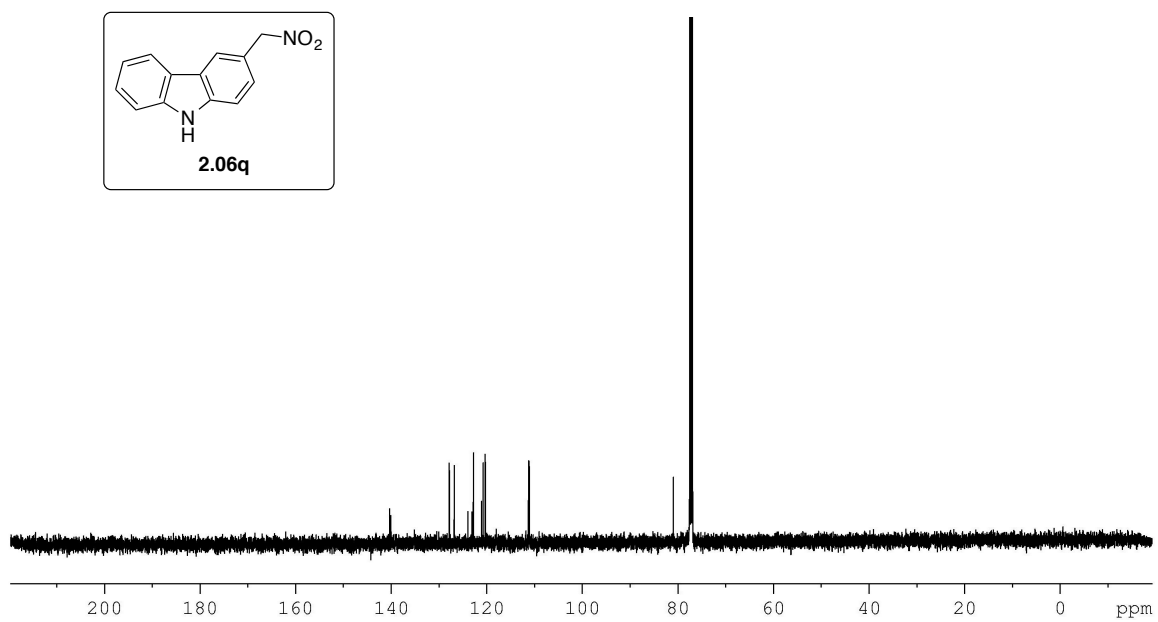

Figure A.2.06i_2 ^{13}C NMR spectrum of compound **2.06i** (125 MHz, CDCl$_3$).
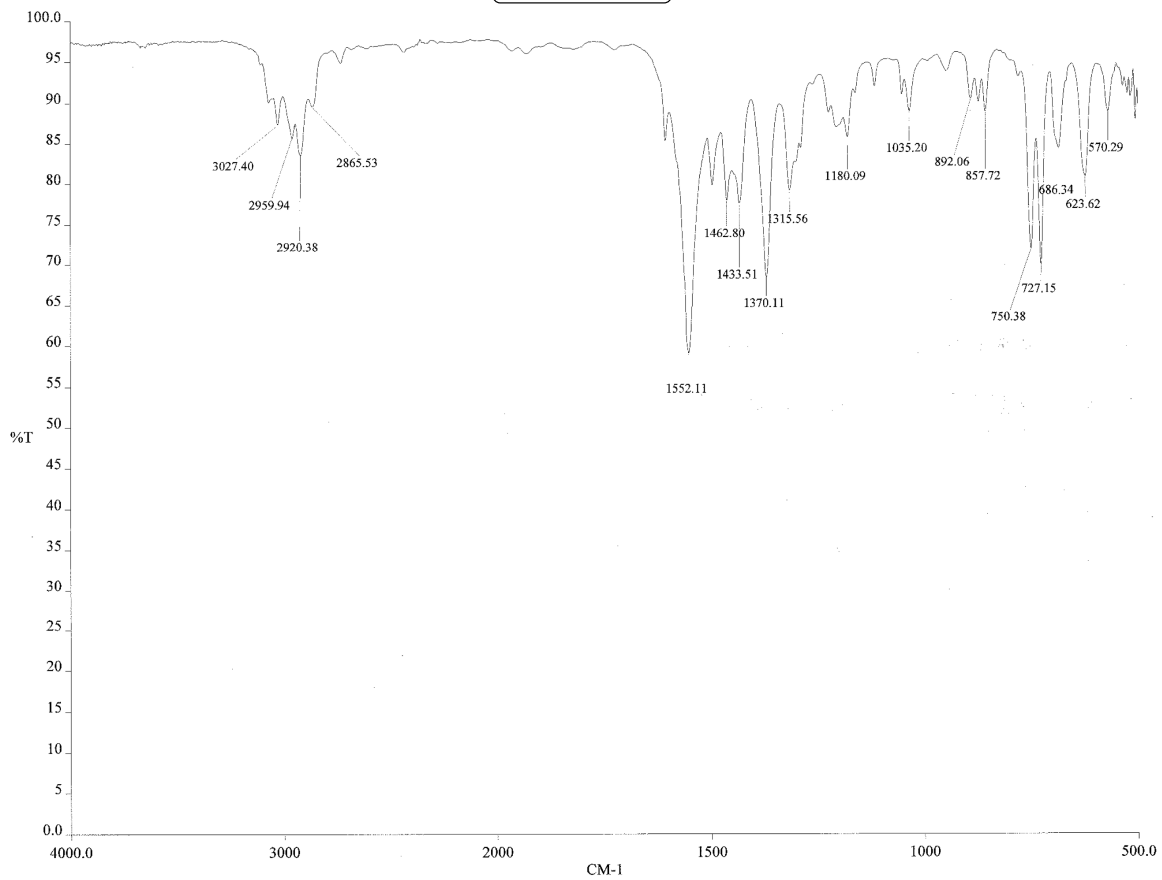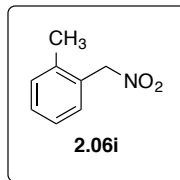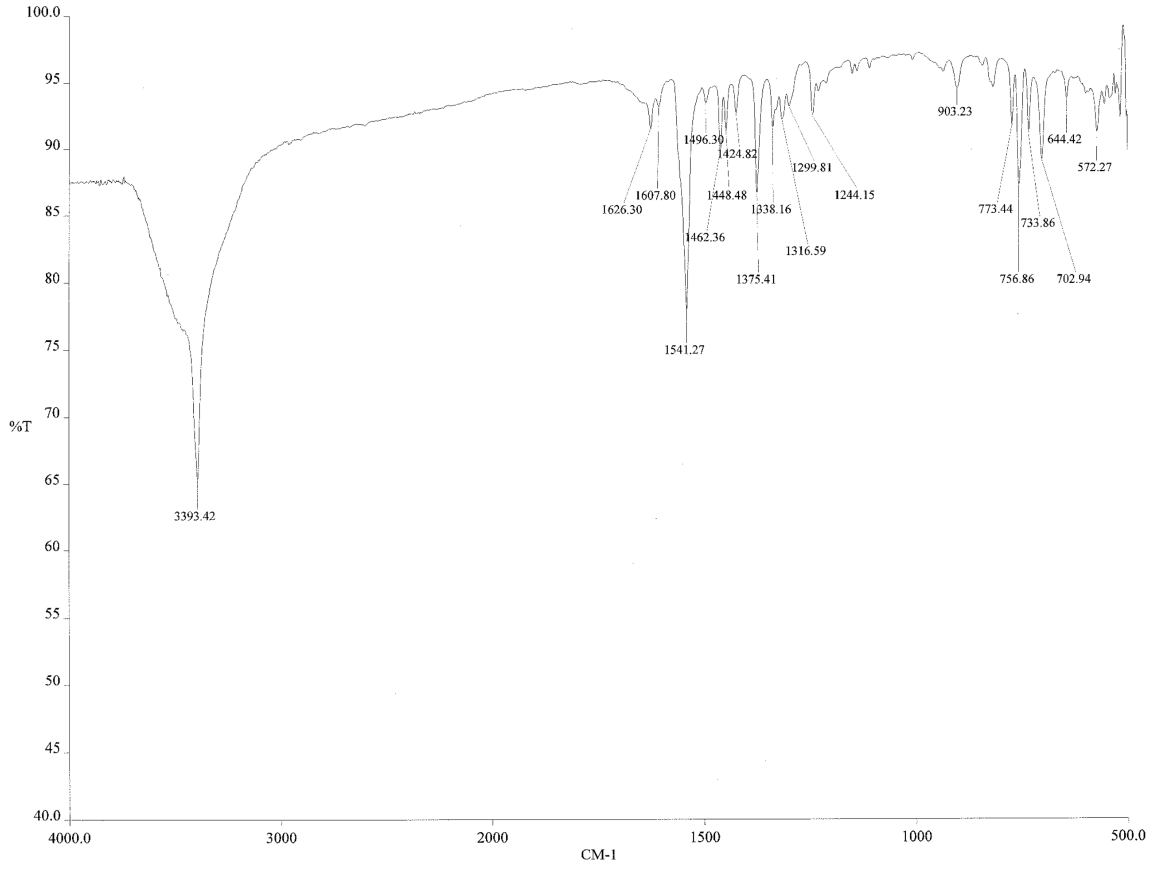
Figure A.2.06i_3 IR spectrum of compound **2.06i**.
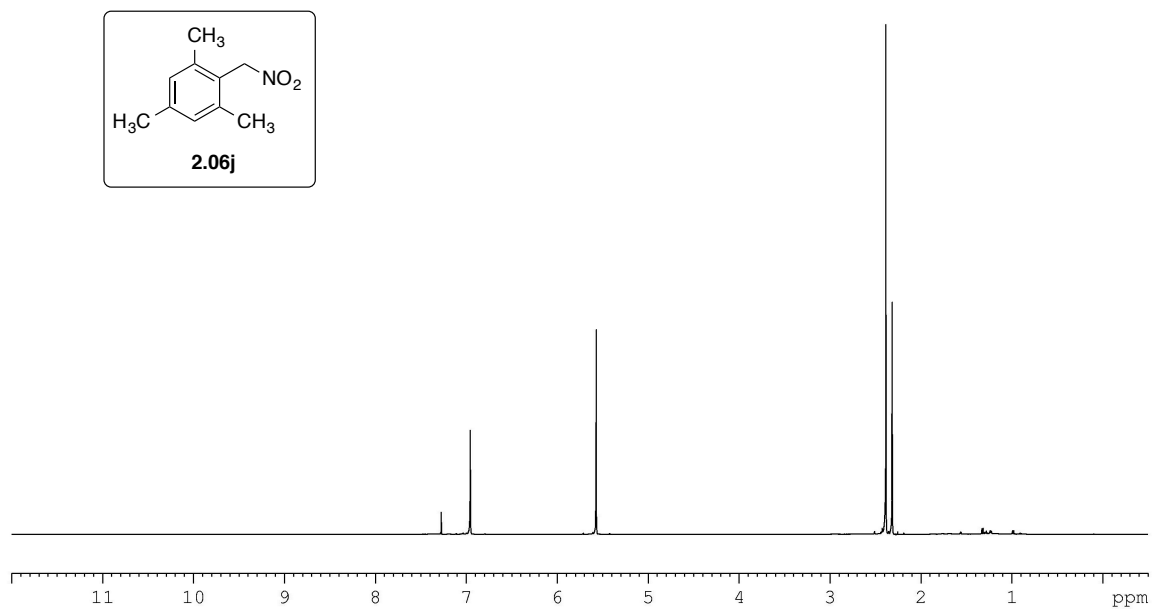
Figure A.2.06j_1 ^{1}H NMR spectrum of compound **2.06j** (500 MHz, CDCl$_3$).

Figure A.2.06j_2 ^{13}C NMR spectrum of compound **2.06j** (125 MHz, CDCl$_3$).
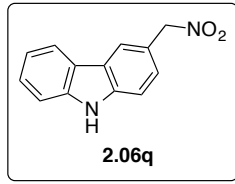
Figure A.2.06j_3 IR spectrum of compound **2.06j**.
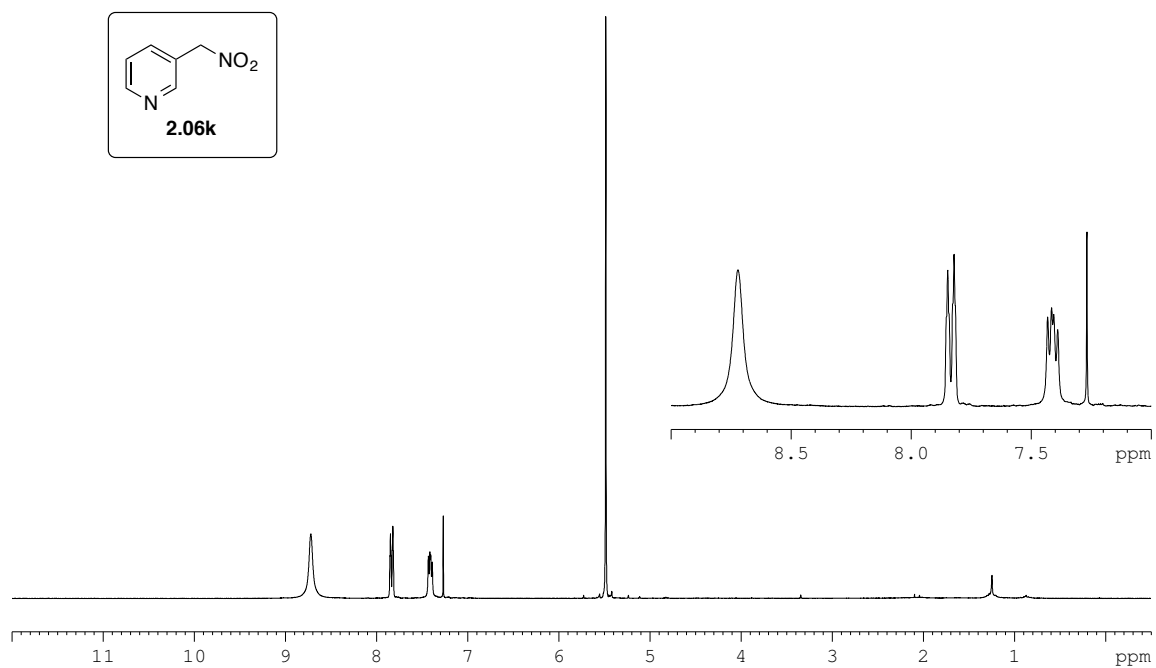
Figure A.2.06k_1 ^{1}H NMR spectrum of compound **2.06k** (500 MHz, CDCl$_3$).

Figure A.2.06k_2 ^{13}C NMR spectrum of compound **2.06k** (125 MHz, CDCl$_3$).

Figure A.2.06k_3 IR spectrum of compound **2.06k**.

Figure A.2.06l_1 ^{1}H NMR spectrum of compound **2.06l** (500 MHz, CDCl$_3$).

Figure A.2.06l_2 ^{13}C NMR spectrum of compound **2.06l** (125 MHz, CDCl$_3$).
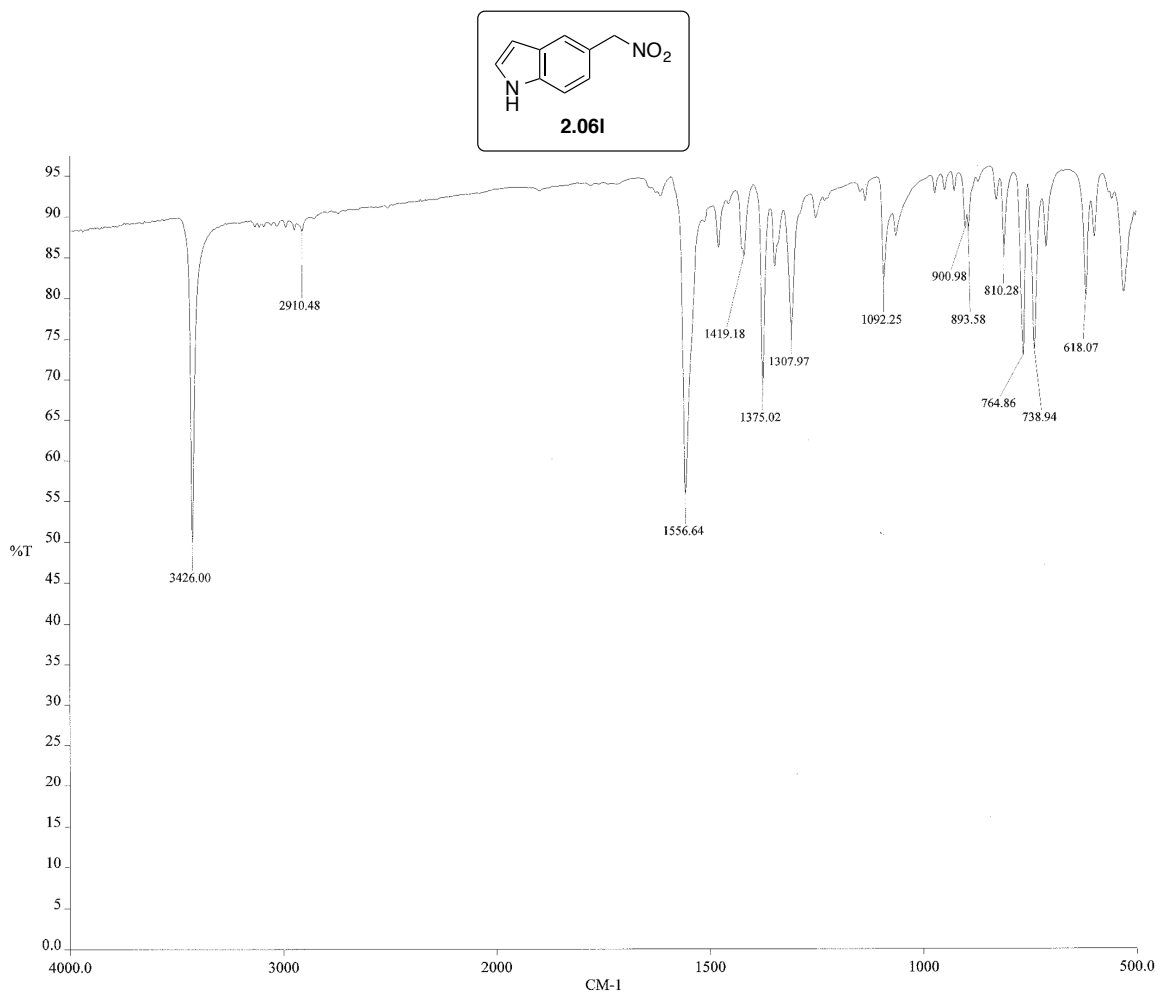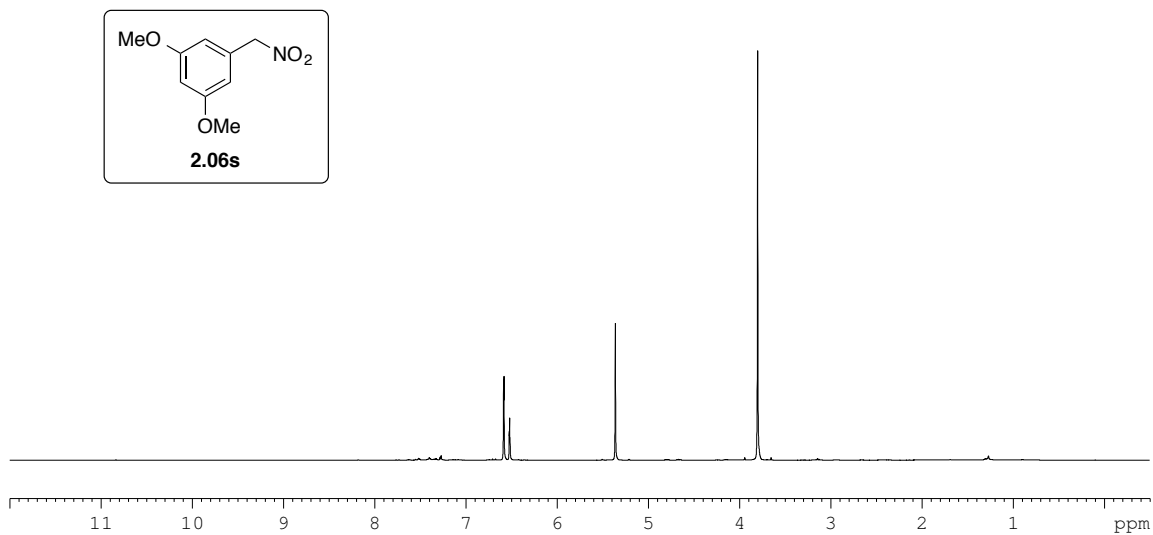
Figure A.2.06l_3 IR spectrum of compound **2.06l**.
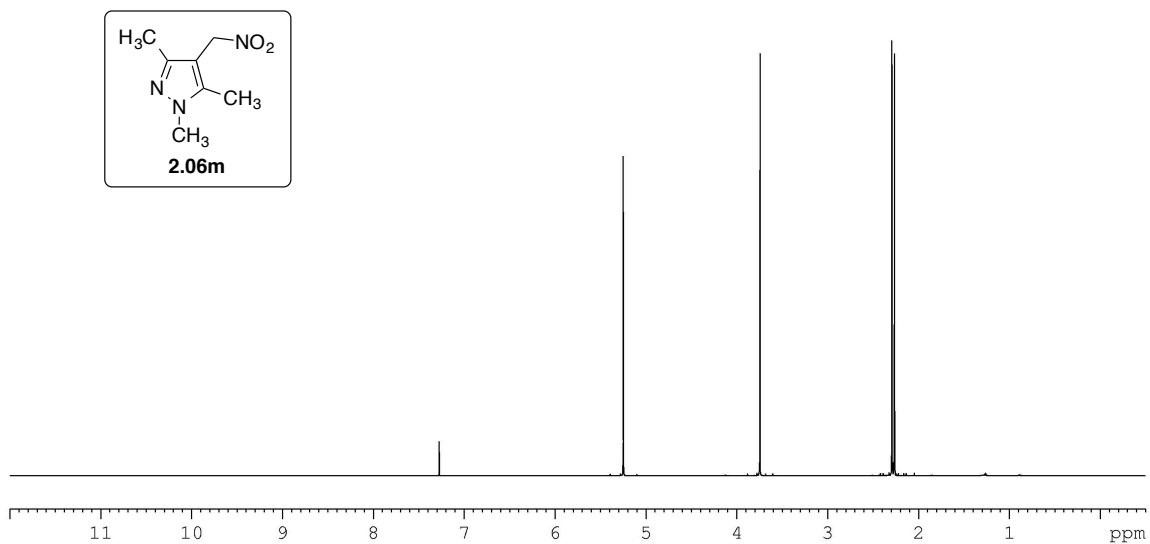
Figure A.2.06m_1 ^{1}H NMR spectrum of compound **2.06m** (500 MHz, CDCl$_3$).
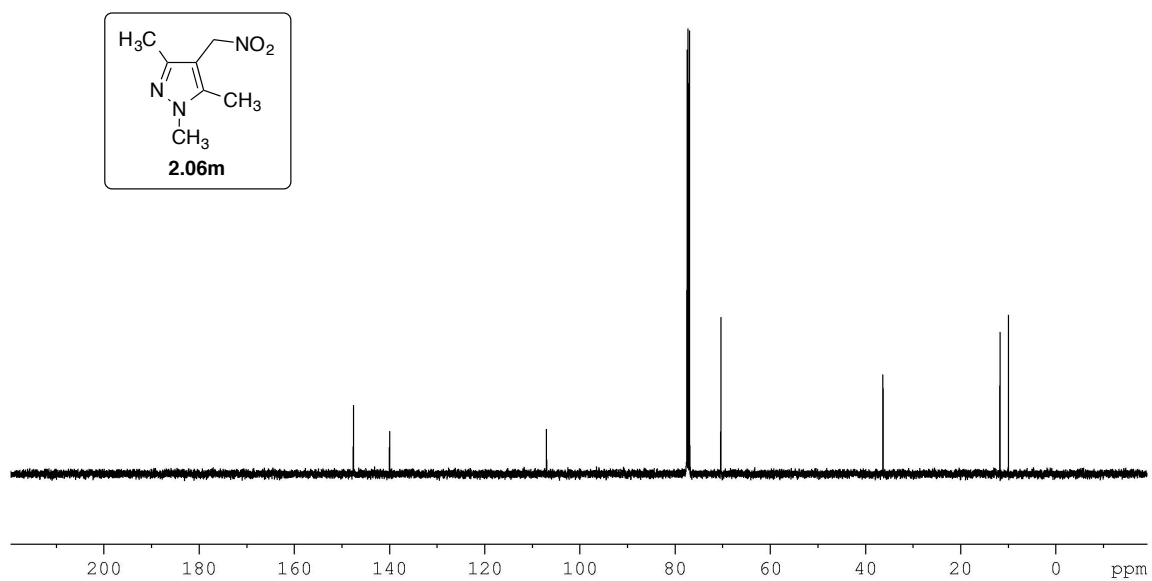
Figure A.2.06m_2 ^{13}C NMR spectrum of compound **2.06m** (125 MHz, CDCl$_3$).
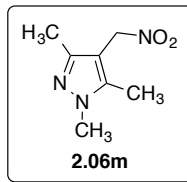
Figure A.2.06m_3 IR spectrum of compound **2.06m**.
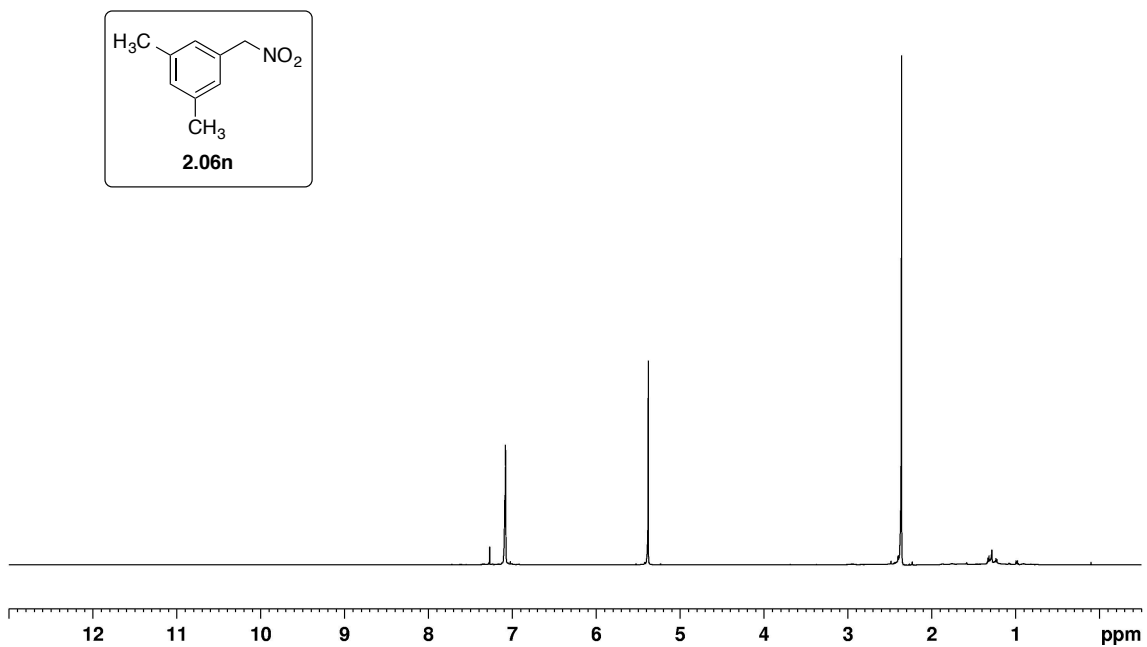
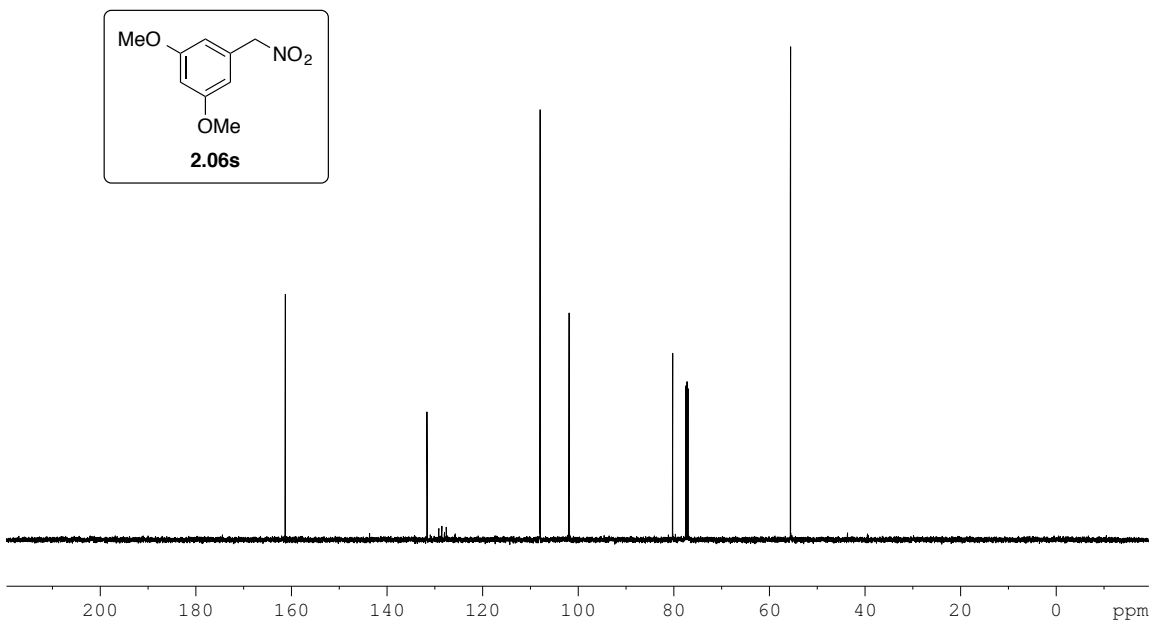**Figure A.2.06n_1** ^{1}H NMR spectrum of compound **2.06n** (500 MHz, CDCl$_3$).
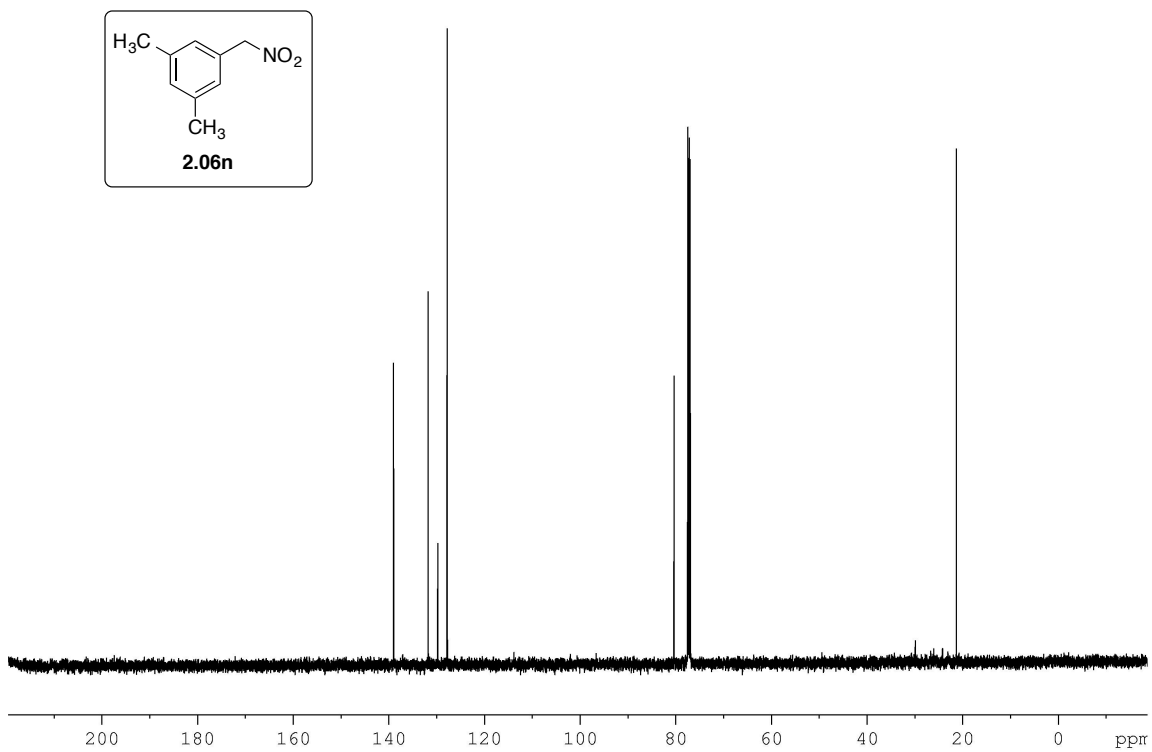
Figure A.2.06n_2 ^{13}C NMR spectrum of compound **2.06n** (125 MHz, CDCl$_3$).
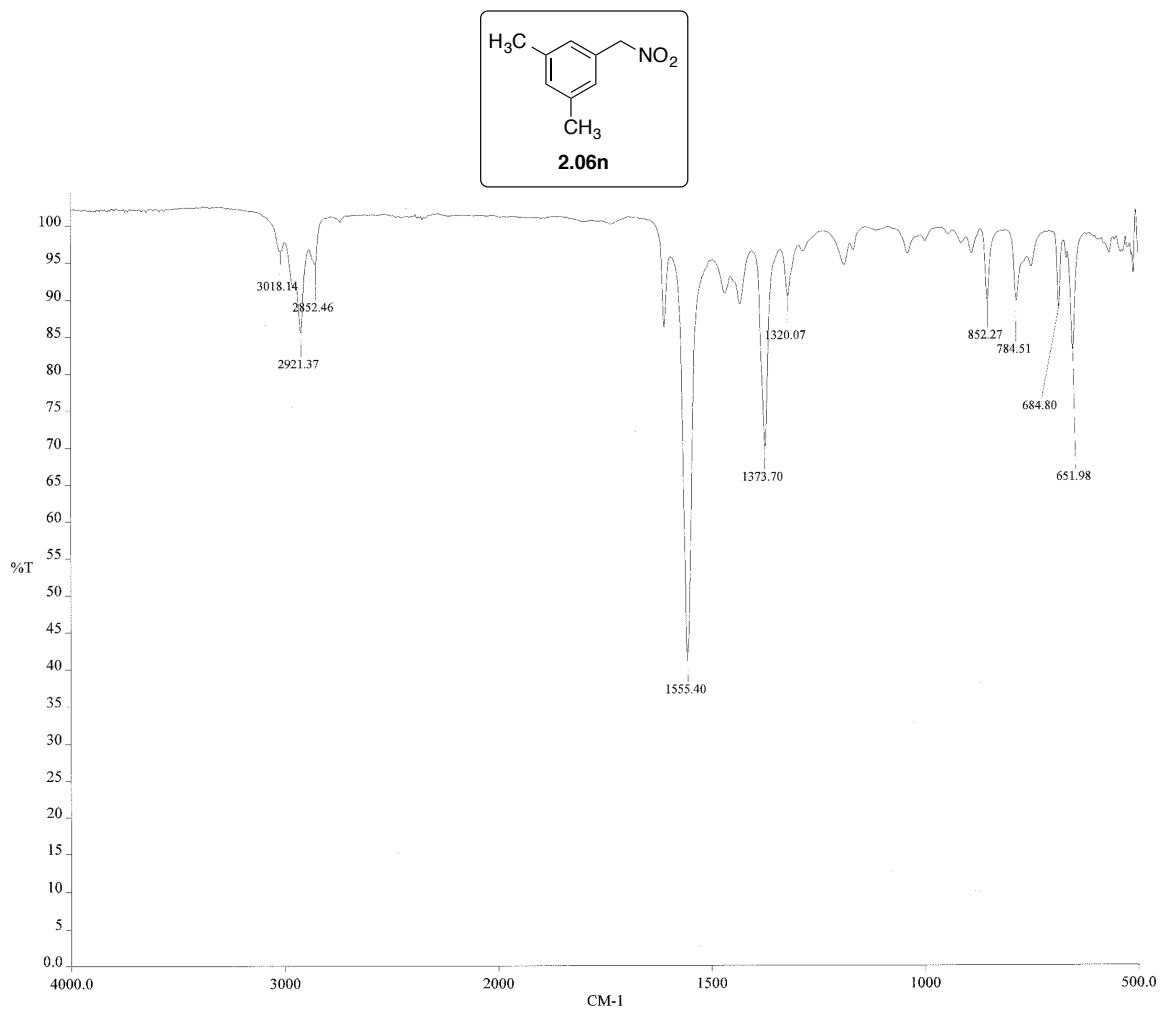
Figure A.2.06n_3 IR spectrum of compound **2.06n**.
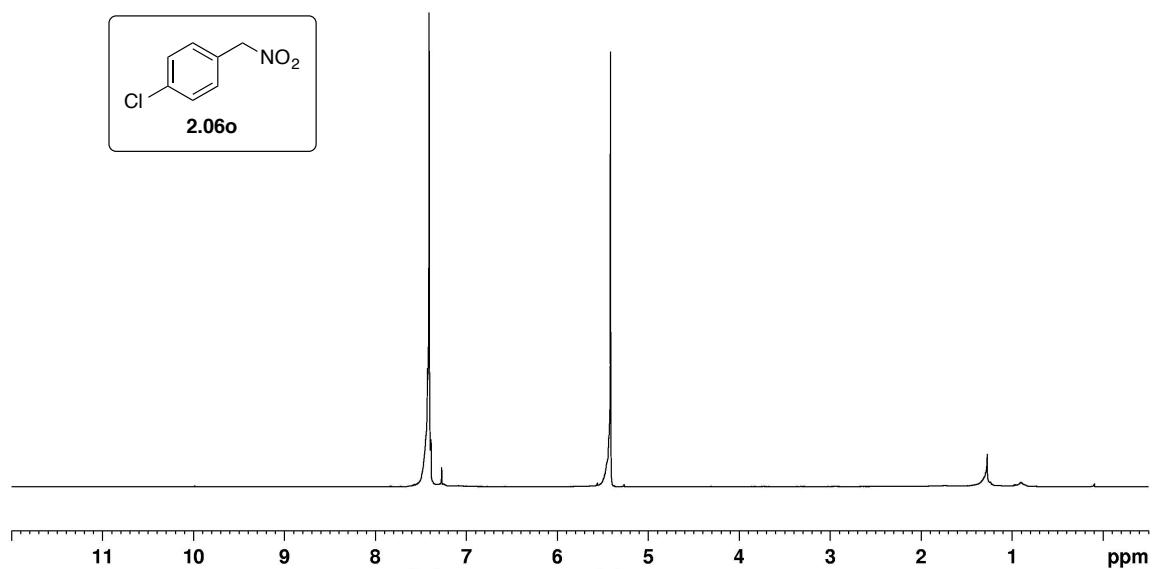
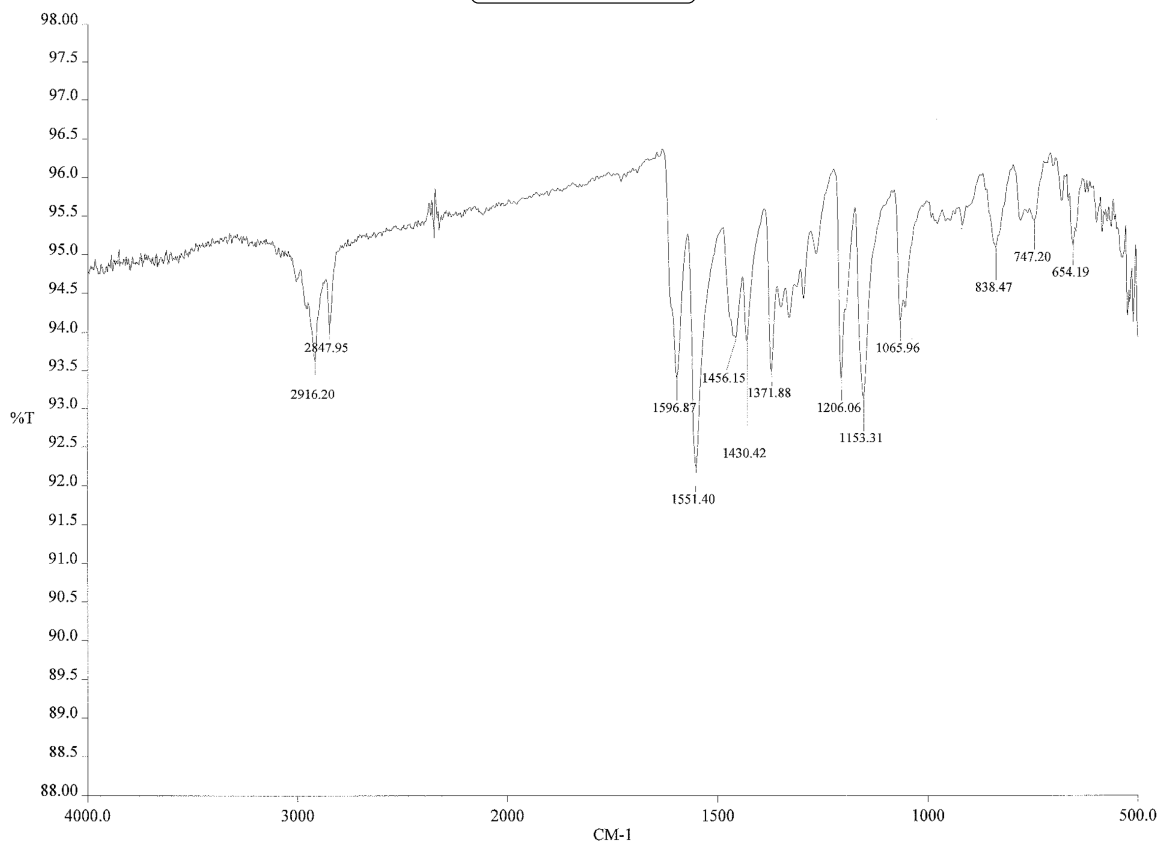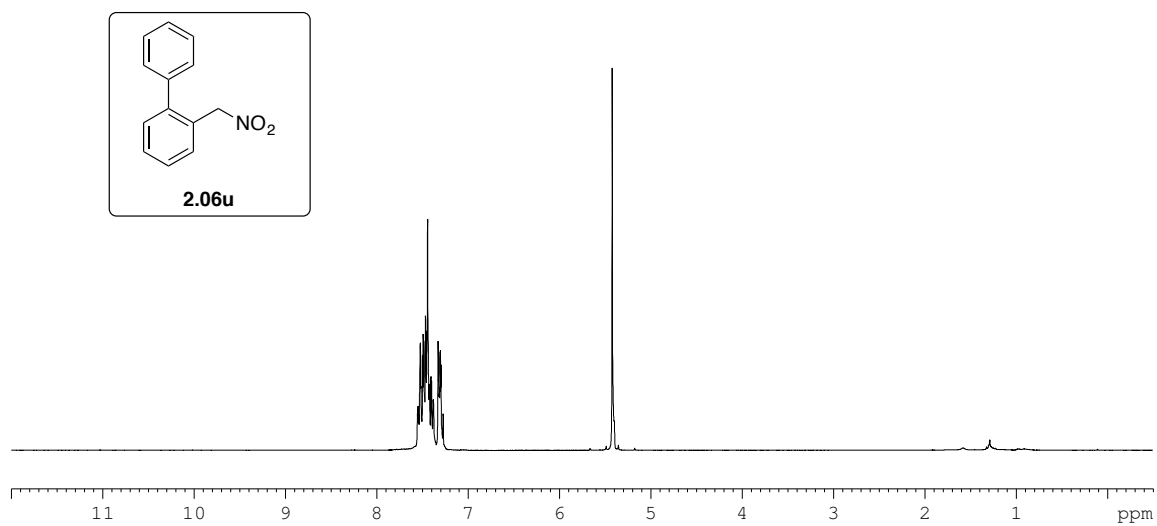**Figure A.2.06o_1** ^{1}H NMR spectrum of compound **2.06o** (500 MHz, CDCl$_3$).
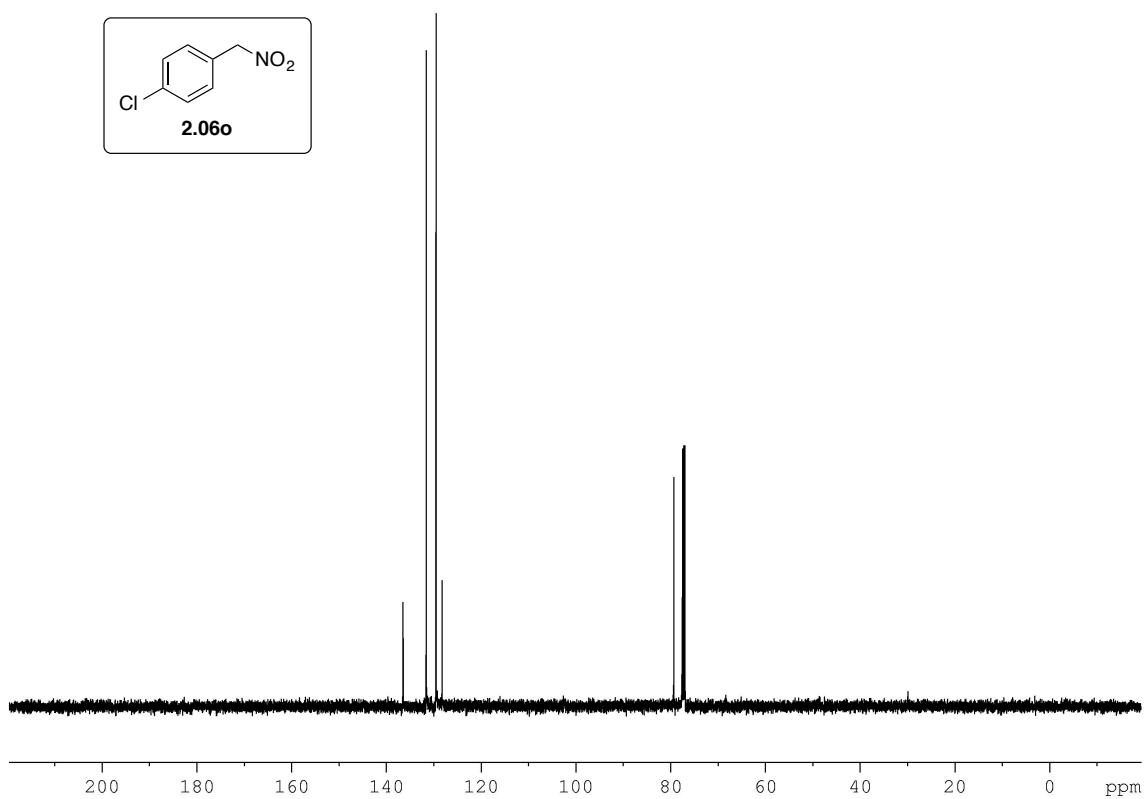
Figure A.2.06o_2 ^{13}C NMR spectrum of compound **2.06o** (125 MHz, CDCl$_3$).

Figure A.2.06o_3 IR spectrum of compound **2.06o**.

Figure A.2.06p_1 ^{1}H NMR spectrum of compound **2.06p** (500 MHz, CDCl$_3$).
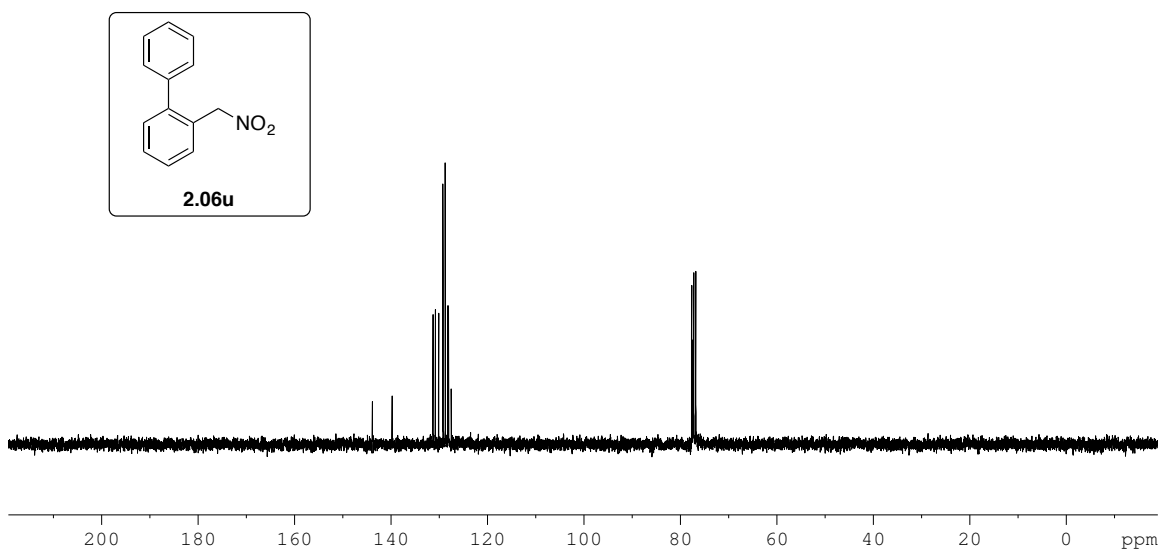

Figure A.2.06p_2 ^{13}C NMR spectrum of compound **2.06p** (125 MHz, CDCl$_3$).
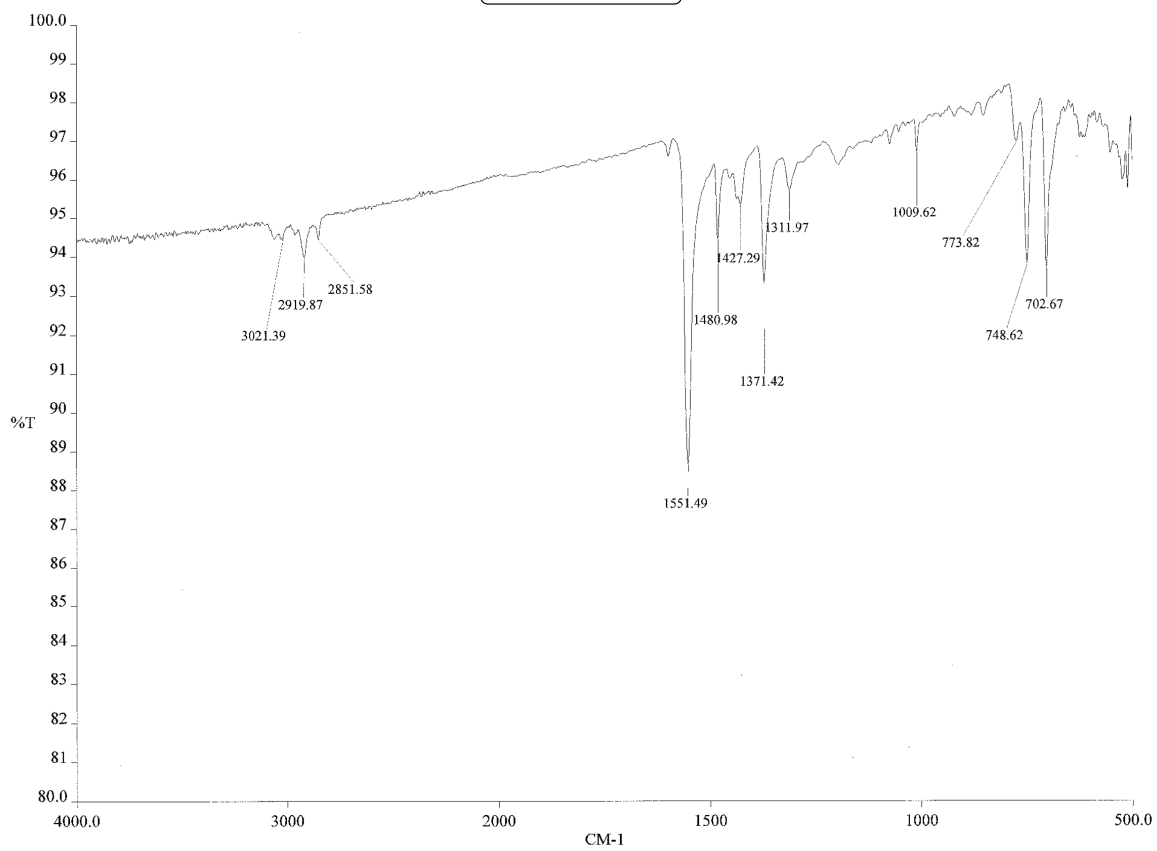
Figure A.2.06p_3 IR spectrum of compound **2.06p**.

Figure A.2.06q_1 ^{1}H NMR spectrum of compound **2.06q** (500 MHz, CDCl$_3$).

Figure A.2.06q_2 ^{13}C NMR spectrum of compound **2.06q** (125 MHz, CDCl$_3$).
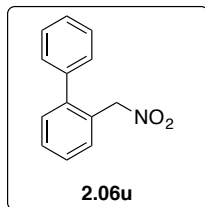
Figure A.2.06q_3 IR spectrum of compound **2.06q**.

Figure A.2.06s_1 ^{1}H NMR spectrum of compound **2.06s** (500 MHz, CDCl$_3$).

Figure A.2.06s_2 ^{13}C NMR spectrum of compound **2.06s** (125 MHz, CDCl$_3$).
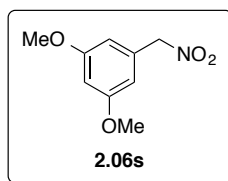
Figure A.2.06s_3 IR spectrum of compound **2.06s**.

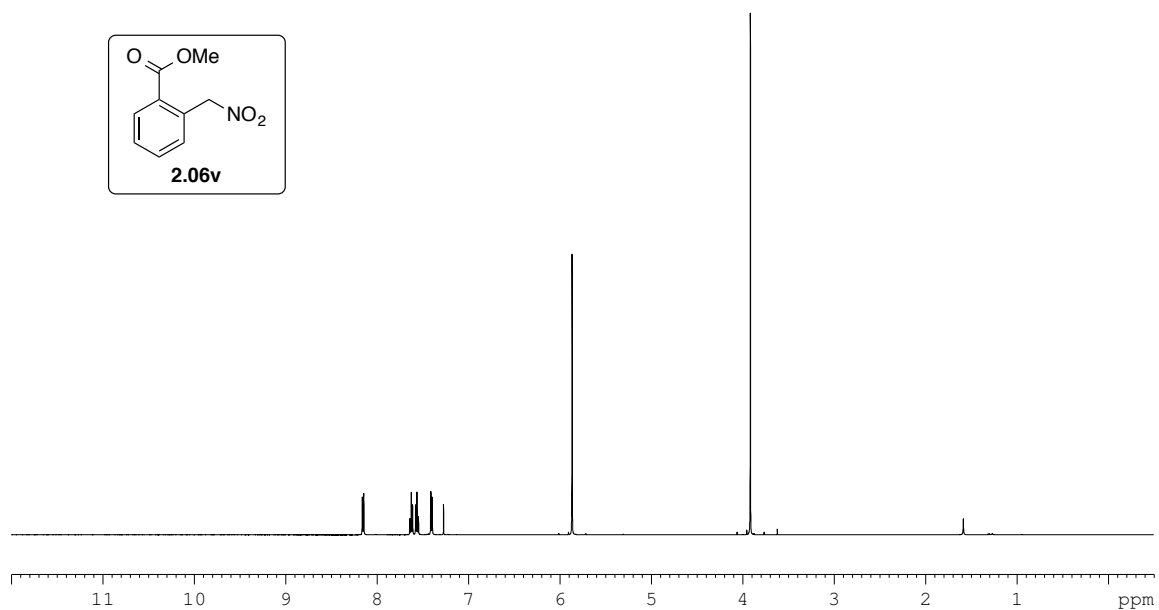**Figure A.2.06u_1** ^{1}H NMR spectrum of compound **2.06u** (300 MHz, CDCl$_3$).

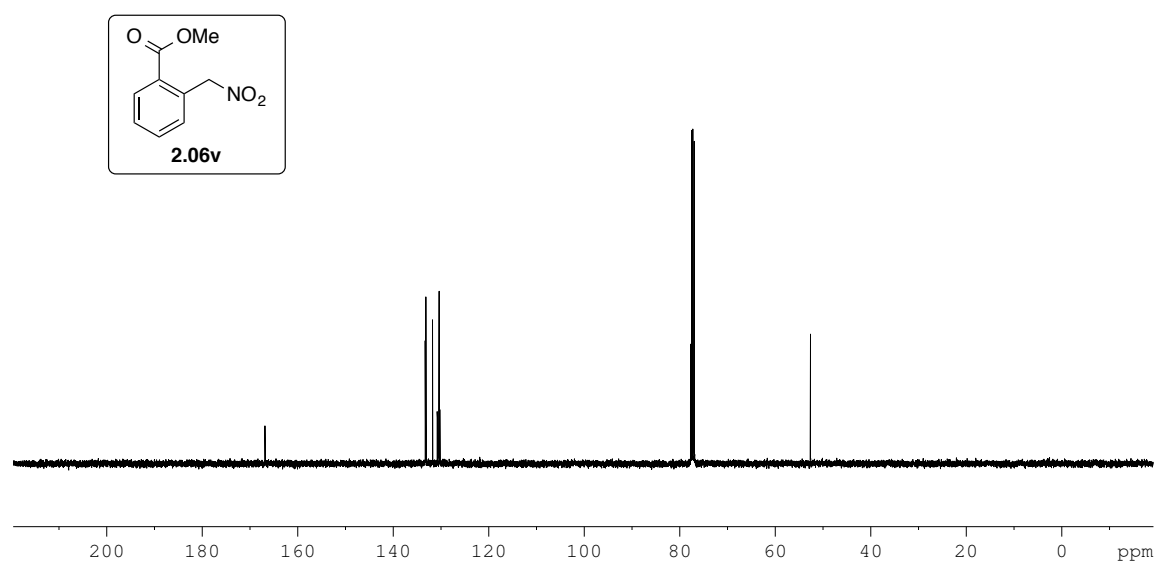**Figure A.2.06u_2** ^{13}C NMR spectrum of compound **2.06u** (75 MHz, CDCl$_3$).
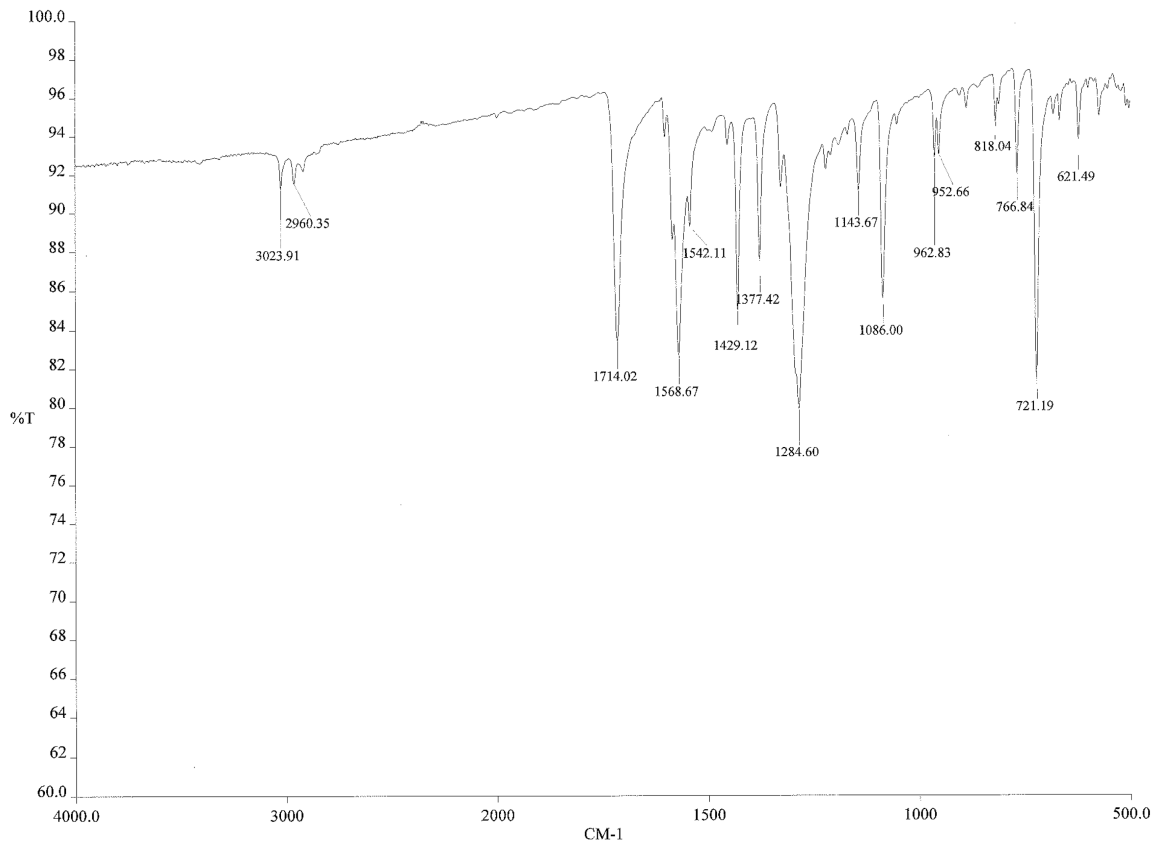
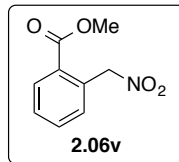**Figure A.2.06u_3** IR spectrum of compound **2.06u**.

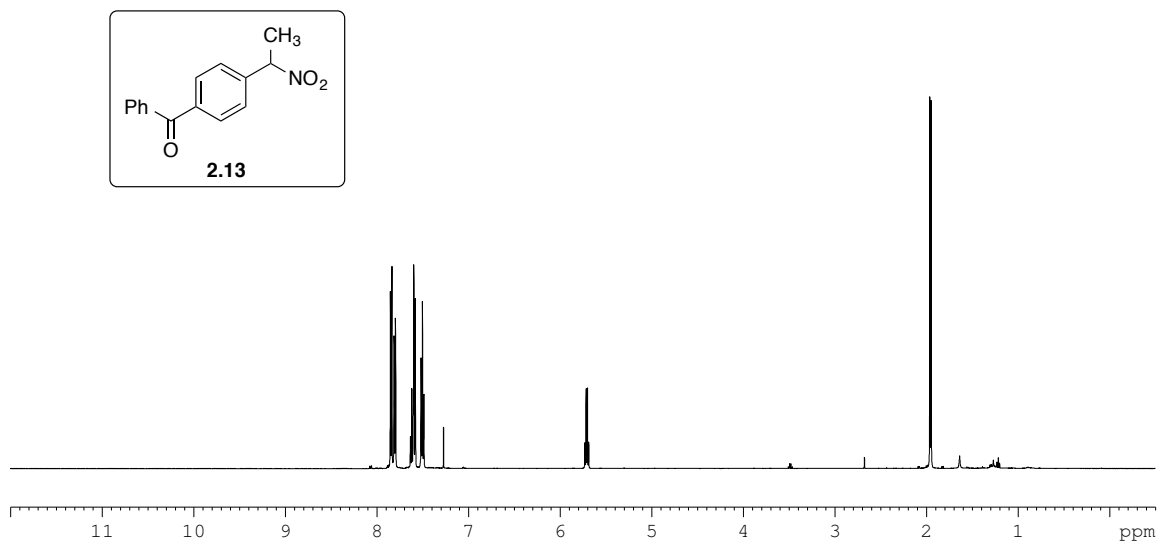**Figure A.2.06v_1** ^{1}H NMR spectrum of compound **2.06v** (500 MHz, CDCl$_3$).

Figure A.2.06v_2 ^{13}C NMR spectrum of compound **2.06v** (125 MHz, CDCl$_3$).

Figure A.2.06v_3 IR spectrum of compound **2.06v**.

Figure A.2.13_1 ^{1}H NMR spectrum of compound **2.13** (500 MHz, CDCl$_3$).
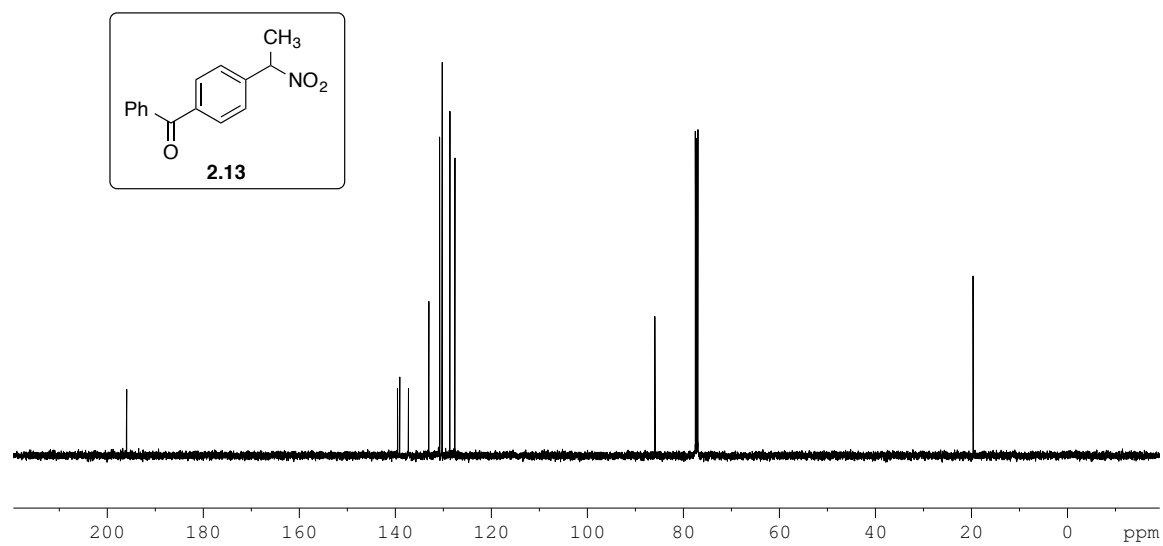
Figure A.2.13_2 ^{13}C NMR spectrum of compound **2.13** (125 MHz, CDCl$_3$).
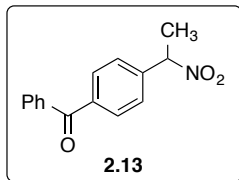
Figure A.2.13_3 IR spectrum of compound **2.13**.
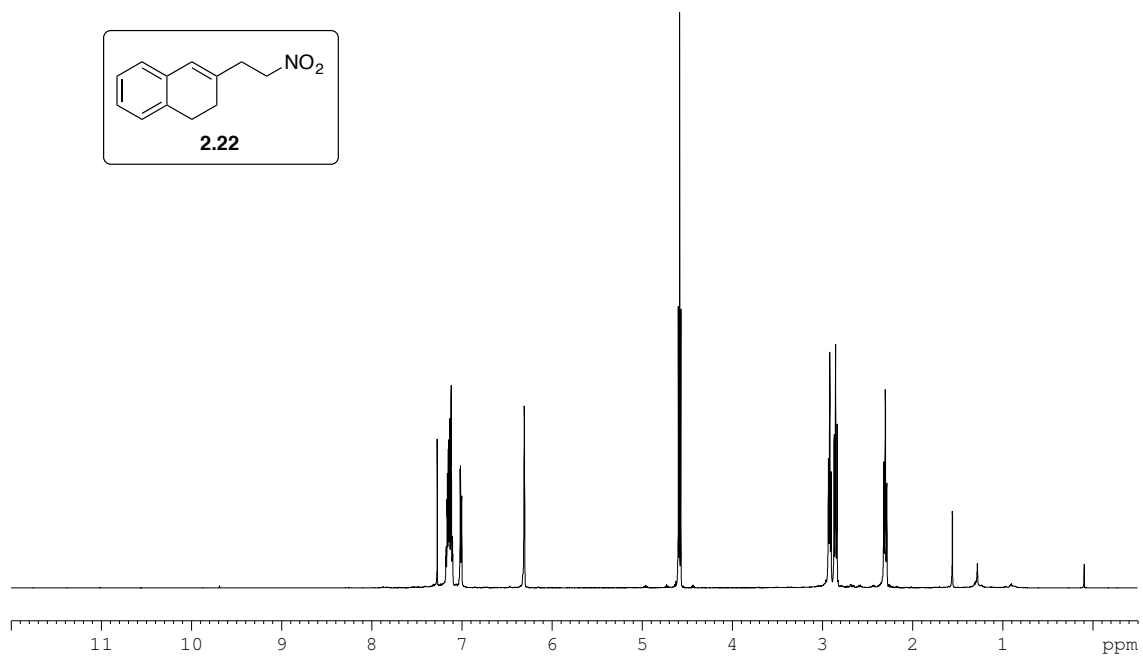
Figure A.2.22_1 ^{1}H NMR spectrum of compound **2.22** (500 MHz, CDCl$_3$).
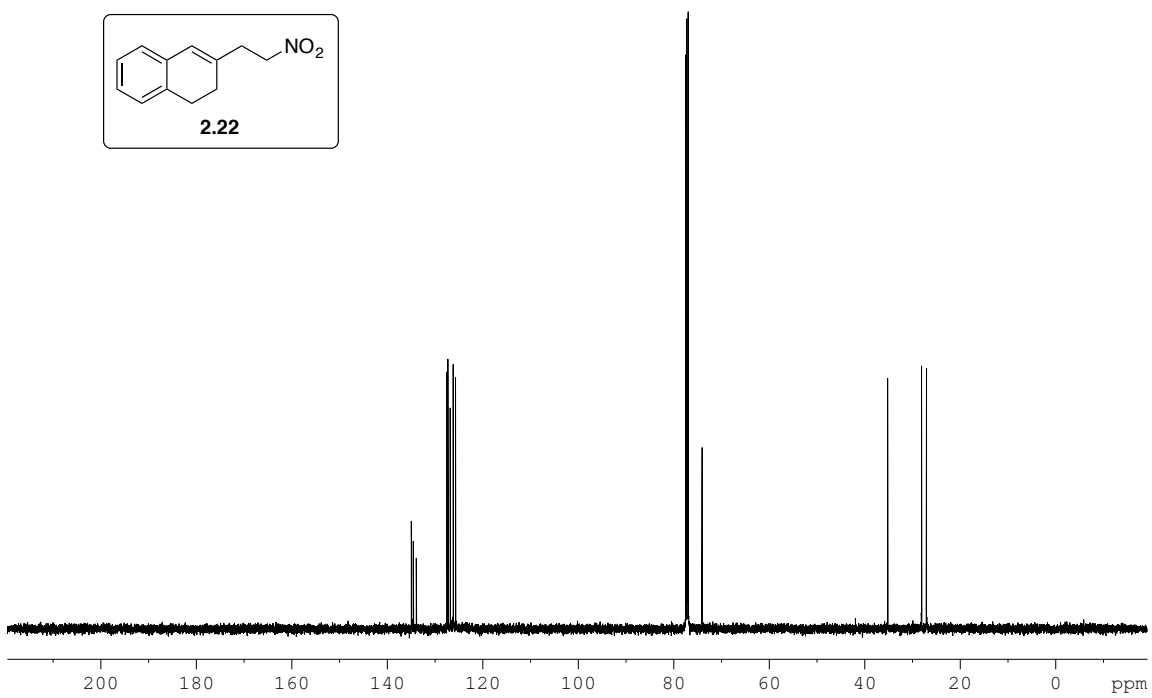
Figure A.2.22_2 ^{13}C NMR spectrum of compound **2.22** (125 MHz, CDCl$_3$).
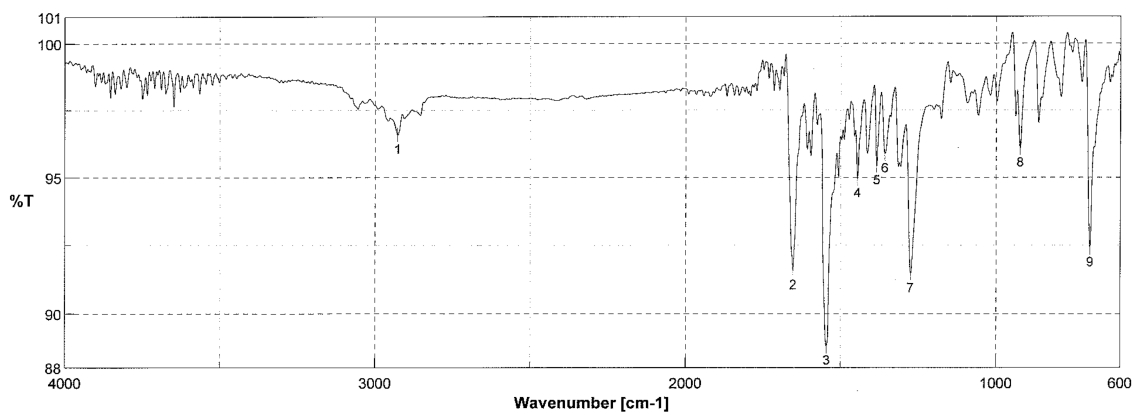
247
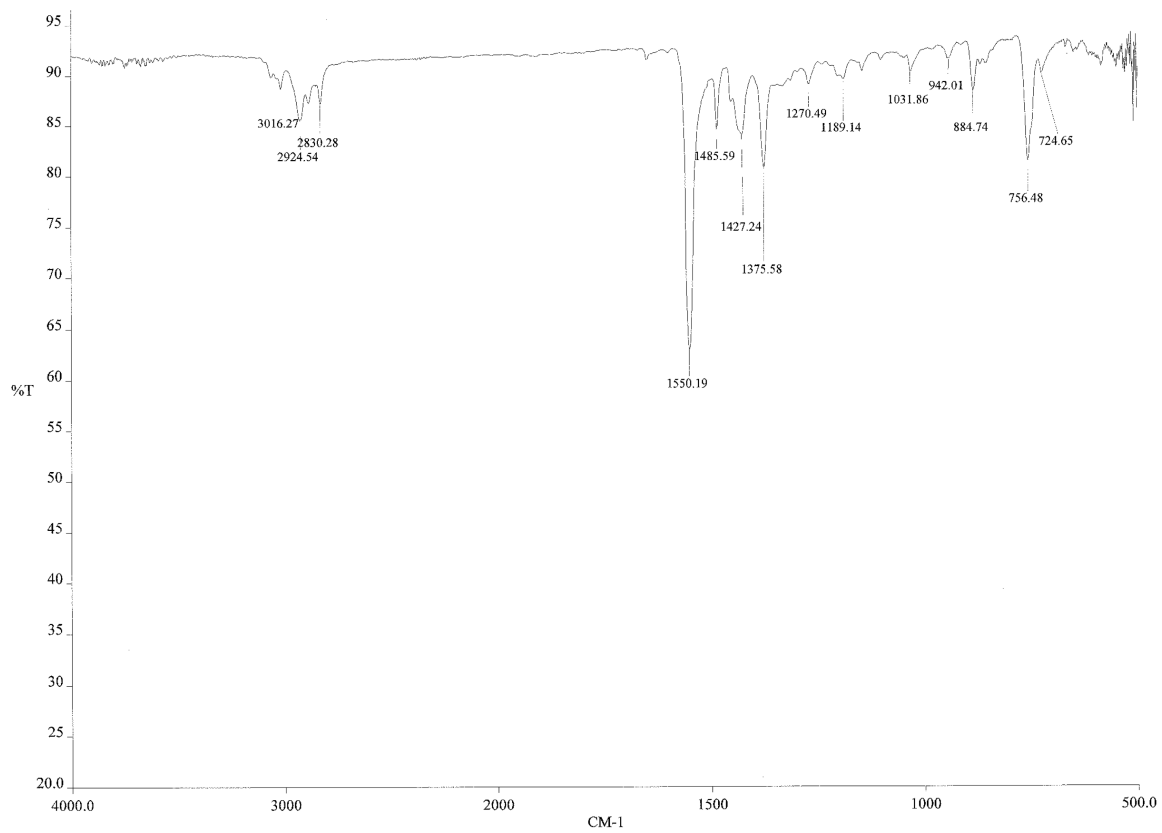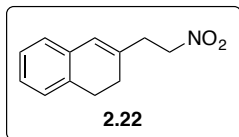
Figure A.2.22_3 IR spectrum of compound **2.22**.
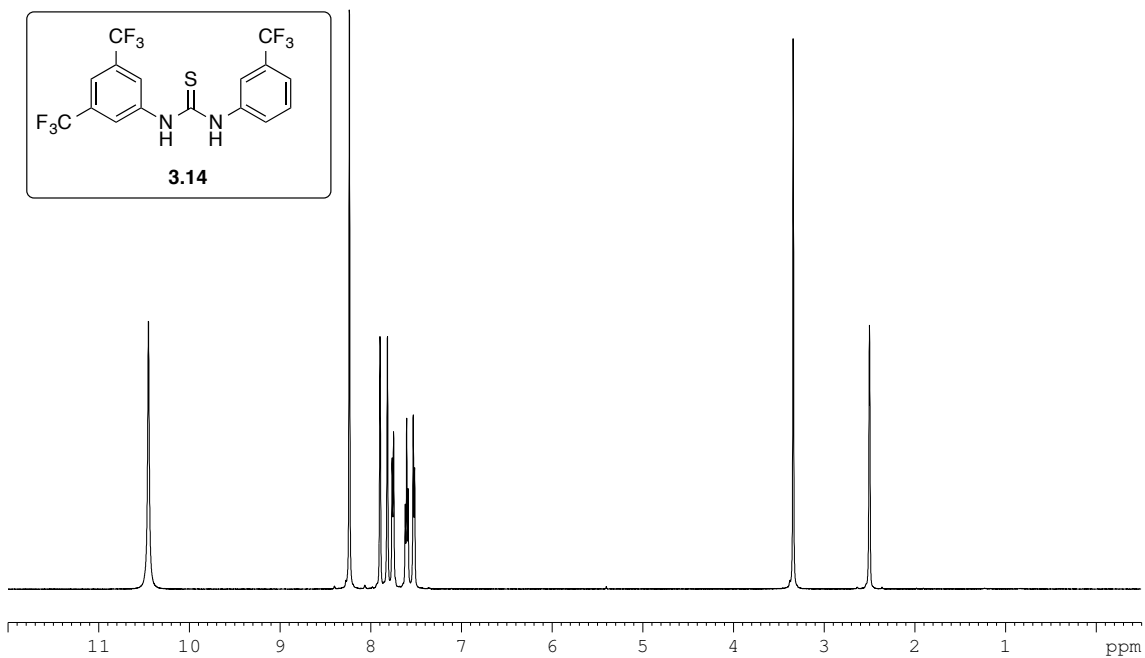
Figure A.3.14_1 ^{1}H NMR spectrum of compound **3.14** (500 MHz, DMSO).
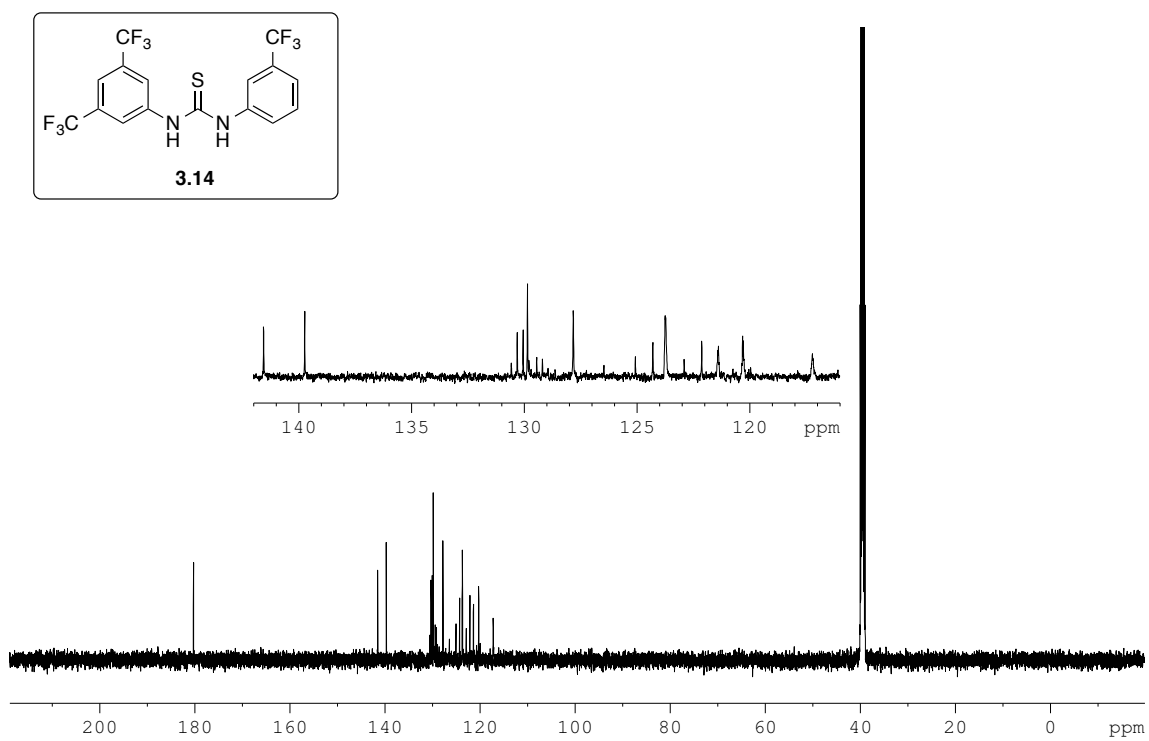
Figure A.3.14_2 ^{13}C NMR spectrum of compound **3.14** (125 MHz, DMSO).
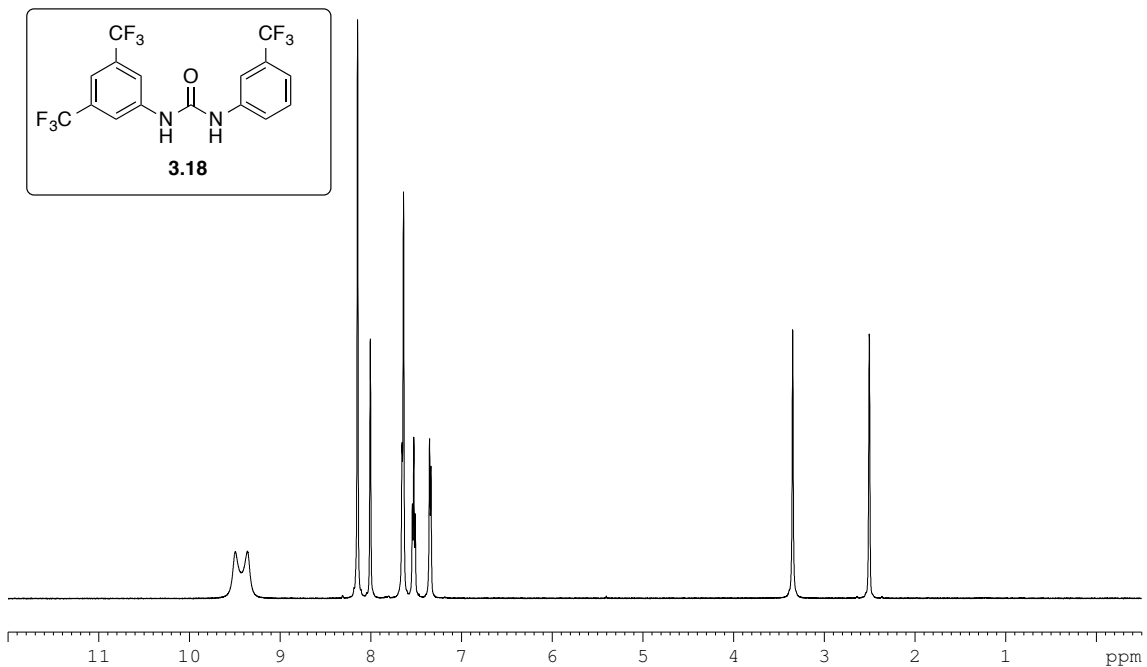
Figure A.3.18_1 ^{1}H NMR spectrum of compound **3.18** (500 MHz, DMSO).
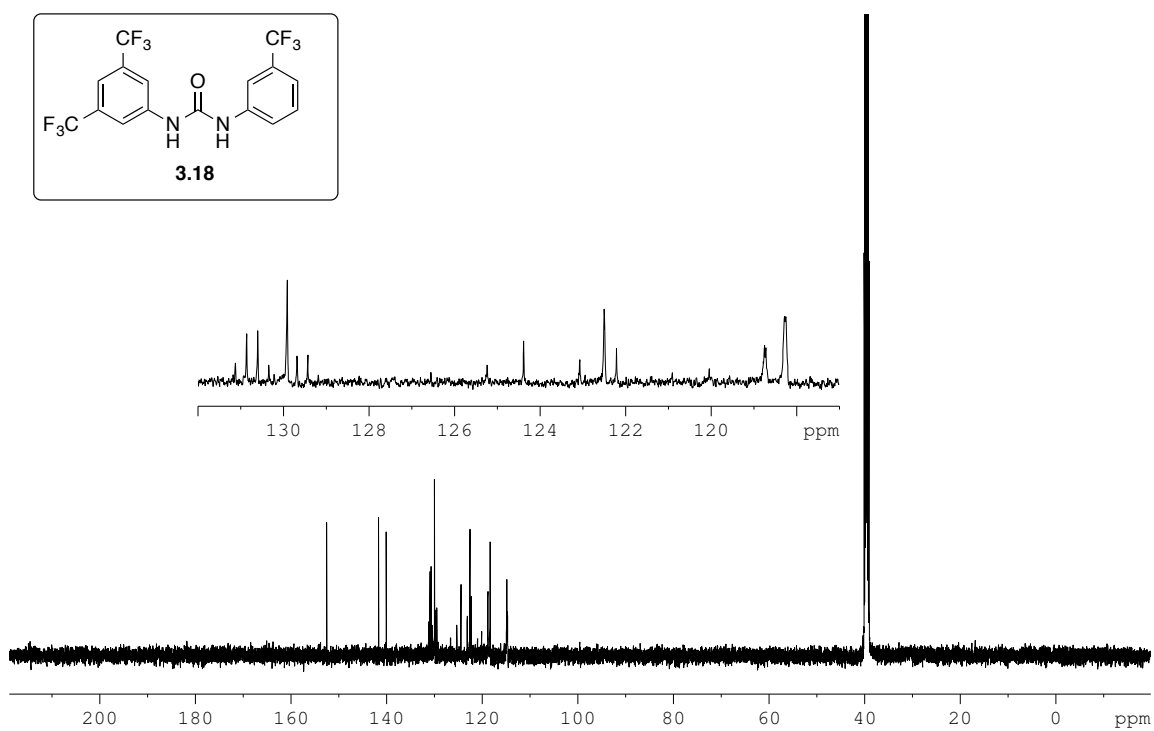
Figure A.3.18_2 ^{13}C NMR spectrum of compound **3.18** (125 MHz, DMSO).

Figure A.3.22_1 ^{1}H NMR spectrum of compound **3.22** (500 MHz, DMSO).
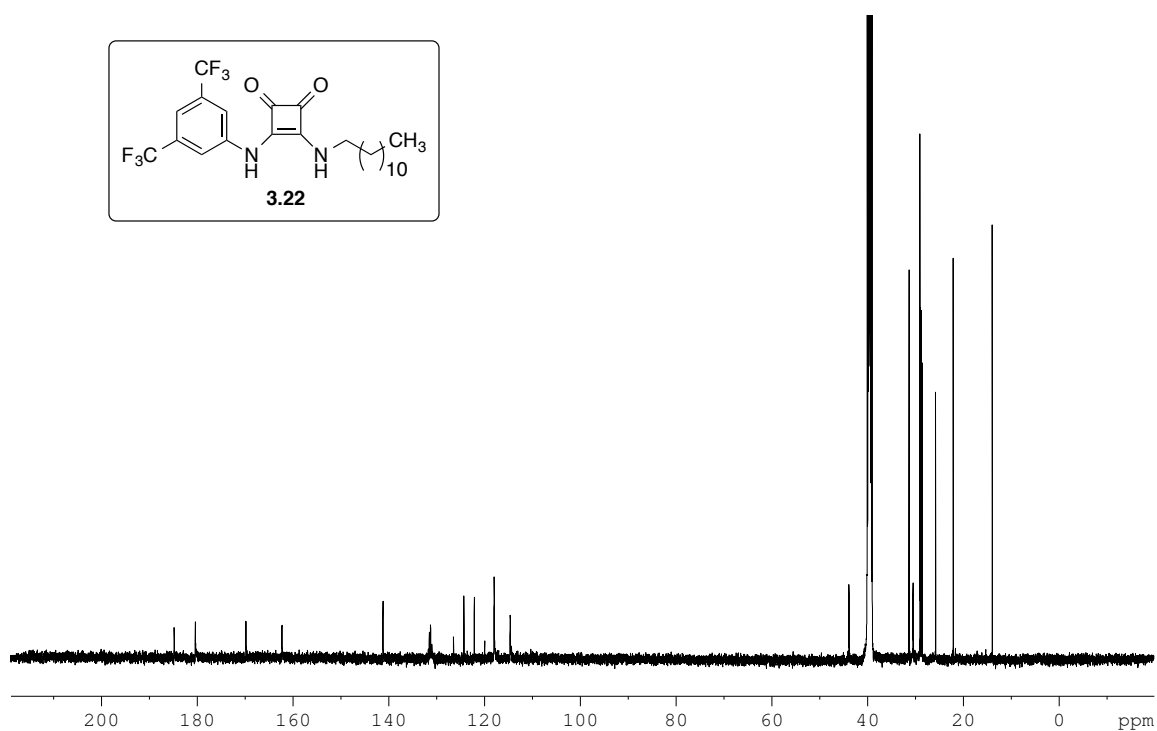
Figure A.3.22_2 ^{13}C NMR spectrum of compound **3.22** (125 MHz, DMSO).
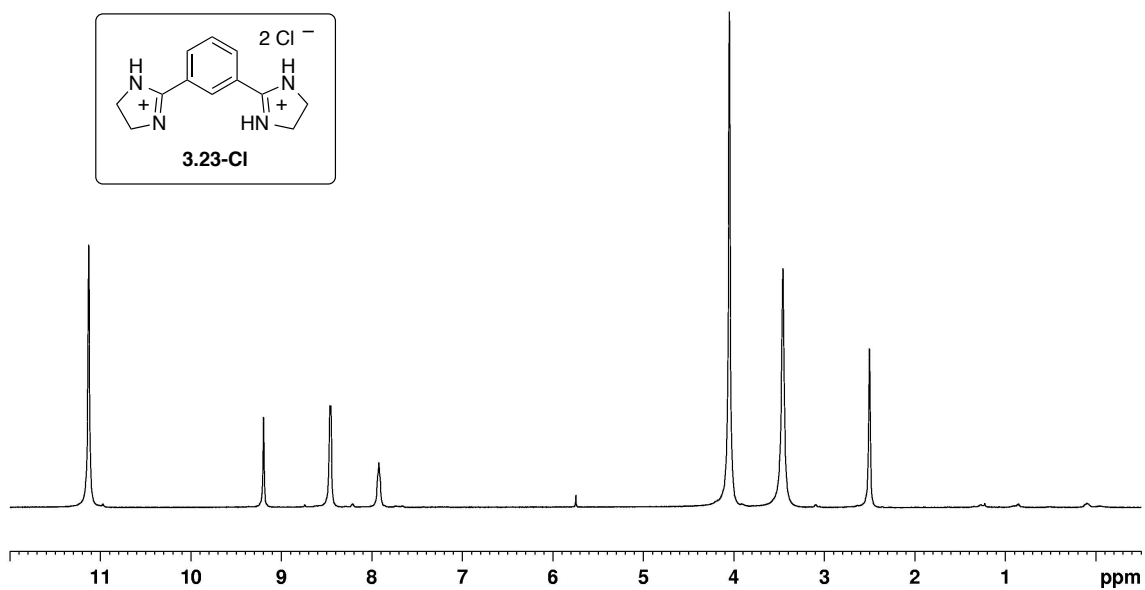
Figure A.3.23-Cl_1 ^{1}H NMR spectrum of compound **3.23-Cl** (500 MHz, DMSO).
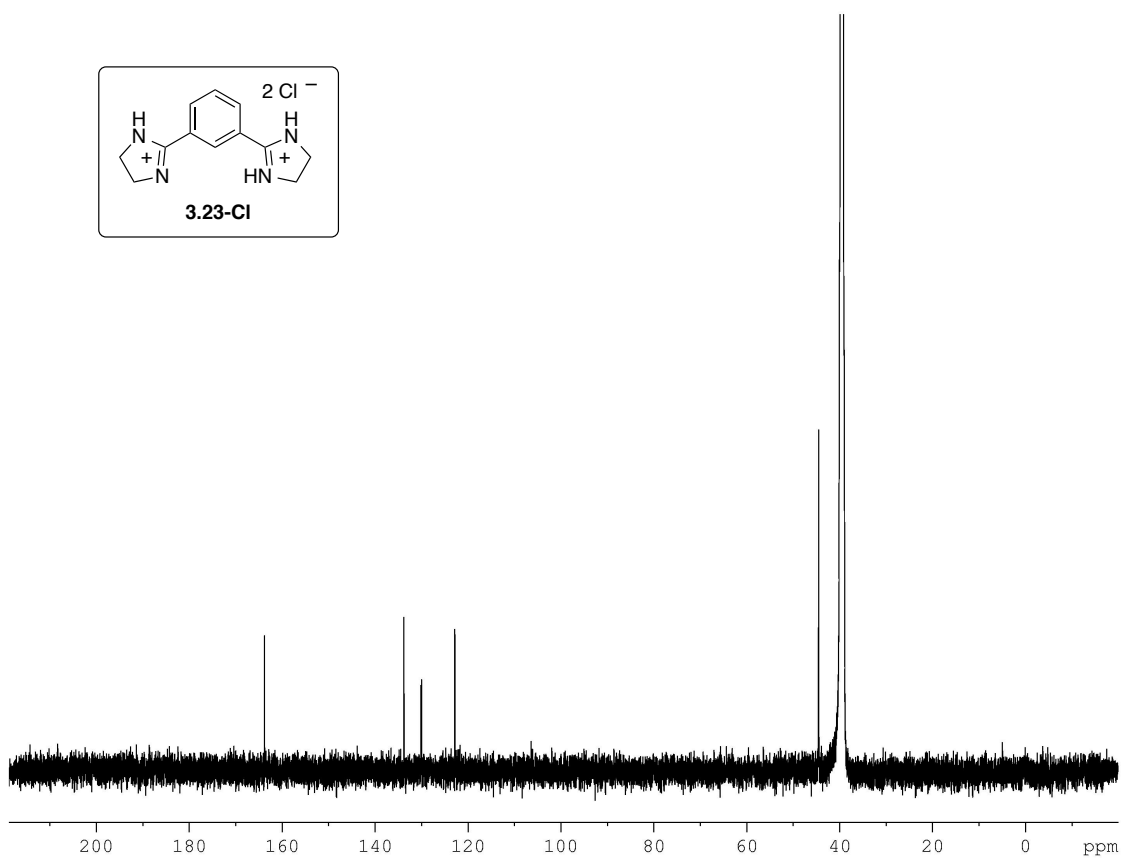
Figure A.3.23-Cl_2 ^{13}C NMR spectrum of compound **3.23-Cl** (125 MHz, DMSO).
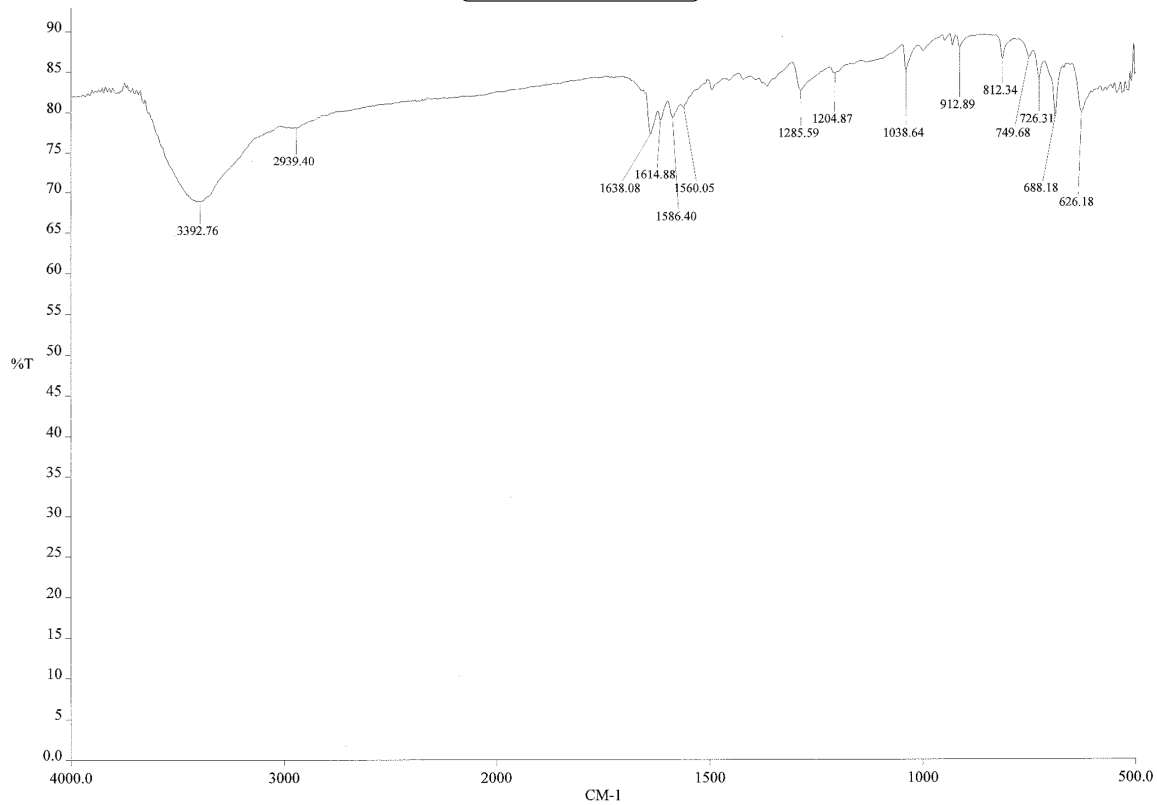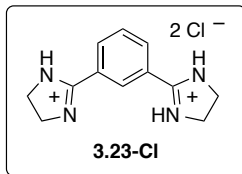
Figure A.3.23-Cl_3 IR spectrum of compound **3.23-Cl**.
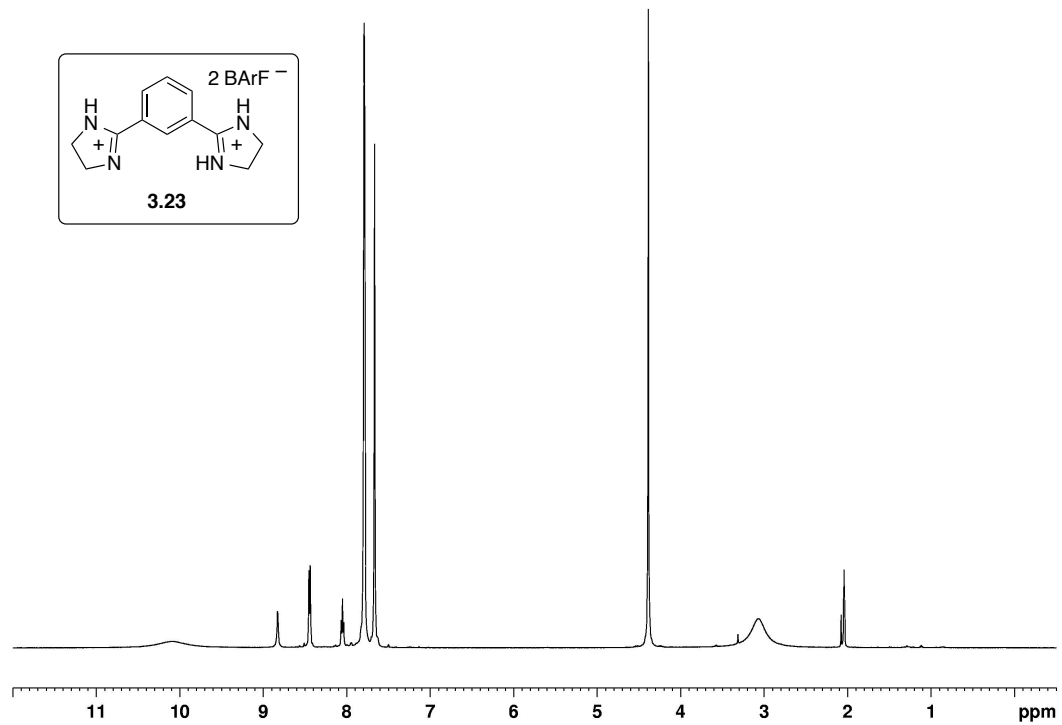
Figure A.3.23_1 ^{1}H NMR spectrum of compound **3.23** (500 MHz, Acetone).
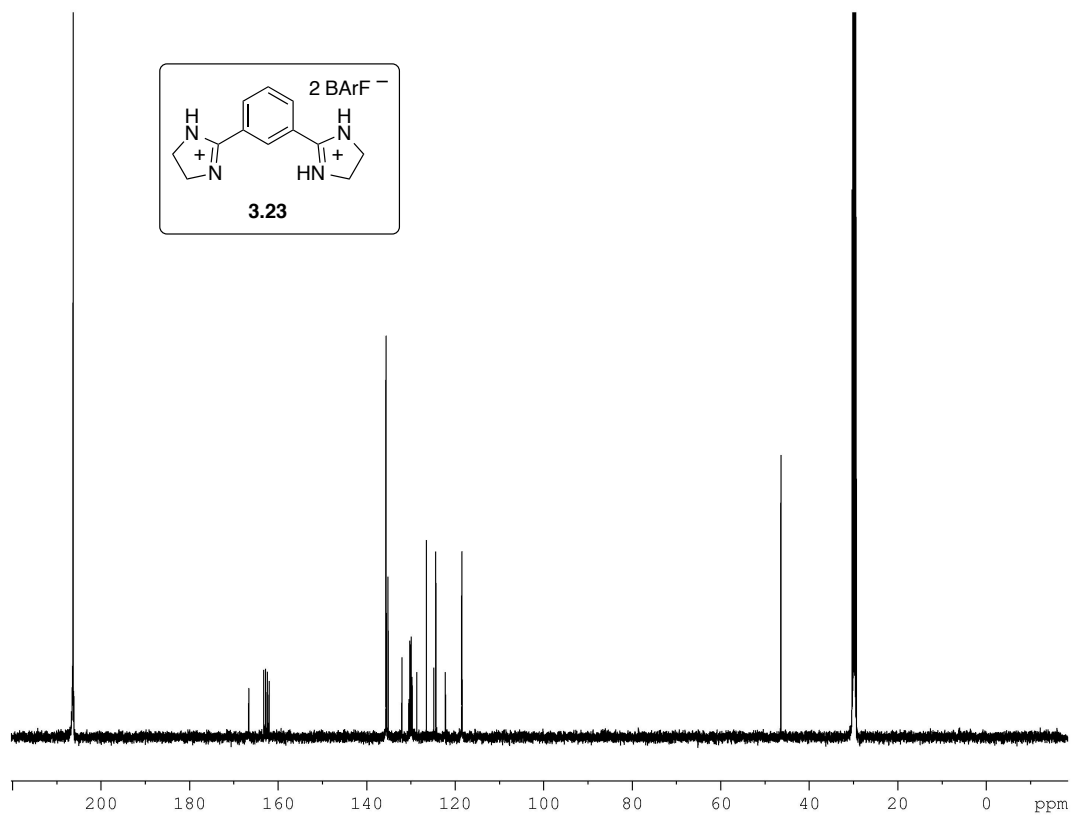
Figure A.3.23_2 ^{13}C NMR spectrum of compound **3.23** (125 MHz, Acetone).
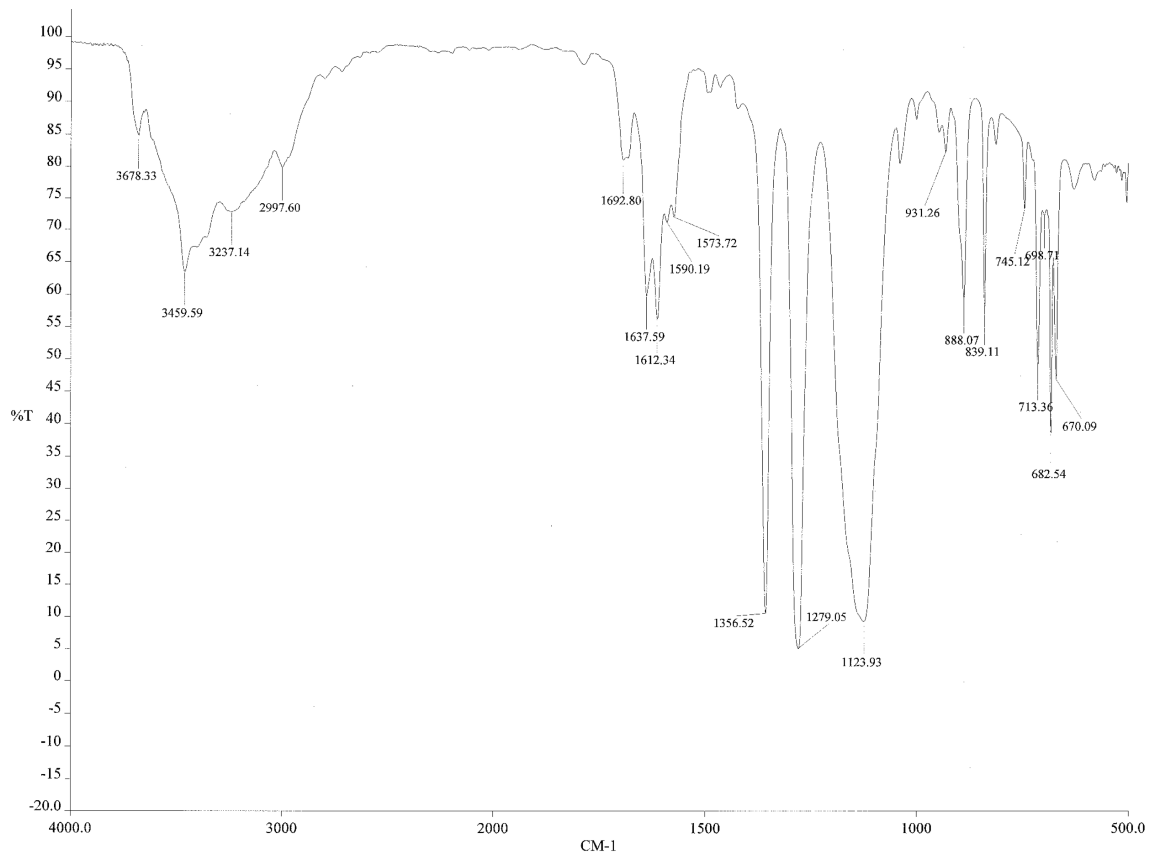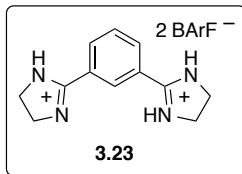
Figure A.3.23_3 IR spectrum of compound **3.23**.
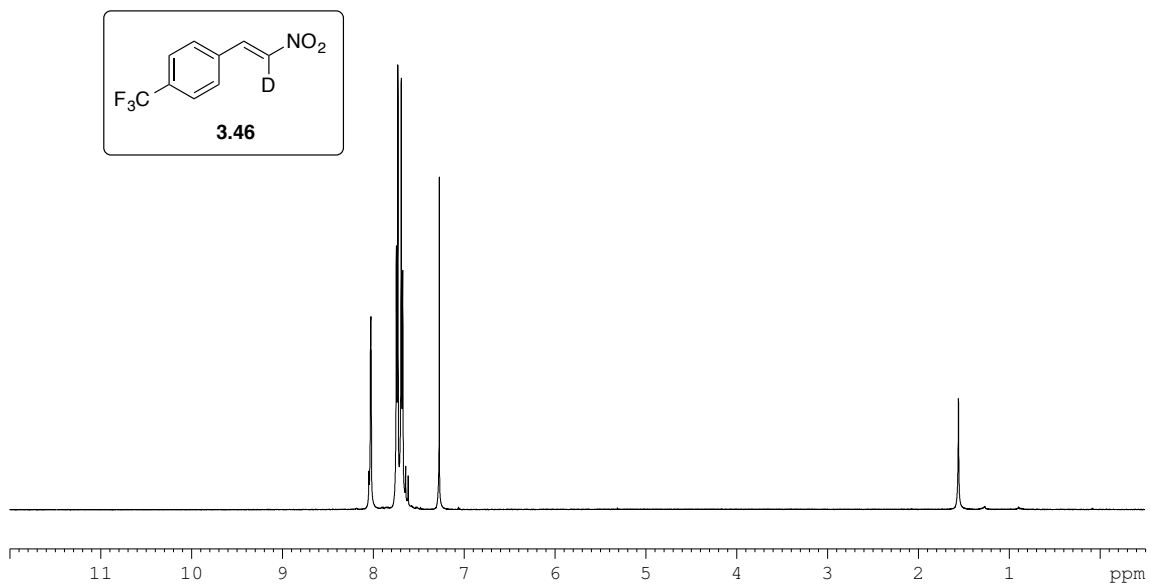
Figure A.3.46_1 ^{1}H NMR spectrum of compound **3.46** (500 MHz, CDCl$_3$).
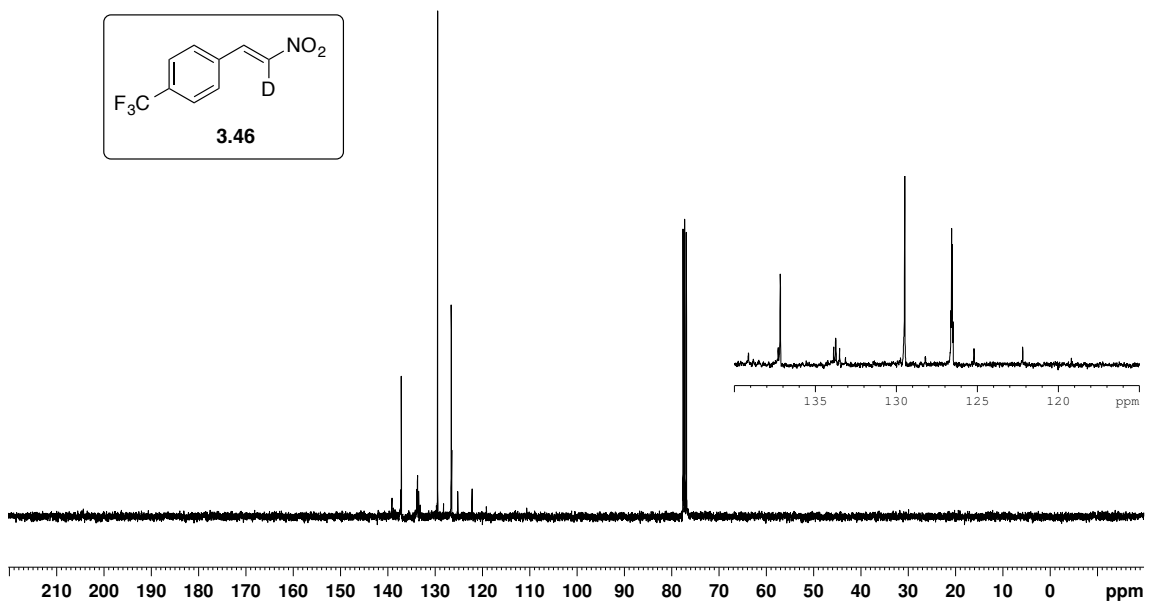
Figure A.3.46_2 ^{13}C NMR spectrum of compound **3.46** (90 MHz, CDCl$_3$).
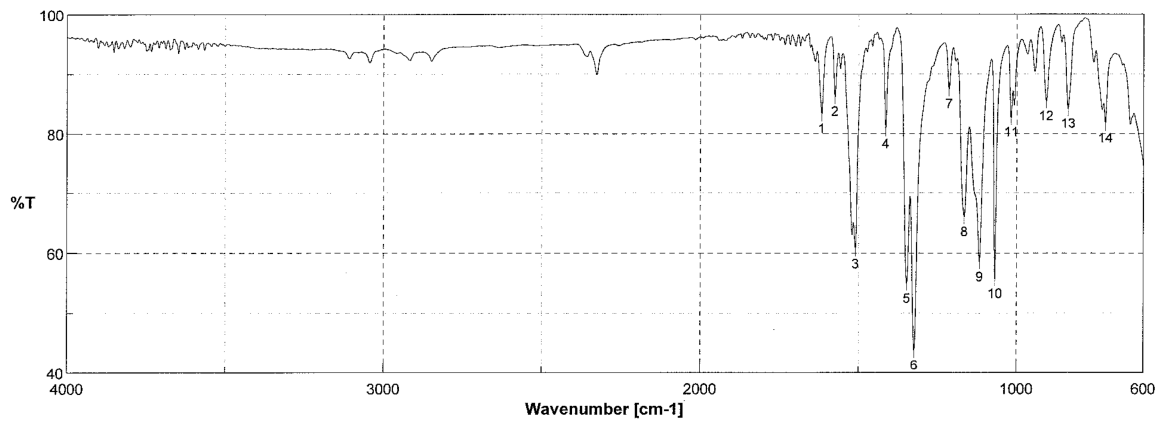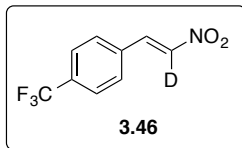
Figure A.3.46_3 IR spectrum of compound **3.46**.
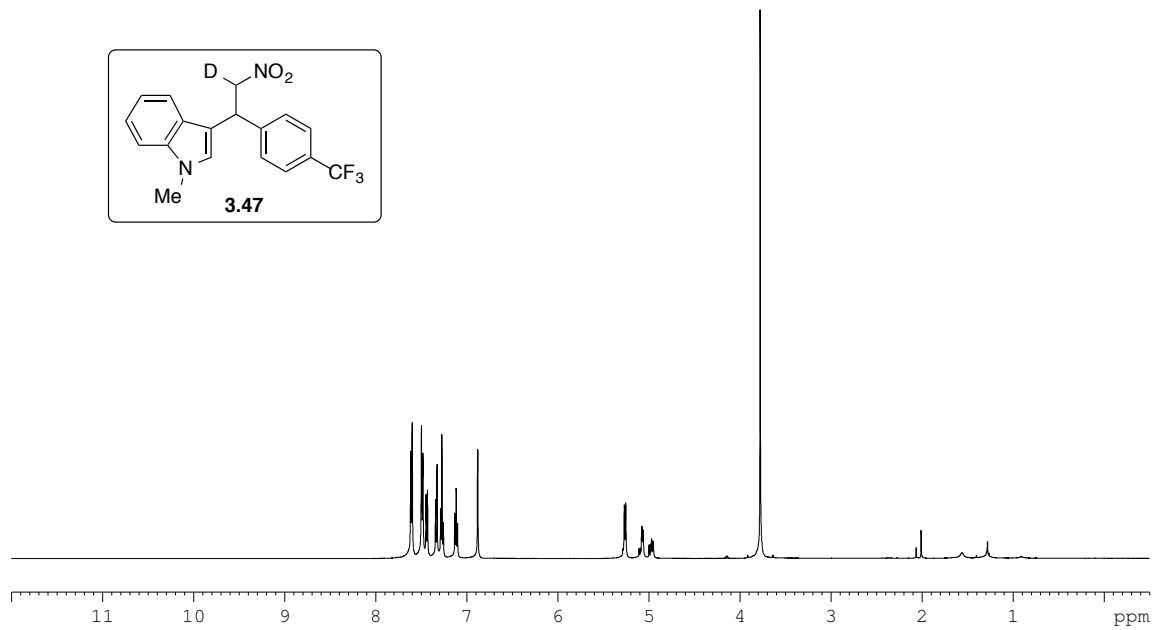
Figure A.3.47_1 ^{1}H NMR spectrum of compound **3.47** (500 MHz, CDCl$_3$).
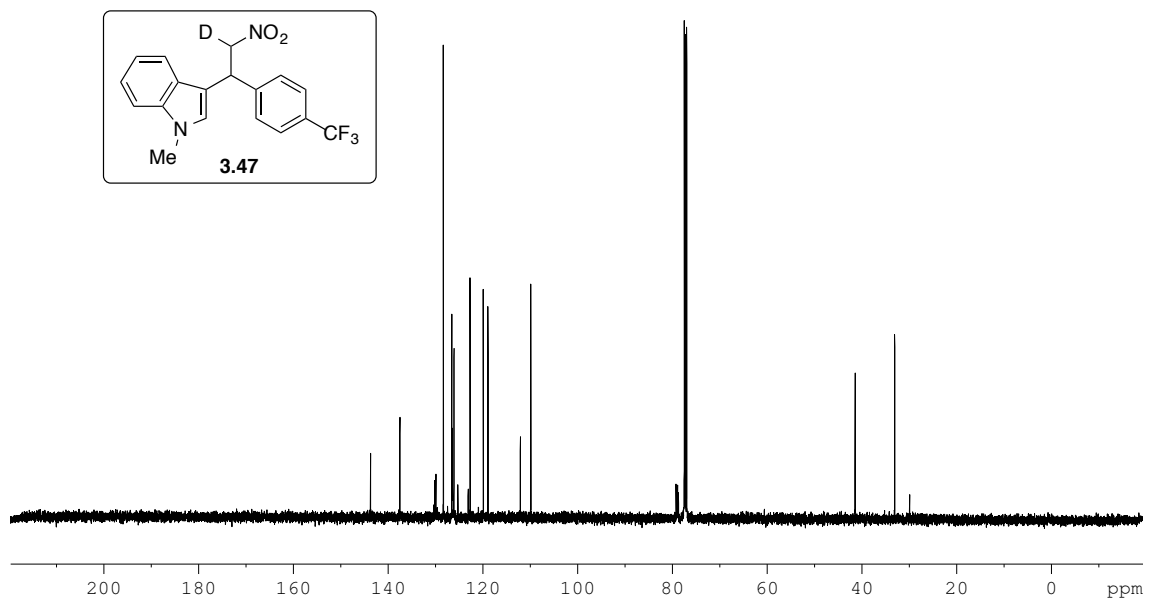
Figure A.3.47_2 ^{13}C NMR spectrum of compound **3.47** (125 MHz, CDCl$_3$).
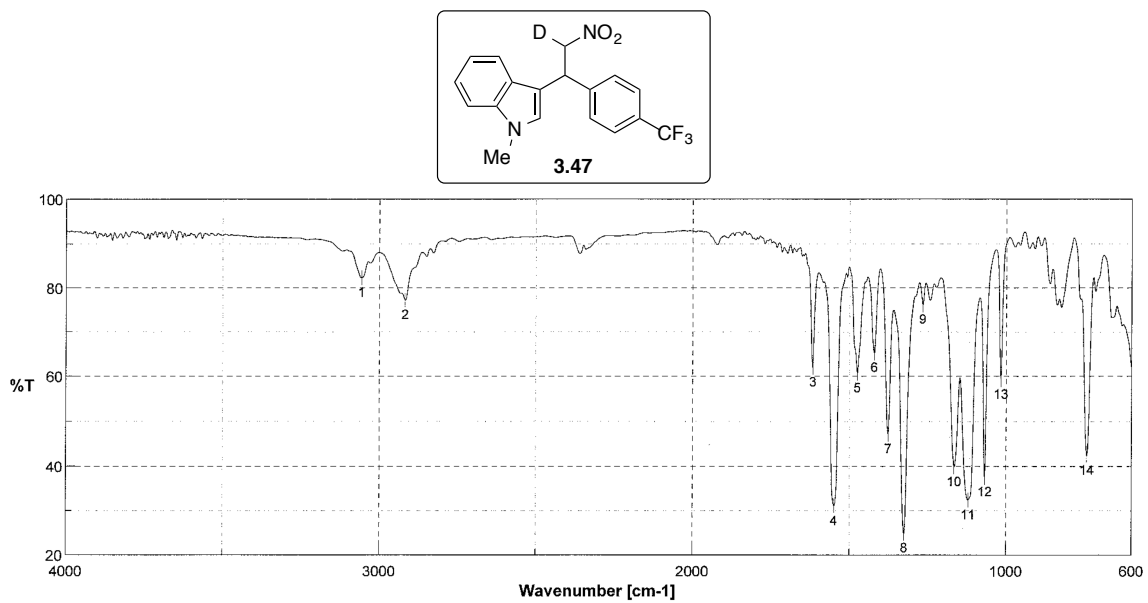
Figure A.3.47_3 IR spectrum of compound **3.47**.
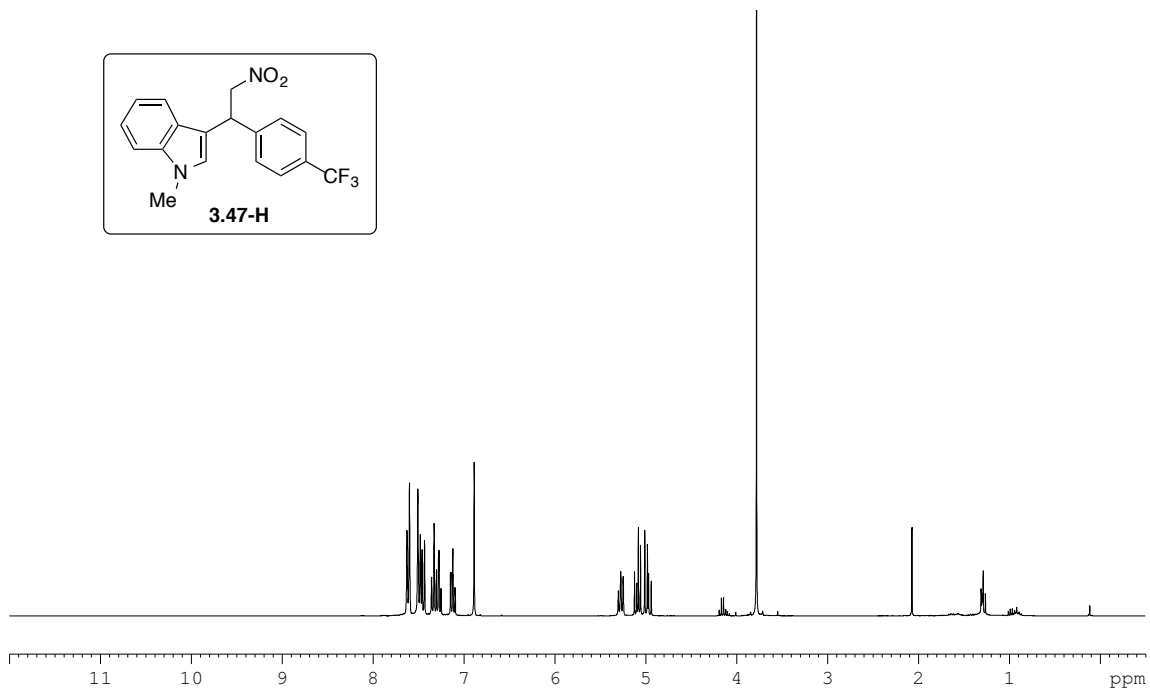
Figure A.3.47-H_1 ^{1}H NMR spectrum of compound **3.47-H**.
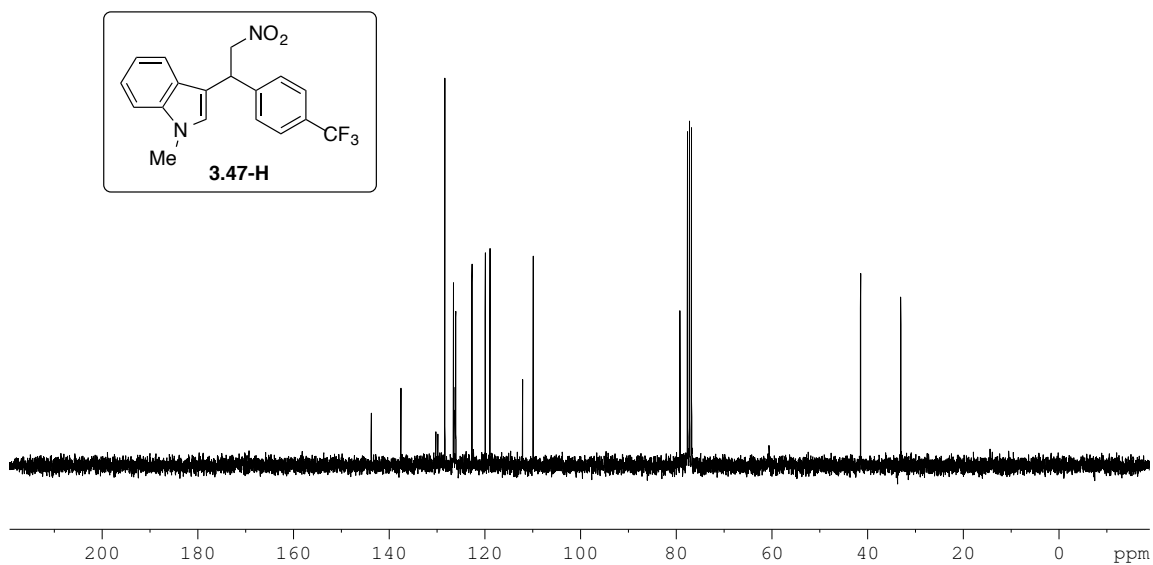
Figure A.3.47-H_2 ^{13}C NMR spectrum of compound **3.47-H**.
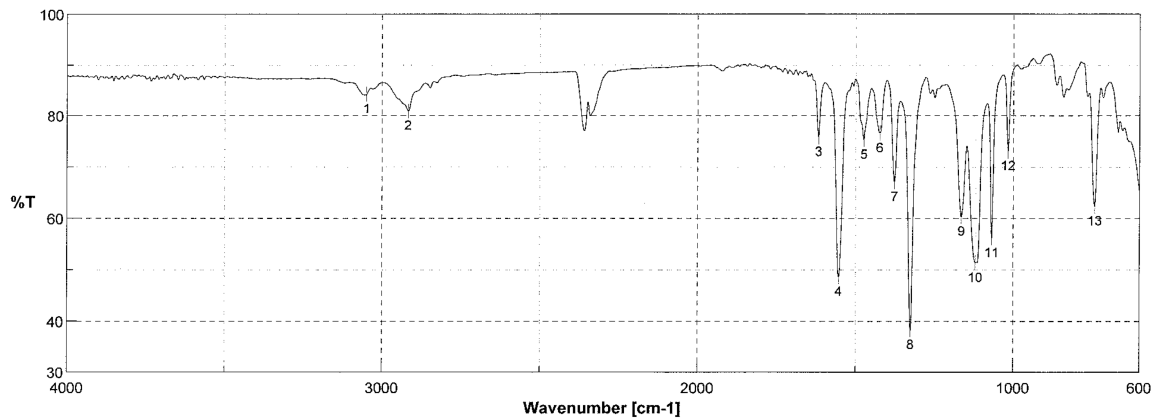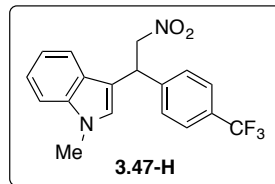
Figure A.3.47-H_3 IR spectrum of compound **3.47-H**.

261
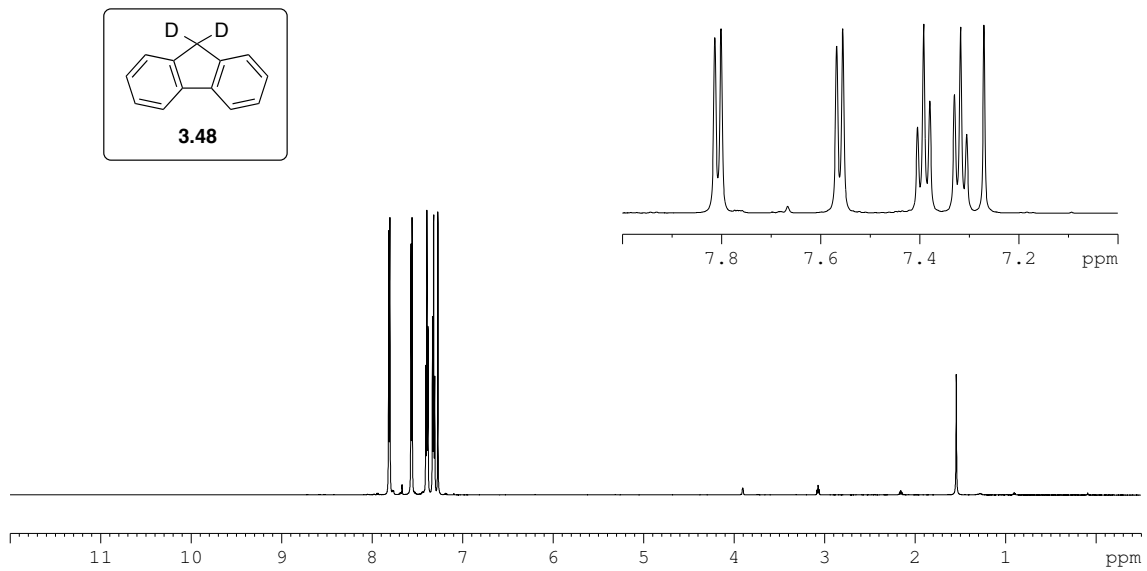
Figure A.3.48_1 ^{1}H NMR spectrum of compound **3.48** (600 MHz, CDCl$_3$).
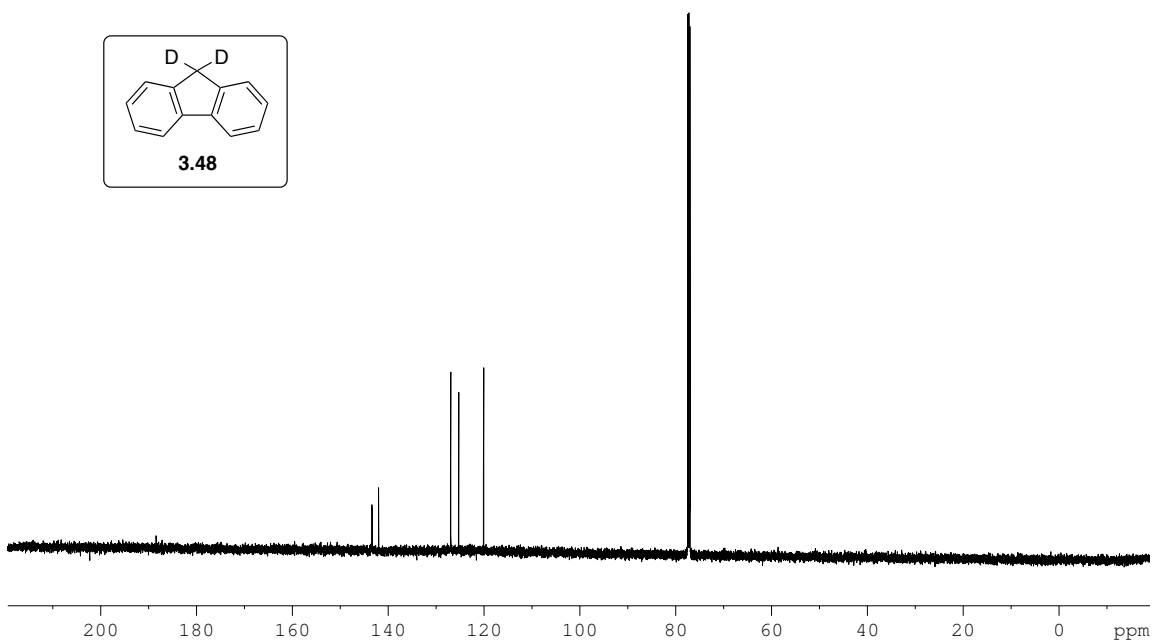
Figure A.3.48_2 ^{13}C NMR spectrum of compound **3.48** (150 MHz, CDCl$_3$).
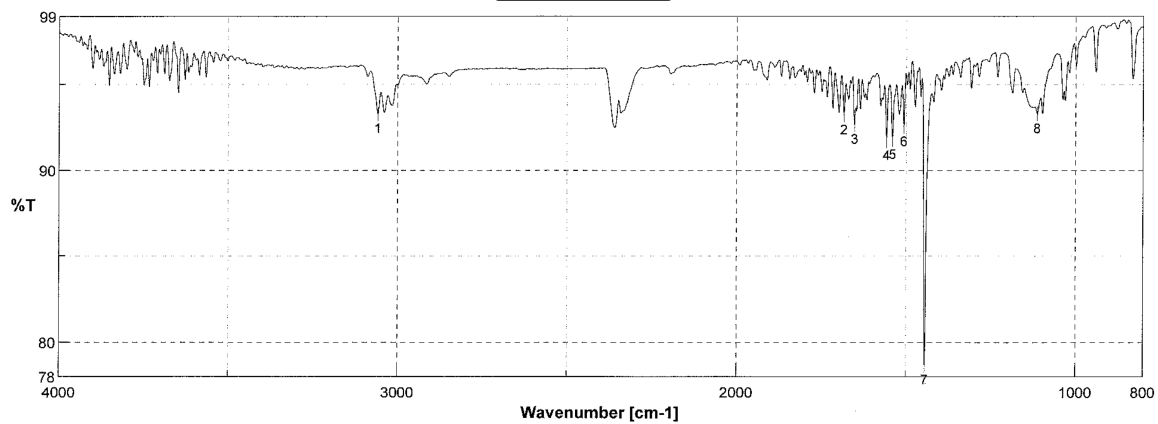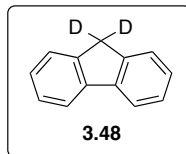
Figure A.3.48_3 IR spectrum of compound **3.48**.
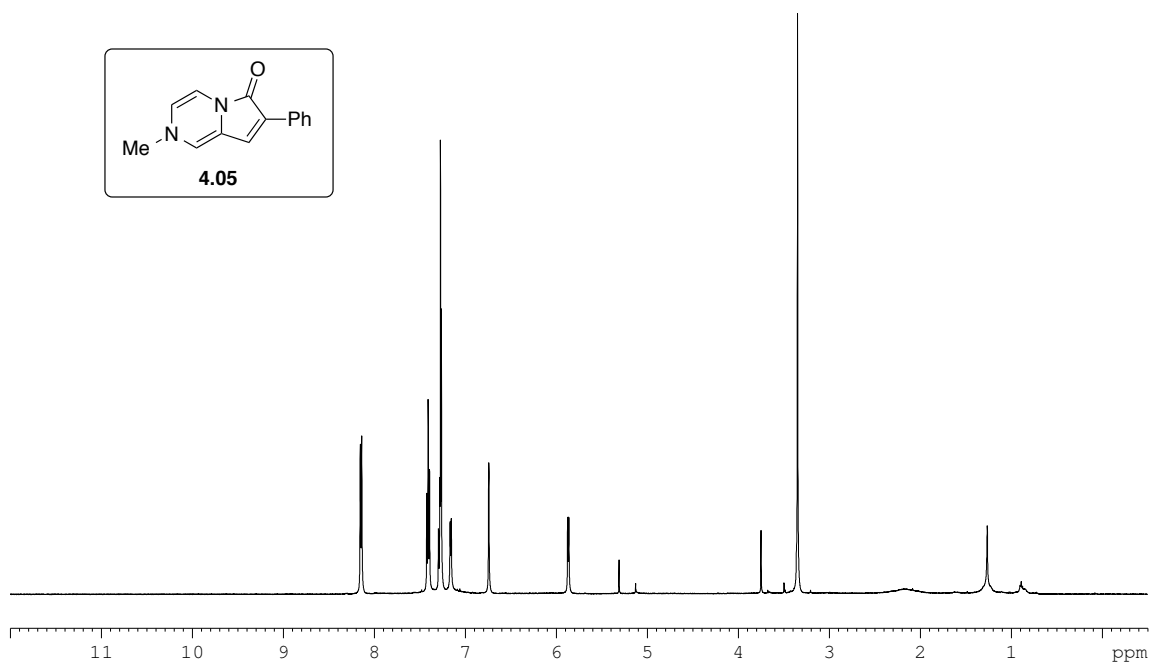
Figure A.4.05_1 ^{1}H NMR spectrum of compound **4.05** (500 MHz, CDCl$_3$).
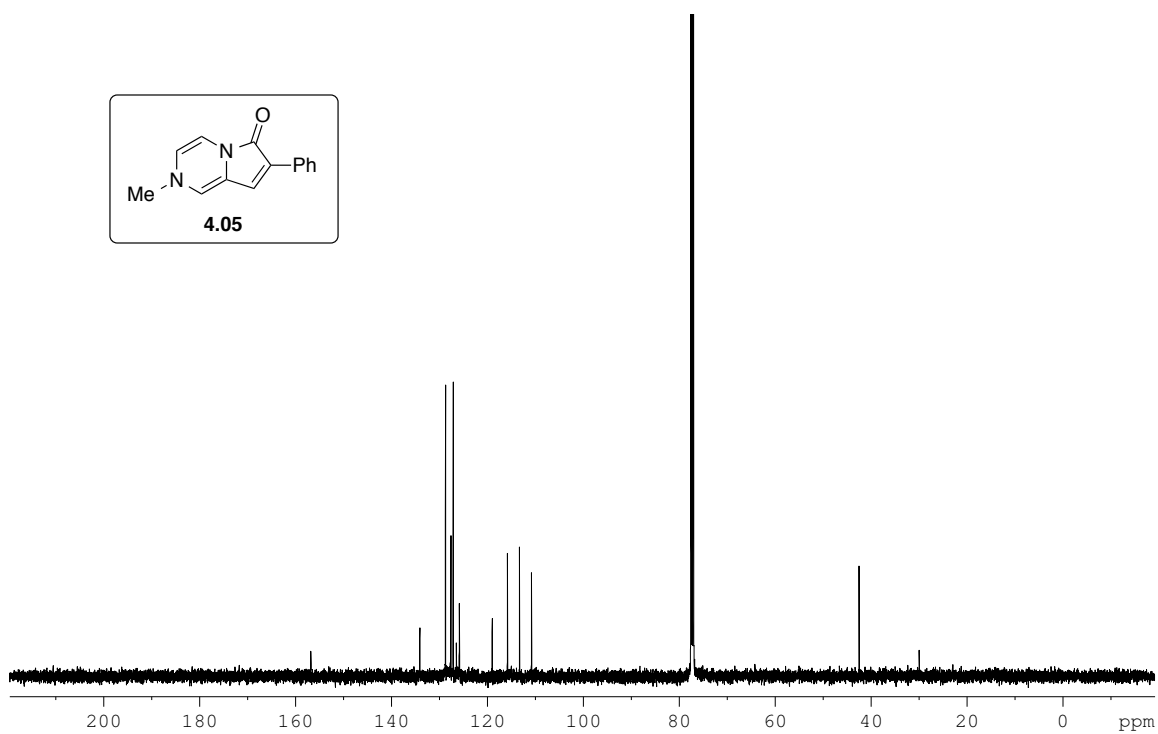
Figure A.4.05_2 ^{13}C NMR spectrum of compound **4.05** (125 MHz, CDCl$_3$).
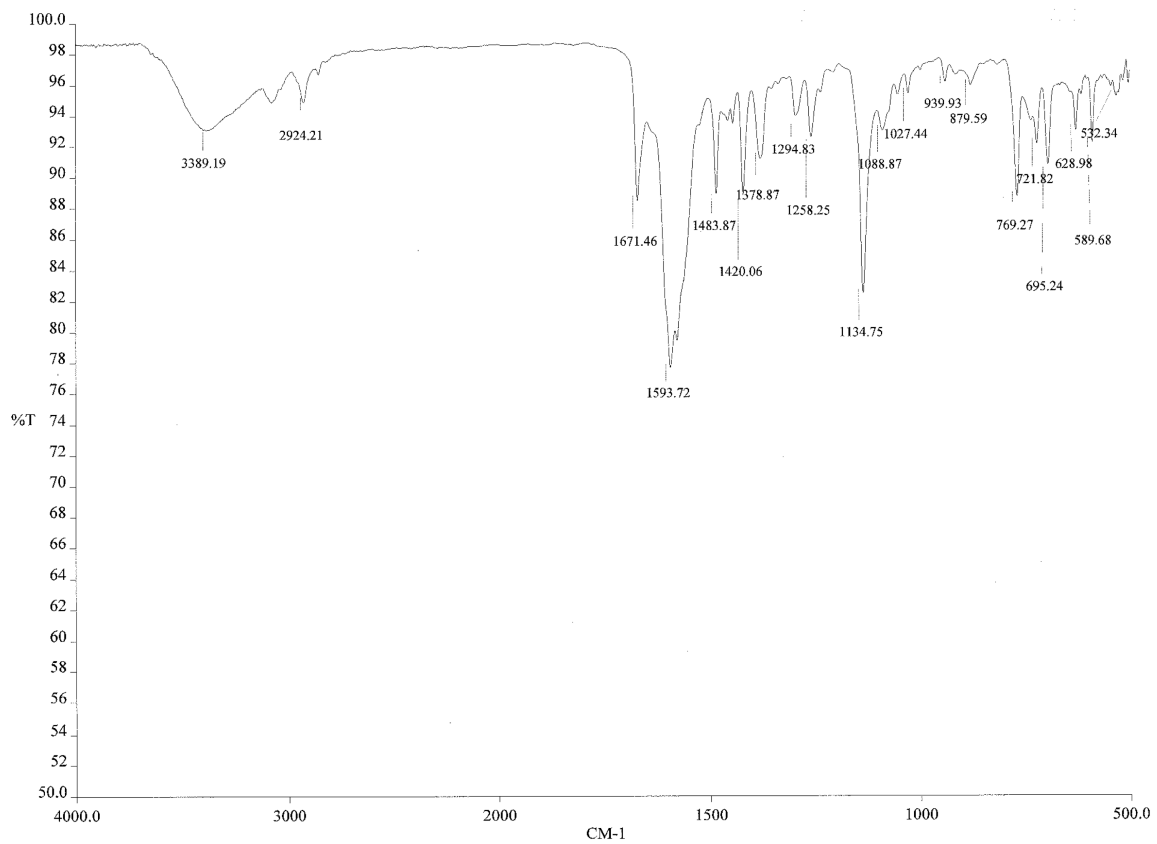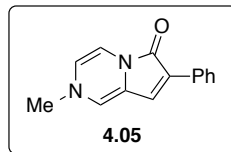
Figure A.4.05_3 IR spectrum of compound **4.05**.
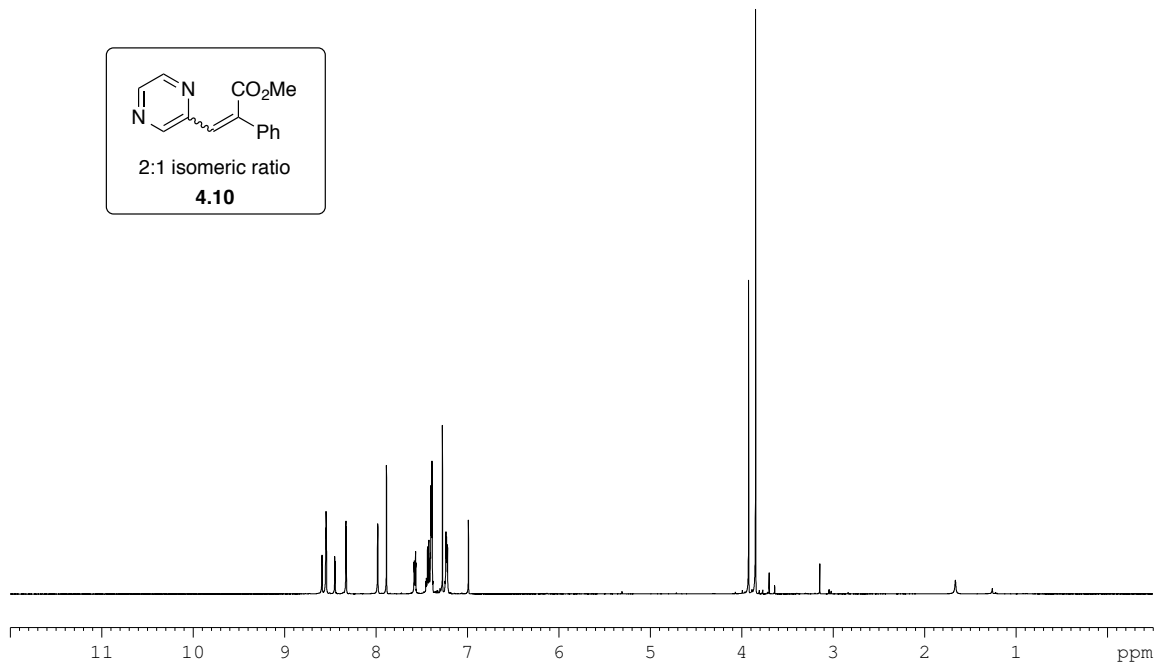
Figure A.4.10_1 ^{1}H NMR spectrum of compound **4.10** (500 MHz, CDCl$_3$).
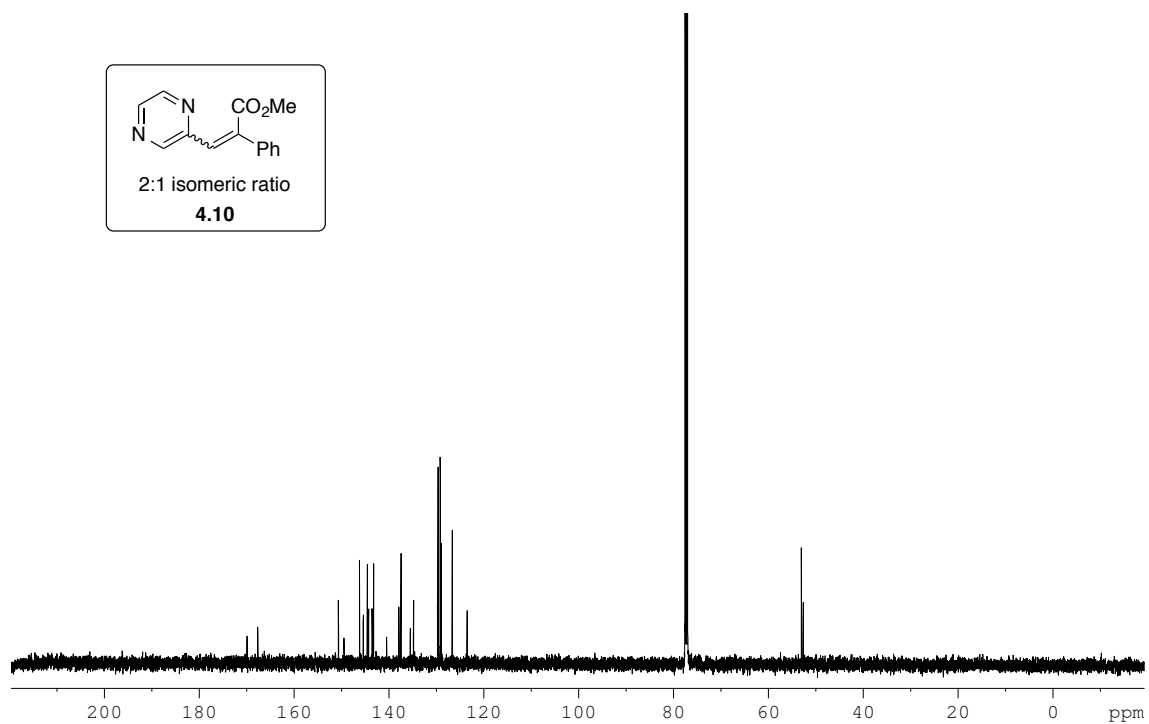
Figure A.4.10_2 ^{13}C NMR spectrum of compound **4.10** (125 MHz, CDCl$_3$).
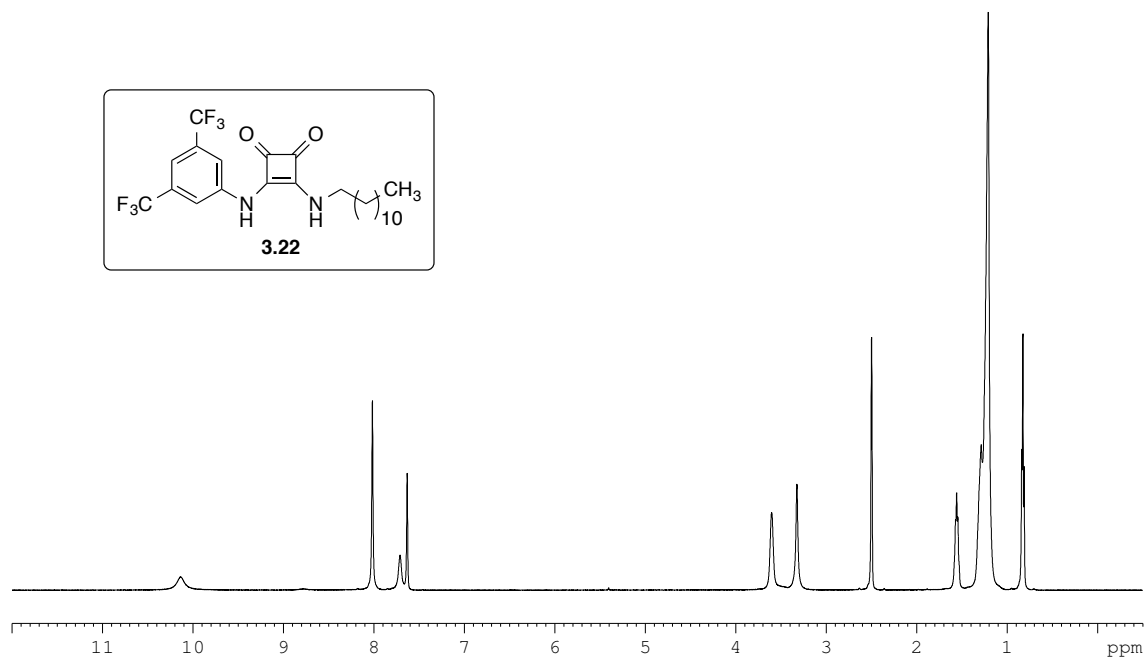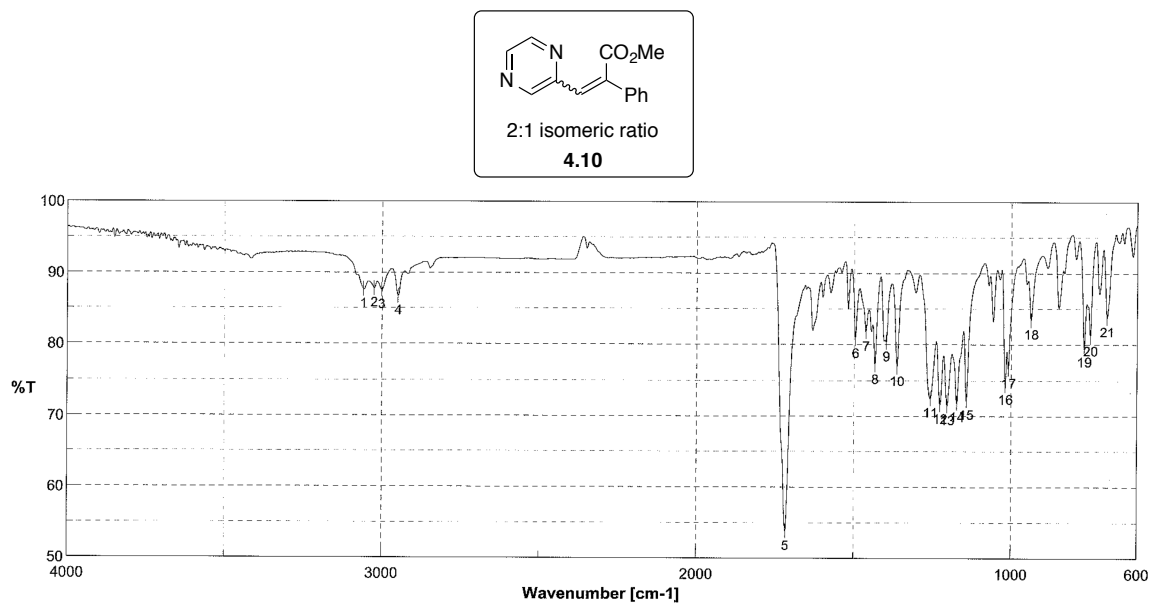
Figure A.4.10_3 IR spectrum of compound **4.10**.

Figure A.4.11_1 ^{1}H NMR spectrum of compound **4.11** (500 MHz, CDCl$_3$).

Figure A.4.11_2 ^{13}C NMR spectrum of compound **4.11** (125 MHz, CDCl$_3$).
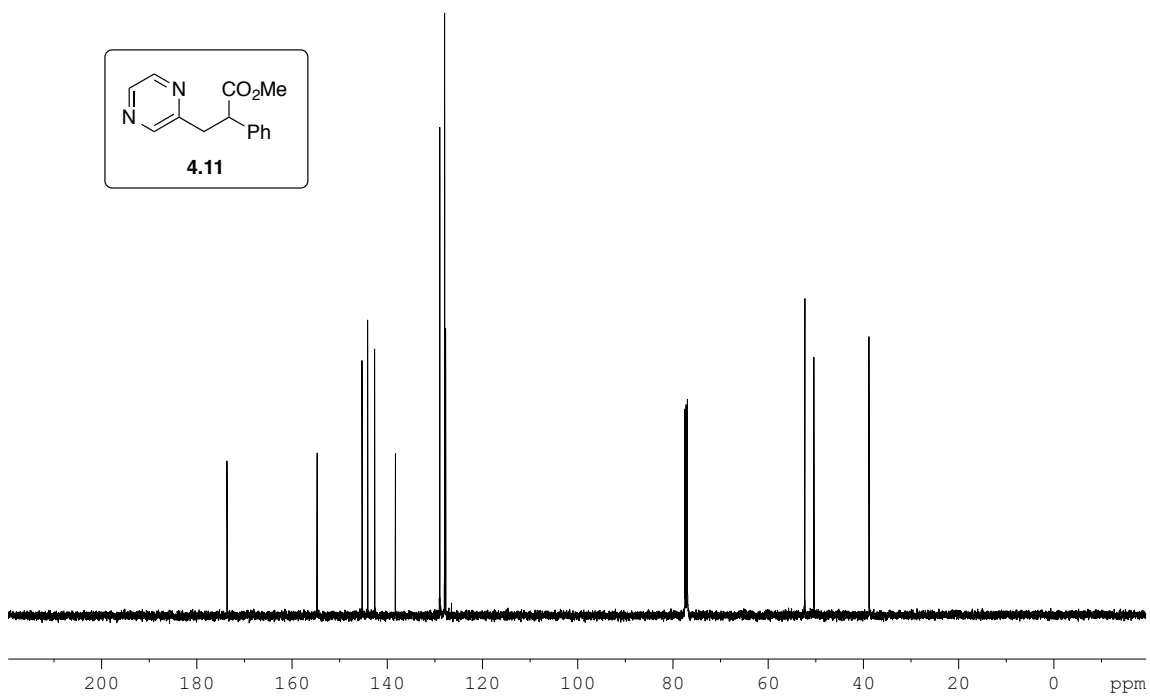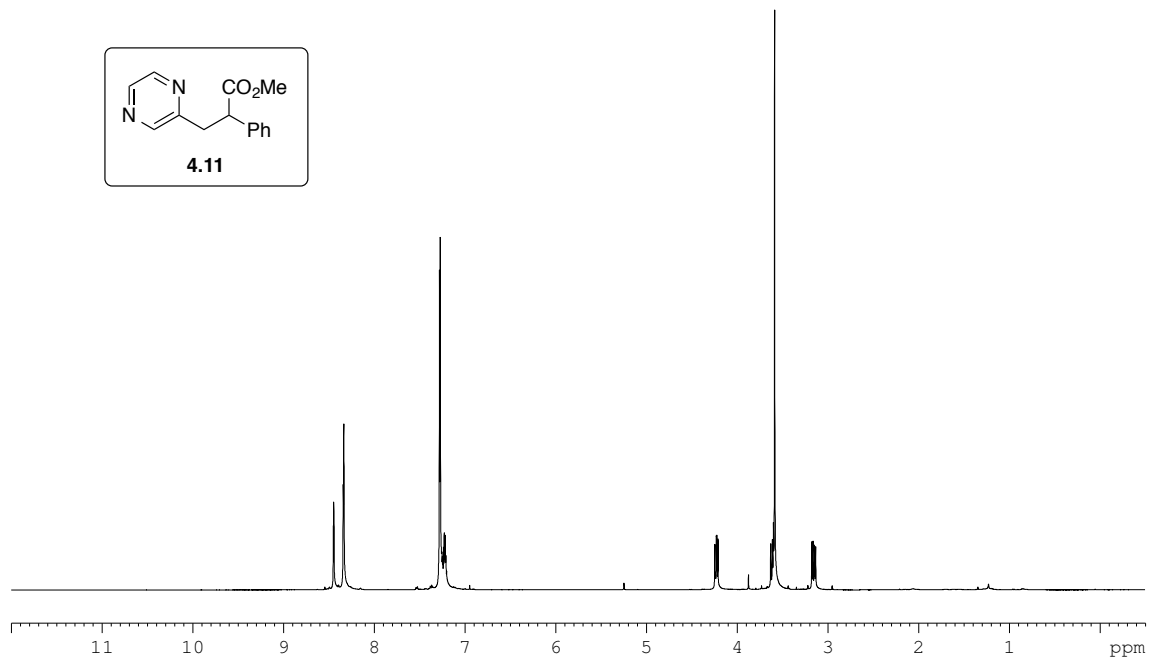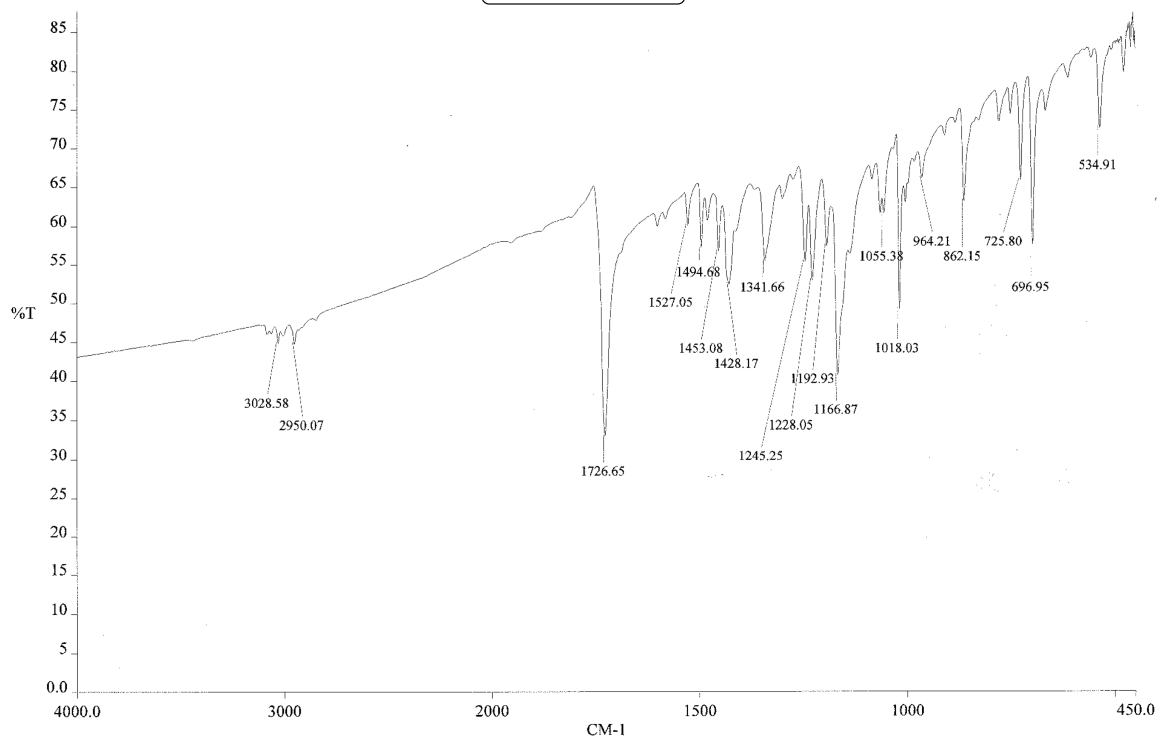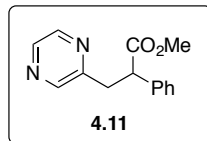
Figure A.4.11_3 IR spectrum of compound **4.11**.
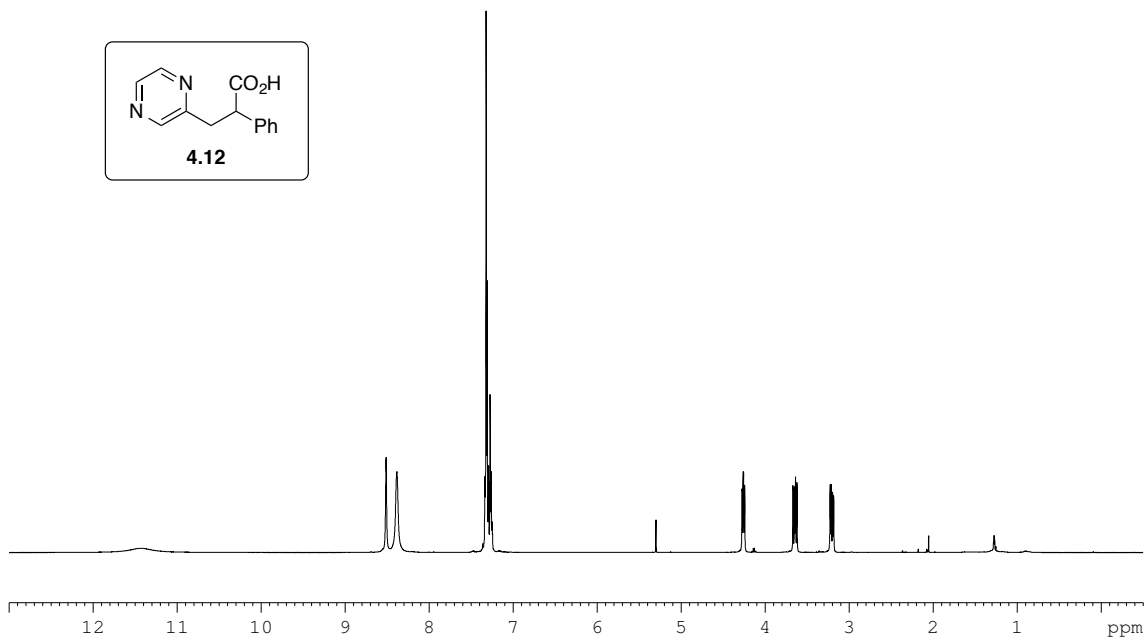
Figure A.4.12_1 ^{1}H NMR spectrum of compound **4.12** (500 MHz, CDCl$_3$).
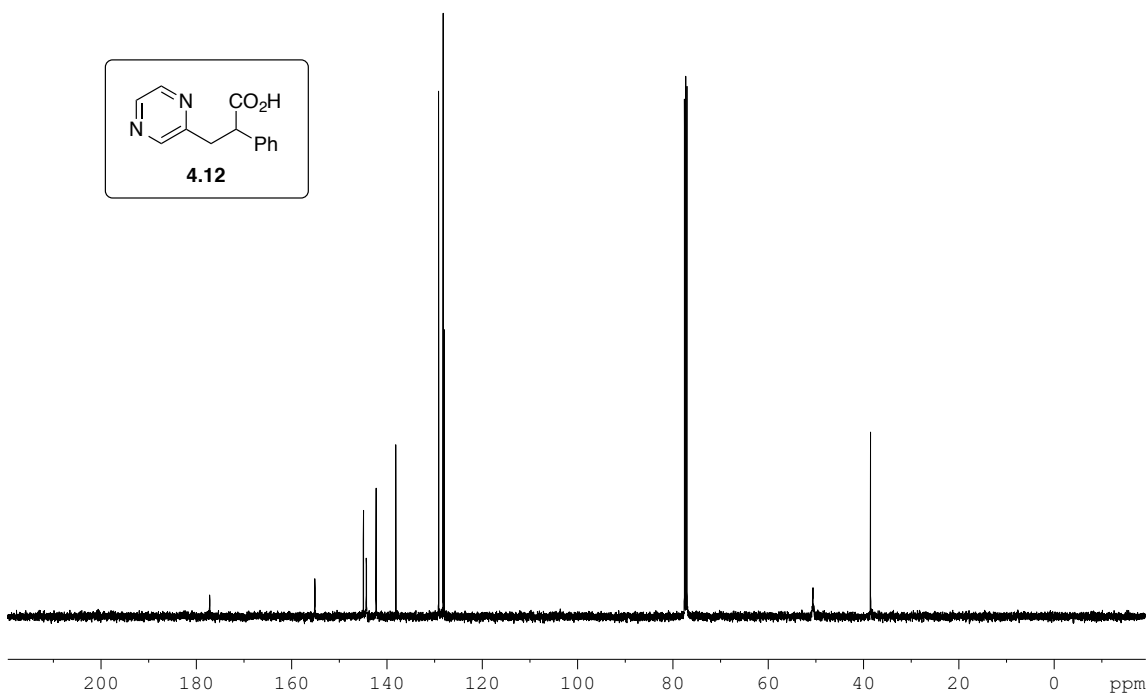
Figure A.4.12_2 ^{13}C NMR spectrum of compound **4.12** (125 MHz, CDCl$_3$).
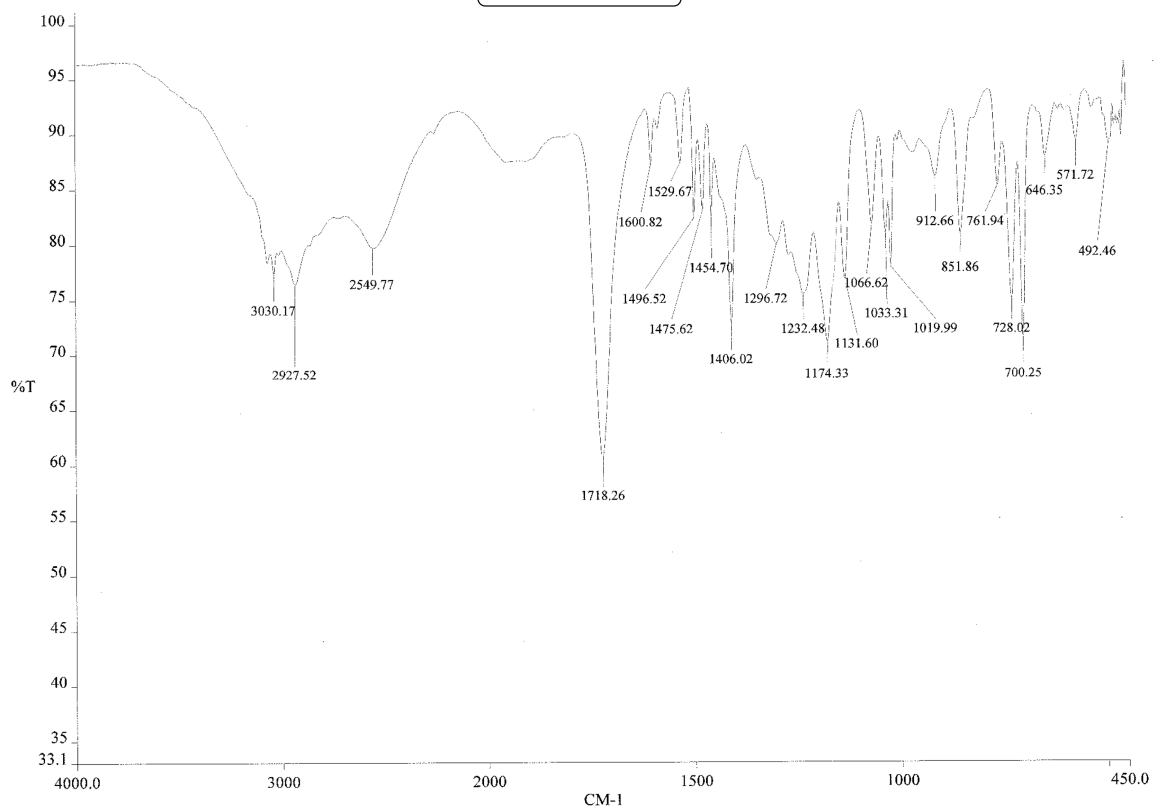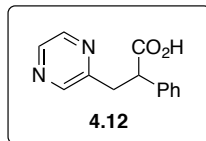
Figure A.4.12_3 IR spectrum of compound **4.12**.
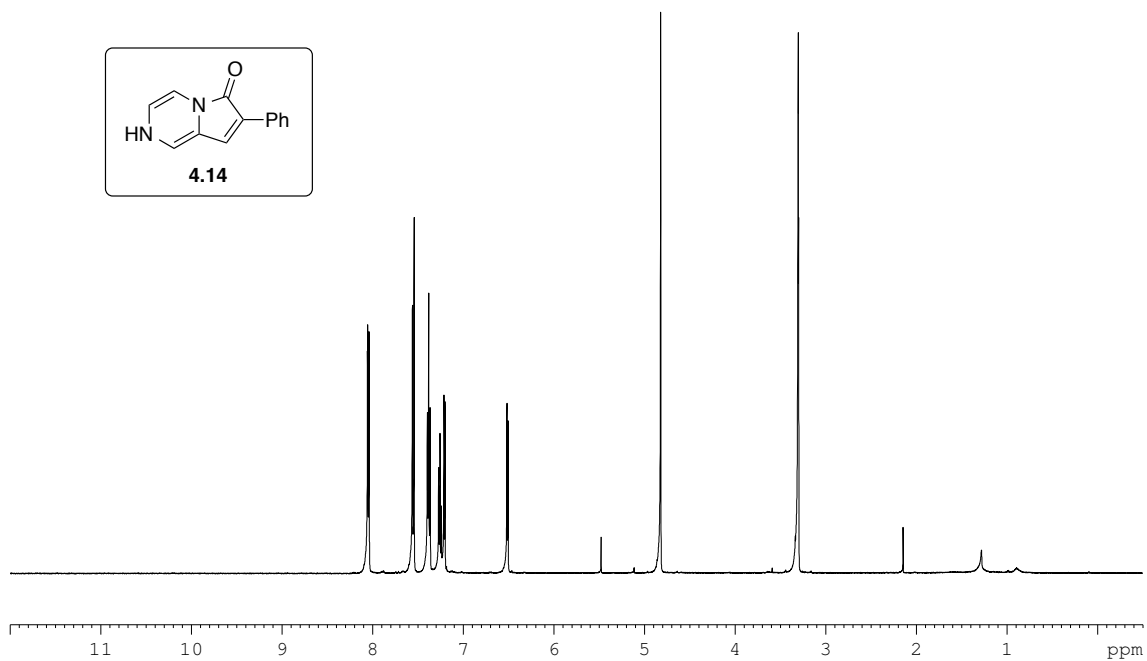
Figure A.4.14_1 ^{1}H NMR spectrum of compound **4.14** (500 MHz, MeOD).
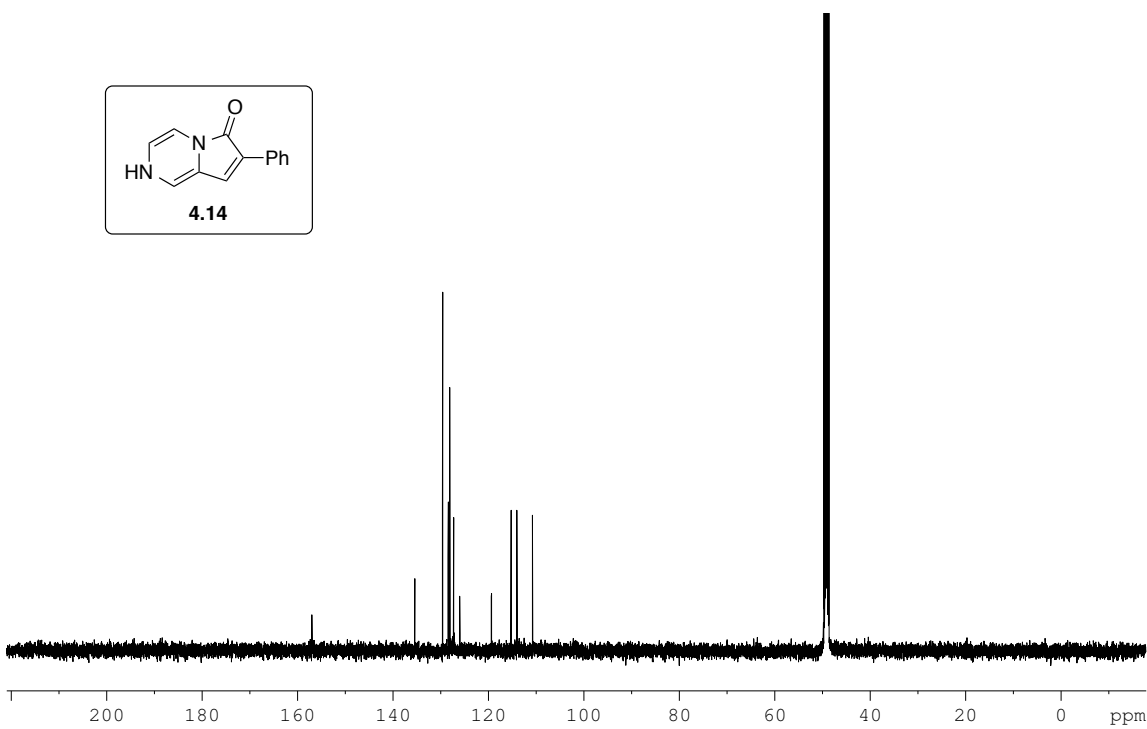
Figure A.4.14_2 ^{13}C NMR spectrum of compound **4.14** (125 MHz, MeOD).
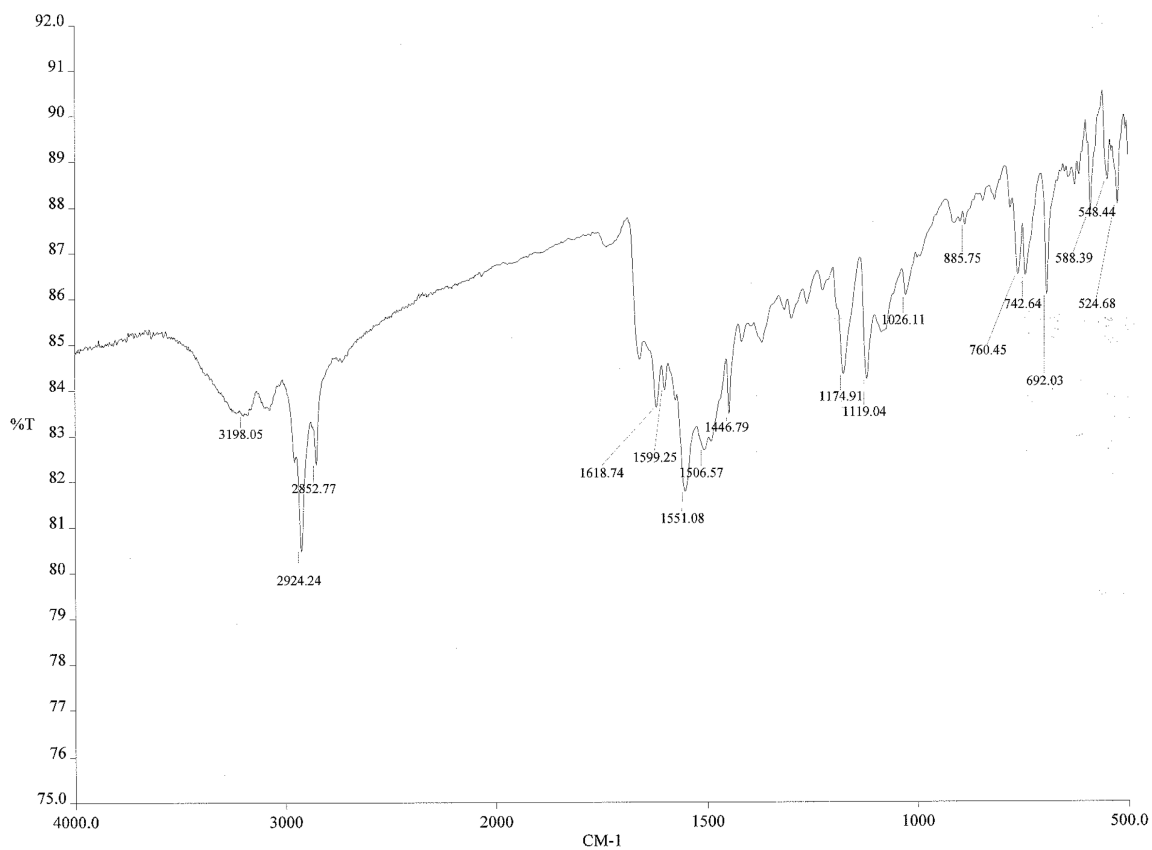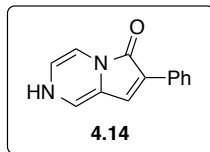
Figure A.4.14_3 IR spectrum of compound **4.14**.

APPENDIX B: X-Ray Crystallographic Data

X-ray Structure Determination of Compound 1.09ab

1.09ab
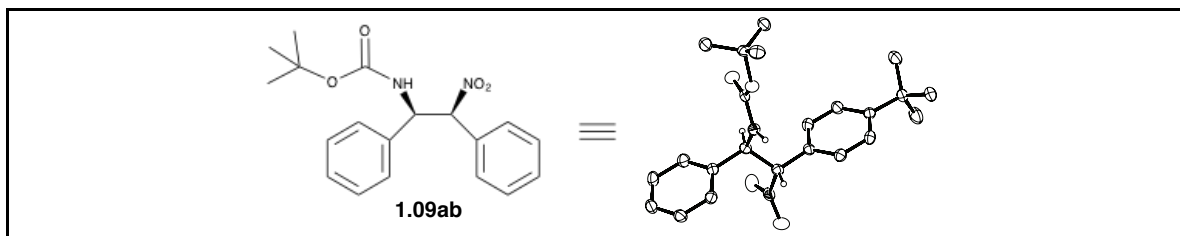
Compound 8036, $C_{23}H_{30}N_2O_4$, crystallizes in the monoclinic space group $P2_1$ (systematic absences 0k0: k=odd) with a=5.7903(2)Å, b=18.8269(7)Å, c=10.1602(4)Å, β=100.963(3)°, V=1087.38(7)Å^3, Z=2, and d_{calc}=1.217 g/cm^3 . X-ray intensity data were collected on a Bruker APEXII CCD area detector employing graphite-monochromated Cu-Kα radiation (λ=1.54178 Å) at a temperature of 100(1)K. Preliminary indexing was performed from a series of ninety 0.5° rotation frames with exposures of 10 seconds. A total of 4308 frames were collected with a crystal to detector distance of 37.4 mm, rotation widths of 0.5° and exposures of 30 seconds:

scan type	2θ	ω	φ	χ	frames
φ	92.00	88.66	348.71	-26.26	739
φ	82.00	30.51	90.66	52.47	511
φ	47.00	51.38	61.25	-33.72	216
ω	-13.00	28.17	42.00	-30.00	102
ω	2.00	5.06	204.72	-61.99	65
ω	92.00	153.27	266.47	-93.68	155
ω	-23.00	20.42	256.68	-41.06	108
ω	77.00	75.35	55.96	-51.77	77
φ	7.00	357.96	6.02	83.36	103
ω	-28.00	359.19	295.26	-33.72	92

ω	77.00	21.87	182.82	78.00	89
ω	-18.00	262.88	41.87	38.14	94
ω	-58.00	329.29	112.78	-71.55	129
φ	-13.00	23.90	93.03	-71.55	142
φ	87.00	172.05	87.56	-55.24	369
φ	92.00	132.53	350.39	-22.49	739
φ	87.00	76.65	37.22	62.65	578

Rotation frames were integrated using SAINT,[162] producing a listing of unaveraged F^2 and $\sigma(F^2)$ values which were then passed to the SHELXTL[163] program package for further processing and structure solution. A total of 9257 reflections were measured over the ranges 4.43 $\leq \theta \leq$ 63.85°, -6 $\leq$ h $\leq$ 6, -20 $\leq$ k $\leq$ 21, -11 $\leq$ l $\leq$ 11 yielding 3362 unique reflections (Rint = 0.0345). The intensity data were corrected for Lorentz and polarization effects and for absorption using SADABS[164] (minimum and maximum transmission 0.6698, 0.7524).

The structure was solved by direct methods (SHELXS-97[165]). Refinement was by full-matrix least squares based on F^2 using SHELXL-97.[165] All reflections were used during refinement. The weighting scheme used was w=1/[$\sigma^2(F_o^2$)+ (0.0318P)^2 + 0.1213P] where P = (F_o^2 + 2F_c^2)/3. Non-hydrogen atoms were refined anisotropically and hydrogen atoms were refined using a riding model. Refinement converged to R1=0.0294 and wR2=0.0674 for 3140 observed reflections for which F > 4σ(F) and R1=0.0331 and wR2=0.0693 and GOF =1.028 for all 3362 unique, non-zero reflections and 269 variables.[166] The maximum Δ/σ in the final cycle of least squares was 0.001 and the two most prominent peaks in the final difference Fourier were +0.137

162) Bruker (2009) SAINT. Bruker AXS Inc., Madison, Wisconsin, USA.
163) Bruker (2009) SHELXTL. Bruker AXS Inc., Madison, Wisconsin, USA.
164) Sheldrick, G.M. (2007) SADABS. University of Gottingen, Germany.
165) Sheldrick, G.M. (2008) Acta Cryst. A64,112-122.
166) R1 = S||F$_o$| - |F$_c$|| / S |F$_o$|
   wR2 = [Sw(F$_o^2$ - F$_c^2$)^2/Sw(F$_o^2$)^2]$^{1/2}$
   GOF = [Sw(F$_o^2$ - F$_c^2$)^2/(n - p)]$^{1/2}$
   where n = the number of reflections and p = the number of parameters refined.

and -0.128 e/Å^3. The Hooft absolute structure parameter y[167] was calculated using PLATON.[168] The resulting value was y = 0.13(12) indicating that the absolute structure has been assigned correctly.

Table B.1. lists cell information, data collection parameters, and refinement data. Final positional and equivalent isotropic thermal parameters are given in Tables B.2. and B.3. Anisotropic thermal parameters are in Table B.4. Tables B.5. and B.6. list bond distances and bond angles. Figure B.1. is an ORTEP[169] representation of the molecule with 50% probability thermal ellipsoids displayed.
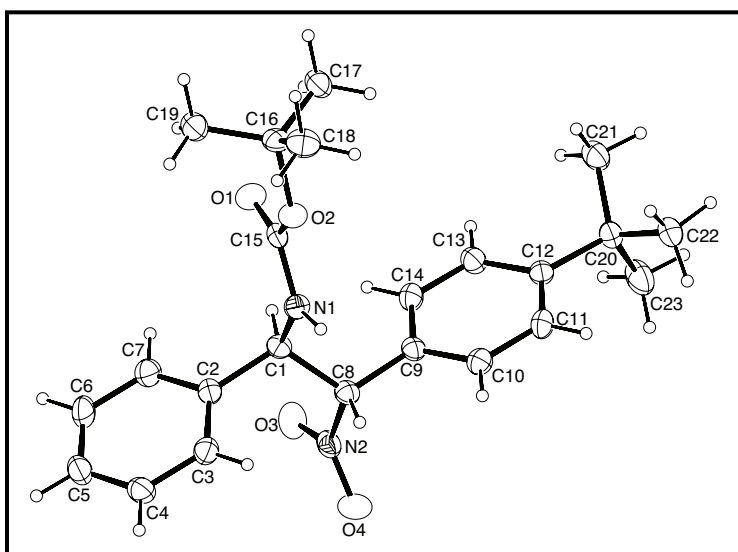
Figure B.1. ORTEP drawing of the title compound with 50% probability thermal ellipsoids.

167) Hooft, R.W.W., Straver, L.H., Spek, A.L. (2008) J. Appl.Cryst., 41, 96-103.
168) Spek, A.L., Acta Cryst., (2009) D65, 148-155.
169) "ORTEP-II: A Fortran Thermal Ellipsoid Plot Program for Crystal Structure Illustrations". C.K. Johnson (1976) ORNL-5138.

Table B.1. Summary of Structure Determination of Compound **1.09ab**.

Empirical formula	$C_{23}H_{30}N_2O_4$
Formula weight	398.49
Temperature	100(1) K
Wavelength	1.54178 Å
Crystal system	monoclinic
Space group	$P2_1$
Cell constants:	
a	5.7903(2) Å
b	18.8269(7) Å
c	10.1602(4) Å
β	100.963(3)°
Volume	1087.38(7) Å^3
Z	2
Density (calculated)	1.217 Mg/m^3
Absorption coefficient	0.671 mm^{-1}
F(000)	428
Crystal size	0.38 x 0.12 x 0.03 mm^3
Theta range for data collection	4.43 to 63.85°
Index ranges	$-6 \leq h \leq 6$, $-20 \leq k \leq 21$, $-11 \leq l \leq 11$
Reflections collected	9257
Independent reflections	3362 [R(int) = 0.0345]
Completeness to theta = 63.85°	98.4 %

Absorption correction	Semi-empirical from equivalents
Max. and min. transmission	0.7524 and 0.6698
Refinement method	Full-matrix least-squares on F^2
Data / restraints / parameters	3362 / 1 / 269
Goodness-of-fit on F^2	1.028
Final R indices [I>2sigma(I)]	R1 = 0.0294, wR2 = 0.0674
R indices (all data)	R1 = 0.0331, wR2 = 0.0693
Absolute structure parameter	-0.10(17)
Largest diff. peak and hole	0.137 and -0.128 e.$\mathring{A}^{-3}$

Table B.2. Refined Positional Parameters for Compound **1.09ab**.

Atom	x	y	z	U_{eq}, $\mathring{A}^2$
C1	0.5324(3)	0.41034(10)	0.60056(16)	0.0199(4)
C2	0.5707(3)	0.48885(9)	0.57767(16)	0.0203(4)
C3	0.7596(3)	0.51202(10)	0.52250(18)	0.0252(4)
C4	0.7882(3)	0.58408(10)	0.49880(18)	0.0289(4)
C5	0.6277(4)	0.63299(10)	0.5298(2)	0.0327(5)
C6	0.4424(4)	0.61024(11)	0.5858(2)	0.0332(5)
C7	0.4141(3)	0.53868(10)	0.60993(18)	0.0275(4)
C8	0.7471(3)	0.37322(10)	0.68477(16)	0.0211(4)
C9	0.7012(3)	0.29942(10)	0.73131(16)	0.0201(4)
C10	0.8440(3)	0.24373(10)	0.70831(17)	0.0237(4)
C11	0.8109(3)	0.17585(10)	0.75503(18)	0.0249(4)
C12	0.6349(3)	0.16098(10)	0.82740(17)	0.0216(4)
C13	0.4914(3)	0.21825(10)	0.84872(18)	0.0251(4)
C14	0.5221(3)	0.28549(10)	0.80170(18)	0.0253(4)

C15	0.2502(3)	0.35652(9)	0.41471(16)	0.0187(4)
C16	0.0219(3)	0.30682(10)	0.20645(17)	0.0241(4)
C17	-0.1038(3)	0.25087(11)	0.27391(19)	0.0289(4)
C18	0.1055(4)	0.27598(12)	0.08600(18)	0.0322(5)
C19	-0.1287(3)	0.37210(11)	0.16758(18)	0.0297(4)
C20	0.6073(3)	0.08755(10)	0.88741(18)	0.0252(4)
C21	0.3487(3)	0.06964(11)	0.8824(2)	0.0331(5)
C22	0.7089(3)	0.02859(10)	0.8115(2)	0.0333(5)
C23	0.7353(4)	0.08808(11)	1.03419(19)	0.0386(5)
N1	0.4753(2)	0.37082(8)	0.47488(14)	0.0218(3)
N2	0.8398(3)	0.41763(9)	0.80758(14)	0.0254(3)
O1	0.0794(2)	0.36812(7)	0.46521(12)	0.0267(3)
O2	0.2473(2)	0.32708(7)	0.29439(11)	0.0239(3)
O3	0.6979(2)	0.44455(7)	0.86724(12)	0.0335(3)
O4	1.0552(2)	0.42126(8)	0.84314(13)	0.0385(4)

$U_{eq} = \frac{1}{3}[U_{11}(aa^*)^2 + U_{22}(bb^*)^2 + U_{33}(cc^*)^2 + 2U_{12}aa^*bb^*\cos\gamma + 2U_{13}aa^*cc^*\cos\beta + 2U_{23}bb^*cc^*\cos\alpha]$

Table B.3. Positional Parameters for Hydrogens in Compound **1.09ab**.

Atom	x	y	z	U_{iso}, Å^2
H1	0.4002	0.4057	0.6475	0.026
H3	0.8671	0.4793	0.5013	0.033
H4	0.9151	0.5994	0.4622	0.038
H5	0.6453	0.6810	0.5127	0.044
H6	0.3357	0.6431	0.6075	0.044
H7	0.2886	0.5239	0.6482	0.037
H8	0.8701	0.3702	0.6308	0.028
H10	0.9639	0.2518	0.6609	0.031
H11	0.9088	0.1393	0.7375	0.033
H13	0.3714	0.2105	0.8962	0.033

H14	0.4223	0.3220	0.8171	0.034
H17a	-0.0041	0.2100	0.2943	0.043
H17b	-0.2467	0.2373	0.2149	0.043
H17c	-0.1401	0.2698	0.3553	0.043
H18a	0.1904	0.3116	0.0470	0.048
H18b	-0.0277	0.2606	0.0209	0.048
H18c	0.2067	0.2362	0.1137	0.048
H19a	-0.1716	0.3924	0.2462	0.045
H19b	-0.2683	0.3589	0.1052	0.045
H19c	-0.0415	0.4063	0.1267	0.045
H21a	0.2809	0.1039	0.9338	0.050
H21b	0.3364	0.0231	0.9191	0.050
H21c	0.2661	0.0706	0.7910	0.050
H22a	0.6433	0.0321	0.7176	0.050
H22b	0.6703	-0.0168	0.8444	0.050
H22c	0.8768	0.0335	0.8250	0.050
H23a	0.8984	0.0990	1.0383	0.058
H23b	0.7216	0.0422	1.0732	0.058
H23c	0.6660	0.1233	1.0829	0.058
H1a	0.5881	0.3561	0.4377	0.029

Table B.4. Refined Thermal Parameters (U's) for Compound **1.09ab**.

Atom	U_{11}	U_{22}	U_{33}	U_{23}	U_{13}	U_{12}
C1	0.0219(9)	0.0200(10)	0.0175(8)	-0.0027(7)	0.0032(7)	-0.0014(8)
C2	0.0248(9)	0.0193(10)	0.0148(8)	-0.0012(7)	-0.0012(7)	0.0002(8)
C3	0.0250(10)	0.0242(11)	0.0252(9)	0.0005(8)	0.0021(8)	0.0028(8)
C4	0.0290(10)	0.0263(11)	0.0294(9)	0.0051(8)	0.0004(8)	-0.0057(9)
C5	0.0370(12)	0.0197(11)	0.0364(11)	0.0017(9)	-0.0061(9)	-0.0015(9)
C6	0.0343(11)	0.0205(11)	0.0428(11)	-0.0044(9)	0.0022(9)	0.0078(9)
C7	0.0266(10)	0.0249(11)	0.0305(10)	-0.0037(9)	0.0043(8)	0.0019(9)
C8	0.0229(9)	0.0203(10)	0.0192(8)	-0.0023(7)	0.0022(7)	-0.0016(8)
C9	0.0227(10)	0.0186(9)	0.0175(8)	-0.0019(7)	0.0002(7)	-0.0016(8)
C10	0.0240(10)	0.0251(11)	0.0214(9)	0.0004(8)	0.0030(8)	0.0011(8)
C11	0.0268(10)	0.0211(10)	0.0270(10)	-0.0008(8)	0.0053(8)	0.0062(8)
C12	0.0224(9)	0.0203(10)	0.0199(9)	-0.0014(8)	-0.0013(7)	-0.0007(8)
C13	0.0254(10)	0.0214(10)	0.0300(10)	0.0002(8)	0.0090(8)	-0.0007(8)
C14	0.0247(10)	0.0213(11)	0.0305(10)	-0.0009(8)	0.0070(8)	0.0036(8)
C15	0.0240(9)	0.0138(9)	0.0181(8)	0.0000(7)	0.0031(7)	-0.0001(7)
C16	0.0237(10)	0.0256(11)	0.0208(9)	-0.0030(8)	-0.0015(8)	-0.0045(8)
C17	0.0335(11)	0.0218(10)	0.0291(10)	0.0004(8)	-0.0001(9)	-0.0042(9)
C18	0.0345(11)	0.0370(12)	0.0237(10)	-0.0073(9)	0.0020(8)	-0.0057(9)
C19	0.0337(10)	0.0253(11)	0.0268(9)	0.0026(8)	-0.0029(8)	-0.0025(9)
C20	0.0268(10)	0.0189(10)	0.0288(9)	0.0022(8)	0.0026(8)	0.0000(8)
C21	0.0339(11)	0.0239(11)	0.0432(11)	0.0047(9)	0.0117(9)	-0.0030(9)
C22	0.0316(11)	0.0195(11)	0.0487(12)	-0.0009(9)	0.0069(9)	0.0009(9)
C23	0.0534(13)	0.0258(11)	0.0322(10)	0.0057(9)	-0.0027(10)	-0.0033(11)
N1	0.0205(7)	0.0222(8)	0.0231(7)	-0.0054(7)	0.0051(6)	0.0007(7)
N2	0.0311(9)	0.0189(8)	0.0233(7)	0.0031(6)	-0.0019(7)	-0.0019(7)
O1	0.0230(6)	0.0331(8)	0.0244(6)	-0.0057(6)	0.0061(5)	-0.0005(6)
O2	0.0235(6)	0.0272(7)	0.0200(6)	-0.0068(5)	0.0019(5)	-0.0021(5)
O3	0.0470(8)	0.0284(8)	0.0243(7)	-0.0044(6)	0.0052(6)	0.0069(7)
O4	0.0312(8)	0.0373(9)	0.0410(8)	-0.0022(7)	-0.0079(6)	-0.0098(7)

The form of the anisotropic displacement parameter is:

281

$$\exp[-2\pi^2(a^{*2}U_{11}h^2+b^{*2}U_{22}k^2+c^{*2}U_{33}l^2+2b^*c^*U_{23}kl+2a^*c^*U_{13}hl+2a^*b^*U_{12}hk)]$$

Table 5. Bond Distances in Compound 1.09ab, **Å**

C1-N1	1.460(2)	C1-C2	1.519(3)	C1-C8	1.536(2)
C2-C7	1.387(3)	C2-C3	1.391(3)	C3-C4	1.393(3)
C4-C5	1.386(3)	C5-C6	1.375(3)	C6-C7	1.385(3)
C8-C9	1.507(3)	C8-N2	1.513(2)	C9-C10	1.382(3)
C9-C14	1.392(2)	C10-C11	1.389(3)	C11-C12	1.393(3)
C12-C13	1.403(3)	C12-C20	1.531(3)	C13-C14	1.377(3)
C15-O1	1.217(2)	C15-O2	1.339(2)	C15-N1	1.357(2)
C16-O2	1.485(2)	C16-C18	1.515(3)	C16-C19	1.515(3)
C16-C17	1.516(3)	C20-C21	1.526(3)	C20-C22	1.532(3)
C20-C23	1.534(3)	N2-O3	1.2204(19)	N2-O4	1.2327(19)

Table 6. Bond Angles in Compound 1.09ab, °

N1-C1-C2	112.16(13)	N1-C1-C8	106.26(14)	C2-C1-C8	113.69(14)
C7-C2-C3	118.87(17)	C7-C2-C1	120.08(16)	C3-C2-C1	121.04(16)
C2-C3-C4	120.26(18)	C5-C4-C3	120.02(18)	C6-C5-C4	119.77(18)
C5-C6-C7	120.31(19)	C6-C7-C2	120.75(18)	C9-C8-N2	107.86(13)
C9-C8-C1	114.96(14)	N2-C8-C1	109.31(14)	C10-C9-C14	118.15(17)
C10-C9-C8	119.98(15)	C14-C9-C8	121.84(16)	C9-C10-C11	120.95(17)
C10-C11-C12	121.83(17)	C11-C12-C13	116.17(17)	C11-C12-C20	122.27(17)
C13-C12-C20	121.48(15)	C14-C13-C12	122.25(17)	C13-C14-C9	120.65(17)
O1-C15-O2	126.07(15)	O1-C15-N1	124.20(15)	O2-C15-N1	109.73(14)
O2-C16-C18	101.84(14)	O2-C16-C19	110.17(15)	C18-C16-C19	110.90(16)
O2-C16-C17	110.43(14)	C18-C16-	110.71(16)	C19-C16-	112.32(15)

		C17		C17	
C21-C20-C12	111.25(15)	C21-C20-C22	106.94(16)	C12-C20-C22	111.99(15)
C21-C20-C23	108.89(16)	C12-C20-C23	108.26(15)	C22-C20-C23	109.47(16)
C15-N1-C1	122.24(14)	O3-N2-O4	124.82(15)	O3-N2-C8	118.16(14)
O4-N2-C8	116.94(15)	C15-O2-C16	120.83(13)		

APPENDIX C: High Throughput Experimentation Data

The nitromethane coupling screen illustrated in Figure 2.1 followed the standard HTE procedure using 20 μmol p-bromoanisole, 5 mol% Pd$_2$dba$_3$, 20 mol% ligand, 2 equiv MeNO$_2$, annd 0.2 M in solvent. Conditions tested: 19 sets of ligands, 4 bases, and 4 solvents.

Ligands:

PPh$_3$	P(o-tol)$_3$	PCy$_3$
P(t-Bu)$_3$·HBF$_4$	cataCXium A	DavePhos
SPhos	RuPhos	XPhos
BrettPhos	AtaPhos	DTBPF
QPhos	JohnPhos	cataCXium POMetB
t-BuMePhos	di-t-BuXPhos	di-t-BuBrettPhos
tetramethyl di-t-BuXPhos		

Bases:

NaOt-Bu, K$_3$PO$_4$, Cs$_2$CO$_3$, CsHCO$_3$

Solvents:

Toluene, 1,4-Dioxane, THF, DME
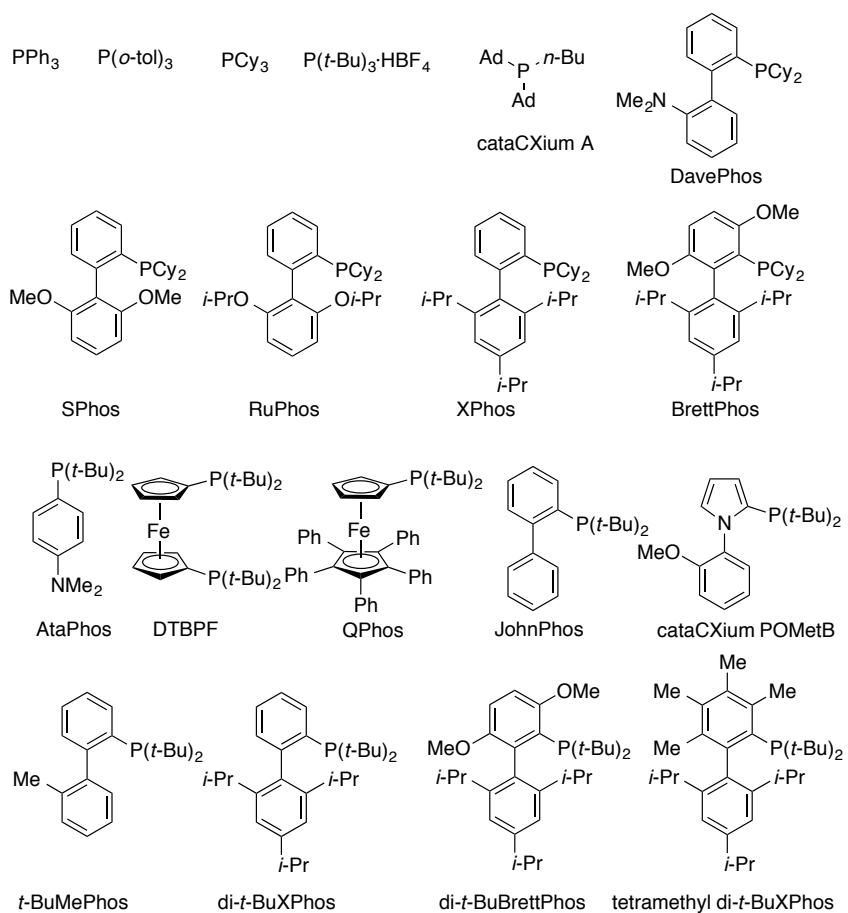
Figure C 1. Ligand structures used in the HTE screen.

Ligand	solvent	base	P / IS
PPh$_3$	DME	CsHCO$_3$	0.0000
PPh$_3$	DME	Cs$_2$CO$_3$	0.0000
PPh$_3$	DME	K$_3$PO$_4$	0.0000
PPh$_3$	DME	NaOt-Bu	0.0000
PPh$_3$	THF	CsHCO$_3$	0.0000
PPh$_3$	THF	Cs$_2$CO$_3$	0.0000
PPh$_3$	THF	K$_3$PO$_4$	0.0000
PPh$_3$	THF	NaOt-Bu	0.0000
PPh$_3$	1,4-dioxane	CsHCO$_3$	0.0000
PPh$_3$	1,4-dioxane	Cs$_2$CO$_3$	0.0000
PPh$_3$	1,4-dioxane	K$_3$PO$_4$	0.0000

PPh$_3$	1,4-dioxane	NaOt-Bu	0.0000
PPh$_3$	toluene	CsHCO$_3$	0.0000
PPh$_3$	toluene	Cs$_2$CO$_3$	0.0000
PPh$_3$	toluene	K$_3$PO$_4$	0.0000
PPh$_3$	toluene	NaOt-Bu	0.0000
P(o-tol)$_3$	DME	CsHCO$_3$	0.0000
P(o-tol)$_3$	DME	Cs$_2$CO$_3$	0.0000
P(o-tol)$_3$	DME	K$_3$PO$_4$	0.0000
P(o-tol)$_3$	DME	NaOt-Bu	0.0000
P(o-tol)$_3$	THF	CsHCO$_3$	0.0000
P(o-tol)$_3$	THF	Cs$_2$CO$_3$	0.0000
P(o-tol)$_3$	THF	K$_3$PO$_4$	0.2423
P(o-tol)$_3$	THF	NaOt-Bu	0.0000
P(o-tol)$_3$	1,4-dioxane	CsHCO$_3$	0.0000
P(o-tol)$_3$	1,4-dioxane	Cs$_2$CO$_3$	0.0000
P(o-tol)$_3$	1,4-dioxane	K$_3$PO$_4$	0.0000
P(o-tol)$_3$	1,4-dioxane	NaOt-Bu	0.0000
P(o-tol)$_3$	toluene	CsHCO$_3$	0.0000
P(o-tol)$_3$	toluene	Cs$_2$CO$_3$	0.2030
P(o-tol)$_3$	toluene	K$_3$PO$_4$	0.5398
P(o-tol)$_3$	toluene	NaOt-Bu	0.0000
PCy$_3$	DME	CsHCO$_3$	0.0000
PCy$_3$	DME	Cs$_2$CO$_3$	0.0000
PCy$_3$	DME	K$_3$PO$_4$	0.0000
PCy$_3$	DME	NaOt-Bu	0.0000
PCy$_3$	THF	CsHCO$_3$	0.0000
PCy$_3$	THF	Cs$_2$CO$_3$	0.0000
PCy$_3$	THF	K$_3$PO$_4$	0.0000
PCy$_3$	THF	NaOt-Bu	0.0000
PCy$_3$	1,4-dioxane	CsHCO$_3$	0.0000

PCy$_3$	1,4-dioxane	Cs$_2$CO$_3$	0.0000
PCy$_3$	1,4-dioxane	K$_3$PO$_4$	0.0000
PCy$_3$	1,4-dioxane	NaOt-Bu	0.0000
PCy$_3$	toluene	CsHCO$_3$	0.0000
PCy$_3$	toluene	Cs$_2$CO$_3$	0.0000
PCy$_3$	toluene	K$_3$PO$_4$	0.0000
PCy$_3$	toluene	NaOt-Bu	0.0000
PtBu$_3$HBF$_4$	DME	CsHCO$_3$	0.0374
PtBu$_3$HBF$_4$	DME	Cs$_2$CO$_3$	0.0413
PtBu$_3$HBF$_4$	DME	K$_3$PO$_4$	0.4559
PtBu$_3$HBF$_4$	DME	NaOt-Bu	0.0445
PtBu$_3$HBF$_4$	THF	CsHCO$_3$	0.0000
PtBu$_3$HBF$_4$	THF	Cs$_2$CO$_3$	0.9993
PtBu$_3$HBF$_4$	THF	K$_3$PO$_4$	0.0473
PtBu$_3$HBF$_4$	THF	NaOt-Bu	0.3442
PtBu$_3$HBF$_4$	1,4-dioxane	CsHCO$_3$	0.1595
PtBu$_3$HBF$_4$	1,4-dioxane	Cs$_2$CO$_3$	0.3700
PtBu$_3$HBF$_4$	1,4-dioxane	K$_3$PO$_4$	0.4430
PtBu$_3$HBF$_4$	1,4-dioxane	NaOt-Bu	0.6745
PtBu$_3$HBF$_4$	toluene	CsHCO$_3$	0.0000
PtBu$_3$HBF$_4$	toluene	Cs$_2$CO$_3$	0.3471
PtBu$_3$HBF$_4$	toluene	K$_3$PO$_4$	0.4092
PtBu$_3$HBF$_4$	toluene	NaOt-Bu	0.2402
CataXCiumA	DME	CsHCO$_3$	0.0000
CataXCiumA	DME	Cs$_2$CO$_3$	0.0000
CataXCiumA	DME	K$_3$PO$_4$	0.0000
CataXCiumA	DME	NaOt-Bu	0.0000
CataXCiumA	THF	CsHCO$_3$	0.0000
CataXCiumA	THF	Cs$_2$CO$_3$	0.0480
CataXCiumA	THF	K$_3$PO$_4$	0.0000

CataXCiumA	THF	NaOt-Bu	0.0000
CataXCiumA	1,4-dioxane	CsHCO$_3$	0.0000
CataXCiumA	1,4-dioxane	Cs$_2$CO$_3$	0.0000
CataXCiumA	1,4-dioxane	K$_3$PO$_4$	0.0000
CataXCiumA	1,4-dioxane	NaOt-Bu	0.0000
CataXCiumA	toluene	CsHCO$_3$	0.0000
CataXCiumA	toluene	Cs$_2$CO$_3$	0.0000
CataXCiumA	toluene	K$_3$PO$_4$	0.0000
CataXCiumA	toluene	NaOt-Bu	0.0000
DavePhos	DME	CsHCO$_3$	0.4551
DavePhos	DME	Cs$_2$CO$_3$	0.5370
DavePhos	DME	K$_3$PO$_4$	0.5071
DavePhos	DME	NaOt-Bu	0.0718
DavePhos	THF	CsHCO$_3$	0.8191
DavePhos	THF	Cs$_2$CO$_3$	0.3616
DavePhos	THF	K$_3$PO$_4$	0.6701
DavePhos	THF	NaOt-Bu	0.0416
DavePhos	1,4-dioxane	CsHCO$_3$	0.6652
DavePhos	1,4-dioxane	Cs$_2$CO$_3$	0.3804
DavePhos	1,4-dioxane	K$_3$PO$_4$	0.5294
DavePhos	1,4-dioxane	NaOt-Bu	0.0678
DavePhos	toluene	CsHCO$_3$	0.1948
DavePhos	toluene	Cs$_2$CO$_3$	0.1733
DavePhos	toluene	K$_3$PO$_4$	0.3848
DavePhos	toluene	NaOt-Bu	0.0000
Sphos	DME	CsHCO$_3$	0.2418
Sphos	DME	Cs$_2$CO$_3$	0.0417
Sphos	DME	K$_3$PO$_4$	0.3359
Sphos	DME	NaOt-Bu	0.0353
Sphos	THF	CsHCO$_3$	0.3327

Sphos	THF	Cs_2CO_3	0.0000
Sphos	THF	K_3PO_4	0.5280
Sphos	THF	NaO*t*-Bu	0.0000
Sphos	1,4-dioxane	$CsHCO_3$	0.3214
Sphos	1,4-dioxane	Cs_2CO_3	0.0000
Sphos	1,4-dioxane	K_3PO_4	0.3245
Sphos	1,4-dioxane	NaO*t*-Bu	0.0244
SPhos	toluene	$CsHCO_3$	0.1717
SPhos	toluene	Cs_2CO_3	0.0000
SPhos	toluene	K_3PO_4	0.1539
SPhos	toluene	NaO*t*-Bu	0.0000
RuPhos	DME	$CsHCO_3$	0.3208
RuPhos	DME	Cs_2CO_3	0.0617
RuPhos	DME	K_3PO_4	0.3828
RuPhos	DME	NaO*t*-Bu	0.0000
RuPhos	THF	$CsHCO_3$	0.4512
RuPhos	THF	Cs_2CO_3	0.0000
RuPhos	THF	K_3PO_4	0.4168
RuPhos	THF	NaO*t*-Bu	0.0000
RuPhos	1,4-dioxane	$CsHCO_3$	0.3436
RuPhos	1,4-dioxane	Cs_2CO_3	0.0318
RuPhos	1,4-dioxane	K_3PO_4	0.2732
RuPhos	1,4-dioxane	NaO*t*-Bu	0.0000
RuPhos	toluene	$CsHCO_3$	0.6149
RuPhos	toluene	Cs_2CO_3	0.0000
RuPhos	toluene	K_3PO_4	0.6059
RuPhos	toluene	NaO*t*-Bu	0.0000
XPhos	DME	$CsHCO_3$	0.7810
XPhos	DME	Cs_2CO_3	0.4298
XPhos	DME	K_3PO_4	1.1413

XPhos	DME	NaOt-Bu	0.2751
Xphos	THF	CsHCO$_3$	0.7064
Xphos	THF	Cs$_2$CO$_3$	1.5541
Xphos	THF	K$_3$PO$_4$	1.9575
Xphos	THF	NaOt-Bu	0.2370
XPhos	1,4-dioxane	CsHCO$_3$	1.3986
XPhos	1,4-dioxane	Cs$_2$CO$_3$	0.5031
XPhos	1,4-dioxane	K$_3$PO$_4$	1.9303
XPhos	1,4-dioxane	NaOt-Bu	0.4374
XPhos	toluene	CsHCO$_3$	0.7446
XPhos	toluene	Cs$_2$CO$_3$	0.7085
XPhos	toluene	K$_3$PO$_4$	1.6426
XPhos	toluene	NaOt-Bu	0.0000
BrettPhos	DME	CsHCO$_3$	0.9239
BrettPhos	DME	Cs$_2$CO$_3$	0.1700
BrettPhos	DME	K$_3$PO$_4$	1.7524
BrettPhos	DME	NaOt-Bu	0.5349
BrettPhos	THF	CsHCO$_3$	1.6570
BrettPhos	THF	Cs$_2$CO$_3$	1.6611
BrettPhos	THF	K$_3$PO$_4$	0.0000
BrettPhos	THF	NaOt-Bu	0.6289
BrettPhos	1,4-dioxane	CsHCO$_3$	1.4623
BrettPhos	1,4-dioxane	Cs$_2$CO$_3$	0.6509
BrettPhos	1,4-dioxane	K$_3$PO$_4$	1.8154
BrettPhos	1,4-dioxane	NaOt-Bu	0.1104
BrettPhos	toluene	CsHCO$_3$	1.4422
BrettPhos	toluene	Cs$_2$CO$_3$	0.2813
BrettPhos	toluene	K$_3$PO$_4$	0.0000
BrettPhos	toluene	NaOt-Bu	0.0000
AtaPhos	DME	CsHCO$_3$	0.0000

AtaPhos	DME	Cs_2CO_3	0.0000
AtaPhos	DME	K_3PO_4	0.1367
AtaPhos	DME	NaOt-Bu	0.0000
AtaPhos	THF	$CsHCO_3$	0.0000
AtaPhos	THF	Cs_2CO_3	0.1455
AtaPhos	THF	K_3PO_4	0.0000
AtaPhos	THF	NaOt-Bu	0.1730
AtaPhos	1,4-dioxane	$CsHCO_3$	0.0000
AtaPhos	1,4-dioxane	Cs_2CO_3	0.0000
AtaPhos	1,4-dioxane	K_3PO_4	0.0000
AtaPhos	1,4-dioxane	NaOt-Bu	0.0000
AtaPhos	toluene	$CsHCO_3$	0.0000
AtaPhos	toluene	Cs_2CO_3	0.0000
AtaPhos	toluene	K_3PO_4	0.0000
AtaPhos	toluene	NaOt-Bu	0.0000
DTBPF	DME	$CsHCO_3$	0.0000
DTBPF	DME	Cs_2CO_3	0.0786
DTBPF	DME	K_3PO_4	0.0000
DTBPF	DME	NaOt-Bu	0.0000
DTBPF	THF	$CsHCO_3$	0.0208
DTBPF	THF	Cs_2CO_3	0.1544
DTBPF	THF	K_3PO_4	0.4039
DTBPF	THF	NaOt-Bu	0.0396
DTBPF	1,4-dioxane	$CsHCO_3$	0.0000
DTBPF	1,4-dioxane	Cs_2CO_3	0.0000
DTBPF	1,4-dioxane	K_3PO_4	0.0785
DTBPF	1,4-dioxane	NaOt-Bu	0.0514
DTBPF	toluene	$CsHCO_3$	0.0000
DTBPF	toluene	Cs_2CO_3	0.0000
DTBPF	toluene	K_3PO_4	0.4001

DTBPF	toluene	NaOt-Bu	0.0000
Qphos	DME	CsHCO$_3$	0.0000
Qphos	DME	Cs$_2$CO$_3$	0.2611
Qphos	DME	K$_3$PO$_4$	0.1727
Qphos	DME	NaOt-Bu	0.4408
Qphos	THF	CsHCO$_3$	0.4189
Qphos	THF	Cs$_2$CO$_3$	0.3103
Qphos	THF	K$_3$PO$_4$	0.4018
Qphos	THF	NaOt-Bu	0.0944
Qphos	1,4-dioxane	CsHCO$_3$	0.1544
Qphos	1,4-dioxane	Cs$_2$CO$_3$	0.0000
Qphos	1,4-dioxane	K$_3$PO$_4$	0.6536
Qphos	1,4-dioxane	NaOt-Bu	0.2914
Qphos	toluene	CsHCO$_3$	0.0000
Qphos	toluene	Cs$_2$CO$_3$	0.4152
Qphos	toluene	K$_3$PO$_4$	0.4236
Qphos	toluene	NaOt-Bu	0.6983
JohnPhos	DME	CsHCO$_3$	0.0000
JohnPhos	DME	Cs$_2$CO$_3$	0.2656
JohnPhos	DME	K$_3$PO$_4$	0.0347
JohnPhos	DME	NaOt-Bu	0.1898
JohnPhos	THF	CsHCO$_3$	0.3428
JohnPhos	THF	Cs$_2$CO$_3$	0.1961
JohnPhos	THF	K$_3$PO$_4$	0.5517
JohnPhos	THF	NaOt-Bu	0.0338
JohnPhos	1,4-dioxane	CsHCO$_3$	0.9195
JohnPhos	1,4-dioxane	Cs$_2$CO$_3$	0.3401
JohnPhos	1,4-dioxane	K$_3$PO$_4$	1.8730
JohnPhos	1,4-dioxane	NaOt-Bu	0.6672
JohnPhos	toluene	CsHCO$_3$	0.1652

JohnPhos	toluene	Cs_2CO_3	0.1535
JohnPhos	toluene	K_3PO_4	0.1044
JohnPhos	toluene	NaO*t*-Bu	0.5335
CataXCium PtBu	DME	$CsHCO_3$	0.6350
CataXCium PtBu	DME	Cs_2CO_3	0.7689
CataXCium PtBu	DME	K_3PO_4	1.5988
CataXCium PtBu	DME	NaO*t*-Bu	0.1010
CataXCium PtBu	THF	$CsHCO_3$	0.4143
CataXCium PtBu	THF	Cs_2CO_3	0.4172
CataXCium PtBu	THF	K_3PO_4	0.5033
CataXCium PtBu	THF	NaO*t*-Bu	0.1847
CataXCium PtBu	1,4-dioxane	$CsHCO_3$	0.9014
CataXCium PtBu	1,4-dioxane	Cs_2CO_3	0.7584
CataXCium PtBu	1,4-dioxane	K_3PO_4	1.9300
CataXCium PtBu	1,4-dioxane	NaO*t*-Bu	2.3957
CataXCium PtBu	toluene	$CsHCO_3$	0.0000
CataXCium PtBu	toluene	Cs_2CO_3	0.3615
CataXCium PtBu	toluene	K_3PO_4	0.6423
CataXCium PtBu	toluene	NaO*t*-Bu	0.7010
tBu-MePhos	DME	$CsHCO_3$	0.2629
tBu-MePhos	DME	Cs_2CO_3	0.0000
tBu-MePhos	DME	K_3PO_4	0.6887
tBu-MePhos	DME	NaO*t*-Bu	0.3007
tBu-MePhos	THF	$CsHCO_3$	0.4366
tBu-MePhos	THF	Cs_2CO_3	0.1773
tBu-MePhos	THF	K_3PO_4	0.0594
tBu-MePhos	THF	NaO*t*-Bu	0.1119
tBu-MePhos	1,4-dioxane	$CsHCO_3$	0.1852
tBu-MePhos	1,4-dioxane	Cs_2CO_3	0.0000
tBu-MePhos	1,4-dioxane	K_3PO_4	0.4352

293

tBu-MePhos	1,4-dioxane	NaO*t*-Bu	0.5511
tBu-MePhos	toluene	CsHCO$_3$	0.0000
tBu-MePhos	toluene	Cs$_2$CO$_3$	0.0000
tBu-MePhos	toluene	K$_3$PO$_4$	0.1711
tBu-MePhos	toluene	NaO*t*-Bu	0.4021
tBu-Xphos	DME	CsHCO$_3$	0.0000
tBu-Xphos	DME	Cs$_2$CO$_3$	0.0000
tBu-Xphos	DME	K$_3$PO$_4$	0.1504
tBu-Xphos	DME	NaO*t*-Bu	0.0000
tBu-Xphos	THF	CsHCO$_3$	0.0000
tBu-Xphos	THF	Cs$_2$CO$_3$	0.0000
tBu-Xphos	THF	K$_3$PO$_4$	0.0889
tBu-Xphos	THF	NaO*t*-Bu	0.0749
tBu-Xphos	1,4-dioxane	CsHCO$_3$	0.0000
tBu-Xphos	1,4-dioxane	Cs$_2$CO$_3$	0.0000
tBu-Xphos	1,4-dioxane	K$_3$PO$_4$	0.0000
tBu-Xphos	1,4-dioxane	NaO*t*-Bu	0.0000
tBu-Xphos	toluene	CsHCO$_3$	0.0000
tBu-Xphos	toluene	Cs$_2$CO$_3$	0.0000
tBu-Xphos	toluene	K$_3$PO$_4$	0.0000
tBu-Xphos	toluene	NaO*t*-Bu	0.0000
tBu-BrettPhos	DME	CsHCO$_3$	0.0000
tBu-BrettPhos	DME	Cs$_2$CO$_3$	0.0000
tBu-BrettPhos	DME	K$_3$PO$_4$	0.1587
tBu-BrettPhos	DME	NaO*t*-Bu	0.0000
tBu-BrettPhos	THF	CsHCO$_3$	0.0898
tBu-BrettPhos	THF	Cs$_2$CO$_3$	0.1502
tBu-BrettPhos	THF	K$_3$PO$_4$	0.0000
tBu-BrettPhos	THF	NaO*t*-Bu	0.0529
tBu-BrettPhos	1,4-dioxane	CsHCO$_3$	0.0000

tBu-BrettPhos	1,4-dioxane	Cs_2CO_3	0.0000
tBu-BrettPhos	1,4-dioxane	K_3PO_4	0.0000
tBu-BrettPhos	1,4-dioxane	NaO*t*-Bu	0.0000
tBu-BrettPhos	toluene	$CsHCO_3$	0.0000
tBu-BrettPhos	toluene	Cs_2CO_3	0.0000
tBu-BrettPhos	toluene	K_3PO_4	0.0000
tBu-BrettPhos	toluene	NaO*t*-Bu	0.0000
Me4-tBuXphos	DME	$CsHCO_3$	0.0000
Me4-tBuXphos	DME	Cs_2CO_3	0.0000
Me4-tBuXphos	DME	K_3PO_4	0.0806
Me4-tBuXphos	DME	NaO*t*-Bu	0.0000
Me4-tBuXphos	THF	$CsHCO_3$	0.0330
Me4-tBuXphos	THF	Cs_2CO_3	0.0000
Me4-tBuXphos	THF	K_3PO_4	0.0000
Me4-tBuXphos	THF	NaO*t*-Bu	0.0822
Me4-tBuXphos	1,4-dioxane	$CsHCO_3$	0.0000
Me4-tBuXphos	1,4-dioxane	Cs_2CO_3	0.0000
Me4-tBuXphos	1,4-dioxane	K_3PO_4	0.0000
Me4-tBuXphos	1,4-dioxane	NaO*t*-Bu	0.0000
Me4-tBuXphos	toluene	$CsHCO_3$	0.0000
Me4-tBuXphos	toluene	Cs_2CO_3	0.0000
Me4-tBuXphos	toluene	K_3PO_4	0.0000
Me4-tBuXphos	toluene	NaO*t*-Bu	0.0000

Table C 1. Raw product to internal standard values for the HTE screen in **Figure 2.1**.

APPENDIX D: UV-Vis Spectroscopic Titration Data
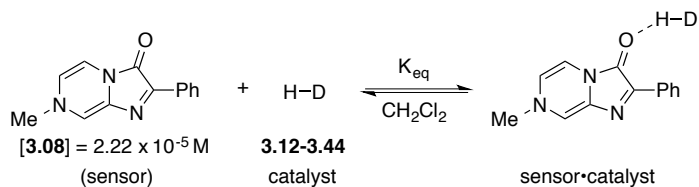
Titrations of Hydrogen-Bonding Catalysts 3.12-3.44 with Sensor 3.08.

Diphenylthiourea **(3.12)**

equiv cat	[catalyst] M	λ_{max} (nm)
0	0	498.6
500	0.0111	497.4
1000	0.0222	496.8
1500	0.0333	496.0
2000	0.0444	495.6
2500	0.0555	494.6
3000	0.0666	493.6
3500	0.0777	493.6
4000	0.0888	493.2
4500	0.0999	492.4
5000	0.111	492.0
5500	0.1221	491.2
6000	0.1332	490.2
6500	0.1443	490.8
7000	0.1554	490.2
7500	0.1665	490.0

8000	0.1776	490.0

(CF₃)₂-Thiourea **(3.13)**

equiv cat	[catalyst] M	λ_{max} (nm)
0	0	498.6
25	0.000554	498.0
50	0.001108	497.4
75	0.001662	496.8
100	0.002216	496.2
125	0.00277	495.0
150	0.003324	494.8
200	0.004432	494.2
250	0.00554	493.0
299	0.006648	493.0
349	0.007756	493.0
399	0.008864	492.2
499	0.01108	488.2
599	0.013296	487.0
699	0.015512	485.4
799	0.017728	484.6
898	0.019944	484.4
998	0.02216	484.2
1098	0.024376	484.0
1198	0.026592	484.4

(CF₃)₃-Thiourea **(3.14)**

equiv cat	[catalyst] M	λ_{max} (nm)
0.00	0	498.6
13.51	0.0003	497.8
27.03	0.0006	496.0
40.54	0.0009	494.0
54.05	0.0012	493.8
81.08	0.0018	492.6
108.11	0.0024	487.8
135.14	0.003	485.6
162.16	0.0036	484.6
189.19	0.0042	483.2
216.22	0.0048	483.2
243.24	0.0054	482.2
270.27	0.006	481.8
337.84	0.0075	481.6
405.41	0.009	480.8
472.97	0.0105	480.2
540.54	0.012	479.8
608.11	0.0135	479.8
675.68	0.015	479.6

(CF$_3$)$_4$-Thiourea **(3.15)**

equiv cat	[catalyst] M	λ_{max} (nm)
0	0	498.6
5	0.000111	499.0
10	0.000222	495.6
15	0.000333	493.8
20	0.000444	491.2
25	0.000555	488.2
30	0.000666	487.2
35	0.000777	485.2
40	0.000888	484.4
45	0.000999	483.2
50	0.00111	483.0
75	0.001665	480.8
100	0.00222	479.8
125	0.002775	479.4
150	0.00333	478.8
175	0.003885	478.4
200	0.00444	478.4
225	0.004995	478.0
250	0.00555	477.8
275	0.006105	477.8
300	0.00666	477.6
325	0.007215	477.4
350	0.00777	477.4

Sulfonamide **(3.16)**

equiv cat	[catalyst] M	λ_{max} (nm)
0.00	0	498.6
5.00	0.000111	497.2
10.00	0.000222	496.4
20.00	0.000444	494.0
30.00	0.000666	493.0
50.00	0.00111	489.2
70.00	0.001554	486.4
90.00	0.001998	484.8
110.00	0.002442	484.0
130.00	0.002886	483.6
150.00	0.00333	483.2
170.00	0.003774	483.0
190.00	0.004218	483.0
210.00	0.004662	482.6
230.00	0.005106	482.2
250.00	0.00555	482.2
270.00	0.005994	482.4

(CF₃)₂-Urea **(3.17)**

equiv cat	[catalyst] M	λ_{max} (nm)
0	0	498.6
50	0.001104	488.2
99	0.002208	484.0
149	0.003312	483.8
199	0.004416	482.2
249	0.00552	481.8
298	0.006624	480.4
348	0.007728	480.6

(CF₃)₃-Urea **(3.18)**

equiv cat	[catalyst] M	λ_{max} (nm)
0.00	0	498.6
13.42	0.000298	492.8
20.14	0.000447	487.8
26.85	0.000596	485.0
33.56	0.000745	484.4
40.27	0.000894	483.2
46.98	0.001043	482.6
53.69	0.001192	482.4
67.12	0.00149	481.8
80.54	0.001788	481.2
93.96	0.002086	481.2
114.10	0.002533	480.4

134.23	0.00298	480.4
154.37	0.003427	480.4
174.50	0.003874	480.0
201.35	0.00447	479.6
234.91	0.005215	479.8
268.47	0.00596	479.6

(CF₃)₄-Urea **(3.19)**

equiv cat	[catalyst] M	λ_{max} (nm)
0	0	498.6
7	0.000148	486.8
13	0.000296	482.0
20	0.000444	481.0
27	0.000592	481.2
33	0.00074	481.2
47	0.001036	480.8
60	0.001332	480.2
73	0.001628	479.8
87	0.001924	480.0

BF$_2$-Urea **(3.20)**

equiv cat	[catalyst] M	λ_{max} (nm)
0.00	0	498.6
0.50	0.0000111	497.0
1.00	0.0000222	494.8
1.50	0.0000333	492.0
2.00	0.0000444	488.0
2.50	0.0000555	484.4
3.00	0.0000666	481.8
3.50	0.0000777	481.0
4.00	0.0000888	479.4
5.00	0.000111	478.8
6.00	0.0001332	477.8
8.00	0.0001776	476.6
10.00	0.000222	476.2
12.00	0.0002664	475.4
14.00	0.0003108	475.4
16.00	0.0003552	475.0
18.00	0.0003996	474.4
20.00	0.000444	474.4
22.00	0.0004884	474.4

Guanidinium **(3.21)**

equiv cat	[catalyst] M	λ_{max} (nm)
0	0.00E+00	498.6
1	2.22E-05	496.0
2	4.44E-05	491.6
3	6.66E-05	485.6
4	8.88E-05	482.0
5	1.11E-04	480.0
6	1.33E-04	479.2
7	1.55E-04	478.0
8	1.78E-04	477.0
9	2.00E-04	476.8
10	2.22E-04	476.4
20	4.44E-04	474.6
30	6.66E-04	473.2
40	8.88E-04	473.8
50	1.11E-03	473.2

Squaramide **(3.22)**

Due to the very low solubility of **3.22** in CH_2Cl_2, the titration was performed heterogeneously. After ~25 equiv addition, the background absorbance overlapped with the sensor absorbance, leading to lower λ_{max} values not associated with the sensor. Based on the curve, a saturated λ_{max} value is approximated at ~480 nm. Catalyst equivalent is approximate in the table below, since the stock solution was a fine slurry.

equiv cat	[catalyst] M	λ_{max} (nm)
0.00	0.00E+00	498.6
4.67	1.04E-04	494.6
9.33	2.07E-04	484.4
14.00	3.11E-04	481.4
18.67	4.14E-04	480.2
23.33	5.18E-04	480.0
28.00	6.22E-04	479.2
37.33	8.29E-04	479.0
46.67	1.04E-03	477.2
65.33	1.45E-03	475.4
84.00	1.86E-03	472.0

BisAmidinium **(3.23)**

equiv cat	[catalyst] M	λ_{max} (nm)
0	0.00E+00	498.2
0.1	2.22E-06	497.2
0.2	4.44E-06	496.4
0.3	6.66E-06	494.6
0.4	8.88E-06	493.2
0.5	1.11E-05	489.2
0.6	1.33E-05	482.8
0.7	1.55E-05	479.8
0.8	1.78E-05	476.6
0.9	2.00E-05	473.3

1	2.22E-05	473.0
1.2	2.66E-05	471.2
1.4	3.11E-05	469.8
1.6	3.55E-05	468.8
1.8	4.00E-05	468.6
2	4.44E-05	468.0
3	6.66E-05	466.4
4	8.88E-05	466.0
6	1.33E-04	465.4
8	1.78E-04	465.2
10	2.22E-04	465.0
15	3.33E-04	464.8
20	4.44E-04	464.6
30	6.66E-04	464.6

MonoAmidinium **(3.24)**

equiv cat	[catalyst] M	λ_{max} (nm)
0	0.00E+00	498.8
5	1.11E-04	495.4
10	2.22E-04	490.6
15	3.33E-04	485.0
20	4.44E-04	482.8
25	5.55E-04	480.8
30	6.66E-04	479.6
35	7.77E-04	478.8

40	8.88E-04	478.2
45	9.99E-04	477.6
50	1.11E-03	477.4
75	1.67E-03	475.2
100	2.22E-03	474.6
125	2.78E-03	473.8
150	3.33E-03	473.6
175	3.89E-03	473.4
200	4.44E-03	473.0
225	5.00E-03	473.0
250	5.55E-03	473.0

Benzotriazole **(3.26)**

equiv cat	[catalyst] M	λ_{max} (nm)
0	0.00E+00	498.6
200	4.44E-03	495.8
400	8.88E-03	493.4
600	1.33E-02	492.6
800	1.78E-02	489.8
1000	2.22E-02	488.8
1200	2.66E-02	488.8
1600	3.55E-02	486.8
2000	4.44E-02	486.8
2400	5.33E-02	485.8
2800	6.22E-02	485.4

3200	7.10E-02	484.2
4000	8.88E-02	484.6
4800	1.07E-01	484.2
5600	1.24E-01	484.2

Thiophosphoramide **(2.27)**

equiv cat	[catalyst] M	λ_{max} (nm)
0.00	0.00E+00	498.6
10.00	2.22E-04	490.8
20.00	4.44E-04	482.8
30.00	6.66E-04	479.2
40.00	8.88E-04	477.8
50.00	1.11E-03	477.8
60.00	1.33E-03	477
80.00	1.78E-03	476.2
100.00	2.22E-03	476
120.00	2.66E-03	475.6
140.00	3.11E-03	475
160.00	3.55E-03	475.2
200.00	4.44E-03	474.8

2-Me-BzOH **(3.28)**

equiv cat	[catalyst] M	λ_{max} (nm)
0	0.00E+00	498.8
200	4.44E-03	496.4
400	8.88E-03	495.2
600	1.33E-02	492.8
800	1.78E-02	491.0
1000	2.22E-02	491.2
1200	2.66E-02	490.6
1400	3.11E-02	489.2
1600	3.55E-02	488.8
1800	4.00E-02	488.0
2000	4.44E-02	487.8
2500	5.55E-02	486.4
3000	6.66E-02	486.4
3500	7.77E-02	486.2

BzOH **(3.29)**

equiv cat	[catalyst] M	λ_{max} (nm)
0	0.00E+00	498.2
200	4.44E-03	495.8
400	8.88E-03	493.4
600	1.33E-02	491.4
800	1.78E-02	490.2
1000	2.22E-02	489.4

1200	2.66E-02	488.4
1400	3.11E-02	487.8
1600	3.55E-02	486.6
1800	4.00E-02	486.6
2000	4.44E-02	486.4
2500	5.55E-02	485.4
3000	6.66E-02	485.4

2-Cl-BzOH **(3.30)**

equiv cat	[catalyst] M	λ_{max} (nm)
0	0.00E+00	498.6
100	2.22E-03	494.4
200	4.44E-03	491.0
300	6.66E-03	487.6
400	8.88E-03	487.0
500	1.11E-02	485.2
600	1.33E-02	485.2
700	1.55E-02	484.6
800	1.78E-02	484.4
900	2.00E-02	483.2
1000	2.22E-02	483.8
1100	2.44E-02	483.2
1300	2.89E-02	482.6
1500	3.33E-02	482.6

2-NO$_2$-BzOH **(3.31)**

equiv cat	[catalyst] M	λ_{max} (nm)
0	0.00E+00	498.6
40	8.88E-04	491.2
80	1.78E-03	486.0
120	2.66E-03	483.6
160	3.55E-03	481.8
200	4.44E-03	480.8
240	5.33E-03	480.6
280	6.22E-03	480.8
320	7.10E-03	480.4
360	7.99E-03	480.0
400	8.88E-03	480.2

3,5-(NO$_2$)$_2$-BzOH **(3.32)**

equiv cat	[catalyst] M	λ_{max} (nm)
0	0.00E+00	498.6
20	4.44E-04	495.4
40	8.88E-04	489.2
60	1.33E-03	485.4
80	1.78E-03	484.0
100	2.22E-03	482.0
150	3.33E-03	480.4
200	4.44E-03	479.8
250	5.55E-03	479.0

300	6.66E-03	478.4
350	7.77E-03	478.0

F$_5$-BzOH (3.33)

equiv cat	[catalyst] M	λ_{max} (nm)
0	0.00E+00	499.0
20	4.44E-04	492.0
40	8.88E-04	485.4
60	1.33E-03	481.6
80	1.78E-03	480.6
100	2.22E-03	480.0
150	3.33E-03	478.4
200	4.44E-03	477.8
250	5.55E-03	477.2
300	6.66E-03	477.4

Trifluoroacetic acid **(3.34)**

equiv cat	**[catalyst] M**	λ_{max} **(nm)**
0.00	0.00E+00	498.6
0.20	4.44E-06	498.4
0.40	8.88E-06	497.6
0.60	1.33E-05	497.6
0.80	1.78E-05	497.6
1.00	2.22E-05	497.4

3.00	6.66E-05	495.6
5.00	1.11E-04	492.4
7.00	1.55E-04	487.6
9.00	2.00E-04	483.8
11.00	2.44E-04	480.2
15.00	3.33E-04	477.0
19.00	4.22E-04	474.4
23.00	5.11E-04	473.4
27.00	5.99E-04	472.6
31.00	6.88E-04	472.4
35.00	7.77E-04	472.0
39.00	8.66E-04	471.0
43.00	9.55E-04	471.2
47.00	1.04E-03	470.8
51.00	1.13E-03	470.6
55.00	1.22E-03	470.0
59.00	1.31E-03	470.0
63.00	1.40E-03	470.2

Spiroligozyme **(3.35)**

equiv cat	[catalyst] M	λ_{max} (nm)
0	0.00E+00	498.6
15	3.33E-04	496.6
30	6.66E-04	494.4
45	9.99E-04	493.4

313

60	1.33E-03	491.4
75	1.67E-03	488.8
90	2.00E-03	488.0
105	2.33E-03	484.8
120	2.66E-03	484.2
135	3.00E-03	483.2
150	3.33E-03	481.6
165	3.66E-03	482.0
180	4.00E-03	481.4
195	4.33E-03	480.8
210	4.66E-03	480.2
225	5.00E-03	480.2
240	5.33E-03	480.0
255	5.66E-03	480.0

(R)-BINOL **(3.36)**

equiv cat	[catalyst] M	λ_{max} (nm)
0	0.00E+00	498.6
500	1.11E-02	496.8
1000	2.22E-02	494.6
1500	3.33E-02	492.2
2000	4.44E-02	491.4
2500	5.55E-02	490.4
3000	6.66E-02	489.4
3500	7.77E-02	488.6

314

4000	8.88E-02	488.8
4500	9.99E-02	488.0
5000	1.11E-01	488.0
5500	1.22E-01	487.8
6000	1.33E-01	487.2
6500	1.44E-01	487.4
7000	1.55E-01	487.0
7500	1.67E-01	486.6
8000	1.78E-01	486.6
8500	1.89E-01	486.0
9000	2.00E-01	486.8
9500	2.11E-01	486.4

4-t-Bu-Phenol **(3.27)**

equiv cat	[catalyst] M	λ_{max} (nm)
0	0.00E+00	498.4
100	2.22E-03	497.2
200	4.44E-03	496.5
300	6.66E-03	495.2
400	8.88E-03	494.8
500	1.11E-02	494
600	1.33E-02	493.5
800	1.78E-02	493.3
1000	2.22E-02	492.7
1500	3.33E-02	489.6

2000	4.44E-02	488.8
2500	5.55E-02	488
3000	6.66E-02	487.5
4000	8.88E-02	486.7
5000	1.11E-01	486.2

4-Br-Phenol (**3.28**)

equiv cat	[catalyst] M	λ_{max} (nm)
0	0	498.6
200	0.00444	493.6
400	0.00888	489.6
600	0.01332	487.4
800	0.01776	486.4
1200	0.02664	485.4
1600	0.03552	484.8
2000	0.0444	484.0
2400	0.05328	484.4
2800	0.06216	484.2

4-NO₂-Phenol **(3.29)**

equiv cat	[catalyst] M	λ_{max} (nm)
0	0.00E+00	498.6
80	1.78E-03	489.2
160	3.55E-03	486.2
240	5.33E-03	484.2
320	7.10E-03	483.0
480	1.07E-02	482.2
640	1.42E-02	481.8
800	1.78E-02	481.6
1000	2.22E-02	481.0
1200	2.66E-02	481.2

F₅-Phenol **(4.40)**

equiv cat	[catalyst] M	λ_{max} (nm)
0.00	0.00E+00	498.6
23.33	5.18E-04	496.6
70.00	1.55E-03	493.0
116.67	2.59E-03	486.0
163.33	3.63E-03	483.0
210.00	4.66E-03	482.8
256.67	5.70E-03	481.6
303.33	6.73E-03	481.2
350.00	7.77E-03	480.8
396.67	8.81E-03	481.0

(R,R)-TADDOL **(4.41)**

equiv cat	[catalyst] M	λ_{max} (nm)
0	0.00E+00	498.6
500	1.11E-02	498.6
1000	2.22E-02	498.6
1500	3.33E-02	498.2
2000	4.44E-02	495.6
2500	5.55E-02	495.0
3000	6.66E-02	494.6
3500	7.77E-02	494.0
4000	8.88E-02	494.0
4500	9.99E-02	493.0
5000	1.11E-01	493.0
5500	1.22E-01	492.6
6000	1.33E-01	492.2
6500	1.44E-01	492.2
7000	1.55E-01	491.8
7500	1.67E-01	491.8
8000	1.78E-01	491.4
8500	1.89E-01	491.4
9000	2.00E-01	491.2
9500	2.11E-01	490.6
10000	2.22E-01	491
10500	2.33E-01	490.8
11000	2.44E-01	490.6

t-BuMe₂SiOH **(3.42)**

equiv cat	[catalyst] M	λ$_{max}$ (nm)
0	0	498.8
2000	0.0444	498.0
4000	0.0888	496.8
6000	0.1332	496.4
8000	0.1776	495.0
10000	0.222	494.2
12000	0.2664	494.2
14000	0.3108	493.4
16000	0.3552	492.8
18000	0.3996	492.4
20000	0.444	491.8
25000	0.555	491.6
30000	0.666	491.2
35000	0.777	490.4
40000	0.888	490.4

SilaneDiol **(3.43)**

equiv cat	[catalyst] M	λ_{max} (nm)
0.00	0.00E+00	498.2
1.00	2.22E-05	498.8
3.00	6.66E-05	498.6
5.00	1.11E-04	498
15.00	3.33E-04	498.2
35.00	7.77E-04	498.2
55.00	1.22E-03	497.2
95.00	2.11E-03	497.2
135.00	3.00E-03	497.2
195.00	4.33E-03	496.2
255.00	5.66E-03	496
355.00	7.88E-03	494.8
455.00	1.01E-02	494.2
555.00	1.23E-02	493
655.00	1.45E-02	492.4
755.00	1.68E-02	491.4
855.00	1.90E-02	490.4
955.00	2.12E-02	490.6
1055.00	2.34E-02	488.8
1155.00	2.56E-02	489.2
1255.00	2.79E-02	488.4
1355.00	3.01E-02	487.8
1455.00	3.23E-02	487.2
1555.00	3.45E-02	487.2

Water **(3.44)**

equiv cat	[catalyst] M	λ_{max} (nm)
0	0.00E+00	498.6
5000	1.11E-01	498.6
10000	2.22E-01	498.6
15000	3.33E-01	498.0
20000	4.44E-01	496.0
25000	5.55E-01	495.6
30000	6.66E-01	495.2
35000	7.77E-01	495.2
40000	8.88E-01	495.2

PPTS **(4.02)**

equiv cat	[catalyst] M	λ_{max} (nm)
0.00	0.00E+00	498.6
0.25	5.56E-06	498.8
0.50	1.11E-05	498.6
1.00	2.22E-05	498.8
2.50	5.56E-05	498.8
7.5	1.67E-04	500.0
12.5	2.78E-04	500.2
23	5.00E-04	500.2
33	7.23E-04	500.2
83	1.83E-03	503.0
133	2.95E-03	505.6

183	4.06E-03	506.8
233	5.17E-03	507.8
333	7.39E-03	509.8
433	9.62E-03	511.0
533	1.18E-02	512.2
784	1.74E-02	510.6

(+)-CSA **(4.03)**

equiv cat	[catalyst] M	λ_{max} (nm)
0.00	0.00E+00	498.4
0.25	5.56E-06	498.2
0.50	1.11E-05	498.6
1.0	2.22E-05	500.0
2.5	5.56E-05	501.8
5	1.11E-04	506.8
7.5	1.67E-04	511.0
10	2.22E-04	512.8
15	3.34E-04	515.2
20	4.45E-04	516.0
30	6.67E-04	516.8
40	8.90E-04	517.2
50	1.11E-03	518.0
75	1.67E-03	518.6

TfNH₂ **(4.04)**

equiv cat	[catalyst] M	λ_{max} (nm)
0.00	0.00E+00	498.4
0.25	5.56E-06	498.6
0.50	1.11E-05	498.4
1.00	2.22E-05	498.2
2.5	5.56E-05	497.8
7.5	1.67E-04	498.0
12.5	2.78E-04	497.8
22.5	5.00E-04	497.4
72.6	1.61E-03	496.8
123	2.72E-03	501.0
223	4.95E-03	525.2
323	7.17E-03	527.0
423	9.40E-03	527.0

APPENDIX E: Diels Alder and Friedel Crafts Rate Plots

Diels Alder Kinetic Plots for All Catalysts

Diphenylthiourea **(3.12)** - 20 mol%
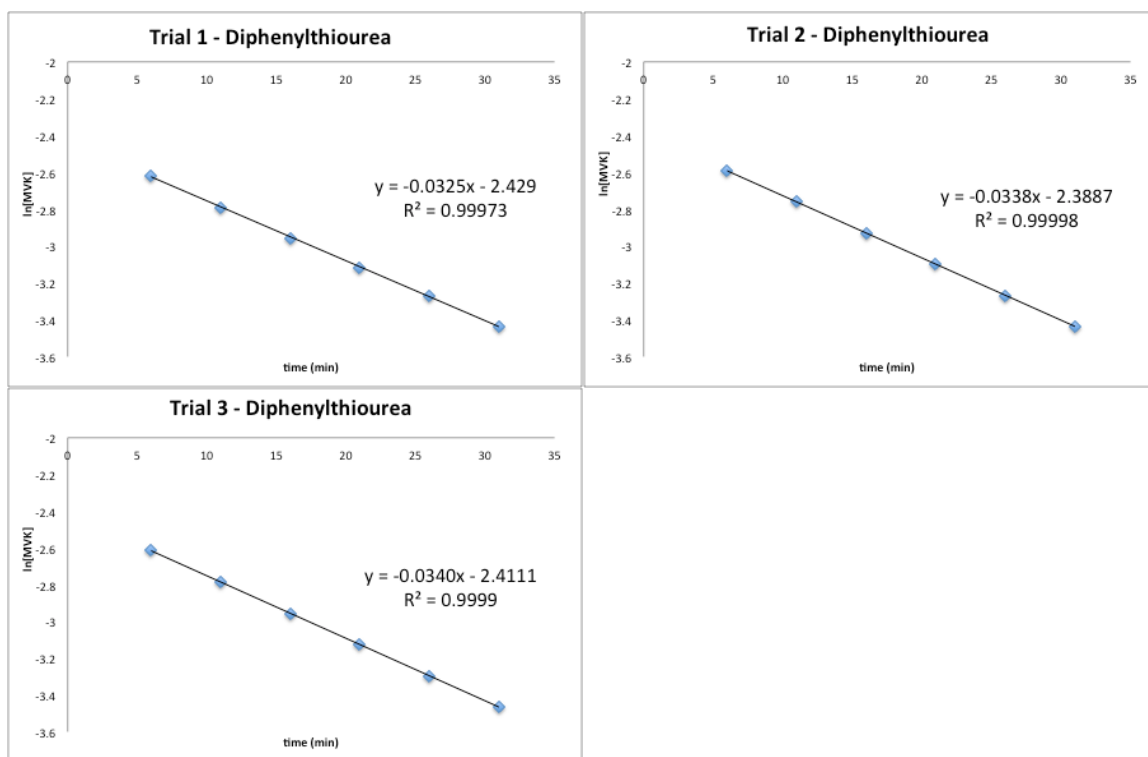
(CF$_3$)$_2$-thiourea **(3.13)** - 10 mol%
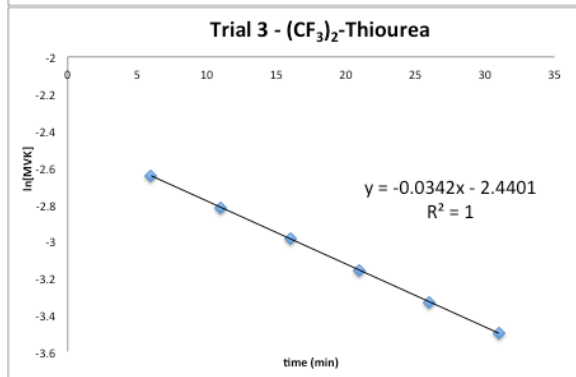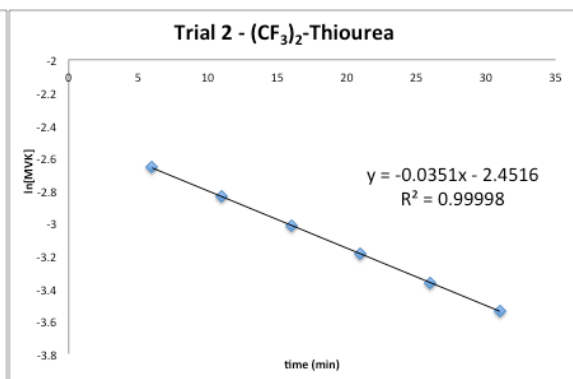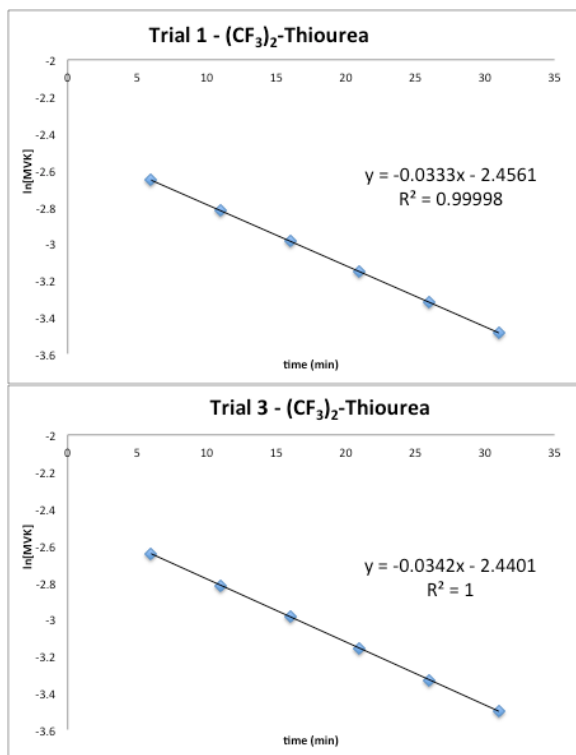
(CF$_3$)$_3$-thiourea **(3.14)** - 5 mol%

(CF₃)₄-thiourea **(3.15)** - 5 mol%

Trial 1 - (CF₃)₄-Thiourea

$y = -0.0514x - 2.4654$
$R^2 = 0.9998$

Trial 2 - (CF₃)₄-Thiourea

$y = -0.0533x - 2.4983$
$R^2 = 0.99986$

Trial 3 - (CF₃)₄-Thiourea

$y = -0.0526x - 2.4212$
$R^2 = 0.99983$

Sulfonamide **(3.16) -** 1 mol%

Trial 1 - Sulfonamide

$y = -0.0337x - 2.5094$
$R^2 = 0.99994$

Trial 2 - Sulfonamide

$y = -0.0336x - 2.5016$
$R^2 = 0.99997$

Trial 3 - Sulfonamide

$y = -0.0337x - 2.5512$
$R^2 = 0.99995$

(CF₃)₂-urea **(3.17)** - 5 mol%

Trial 1 - (CF₃)₂-Urea

y = -0.0450x - 2.3054
R² = 0.9999

ln[MVK]

time (min)

Trial 2 - (CF₃)₂-Urea

y = -0.0443x - 2.3651
R² = 0.99988

ln[MVK]

time (min)

Trial 3 - (CF₃)₂-Urea

y = -0.0440x - 2.3816
R² = 0.99996

ln[MVK]

time (min)

Guanidinium **(3.21)** – 2 mol%

Trial 1 - Guanidinium

y = -0.0512x - 2.4688
R² = 0.99956

ln[MVK]

time (min)

Trial 2 - Guanidinium

y = -0.0495x - 2.4703
R² = 0.99967

ln[MVK]

time (min)

Trial 3 - Guanidinium

y = -0.0521x - 2.4132
R² = 0.99985

ln[MVK]

time (min)

BisAmidinium **(3.23)** – 0.25 mol%

Trial 1 - BisAmidinium

$y = -0.0550x - 2.4419$
$R^2 = 0.9999$

Trial 2 - BisAmidinium

$y = -0.0673x - 2.2257$
$R^2 = 0.99676$

MonoAmidinium **(3.24)** – 5 mol%

Trial 1 - MonoAmidinium

$y = -0.1051x - 2.5607$
$R^2 = 0.99972$

Trial 2 - MonoAmidinium

$y = -0.094x - 2.4961$
$R^2 = 0.9999$

Trial 3 - MonoAmidinium

$y = -0.0789x - 2.4871$
$R^2 = 0.99993$

Azaindolium **(3.25)** – 0.25 mol%

Trial 1 - Azaindolium

$y = -0.0469x - 2.469$
$R^2 = 0.99958$

Trial 2 - Azaindolium

$y = -0.0409x - 2.3654$
$R^2 = 0.99972$

Trial 3 - Azaindolium

$y = -0.0396x - 2.3383$
$R^2 = 0.99992$

Thiophosphoramide **(3.27)** – 2 mol%

Trial 1 - Thiophosphoramide

$y = -0.0403x - 2.5759$
$R^2 = 0.99992$

Trial 2 - Thiophosphoramide

$y = -0.0407x - 2.5489$
$R^2 = 0.99995$

Trial 3 - Thiophosphoramide

$y = -0.0407x - 2.5225$
$R^2 = 0.99979$

BzOH **(3.29)** – 10 mol%

2-NO$_2$-BzOH **(3.31)** – 5 mol%

F₅-BzOH **(3.33)** – 1 mol%

Trial 1 - F₅-BzOH

$y = -0.034x - 2.4098$
$R^2 = 0.99996$

Trial 2 - F₅-BzOH

$y = -0.0372x - 2.403$
$R^2 = 0.99997$

Trial 3 - F₅-BzOH

$y = -0.0367x - 2.3845$
$R^2 = 0.99997$

(R)-BINOL **(3.36)** – 20 mol%

Trial 1 - *(R)*-BINOL

$y = -0.0352x - 2.3756$
$R^2 = 0.99997$

Trial 2 - *(R)*-BINOL

$y = -0.0337x - 2.4453$
$R^2 = 0.99933$

Trial 3 - *(R)*-BINOL

$y = -0.0354x - 2.1386$
$R^2 = 0.99995$
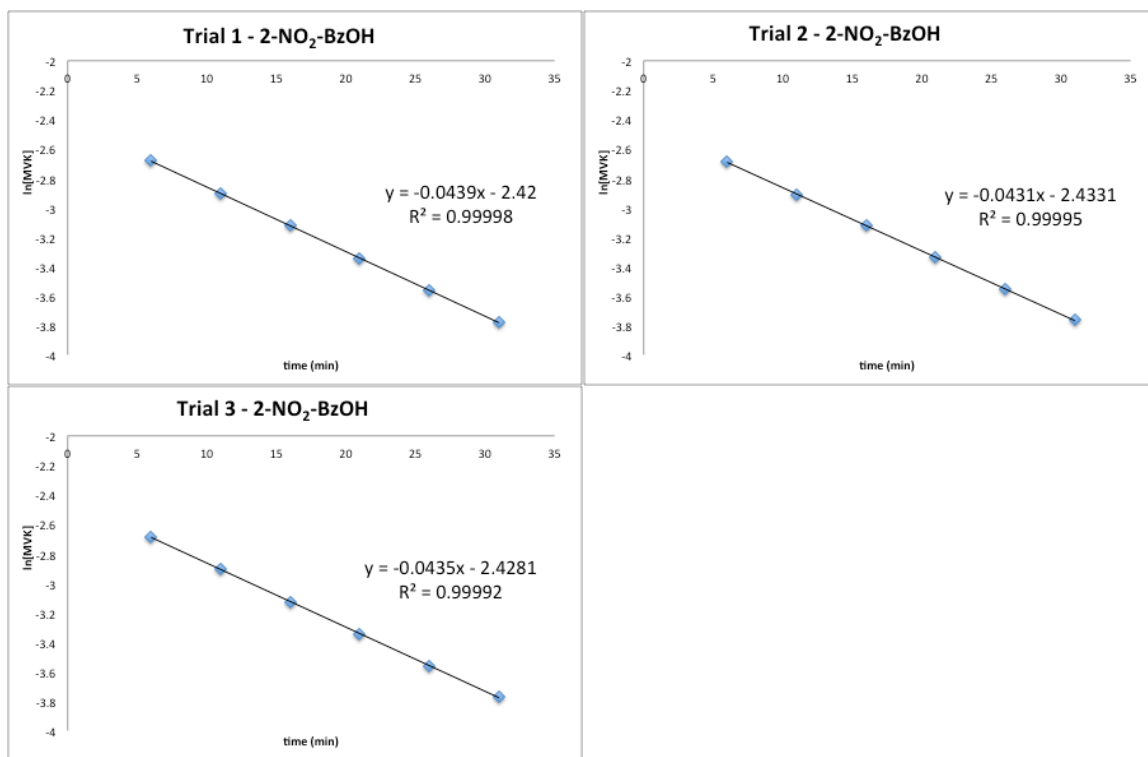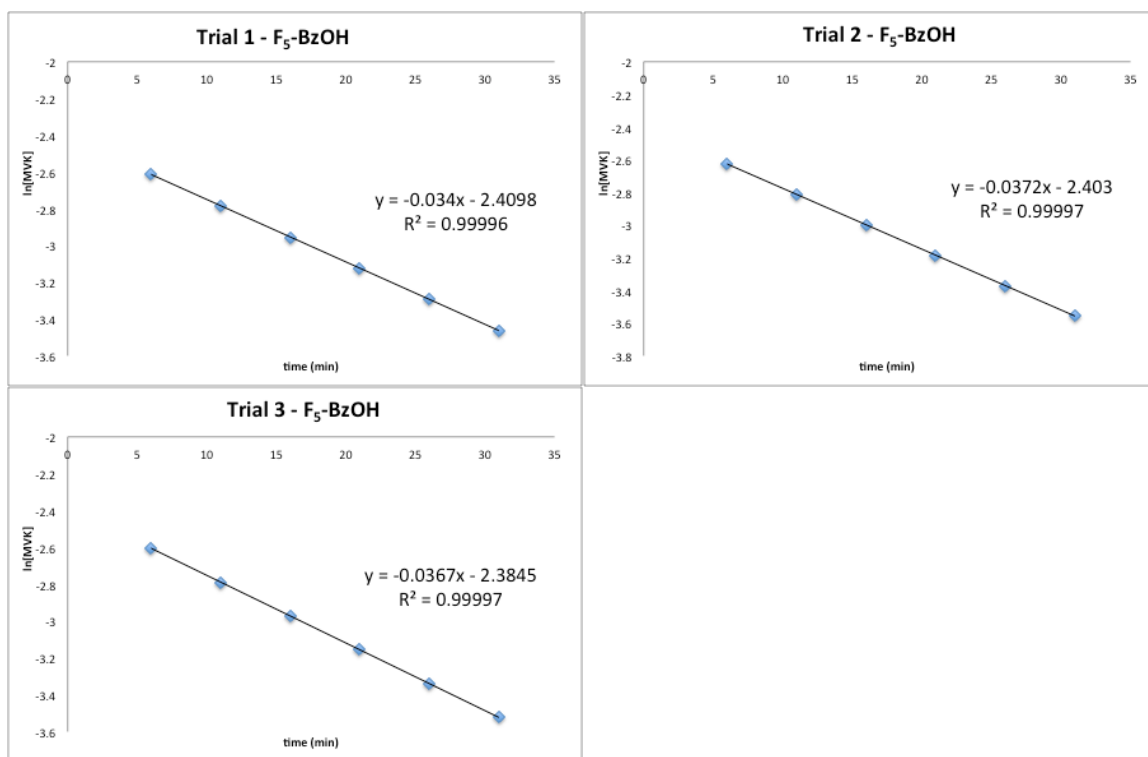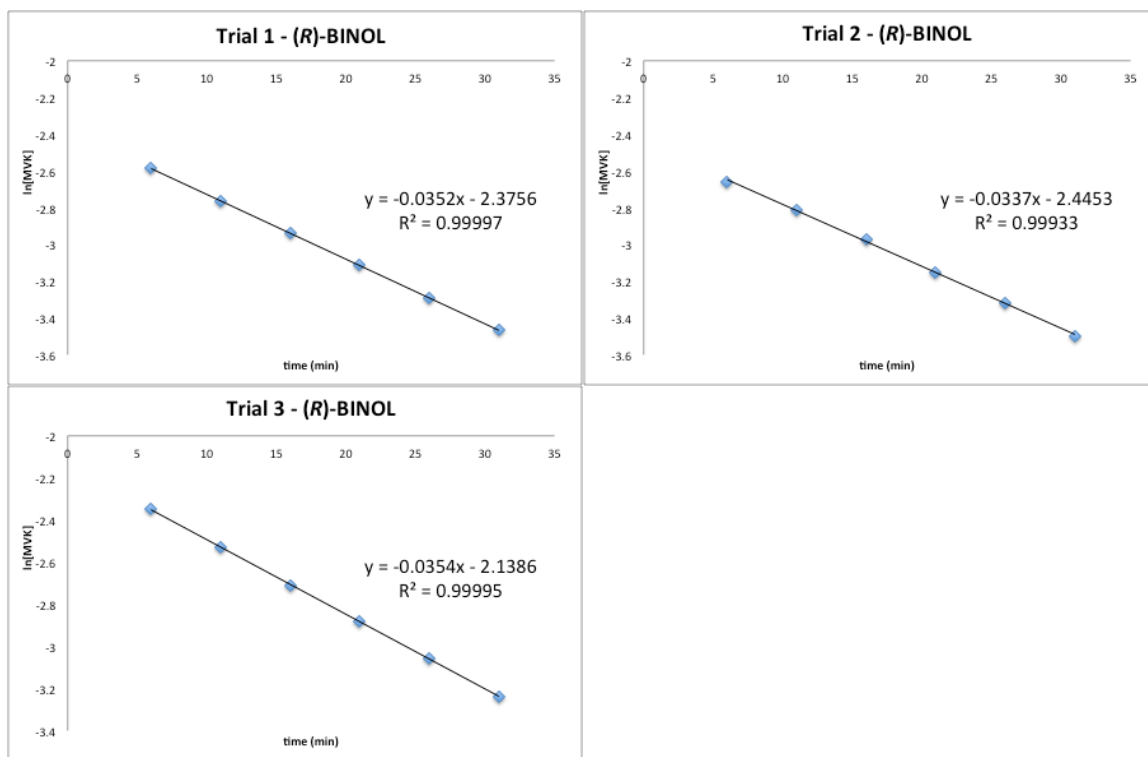
4-Br-Phenol **(3.38)** – 20 mol%
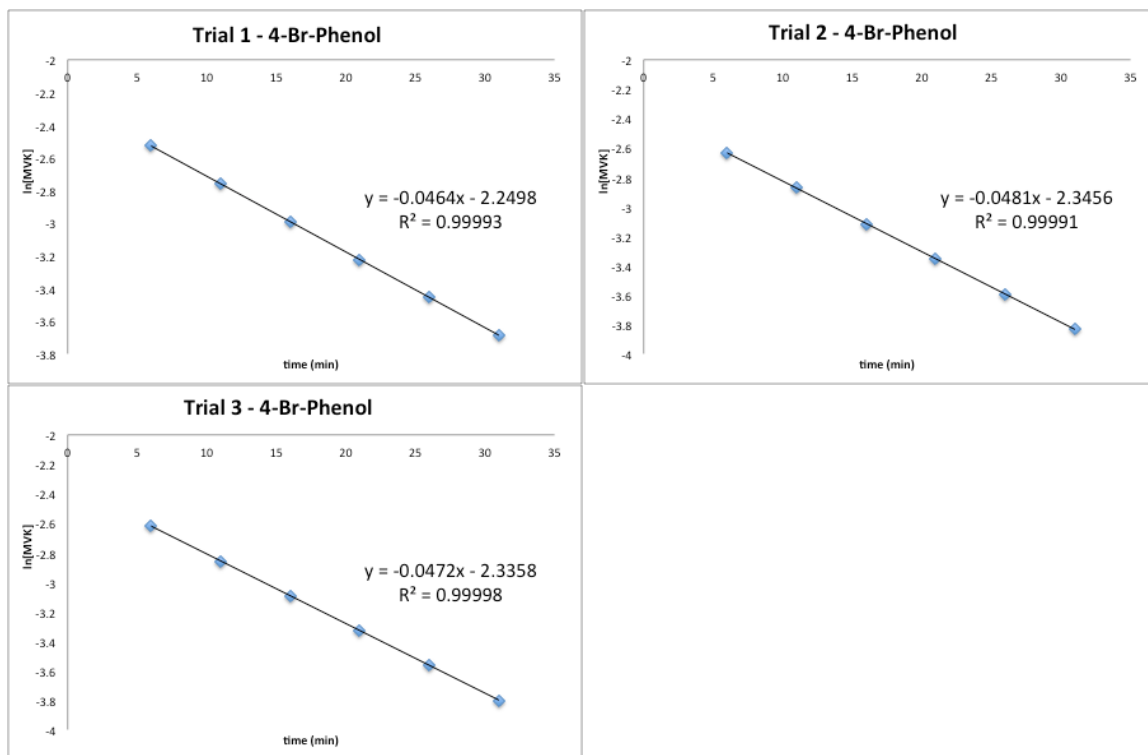
4-NO₂-Phenol **(3.39)** – 10 mol%
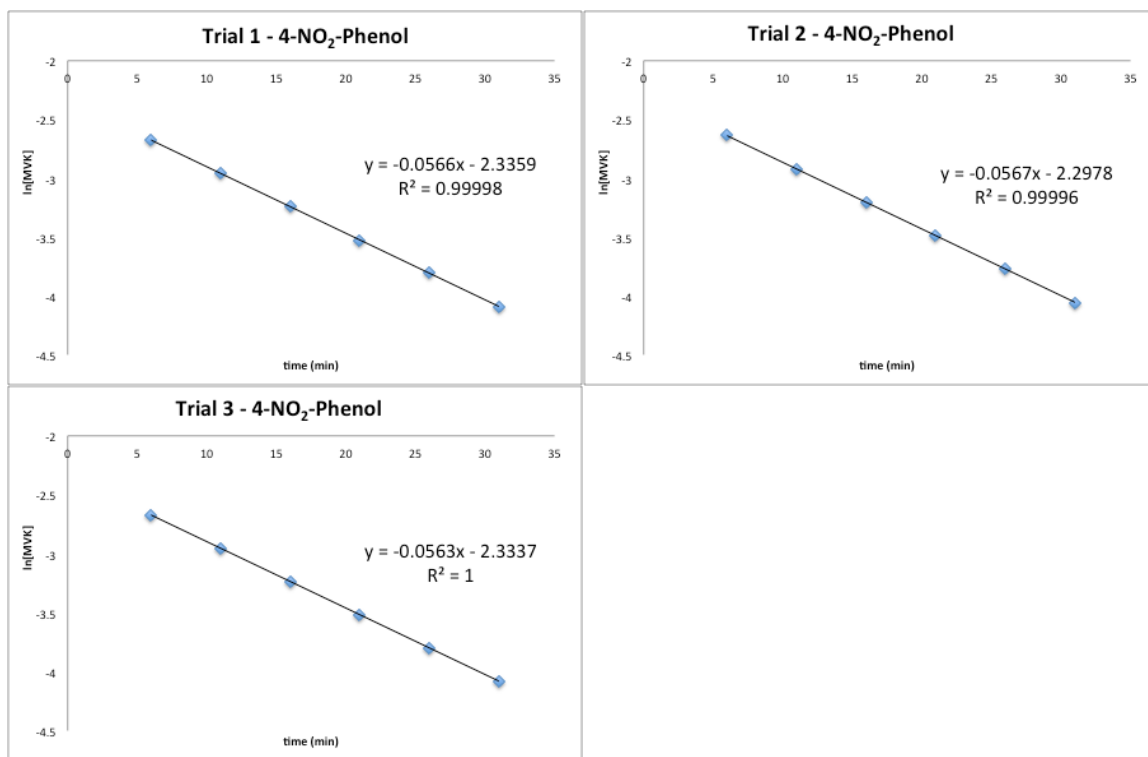
(R,R)-TADDOL **(3.41)** -20 mol%
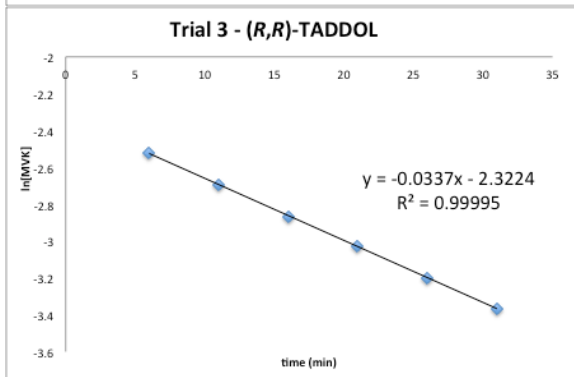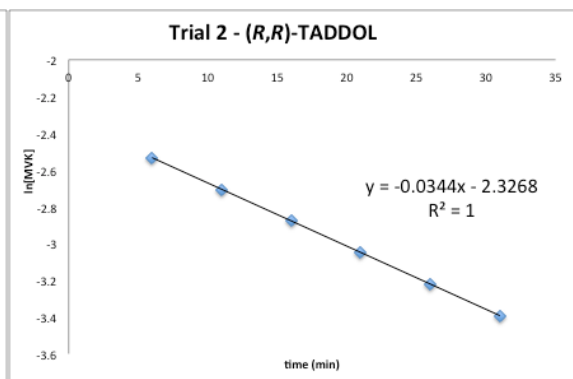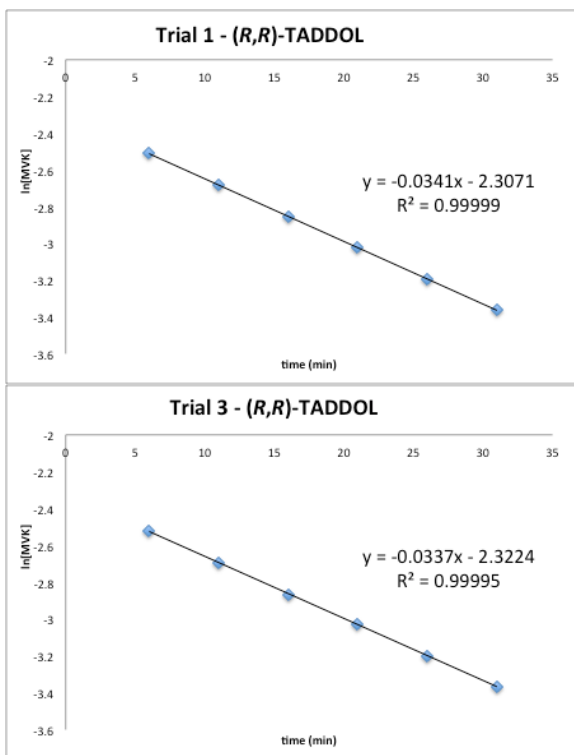
Diphenylphosphate **(4.01)** – 1 mol%
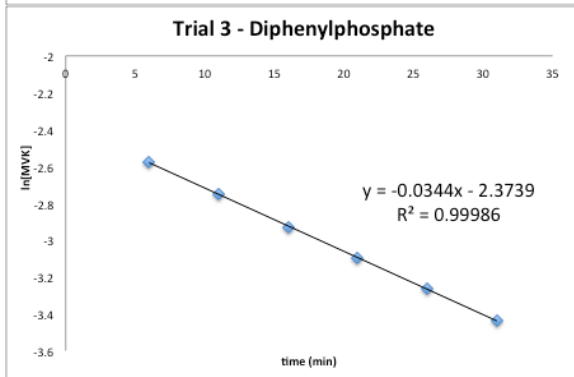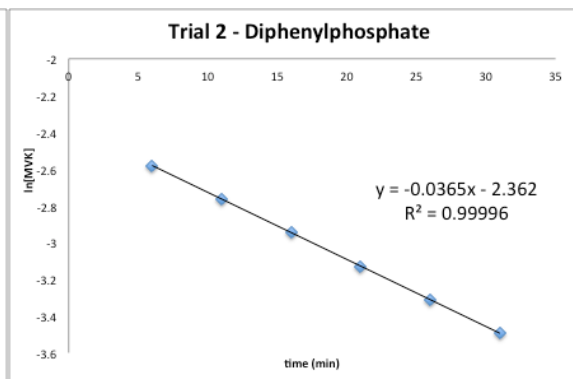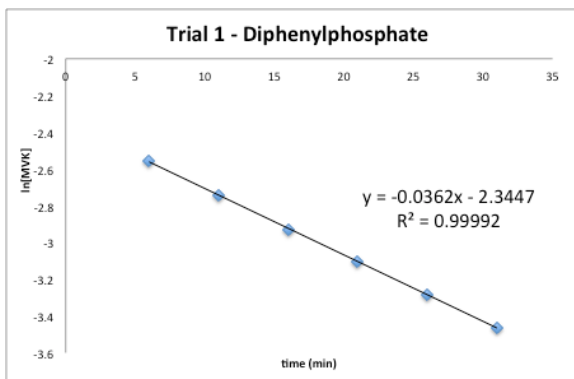
PPTS **(4.02)** – 5 mol%
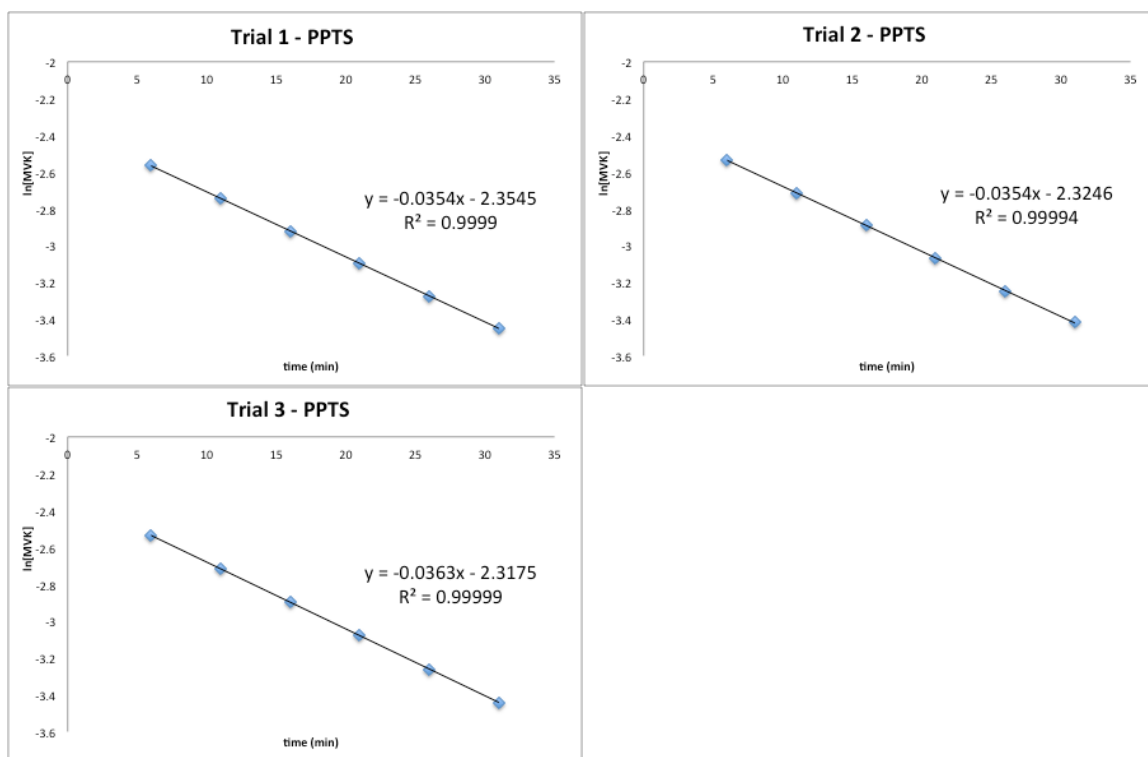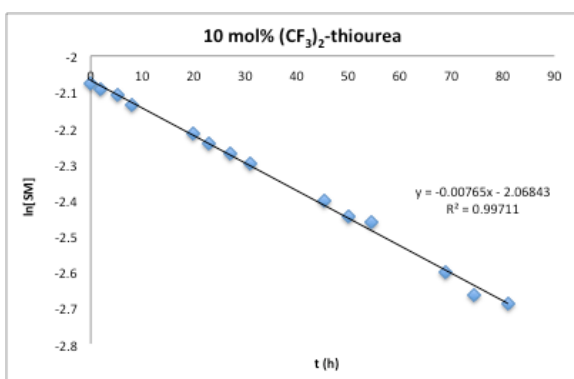

(+) –(CSA) **(4.03)** – 1 mol%
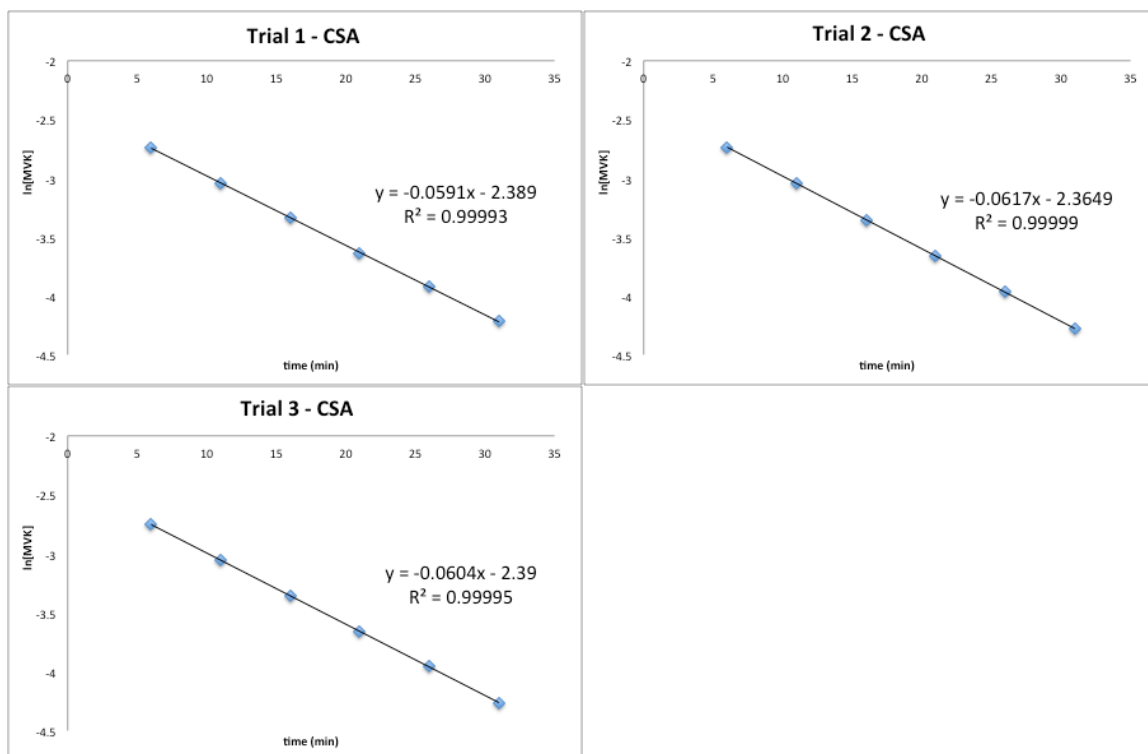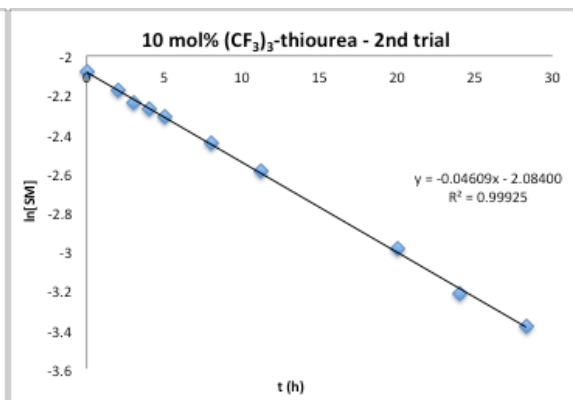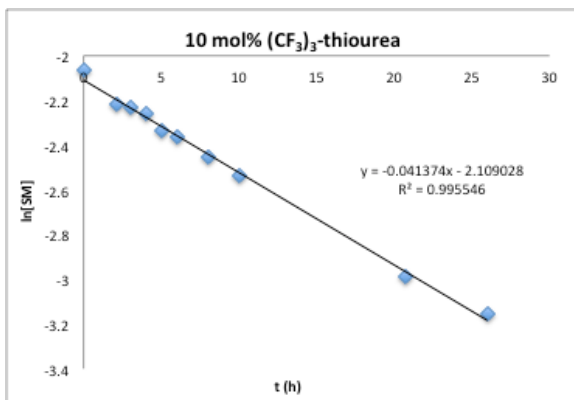
Background
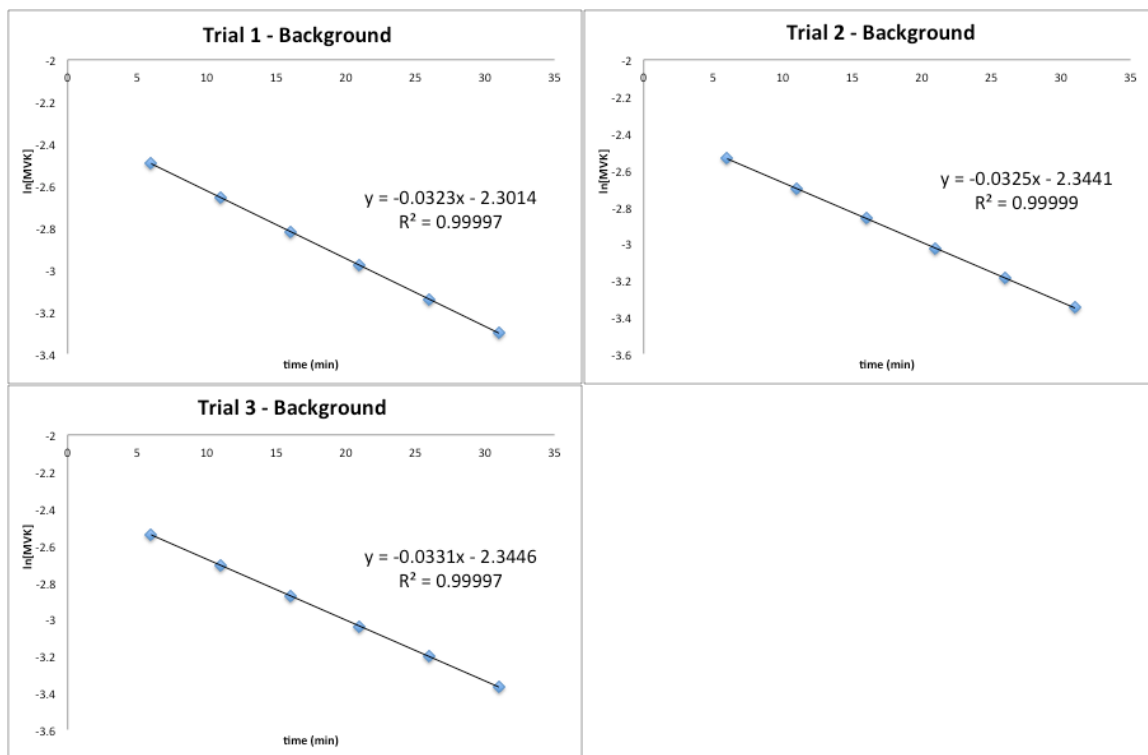
Friedel Crafts Kinetic Plots for All Catalysts

Diphenylthiourea **(3.12)** - 10 mol%
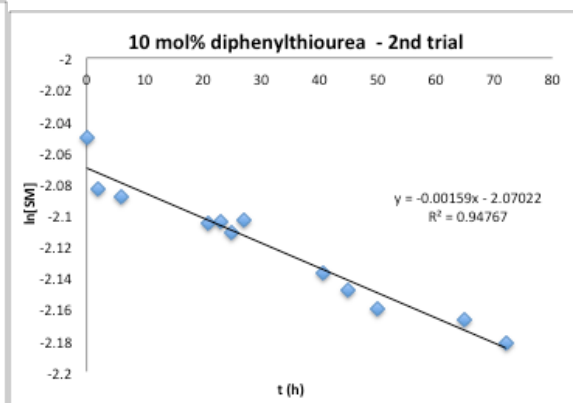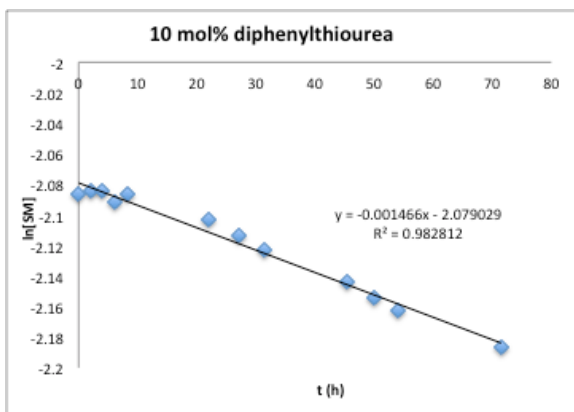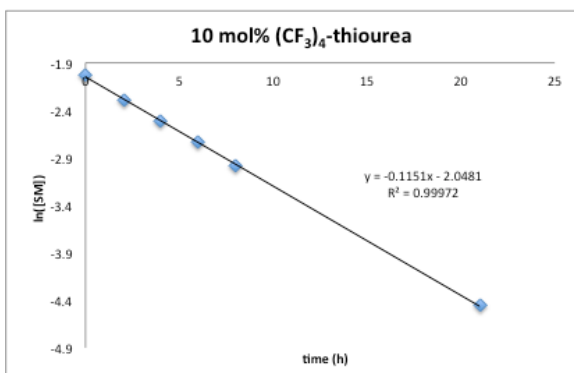

(CF₃)₂-thiourea **(3.13)** - 10 mol%
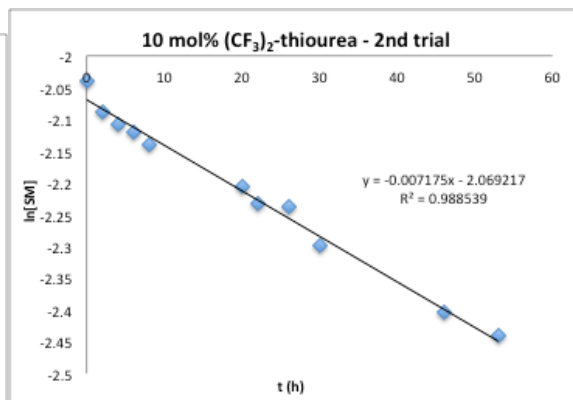
(CF₃)₃-thiourea **(3.14)** - 10 mol%

(CF$_3$)$_4$-thiourea **(3.15)** - 10 mol%(1st trial), 5 mol% (2nd trial)
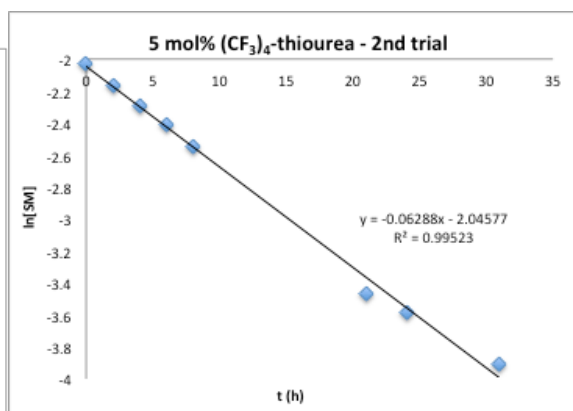
Sulfonamide **(3.16)** - 5 mol%
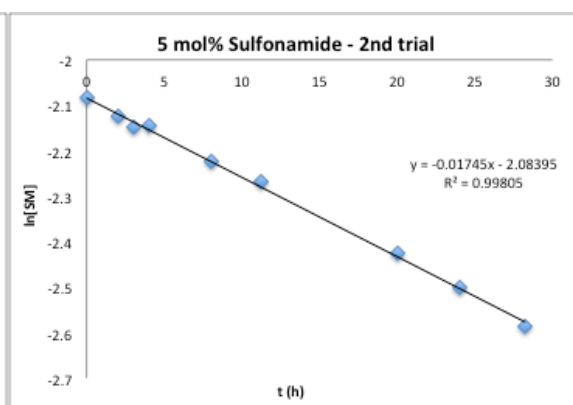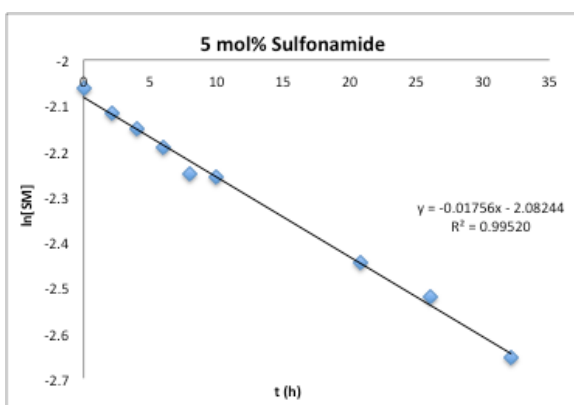
(CF$_3$)$_2$-urea **(3.17)** - 5 mol%
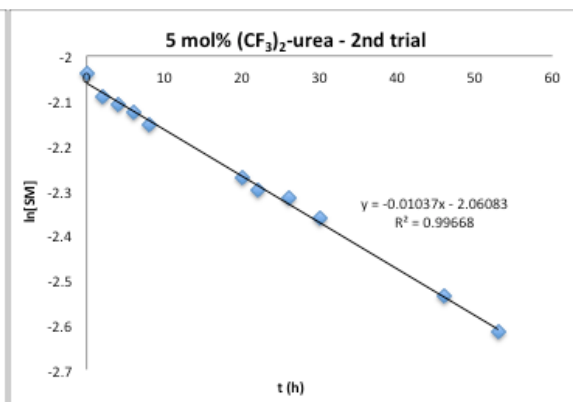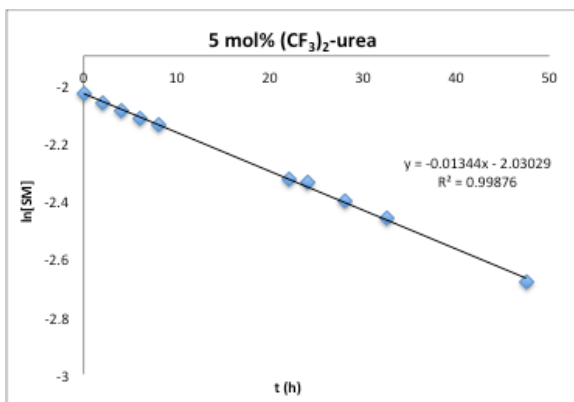
(CF₃)₃-urea **(3.18)** - 5 mol%
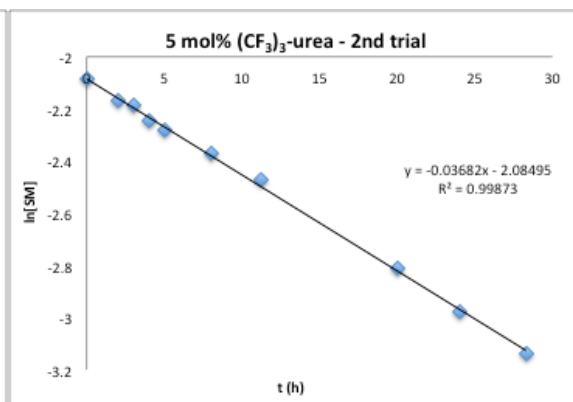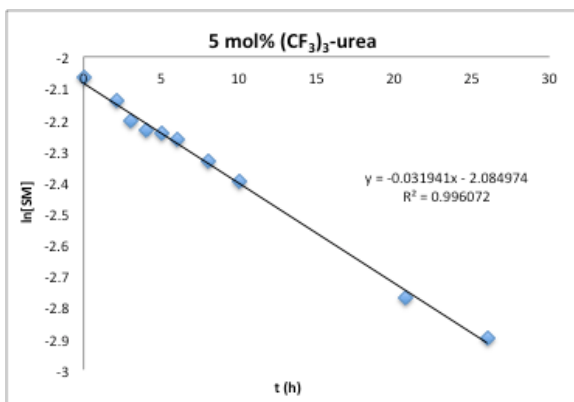
(CF₃)₄-urea **(3.19)** - 5 mol%
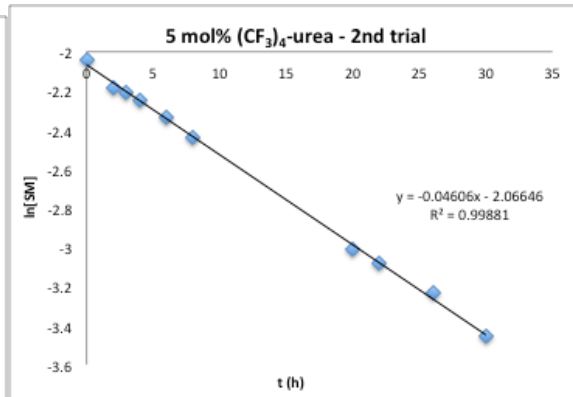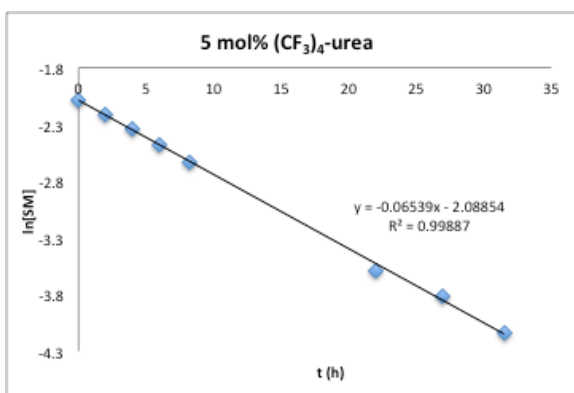
BF₂-urea **(3.20)** – 1 mol%
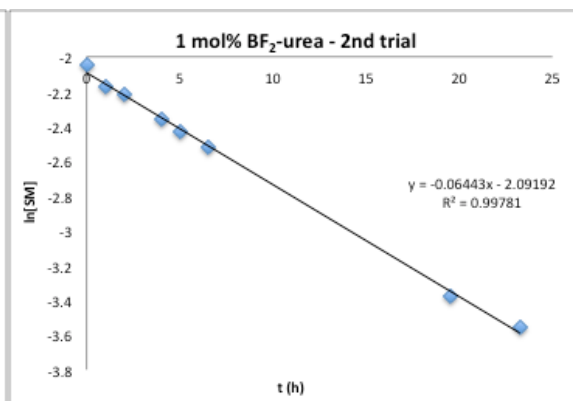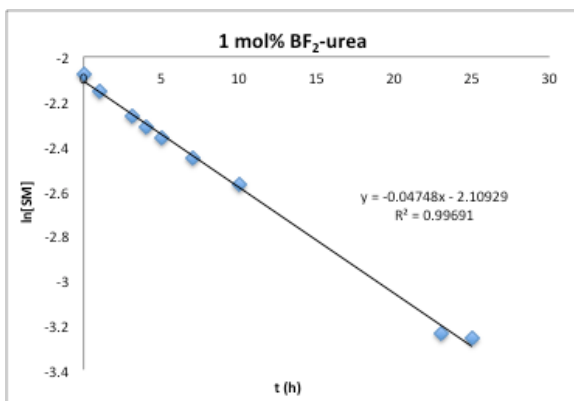
Guanidinium **(3.21)** – 0.5 mol%
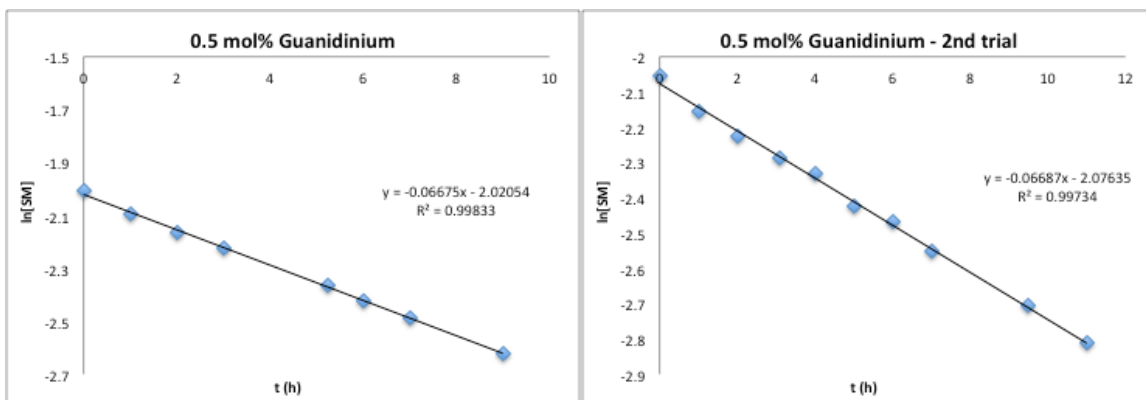
Squaramide **(3.22)** – 5 mol%* (heterogeneous reaction)
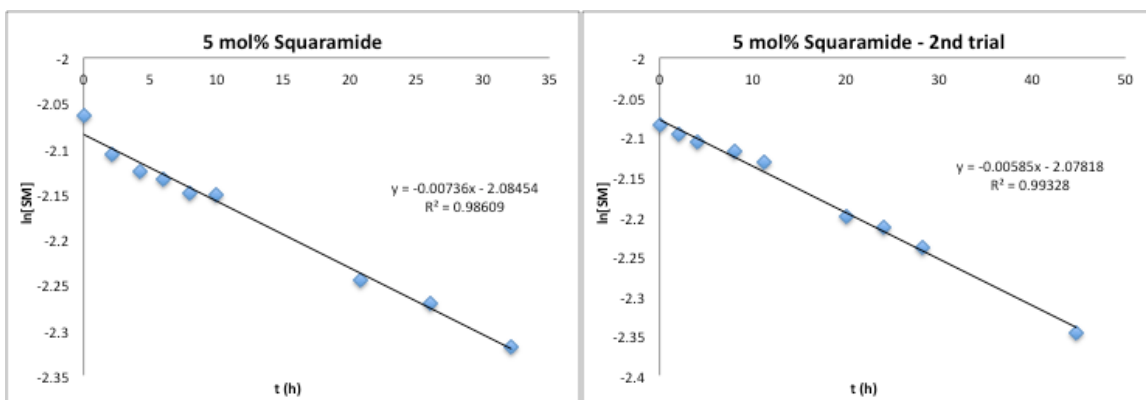
BisAmidinium **(3.23)** – 0.2 mol%
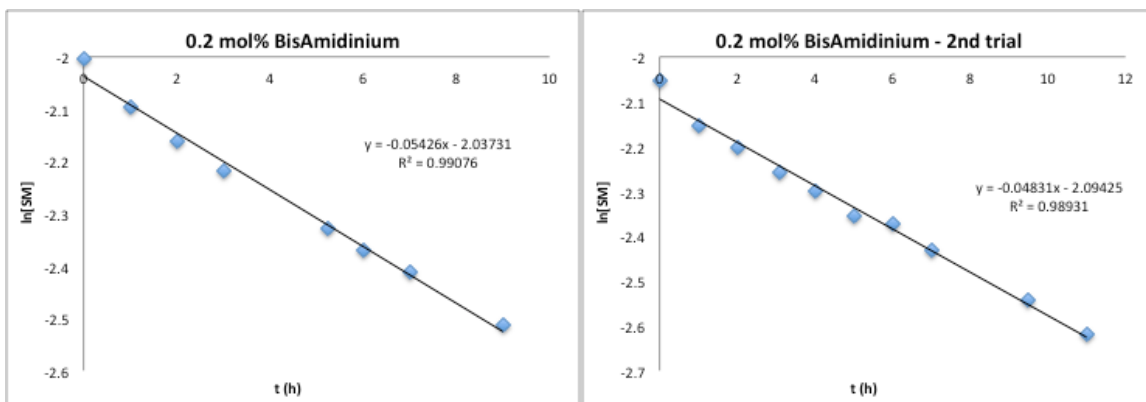
MonoAmidinium **(3.24)** – 0.5 mol%
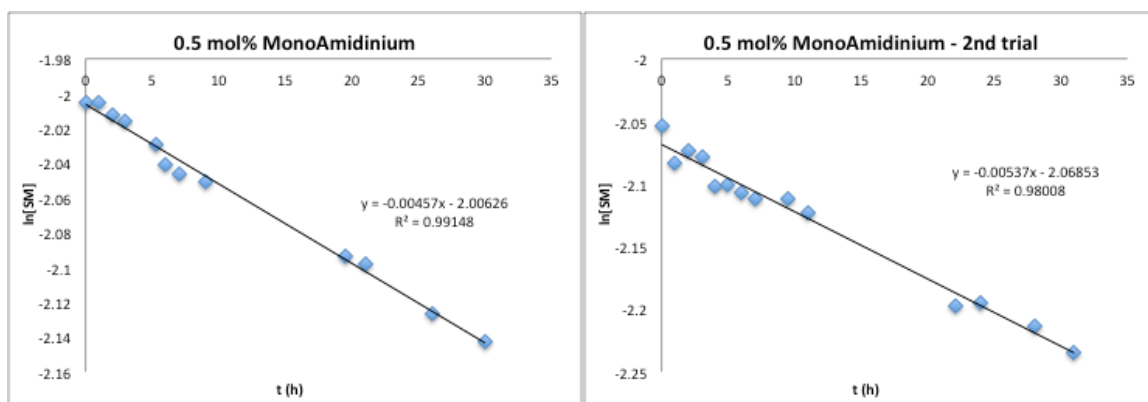
Azaindolium **(3.25)** – 0.69 mol%
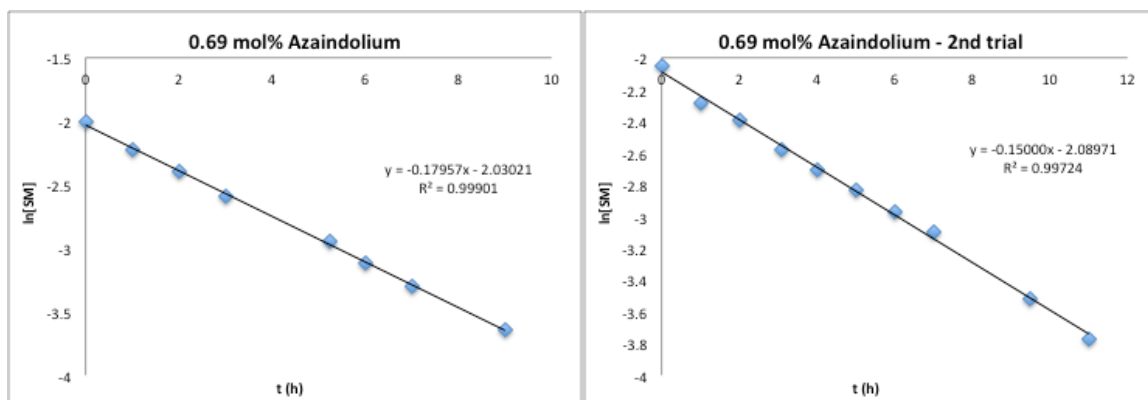
Benzotriazole **(3.26)** – 10 mol%
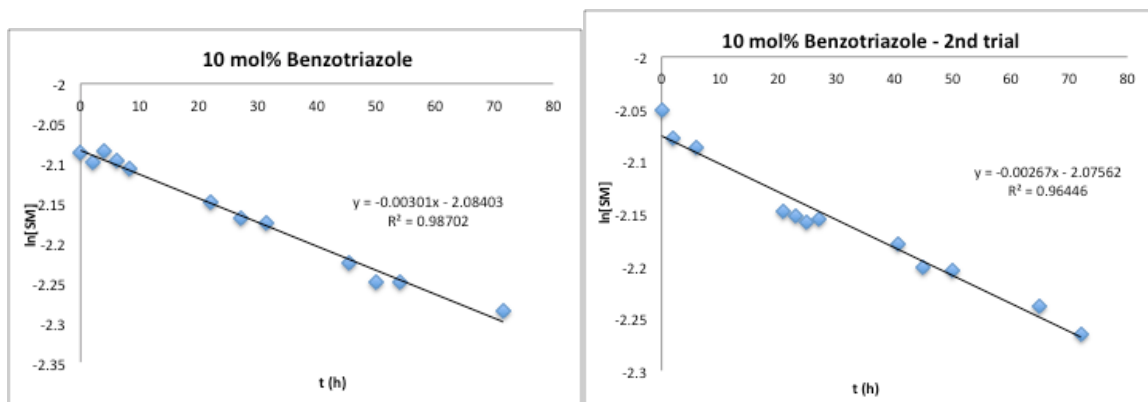
Thiophosphoramide **(3.27)** – 5 mol%
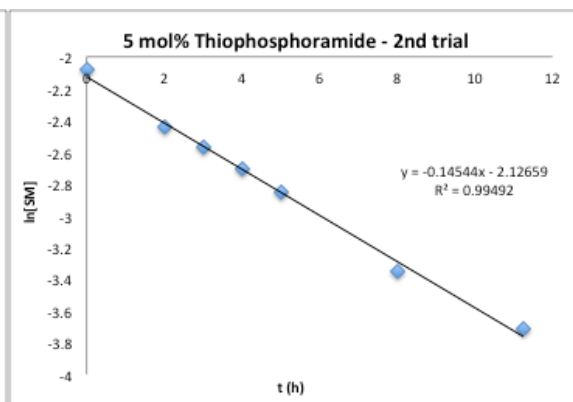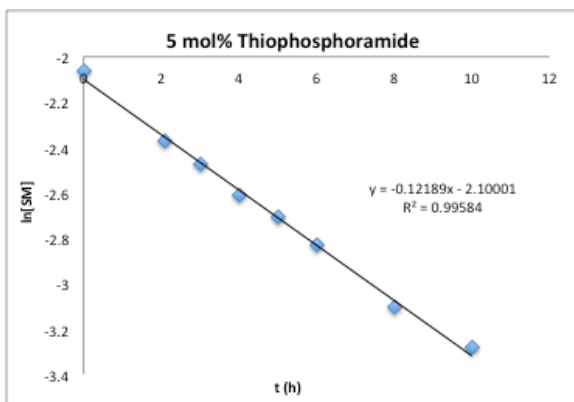
2-Me-BzOH **(3.28)** – 10 mol%
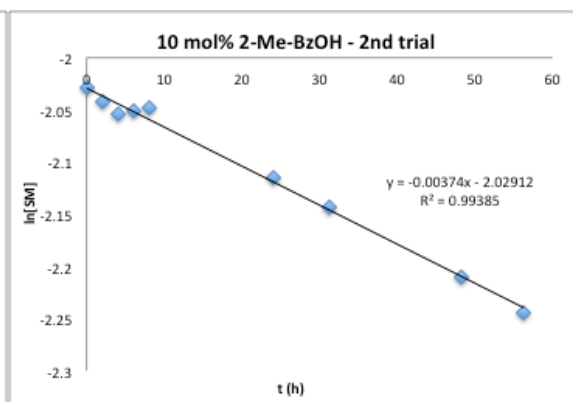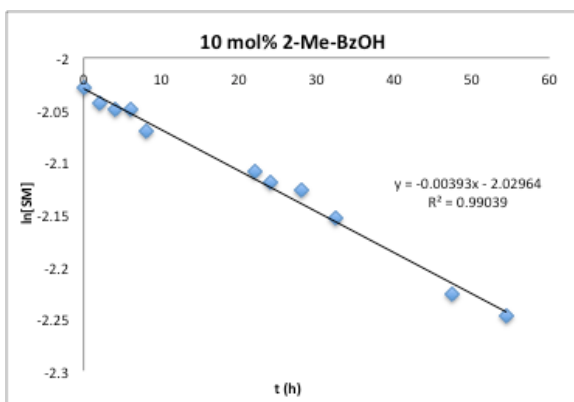
BzOH **(3.29)** – 10 mol%
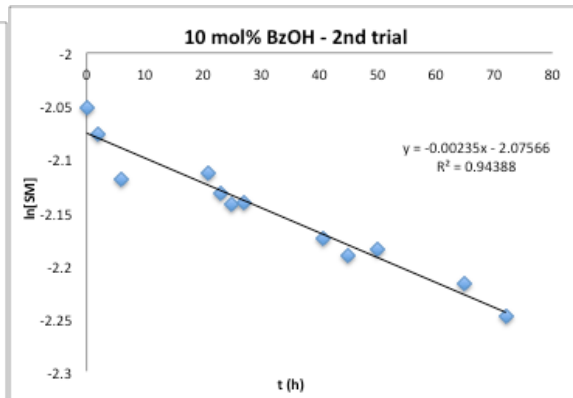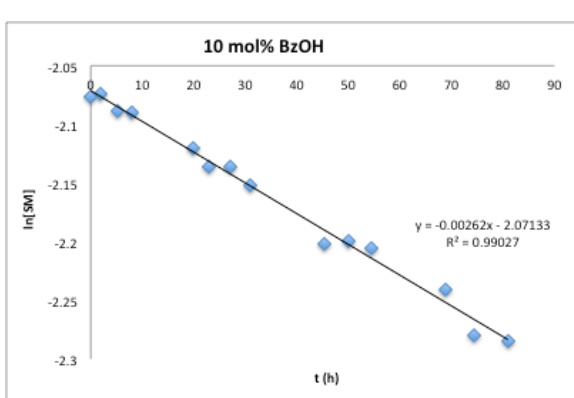
2-Cl-BzOH **(3.30)** – 10 mol%
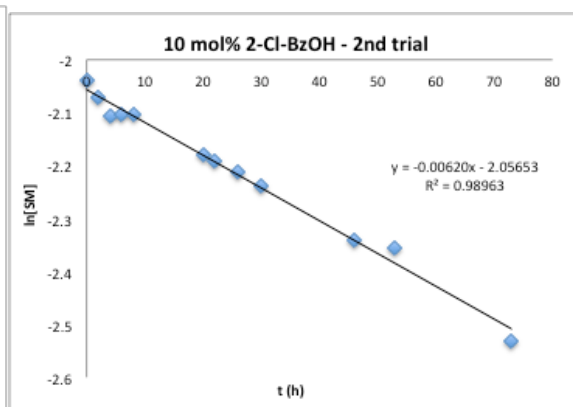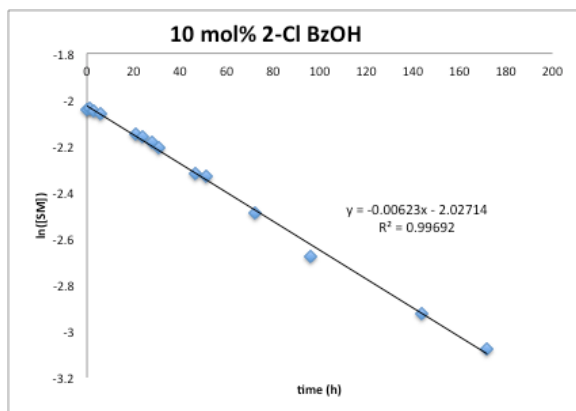
2-NO₂-BzOH **(3.31)** – 10 mol%
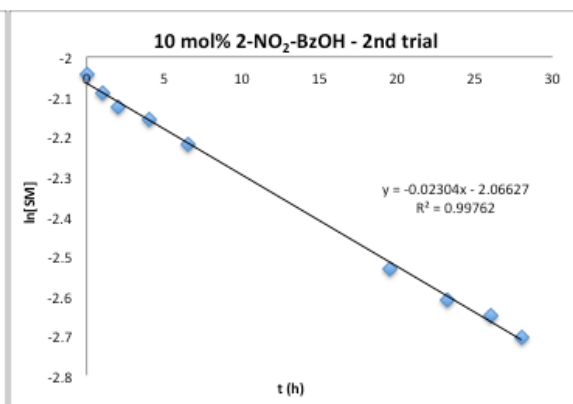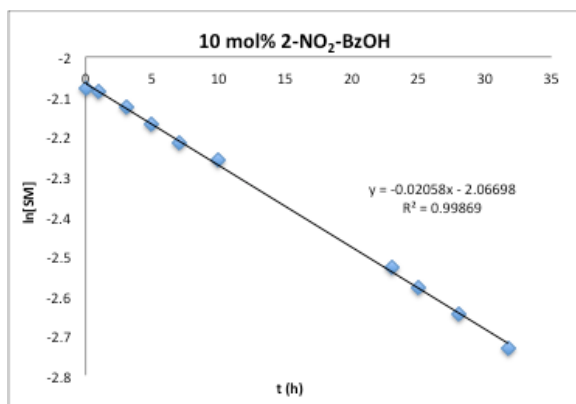
F₅-BzOH **(3.33)** – 10 mol%
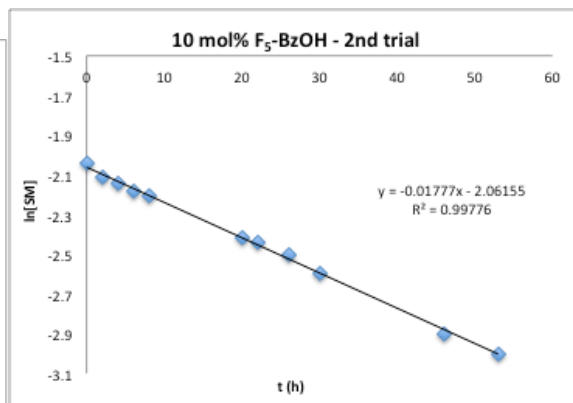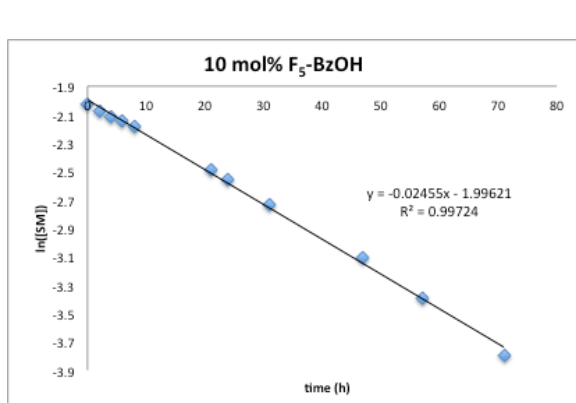
(R)-BINOL **(3.36)** – 10 mol%
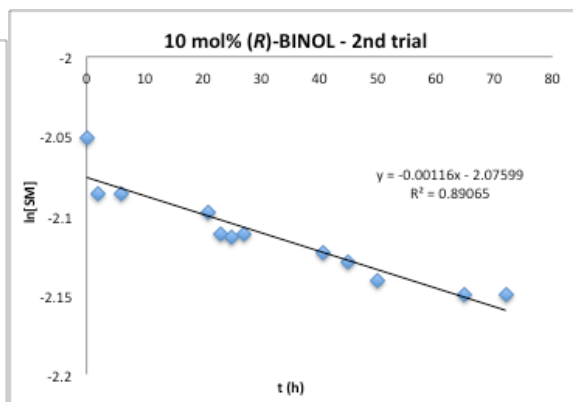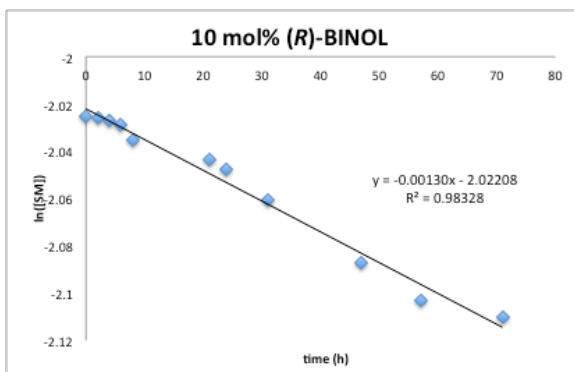
4-t-Bu-Phenol **(3.37)** – 10 mol%
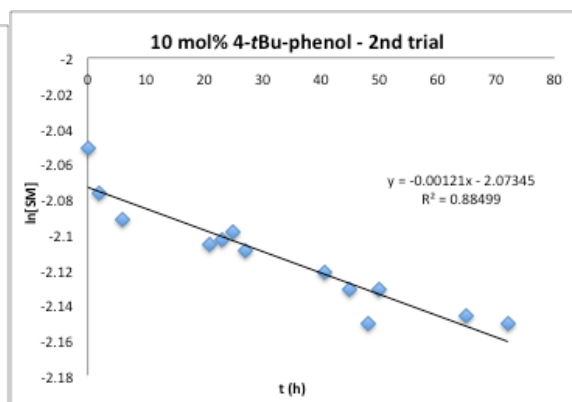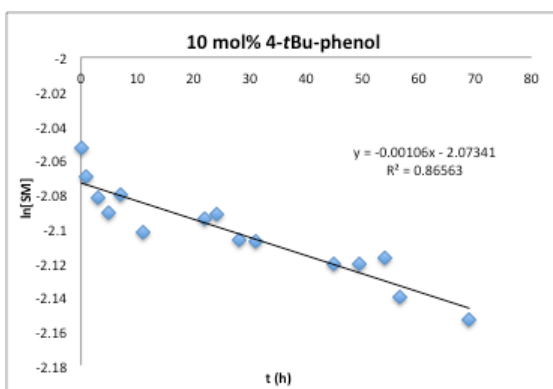
4-Br-Phenol **(3.38)** – 10 mol%
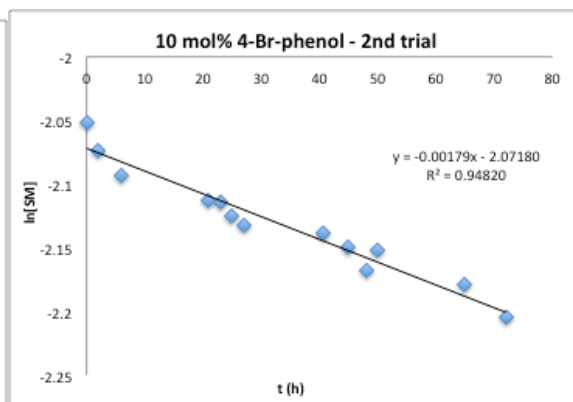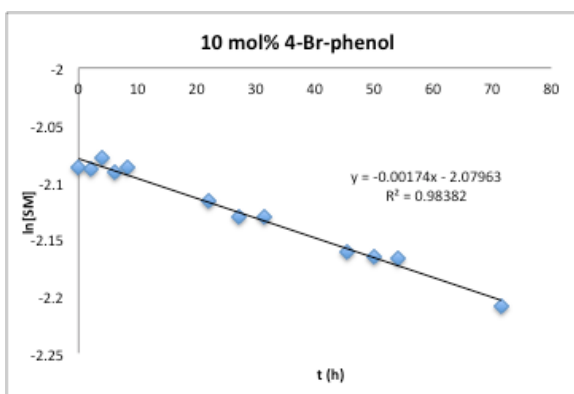
4-NO₂-Phenol **(3.39)** – 10 mol%
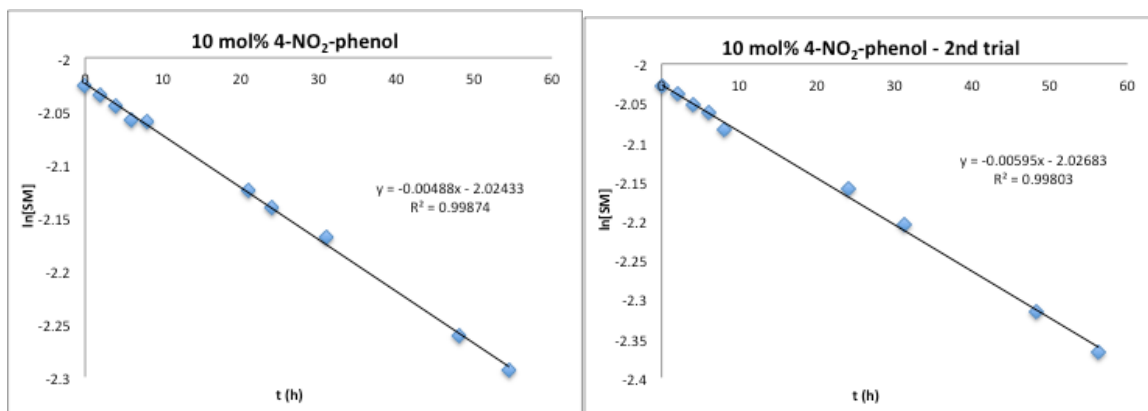
F₅-Phenol **(3.40)** – 10 mol%
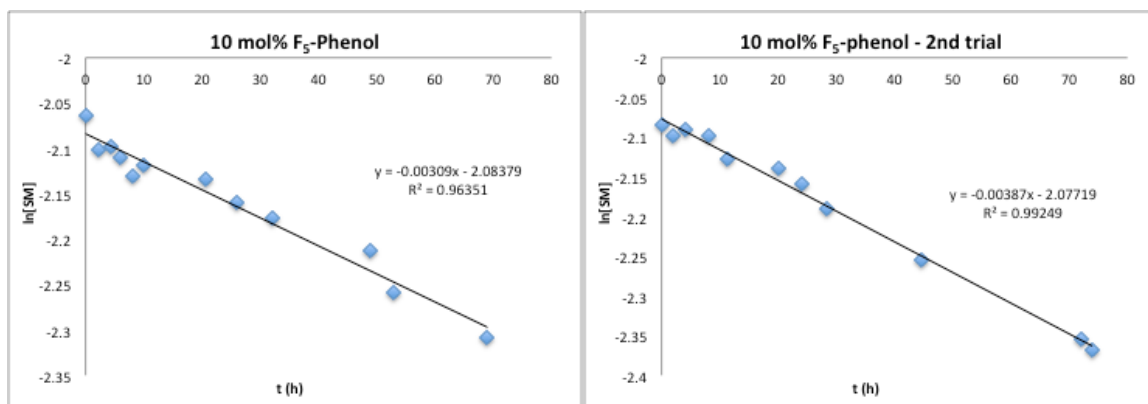
(R,R)-TADDOL **(3.41)** -10 mol%
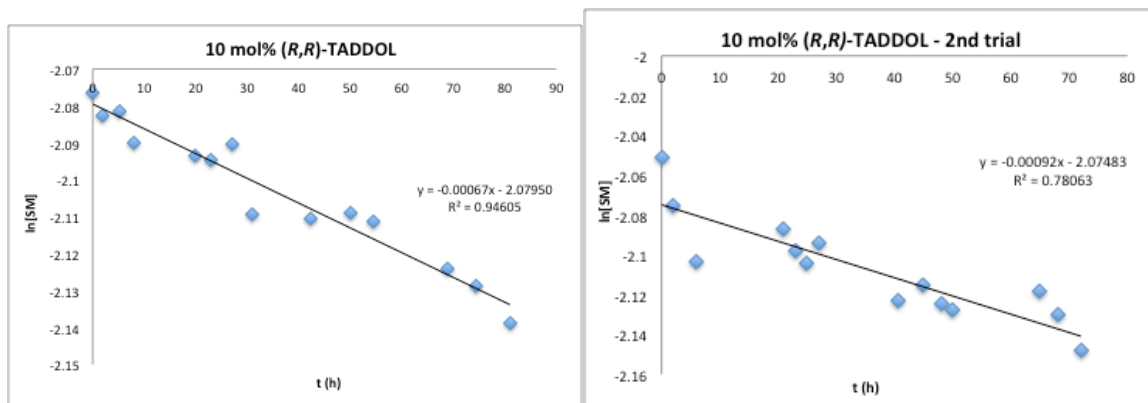
The average k'obs indicates no rate enhancement, or even slight inhibition, within error.

Silanediol **(3.43)** – 5 mol% (1st trial), 10 mol% (2nd trial)
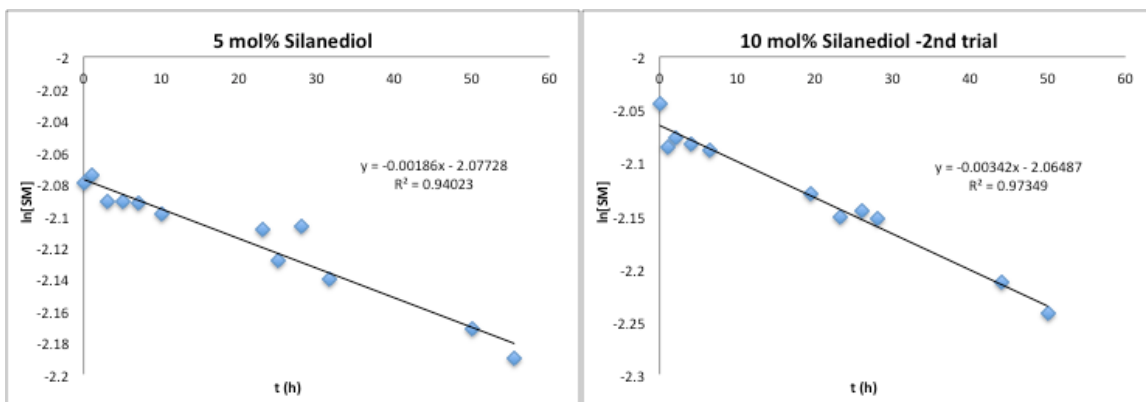
Diphenylphosphate **(4.01)** – 5 mol%

PPTS **(4.02)** – 1 mol%

345
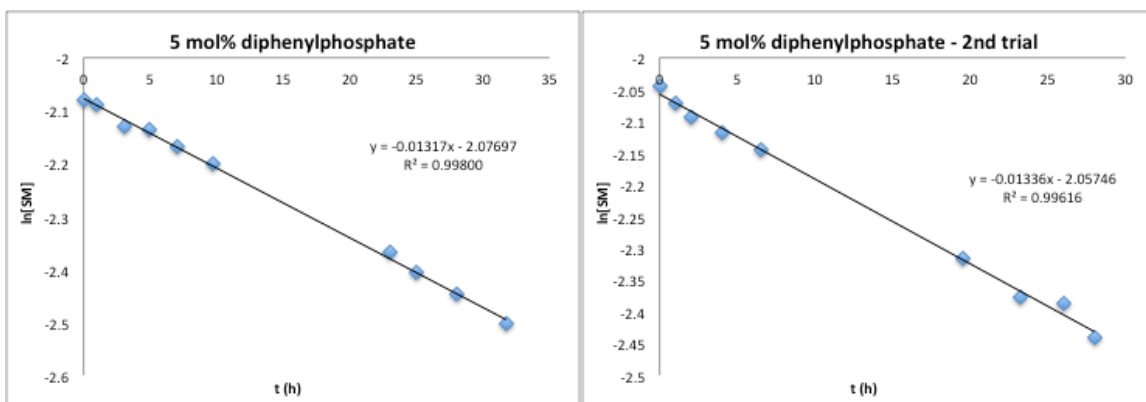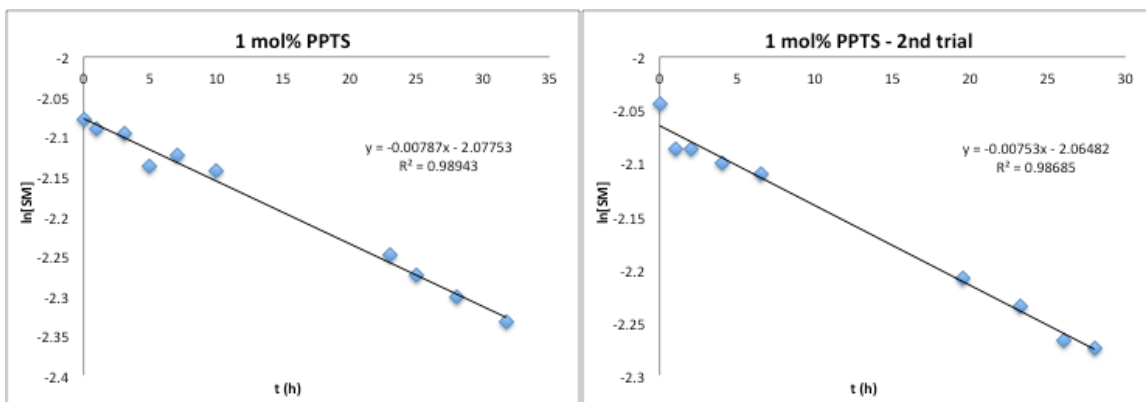
(+) –(CSA) **(4.03)** – 1 mol%
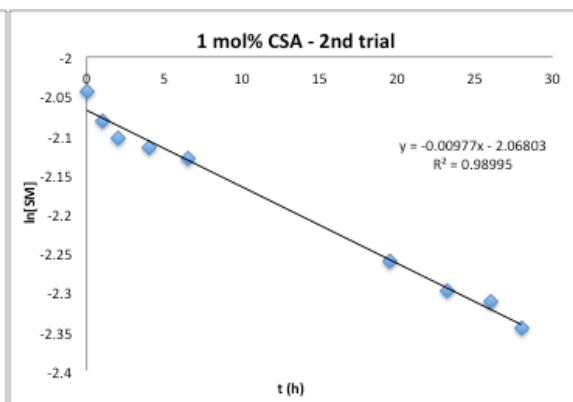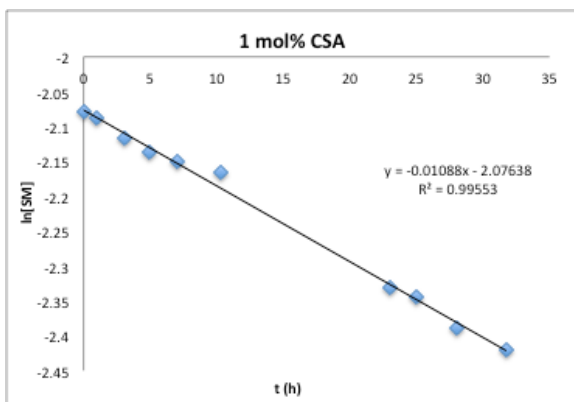
Background
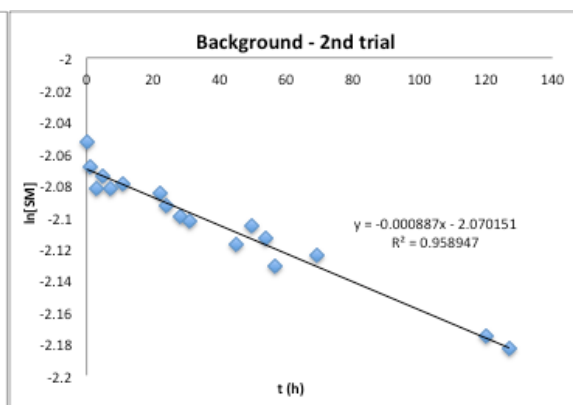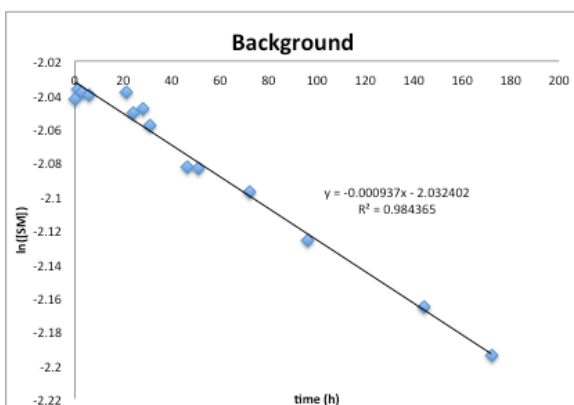
Friedel Crafts Reaction - Rate Order Studies

The Friedel Crafts reaction was studied under standard conditions employing [**3.45**] = 1.33 M, catalyst [**3.15**] = 2.66 x 10^{-3}M and varying starting material [**3.46**] (from 0.0444 M to 0.267 M). Initial rates were determined, and the resulting ln(initial rate) vs ln(initial [**3.46**]) displayed first order dependency in substrate.
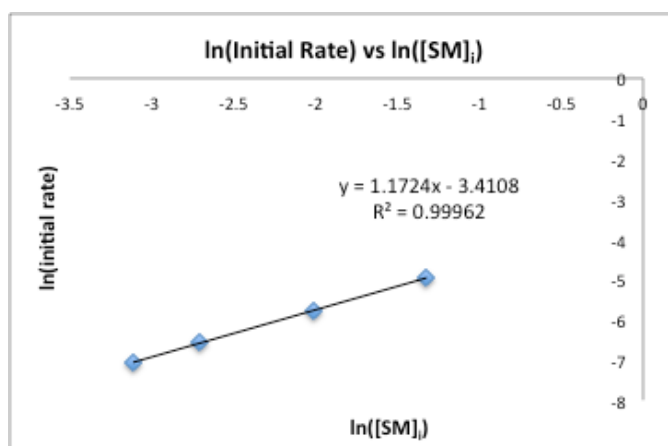
The Friedel Crafts reaction was studied under standard conditions employing [**3.45**] = 1.33 M, catalyst [**3.46**] = 0.133 M and varying catalyst [**3.15**] (2 mol%, 5 mol%, 10 mol%). Initial rates were determined, and the resulting ln(initial rate) vs ln[**3.15**] displayed first order dependency in catalyst.
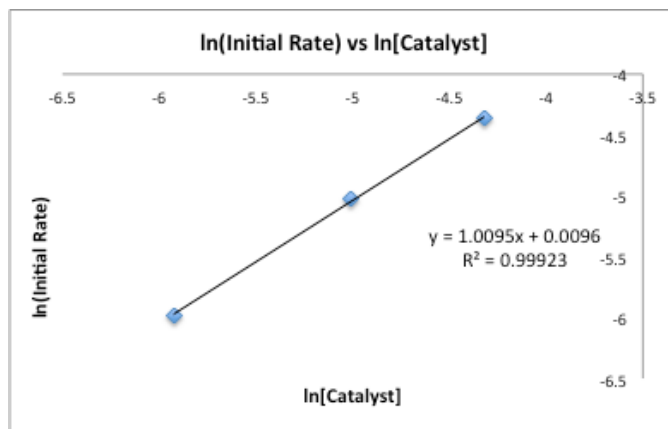
BIBLIOGRAPHY

Akiyama, T. "Stronger Brønsted Acids" *Chem. Rev.* **2007**, *107*, 5744-5758.

Akiyama, T.; Itoh, J.; Fuchibe, K. "Recent Progress in Chiral Brønsted Acid Catalysis" *Adv. Synth. Catal.* **2006**, *348*, 999-1010.

Akiyama, T.; Morita, H.; Itoh, J.; Fuchibe, K. "Chiral Brønstend Acid Catalyzed Enantioselective Hydrophosphonylation of Imines: Asymmetric Synthesis of *α*-Amino Phosphonates" *Org. Lett.* **2005**, *7*, 2583-2585.

Aleman, J.; Parra, A.; Jiang, H.; Jørgensen, K. A. "Squaramides: Bridging from Molecular Recognition to Bifunctional Organocatalysis" *Chem. Eur. J.* **2011**, *17*, 6890-6899.

Anderson, J. C.; Howell, G. P.; Lawrence, R. M.; Wilson, C. S. "An Asymmetric Nitro-Mannich Reaction Applicable to Alkyl, Aryl, and Heterocyclic Imines" *J. Org. Chem.* **2005**, *70*, 5665-5670.

Ando, K.; Shimazu, Y.; Seki, N.; Yamataka, H. "Kinetic Study of Proton-Transfer Reactions of Phenylnitromethanes. Implication for the Origin of Nitroalkane Anomaly" *J. Org. Chem.* **2011**, *76*, 3937-3945.

Annamalai, V. R.; Linton, E. C.; Kozlowski, M. C. "Design of a Bisamidinium Claisen Rearrangement Catalyst for Monodentate Substrates" *Org. Lett.* **2009**, *11*, 621-624.

Annamalai, V.; DiMauro, E. F.; Carroll, P. J.; Kozlowski, M. C. "Catalysis of the Michael Addition Reaction by Late Transition Metal Complexes of BINOL-Derived Salens" *J. Org. Chem.* **2003**, *68*, 1973-1981.

Asaro, M. F.; Nakayama, I.; Wilson, Jr., R. B. "Formation of Sterically Hindered Primary Vicinal Diamines from Vicinal and Geminal Dinitro Compounds" *J. Org. Chem.* **1992**, *57*, 778-782.

Auvil, T. J.; Schafer, A. G.; Mattson, A. E. "Design Strategies for Enhanced Hydrogen-Bond Donor Catalysts" *Eur. J. Org. Chem.* **2014**, 2633-2646

Baillargeon, V. P.; Stille, J. K. "Palladium-Catalyzed Formylation of Organic Halides with Carbon Monoxide and Tin Hydride" *J. Am. Chem. Soc.* **1986**, *108*, 452-461.

Ballini, R.; Bosica, G.; Fiorini, D.; Palmieri, A.; Petrini, M. "Conjugate Additions of Nitroalkanes to Electron-Poor Alkenes: Recent Results" *Chem. Rev.* **2005**, *105*, 933-971.

Ballini, R.; Palmieri, A.; Righi, P. "Highly efficient one- or two-step sequences for the synthesis of fine chemicals from versatile nitroalkanes" *Tetrahedron* **2007**, *63*, 12099–12121.

Ballini, R.; Petrini, M. "Recent synthetic developments in the nitro to carbonyl conversion (Nef reaction)" *Tetrahedron* **2004**, *60*, 1017-1047.

Barlin, G. B.; Brown, D. J.; Kadunc, Z.; Petric, A.; Stanovnik, B.; Tiler, M. "Imidazo[1,2-*b*]pyridines and an Imidazo[1,2-*a*]pyrazine from Pyridazin- and Pyrazin-amines" *Aust. J. Chem.* **1983**, *36*, 1215-1220.

Barr, L.; Easton, C. J.; Lee, K.; Lincoln, S. F. "Aminocyclodextrins to facilitate the deprotonation of 4-*tert*-butyl-α-nitrotoluene" *Org. Biomol. Chem.* **2005**, *3*, 2990-2993.

Barton, D. H. R.; Motherwell, W. B.; Zard, S. Z. "A simple and economic synthesis of the corticosteroid side chain from 17-oxo-steroids" *Bull. Soc. Chim. Fr.* **1983**, 61-65.

Bartra, M.; Romea, P.; Urpi, F.; Vilarrasa, J. "A Fast Procedure for the Reduction of Azides and Nitro Compounds Based on the Reducing Ability of Sn(SR)$_3^-$ Species" *Tetrahedron* **1990**, *46*, 587-594.

Base, S.; Vanajatha, G. "A Versatile Method for the Conversion of Oximes to Nitroalkanes" *Synth. Commun.* **1998**, *28*, 4531-4535.

Beletskaya, I. P.; Cheprakov, A. V. "The Heck Reaction as a Sharpening Stone of Palladium Catalysis" *Chem. Rev.* **2000**, *100*, 3009-3066.

Beletskiy, E. V.; Schmidt, J.; Wang, X.-B.; Kass, S. R. "Three Hydrogen Bond Donor Catalysts: Oxyanion Hole Mimics and Transition State Analogues" *J. Am. Chem. Soc.* **2012**, *134*, 18534-18537.

Black, A. P.; Babers, F. H. "Phenylnitromethane" *Org. Synth.* **1939**, *19*, 73-76.

Borovika, A.; Tang, P.-I.; Klapman, S.; Nagorny, P. "Thiophosphoramide-Based Cooperative Catalysts for Bønsted Acid Promoted Ionic Diels–Alder Reactions" *Angew. Chem. Int. Ed.* **2013**, *52*, 13424-13428.

Bretherick, L. *Bretherick's Handbook of Reactive Chemical Hazards*, 4th ed.; Butterworths: Boston, 1990.

Bruker (2009) SAINT. Bruker AXS Inc., Madison, Wisconsin, USA.

Bruker (2009) SHELXTL. Bruker AXS Inc., Madison, Wisconsin, USA.

Bug, T.; Lemek, T.; Mayr, H. "Nucleophilicities of Nitroalkyl Anions" *J. Org. Chem.* **2004**, *69*, 7565-7576.

Burkhard, J. A.; Tchitchanov, B. H.; Carreira, E. M. "Cascade Formation of Isoxazoles: Facile Base-Mediated Rearrangement of Substituted Oxetanes" *Angew. Chem. Int. Ed.* **2011**, *50*, 5379–5382.

Cai, Q.; Liu, C.; Liang, X.-W.; You, S.-L. "Enantioselective Construction of Pyrroloindolines via Chiral Phosphoric Acid Catalyzed Cascade Michael Addition–Cyclization of Tryptamines" *Org. Lett.* **2012**, *14*, 4588-4590.

Carey, F. A.; Sundberg, R. J. *Advanced Organic Chemistry, Part A: Structure and Mechanisms*, 5th ed.; Springer: New York, 2007; 348-354.

Cecchi, L.; De Sarlo, F.; Machetti, F. "1,4-Diazabicyclo[2.2.2]octane (DABCO) as an Efficient Reagent for the Synthesis of Isoxazole Derivatives from Primary Nitro Compounds and Dipolarophiles: The Role of the Base" *Eur. J. Org. Chem.* **2006**, 4852-4860.

Chin, J.; Mancin, F.; Thavarajah, N.; Lee, D.; Lough, A.; Chung, D. S. "Controlling Diaza-Cope Rearrangement Reactions with Resonance-Assisted Hydrogen Bonds" *J. Am. Chem. Soc.* **2003**, *125*, 15276-15277.

Connon, S. J. "Organocatalysis Mediated by (Thio)urea Derivatives" *Chem. Eur. J.* **2006**, *12*, 5418-5427.

Connon, S. J. "The Design of Novel, Synthetically Useful (Thio)urea-Based Organocatalysts" *Synlett* **2009**, 354-376.

Corey, E. J.; Lee, D.-H.; Sarshar, S. "Convenient Routes to Symmetrical Benzils and Chiral 1,2-Diaryl-1,2-diaminoethanes, Useful Controllers and Probes for Enantioselective Synthesis" *Tetrahedron: Asymmetry* **1995**, *6*, 3-6.

Cranwell, P.B.; Hiscock, J. R.; Haynes, C. J. E.; Light, M. E.; Wells, N. J., Gale, P. A. "Anion recognition and transport properties of sulfamide-, phosphoric triamide- and thiophosphoric triamide-based receptors" *Chem. Commun.* **2013**, *49*, 874-879.

Cui, Y.; Evans, O. R.; Ngo, H. L.; White, P. S.; Lin, W. "Rational Design of Homochiral Solids Based on Two-Dimensional Metal Carboxylates" *Angew. Chem. Int. Ed.* **2002**, *41*, 1159-1162.

Culkin, D. A.; Hartwig, J. F. "Palladium-catalyzed alpha-arylation of carbonyl compounds and nitriles." *Acc. Chem. Res.* **2003**, *36*, 234-245. (b) Biscoe, M. R.; Buchwald, S. L. "The Selective Monoarylation of Acetate Esters and Aryl Methyl Ketones Using Aryl Chlorides." *Org. Lett.* **2009**, *11*, 1773-1775.

Curran, D. P.; Kuo, L. H. "Acceleration of a Dipolar Claisen Rearrangement by Hydrogen Bonding to a Soluble Diaryl Urea" *Tetrahedron Letters* **1995**, *36*, 6647-6650.

Curran, D. P.; Kuo, L. H. "Altering the Stereochemistry of Allylation Reactions of Cyclic α-Sulfinyl Radicals with Diarylureas" *J. Org. Chem.* **1994**, *59*, 3259-3261.

Davis, T. A.; Johnston, J. N. "Catalytic, enantioselective synthesis of silbene *cis*-diamines: A concise preparation of (–)-Nutlin 3, a potent p53/MDM2 inhibitor" *Chem. Sci.* **2011**, *2*, 1076-1079.

Davis, T. A.; Vilgelm, A. E.; Richmond, A.; Johnston, J. N. "Preparation of (–)-Nutlin-3 Using Enantioselective Organocatalysis at Decagram Scale" *J. Org. Chem.* **2013**, *78*, 10605-10616.

Deardoff, D. R.; Savin, K. A.; Justman, C. J.; Karanjawala, Z. E.; Sheppeck, J. E., II; Hager, D. C.; Aydin, N. "Conversion of Allylic Alcohols into Allylic Nitromethyl Compounds via a Palladium-Catalyzed Solvolysis: An Enantioselective Synthesis of an Advanced Carbocyclic Nucleoside Precursor" *J. Org. Chem.* **1996**, *61*, 3616–3622.

Denmark, S. E.; Su, X.; Nishigaichi, Y.; Coe, D. M.; Wong, K.-T.; Winter, S. B. D.; Choi, J. Y. "Synthesis of Phosphoramides for the Lewis Base-Catalyzed Allylation and Aldol Addition Reactions" *J. Org. Chem.* **1999**, *64*, 1958-1967.

Denoyelle, S.; Chen, T.; Chen, L.; Wang, Y.; Klosi, E.; Halperin, J. A.; Aktas, B. H.; Chorev, M. "In vitro inhibition of translation initiation by N,N'-diarylureas--potential anti-cancer agents." *Bioorg. Med. Chem. Lett.* **2012**, *22*, 402-409.

Deters, J. F.; McCusker, P. A.; Pilger, Jr., R. C. "A Scale of Relative Lewis Acidities from Proton Magnetic Resonance Data" *J. Am. Chem. Soc.* **1968**, *90*, 4583-4585.

Di Nunno, L.; Vitale, P.; Scilimati, A. "Effect of the aryl group substituent in the dimerization of 3-arylisoxazoles to *syn* 2,6-diaryl-3,7-diazatricyclo[4.2.0.0^{2,5}]octan-4,8-diones induced by LDA" *Tetrahedron* **2008**, *64*, 11198-11204.

DiMauro, E. F.; Kozlowski, M. C. "BINOL-Salen Metal Catalysts Incorporating a Bifunctional Design" *Org. Lett.* **2001**, *3*, 1641-1644.

DiMauro, E. F.; Kozlowski, M. C. "Late-Transition-Metal Complexes of BINOL-Derived Salens: Synthesis, Structure, and Reactivity" *Organometallics* **2002**, *21*, 1454-1461.

Do, H.-Q.; Tran-Vu, H.; Daugulis, O. "Copper-Catalyzed Homodimerization of Nitronates and Enolates under an Oxygen Atmosphere" *Organometallics* **2012**, *31*, 7816.

Doyle, A. G.; Jacobsen, E. N. "Small-Molecule H-Bond Donors in Asymmetric Catalysis" *Chem. Rev.* **2007**, *107*, 5713-5743.

Dreher, S. D.; Dormer, P. G.; Sandrock, D. L.; Molander, G. A. "Efficient Cross-Coupling of Secondary Alkyltrifluoroborates with Aryl Chlorides–Reaction

Discovery Using Parallel Microscale Experimentation" *J. Am. Chem. Soc.* **2008**, *130*, 9257-9259.

Emmons, W. D.; Pagano, A. S. "Peroxytrifluoroacetic Acid. VI. The Oxidation of Oximes to Nitroparaffins" *J. Am. Chem. Soc.* **1955**, *77*, 4557-4559. (b) Bose, D. S.; Vanajatha, G. "A Versatile Method for the Conversion of Oximes to Nitroalkanes" *Synth. Commun.* **1998**, *28*, 4531-4535.

Etter, M. C.; Urbanczyk-Kipkowska, Z.; Zia-Ebrahimi, M.; Panunto, T. W. "Hydrogen Bond Directed Cocrystallization and Molecular Recognition Properties of Diarylureas" *J. Am. Chem. Soc.* **1990**, *112*, 8415-8426.

Fessard, T. C.; Motoyoshi, H.; Carreira, E. M. "Pd-catalyzed cleavage of benzylic nitro bonds: New opportunities for asymmetric synthesis" *Angew Chem. Int. Ed.* **2007**, *46*, 2078-2081.

Feuer, H., Nielsen, A. T., Eds. In *Nitro Compounds: Recent Advances in Synthesis and Chemistry*; VCH Publishers: New York, 1990; Chapters 1-2.

Fini, F.; Sgarzani, V.; Pettersen, D.; Herrera, R. P.; Bernardi, L.; Ricci, A. "Phase-Transfer-Catalyzed Asymmetric Aza-Henry Reaction Using *N*-Carbamoyl Imines Generated In Situ from α-Amido Sulfones" *Angew. Chem. Int. Ed.* **2005**, *44*, 7975-7978.

Fischer, P. M.; Lane, D. P. "Small-molecule inhibitors of the p53 suppressor HDM2: have protein-protein interactions come of age as drug targets?" *Trends Pharmacol. Sci.* **2004**, *25*, 343-346.

Fleming, E. M.; McCabe, T.; Connon, S. J. "Novel axially chiral bis-arylthiourea-based organocatalysts" *Tetrahedron Lett.* **2006**, *47*, 7037-7042.

Fox, J. M.; Huang, X.; Chieffi, A.; Buchwald, S. L. "Highly Active and Selective Catalysts for the Formation of α-Aryl Ketones" *J. Am. Chem. Soc.* **2000**, *122*, 1360-1370.

Fukuzumi, S.; Ohkubo, K. "Fluorescence of Maxima of 10-Methylacridone–Metal Ion Salt Complexes: A Convenient and Quantitative Measure of Lewis Acidity of Metal Ion Salts" *J. Am. Chem. Soc.* **2002**, *124*, 10270-10271.

Fukuzumi, S.; Ohkubo, K. "Quantitative Evaluation of Lewis Acidity of Metal Ions Derived from the *g* Values of ESR Spectra of Superoxide: Metal Ion Complexes in Relation to the Promoting Effects in Electron Transfer Reactions" *Chem. Eur. J.* **2000**, *6*, 4532-4535.

Gilli, P.; Pretto, L.; Bertolasi, V.; Gilli, G. "Predicting Hydrogen-Bond Strengths from Acid–Base Molecular Properties. The pK_a Slide Rule: Toward the Solution of a Long-Lasting Problem" *Acc. Chem. Res.* **2009**, *42*, 33-44.

Gomez-Bengoa, E.; Linden, A.; Lopez, R.; Mugica-Mendiola, I.; Oiarbide, M.; Palomo, C. "Asymmetric Aza-Henry Reaction Under Phase Transfer Catalysis: An Experimental and Theoretical Study" *J. Am. Chem. Soc.* **2008**, *130*, 7955-7966.

Greger, J. G.; Yoon-Miller, S. J. P.; Bechtold, N. R.; Flewelling, S. A.; MacDonald, J. P.; Downey, C. R.; Cohen, E. A.; Pelkey, E. T. "Synthesis of Unsymmetrical 3,4-Diaryl-3-pyrrolin-2-ones Utilizing Pyrrole Weinreb Amides" *J. Org. Chem.* **2011**, *76*, 8203-8214.

Gupta, K. C.; Sutar, A. K. "Catalytic activities of Schiff base transition metal complexes" *Coord. Chem. Rev.* **2008**, *252*, 1420-1450.

Hallet, A. J.; Kwant, G. J.; de Vries, J. G. "Continuous Separation of Racemic 3,5-Dinitrobenzoyl-Amino Acids in a Centrifugal Contact Separator with the Aid of Cinchona-Based Chiral Host Compounds" *Chem. Eur. J.* **2009**, *15*, 2111-2120.

Handa, S.; Gnanadesikan, V.; Masunaga, S.; Shibasaki, M. "*syn*-Selective Catalytic Asymmetric Nitro-Mannich Reactions Using a Heterobimetallic Cu–Sm–Schiff Base Complex" *J. Am. Chem. Soc.* **2007**, *129*, 4900-4901.

Handa, S.; Gnanadesikan, V.; Matsunaga, S.; Shibasaki, M. "Heterobimetallic Transition Metal/Rare Earth Metal Bifunctional Catalysis: A Cu/Sm/Schiff Base Complex for *Syn*-Selective Catalytic Asymmetric Nitro-Mannich Reaction" *J. Am. Chem. Soc.* **2010**, *132*, 4925-4934.

Hardman, A. M.; So, S. S.; Mattson, A. E. "Urea-catalyzed Construction of Oxazinanes " *Org. Biomol. Chem.* **2013**, *11*, 5793-5797.

Harper, K. C.; Sigman, M. S. "Using Physical Organic Parameters to Correlate Asymmetric Catalyst Performance" *J. Org. Chem.* **2013**, *78*, 2813-2818.

Hauser, F. M.; Baghdanov, V. M. "A Convenient Preparation of Ring-Methoxylated Phenylnitromethanes" *J. Org. Chem.* **1998**, *53*, 2872-2873.

Henseler, A.; Kato, M.; Mori, K.; Akiyama, T. "Chiral Phosphoric Acid Catalyzed Transfer Hydrogenation: Facile Synthetic Access to Highly Optically Active Trifluoromethylated Amines" *Angew. Chem. Int. Ed.* **2011**, *50*, 8180-8183.

Hilgraf, R.; Pfaltz, A. "Chiral Bis(*N*-sulfonylamino)phosphine- and TADDOL-Phosphite-Oxazoline Ligands: Synthesis and Application in Asymmetric Catalysis" *Adv. Synth. Catal.* **2005**, *347*, 61-77.

356

Hilt, G.; Puenner, F.; Moebus, J.; Naseri, V.; Bohn, M. A. "A Lewis Acidity Scale in Relation to Rate Constants of Lewis Acid Catalyzed Organic Reactions" *Eur. J. Org. Chem.* **2011**, 5962-5966.

Hine, J.; Ahn, K.; Gallucci, J. C.; Linden, S.-M. "1,8-Biphenylenediol Forms Two Strong Hydrogen Bonds to the Same Oxygen Atom" *J. Am. Chem. Soc.* **1984**, *106*, 7980-7981.

Hine, J.; Linden, S.-M.; Kanagasabapathy, V. M. "1,8-Biphenylenediol is a Double-Hydrogen-Bonding Catalyst for Reaction of an Epoxide with a Nucleophile" *J. Am. Chem. Soc.* **1985**, *107*, 1082-1083.

Hine, J.; Linden, S.-M.; Kanagasabapathy, V. M. "Double-Hydrogen-Bonding Catalysis of the Reaction of Phenyl Glycidyl Ether with Diethylamine by 1,8-Biphenylenediol" *J. Org. Chem.* **1985**, *50*, 5096-5097.

Hirano, T.; Sekiguchi, T.; Hashizume, D.; Ikeda, H.; Maki, S.; Niwa, H. "Colorimetric and fluorometric sensing of the Lewis acidity of a metal ion by metal-ion complexation of imidazo[1,2-*a*]pyrazin-3(7*H*)-ones" *Tetrahedron* **2010**, *66*, 3842-3848.

Hooft, R.W.W., Straver, L.H., Spek, A.L. (2008) J. Appl.Cryst., 41, 96-103.

Huang, Y.; Unni, A.K.; Thadani, A. N.; Rawal, V. H. "Single enantiomers from a chiral-alcohol catalyst" *Nature* **2003**, *424*, 146.

Huynh, P. Correlation of Reaction Rates with LUMO Lowering Ability. M.S. Thesis, University of Pennsylvania, Philadelphia, PA, June 2012.

Huynh, P. N. H.; Walvoord, R. R.; Kozlowski, M. C. "Rapid Quantification of the Activating Effects of Hydrogen-Bonding Catalysts with a Colorimetric Sensor" *J. Am. Chem. Soc.* **2012**, *134*, 15621-15623.

Irving, H.; Williams, R. J. P. "Order of Stability of Metal Complexes" *Nature*, **1948**, *162*, 746-747.

Irving, H.; Williams, R. J. P. "The Stability of Transition-metal Complexes" *J. Chem. Soc.* **1953**, 3192-3210.

Jakab, G.; Tancon, C.; Zhang, Z.; Lippert, K. M.; Schreiner, P. R. "(Thio)urea Organocatalyst Equilibrium Acidities in DMSO" *Org. Lett.* **2012**, *14*, 1724-1727.

Jakubec, P.; Hawkins, A.; Felzmann, W.; Dixon, D. J. "Total Synthesis of Manzamine A and Related Alkaloids" *J. Am. Chem. Soc.* **2012**, *134*, 17482-17485.

Jamieson, E. R.; Lippard, S. J. "Structure, Recognition, and Processing of Cisplatin–DNA Adducts" *Chem. Rev.* **1999**, *99*, 2467-2498.

Jencks, W. P.; Regenstein, J. "Ionization Constants of Acids and Bases" In *Handbook of Biochemistry and Molecular Biology*, 3rd ed.; Fassman, G. D., Ed.; CRC Press: Ohio, 1975; Vol. 1, pp 305-351.

Jensen, K. H.; Sigman, M. S. "Evaluation of Catalyst Acidity and Substrate Electronic Effects in a Hydrogen Bond-Catalyzed Enantioselective Reaction" *J. Org. Chem.* **2010**, *75*, 7194-7201.

Jensen, K. H.; Sigman, M. S. "Systematically Probing the Effect of Catalyst Acidity in a Hydrogen-Bond-Catalyzed Enantioselective Reaction" *Angew. Chem. Int. Ed.* **2007**, *46*, 4748-4750.

Jiang, J.; Xu, H.-D.; Xi, J.-B.; Ren, B.-Y.; Lv, F.-P.; Guo, X.; Jiang, L.-Q.; Zhang, Z.-Y.; Hu, W.-H. "Diastereoselectively Switchable Enantioselective Trapping of Carbamate Ammonium Ylides with Imines" *J. Am. Chem. Soc.* **2011**, *133*, 8428-8431.

Jiang, X.; Zhang, Y.; Wu, L.; Zhang, G.; Liu, X.; Zhang, H.; Fu, D.; Wang, R. "Doubly Stereocontrolled Asymmetric Aza-Henry Reaction with *in situ* Generation of *N*-Boc-Imines Catalyzed by Novel Rosin-Derived Amine Thiourea Catalysts" *Adv. Synth. Catal.* **2009**, *351*, 2096-2100.

Kamlet, M. .; Abboud, J.-L. M.; Abraham, M. H.; Taft, R. W. "Linear Solvation Energy Relationship. 23. A Comprehensive Collection of the Solvatochromic Parameters, π^*, α, and β, and Some Methods for Simplifying the Generalized Solvatochromic Equation" *J. Org. Chem.* **1983**, *48*, 2877-2887.

Kantlehner, W. "New Methods for the Preparation of Aromatic Aldehydes" *Eur. J. Org. Chem.* **2003**, 2530-2546.

Kelly, T. R.; Meghani, P.; Ekkundi, V. S. "Diels-Alder Reactions: Rate Acceleration Promoted by a Biphenylenediol" *Tetrahedron Lett.* **1990**, *31*, 3381-3384.

Kim, H.-J.; Kim, H.; Alhakimi, G.; Jeong, E. J.; Thavarajah, N.; Studnicki, L.; Koprianiuk, A.; Lough, A. J.; Suh, J.; Chin, J. "Preorganization in Highly Enantioselective Diaza-Cope Rearrangement Reaction" *J. Am. Chem. Soc.* **2005**, *127*, 16370-16371.

Kim, H.; Nguyen, Y.; Yen, C. P.-H.; Chagal, L.; Lough, A. J.; Kim, B. M.; Chin, J. "Stereospecific Synthesis of C_2 Symmetric Diamines from the Mother Diamine by Resonance-Assisted Hydrogen-Bond Directed Diaza-Cope Rearrangment" *J. Am. Chem. Soc.* **2008**, *130*, 12184-12191.

Klaus, S.; Neumann, H.; Zapf, A.; Strübing, D.; Hübner, S.; Almena, J.; Riermeier, T.; Gross, P.; Sarich, M.; Krahnert, W.-R.; Rossen, K.; Beller, M. "A General and Efficient Method for the Formylation of Aryl and Heteroaryl Bromides" *Ang. Chem. Int. Ed.* **2006**, *45*, 154-158.

Knudsen, K. R.; Risgaard, T.; Nishiwaki, N.; Gothelf, K. F.; Jørgensen, K. A. "The First Catalytic Asymmetric Aza-Henry Reaction of Nitronates with Imines: A Novel Approach to Optically Active *β*-Nitro-*α*-Amino Acid- and *α,β*-Diamino Acid Derivatives" *J. Am. Chem. Soc.* **2001**, *123*, 5843-5844.

Kolb, H. C.; VanNieuwenhze, M. S.; Sharpless, K. B. "Catalytic Asymmetric Dihydroxylation" *Chem. Rev.* **1994**, *94*, 2483-2547.

Konishi, H.; Lam, T. Y.; Malerich, J. P.; Rawal, V. H. "Enantioselective α-Amination of 1,3-Dicarbonyl Compounds Using Squaramide Derivatives as Hydrogen Bonding Catalysts" *Org. Lett.* **2010**, *12*, 2028-2031.

Kornblum, N.; Brown, R. A. "The Action of Acids on Nitronic Esters and Nitroparaffin Salts. Concerning the Mechanisms of the Nef and the Hydroxamic Acid Forming Reactions of Nitroparaffins" *J. Am. Chem. Soc.* **1965**, *87*, 1742-1747.

Kornblum, N.; Erickson, A. S.; Kelly, W. J.; Henggeler, B. "Conversion of Nitro Paraffins into Aldehydes and Ketones" *J. Org. Chem.* **1982**, *47*, 4534-4538.

Kornblum, N.; Graham, G. E. "The Regeneration of Nitroparaffins from Their Salts" *J. Am. Chem. Soc.* **1951**, *73*, 4041-443.

Kornblum, N.; Larson, H. O.; Blackwood, R. K.; Mooberry, D. D.; Oliveto, E. P.; Graham, G. E. "A new Method for the Synthesis of Aliphatic Nitro Compounds" *J. Am. Chem. Soc.* **1956**, *78*, 1497-1501.

Kornblum, N.; Powers, J. W. "Synthesis of Aliphatic Nitro Compounds" *J. Org. Chem.* **1957**, *22*, 455-456

Kornblum, N.; Smiley, R. A.; Blackwood, R. K.; Iffland, D. C. "The Mechanism of the Reaction of Silver Nitrite with Alkyl Halides. The Contrasting Reactions of Silver and Alkali Metal Salts with Alkyl Halides. The Alkylation of Ambident Anions" *J. Am. Chem. Soc.* **1955**, *77*, 6269-6280.

Kornblum, N.; Taub, B.; Ungnade, H. E. "The Reaction of Silver Nitrite with Primary Alkyl Halides" *J. Am. Chem. Soc.* **1954**, *76*, 3209-3211.

Kumaraswamy, G.; Sastry, M. N. V.; Jena, N.; Kumar, K. R.; Vairamani, M. "Enantioenriched (*S*)-6,6'-diphenylBinol-Ca: a novel and efficient chirally modified metal complex for asymmetric epoxidation of α,β-unsaturated enones" *Tetrahedron: Asymmetry* **2003**, *14*, 3797-3803.

Kwong, F. Y.; Lai, C. W.; Chan, K. S. "Catalytic Solvent-Free Arsination: First Catalytic Application of Pd–Ar/As–Ph Exchange in the Synthesis of Functionalized Aryl Arsines" *J. Am. Chem. Soc.* **2001**, *123*, 8864-8865.

Li, X.; Deng, H.; Luo, S.; Cheng, J.-P. "Organocatalytic Three-Component Reactions of Pyruvate, Aldehyde, and Aniline by Hydrogen-Bonding Catalysts" *Eur. J. Org. Chem.* **2008**, 4350-4356.

Li, X.; Deng, H.; Zhang, B.; Li, J.; Zhang, L.; Luo, S.; Cheng, J.-P. "Physical Organic Study of Structure-Activity-Enantioselectivity Relationships in Asymmetric Bifunctional Thiourea Catalysis: Hints for the Design of New Organocatalysts" *Chem. Eur. J.* **2010**, *16*, 450-455.

Ligiero, C. B. P.; Visentin, L. C.; Giacomini, R.; Filgueiras, C. A. L.; Miranda, P. C. M. L. "2,3,5,6-Tetra(pyrazin-2-yl)pyrazine: a novel bis-bidentate, bis-tridentate chelator" *Tetrahedron Lett*. **2009**, *50*, 4030-4032.

Lindholm, A.; Maki-Arvela, P.; Toukonitty, E.; Pakkanen, T. A.; Hirvi, J. T.; Salmi, T.; Murzin, D. Y.; Sjöholm, R.; Leino, R. "Hydrosilylation of cinchonidine and 9-*O*-TMS-cinchonidine with triethoxysilane: application of 11-(triethoxysilyl)-10-11-dihydrocinchonidine as a chiral modifier in the enantioselective hydrogenation of 1-phenylpropane-1,2-dione" *J. Chem. Soc., Perkin Trans. 1* **2002**, 2605-2612.

Lippert, K. M.; Hof, K.; Gerbit, D.; Ley, D.; Hausmann, H.; Guenther, S.; Schreiner, P. R. *Eur. J. Org. Chem.* **2012**, 5919-5927.

Lowe, S. W.; Cepero, E.; Evan, G. "Intrinsic tumour suppression" *Nature* **2004**, *432*, 307-315.

Lucet, D.; Le Gall, T.; Mioskowski, C. "The Chemistry of Vicinal Diamines" *Angew. Chem. Int. Ed.* **1998**, *37*, 2580-2627.

Luzzio, F. A. "The Henry reaction: recent examples" *Tetrahedron* **2001**, *57*, 915-945.

M. Pouchart, C. J. *The Alrich Library of NMR Spectra,* 2nd ed.; Aldrich Chemical Company: Milwaukee, WI, 1983; Vol. 2.

Malerich, J. P.; Hagihara, K.; Rawal, V. H. "Chiral Squaramide Derivatives are Excellent Hydrogen Bond Donor Catalysts" *J. Am. Chem. Soc.* **2008**, *130*, 14416-14417.

Markofsky, S. B. "Nitro Compounds, Aliphatic", Ullmann's Encyclopedia of Industrial Chemistry, Electronic Release, Wiley-VCH, Weinheim October 2011.

Marques-Lopez, E.; Merino, P.; Tejero, T.; Herrera, R. P. "Catalytic Enantioselective Aza-Henry Reactions" *Eur. J. Org. Chem.* **2009**, 2401-2420.

Marsh, G. P.; Parson, P. J.; McCarthy, C.; Coniquet, X. G. "An Efficient Synthesis of Nitroalkenes by Alkene Cross Metathesis: Facile Access to Small Ring Systems" *Org. Lett.* **2007**, *9*, 2613-2616.

McDaniel, D. H.; Brown, H. C. "An Extended Table of Hammett Substituent Constants Based on the Ionization of Substituted Benzoic Acids" *J. Org. Chem.* **1958**, *23*, 420-427.

McKittrick, D. S.; Irvine, R. J.; Bergsteinsson, I. "Nitromethane – Potential Hazards in Use" *Ind. Eng. Chem., Anal. Ed.* **1938**, *10*, 630-631.

Meng, Q.; Thibblin, A. "Solvent-Promoted E2 Reaction Competing with SN2 Reaction and Stepwise Solvolytic Elimination and Substitution Reactions" *J. Am. Chem. Soc.* **1995**, *117*, 9399-9407.

Metz, A. E.; Berritt, S.; Dreher, S. D.; Kozlowski, M. C. "Efficient Palladium-Catalyzed Cross-Coupling of Highly Acidic Substrates, Nitroacetates" *Org. Lett.* **2012**, *14*, 760-763.

Metz, A. E.; Kozlowski, M. C. "2-Aryl-2-nitroacetates as Central Precursors to Aryl Nitromethanes, α-Ketoesters, and α-Amino Acids" *J. Org. Chem.* **2013**, *78*, 717-722 .

Meyer, V.; Stüber, O. "Vorläufige Mittheilung" *Chem. Ber.* **1872**, *5*, 203-205.

Michalson, E. T.; Szmuszkovicz, J. "Medicinal agents incorporating the 1,2-diamine functionality" *Prog. Drug. Res.* **1989**, *33*, 135-149.

Mikami, K.; Kakuno, H.; Aikawa, K. "Enantiodiscrimination and Enantiocontrol of Neutral and Cationic Pt[II] Complexes Bearing the *Tropos* Biphep Ligand: Application to Asymmetric Lewis Acid Catalysis" *Angew. Chem. Int. Ed.* **2005**, *44*, 7257-7260.

Miyano, S.; Nawa, M.; Mori, A.; Hashimoto, H. "Axially Dissymmetric Bis(aminophosphine)s Derived from 2,2'-Diamino-1,1'-binaphthyl. Synthesis and Application to Rhodium(I)-Catalyzed Asymmetric Hydrogenations" *Bull. Chem. Soc. Jpn.* **1984**, *57*, 2171-2176.

Miyaura, N.; Suzuki, A. "Palladium-Catalyzed Cross-Coupling Reactions of Organoboron Compounds" *Chem. Rev.* **1995**, *95*, 2457-2483.

Nakai, S.; Yasui, M.; Nakazato, M.; Iwasaki, F.; Maki, S.; Niwa, H.; Ohashi, M.; Hirano, T. "Fundamental Studies on the Structures and Spectroscopic Properties of Imidazo[1,2-*a*]pyrazin-3(7*H*)-one Derivatibes" *Bull Chem. Soc. Jpn.* **2003**, *76*, 2361-2387.

Natarajan, A.; Guo, Y.; Arthanari, H.; Wagner, G.; Halperin, J. A.; Chorev, M. "Synthetic Studies toward Aryl-(4-aryl-4*H*-[1,2,4]triazole-3-yl)-amine from 1,3-Diarylthiourea as Urea Mimetics" *J. Org. Chem.* **2005**, *70*, 6362-6368.

Nef, J. U. "Ueber die Constitution der Salze der Nitroparaffine" *Liebigs Ann. Chem.* **1894**, *280*, 263-291.

Ni, X.; Li, X.; Wang, Z.; Cheng, J.-P. "Squaramide Equilibrium Acidities in DMSO" *Org. Lett.* **2014**, *16*, 1786-1789.

Nickerson, D. M.; Angeles, V. V.; Auvil, T. J.; So, S. S.; Mattson, A. E. "Internal Lewis Acid Assisted Ureas: Tunable Hydrogen Bond Donor Catalysts" *Chem. Commun.* **2013**, *49*, 4289-4291.

Nicolaou, K. C.; Bulger, P. G.; Sarlah, D. "Palladium-Catalyzed Cross-Coupling Reactions in Total Synthesis" *Angew. Chem. Int. Ed.* **2005**, *44*, 4442-4489.

Nugent, B. M.; Yoder, R. A.; Johnston, J. N. "Chiral Proton Catalysis: A Catalytic Enantioselective Direct Aza-Henry Reaction" *J. Am. Chem. Soc.* **2004**, *126*, 3418-3419.

Okino, T.; Hoashi, Y.; Takemoto, Y. "Enantioslelective Michael Reaction of Malonates to Nitroolefins Catalyzed by Bifunctional Organocatalysts" *J. Am. Chem. Soc.* **2003**, *125*, 12672-12673.

Okino, T.; Nakamura, S.; Furukawa, T.; Takemoto, Y. "Enantioselective Aza-Henry Reaction Catalyzed by a Bifunctional Organocatalyst" *Org. Lett.* **2004**, *6*, 625-627.

Olah, G. A.; Arvanaghi, M.; Vankar, Y. D.; Prakash, G. K. S. "Synthetic Methods and Reactions; 89. Improved Transformation of Nitro Compounds into Carbonyl Compounds by Hydrogen Peroxide/Potassium Carbonate" *Synthesis* **1980**, 662-663.

Olah, G. A.; Ohannesian, L.; Arvanaghi, M. "Formylating Agents" *Chem. Rev.* **1987**, *87*, 671-686.

Ono, N. *The Nitro Group in Organic Synthesis*; Wiley-VCH: New York, 2001.

Ono, N.; Hamamoto, I.; Kaji, A. "Palladium-catalysed Allylic Alkylations of Allylic Nitro-compounds" *J. Chem. Soc., Chem. Commun.* **1982**, 821–822.

"ORTEP-II: A Fortran Thermal Ellipsoid Plot Program for Crystal Structure Illustrations". C.K. Johnson (1976) ORNL-5138.

Padilla-Salinas, R. Part II: Nitroethylation of Vinyl Triflates and Vinyl Bromides. Ph.D. Thesis, University of Pennsylvania, Philadelphia, PA, June 2014.

Padilla-Salinas, R.; Walvoord, R. R.; Tcyrulnikov, S.; Kozlowski, M. C. "Nitroethylation of Vinyl Triflates and Bromides" *Org. Lett.* **2013**, *15*, 3966-3969.

Padwa, A. In *1,3-Dipolar Cycloaddition Chemistry*; Taylor, E. C., Weissberger, A., Eds.; Wiley & Sons: New York, 1984; Chapter 10.

Pagano, A. H.; Shechter, H. "Oxidation of Nitronates with Persulfate and with Silver Ions" *J. Org. Chem.* **1970**, *35*, 295-303.

Palomo, C.; Oiarbide, M.; Laso, A.; Lopez, R. "Catalytic Enantioselective Aza-Henry Reaction with Broad Substrate Scope" *J. Am. Chem. Soc.* **2005**, *127*, 17622-17623.

Parker, M. F. L.; Osuna, S.; Bollot, G.; Vaddypally, S.; Zdilla, M. J.; Houk, K. N.; Schafmeister, C. E. "Acceleration of an Aromatic Claisen Rearrangement via a Designed Spiroligozyme Catalyst that Mimics the Ketosteroid Isomerase Catalytic Dyad" *J. Am. Chem. Soc.* **2014**, *136*, 3817-3827.

Piermarini, G. J.; Block, S.; Miller, P. J. "Effects of pressure on the thermal decomposition kinetics and chemical reactivity of nitromethane" *J. Phys. Chem.* **1989**, *93*, 457-462.

Pikul, S.; Corey, E. J. "(1R,2R)-(+)- and (1S,2S)-(−)-1,2-diphenyl-1,2-ethylenediamine" *Org. Synth.* **1998**, *71*, 22-26.

Prim, D.; Campagne, J.-M.; Joseph, D.; Andrioletti, B. "Palladium-catalysed reactions of aryl halides with soft, non-organometallic nucleophiles" *Tetrahedron* **2002**, *58*, 2041-2075.

Pytela, O.; Liska, J. "Chemometrical Analysis of Substituent Effects. V. *ortho* Effect" *Collect. Czech. Chem. Commmun.* **1994**, *59*, 2005-2021.

Rampalakos, C.; Wulff, W. D. "A Novel Bis-Thiourea Organocatalyst for the Asymmetric Aza-Henry Reaction" *Adv. Synth. Catal.* **2008**, *350*, 1785-1790.

Ray, J. D.; Ogg, Jr., R. A. "The Heat of Formation of Methyl Nitrate" *J. Phys. Chem.* **1959**, *63*, 1522-1523.

Raymond, E.; Chaney, S. G.; Taamma, A.; Cvitkovic, E. "Oxaliplatin: A review of preclinical and clinical studies" *Ann. Oncol.* **1998**, *9*, 1053-1071.

Reuping, M.; Antonchick. A. P. "Brønsted-Acid-Catalyzed Activation of Nitroalkanes: A Direct Enantioselective Aza-Henry Reaction" *Org. Lett.* **2008**, *10*, 1731-1734.

Rieck, H.; Helmchen, G. "Palladium Complex Catalyzed Asymmetric Allylic Substitutions with Nitromethane: Enantioselectivities Exceeding 99.9%ee" *Angew. Chem. Int. Ed.* **1996**, *34*, 2687–2689.

Robak, M.; Trincado, M.; Ellman, J. A. "Enantioselective Aza-Henry Reactions with an *N*-Sulfinyl Urea Organocatalyst" *J. Am. Chem. Soc.* **2007**, *129*, 15110-15111.

Rodriguez, A. A.; Yoo, H.; Ziller, J. W.; Shea, K. J. "New architectures in hydrogen bond catalysis" *Tetrahedron Lett.* **2009**, *50*, 6830-6833.

Rosini, G.; Ballini, R. "Functionalized Nitroalkanes as Useful Reagents for Alkyl Anion Synthons" *Synthesis* **1988**, 833-847.

Roskamp, E. J.; Pedersen, S. F. "Convenient Routes to Vicinal Diamines. Coupling of Nitriles or *N*-(Trimethylsilyl)imines Promoted by $NbCl_4(THF)_2$" *J. Am. Chem. Soc.* **1987**, *109*, 3152-3154.

Rozen, S.; Kol, M. "Oxidation of Aliphatic Amines by HOF•CH₃CN Complex Made Directly from F_2 and Water" *J. Org. Chem.* **1992**, *57*, 7342-7344.

Sasaki, H.; Irie, R.; Hamada, T.; Suzuki, K.; Katsuki, T. "Rational Design of Mn-Salen Catalyst (2): Highly Enantioselective Epoxidation of Conjugated *cis*-Olefins" *Tetrahedron* **1994**, *50*, 11827-11838.

Schafer, A. G.; Wieting, J. M.; Fisher, T. J.; Mattson, A. E. "Chiral Silanediols in Anion-Binding Catalysis" *Angew. Chem. Int. Ed.* **2013**, *52*, 11321-11324.

Schafer, A. G.; Wieting, J. M.; Mattson, A. E. "Silanediols: A New Class of Hydrogen Bond Donor Catalysts" *Org. Lett.* **2011**, *13*, 5228-5231.

Schenker, S.; Zamfir, A.; Freund, M.; Tsogoeva, S. B. "Developments in Chiral Binaphthyl-Derived Brønsted/Lewis Acids and Hydrogen-Bond-Donor Organocatalysis" *Eur. J. Org. Chem.* **2011**, 2209-2222.

Schreiner, P. R. "Metal-free organocatalysis through explicit hydrogen bonding interactions" *Chem. Soc. Rev.* **2003**, *32*, 289-296.

Seebach, D.; Colvin, E. W.; Lehr, F.; Weller, T. "Nitroaliphatic Compounds − Ideal Intermediates in Organic Synthesis" *Chimia* **1979**, *33*, 1–18.

Sekiguchi, T.; Maki, S.; Niwa, H.; Ikeda, H.; Hirano, T. "Metal-ion complexation of imidazo[1,2-*a*]pyrazin-3(7*H*)-ones: continuous changes in absorption spectra of complexes depending on the Lewis acidity of the metal ion" *Tetrahedron Lett.* **2004**, *45*, 1065-1069.

Sheldrick, G.M. (2007) SADABS. University of Gottingen, Germany.

Sheldrick, G.M. (2008) Acta Cryst. A64,112-122.

Shoenberg, A.; Heck, R. F. "Palladium-Catalyzed Formylation of Aryl, Heterocyclic, and Vinylic Halides" *J. Am. Chem. Soc.* **1974**, *96*, 7761-7764.

Shokri, A.; Wang, Y.; O'Doherty, G. A.; Wang, X.-B.; Kass, S. R. "Hydrogen-Bond Networks: Strengths of Different Types of Hydrogen Bonds and An Alternative to the Low Barrier Hydrogen-Bond Proposal" *J. Am. Chem. Soc.* **2013**, *135*, 17919-17924.

Sice, J. "Preparation and Reactions of 2-Methoxythiophene" *J. Am. Chem. Soc.* **1953**, *75*, 3697-3700.

Sigman, M. S.; Jacobsen, E. N. "Schiff Base Catalysts for the Asymmetric Strecker Reaction Identified and Optimized from Parallel Synthetic Libraries" *J. Am. Chem. Soc.* **1998**, *120*, 4901-4902.

Skoda-Foeldes, R.; Kollar, L. "Synthetic Applications of Palladium Catalysed Carbonylation of Organic Halides" *Curr. Org. Chem.* **2002**, *6*, 1097-1119.

So, S. S.; Auvil, T. J.; Garza, V. J.; Mattson, A. E. "Boronate Urea Activation of Nitrocyclopropane Carboxylates" *Org. Lett.* **2012**, *14*, 444-447.

So, S. S.; Burkett, J. A.; Mattson, A. E. "Internal Lewis Acid Assisted Hydrogen Bond Donor Catalysis" *Org. Lett.* **2011**, *13*, 716-719.

Sohtome, Y.; Nagasawa, K. "The Design of Chiral Double Hydrogen Bonding Networks and Their Applications to Catalytic Asymmetric Carbon-Carbon and Carbon-Oxygen Bond-Forming Reactions" *Synlett* **2010**, 1-22.

Spek, A.L., Acta Cryst., (2009) D65, 148-155.

Steiner, T. "The Hydrogen Bond in the Solid State" *Angew. Chem. Int. Ed.* **2002**, *41*, 48-76.

Suzuki, H.; Murashima, T.; Kozai, I.; Mori, T. "Ozone-mediated Nitration of Alkylbenzenes and Related Compounds with Nitrogen Dioxide" *J. Chem. Soc., Perkin Trans. 1* **1993**, 1591-1597.

Takamuki, Y.; Maki, S.; Niwa, H.; Ikeda, H.; Hirano, T. "Substituent Effects on the Solvatochromism of 2-Phenylimidazopyrazinones: Effective Control of the Color Variation Range and Sensitivity toward an Indication of the Proton-donor Ability of

Solvents by an Electron-withdrawing Group Substitution" *Chem. Lett.* **2004**, *33*, 1484-1485.

Takamuki, Y.; Maki, S.; Niwa, H.; Ikeda, H.; Hirano, T. "Substituent effects on the spectroscopic properties of solvatochromic 2-phenylimidazo[1,2-*a*]pyrazin-3(7*H*)-ones: an effective control for the colorimetric sensor properties" *Tetrahedron* **2005**, *61*, 10073-10080.

Takenaka, N.; Sarangthem, R. S.; Seerla, S. K. "2-Aminopyridinium Ions Activate Nitroalkenes through Hydrogen Bonding" *Org. Lett.* **2007**, *9*, 2819-2822.

Tamura, R.; Hegedus, L. S. "Palladium(0)-catalyzed allylic alkylation and amination of allylnitroalkanes" *J. Am. Chem. Soc.* **1982**, *104*, 3727–3729.

Tamura, R.; Kamimura, A.; Ono, N. "Displacement of Aliphatic Nitro Groups by Carbon and Heteroatom Nucleophiles" *Synthesis* **1991**, 423–434.

Taylor, E. C.; Cheeseman, G. W. H. "Synthesis and Properties of Pyrrolo(1,2-*a*)quinoxalines" *J. Am. Chem. Soc.* **1964**, *86*, 1830-1835.

Taylor, M. S.; Jacobsen, E. N. "Asymmetric Catalysis by Chiral Hydrogen-Bond Donors" *Angew. Chem. Int. Ed.* **2006**, *45*, 1520-1543.

Tran, N. T.; Wilson, S. O.; Franz, A. K. "Cooperative Hydrogen-Bonding Effects in Silanediol Catalysis" *Org. Lett.* **2012**, *14* 186-189.

Trost, B. M; Lupton, D. W. "Dinuclear Zinc-Catalyzed Enantioselective Aza-Henry Reaction" *Org. Lett.* **2007**, *9*, 2023-2026.

Trost, B. M.; Surivet, J. "Asymmetric Alkylation of Nitroalkanes" *Angew. Chem. Int. Ed.* **2000**, *39*, 3122–3124.

Tuerkmen, Y. E.; Rawal, V. H. "Exploring the Potential of Diarylacetylenediols as Hydrogen Bonding Catalysts" *J. Org. Chem.* **2013**, *78*, 8340-8353.

Uozumi, Y.; Suzuka, T. "π-Allylic C1-Substitution in Water with Nitromethane Using Amphiphilic Resin-Supported Palladium Complexes" *J. Org. Chem.* **2006**, *71*, 8644–8646

Uraguchi, D.; Koshimoto, K.; Ooi, T. "Chiral Ammonium Betaines: A Bifunctional Organic Base Catalyst for Asymmetric Mannich-Type Reaction of *α*-Nitrocarboxylates" *J. Am. Chem. Soc.* **2008**, *130*, 10878-10879.

Urpi, F.; Vilarrasa, J. "New Synthetic 'Tricks'. A Novel One-Pot Procedure for the Conversion of Primary Nitro Groups into Aldehydes" *Tetrahedron Lett.* **1990**, *31*, 7499-7500.

Uyeda, C.; Jacobsen, E. N. "Enantioselective Claisen Rearrangements with a Hydrogen-Bond Donor Catalyst" *J. Am. Chem. Soc.* **2008**, *130*, 9228-9229.

Veitch, G. E.; Jacobsen, E. N. "Tertiary Aminourea-Catalyzed Enantioselective Iodolactonization" *Angew. Chem. Int. Ed.* **2010**, *49*, 7332-7335.

Voets, M.; Antes, I.; Schere, C.; Mueller-Viera, U.; Biemel, K.; Marchais-Oberwinkler, S.; Hartmann, R. W. "Synthesis and Evaluation of Heteroaryl-Substituted Dihydronaphthalenes and Indenes: Potent and Selective Inhibitors of Aldosterone Synthase (CYP11B2) for the Treatment of Congestive Heart Failure and Myocardial Fibrosis" *J. Med. Chem.* **2006**, *49*, 2222-2231.

Vogl, E. M.; Buchwald, S. L. "Palladium-Catalyzed Monoarylation of Nitroalkanes" *J. Org. Chem.* **2002**, *67*, 106-111.

Wade, P. A.; Morrow, S. D.; Hardinger, S. A. "Palladium Catalysis as a Means for Promoting the Allylic C-Alkylation of Nitro Compounds" *J. Org. Chem.* **1982**, *47*, 365– 367.

Wakefield, B. J. *Organolithium Methods*; Academic Press: San Diego, CA, 1988.

Walsh, P. W.; Kozlowski, M. C. Fundamentals of Asymmetric Catalysis; University Science Books: Sausalito, CA, 2009.

Walvoord, R. R.; Berritt, S.; Kozlowski, M. C. "Palladium-Catalyzed Nitromethylation of Aryl Halides: An Orthogonal Formylation Equivalent" *Org. Lett.* **2012**, *14*, 4086-4089.

Walvoord, R. R.; Kozlowksi, M. C. "Minimizing the Amount of Nitromethane in Palladium-Catalyzed Cross-Coupling with Aryl Halides" *J. Org. Chem.* **2013**, *78*, 8859-8864.

Wang, D.; Lipard, S. J. "Cellular Processing of Platinum Anticancer Drugs" *Nat. Rev. Drug Discovery* **2005**, *4*, 307-320.

Wei, Y.; He, W.; Liu, Y.; Liu, P.; Zhang, S. "Highly Enantioselective Nitro-Mannich Reaction Catalyzed by *Cinchona* Alkaloids and *N*-Benzotriazole Derived Ammonium Salts" *Org. Lett.* **2012**, *14*, 704-707.

Wenzel, A. G.; Jacobsen, E. N. "Asymmetric Catalytic Mannich Reactions Catalyzed by Urea Derivatives: Enantioselective Synthesis of β-Aryl-β-Amino Acids" *J. Am. Chem. Soc.* **2002**, *124*, 12964-12965.

Westermann, B. "Asymmetric Catalytic Aza-Henry Reactions Leading to 1,2-Diamines and 1,2-Diaminocarboxylic Acids" *Angew. Chem. Int. Ed.* **2003**, *42*, 151-153.

Wheate, N. J.; Walker, S.; Craig, G. E.; Oun, R. "The status of platinum anticancer drugs in the clinic and in clinical trials" *Dalton Trans.* **2010**, *39*, 8113-8127.

Wittkopp, A.; Schreiner, P. R. "Metal-Free, Noncovalent Catalysis of Diels-Alder Reactions by Neutral Hydogen Bond Donors in Organic Solvents and in Water" *Chem. Eur. J.* **2003**, *9*, 407-414.

Wu, R.; Chang, X.; Lu, A.; Wang, Y.; Wu, G.; Song, H.; Zhou, Z.; Tang, C. "Chiral (thio)phosphorodiamides as excellent hydrogen bond donor catalysts in the asymmetric Michael addition of 2-hydroxy-1,4-naphthoquinone to nitroolefins" *Chem. Commun.* **2011**, *47*, 5034-5036.

Yamada, K.; Harwood, S. J.; Gröger, H.; Shibasaki, M. "The First Catalytic Asymmetric Nitro-Mannich-Type Reaction Promoted by a New Heterobimetallic Complex" *Angew. Chem. Int. Ed.* **1999**, *38*, 3504-3506.

Yoon, T. P.; Jacobsen, E. N. "Highly Enantioselective Thiourea-Catalyzed Nitro-Mannich Reactions" *Angew. Chem. Int. Ed.* **2005**, *44*, 466-468.

Zhang, Z.; Yu, A.; Zhou, W. "Synthesis and structure-activity relationship of 7-(substituted)-aminomethyl-4-quinolone-3-carboxylic acid derivatives" *Bioorg. Med. Chem.* **2007**, *15*, 7274-7280.

Zhong, Y.-W.; Izumi, K.; Xu, M.-H.; Lin, G.-Q. "Highly Diastereoselective and Enantioselective Synthesis of Enantiopure C_2-Symmetrical Vicinal Diamines by Reductive Homocoupling of Chiral *N-tert*-Butansulfinyl Imines" *Org. Lett.* **2004**, *6*, 4747-4750.

Zhu, Y.; Malerich, J. P.; Rawal, V. H. "Squaramide-Catalyzed Enantioselective Michael Addition of Diphenyl Phosphite to Nitroalkenes" *Angew. Chem. Int. Ed.* **2010**, *49*, 153-156.